HYDROPIC EAR DISEASE: IMAGING AND FUNCTIONAL EVALUATION

EDITED BY: Robert Gürkov, Shinji Naganawa and Ilmari Pyykkö
PUBLISHED IN: Frontiers in Surgery

frontiers Research Topics

ISSN 1664-8714
ISBN 978-2-88976-186-9
DOI 10.3389/978-2-88976-186-9

About Frontiers

Frontiers is more than just an open-access publisher of scholarly articles: it is a pioneering approach to the world of academia, radically improving the way scholarly research is managed. The grand vision of Frontiers is a world where all people have an equal opportunity to seek, share and generate knowledge. Frontiers provides immediate and permanent online open access to all its publications, but this alone is not enough to realize our grand goals.

Frontiers Journal Series

The Frontiers Journal Series is a multi-tier and interdisciplinary set of open-access, online journals, promising a paradigm shift from the current review, selection and dissemination processes in academic publishing. All Frontiers journals are driven by researchers for researchers; therefore, they constitute a service to the scholarly community. At the same time, the Frontiers Journal Series operates on a revolutionary invention, the tiered publishing system, initially addressing specific communities of scholars, and gradually climbing up to broader public understanding, thus serving the interests of the lay society, too.

Dedication to Quality

Each Frontiers article is a landmark of the highest quality, thanks to genuinely collaborative interactions between authors and review editors, who include some of the world's best academicians. Research must be certified by peers before entering a stream of knowledge that may eventually reach the public - and shape society; therefore, Frontiers only applies the most rigorous and unbiased reviews.
Frontiers revolutionizes research publishing by freely delivering the most outstanding research, evaluated with no bias from both the academic and social point of view. By applying the most advanced information technologies, Frontiers is catapulting scholarly publishing into a new generation.

What are Frontiers Research Topics?

Frontiers Research Topics are very popular trademarks of the Frontiers Journals Series: they are collections of at least ten articles, all centered on a particular subject. With their unique mix of varied contributions from Original Research to Review Articles, Frontiers Research Topics unify the most influential researchers, the latest key findings and historical advances in a hot research area! Find out more on how to host your own Frontiers Research Topic or contribute to one as an author by contacting the Frontiers Editorial Office: frontiersin.org/about/contact

HYDROPIC EAR DISEASE: IMAGING AND FUNCTIONAL EVALUATION

Topic Editors:
Robert Gürkov, Bielefeld University, Germany
Shinji Naganawa, Nagoya University, Japan
Ilmari Pyykkö, Tampere University, Finland

Citation: Gürkov, R., Naganawa, S., Pyykkö, I., eds. (2022). Hydropic Ear Disease: Imaging and Functional Evaluation. Lausanne: Frontiers Media SA. doi: 10.3389/978-2-88976-186-9

Table of Contents

05 ***Editorial: Hydropic Ear Disease: Imaging and Functional Evaluation***
Shinji Naganawa

07 ***Is Vestibular Meniere's Disease Associated With Endolymphatic Hydrops?***
Yuka Morita, Kuniyuki Takahashi, Shinsuke Ohshima, Chihiro Yagi, Meiko Kitazawa, Tatsuya Yamagishi, Shuji Izumi and Arata Horii

14 ***Effects of Glucocorticoids on the Inner Ear***
Taizo Takeda, Setsuko Takeda and Akinobu Kakigi

20 ***Endolymphatic Hydrops in Patients With Intralabyrinthine Schwannomas***
Yibo Zhang, Feitian Li, Chunfu Dai and Wuqing Wang

30 ***Case Report: Positive Pressure Therapy Combined With Endolymphatic sac Surgery in a Patient With Ménière's Disease***
Munehisa Fukushima, Shiro Akahani, Hidenori Inohara and Noriaki Takeda

35 ***Enhanced Eye Velocity in Head Impulse Testing—A Possible Indicator of Endolymphatic Hydrops***
Ian S. Curthoys, Leonardo Manzari, Jorge Rey-Martinez, Julia Dlugaiczyk and Ann M. Burgess

46 ***A Synchrotron and Micro-CT Study of the Human Endolymphatic Duct System: Is Meniere's Disease Caused by an Acute Endolymph Backflow?***
Hao Li, Gunesh P. Rajan, Jeremy Shaw, Seyed Alireza Rohani, Hanif M. Ladak, Sumit Agrawal and Helge Rask-Andersen

63 ***Endolymphatic Hydrops in Fluctuating Hearing Loss and Recurrent Vertigo***
Pablo Domínguez, Raquel Manrique-Huarte, Víctor Suárez-Vega, Nieves López-Laguna, Carlos Guajardo and Nicolás Pérez-Fernández

76 ***Vestibular Endolymphatic Hydrops Visualized by Magnetic Resonance Imaging and Its Correlation With Vestibular Functional Test in Patients With Unilateral Meniere's Disease***
Yupeng Liu, Fan Zhang, Baihui He, Jingchun He, Qing Zhang, Jun Yang and Maoli Duan

87 ***MRI With Intratympanic Gadolinium: Comparison Between Otoneurological and Radiological Investigation in Menière's Disease***
Giampiero Neri, Armando Tartaro and Letizia Neri

94 ***Cochlear Meniere's: A Distinct Clinical Entity With Isolated Cochlear Hydrops on High-Resolution MRI?***
Jose E. Alonso, Gail P. Ishiyama, Rance J. T. Fujiwara, Nancy Pham, Luke Ledbetter and Akira Ishiyama

104 ***Visualization of Endolymphatic Hydrops in Patients With Unilateral Idiopathic Sudden Sensorineural Hearing Loss With Four Types According to Chinese Criterion***
Huan Qin, Baihui He, Hui Wu, Yue Li, Jianyong Chen, Wei Wang, Fan Zhang, Maoli Duan and Jun Yang

113 ***Novel Magnetic Resonance Imaging-Based Method for Accurate Diagnosis of Meniere's Disease***

Taeko Ito, Takashi Inoue, Hiroshi Inui, Toshiteru Miyasaka, Toshiaki Yamanaka, Kimihiko Kichikawa, Noriaki Takeda, Masato Kasahara, Tadashi Kitahara and Shinji Naganawa

120 ***MR Imaging of Cochlear Modiolus and Endolymphatic Hydrops in Patients With Menière's Disease***

Rita Sousa, Carla Guerreiro, Tiago Eça, Jorge Campos and Leonel Luis

128 ***Advanced Imaging of the Vestibular Endolymphatic Space in Ménière's Disease***

Diego Zanetti, Giorgio Conte, Elisa Scola, Silvia Casale, Giorgio Lilli and Federica Di Berardino

137 ***Measurements From Ears With Endolymphatic Hydrops and 2-Hydroxypropyl-Beta-Cyclodextrin Provide Evidence That Loudness Recruitment Can Have a Cochlear Origin***

Shannon M. Lefler, Robert K. Duncan, Shawn S. Goodman, John J. Guinan Jr and Jeffery T. Lichtenhan

155 ***The Additional Value of Endolymphatic Hydrops Imaging With Intratympanic Contrast for Diagnostic Work-Up—Experience From a Neurotology Center in Austria***

Lennart Weitgasser, Anna O'Sullivan, Alexander Schlattau and Sebastian Roesch

161 ***Hydropic Ear Disease: Correlation Between Audiovestibular Symptoms, Endolymphatic Hydrops and Blood-Labyrinth Barrier Impairment***

Lisa M. H. de Pont, Josephine M. van Steekelenburg, Thijs O. Verhagen, Maartje Houben, Jelle J. Goeman, Berit M. Verbist, Mark A. van Buchem, Claire C. Bommeljé, Henk M. Blom and Sebastiaan Hammer

172 ***Enhanced Eye Velocity With Backup Saccades in vHIT Tests of a Menière Disease Patient: A Case Report***

Maria Montserrat Soriano-Reixach, Jorge Rey-Martinez, Xabier Altuna and Ian Curthoys

178 ***Imaging Analysis of Patients With Meniere's Disease Treated With Endolymphatic Sac-Mastoid Shunt Surgery***

Yawei Li, Yafeng Lv, Na Hu, Xiaofei Li, Haibo Wang and Daogong Zhang

184 ***Vestibular Aqueduct Morphology and Meniere's Disease—Development of the "Vestibular Aqueduct Score" by 3D Analysis***

Laurent Noyalet, Lukas Ilgen, Miriam Bürklein, Wafaa Shehata-Dieler, Johannes Taeger, Rudolf Hagen, Tilmann Neun, Simon Zabler, Daniel Althoff and Kristen Rak

194 ***Consensus on MR Imaging of Endolymphatic Hydrops in Patients With Suspected Hydropic Ear Disease (Meniere)***

Yupeng Liu, Ilmari Pyykkö, Shinji Naganawa, Pedro Marques, Robert Gürkov, Jun Yang and Maoli Duan

frontiers | Frontiers in Surgery

EDITORIAL
published: 27 April 2022
doi: 10.3389/fsurg.2022.913741

Editorial: Hydropic Ear Disease: Imaging and Functional Evaluation

*Shinji Naganawa**

Department of Radiology, Graduate School of Medicine, Nagoya University, Nagoya, Japan

Keywords: magnetic resonance imaging (MRI), Meniere's disease, Endolymphatic hydrops-related disease, Gadolilnium, Hydropic ear disease

Editorial on the Research Topic

Hydropic Ear Disease: Imaging and functional evaluation

Recent developments and advances in the objective methods of evaluating endolymphatic hydrops and its related inner ear diseases have led to a better understanding of inner ear disease. Twenty-one valuable articles have been published in this issue of the research topic "Hydropic Ear Disease: Imaging and functional evaluation" on the advances in diagnostic imaging and techniques for measuring the function of the six sensory organs present in the inner ear. As of the beginning of April 2022, it has already recorded more than 47,500 views, which means that readers are very interested in this project. Fifteen out of the 21 papers report on magnetic resonance imaging (MRI) of the patients.

MRI depiction of endolymphatic hydrops in the patients with Meniere's disease was firstly achieved in 2007 with 3D-fluid attenuated inversion recovery (FLAIR) obtained 24 h after intratympanic gadolinium contrast administration (1). A clinically feasible method using a heavily T2-weighted 3D-FLAIR after 4 hours of intravenous injection of a standard dose of gadolinium contrast agent was achieved in 2010 (2). After these developments, many technical improvements have been reported including the development of HYDROPS (HYbriD of Reversed image Of Positive endolymph signal and native image of positive perilymph Signal) technique, which utilized the subtraction of two kinds of images (3). After these developments, many institutions began to acquire the MR imaging of endolymphatic hydrops. Subsequently, an update of endolymphatic hydrops assessment using MR imaging has been proposed for the management of inner ear disease (4–7).

A number of attempts have been made to perform the assessment of endolymphatic hydrops by MRI without the use of gadolinium contrast media (8–12). However, these are unfortunately unreliable because they do not adequately distinguish between artifact and imaging findings (13–15). Recognition of the endolymphatic space on non-contrast MRI is still possible only in very exceptional cases. These exceptional cases include hemorrhage into the ampulla (16), reflux of proteinous fluid in the enlarged endolymphatic duct and sac syndrome (17), and the compositional change of perilymph due to vestibular schwannomas (18). In general, contrast-enhanced MRI evaluation of endolymphatic hydrops is the most reliable method of examination at this time.

In this research topic, Fukushima et al. have reported on the use of MRI of endolymphatic hydrops to observe the effect of positive pressure therapy in a Meniere's disease patient (https://www.frontiersin.org/articles/10.3389/fsurg.2021. 606100/full). Although this is a case report, this

OPEN ACCESS

Edited by:
Pavel Dulguerov, Geneva University Hospitals (HUG), Switzerland

****Correspondence:***
Shinji Naganawa
naganawa@med.nagoya-u.ac.jp

Speciality section:
This article was submitted to Otorhinolaryngology - Head and Neck Surgery, a section of the journal Frontiers in Surgery

Received: *06 April 2022*
Accepted: *08 April 2022*
Published: *27 April 2022*

Citation:
Naganawa S (2022) Editorial: Hydropic Ear Disease: Imaging and Functional Evaluation. Front. Surg. 9:913741. doi: 10.3389/fsurg.2022.913741

is a new and interesting proposal for the valuable and practical use of the MR imaging of endolymphatic hydrops.

In a review article of this research topic, that is co-authored by Topic editors, the authors tried to discuss and present a consensus on patient selection, imaging techniques, and evaluation methods at the occasion of 15 years after the invention of the MR imaging of the endolymphatic hydrops (https://www.frontiersin.org/articles/10.3389/fsurg.2022.874971/abstract).

It is expected that this issue of research topic will stimulate more interest in this field of research, encourage more researchers to enter the field, and ultimately help bring good news to patients suffering from the hydropics ear disease.

AUTHOR CONTRIBUTIONS

The author wrote this manuscript and aproved it alone.

REFERENCES

1. Nakashima T, Naganawa S, Sugiura M, Teranishi M, Sone M, Hayashi H, et al. Visualization of endolymphatic hydrops in patients with Meniere's disease. *Laryngoscope*. (2007) 117:415–20. doi: 10.1097/MLG.0b013e31802c300c
2. Naganawa S, Yamazaki M, Kawai H, Bokura K, Sone M, Nakashima T. Visualization of endolymphatic hydrops in Ménière's disease with single-dose intravenous gadolinium-based contrast media using heavily T(2)-weighted 3D-FLAIR. *Magn Reson Med Sci*. (2010) 9:237–42. doi: 10.2463/mrms.9.237
3. Naganawa S, Yamazaki M, Kawai H, Bokura K, Sone M, Nakashima T. Imaging of Ménière's disease after intravenous administration of single-dose gadodiamide: utility of subtraction images with different inversion time. *Magn Reson Med Sci*. (2012) 11:213–19. doi: 10.2463/mrms.11.213
4. Nakashima T, Pyykkö I, Arroll MA, Casselbrant ML, Foster CA, Manzoor NF, et al. Meniere's disease. *Nat Rev Dis Primers*. (2016) 2:16028. doi: 10.1038/nrdp.2016.28
5. Gürkov R. Menière and friends: imaging and classification of hydropic ear disease. *Otol Neurotol*. (2017) 38:e539–e544. doi: 10.1097/MAO.0000000000001479
6. Iwasaki S, Shojaku H, Murofushi T, Seo T, Kitahara T, Origasa H, et al. Committee for clinical practice guidelines of Japan Society for equilibrium research. Diagnostic and therapeutic strategies for Meniere's disease of the Japan Society for Equilibrium Research. *Auris Nasus Larynx*. (2021) 48:15–22. doi: 10.1016/j.anl.2020.10.009
7. Pyykkö I, Nakashima T, Yoshida T, Zou J, Naganawa S. Meniere's disease: a reappraisal supported by a variable latency of symptoms and the MRI visualisation of endolymphatic hydrops. *BMJ Open*. (2013) 3(2):e001555. doi: 10.1136/bmjopen-2012-001555
8. Fukutomi H, Hamitouche L, Yamamoto T, Denat L, Zhang L, Zhang B, et al. Visualization of the saccule and utricle with non-contrast-enhanced FLAIR sequences. *Eur Radiol*. (2021). doi: 10.1007/s00330-021-08403-w
9. Keller JH, Hirsch BE, Marovich RS, Branstetter 4th BF. Detection of endolymphatic hydrops using traditional MR imaging sequences. *Am J Otolaryngol*. (2017) 38:442–6. doi: 10.1016/j.amjoto.2017.01.038
10. Simon F, Guichard J-P, Kania R, Franc J, Herman P, Hautefort C. Saccular measurements in routine MRI can predict hydrops in Menière's disease. *Eur Arch Otorhinolaryngol*. (2017) 274:4113–20. doi: 10.1007/s00405-017-4756-8
11. van der Lubbe MFJA, Vaidyanathan A, de Wit M, van den Burg EL, Postma AA, Bruintjes TD, et al. A non-invasive, automated diagnosis of Menière's disease using radiomics and machine learning on conventional magnetic resonance imaging: a multicentric, case-controlled feasibility study. *Radiol Med*. (2022) 127:72–82. doi: 10.1007/s11547-021-01425-w
12. Venkatasamy A, Veillon F, Fleury A, Eliezer M, Abu Eid M, Romain B, et al. Imaging of the saccule for the diagnosis of endolymphatic hydrops in Meniere disease, using a three-dimensional T2-weighted steady state free precession sequence: accurate, fast, and without contrast material intravenous injection. *Eur Radiol Exp*. (2017) 1(14). doi: 10.1186/s41747-017-0020-7
13. Naganawa S, Ito R, Taoka T, Yoshida T, Sone M. Letter to editor on the article "A non-invasive, automated diagnosis of Menière's disease using radiomics and machine learning on conventional magnetic resonance imaging: a multicentric, case-controlled feasibility study" by van der Lubbe Mfja et al. *Radiol Med*. (2022). doi: 10.1007/s11547-022-01486-5
14. Naganawa S, Sone M. Letter to Editors: Detection of endolymphatic hydrops using traditional MR imaging sequences. *Am J Otolaryngol*. (2017) 38:637–8. doi: 10.1016/j.amjoto.2017.06.014
15. Dominguez P, Naganawa S. Letter to the editor on the article "Saccular measurements in routine MRI can predict hydrops in Ménière's disease" by Simon F, et al. *Eur Arch Otorhinolaryngol*. (2018) 275:311–12. doi: 10.1007/s00405-017-4794-2
16. Naganawa S, Ishihara S, Iwano S, Sone M, Nakashima T. Detection of presumed hemorrhage in the ampullar endolymph of the semicircular canal: a case report. *Magn Reson Med Sci*. (2009) 8:187–91. doi: 10.2463/mrms.8.187
17. Naganawa S, Sone M, Otake H, Nakashima T. Endolymphatic hydrops of the labyrinth visualized on noncontrast MR imaging: a case report. *Magn Reson Med Sci*. (2009) 8:43–6. doi: 10.2463/mrms.8.43
18. Yamazaki M, Naganawa S, Kawai H, Nihashi T, Fukatsu H, Nakashima T. Increased signal intensity of the cochlea on pre- and post-contrast enhanced 3D-FLAIR in patients with vestibular schwannoma. *Neuroradiology*. (2009) 51:855–63. doi: 10.1007/s00234-009-0588-6

Conflict of Interest: The authors declare that the research was conducted in the absence of any commercial or financial relationships that could be construed as a potential conflict of interest.

frontiers in Surgery

ORIGINAL RESEARCH
published: 18 December 2020
doi: 10.3389/fsurg.2020.601692

Is Vestibular Meniere's Disease Associated With Endolymphatic Hydrops?

Yuka Morita, Kuniyuki Takahashi, Shinsuke Ohshima, Chihiro Yagi, Meiko Kitazawa, Tatsuya Yamagishi, Shuji Izumi and Arata Horii*

Department of Otolaryngology, Head and Neck Surgery, Graduate School of Medical and Dental Sciences, Niigata University, Niigata, Japan

OPEN ACCESS

Edited by:
Robert Gürkov, Bielefeld University, Germany

Reviewed by:
Jeremy Hornibrook, University of Canterbury, New Zealand
Hans Thomeer, University Medical Center Utrecht, Netherlands
Bert De Foer, Sint Augustinus Hospital, Belgium

***Correspondence:**
Yuka Morita
yukam@med.niigata-u.ac.jp

Specialty section:
This article was submitted to Otorhinolaryngology - Head and Neck Surgery, a section of the journal Frontiers in Surgery

Received: *01 September 2020*
Accepted: *02 November 2020*
Published: *18 December 2020*

Citation:
Morita Y, Takahashi K, Ohshima S, Yagi C, Kitazawa M, Yamagishi T, Izumi S and Horii A (2020) Is Vestibular Meniere's Disease Associated With Endolymphatic Hydrops? Front. Surg. 7:601692. doi: 10.3389/fsurg.2020.601692

Background: Vestibular Meniere's disease (American Academy of Ophthalmology and Otolaryngology, 1972) also known as possible Meniere's disease (American Academy of Otolaryngology Head and Neck Surgery, 1995) or vestibular type of atypical Meniere's disease (V-AMD) (Japan Society for Equilibrium Research, 2017) is characterized by an episodic vertigo without hearing loss. Though named as Meniere's disease (MD), this entity may not be caused solely by endolymphatic hydrops (EH).

Objective: To estimate the role of EH in vestibular Meniere's disease in comparison with definite Meniere's disease.

Methods: Thirty patients with unilateral definite MD and 16 patients with vestibular Meniere's disease were included. Those who met the criteria for definite or probable vestibular migraine were excluded. All patients underwent vestibular assessments including inner ear MRI 4 h after intravenous gadolinium injection, bithermal caloric testing, directional preponderance of vestibulo-ocular reflex in rotatory chair test, cervical- and ocular-vestibular evoked myogenic potential, stepping test, dizziness handicap inventory (DHI), and hospital anxiety and depression scale (HADS). All above tests and frequency/duration of vertigo spells were compared between vestibular Meniere's disease and MD.

Results: Even in unilateral MD, cochlear and vestibular endolymphatic hydrops (c-, v-EH) were demonstrated not only in the affected side but also in the healthy side in more than half of patients. Positive rate of v-EH in vestibular Meniere's disease (68.8%) was as high as that of MD (80%). In vestibular Meniere's disease, the number of bilateral EH was higher in the vestibule (56.3%) than that in the cochlea (25.0%). There were no differences in vestibular tests and DHI between vestibular Meniere's disease and MD; however, the frequency of vertigo spells was lower in vestibular Meniere's disease ($p = 0.001$). The total HADS score in the MD group was significantly higher than that in the vestibular Meniere's disease group.

Conclusions: MD is a systemic disease with bilateral involvement of inner ears. V-EH is a major pathophysiology of vestibular Meniere's disease, which would precede c-EH in the development of vestibular Meniere's disease, a milder subtype of MD. MRI is useful for differentiating MD from other vertigo attacks caused by different pathologies in bringing EH into evidence.

Keywords: Meniere's disease, endolymphatic hydrops (EH), episodic vertigo, magnetic resonance imaging, diagnosis

INTRODUCTION

Meniere's disease is characterized by episodic vertigo, fluctuating progressive sensorineural hearing loss, and other cochlear symptoms such as tinnitus and aural fullness. The American Academy of Ophthalmology and Otolaryngology (AAOO) defined vestibular Meniere's disease as showing only episodic vertigo without hearing loss in 1972 (1). Paparella and Mancini reported two subgroups of vestibular Meniere's disease that had distinctive clinical profiles. In one subgroup, patients subsequently develop hearing loss and typical Meniere's disease with aural pressure, whereas those in the other subgroup do not (2). This suggests that subvarieties that include not only endolymphatic hydrops (EH) but also other pathophysiologies may be involved in vestibular Meniere's disease. Twenty-three years later, the term "vestibular Meniere's disease" was withdrawn from the American Academy of Otolaryngology-Head and Neck Surgery (AAO-HNS) definitions of Meniere's disease (3), probably because "vestibular Meniere's disease" had been thought to be not solely caused by endolymphatic hydrops. As a result, the formerly known vestibular Meniere's disease (1, 2) was placed into a category of "possible Meniere's disease" on the AAO-HNS 1995 criteria. Later definitions of Meniere's disease that were proposed by the Barany Society 2015 (4) and AAO-HNS 2000 (5) did not include the subvarieties of Meniere's disease, such as vestibular and cochlear Meniere's disease, whereas the definition by the Japan Society for Equilibrium Research (JSER) in 2017 included the vestibular type of atypical Meniere's disease (6), which is basically the same concept as that of vestibular Meniere's disease (1, 2).

Until 2007 when Nakashima et al. published the first report on visualization of endolymphatic hydrops in Meniere's patients (7), EH could only be evidenced by postmortem histology. To examine whether vestibular Meniere's disease is associated with EH, we conducted a comparative study to differentiate vestibular Meniere's disease from definite Meniere's disease by inner ear magnetic resonance imaging (MRI) studies as well as several assessments including demographic and clinical characteristics and vestibular function tests.

MATERIALS AND METHODS

The studies involving human participants were reviewed and approved by the Institutional Review Board of Niigata University Hospital (No. 2015-2440).

Thirty patients with unilateral definite Meniere's disease (Barany Society definition) (4) and 16 patients with vestibular Meniere's disease (AAOO-1972, Paparella and Mancini) (1, 2), diagnosed between 2015 and 2019, were included in this study. The side affected by definite Meniere's disease, that is, the side with a higher hearing threshold, was decided on the basis of an audiogram. In cases of vestibular Meniere's disease, we did not discuss the affected side but only concentrated whether the EH was identified unilaterally or bilaterally. All 16 patients with vestibular Meniere's disease did not meet the diagnostic criteria for both definite and probable vestibular migraine (VM) (8).

Demographic and clinical data, including age, sex, period from disease onset to consultation, frequency of vertigo spells, and duration of vertigo attack, were obtained from the patients' medical records.

All the patients underwent inner ear imaging studies using a 3-T MR unit after receiving intravenous contrast injections as described by Naganawa et al. (9). Briefly, MRI measurements were performed 4 h after intravenous administration of a single dose (0.2 ml/kg or 0.1 mmol/kg of body weight) of gadolinium-diethylenetriaminepentaacetic acid dimethylamide (Gadovist, Bayer Healthcare, Leverkusen, Germany) using a 3-T MR unit (MAGNETOM Prisma; Siemens, Erlangen, Germany) with a 64-channel array head coil. Heavily T2-weighted MR cisternography was obtained as the anatomical reference of the total lymph fluid, and heavily T2-weighted(hT2W)-3D-FLAIR with inversion time (TI) of 2,250 ms (PPI) and hT2W-3D-inversion recovery with TI of 2,050 ms (PEI) were obtained as the methods proposed by Naganawa et al. (9). Two head and neck radiologists with 30 and 22 years of experience who were blinded to the clinical data independently assessed the cochlear and vestibular endolymphatic hydropses (c-EH and v-EH) as none, mild, or significant, using a grading system proposed by Nakashima et al. (10) (**Figure 1**). Mild or significant hydrops was defined as positive hydrops. Discrepant interpretations were resolved by discussion between the radiologists.

The patients also underwent vestibular assessments, including bithermal caloric testing, cervical and ocular-vestibular-evoked myogenic potentials (VEMP), stepping test, and rotatory chair test. The validated Japanese versions of the Dizziness Handicap Inventory and Hospital Anxiety and Depression Scale were used for the evaluation of subjective symptoms and psychological state.

Caloric Test

An alternate bithermal (26 and 45°C) air caloric test was performed. The maximum slow phase velocity of the nystagmus was measured on electronystagmography, and the canal paresis % (CP%) was calculated using the formula of Jongkees (11). A

	none	mild	significant
		Displacement of Reissner's membrane	
cochlea	No displacement of Reissner's membrane	Area of cochlear duct ≦ area of the scala vestibuli	Area of the cochlear duct exceeds the area of the scala vestibuli
vestibule (area ratio*)	≦ 33.3%	>33.3%, ≦ 50%	>50%

FIGURE 1 | The grading system of endolymphatic hydrops [Nakashima et al. (10)]. In the vestibule, the grading was determined by the ratio of the area of endolymphatic space to the vestibular fluid space (sum of the endolymphatic and perilymphatic spaces). Patients with no hydrops have a ratio of one-third or less, those with mild hydrops have between one-third and a half, and those with significant hydrops have a ratio of more than 50%. In the cochlea, patients classified as having no hydrops show no displacement of Reissner's membrane; those with mild hydrops show displacement of Reissner's membrane, but the area of the endolymphatic space does not exceed the area of the scala vestibuli; and in those with significant hydrops, the area of the endolymphatic space exceeds the area of the scala vestibuli. *Ratio of the area of the endolymphatic space to that of the fluid space (sum of the endolymphatic and perilymphatic spaces) in the vestibule measured on image tracings.

CP of >20% was considered to indicate a significant unilateral caloric weakness.

VEMP

To quantify otolithic function, cervical VEMP (cVEMP) and ocular VEMP (oVEMP) were recorded using the Neuropack system (Nihon Koden, Japan). During the recording for cVEMP, the subjects were asked to lie in the supine position with their heads raised. The click (0.1-ms rarefactive square waves of 105-dB nHL) was used to induce cVEMP. For the recording of oVEMP, a hand-held electromechanical vibrator (Minishaker, Bruel & Kjaer, Denmark) fitted with a short bolt terminating in a plastic cap was used. The vibrator delivered a 500-Hz tone burst (4-ms plateau and 1-ms rise and fall) on the subject's skull at the Fz (midline of the hairline). The subjects were in the supine position during the measurement and asked to stare 30° upward and fix their gaze on a specific mark in front of them. The interaural asymmetry ratios (IAARs) of cVEMP and oVEMP were obtained using the following formula:

$$\mathrm{IAAR} = (\mathrm{Ar} - \mathrm{Al})/(\mathrm{Ar} + \mathrm{Al}) \times 100$$

Ar: normalized amplitude (p13-n23 or n10-p15) on the right side
Al: normalized amplitude (p13-n23 or n10-p15) on the left side

A |AR| of >33.3% was defined as a unilateral saccular (cVEMP) or utricular (oVEMP) dysfunction.

Stepping Test

The subject was asked to stand upright with the feet close together in the centers of circles with radii of 0.5 and 1 m that were drawn on the floor. The subject was then blindfolded and instructed to stretch both arms straight forward and to step in place at a normal walking speed (∼110 steps/min) for a total of 100 steps. The abnormality threshold was set as a rotational deviation >45°.

Rotatory Chair Test

The rotatory chair test was performed using Nistamo21 IRN 2 (Morita, Japan). The patients sat in a rotatory chair to which a pendulum-like rotation was applied so that the maximum head angular velocity was 50°/s at a stimulation frequency of 0.1 Hz. The angular velocity of eye movements was monitored and analyzed. The vestibulo-ocular reflex directional preponderance (VOR-DP) was calculated, and a VOR-DP of >12% was considered a significant DP.

Dizziness Handicap Inventory

The Dizziness Handicap Inventory (DHI) is a standard questionnaire that quantitatively evaluates the degree of handicap in the daily life of patients with vestibular disorders; it consists of 25 questions (12, 13). The total score ranges from 0 (no disability) to 100 (severe disability).

Hospital Anxiety and Depression Scale

The Hospital Anxiety and Depression Scale (HADS) is a 14-item questionnaire that is comprised of two subscales for assessing non-somatic symptoms of anxiety (HADS-A) and depression (HADS-D). Each item of the questionnaire is rated from 0 to 3. The scores in the two subscales range from 0 (no sign of anxiety or depression) to 21 (maximum level of anxiety or depression). A score of ≥11 is indicative of probable anxiety or depression (14).

Statistical analyses were conducted using the SPSS version 21 package software. Described statistics are summarized in number, percentage, median and range, or mean and standard deviation. Intergroup comparisons were performed using the Mann–Whitney *U*-test. Intergroup comparisons of the qualitative variables were performed using the Fisher exact test. A threshold of $p < 0.05$ was set to evaluate statistical significance.

TABLE 1 | Demographic and clinical characteristics and vestibular assessments of the patients with Meniere's disease (MD) and vestibular Meniere's disease (VMD).

	MD	VMD	*p*-value
Age	46 (19–83)	45 (25–71)	0.972
Male/female	15/15	2/14	0.014*
Period from onset, median (range)	33 (2–408)	72 (2–552)	0.008*
Duration of vertigo attack			0.329
<1 h	5	3	
<6 h	14	9	
<12 h	0	0	
>12 h	2	4	
Unknown	9	0	
Frequency of vertigo spells			0.001**
Every day	2	0	
1 or 2/week	1	0	
1 or 2/month	13	2	
5 or 6/year	5	2	
1 or 2/year	7	12	
Unknown	2	0	
DHI (mean ± *SD*)	41.1 ± 19.1	34.6 ± 15.0	0.321
P	10.8 ± 6.7	11.4 ± 3.8	0.624
E	14.5 ± 7.0	10.5 ± 7.3	0.059
F	15.7 ± 8.7	12.8 ± 7.2	0.186
HADS-total (mean ± *SD*)	15.2 ± 5.2	10.1 ± 5.9	0.008**
HADS-A	7.4 ± 3.4	5.1 ± 3.8	0.062
HADS-D	7.8 ± 3.3	5.1 ± 3.2	0.01*
Vestibular Assessments			
CP% > 20%	15 (50%)	4 (25%)	0.132
cVEMP asymmetry > 33.3%	9 (30%)	3 (18.8%)	0.323
oVEMP asymmetry > 33.3%	5 (16.7%)	1 (6.25%)	0.307
Stepping test positive	12 (40%)	9 (56.3%)	0.563
VOR-DP > 12%	12 (40%)	5 (31.3%)	0.502

** values indicates the statistical significant. *$p < 0.05$ and **$p < 0.01$.*

RESULTS

Table 1 shows the demographic and clinical characteristics and vestibular assessments of the patients with Meniere's disease and vestibular Meniere's disease. Vestibular Meniere's disease was female-dominant ($p = 0.014$) as compared with Meniere's disease. The period from the onset of the first vertigo attack to consultation in vestibular Meniere's disease (median: 72 months, range: 2–552 months) was significantly longer than that in Meniere's disease (median: 33 months, range: 2–408 months; $p = 0.008$). Vertigo spells usually occur once or twice a month in Meniere's disease but are significantly less frequent in vestibular Meniere's disease ($p = 0.001$). The total HADS score in the Meniere's disease group (15.2 ± 5.2) was significantly higher than that in the vestibular Meniere's disease group (10.1 ± 5.9). No significant differences in age, duration of vertigo attack, and DHI score were found.

The vestibular function test revealed no significant differences in CP%, c-VEMPs, o-VEMPs, VOR-DP in the rotatory chair test, and stepping test score between the Meniere's disease and vestibular Meniere's disease groups.

Figure 2 shows the statuses of (A) the cochlear EH (c-EH) and (**B**) vestibular EH (v-EH) of the affected and healthy sides of the patients in the Meniere's disease group. Even on the healthy side, c-EH and v-EH (significant + mild) were demonstrated in 66.7% (13.3 + 53.4%; **Figure 2A**, healthy side) and 50% (13.3 + 36.7%; **Figure 2B**, healthy side) of the patients in the Meniere's disease group, respectively. The proportion of significant EH was higher on the affected side of the cochlea (**Figure 2A**; $p = 0.028$) and vestibule (**Figure 2B**; $p = 0.021$) than on the healthy side in the Meniere's disease group.

Figure 3 shows the status of EH (bilateral, unilateral, or none) in the (A) Meniere's disease and (B) vestibular Meniere's disease groups. The number of bilateral v-EH cases in the v-EH-positive vestibular Meniere's disease group was higher than that of bilateral c-EH in the c-EH-positive vestibular Meniere's disease group ($p < 0.05$; **Figure 3B**). By contrast, the number proportion of bilateral v-EH was not different from that of bilateral c-EH in the Meniere's disease group (**Figure 3A**).

c-EH and/or v-EH was found in 93.3% of the patients with Meniere's disease and 87.5% of the patients with vestibular Meniere's disease (**Table 2**). While the positivity rate of c-EH in vestibular Meniere's disease (62.5%) was significantly lower than that in Meniere's disease (90%), the positivity rate of v-EH in vestibular Meniere's disease (68.8%) was as high as that in Meniere's disease (80%; **Table 2**).

DISCUSSION

EH in Meniere's Disease

In general, Meniere's disease affects one side of the ears. Several studies reported that the incidence of bilateral Meniere's disease was 2–47%, depending on the length of follow-up and strictness of adherence to the criteria for diagnosis (15, 16). Recently, inner ear MRI scans have demonstrated the existence of EH in the unaffected ear in patients with Meniere's disease. Yoshida et al. reported that the incidence rates of EH in the cochlea and vestibule on the healthy side of patients with Meniere's disease were 46.9 and 53.2%, respectively (17). In our study, even on the healthy side, c-EH (**Figure 2A**, healthy side) and v-EH (**Figure 2B**, healthy side) were demonstrated in 66.7 and 50% of the patients with Meniere's disease, respectively. Taken together, these findings could imply that Meniere's disease is a systemic disorder or that an abnormal process affecting one ear can affect the other ear after time. As EH on the affected side was more severe than that on the healthy side (**Figure 2A** for c-EH and **Figure 2B** for v-EH), Meniere's disease may not have bilateral EH from the early stage but could progress from a unilateral disease to a bilateral disease.

EH in Vestibular Meniere's Disease

As shown in **Table 2**, inner ear MRI studies demonstrated that v-EH was present in most patients (68.8%) with vestibular Meniere's disease. Kato et al. also reported that the positivity rate of v-EH in patients with vestibular Meniere's disease was

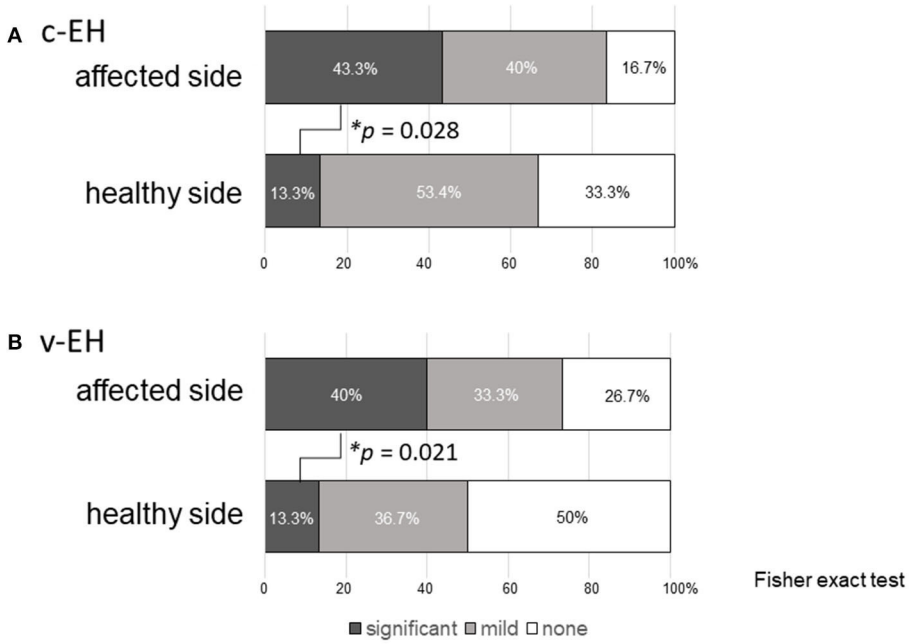

FIGURE 2 | Endolymphatic hydrops in the affected and healthy side of Meniere's disease. **(A)** Cochlea endolymphatic hydrops (c-EH) and **(B)** vestibular endolymphatic hydrops (v-EH). Even on the healthy side, c-EH and v-EH (significant + mild) were demonstrated in 66.7% (13.3 + 53.4%; **A**, healthy side) and 50% (13.3 + 36.7%) of the patients in the Meniere's disease group (**B**, healthy side), respectively. The proportion of significant EH was higher on the affected side of the cochlea (**A**; $p = 0.028$) and vestibule (**B**; $p = 0.021$) than on the healthy side in the Meniere's disease group. c-EH, cochlea endolymphatic hydrops; v-EH, vestibular endolymphatic hydrops.

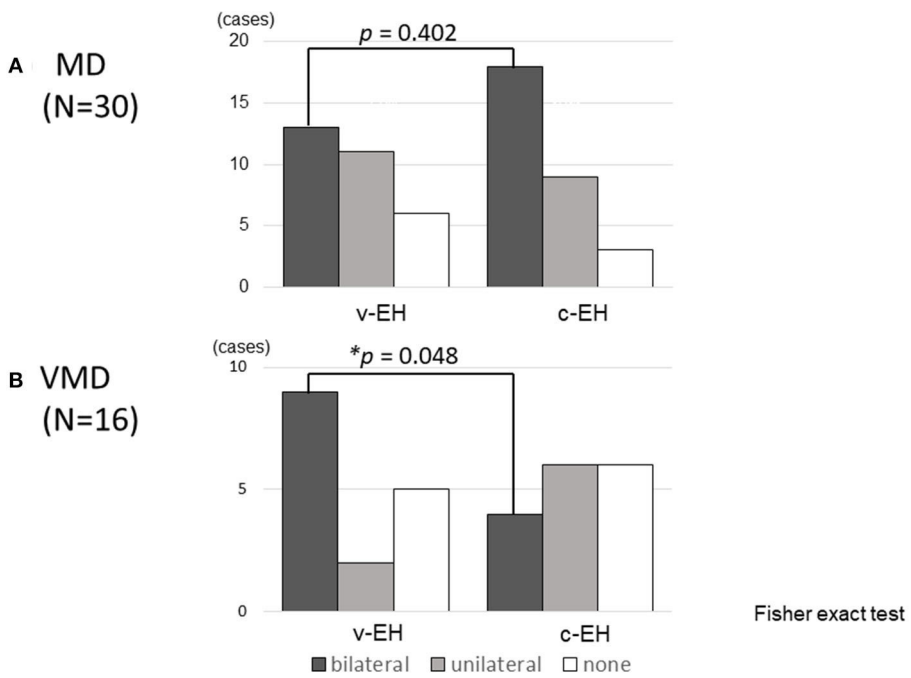

FIGURE 3 | Cochlear and vestibular endolymphatic hydrops in **(A)** Meniere's disease (MD) and **(B)** vestibular Meniere's disease (VMD). **(A)** The number of bilateral v-EH was not different from bilateral c-EH in Meniere's disease. **(B)** The number of bilateral v-EH in v-EH-positive VMD patients was higher than that of bilateral c-EH in c-EH-positive VMD patients ($p < 0.05$). v-EH, vestibular endolymphatic hydrops; c-EH, cochlea endolymphatic hydrops.

TABLE 2 | Endolymphatic hydrops in Meniere's disease (MD) and vestibular Meniere's disease (VMD).

	MD	VMD	*p*-value
c-EH positive	27 (90%)	10 (62.5%)	0.034*
v-EH positive	24 (80%)	11 (68.8%)	0.308
c-EH and/or v-EH positive	28 (93.3%)	14 (87.5%)	0.221

*c-EH, cochlear endolymphatic hydrops; v-EH, vestibular endolymphatic hydrops. * value indicate the statistical significant. *$p < 0.05$.*

83% (18). Although healthy controls were not enrolled in this study, a previous report demonstrated that v-EH is rarely found (7%) in controls without audiovestibular diseases (17), suggesting that most patients with vestibular Meniere's disease are actually associated with v-EH. c-EH was also demonstrated in 62.5% of the patients with vestibular Meniere's disease, resulting in an EH-positivity rate of 87.5% in the vestibule and/or cochlea in patients with vestibular Meniere's disease. This rate was as high as that of definite Meniere's disease (93.3%; **Table 2**), which suggests that vestibular Meniere's disease is a vestibular type of primary hydropic ear disease (19). Attyé et al. also reported that half of the patients with repeated peripheral vertigo that lasted 20 min without hearing loss, which seems to have the same symptoms as vestibular Meniere's disease, showed v-EH and/or c-EH on MRI, which suggests an association of v-EH with vestibular Meniere's disease (20).

Not only v-EH but also c-EH was found in 62.5% of the patients with vestibular Meniere's disease (**Table 2**), which suggests that vestibular Meniere's disease could potentially develop to Meniere's disease. As shown in **Figure 3B**, the number of bilateral v-EH cases was higher than that of bilateral c-EH cases in patients with vestibular Meniere's disease, which suggests that v-EH precedes c-EH in the development of vestibular Meniere's disease. When c-EH starts to exert cochlear symptoms, vestibular Meniere's disease would develop into definite Meniere's disease.

Differential Diagnosis of Vestibular Meniere's Disease

As a differential diagnosis of vestibular Meniere's disease, vestibular migraine (VM), which also shows episodic vertigo plus migraine, is most challenging to diagnose in clinical settings. Although we excluded patients with VM from the study by carefully interviewing patients regarding headache and migraine, patients with similar but not exactly the same pathophysiology as VM might be included in the study group. Our female-dominant study population (**Table 1**) would be partly consistent with the demographic characteristics of VM (21). This would account for the v-EH-negative populations of patients with vestibular Meniere's disease, which accounted for 31.2% of the patients with vestibular Meniere's disease (**Table 2**). According to a previous report that focused on the inner ear MRI of patients with VM, the positivity rate of EH in patients with VM was significantly lower than that in vestibular Meniere's disease (22). Taken together, the v-EH on inner ear MRI could be a useful sign for the discrimination of EH-associated vestibular Meniere's disease from VM.

Vestibular Meniere's disease might have two variants: one that subsequently develops into definite Meniere's disease and another that does not (2). The former group would be associated with EH, whereas the latter group may have a VM-related pathophysiology. Comparative studies to examine clinical courses such as future development into Meniere's disease or VM should be conducted in EH-positive and EH-negative episodic vertigo patients without hearing loss. Because treatment strategy is totally different between the two variants (i.e., the same treatment as the definite Meniere's disease for EH-positive variants and calcium blockers for the VM-related pathologies, inner ear MRI is quite important not only to diagnose vestibular Meniere's disease but also to select the appropriate treatment).

Clinical Characteristics and Vestibular Function of Patients With Vestibular Meniere's Disease

In this study, we conducted a comparative study to differentiate vestibular Meniere's disease from definite Meniere's disease by assessing several factors, including not only EH imaging studies but also demographic and clinical characteristics and vestibular tests. Among these distinguishing features, a longer period from onset to consultation, lower frequency of vertigo spells, and lower total HADS score were found in the vestibular Meniere's disease group as compared with the definite Meniere's disease group (**Table 1**). These results suggest that the overall symptoms of vestibular Meniere's disease are mild as compared with those of definite Meniere's disease. In parallel with these symptom scales, the positivity rate of c-EH was lower in the vestibular Meniere's disease group (62.5%) than in the definite Meniere's disease group (90%; **Table 2**). All these findings suggest that vestibular Meniere's disease may be a milder subtype of Meniere's disease.

Limitations and Conclusions

One limitation of the study was that no control participants were enrolled. For instance, the positivity rate of v-EH in vestibular Meniere's disease should have been compared with that in control patients. However, at present, contrast-enhanced MRI is difficult to perform in healthy volunteers. Instead, we performed a comparative study with definite Meniere's disease to show the similarity of inner ear status between vestibular and of definite Meniere's disease. Nonetheless, according to the previous reports using the same inner ear MRI methods as the present study, the positivity rate of EH in healthy groups was 38.1% for c-EH and 7.1% for v-EH (16). Therefore, the positivity rates of c-EH (62.5%) and v-EH (68.8%) in our patients with vestibular Meniere's disease seem sufficiently higher than those in healthy controls.

In conclusion, V-EH is a major pathophysiology of vestibular Meniere's disease, which would precede c-EH in the development of vestibular Meniere's disease, a milder subtype of Meniere's disease in terms of clinical symptoms and hydrops. Inner ear MRI

is useful for the differential diagnosis of episodic vertigo without hearing loss.

DATA AVAILABILITY STATEMENT

The original contributions presented in the study are included in the article/supplementary materials, further inquiries can be directed to the corresponding author/s.

ETHICS STATEMENT

The studies involving human participants were reviewed and approved by the institutional review board of Niigata University Hospital (No. 2015-2440). The patients/participants provided their written informed consent to participate in this study.

AUTHOR CONTRIBUTIONS

YM and AH contributed to the conception and design of the manuscript. KT, SO, CY, MK, TY, and SI made substantial contributions to the conception of the work and were responsible for data collection. YM wrote the manuscript. All authors contributed to manuscript revision, read, and approved the submitted version.

FUNDING

This work was partly supported by Grants-in-Aid from the Ministry of Education, Culture, Sports, Science and Technology of Japan (18K09371) and Japan Agency for Medical Research and Development (18059460).

REFERENCES

1. Alford BR. Committee on hearing and equilibrium, report on subcommittee on equilibrium and its measurement, Meniere's disease: criteria for diagnosis and evaluation of therapy for reporting. *Trans Am Acad Ophthalmol Otolaryngol.* (1972) 76:1462–4.
2. Paparella MM, Mancini F. Vestibular Meniere disease. *Otolaryngol Head Neck Surg.* (1985) 93:148–51. doi: 10.1177/019459988509300203
3. Committeee on Hearing and Equilibrium. Committee on hearing and equilibrium guidelines for the diagnosis and evaluation of therapy in Menière's disease, American Academy of Otolaryngology-Head and Neck Foundation, Inc. *Otolaryngol Head Neck Surg.* (1995) 113:181–5. doi: 10.1016/S0194-5998(95)70102-8
4. Lopez-Escamez JA, Carey J, Chung WH, Goebel JA, Magnusson M, Mandala M, et al. Diagnostic criteria for Ménière's disease. *J Vestib Res.* (2015) 25:1–7. doi: 10.3233/VES-150549
5. Basura GJ, Adams ME, Monfared A, Schwartz SR, Antonelli PJ, Burkard R, et al. Clinical practice guideline: Meniere's disease. *Otolaryngol Head Neck Surg.* (2020) 162:S1–55. doi: 10.1177/0194599820909438
6. Japan Society for Equilibrium Research. Diagnostic criteria of Meniere's disease. *Equilibrium Res.* (2017) 76:233–41. doi: 10.3757/jser.76.302
7. Nakashima T, Naganawa S, Sugiura M, Teranishi M, Sone M, Hayashi H, et al. Visualization of endolymphatic hydrops in patients with Meniere's disease. *Laryngoscope*. (2007) 117:415–20. doi: 10.1097/MLG.0b013e31802c300c
8. Lempert T, Olesen J, Furman J, Waterston J, Seemungal B, Carey J, et al. Vestibular migraine: diagnostic criteria. *J Vestibular Res.* (2012) 22:167–72. doi: 10.3233/VES-2012-0453
9. Naganawa S, Yamazaki M, Kawai H, Bokura K, Sone M, Nakashima T. Imaging of Menière's disease after intravenous administration of single-dose gadodiamide: utility of multiplication of MR cisternography and HYDROPS image. *Magn Reson Med Sci.* (2013) 12:63–8. doi: 10.2463/mrms.2012-0027
10. Nakashima T, Naganawa S, Pyykkö I, Gibson WPR, Sone M, Nakata S, et al. Grading of endolymphatic hydrops using magnetic resonance imageing. *Acta Otolaryngol Suppl.* (2009) 560:5–8. doi: 10.1080/00016480902729827
11. Jongkees LB, Maas JP, Philipszoon AJ. Clinical nystamography; a detailed study of electro-nystamography in 341 patients with vertigo. *Pract Otorhinolaryngol.* (1962) 24:65–93. doi: 10.1159/000274383
12. Goto F, Tsutsumi T, Ogawa K. The Japanese version of the Dizziness Handicap Inventory as an index of treatment success; exploratory factor analysis. *Acta Otolaryngol.* (2011) 131:817–5. doi: 10.3109/00016489.2011.565423
13. Jacobson GP, Newman CW. The development of the Dizziness Handicap Inventory. *Arch Otolaryngol Head Neck Surg.* (1990) 116:424–7. doi: 10.1001/archotol.1990.01870040046011
14. Zigmond AS, Snaith RP. The hospital anxiety and depression scale. *Acta Psychiatr Scand.* (1983) 67:361–70. doi: 10.1111/j.1600-0447.1983.tb09716.x
15. Huppert D, Strupp M, Brandt T. Long term course of Meniere's disease revisited. *Acta Otolaryngol.* (2010) 130:356–62. doi: 10.3109/00016480903382808
16. Suh MJ, Jeong J, Kim HJ, Jung J, Kim SH. Clinical characteristics of bilateral Meniere's disease in a single Asian ethnic group. *Laryngoscope.* (2019) 129:1191–6. doi: 10.1002/lary.27423
17. Yoshida T, Sugimoto S, Teranishi M, Otake H, Yamazaki M, Naganawa S, et al. Imaging of the endolymphatic space in patients with Ménière's disease. *Auris Nasus Larynx.* (2018) 45:33–8. doi: 10.1016/j.anl.2017.02.002
18. Kato M, Sugiura M, Shimono M, Yoshida T, Otake H, Kato K, et al. Endolymphatic hydrops revealed by magnetic resonance imaging in patients with atypical Meniere's disease. *Acta Otolaryngol.* (2013) 133:123–9. doi: 10.3109/00016489.2012.726374
19. Gürkov R, Pyykö I, Zou J, Kentala E. What is Meniere's disease? A contemporary re-evaluation of endolymphatic hydrops. *J Neurol.* (2016) 263:71–81. doi: 10.1007/s00415-015-7930-1
20. Attye A, Dumas G, Troprès I, Roustit M, Karkas A, Banciu E, et al. Recurrent peripheral vestibulopathy: is MRI useful for the diagnosis of endolymphatic hydrops in clinical practice? *Eur Radiol.* (2015) 25:3043–9. doi: 10.1007/s00330-015-3712-5
21. Furman JM, Marcus DA, Balaban CD. Vestibular migraine: clinical aspects and pathophysiology. *Lancet Neurol.* (2013) 12:706–5. doi: 10.1016/S1474-4422(13)70107-8
22. Nakada T, Yoshida T, Suga K, Kato M, Otake H, Kato K, et al. Endolymphatic space size in patients with vestibular migraine and Menière's disease. *J Neurol.* (2014) 261:2079–84. doi: 10.1007/s00415-014-7458-9

Conflict of Interest: The authors declare that the research was conducted in the absence of any commercial or financial relationships that could be construed as a potential conflict of interest.

frontiers in Surgery

ORIGINAL RESEARCH
published: 11 January 2021
doi: 10.3389/fsurg.2020.596383

Effects of Glucocorticoids on the Inner Ear

Taizo Takeda[1], *Setsuko Takeda*[1] *and Akinobu Kakigi*[2]*

[1] Kochi Medical School, Kochi, Japan, [2] Department of Otorhinolaryngology Head and Neck Surgery, Graduate School of Medicine, Kobe University, Kobe, Japan

Hypothesis: Recently, several lines of evidence have suggested that the inner ear is under hormonal control. It is likely that steroids have some influence on the inner ear.

Background: Many clinicians have been empirically using steroids for the treatment of diseases associated with endolymphatic hydrops. The theoretical grounds for this are not clear, and there have been a number of debates on the effectiveness of steroid treatment. Furthermore, there are few reports on histological observations of the influences of steroids on the cochlea.

Method: Fifteen guinea pigs (30 ears) were divided into three groups. In the control group, physiological saline solution was administered intra-peritoneally for 3 days. In two steroid groups, 40 mg/kg/day of hydrocortisone or 4 mg/kg/day of dexamethasone was administered intra-peritoneally for 3 days. Extension of Reissner's membrane and volume change of the scala media were checked 6 h after the last administration. The degree of Reissner's membrane extension and volumetric change of the scala media were quantitatively measured with the use of a video-digitizer.

Results: We did not identify any distinct changes in the cochlea of the control group. In contrast, the extension of Reissner's membrane and endolymphatic hydrops were observed in the animals in the steroid groups. Statistical analysis revealed that Reissner's membrane extended significantly in the steroid groups, and that the volume of the scala media also increased significantly.

Conclusion: This is the first report to investigate the effects of systemic administration of glucocorticoids on guineapig cochlea. The extension of Reissner's membrane and dilated endolymphatic space were evident in the steroid groups. However, the underlying mechanism of histological changes was not clear, marked care needs to be taken when administering steroids to patients with Meniere's disease whose histological feature is endolymphatic hydrops.

Keywords: hydrocortisone, dexamehtasone, endolymphatic hydrops (EH), sudden deafness, Meniere's disease, steroid therapy

OPEN ACCESS

Edited by:
Robert Gürkov,
Bielefeld University, Germany

Reviewed by:
Daniel John Brown,
Curtin University, Australia
Angela Schell,
University of Heidelberg, Germany

***Correspondence:**
Akinobu Kakigi
kakigia@gmail.com

Specialty section:
This article was submitted to Otorhinolaryngology - Head and Neck Surgery, a section of the journal Frontiers in Surgery

Received: *19 August 2020*
Accepted: *07 December 2020*
Published: *11 January 2021*

Citation:
Takeda T, Takeda S and Kakigi A (2021) Effects of Glucocorticoids on the Inner Ear. Front. Surg. 7:596383. doi: 10.3389/fsurg.2020.596383

INTRODUCTION

An allergic reaction had been suspected to be one of the contributing factors to Meniere's disease. Based on the allergy theory, Hauser (1) treated two cases of Meniere's disease with corticosteroids in 1959 and obtained favorable results. However, steroid therapy received little attention, and its use did not progress markedly in the treatment of Meniere's disease (2). Also, serologic test

results did not support the allergy theory (3). In 1986, Beck (4) concluded that corticosteroid therapy, which is very effective for allergic diseases, had no marked effect against Meniere's disease. Based on this result, he did not support the allergy theory of Meniere's disease. Additionally, Stahle (2) also disagreed with the allergy theory. Since that time, there have been few advances and discussions regarding steroid therapy based on allergy.

Since McCabe (5) proposed the new concept of "autoimmune sensorineural hearing loss," it has been highlighted that some cases of Meniere's disease might be caused by autoimmune factors. This concept encouraged the use of steroids in the treatment of Meniere's disease. Shea (6) reported that about 10% of patients with typical Meniere's disease showed improved hearing and decreased dizziness following dexamethasone treatment. Further, Shea Jr. (7) achieved better results by administering dexamethasone by perfusion *via* the round window plus intravenously. In contrast, Silverstein (8) obtained different results from a double-blind, crossover trial of dexamethasone inner ear perfusion. Intratympanic administration of dexamethasone to patients with Meniere's disease led to no benefit over a placebo for the treatment of hearing loss and tinnitus.

As evident in the literature, corticosteroids have often been used for the treatment of Meniere's disease. However, many clinical trials failed to show the conclusive efficacy of steroid therapy regardless of whether steroid was administered systemically or intratympanically (9–12). Further, the rationality for this use is still controversial. In fact, there is no experimental evidence that this treatment is beneficial. In the present study, we administered hydrocortisone and dexamethasone serially to normal guinea pigs and investigated the histological changes in the inner ear.

MATERIALS AND METHODS

Fifteen Hartley guinea pigs with a positive Preyer's reflex, weighing between 300 g and 400 g, were used.

Experimental animals: Fifteen guinea pigs were divided into three groups (**Table 1**): Control group: five animals (10 ears) were administered physiological saline aqueous solution (0.2 ml) intra-peritoneally twice a day for 3 days. Steroid group: this group was composed of two groups, hydrocortisone and dexamethasone groups. The hydrocortisone group (5 animals, 10 ears) were administered 20 mg/kg of hydrocortisone intra-peritoneally. Hydrocortisone was also given twice a day for 3 days. Twenty mg/kg of hydrocortisone was reported to be an effective dose (ED50) for anti-inflammatory activity in rats (13). The dexamethasone group (5 animals, 10 ears) was intra-peritoneally administered 2 mg/kg of dexamethasone twice a day for 3 days. The effective dose (ED50) for anti-anaphylaxis activity in rats was reported to be 1.8 mg/kg (14). All animals were sacrificed 6 h after the last administration to observe histological changes in Reissner's membrane.

Preparation procedure: We obtained both sides of the temporal bones immediately following fixation with perfusion of 10% formalin solution under deep anesthesia with intra-peritoneal injections of pentobarbital. We kept the temporal bones in 10% formalin solution for 10 days or more. They were decalcified with 5% trichloroacetic acid and dehydrated with alcohol in increasing concentrations, and were then embedded in paraffin and celloidin. The prepared blocks were cut into 6 μm horizontal sections. The sections were stained with hematoxylin and eosin and studied under a light microscope.

TABLE 1 | Extension ratios of Reissner's membrane (ER-R) (%) and increase ratios of the cross-sectional area of the scala media (IR-S) (%) of control and steroid groups.

	Control ($n = 10$)	Hydrocortisone ($n = 10$)	Dexamethasone ($n = 10$)
ER-R (%)	2.4 ± 1.5	7.6 ± 2.6	5.0 ± 1.5
	P<0.001		
	P<0.01		
IR-S (%)	5.5 ± 1.7	16.9 ± 1.3	12.3 ± 2.5
	P<0.001		
	P<0.001		

Both ER-R and IR-S of the steroid groups were significantly higher than those of the control group using Student's t-test.

Measurement procedure: The extension of Reissner's membrane and increase of the endolymphatic space were quantitatively analyzed in addition to conventional observations of the morphological changes in the cochlea and endolymphatic sac. For this analysis, the following four parameters were measured (**Figure 1**) from the mid-modiolar sections of the cochlea: (1) the length of the extended Reissner's membrane (L), (2) the cross-sectional area of the bulged scala media (dotted area, S), (3) the reference length of Reissner's membrane (Lo), and (4) the cross-sectional area of the reference space of the scala media (So). The measurement system was composed of a video camera, a computer, and a digitizer (Video Micro Meter VM-30, Olympus Co., Tokyo, Japan). The second author measured those parameters without any notice about which specimen is which group.

From these parameters measured at all turns, the extension ratios (%) of Reissner's membrane and increase ratios (%) of the cross-sectional area of the scala media were calculated according to the formula described below:

Extension ratio of Reissner's membrane (ER-R) (%) $= 100 \times (\Sigma L - \Sigma L0)/\Sigma L0$

Increase ratio of the cross-sectional area of the scala media (IR-S) (%) $= 100 \times (\Sigma S - \Sigma S0)/\Sigma S0$

Σ means the summation of the values of four turns.

This study was approved by the Kochi Medical School Animal Care and Use Committee (Approval No. B-00094) and conformed to the Animal Welfare Act and the guiding principles for animal care produced by the Ministry of Education, Culture, Sports, Science and Technology, Japan.

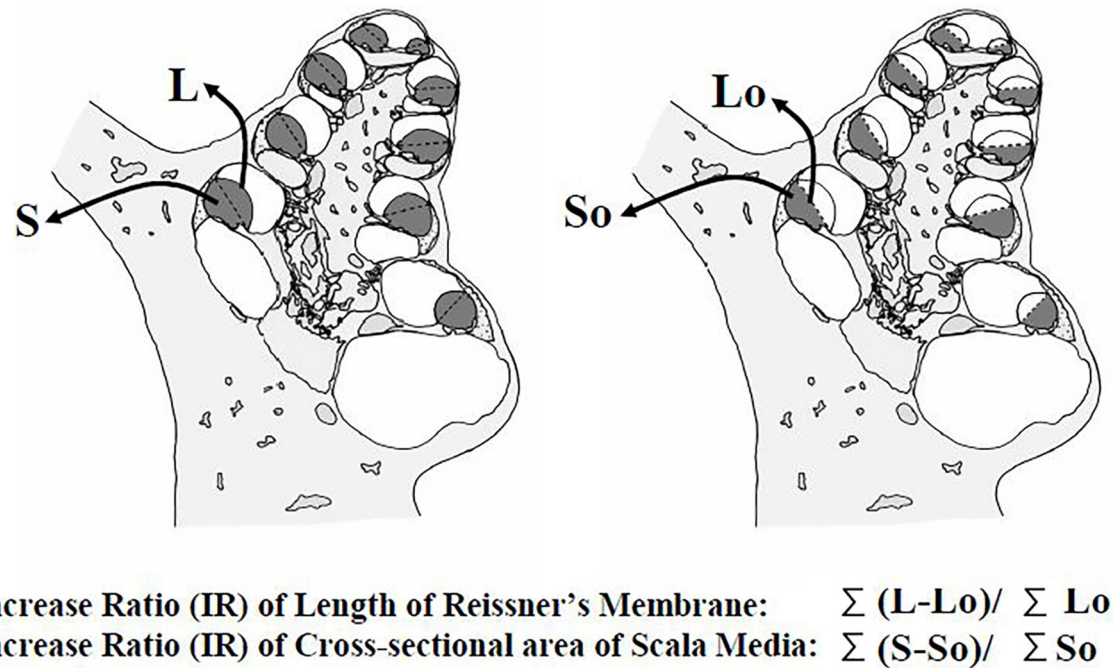

FIGURE 1 | Four parameters for assessment of the extension of Reissner's membrane and dilation of the scala media. The length of the extended Reissner's membrane (L), the cross-sectional area of the bulging scala media (dotted area, S), the reference length of Reissner's membrane (Lo); the length between the points of attachment of the stria vascularis and of attachment of the basilar membrane, and the cross-sectional area of the reference scala media (So), enclosed by the reference Reissner's membrane. Extension ratios of Reissner's membrane and increase ratios of the scala media were calculated from these data.

RESULTS

Reissner's membranes were extended and slight endolymphatic hydrops was found in 17 (85.0 %) of 20 ears following the administration of hydrocortisone. **Figure 2** shows representative histological findings from normal and steroid groups. The extension of Reissner's membrane and dilated endolymphatic space were evident in the steroid groups.

Extension ratios of Reissner's membrane (ER-R) (%) and increase ratios of the cross-sectional area of the scala media (IR-S) (%) of the 3 groups (Mean ± S.D.) are shown in **Table 1**. These three sample data were considered to come from a population with a normal distribution, hence the null hypothesis of normality assumption was rejected by the Kolmogorov-Smirnov normality test ($p > 0.05$). Thus, the *t*-test was applied for the statistical analysis of these data. ER-R and IR-S of the hydrocortisone group were significantly higher than those of the control group ($P < 0.001$, *t*-test), and ER-R and IR-S of the glucocorticoid group were also significantly higher than those of the control group ($P < 0.001$, *t*-test). Statistical analysis was performed with the use of the commercially available software StatMate V (ATMS Co. Tokyo, Japan).

Steroid administration led to no marked histological change other than the volumetric changes of the scala media. Neither vacuolization nor atrophic change was noted in the stria vascularis or vestibular sensory epithelium. The endolymphatic sac also had a normal appearance light-microscopically. No abnormal infiltration was observed in the lumen of the endolymphatic sac.

DISCUSSION

This is the first report to investigate the effects of systemic administration of glucocorticoids on guineapig cochlea. The extension of Reissner's membrane and dilated endolymphatic space were evident in the steroid groups. Recently, receptors of gluco- and mineralocolcicoid hormones were detected in the inner ear by different techniques (15, 16). A more detailed investigation by an Enzyme Linked Immuno-Sorbent Assay (ELISA) revealed that glucocorticoid receptors were distributed not only in the spiral ligament but also in the stria vascularis, although at lower levels (17). The localization of glucocorticoid receptors was also confirmed by *in situ* hybridization histochemical studies (18). Furthermore, the expression of mineralocorticoid type I receptor mRNA was also demonstrated in marginal cells of the stria vascularis by *in situ* hybridization histochemistry (19). These facts support the suggestion that adrenocorticoids play a biological role in the inner ear function.

It is worthy of attention that adrenal steroid receptors are present in the stria vascularis, which is considered to participate in ion and fluid homeostasis in the inner ear. Although we have little information available on the mechanism of action

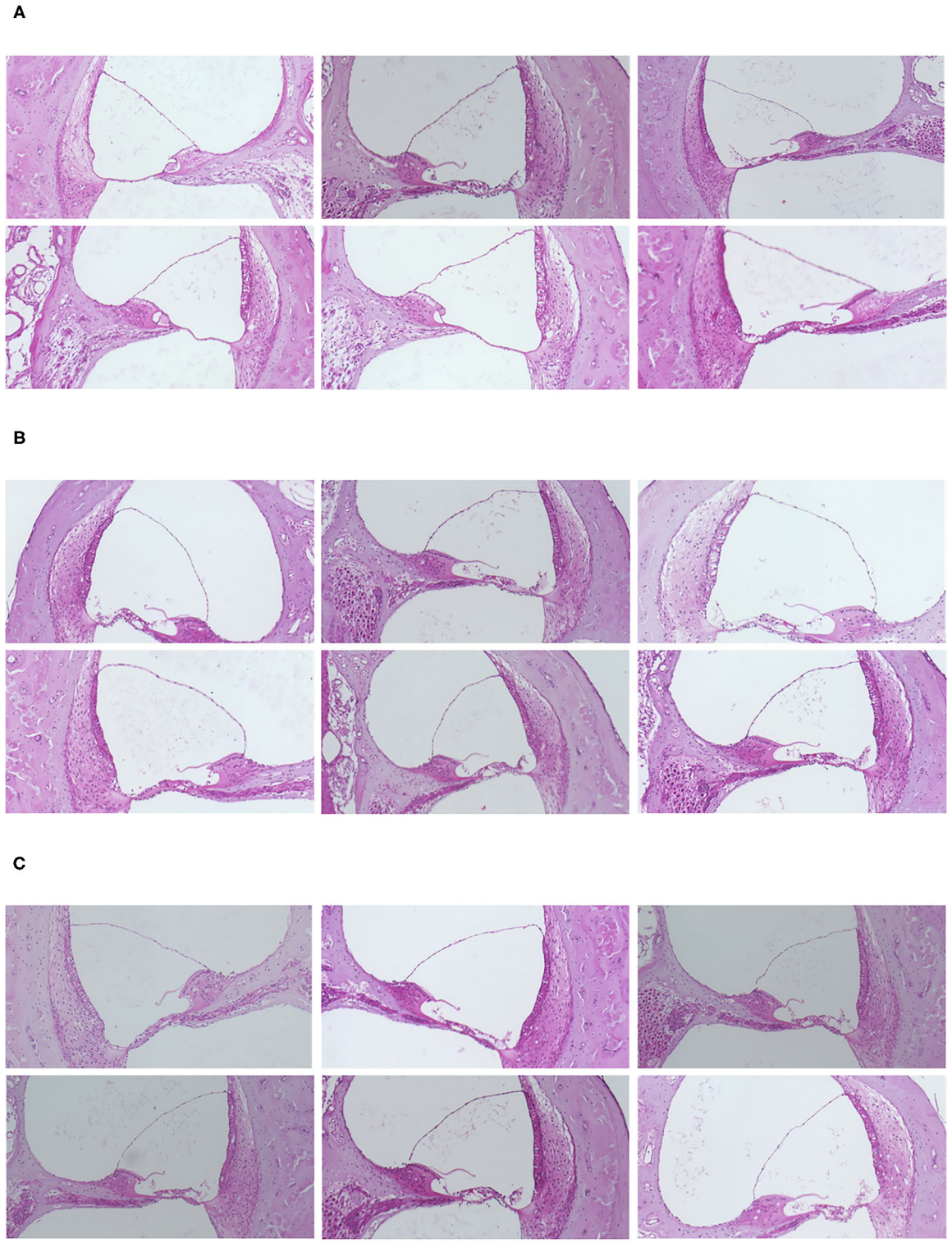

FIGURE 2 | (A) Representative histological findings in the normal and steroid groups. Slight but distinct endolymphatic hydrops was observed in the steroid groups. **(A)** Control group. **(B)** Hydrocortisone group. **(C)** Dexamethasone group.

of these steroid hormones in the inner ear, it is likely that the excess of adrenal steroids might have some influence on ion and fluid homeostasis in the inner ear. In support of this, it has been reported that endolymphatic hydrops was induced with aldosterone (20).

In the present study, serial administration of the synthetic glucocorticoid hydrocortisone also resulted in the extension of Reissner's membrane and slight endolymphatic hydrops. The stria vascularis and spiral ligament are well-known to contain varying levels of Na, K-ATPase, which is considered to be an important enzyme involved in ion and fluid transport (21–23). Elevated serum levels of glucocorticoid have been reported to be correlated with significant increases in Na, K-ATPase α-subunit levels, both in the stria vascularis and spiral ligament (24). This increase in the activity of Na, K-ATPase is likely to be one of the possible factors contributing to the steroid-induced hydrops formation observed in the present study. Another possible factor is steroid-induced upregulation of aquaporin 3 (25, 26). Aquaporins are known to play roles in the homeostatic mechanism regulating water and ionic balance in the inner ear fluids (27, 28). Therefore, the present hydrops formation may have resulted from the acceleration of endolymphatic water homeostasis via glucocorticoid-enhanced AQP3 in the inner ear.

Although no morphologic changes except extension of Reissner's membrane were observed in the present study under a light microscope, there is some evidence that changes in levels of circulating adrenal steroids influence the inner ear ultra-structurally as well as functionally (29–32). An increase in the intercellular space and a decrease in basolateral infoldings in the stria vascularis and dark cells of the vestibular epithelium were observed in adrenalectomized animals (29, 30). Furthermore, the restoration of circulating adrenocorticosteroids levels resulted in recovery of the cellular architecture of the stria vascularis and dark cells of the vestibular epithelium in adrenalectomized animals (31, 32). These findings provide indirect evidence that adrenal steroids are involved in the cellular regulations of inner ear tissues concerned with fluid and ionic microhomeostasis.

As mentioned above, it has been reported that under an abnormal state of adrenal steroids, ultrastructural changes in sensory and non-sensory cells of the cochlea and vestibular organs, although small, have been detected (33). It is unknown whether these changes are pathologic. Regarding functional aspects of the inner ear, however, glucocorticoid intake was reported to induce an elevated threshold of human auditory evoked responses (34, 35).

Glucocorticoids with a strong anti-inflammatory action have been prescribed empirically for Meniere's disease (1, 6–12). It is unknown how many dosages in a human correspond to the 20 mg/kg of hydrocortisone and 2 mg/kg of dexamethasone used in the present study. The dosage is the effective dose (ED50) for anti-inflammatory action or anti-anaphylaxis action in rats, and is not excessive in rodent. However, the development of endolymphatic hydrops induced by the serial administration of hydrocortisone or dexamethasone with such dosage provides a puzzling problem in the treatment of Meniere's. Of course, the present results do not clarify the effects of steroids on pathological conditions, such as Meniere's disease, but do not support the concept that endolymphatic hydrops can be reduced by glucocorticoid intake. The present results are compatible with those of Silverstein's clinical trial (7).

The limitation of this study is as follows. Samples were only taken at one time-point, 6 h after the last injection. So, it is not clear if the mild hydrops is an acute response or a more chronic imbalance. To investigate the hydrops, we selected light microscopy. So, we couldn't investigate the cellular damage in the inner ear. Recently, intratympanic administration of steroid therapy is performed to treat an acute sensorineural hearing loss. To conclude the efficacy of steroid therapy, we should compare the results between intratympanically and systemically administered steroids. Further studies are needed to conclude that glucocorticoid therapy affects inner ear fluid homeostasis negatively.

DATA AVAILABILITY STATEMENT

The original contributions presented in the study are included in the article/**Supplementary Materials**, further inquiries can be directed to the corresponding author/s.

ETHICS STATEMENT

The animal study was reviewed and approved by Kochi Medical School Animal Care and Use Committee (Approval No. B-00094).

AUTHOR CONTRIBUTIONS

All authors listed have made a substantial, direct and intellectual contribution to the work, and approved it for publication.

SUPPLEMENTARY MATERIAL

The Supplementary Material for this article can be found online at: https://www.frontiersin.org/articles/10.3389/fsurg.2020.596383/full#supplementary-material

REFERENCES

1. Hauser E. Meniere's disease; a new therapeutic approach. *J Am Geriatr Soc*. (1959) 7:874–6. doi: 10.1111/j.1532-5415.1959.tb00357.x
2. Stahle J. Allergy, immunology, psychosomatic, hypo- and hypertonus. *Arch Otorhinolaryngol*. (1976) 212:287–92. doi: 10.1007/BF00453676
3. Taillens JP. Cortisone in clinical otorhino-laryngology. *Adv Otorhinolaryngol*. (1968) 15:32–63. doi: 10.1159/000385358
4. Beck C. "Controversial aspects of Meniere's disease" in ed C. R. Pfaltz *Georg Thieme Verlag Stuttgart and Thieme Inc*. (1986).
5. McCabe BF. Autoimmune sensorineural hearing loss. *Ann Otol Rhinol Laryngol*. (1979) 88:585–9. doi: 10.1177/000348947908800501

6. Shea JJ. Autoimmune sensorineural hearing loss as an aggravating factor in Meniere's disease. *Adv Otorhinolaryngol*. (1983) 30:254–7. doi: 10.1159/000407651
7. Shea JJ Jr, Ge X. Dexamethasone perfusion of the labyrinth plus intravenous dexamethasone for Meniere's disease. *Otolaryngol Clin North Am*. (1996) 29:353–8. doi: 10.1016/S0030-6665(20)30398-4
8. Silverstein H, Isaacson JE, Olds MJ, Rowan PT, Rosenberg S. Dexamethasone inner ear perfusion for the treatment of Meniere's disease: a prospective, randomized, double-blind, crossover trial. *Am J Otol*. (1998) 19:196–201.
9. Dodson KM, Woodson E, Sismanis A. Intratympanic steroid perfusion for the treatment of Ménière's disease: a retrospective study. *Ear Nose Throat J*. (2004) 83:394–8. doi: 10.1177/014556130408300611
10. Doyle KJ, Bauch C, Battista R, Beatty C, Hughes GB, Mason J, et al. Intratympanic steroid treatment: a review. *Otol Neurotol*. (2004) 25:1034–9. doi: 10.1097/00129492-200411000-00031
11. Casani AP, Piaggi P, Cerchiai N, Seccia V, Franceschini SS, Dallan I. Intratympanic treatment of intractable unilateral Meniere disease: gentamicin or dexamethasone? A randomized controlled trial otolaryngol. *Head Neck Surg*. (2012) 146:430–7. doi: 10.1177/0194599811429432
12. Fisher LM, Derebery MJ, Friedman RA. Oral steroid treatment for hearing improvement in Ménière's Disease and endolymphatic hydrops. *Otol Neurotol*. (2012) 33:1685–691. doi: 10.1097/MAO.0b013e31826dba83
13. Sofia RD, Nalepa SD, Vassar HB, Knobloch LC. Comparative anti-phlogistic activity of Δ9-tetrahydrocannabinol, hydrocortisone and aspirin in various rat paw edema models. *Life Sci*. (1974) 15:251–60. doi: 10.1016/0024-3205(74)90214-8
14. Church MK, Miller P. Time courses of the anti-anaphylactic and anti-inflammatory effects of dexamethasone in the rat and mouse. *Br J Pharmacol*. (1978) 62:481–6. doi: 10.1111/j.1476-5381.1978.tb07751.x
15. Rarey KE, Luttge WG. Presence of type I and type II/IB receptors for adrenocorticosteroid hormones in the inner ear. *Hear Res*. (1989) 41:217–22. doi: 10.1016/0378-5955(89)90013-0
16. ten Cate WJ, Curtis LM, Rarey KE. Immunochemical detection of glucocorticoid receptors within rat cochlea vestibular tissues. *Hear Res*. (1992) 60:199–204. doi: 10.1016/0378-5955(92)90021-E
17. Rarey KE, Curtis LM, ten Cate WJ. Tissue specific levels of glucocorticoid receptor within the rat inner ear. *Hear Res*. (1993) 64:205–10. doi: 10.1016/0378-5955(93)90007-N
18. ten Cate WJ, Curtis LM, Small GM, Rarey KE. Localization of glucocorticoid receptors and glucocorticoid receptor mRNA in the rat cochlea. *Laryngoscope*. (1993) 103:865–71. doi: 10.1288/00005537-199308000-00007
19. Furuta H, Mori N, Sato C, Hoshikawa H, Sakai S, Iwakura S, et al. Mineralocorticoid type I receptors in the rat cochlea: mRNA identification by polymerase chain reaction (PCR) and in situ hybridization. *Hear Res*. (1994) 78:175–80. doi: 10.1016/0378-5955(94)90023-X
20. Dunnebier EA, Segenhout JM, Wit HP, Albers WJ. Two-phase endolymphatic hydrops: a new dynamic guinea pig model. *Acta Otolaryngol (Stockh)*. (1997) 117:13–9. doi: 10.3109/00016489709117984
21. Schulte BA, Adams JC. Distribution immunoreactive Na+-K+-ATPase in gerbil cochlea. *J Histochem Cytochem*. (1989) 37:1271–34. doi: 10.1177/37.2.2536055
22. Ryan AF, Watt AG. Expression of mRNA encoding α and β subunit isoforms of the Na, K-ATPase in the rat cochlea. *Mol Cell Neurosci*. (1991) 2:179–87. doi: 10.1016/1044-7431(91)90011-C
23. Spicer SS, Schulte BA. Differentiation of inner ear fibrocytes according to their ion transport related activity. *Hear Res*. (1991) 56:53–64. doi: 10.1016/0378-5955(91)90153-Z
24. Curtis LM, ten Cate WJ, Rarey KE. Dynamics of Na, K-ATPase sites in lateral cochlear wall tissues of the rat. *Eur Arch Otorhinolaryngol*. (1993) 250:265–70. doi: 10.1007/BF00186223
25. Fukushima M, Kitahara T, Fuse Y, Uno Y, Doi K, Kubo T. Changes in aquaporin expression in the inner ear of the rat after i.p. injection of steroids. *Acta Otolaryngol Suppl*. (2004) 553:13–8. doi: 10.1080/03655230410017599
26. Nevoux J, Viengchareun S, Lema I, Lecoq AL, Ferrary E, Lombès M. Glucocorticoids stimulate endolymphatic water reabsorption in inner ear through aquaporin 3 regulation. *Pflugers Arch*. (2015) 467:1931–43. doi: 10.1007/s00424-014-1629-5
27. Beitz E, Zenner HP, Schultz JE. Aquaporin-mediated fluid regulation in the inner ear. *Cell Mol Neurobiol*. (2003) 23:315–29. doi: 10.1023/a:1023636620721
28. Takeda T, Taguchi D. Aquaporins as potential drug targets for Meniere's disease and its related diseases. *Handb Exp Pharmacol*. (2009) 190:171–84. doi: 10.1007/978-3-540-79885-9_8
29. Rarey KE, Tyneway D, Patterson K. Decreased adenosine triphosphatase activity in the absence of adrenocorticosteroids. *Arch Otolaryngol Head Neck Surg*. (1989) 115:817–21. doi: 10.1001/archotol.1989.01860310055022
30. Lohuis PJ, ten Cate WJ, Patterson KE, Rarey KE. Modulation of the stria vascularis in the absence of circulating adrenocorticosteroids. *Acta Otolaryngol (Stockh)*. (1990) 110:348–56. doi: 10.3109/00016489009122559
31. ten Cate WJ, Rarey KE. Plasma membrane modulation of ampullar dark cells by corticosteroids. *Arch Otolaryngol Head Neck Surg*. (1991) 117:96–9. doi: 10.1001/archotol.1991.01870130102025
32. Rarey KE, Lohuis PJ, ten Cate WJ. Response of the stria vascularis to corticosteroids. *Laryngoscope*. (1991) 101:1081–4. doi: 10.1288/00005537-199110000-00009
33. Trevisi M, Mazzoni M, Ricci D. Ultrstructual observations on the guinea pig epithelium in the vestibular apparatus during steroid hormone treatment. *Acta Otolaryngol (Stockh)*. (1980) 90 (Suppl 373):1–23. doi: 10.3109/00016488009136998
34. Born J, Schwab R, Pietrowsky R, Pauschinger P, Fehm HL. Glucocorticoid influence on the auditory brain-stem responses in man. *Electroencephalogr Clin Neurophysiol*. (1989) 74:209–16. doi: 10.1016/0013-4694(89)90007-2
35. Beckwith BE, Lerud K, Antes JR, Reynolds BW. Hydrocortisone reduces auditory sensitivity at high tonal frequency in adult males. *Phamacol Biochem Behav*. (1983) 19:431–33. doi: 10.1016/0091-3057(83)90115-6

Conflict of Interest: The authors declare that the research was conducted in the absence of any commercial or financial relationships that could be construed as a potential conflict of interest.

frontiers in Surgery

ORIGINAL RESEARCH
published: 04 February 2021
doi: 10.3389/fsurg.2020.623078

Endolymphatic Hydrops in Patients With Intralabyrinthine Schwannomas

Yibo Zhang[1,2†], *Feitian Li*[1,2†], *Chunfu Dai*[1,2*] *and Wuqing Wang*[1,2*]

[1] Department of Otology and Skull Base Surgery, Eye, Ear, Nose, and Throat Hospital, Fudan University, Shanghai, China, [2] Key Laboratory of Hearing Medicine, Ministry of Health, Eye, Ear, Nose, and Throat Hospital, Fudan University, Shanghai, China

Purpose: The presence of endolymphatic hydrops (EH) in patients with intralabyrinthine schwannomas (ILSs) is poorly understood. This study aims to determine whether there is a correlation between endolymphatic hydrops and clinical presentations of ILS.

Methods: Data from nine patients with ILSs were retrospectively reviewed between 2007 and 2020. Temporal bone MRI with intratympanic or intravenous injection of gadolinium was applied to detect ILSs and EH.

Results: 3D real inversion recovery (IR) sequence MRI of the temporal bone confirmed ipsilateral EH in four patients (4/6). All four patients with EH on MRI presented with vertigo similar to Meniere's disease. Among these patients with EH, one patient with EH in the cochlea showed moderate sensorineural hearing loss, while three patients with EH in both the vestibule and cochlea showed profound hearing loss. MRI demonstrated a transmacular tumor (TMA) in one patient, intravestibular (IV) in four patients, and vestibulocochlear (VC) in four patients. Two IV cases showed moderated hearing loss, while the TMA and VC cases showed profound hearing loss. Transotic resection of the tumor was applied in five patients; translabyrinthine resection was applied in one patient; two patients were under observation; and one patient was given intratympanic injection of gentamicin (ITG). During follow-up, all of the treated patients reported relief of vertigo, and postoperative MRI was performed in two patients, which showed no tumor recurrence. The two patients under observation showed no deterioration of hearing loss or vertigo. One patient was lost to follow-up.

Conclusion: EH concurrent with ILSs has been underestimated previously. With the extensive application of temporal bone MRI paradigms, such as 3D-real IR sequence MRI, more cases of potential EH in patients with ILS will be identified. The severity of hearing loss may be associated with the location of the tumor and the degree of EH.

Keywords: intralabyrinthine schwannomas, endolymphatic hydrops, vertigo, hearing loss, MRI

OPEN ACCESS

Edited by:
Robert Gürkov,
Bielefeld University, Germany

Reviewed by:
Hans Thomeer,
University Medical Center Utrecht, Netherlands
Marcin Szymanski,
Medical University of Lublin, Poland

***Correspondence:**
Wuqing Wang
wwuqing@189.cn
Chunfu Dai
cfdai66@126.com

†These authors have contributed equally to this work

Specialty section:
This article was submitted to Otorhinolaryngology Head and Neck Surgery, a section of the journal Frontiers in Surgery

Received: *29 October 2020*
Accepted: *31 December 2020*
Published: *04 February 2021*

Citation:
Zhang Y, Li F, Dai C and Wang W (2021) Endolymphatic Hydrops in Patients With Intralabyrinthine Schwannomas. Front. Surg. 7:623078. doi: 10.3389/fsurg.2020.623078

INTRODUCTION

Intralabyrinthine schwannomas (ILSs) are rare benign tumors within the membranous labyrinth that are reported to arise from the distal branches of the cochlear, superior vestibular, or inferior vestibular nerves (1, 2). Mayer described the first ILS case in 1917 (3). ILSs have been historically underdiagnosed, and most of them were unexpectedly identified during labyrinthectomy or cadaver

autopsy (4, 5). With the application of magnetic resonance imaging (MRI), an increasing number of ILSs have been identified at the early stage.

Unilateral progressive hearing loss and recurrent vertigo are the most common symptoms in patients with ILSs (6, 7). These symptoms may mimic patients suffering from other inner ear disorders, such as Meniere's disease, and result in similar findings in acoustic and vestibular function tests, which further lead to the misdiagnosis of ILS at the early stage.

Endolymphatic hydrops (EH) is considered a pathological hallmark of Meniere's disease. However, EH can also be detected in other inner ear diseases, such as delayed endolymphatic hydrops, endolymphatic sac tumors, extralabyrinthine and intralabyrinthine schwannomas (8–10). Shinji Naganawa et al. demonstrated EH in some patients with vestibular schwannomas and concluded that there was no significant correlation between vertigo and vestibular hydrops. However, their cases mainly consisted of extralabyrinthine schwannomas. Anatomically, intralabyrinthine tumors are more likely to result in EH because of the possible mechanical blockade of the endolymph fluid (11). Only a few studies have reported EH in intralabyrinthine schwannomas (12–14), and the correlation between clinical symptoms and EH in ILS is still unclear. In addition, the underlying mechanism of ILS-associated EH remains unknown.

In this study, we retrospectively reviewed the medical records of nine patients with ILS and aimed to (1) demonstrate the occurrence of EH in ILSs; (2) reveal the correlation between clinical symptoms and imaging features of endolymphatic hydrops; and (3) discuss the diagnostic pitfalls of ILS.

METHODS AND PATIENTS

Patients

The clinical data of nine patients with ILS who were treated at the Otology & Skull Base Surgery Department, Fudan University, between 2007 and 2020, were retrospectively reviewed. We retrieved data on age, symptoms, pure tone test, imaging, and management.

The diagnosis in six patients with ILS was confirmed by pathological examination postoperatively, while the other three patients who chose a wait-and-see strategy were diagnosed based on imaging. Six patients underwent both enhanced temporal bone MRI and temporal bone MRI with intratympanic or intravenous injection of gadolinium to detect EH. Patients 1, 2, and 3 only underwent enhanced temporal bone MRI, since MRI with intratympanic or intravenous injection of gadolinium was unavailable at that time in our hospital. According to the anatomic classification developed by Salzman et al. (7), ILSs in the present study are divided into six types, including intracochlear, transmodiolar, intravestibular, transmacular, vestibulocochlear, and transotic types. The tumor size was measured at its largest dimension on MRI.

MRI Acquisition

For the intratympanic injection (IT) method, the patients received bilateral intratympanic injections of gadolinium diluted in saline (v/v 1:7) using a 22-gauge spinal needle and a 1-ml syringe. Gadopentetate dimeglumine was chosen in this research as the gadolinium contrast agent. Following the injections, the patients maintained an upright seated position for 30 min without speaking or swallowing. After 24 h, MRI scans were performed using a 3 T MR unit (Verio, Siemens Healthcare, Erlangen, Germany) with a 32-channel phased-array receive-only head coil. T2-space, 3D-real IR, and 3D-FLAIR sequence MRI images were collected. Briefly, the parameters for the 3D-real IR sequence were as follows: voxel size of 0.4 × 0.4 × 0.8 mm, scan time of 14 min, repetition time (TR) of 9,000 ms, echo time (TE) of 181 ms, inversion time (TI) of 1,730 ms, slice thickness of 0.80 mm, field of view (FOV) of 160 × 160 mm, and matrix size of 3,300 × 918. The parameters for the 3D-FLAIR sequence were as follows: voxel size of 0.7 × 0.7 × 0.6 mm, scan time of 6 min, TR of 6,000 ms, TE of 387 ms, TI of 2,100 ms, slice thickness of 0.60 mm, echo train length of 173, FOV of 220 × 220 mm, and matrix size of 1,701 × 810.

For the intravenous (IV) method, the patients received an intravenous injection of a double dose (0.4 ml/kg body weight) of Gd-HP-DO3A; 4 h later, MRI was performed. All scans were performed on a 3 T MRI scanner (Verio; Siemens Healthcare, Erlangen, Germany) using a 32-channel phased array receive-only coil. T2-space and 3D real-IR sequence MRI scans were applied to collect images. The parameters for the 3D real-IR sequence were as follows: voxel size of 0.17 × 0.17 × 0.6 mm, scan time of 15 min and 20 s, repetition time of 6,000 ms, echo time of 181 ms, inversion time of 1,850 ms, slice thickness of 0.6 mm, field of view of 160 × 160 mm, and matrix size of 768 × 768.

RESULTS

Clinical Characteristics

The clinical characteristics of the study cohort are summarized in **Table 1**. The age of patients at presentation ranged from 35 to 69 years old (50.9 years old on average), and the sex ratio was 2:7 (male to female). Ipsilateral sensorineural hearing loss was observed in all patients. Seven patients presented with profound hearing loss, one patient showed moderate progressive hearing loss, and one patient demonstrated moderate sudden hearing loss. All patients experienced recurrent vertigo attacks with various characteristics (**Table 2**). All patients underwent caloric test, which showed ipsilateral weakness consistent with the tumor side.

Magnetic Resonance Imaging of Intralabyrinthine Schwannomas

Temporal bone MRI with enhancement was performed in nine patients, which revealed a hypointense filling defect within the labyrinthine on T2-weighted images, and enhanced T1-weighted images revealed a homogeneously enhanced mass within the labyrinthine in these patients (**Figure 1**). Intraoperative findings confirmed the final diagnosis (**Figure 2**).

In the present study, MRI demonstrated a transmacular tumor in one patient, intravestibular tumors in four patients, and vestibulocochlear tumors in four patients (**Figure 3**). The mean tumor size in our study was 3.8 mm (**Table 2**).

TABLE 1 | Clinical features of the study population.

Patient	Age	Duration (years)	Tumor side	Symptoms	Caloric tests weaker side	Tentative diagnosis	Final diagnosis
1	44–46	20	R	Profound pSNHL, V,T	R	Sensorineural hearing loss	ILS
2	35–37	4	L	Moderate pSNHL, V, T	L	MD	ILS
3	58–60	10	R	Profound pSNHL, V, T	R	Delayed endolymphatic hydrops	ILS
4	34–36	2	R	Moderate sudden SNHL, EF, V, T	R	Idiopathic hearing loss	ILS
5	68–70	1	R	Profound pSNHL, V, T	R	MD	ILS
6	36–38	12	R	Profound pSNHL, V, T	R	MD	ILS
7	58–60	30	L	Profound pSNHL, V, T	L	Depression, MD	ILS
8	61–63	10	R	Profound pSNHL, V, T	R	ILS	ILS
9	55–57	5	R	Profound pSNHL, V	R	ILS	ILS

pSNHL, progressive sensorineural hearing loss; V, vertigo; T, tinnitus; EF, ear fullness.

TABLE 2 | Correlation between vertigo attacks and magnetic resonance imaging (MRI) presentation.

Patient	Classification by Salzman et al.	Tumor size (mm)	Endolymphatic hydrops	Characteristics of vertigo	Duration per attack	Follow-up (months)
1	TMA	5.0	Only enhanced MRI	Positional vertigo	Seconds to minutes	Lost
2	IV	3.0	Only enhanced MRI	Recurrent vertigo	Several hours	79
3	IV	1.5	Only enhanced MRI	Recurrent vertigo	10 min to several hours	106
4	IV	4.7	Cochlea (IV)	Recurrent vertigo	10 min to several hours	31
5	VC	3.4	Cochlea + vestibule (IV)	Recurrent vertigo	Several hours	7
6	IV	3.8	Cochlea + vestibule (IT)	Recurrent vertigo	Several hours	71
7	VC	2.5	Cochlea + vestibule (IT)	Recurrent vertigo	10 min	65
8	VC	4.6	No EH (IV)	Recurrent vertigo	Several minutes	8
9	VC	5.7	No EH (IV)	Drop attack	10 min to several hours	22

TMA, transmacular; IV, intravestibular; VC, vestibulocochlear; EH, endolymphatic hydrops; IV, intravenous injection of gadolinium; IT, intratympanic injection of gadolinium.

Endolymphatic Hydrops Concurrent With Intralabyrinthine Schwannomas

3D real inversion recovery (IR) sequence MRI of the temporal bone was applied in six patients to demonstrate endolymphatic hydrops, with the IV method applied in four patients and the IT method used in two patients. Four patients showed an intralabyrinthine hypointense mass concurrent with endolymphatic hydrops. Three patients presented with endolymphatic hydrops in both the cochlea and vestibule (**Figures 4A,B**), and one patient presented with endolymphatic hydrops in the cochlea (**Figure 4C**). All four patients with EH on MRI presented with vertigo similar to Meniere's disease.

Surgical Outcomes

Five patients (patients 1, 3, 6, 7, and 8) with profound hearing loss underwent translabyrinthine resection of the tumor. Patient 2 with moderate hearing loss underwent surgery due to intractable vertigo. Patients 4 and 5 with serviceable hearing and tolerable vertigo chose conservative management. Intratympanic injection of low-dose gentamicin was used in patient 9 to relieve vertigo. No postoperative facial paresis, cerebrospinal fluid leakage, or other severe complications were encountered, except patient 7 who had delayed facial paresis 1 week after surgery and recovered completely in 1 month.

Follow-Up

Eight patients were followed up. One patient was lost to follow-up. The mean follow-up time was 48.6 months (range, 7–106 months). During follow-up, five patients who underwent surgery reported no vertigo attacks, and two out of these five underwent MRI surveillance and did not show tumor recurrence (**Figure 5**). Two patients who were under observation and the patient who received ITG did not present with deterioration of hearing loss or vertigo.

DISCUSSION

Prevalence

ILSs are rare disorders, but they may have been underestimated before. Van Abel et al. reported that the average delay between

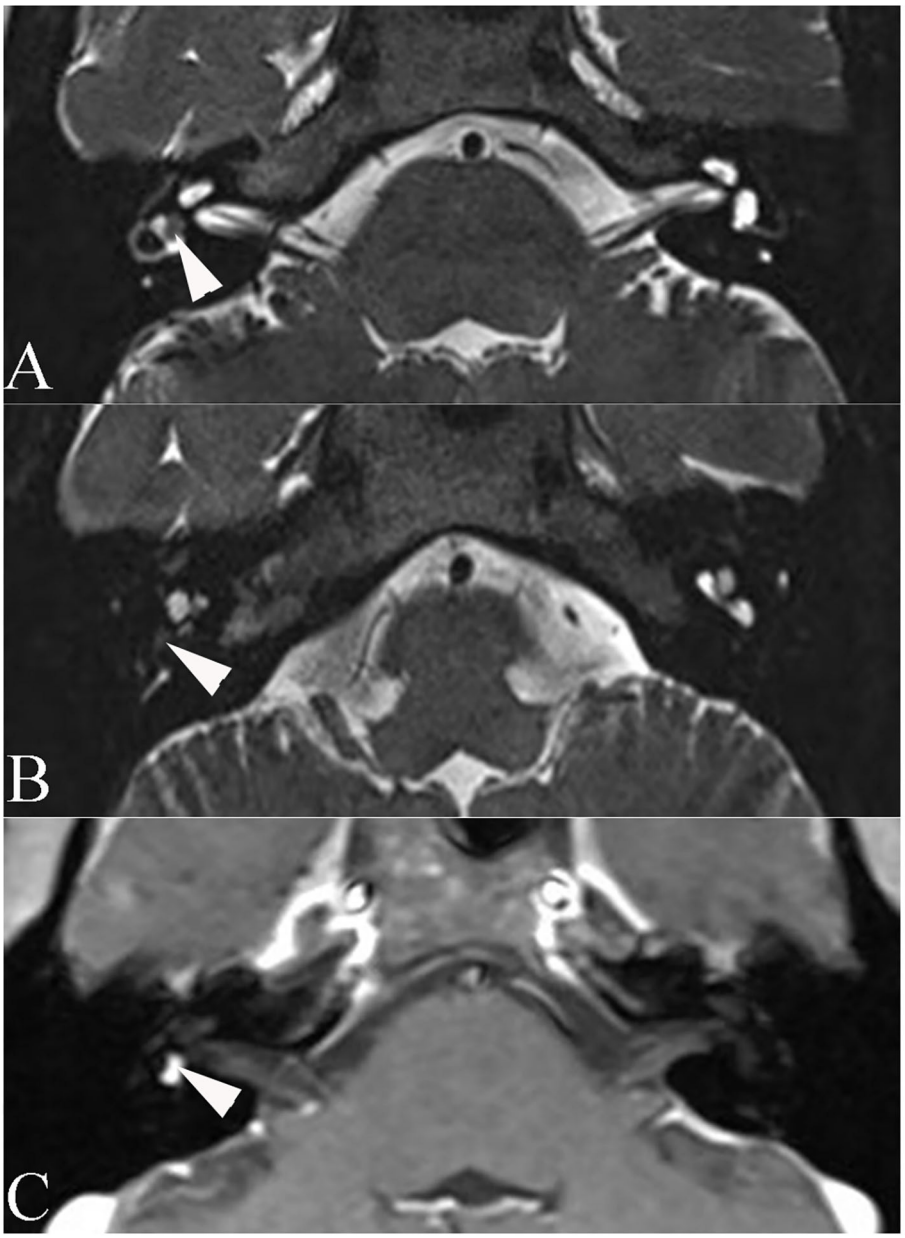

FIGURE 1 | Axial magnetic resonance imaging of patient 6. **(A)** T2-weighted magnetic resonance imaging reveals a hypointense mass within the vestibule (arrowhead). **(B)** T2-weighted MRI reveals a hypointense mass within the basal turn of the cochlea (arrowhead). **(C)** Enhanced T1-weighted MRI reveals signal enhancement of the mass (arrowhead).

symptom onset and diagnosis of ILS was 7.0 ± 8.0 years (15). Currently, with the application of high-resolution MRI scans with or without contrast, more ILSs can be diagnosed at an early stage. It is estimated that the incidence of ILSs exceeds 1 per 100,000 person-years with modern diagnostic imaging (16). The rising incidence of ILSs in recent years most likely reflects an improved capacity for disease detection rather than a true increase in tumor development. According to the meta-analysis by Gosselin et al., no significant difference was found in the sex ratio of patients with ILS (17). Although the sex ratio was 2:7 (male to female) in the present study, no female predilection for this lesion could be drawn because of the limited sample size.

Clinical Characteristics and Misdiagnosis of Intralabyrinthine Schwannomas

ILS is also known as primary inner ear schwannoma, since this term differentiates ILS from extralabyrinthine schwannomas that involve the labyrinthine, thus more precisely describing

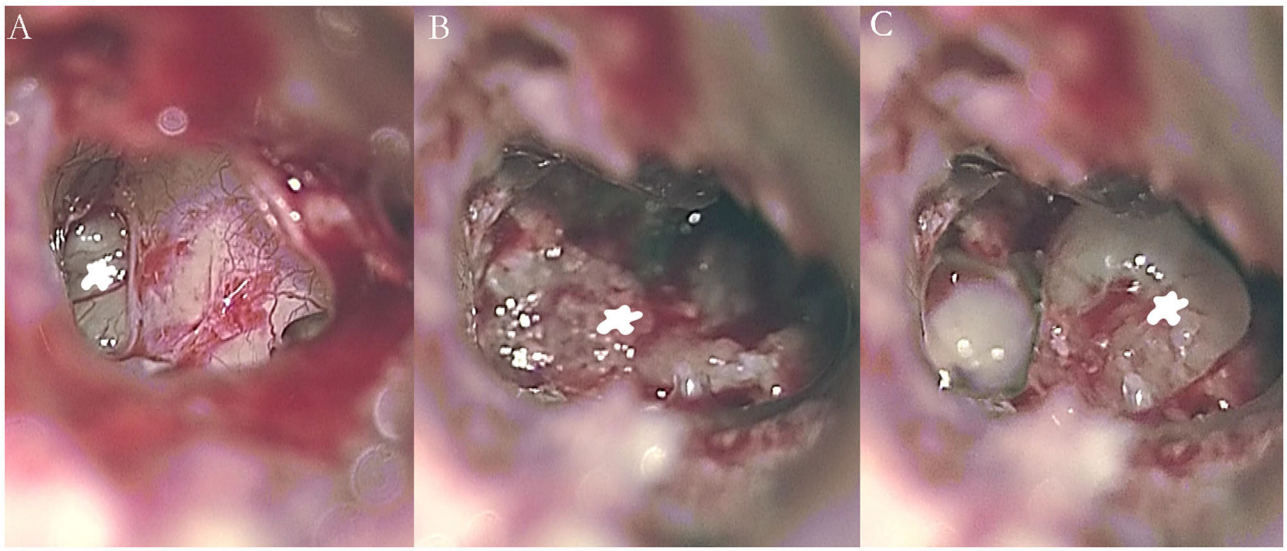

FIGURE 2 | Intraoperative images showing an intralabyrinthine schwannoma in the right vestibule **(A, B)** and cochlea **(C)** of patient 5 (asterisk).

this lesion (15). Kennedy et al. proposed a new classification of ILSs in 2004 (18). On the basis of the Kennedy classification, Salzman et al. excluded the tympanolabyrinthine class because there were no observed cases fitting the description, and there was redundancy with the transotic subtype (7). Furthermore, Van Abel et al. proposed renaming intralabyrinthine schwannoma as primary inner ear schwannoma (PIES) to permit clear subsite categorization and modified the Kennedy classification, which excludes the transotic subtype and adds the translabyrinthine subtype (15). We applied the Salzman classification in this study because no translabyrinthine subtype cases were included. There is no consensus on the method of tumor size measurement, and previous studies have recorded the size of ILS based on MRI; however, a detailed description of the measurement was absent (2, 19). The sizes of ILSs measured in this study may be biased due to the natural growth pattern of ILSs. To determine the exact sizes of ILSs, a prospective study of 3D reconstruction and volumetric quantification of ILS needs to be performed in the future.

Sensorineural hearing loss is one of the most common symptoms of ILSs (20). It can occur as sudden or progressive non-recovering hearing loss. In the present study, moderate to profound sensorineural hearing loss was present in all cases, and the severity of hearing loss seemed to be related to the location of the tumor. Two intravestibular tumor cases showed moderated hearing loss, while all the transmacular and vestibulocochlear tumor cases showed profound hearing loss. Regarding the mechanism of hearing loss, Santos et al. performed a histopathologic study and demonstrated that, in addition to mechanical obstruction, the degeneration of hair cells, spiral ganglion neurons, and stria vascularis may also underlie the various SNHL in ILSs (21). Furthermore, hearing loss may also develop as a result of cochlear aperture obstruction and intralabyrinthine protein accumulation due to the tumor (22). All of our patients complained of tinnitus, which is consistent with a previous study (17).

Recurrent vertigo attacks, which mimic Meniere's disease, is another common symptom of ILSs, and combined with hearing loss and tinnitus, patients with ILS are prone to be misdiagnosed with MD at the early stage. Unfortunately, we still do not know if there are any typical differences in symptoms between patients with MD and patients with ILS, especially at the early stage. Though a differentiating clinical parameter between these two entities might be the extent of hearing loss. In ILS, frequently, total deafness occurs, whereas most MD cases end up with severe sensorineural hearing loss but not total deafness. A cohort study over a long period of time or a meta-analysis between the two groups could be meaningful to reveal the difference.

Correlation Between Magnetic Resonance Imaging Characteristics and Vertigo in Patients With Intralabyrinthine Schwannomas

Jerin et al. reported two cases of ILS presenting with clinical symptoms that were similar to patients suffering from delayed endolymphatic hydrops, but no EH was demonstrated on temporal bone MRI in the two cases. A few studies have reported recurrent vertigo attacks in patients with ILS, mimicking Meniere's disease or delayed endolymphatic hydrops. However, few studies have shown that EH can be identified in patients with ILSs (12–14). Homann et al. first reported the coincidence of EH and intralabyrinthine tumors. However, due to the limited cases (two cases), it is unavailable to provide more information on the correlation of EH and the symptoms of ILS.

In the present study, the intralabyrinthine mass coexisting with EH was identified in four out of six patients using 3D real IR sequence MRI with injection of gadolinium. All four

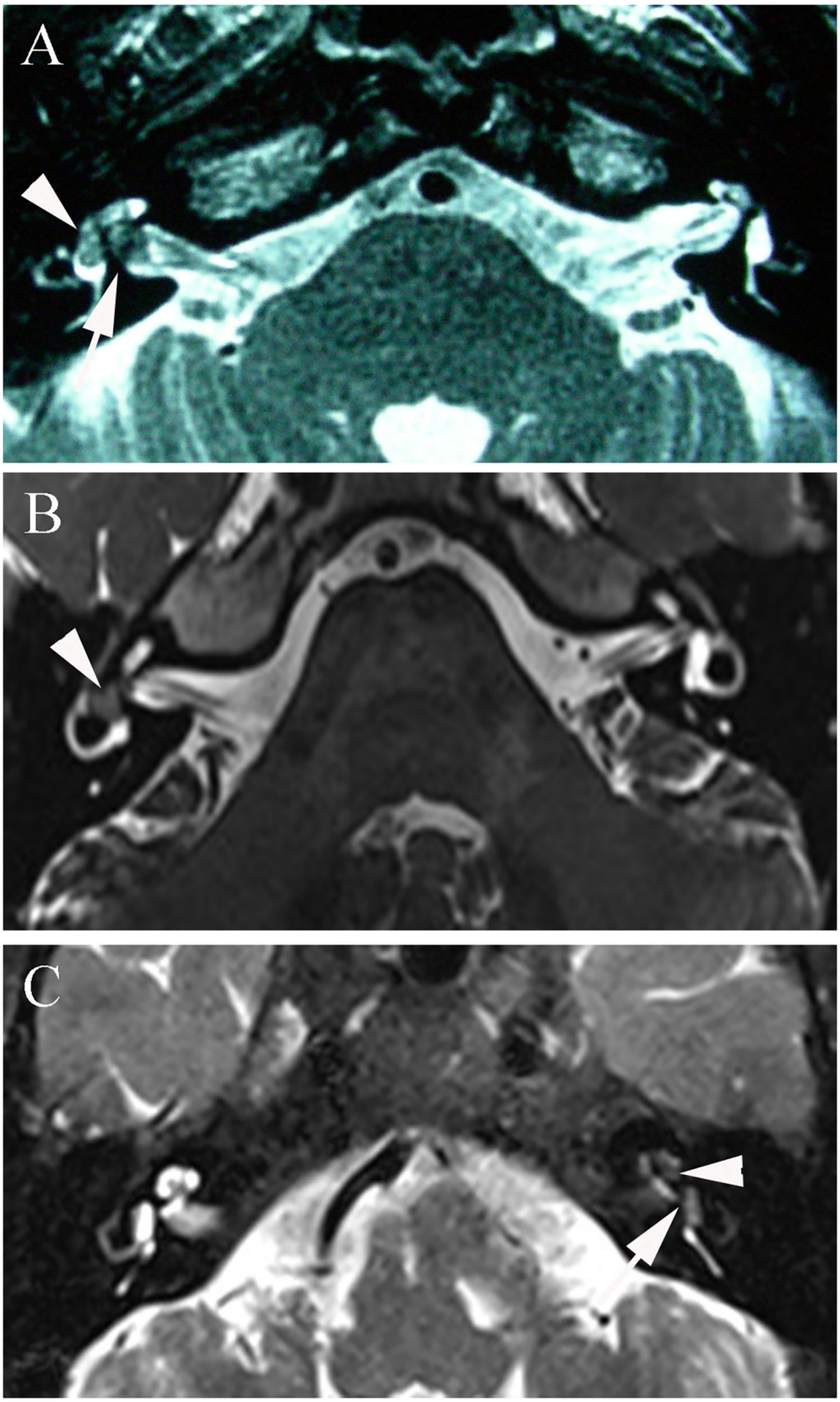

FIGURE 3 | (A) T2-3D-space MRI of patient 1 with a transmacular tumor shows a hypointense mass in the vestibule (arrowhead) and a larger defect in the fundus of the internal auditory canal (arrow). **(B)** T2-3D-space MRI of patient 4 with an intravestibular tumor shows an isolated mass in the right vestibule (arrowhead). **(C)** Patient 7 with a vestibulocochlear tumor shows filling defects in both the vestibule (arrowhead) and cochlea (arrow) on T2-weighted MRI.

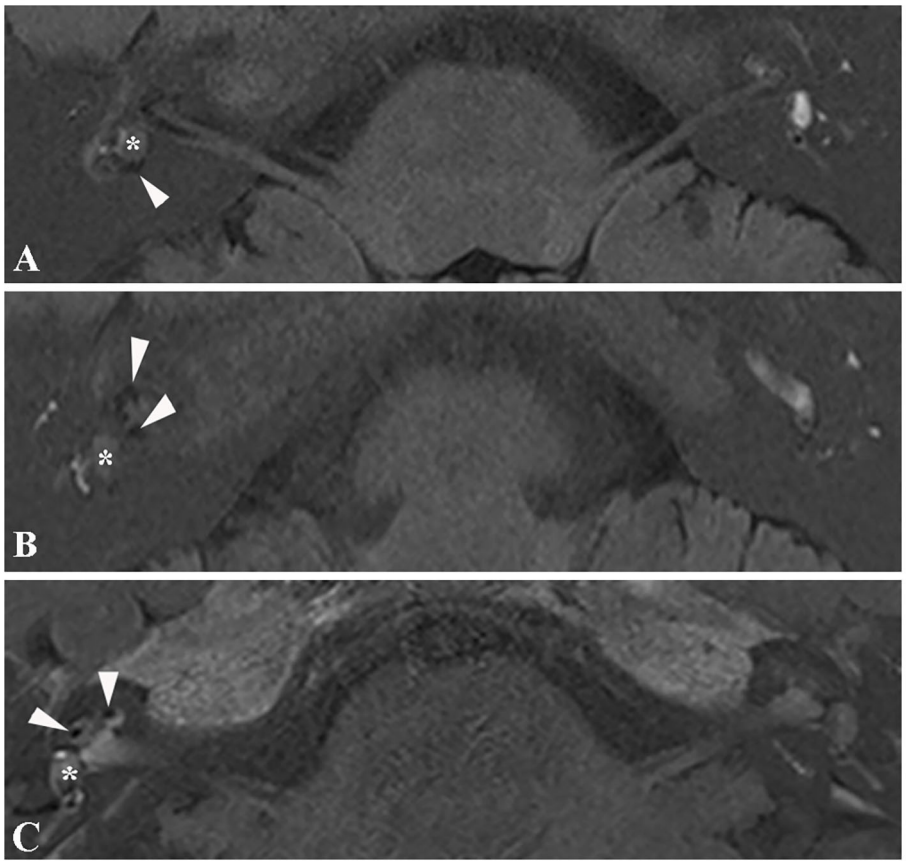

FIGURE 4 | Magnetic resonance image of endolymphatic hydrops. **(A)** 3D real IR MRI of patient 6 shows endolymphatic hydrops in the vestibule (arrowhead) concurrent with an intravestibular tumor (asterisk). **(B)** 3D-real IR MR image of patient 6 with an intravestibular tumor (asterisk), presenting with endolymphatic hydrops in the cochlea (arrowhead). **(C)** 3D-real IR MRI of patient 4 with intravestibular tumor (asterisk) showing endolymphatic hydrops in the basal turn of the cochlea.

patients with EH on MRI presented with vertigo similar to Meniere's disease, so we assumed that EH is one typical imaging characteristic of ILSs, even in the early stage. It is hard to say whether EH or the intralabyrinthine mass is the first thing that can be detected on the MRI. Regarding the mechanism of EH in ILS, we speculated that the tumor may block the longitudinal flow of the endolymph, prevent the flow of the endolymph to the endolymphatic sac, or cause inflammation of the endolymph (23, 24).

In patient 1 with positional vertigo, temporal bone MRI with intratympanic injection of gadolinium revealed that the tumor was located in the vestibular cavity and the fundus of the internal acoustic meatus, and no EH was detected, which is consistent with the presentation. Slattery et al. reported a high proportion of patients displaying positional vertigo and assumed that it may be attributed to the direct effect of the tumor exerted on the cochlear and vestibular end organs (19).

In addition, the severity of hearing loss in the hydropic ears seems to be related to the site of hydrops, as hearing loss in patients with mild endolymphatic hydrops was moderate and profound in patients with both vestibular and cochlear hydrops. Further studies are needed to confirm the association between the symptoms and synchronous EH in ILSs.

Inner ear tumors are easily missed due to their occult location and small size, especially on conventional MRI. From our experience, it is not difficult to identify tumors and EH in the labyrinth of patients with ILS after careful review of high-resolution MRI using the IT or IV method. According to a previous study, there is no difference in the detection rate of EH by the IT or IV method (25). The strength of the IT method is the better contrast and resolution of the obtained pictures, but it is more invasive and could be affected by the external or middle ear condition. However, the IV method is less invasive and allows simultaneous monitoring of both ears (26). Thus, the IV method is now preferred in our hospital. High-resolution T2 MRI sequences are also recommended during follow-up but are sometimes refused by patients in whom vertigo does not recur.

Management

Since vertigo is considered a risk factor for the growth of vestibular schwannomas (27), for patients with intractable vertigo or unserviceable hearing, resection of the tumor via the labyrinth or intratympanic injection of gentamicin is preferred

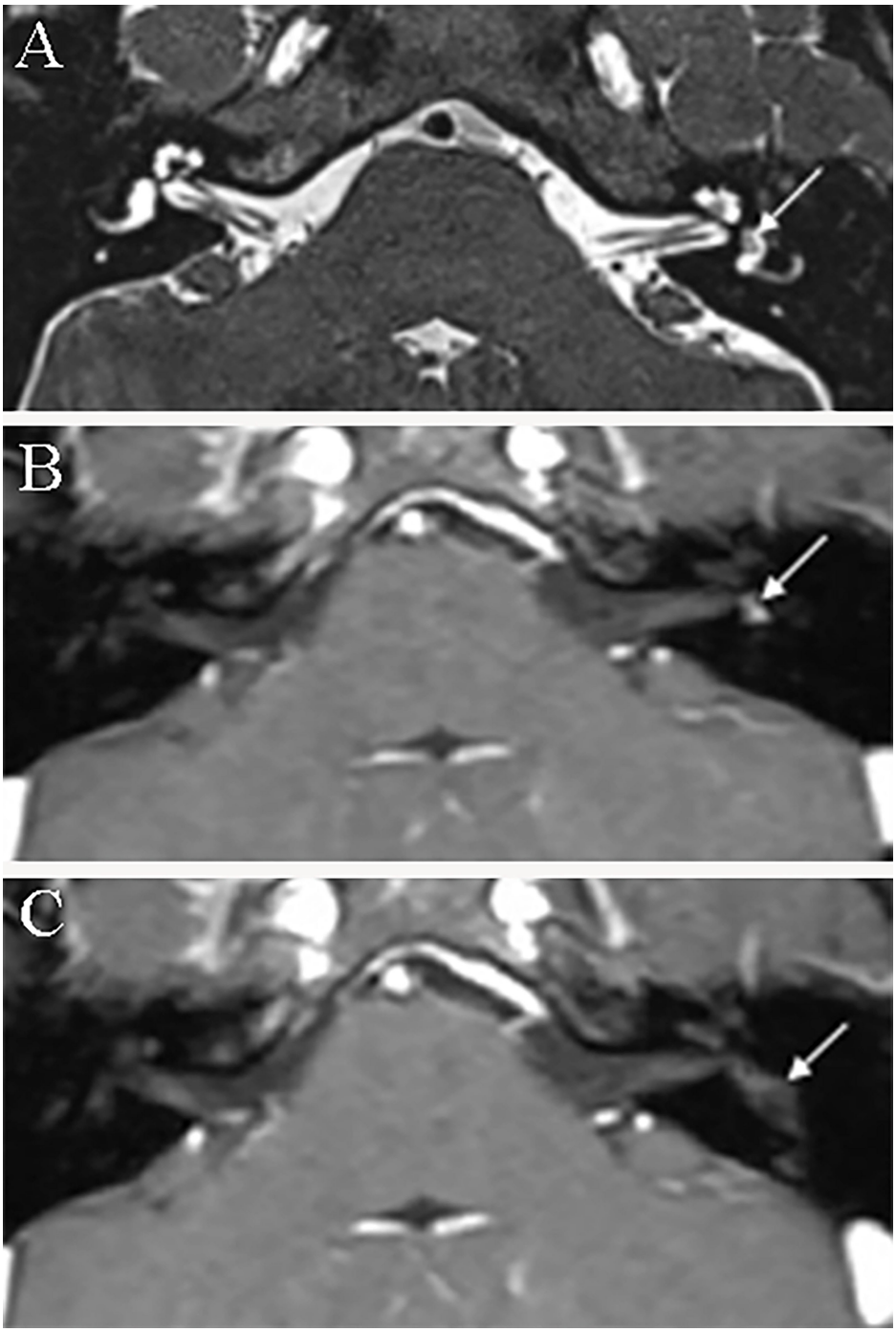

FIGURE 5 | Axial magnetic resonance imaging of patient 4 before and after surgery. **(A)** T2-3D-space MRI reveals a hypointense filling defect within the left vestibule (arrow). **(B)** Enhanced T1-weighted MRI demonstrates a mass (arrow) within the vestibular cavity before surgery. **(C)** Enhanced T1-weighted MRI reveals no enhanced mass within the vestibule (arrowhead) of the tumor at 6 months postoperatively.

(28). For patients with serviceable hearing or tolerable symptoms, a wait-and-see strategy is recommended. In recent years, endoscopic ear surgery has been widely used for its advantages, such as shortening the operation time, reducing the need for mastoidectomy, and reducing postoperative complications (29, 30). Studies have reported that endoscopic ear surgery can also be applied in treating ILS. Pan et al. reported the first documented case of endoscope-assisted resection of an intravestibular schwannoma and demonstrated that an endoscopic approach for tumor resection in the vestibule offered improved visualization

of the vestibule compared to that in an operating microscope (31). Marchioni et al. reported a series of six cases affected by ILSs of the intracochlear type who underwent surgery with an endoscopic transcanal transpromontorial approach and demonstrated that the endoscopic approach should be preferred to other more invasive surgical techniques in patients with intracochlear ILSs (32). Ma et al. reported partial cochlectomy via a transcanal endoscopic approach, and simultaneous cochlear implantation was performed in an intracochlear schwannoma case, which resulted in good audiologic outcomes (33). Taken together, in addition to cholesteatoma removal and tympanoplasty, endoscopic ear surgery is also suitable for patients with ILS, owing to its direct access to hidden recesses, such as vestibules, small incisions, and lower risk of postoperative complications.

The limitation of this study is that the number of cases is small; thus, statistical analysis between symptoms and imaging presentations cannot be performed.

CONCLUSION

EH concurrent with ILSs has been historically underestimated. With the extensive application of clinical MRI paradigms, such as 3D real IR sequence MRI, more potential cases of EH presenting in patients with ILS will be identified. The severity of hearing loss may be related to the location of the tumor and the degree of EH.

DATA AVAILABILITY STATEMENT

The original contributions presented in the study are included in the article/supplementary material, further inquiries can be directed to the corresponding author/s.

ETHICS STATEMENT

The studies involving human participants were reviewed and approved by The medical ethics committee of the Eye, Ear, Nose, and Throat Hospital of Fudan University, Shanghai, China. The patients/participants provided their written informed consent to participate in this study.

AUTHOR CONTRIBUTIONS

YZ conceived the idea and drafted the manuscript, while FL collected the raw data and followed the patients. WW and CD generously provided the material and revised the manuscript. All authors contributed to the article and approved the submitted version.

REFERENCES

1. Hamed A, Linthicum FJ. Intralabyrinthine schwannoma. *Otol Neurotol.* (2005) 26:1085–6. doi: 10.1097/01.mao.0000185064.97210.01
2. Neff BA, Willcox TJ, Sataloff RT. Intralabyrinthine schwannomas. *Otol Neurotol.* (2003) 24:299–307. doi: 10.1097/00129492-200303000-00028
3. Mayer O. Ein Fall von multiplen Tumoren in den Endansbreitungen des Akustikus. *Z Ohrenheilk.* (1917) 75: 95–113.
4. Weymuller EJ. Unsuspected intravestibular schwannoma. *Arch Otolaryngol.* (1975) 101: 630–2. doi: 10.1001/archotol.1975.00780390044012
5. DeLozier HL, Gacek RR, Dana ST. Intralabyrinthine schwannoma. *Ann Otol Rhinol Laryngol.* (1979) 88:187–91. doi: 10.1177/000348947908800207
6. Doyle KJ, Brackmann DE. Intralabyrinthine schwannomas. *Otolaryngol Head Neck Surg.* (1994) 110:517–23. doi: 10.1177/019459989411000608
7. Salzman KL, Childs AM, Davidson HC, Kennedy RJ, Shelton C, Harnsberger HR. Intralabyrinthine schwannomas: imaging diagnosis and classification. *Am J Neuroradiol.* (2012) 33:104–9. doi: 10.3174/ajnr.A2712
8. Butman JA, Nduom E, Kim HJ, Lonser RR. Imaging detection of endolymphatic sac tumor-associated hydrops. *J Neurosurg.* (2013) 119:406–11. doi: 10.3171/2013.2.JNS12608
9. Naganawa S, Kawai H, Sone M, Nakashima T, Ikeda M. Endolympathic hydrops in patients with vestibular schwannoma: visualization by non-contrast-enhanced 3D FLAIR. *Neuroradiology.* (2011) 53:1009–15. doi: 10.1007/s00234-010-0834-y
10. Homann G, Fahrendorf D, Niederstadt T, Nagelmann N, Heindel W, Lütkenhöner B, et al. HR 3 Tesla MRI for the diagnosis of endolymphatic hydrops and differential diagnosis of inner ear tumors—demonstrated by two cases with similar symptoms. *Rofo.* (2014) 186:225–9. doi: 10.1055/s-0033-1356221
11. Schuknecht HF, Rüther A. Blockage of longitudinal flow in endolymphatic hydrops. *Eur Arch Otorhinolaryngol.* (1991) 248(4):209–17. doi: 10.1007/BF00173659
12. Ekram T, Koch SR, Rajan J. Intralabyrinthine schwannomas: review of anatomy, pathology, clinical features from an imaging perspective. *J Clin and Diagn Res.* (2012) 6:915–8.
13. Jerin C, Krause E, Ertl-Wagner B, Gürkov R. Clinical features of delayed endolymphatic hydrops and intralabyrinthine schwannoma: an imaging-confirmed comparative case series. English version. *HNO.* (2017) 65(Suppl 1):41–5. doi: 10.1007/s00106-016-0199-6
14. Venkatasamy A, Bretz P, Karol A, Karch-Georges A, Charpiot A, Veillon F. MRI of endolymphatic hydrops in patients with intralabyrinthine schwannomas: a case-controlled study using non-enhanced T2-weighted images at 3T. *Eur Arch Otorhinolaryngol.* (2020). doi: 10.1007/s00405-020-06271-6. [Epub ahead of print].
15. Van Abel KM, Carlson ML, Link MJ, Neff BA, Beatty CW, Lohse CM, et al. Primary inner ear schwannomas: a case series and systematic review of the literature. *Laryngoscope.* (2013) 123:1957–66. doi: 10.1002/lary.23928
16. Marinelli JP, Lohse CM, Carlson ML. Incidence of intralabyrinthine schwannoma: a population-based study within the United States. *Otol Neurotol.* (2018) 39:1191–4. doi: 10.1097/MAO.0000000000001875
17. Gosselin E, Maniakas A, Saliba I. Meta-analysis on the clinical outcomes in patients with intralabyrinthine schwannomas: conservative management vs. microsurgery. *Eur Arch Otorhinolaryngol.* (2016) 273:1357–67. doi: 10.1007/s00405-015-3548-2
18. Kennedy RJ, Shelton C, Salzman KL, Davidson HC, Harnsberger HR. Intralabyrinthine schwannomas: diagnosis, management, and a new classification system. *Otol Neurotol.* (2004) 25:160–7. doi: 10.1097/00129492-200403000-00014
19. Slattery EL, Babu SC, Chole RA, Zappia JJ. Intralabyrinthine schwannomas mimic cochleovestibular disease: symptoms from tumor mass effect in the labyrinth. *Otol Neurotol.* (2015) 36:167–71. doi: 10.1097/MAO.0000000000000516
20. Dubernard X, Somers T, Veros K, Vincent C, Franco-Vidal V, Deguine O, et al. Clinical presentation of intralabyrinthine schwannomas: a multicenter study of 110 cases. *Otol Neurotol.* (2014) 35:1641–9. doi: 10.1097/MAO.0000000000000415
21. Santos F, Linthicum FH, House JW, Wilkinson EP. Histopathologic markers of hearing loss in intralabyrinthine schwannomas: implications for management. *Otol Neurotol.* (2011) 32:1542–7. doi: 10.1097/MAO.0b013e318238fc63

22. Asthagiri AR, Vasquez RA, Butman JA, Wu T, Morgan K, Brewer CC, et al. Mechanisms of hearing loss in neurofibromatosis type 2. *PLoS ONE.* (2012) 7:e46132. doi: 10.1371/journal.pone.0046132
23. Takano S, Iguchi H, Sakamoto H, Yamane H, Anniko M. Blockage pattern of longitudinal flow in Meniere's disease. *Acta Otolaryngol.* (2013) 133:692–8. doi: 10.3109/00016489.2013.771409
24. Yamane H, Takayama M, Sunami K, Sakamoto H, Imoto T, Anniko M. Blockage of reuniting duct in Meniere's disease. *Acta Otolaryngol.* (2010) 130:233–9. doi: 10.3109/00016480903096648
25. Li Y, Sha Y, Wang F, Lu P, Liu X, Sheng Y, et al. Comprehensive comparison of MR image quality between intratympanic and intravenous gadolinium injection using 3D real IR sequences. *Acta Otolaryngol.* (2019) 139:659–64. doi: 10.1080/00016489.2019.1600719
26. Yamazaki M, Naganawa S, Tagaya M, Kawai H, Ikeda M, Sone M, et al. Comparison of contrast effect on the cochlear perilymph after intratympanic and intravenous gadolinium injection. *AJNR Am J Neuroradiol.* (2012) 33:773–8. doi: 10.3174/ajnr.A2821
27. Artz JC, Timmer FC, Mulder JJ, Cremers CW, Graamans K. Predictors of future growth of sporadic vestibular schwannomas obtained by history and radiologic assessment of the tumor. *Eur Arch Otorhinolaryngol.* (2009) 266:641–6. doi: 10.1007/s00405-008-0791-9
28. Yang J, Jia H, Li G, Huang M, Zhu W, Wang Z, et al. Intratympanic gentamicin for small vestibular schwannomas with intractable vertigo. *Otol Neurotol.* (2018) 39:e699–703. doi: 10.1097/MAO.0000000000001899
29. Kiringoda R, Kozin ED, Lee DJ. Outcomes in endoscopic ear surgery. *Otolaryngol Clin North Am.* (2016) 49:1271–90. doi: 10.1016/j.otc.2016.05.008
30. Marchioni D, Rubini A, Gazzini L, Alicandri-Ciufelli M, Molinari G, Reale M, et al. Complications in endoscopic ear surgery. *Otol Neurotol.* (2018) 39:1012–7. doi: 10.1097/MAO.0000000000001933
31. Pan C, Sewell A, Michaelides E. Endoscope-assisted resection of intravestibular Schwannoma: a video case report. *Laryngoscope.* (2019) 129:986–8. doi: 10.1002/lary.27605
32. Marchioni D, De Rossi S, Soloperto D, Presutti L, Sacchetto L, Rubini A. Intralabyrinthine schwannomas: a new surgical treatment. *Eur Arch Otorhinolaryngol.* (2018) 275:1095–102. doi: 10.1007/s00405-018-4937-0
33. Ma AK, Patel N. Endoscope-assisted partial cochlectomy for intracochlear schwannoma with simultaneous cochlear implantation: a case report. *Otol Neurotol.* (2020) 41:334–8. doi: 10.1097/MAO.0000000000002539

Conflict of Interest: The authors declare that the research was conducted in the absence of any commercial or financial relationships that could be construed as a potential conflict of interest.

frontiers in Surgery

CASE REPORT
published: 25 March 2021
doi: 10.3389/fsurg.2021.606100

Case Report: Positive Pressure Therapy Combined With Endolymphatic sac Surgery in a Patient With Ménière's Disease

Munehisa Fukushima[1]*, *Shiro Akahani*[1], *Hidenori Inohara*[2] and *Noriaki Takeda*[3]

[1] Department of Otolaryngology—Head and Neck Surgery, Kansai Rosai Hospital, Amagasaki, Japan, [2] Department of Otolaryngology—Head and Neck Surgery, Graduate School of Medicine, Osaka University, Osaka, Japan, [3] Department of Otolaryngology, University of Tokushima School of Medicine, Tokushima, Japan

OPEN ACCESS

Edited by:
Ilmari Pyykkö,
Tampere University, Finland

Reviewed by:
Mary Daval,
Fondation Ophtalmologique Adolphe de Rothschild, France
A. B. Zulkiflee,
University Malaya Medical Centre, Malaysia
Ing Ping Tang,
Universiti Malaysia Sarawak, Malaysia
Sebastian Christoph Roesch,
Paracelsus Medical University, Austria
Conrad Riemann,
Bielefeld Clinic, Germany
Neil Donnelly,
University of Cambridge, United Kingdom

***Correspondence:**
Munehisa Fukushima
mfukushima@kansaih.johas.go.jp

Specialty section:
This article was submitted to Otorhinolaryngology - Head and Neck Surgery, a section of the journal Frontiers in Surgery

Received: 14 September 2020
Accepted: 03 March 2021
Published: 25 March 2021

Citation:
Fukushima M, Akahani S, Inohara H and Takeda N (2021) Case Report: Positive Pressure Therapy Combined With Endolymphatic sac Surgery in a Patient With Ménière's Disease. Front. Surg. 8:606100. doi: 10.3389/fsurg.2021.606100

Positive pressure therapy (PPT) is applied for medically-intractable vertigo in Ménière's disease (MD); however, it remains unknown whether PPT affects *in vivo* endolymphatic hydrops (EH). In this case report, we describe a 5-year course of MD in a patient in which EH was repeatedly observed. As the patient experienced recurrent vertigo attacks after endolymphatic sac surgery, he began to use the PPT device additionally and vertiginous episodes decreased in accordance with a decrease in the EH volume. The mechanism of PPT is suggested that the pressure increase in the middle ear inhibits EH development. PPT, if added after surgery, might be more effective to reduce EH volume compared with surgery alone. A larger study group size is required to test these preliminary data concerning EH changes.

Keywords: positive pressure therapy, Ménière's disease, endolymphatic hydrops, endolymphatic sac surgery, magnetic resonance imaging

INTRODUCTION

Ménière's disease (MD) is a common inner ear disease that is characterized by episodic vertigo, fluctuating sensorineural hearing loss, and tinnitus. Twenty percent of patients with MD are refractory to medical therapy (1) and suffer frequent vertigo attacks with progressive profound hearing loss (2). For medically-intractable MD patients, available options other than function-ablative procedures are positive pressure therapy (PPT) or endolymphatic sac surgery (3), although review articles concluded insufficient evidence to support the benefit of both PPT and surgery (4, 5). MD is pathologically defined as idiopathic endolymphatic hydrops (EH) in the inner ear (6, 7), and reducing EH is an hypothesized pathway in these two therapies; however, this has not been directly demonstrated for PPT.

EH is currently easily visualized using 3-Tesla magnetic resonance imaging (MRI) after intravenous administration of gadolinium (Gd) (8). Using this imaging method, we routinely characterize EH enlargement in patients with MD and measure EH volume semi-quantitatively (9). In this short preliminary report, we describe a 5-year course of MD in a patient in which EH volume was repeatedly measured, and demonstrated *in vivo* EH reduction using a PPT device. The significance of these findings is discussed with specific reference to known EH pathophysiology.

Informed consent was obtained from the described patient.

CASE REPORT

A 68-year-old man, a piano instructor, complained of repeated vertigo for a few hours with nausea once per month for 15 years despite taking medications, namely diuretics and difenidol. He suffered from persistent tinnitus in the right ear, and pure-tone audiometry indicated sensorineural hearing loss of 48.8/37.5 dB involving the whole frequency spectrum [right/left ears,

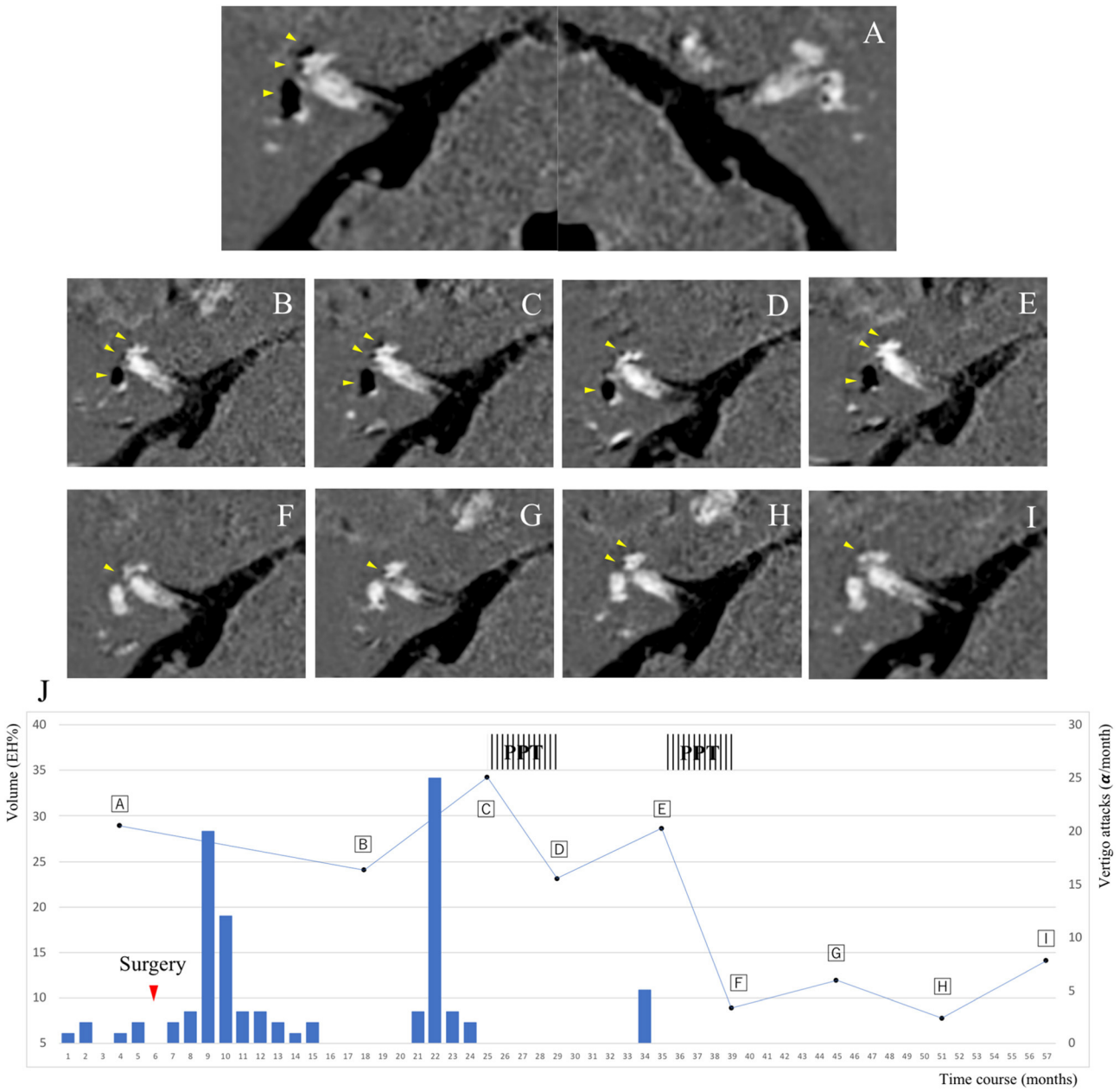

FIGURE 1 | Course of endolymphatic hydrops (EH) and progression of vertigo attacks in a 68-year-old man. The patient's course was semi-quantitatively assessed by gadolinium-enhanced inner ear magnetic resonance images, which are shown in **(A–I)** (axial T2-weighted fluid-attenuated inversion recovery). The y axis on the left indicates the volume ratio of EH to the total inner ear volume in the right ear. **(J)** is a progress chart of the patient's vertigo attacks as frequency per month on the y axis (right-hand side). **(A)** Significant EH in the right vestibule and cochlea. No EH in the left vestibule and cochlea. May 2015. **(B)** Mild EH in the right vestibule and cochlea. July 2016. **(C)** Significant EH in the right vestibule and mild EH in the right cochlea. February 2017. **(D)** Mild EH in the right vestibule and cochlea. June 2017. **(E)** Significant EH in the right vestibule and mild EH in the right cochlea. December 2017. **(F)** No EH in the right vestibule and mild EH in the right cochlea. April 2018. **(G)** October 2018. **(H)** April 2019. **(I)** November 2019. No EH in the right vestibule and mild EH in the right cochlea. The yellow arrowheads indicate EH, and the black areas represent EH in the labyrinth. **(J)** The red inverted triangle in the chart indicates the day of surgery. The vertical stripes indicate the durations of the positive pressure therapy.

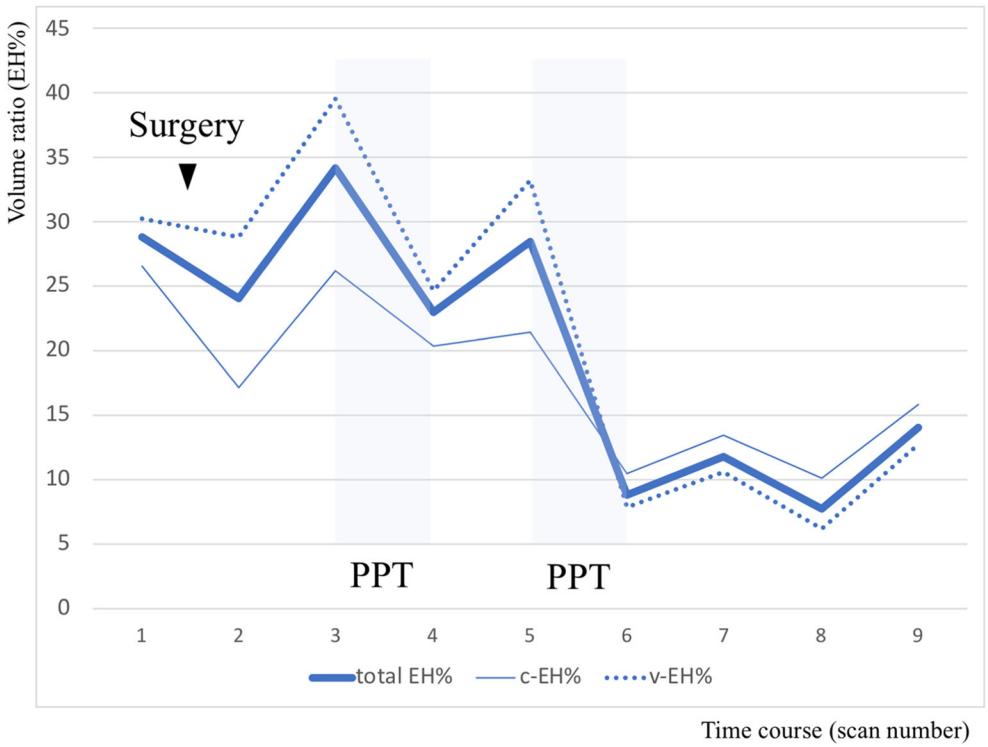

FIGURE 2 | Volume analysis of endolymphatic hydrops (EH) divided into cochlea and vestibule regions. The y axis indicates the volume ratio of EH to the involved part of the inner ear volume in the right ear. In this chart, the bold line indicates the volume ratio of EH relative to total inner ear volume (total EH%), the fine line indicates the volume ratio of EH relative to cochlear volume (c-EH%), and the dotted line indicates the volume ratio of EH relative to vestibular volume (v-EH%).

TABLE 1 | Sequential values of the volume ratio of endolymphatic hydrops (EH) in the right ear according to region.

	1	2	3	4	5	6	7	8	9
total EH%	28.8	24	34.2	23	28.5	8.8	11.8	7.7	14
c-EH%	26.5	17.1	26.2	20.4	21.4	10.4	13.4	10.1	15.8
v-EH%	30.3	28.8	39.5	24.7	33.2	7.8	10.6	6.2	12.7

Total EH%, volume ratio of EH to total inner ear volume; c-EH%, volume ratio of EH to cochlear volume; v-EH%, volume ratio of EH to vestibular volume.

four-tone average according to the AAO-HNS criteria (10)]. He underwent Gd-enhanced MRI of the inner ear and neuro-otological testing. The first MRI scan revealed significant EH in the right vestibule and cochlea (**Figure 1A**); the volume ratio of EH relative to total inner ear volume (EH%) was 28.8%. The bithermal water-irrigation caloric test was used to measure the maximum slow phase velocity, and results showed no response in the right ear. We diagnosed right definite MD (stage 3) (10), educated the patient regarding diet and lifestyle modifications, and prescribed betahistine and diuretics. After 4 months of the additional treatments, the frequency of the vertigo attacks remained constant, and hearing in his right ear worsened to 56.3 dB. We performed endolymphatic sac drainage with steroid instillation (11) on July 2015. We followed the patient to evaluate vertigo and hearing at least once per month and requested that he record the date, severity, and duration of vertigo attacks in a self-check diary (12); the course of the vertigo from the month prior to the first examination is shown in **Figure 1J**. In May 2016, he reported no vertigo, and the second MRI revealed decreased EH (**Figure 1B**, EH% = 24). However, he suffered frequent vertigo attacks beginning in October 2016, hearing in his right ear worsened to 66.3 dB, and the third MRI revealed increased EH (**Figure 1C**, EH% = 34.2). He began to use the PPT device (EFET01, Daiichi Medical Co., Ltd., Japan) for the first time at home three times daily from February 2017 to June 2017. Vertiginous episodes resolved, hearing in his right ear improved to 55 dB, and the fourth MRI revealed decreased EH (**Figure 1D**, EH% = 23). However, vertiginous episodes recurred in November 2017, hearing in his right ear worsened to 65 dB, and the fifth MRI revealed increased EH (**Figure 1E**, EH% = 28.5). The second series of using the PPT device at home was performed from December 2017 to April 2018. Vertiginous

episodes decreased, hearing in his right ear improved to 46.3 dB, and the sixth MRI revealed decreased EH equal to normal volume (**Figure 1F**, EH% = 8.8). For 2 years beginning in December 2017, he reported no vertigo, and the subsequent MRI revealed overall low EH values (**Figures 1G–I**: EH% = 11.8, 7.7, and 14, respectively). The latest hearing level was 47.5/42.5 dB, and he showed no caloric response in his right ear. All nine MRI scans detected no EH in the left inner ear throughout the 5-year observational course.

DISCUSSION

PPT and endolymphatic sac surgery is recommended as a second-line therapy for intractable MD when various medications fail (3). Several reports using MRI described EH volume decrease after sac surgery (13–15); however, to the best of our knowledge, no previous reports have demonstrated the effects of PPT for *in vivo* EH volume change in MD patients. In this patient, the frequency of the vertigo attacks was fully correlated with increases and decreases in EH volume (**Figure 1J**). There is a close association between the vector of the EH volume and MD symptoms, and the decreased EH% values were greater than twice the values after adding PPT (from 34.2 to 23 and from 28.5 to 8.8, respectively) than with surgery only (from 28.8 to 24). As shown in **Figure 2** and **Table 1**, EH volume in the right ear of this case showed almost parallel changes, both when evaluated by total volume and by each region. The frequency of the monthly vertigo attacks increased from 1 to 10 after surgery, but decreased from 10 to 0 after adding PPT; the decrease in vestibular EH might have reflected vestibular symptoms in this case. PPT, which was added 18 months after surgery, might be more effective to reduce the frequency of vertigo and the EH volume compared with surgery alone.

A meta-analysis of PPT reported a reduction in vestibular symptoms in patients with MD (16, 17), but the clinical efficacy of PPT for MD remains controversial (4). Animal studies showed that positive middle ear pressure instantly transferred to inner ear pressure (18), and electrocochleography recordings demonstrated that the summating potential significantly decreased in the PPT group (19). The suggested mechanism of PPT is that the pressure increase in the middle ear improves endolymphatic drainage and inhibits EH development (20), and this hypothesis was proven for the first time, in this study. The PPT device used in our study, unlike the Meniett device, provides intermittent positive pressure without ventilation tube insertion, and vertigo control for MD patients was demonstrated to be as effective as with the Meniett device (21). With these considerations, this remarkable case suggests that local pressure pulse application without oxygenation can affect labyrinthine physiology and induce *in vivo* EH reduction. Regarding our patient's hearing level in the affected ear, the difference between the first and the latest audiometry of 1.3 decibels was considered no change. Although the hearing level in the affected ear is reported to correlate with EH volume (22), the decrease in cochlear EH might not have improved the hearing level in this case. In MD, hearing levels worsen, and EH volume develops over time (23). The EH-reducing effect of a PPT device might have stopped the hearing deterioration, in our patient. Additionally, image data before or after PPT are useful to accurately determine the results of treatment.

In summary, we successfully treated a patient with intractable MD using a PPT device combined with endolymphatic sac surgery. Positive pressure could remedy vertiginous symptoms of MD through EH volume reduction. As this is a single case, and the data are preliminary, a larger study group size is required to evaluate the effect of PPT for *in vivo* EH. We plan to address this limitation in a future study.

DATA AVAILABILITY STATEMENT

The original contributions presented in the study are included in the article/supplementary material, further inquiries can be directed to the corresponding author/s.

ETHICS STATEMENT

Ethical review and approval was not required for the study on human participants in accordance with the local legislation and institutional requirements. The patients/participants provided their written informed consent to participate in this study. Written informed consent was obtained from the individual(s) for the publication of any potentially identifiable images or data included in this article.

AUTHOR CONTRIBUTIONS

MF initiated and performed the surgery. All authors were involved in the writing, reviewing, and editing of the manuscript.

FUNDING

This research was supported in part by the medical research fund of the Hyogo Medical Association and by research funds to promote the hospital functions of the Japan Organization of Occupational Health and Safety.

ACKNOWLEDGMENTS

We thank Jane Charbonneau, DVM, from Edanz Group (https://en-author-services.edanz.com/ac) for editing a draft of this manuscript.

REFERENCES

1. Arenberg IK. Pro position for endolymphatic sac and duct surgery. In: Arenberg IK, Graham MD, editors. *Treatment Options for Ménière's Disease*. San Diego, CA: Singular Publishing Group, Inc. (1998) p. 19–23.
2. Huppert D, Strupp M, Brandt T. Long-term course of Meniere's disease revisited. *Acta Otolaryngol.* (2010) 130:644–51. doi: 10.3109/00016480903382808
3. Sajjadi H, Paparella MM. Meniere's disease. *Lancet.* (2008) 372:406–14. doi: 10.1016/S0140-6736(08)61161-7
4. van Sonsbeek S, Pullens B, van Benthem PP. Positive pressure therapy for Meniere's disease or syndrome. *Cochrane Database Syst Rev.* (2015) Cd008419. doi: 10.1002/14651858.CD008419.pub2
5. Pullens B, Verschuur HP, van Benthem PP. Surgery for Meniere's disease. *Cochrane Database Syst Rev.* (2013) 2013:CD005395. doi: 10.1002/14651858.CD005395.pub3
6. K. Y. Uber die pathologische Veranderung bei einem Meniere-Kraken. *J Otolaryngol Jpn.* (1938) 44:2310–2.
7. Hallpike CS, Cairns H. Observations on the pathology of Meniere's syndrome: (Section Of Otology). *Proc R Soc Med.* (1938) 31:1317–36. doi: 10.1177/003591573803101112
8. Naganawa S, Yamazaki M, Kawai H, Bokura K, Sone M, Nakashima T. Imaging of Meniere's disease after intravenous administration of single-dose gadodiamide: utility of subtraction images with different inversion time. *Magn Reson Med Sci.* (2012) 11:213–9. doi: 10.2463/mrms.11.213
9. Fukushima M, Oya R, Nozaki K, Eguchi H, Akahani S, Inohara H, et al. Vertical head impulse and caloric are complementary but react opposite to Meniere's disease hydrops. *Laryngoscope.* (2019) 129:1660–6. doi: 10.1002/lary.27580
10. Committee on hearing and equilibrium guidelines for the diagnosis and evaluation of therapy in Meniere's disease. American Academy of Otolaryngology-Head and Neck Foundation, Inc. *Otolaryngol Head Neck Surg.* (1995) 113:181–5. doi: 10.1016/S0194-5998(95)70102-8
11. Kitahara T, Kubo T, Okumura S, Kitahara M. Effects of endolymphatic sac drainage with steroids for intractable Meniere's disease: a long-term follow-up and randomized controlled study. *Laryngoscope.* (2008) 118:854–61. doi: 10.1097/MLG.0b013e3181651c4a
12. Fukushima M, Akahani S, Inohara H, Takeda N. Stability of endolymphatic hydrops in meniere disease shown by 3-tesla magnetic resonance imaging during and after vertigo attacks. *JAMA Otolaryngol Head Neck Surg.* (2019) 145:583–5. doi: 10.1001/jamaoto.2019.0435
13. Uno A, Imai T, Watanabe Y, Tanaka H, Kitahara T, Horii A, et al. Changes in endolymphatic hydrops after sac surgery examined by Gd-enhanced MRI. *Acta Otolaryngol.* (2013) 133:924–9. doi: 10.3109/00016489.2013.795290
14. Higashi-Shingai K, Imai T, Okumura T, Uno A, Kitahara T, Horii A, et al. Change in endolymphatic hydrops 2 years after endolymphatic sac surgery evaluated by MRI. *Auris Nasus Larynx.* (2019) 46:335–45. doi: 10.1016/j.anl.2018.10.011
15. Ito T, Inui H, Miyasaka T, Shiozaki T, Matsuyama S, Yamanaka T, et al. Three-dimensional magnetic resonance imaging reveals the relationship between the control of vertigo and decreases in endolymphatic hydrops after endolymphatic sac drainage with steroids for Meniere's disease. *Front Neurol.* (2019) 10:46. doi: 10.3389/fneur.2019.00046
16. Ahsan SF, Standring R, Wang Y. Systematic review and meta-analysis of Meniett therapy for Meniere's disease. *Laryngoscope.* (2015) 125:203–8. doi: 10.1002/lary.24773
17. Zhang SL, Leng Y, Liu B, Shi H, Lu M, Kong WJ. Meniett therapy for Meniere's disease: an updated meta-analysis. *Otol Neurotol.* (2016) 37:290–8. doi: 10.1097/MAO.0000000000000957
18. Feijen RA, Segenhout JM, Wit HP, Albers FW. Monitoring inner ear pressure changes in normal guinea pigs induced by the Meniett20. *Acta Otolaryngol.* (2000) 120:804–9. doi: 10.1080/0001648007500 61633
19. Densert B, Sass K, Arlinger S. Short term effects of induced middle ear pressure changes on the electrocochleogram in Meniere's disease. *Acta Otolaryngol.* (1995) 115:732–7. doi: 10.3109/000164895091 39394
20. Sakikawa Y, Kimura RS. Middle ear overpressure treatment of endolymphatic hydrops in guinea pigs. *ORL J Otorhinolaryngol Relat Spec.* (1997) 59:84–90. doi: 10.1159/000276915
21. Watanabe Y, Shojaku H, Junicho M, Asai M, Fujisaka M, Takakura H, et al. Intermittent pressure therapy of intractable Meniere's disease and delayed endolymphatic hydrops using the transtympanic membrane massage device: a preliminary report. *Acta Otolaryngol.* (2011) 131:1178–86. doi: 10.3109/00016489.2011.600331
22. Fukushima M, Kitahara T, Oya R, Akahani S, Inohara H, Naganawa S, et al. Longitudinal up-regulation of endolymphatic hydrops in patients with Meniere's disease during medical treatment. *Laryngoscope Investig Otolaryngol.* (2017) 2:344–50. doi: 10.1002/lio2.115
23. Fukushima M, Ueno Y, Kitayama K, Akahani S, Inohara H, Takeda N. Assessment of the progression of vertical semicircular canal dysfunction and increased vestibular endolymphatic hydrops in patients with early-stage Meniere disease. *JAMA Otolaryngol Head Neck Surg.* (2020) 146:789–800. doi: 10.1001/jamaoto.2020.1496

Conflict of Interest: The authors declare that the research was conducted in the absence of any commercial or financial relationships that could be construed as a potential conflict of interest.

frontiers in Surgery

ORIGINAL RESEARCH
published: 07 May 2021
doi: 10.3389/fsurg.2021.666390

Enhanced Eye Velocity in Head Impulse Testing—A Possible Indicator of Endolymphatic Hydrops

Ian S. Curthoys[1], Leonardo Manzari[2], Jorge Rey-Martinez[3], Julia Dlugaiczyk[4] and Ann M. Burgess[1]*

[1] Vestibular Research Laboratory, School of Psychology, The University of Sydney, Sydney, NSW, Australia, [2] MSA ENT Academy Center, Cassino, Italy, [3] Otoneurology Unit, Otolaryngology Department, Hospital Universitario Donostia, San Sebastian, Spain, [4] Department of Otorhinolaryngology, Head and Neck Surgery, University Hospital Zurich, University of Zurich, Zürich, Switzerland

Introduction: On video head impulse testing (vHIT) of semicircular canal function, some patients reliably show enhanced eye velocity and so VOR gains >1.0. Modeling and imaging indicate this could be due to endolymphatic hydrops. Oral glycerol reduces membranous labyrinth volume and reduces cochlear symptoms of hydrops, so we tested whether oral glycerol reduced the enhanced vHIT eye velocity.

Study Design: Prospective clinical study and retrospective analysis of patient data.

Methods: Patients with enhanced eye velocity during horizontal vHIT were enrolled (n = 9, 17 ears) and given orally 86% glycerol, 1.5 mL/kg of body weight, dissolved 1:1 in physiological saline. Horizontal vHIT testing was performed before glycerol intake (time 0), then at intervals of 1, 2, and 3 h after the oral glycerol intake. Control patients with enhanced eye velocity (n = 4, 6 ears) received water and were tested at the same intervals. To provide an objective index of enhanced eye velocity we used a measure of VOR gain which captures the enhanced eye velocity which is so clear on inspecting the eye velocity records. We call this measure the initial VOR gain and it is defined as: (the ratio of peak eye velocity to the value of head velocity at the time of peak eye velocity). The responses of other patients who showed enhanced eye velocity during routine clinical testing were analyzed to try to identify how the enhancement occurred.

Results: We found that oral glycerol caused, on average, a significant reduction in the enhanced eye velocity response, whereas water caused no systematic change. The enhanced eye velocity during the head impulses is due in some patients to a compensatory saccade-like response during the increasing head velocity.

Conclusion: The significant reduction in enhanced eye velocity during head impulse testing following oral glycerol is consistent with the hypothesis that the enhanced eye velocity in vHIT may be caused by endolymphatic hydrops.

Keywords: endolymphatic hydrops, Menière's Disease, vHIT, semicircular canal testing, VOR, vestibular

OPEN ACCESS

Edited by:
Robert Gürkov, Bielefeld University, Germany

Reviewed by:
John Allum, University of Basel, Switzerland
Hans Thomeer, University Medical Center Utrecht, Netherlands

****Correspondence:***
Ian S. Curthoys
ian.curthoys@sydney.edu.au

Specialty section:
This article was submitted to Otorhinolaryngology - Head and Neck Surgery, a section of the journal Frontiers in Surgery

Received: *10 February 2021*
Accepted: *12 April 2021*
Published: *07 May 2021*

Citation:
Curthoys IS, Manzari L, Rey-Martinez J, Dlugaiczyk J and Burgess AM (2021) Enhanced Eye Velocity in Head Impulse Testing—A Possible Indicator of Endolymphatic Hydrops. Front. Surg. 8:666390. doi: 10.3389/fsurg.2021.666390

INTRODUCTION

An enhanced eye velocity response to stimulation of the semicircular canals by angular acceleration has been reported in patients with Menière's Disease (MD) (1–3). Evidence for enhanced eye velocity in the video head impulse test (vHIT) of horizontal semicircular canal function (vHIT) with very high angular accelerations (up to 5,000 deg/s^2) has also been reported (4–7). The prevalence of this increased enhanced eye velocity has now been documented by a large study (7) showing a prevalence for enhanced eye velocity in vHIT testing of patients with MD. In these patients the result was not due to poor calibration or artifacts in testing, such as goggle slip (8, 9) since the testers were very experienced clinicians who carefully checked for calibration errors or goggle slip. It was not due to testing with a very close viewing distance—which acts to increase VOR gain (10, 11). Repeated vHIT tests show that enhanced eye velocity is a characteristic response pattern for individual patients, and the consistency of such a response can be seen in the repeated test results of one patient on different occasions (4). In these patients during a head impulse, the eye velocity exceeds the head velocity, resulting in a VOR gain >1.0, where the area VOR gain is defined as (the area under the eye velocity record divided by the area under the head velocity record). It appears that enhanced eye velocity in vHIT testing is rarely found in testing healthy subjects (7).

The focus of the present study was on the possible cause of such enhanced eye velocity. Our hypothesis is that it may be due to endolymphatic hydrops (ELH). Imaging of the labyrinth of two patients with enhanced eye velocity has shown ELH (4). The hypothesis is that ELH alters the hydrodynamic load on the cupula during an angular acceleration and so results in an increased eye velocity (4, 5, 12). That hypothesis is supported by fluid dynamical modeling of the effect of ELH on vHIT responses showing that ELH resulted in enhanced eye velocity responses similar to the enhanced responses actually obtained from patients with MRI-confirmed ELH (4, 5, 12). To further test this hypothesis, we sought in patients showing enhanced eye velocity to modify labyrinth volume experimentally by using oral glycerol and testing what effect that modification had on their enhanced eye velocity response.

There is anatomical evidence from guinea pig studies that glycerol acts to reduce membranous labyrinth volume (13, 14). In patients the glycerol dehydration test has been used to indicate ELH in auditory testing by measuring auditory thresholds before and after oral intake of glycerol. The reduction of thresholds for low frequencies is an indicator of probable ELH (15, 16). Objective measures show that oral glycerol caused changes of the cochlear electrophysiological indicator of ELH (the SP/AP ratio of the ECochG during glycerol) (17). There are vestibular parallels to these auditory changes after glycerol—VEMP amplitude increases (18–22). So, we reasoned that the glycerol test could be used to test whether enhanced eye velocity during vHIT testing is due to ELH, by selecting patients who showed enhanced eye velocity to horizontal head impulses and measuring their eye velocity before and at hourly intervals after oral intake of glycerol. We predicted that the glycerol should act to decrease the ELH and so to decrease the enhanced eye velocity. As a control we tested patients with enhanced eye velocity at hourly intervals before and after oral intake of comparable volumes of water.

Abbreviations: ECochG, electrocochleography; ELH, endolymphatic hydrops; VOR, vestibulo-ocular reflex; HIT, head impulse test; vHIT, video head impulse test.

MATERIALS AND METHODS

Study Design and Participants

Patients were enrolled if they showed enhanced eye velocity on vHIT testing. The criterion level for enrolment was set as an initial VOR gain >1.29. That cutoff level was established by measuring the initial VOR gain in a group of healthy subjects where the mean value of initial VOR gain in 16 healthy asymptomatic subjects (32 ears) was 1.05 ± 0.118 (SD) (see **Table 1** for demographic data on patients and healthy subjects). Thus, an initial VOR gain >1.29 is larger than 95% of the population [mean +2 standard deviations (25)], and so patients in whom the vHIT records for an impulse to one side showed an initial VOR gain >1.29 were enrolled in this study. We enrolled nine test patients (17 ears met criterion) and four control patients (6 ears met criterion). We stress that the inclusion criterion in this study was not based on diagnosis, but on this objective measure of enhanced eye velocity on vHIT testing. **Table 1** shows the demographics of the patients and shows that the usual diagnosis was definite Menière's Disease based on Bárány Society guidelines (23). The diagnosis of Definite Menière's Disease according to the Bárány Society criteria requires (i) at least two episodes of spontaneous vertigo lasting between 20 min and 12 h, (ii) the presence of a low-frequency sensorineural hearing loss in the affected ear (at least 30 dB nHL in two neighboring frequencies <2 kHz) in the pure-tone audiogram before, during or after an attack, (iii) fluctuating auditory symptoms like fullness or tinnitus in the affected ear. In case the patient reports fluctuating hearing loss in the affected ear, but criterion (ii) is not fulfilled, the symptoms are classified as "probable Menière's Disease." Glycerol test patients are G1–G9 and control patients are W1–W4. Two patients who met the inclusion criterion of an initial gain above 1.29 were diagnosed as having Vestibular Migraine according to the diagnostic criteria of the Bárány Society (24). A summary of the demographics of the group of 16 healthy subjects is also shown (**Table 2**).

The patients were tested before and at hourly intervals after oral glycerol intake (test patients) or water intake (control patients). All the test patients were given orally 86% glycerol at a dosage of 1.5 mL/kg of body weight, dissolved 1:1 in physiological saline. The control patients received only water. Because vHIT testing is so fast and is not burdensome to patients, it was possible to test these patients at 4 successive epochs: before oral glycerol (or water) intake (time 0) and 1, 2, and 3 h after the intake. All patients were tested at quiescence.

TABLE 1 | It shows the demographics of the patients and shows that the usual diagnosis was definite Menière's Disease based on Bárány Society guidelines (23).

Patient no.	Gender	Age	Diagnosis	PTA	Ears included
Glycerol					
G1	Female	68	Bilateral definite MD*	78.5–50	L,R
G2	Female	54	Bilateral definite MD*	55–37.5	L,R
G3	Female	42	Vestibular migraine	12.5–10	L,R
G4	Female	43	Vestibular migraine	10–10	L,R
G5	Female	49	Right definite MD* – Left delayed endolymphatic hydrops	73.5–32.5	L,R
G6	Male	49	Right definite MD*	12.5–10	L,R
G7	Female	70	Bilateral definite MD*	35–62.5	L,R
G8	Female	31	Right definite MD*	36.25–10	R
G9	Male	35	Left probable MD	15–27.5	L,R
Water					
W1	Male	48	Right definite MD*	43.75–10	L
W2	Female	65	Bilateral definite MD*	21.25–22.5	L,R
W3	Female	32	Left definite MD*	10–32.5	L,R
W4	Female	44	Left probable MD	10–12.5	R

Glycerol test patients are G1–G9 and control patients are W1–W4. Two patients who met the inclusion criterion of an initial gain above 1.29 were diagnosed as having Vestibular Migraine according to the diagnostic criteria of the Bárány Society (24).
*"Ears included" refers to which sides showed enhanced eye velocity and were included in the statistical analysis. The asterisk * shows which patients had a diagnosis of definite Menière's Disease.*

TABLE 2 | It shows a summary of the demographics of the group of 16 healthy subjects.

Subject no.	Gender	Age
N1	Female	48
N2	Male	35
N3	Male	54
N4	Male	74
N5	Male	35
N6	Female	46
N7	Male	72
N8	Female	55
N9	Male	28
N10	Female	45
N11	Female	51
N12	Male	21
N13	Female	61
N14	Female	18
N15	Female	26
N16	Female	55
N17	Female	43

Ethics

All patients were informed about the procedure and the vestibular tests which were part of their clinical evaluation. The glycerol testing was carried out at the MSA ENT Academy Center in Cassino, and all procedures were performed in accordance with the Helsinki declaration, and were approved by the MSA ENT Academy Institutional Review Board, and all subjects and patients gave informed consent to the investigation and were free to terminate their participation at any time.

The glycerol experiment reported here yielded some results which were puzzling, so we reviewed earlier data from clinical vHIT testing of other patients tested during their routine clinical evaluation at Cassino or Donostia seeking examples of enhanced eye velocity in the responses of these patients. In each case the vHIT testing had been conducted with the patient's approval as part of the standard clinical assessment of their vestibular function. Since no novel or exceptional interventions were performed, simply the routine vHIT testing, only the approval of the local ethical committee for the corresponding institutions was required for the researchers.

vHIT Testing

The function of the horizontal semicircular canals was measured using the horizontal video head impulse test (vHIT) (26) (OtosuiteV®, GN Otometrics, Denmark). Subjects were instructed to fixate an earth-fixed dot on the wall at 1 m distance in front of them. Room lighting conditions were adjusted to ensure that the pupil was small, and the pupil image was not affected by reflections at any point in the range of the head movement. At each testing epoch the clinician (LM) applied about 20 brief, rapid, horizontal head turns (head impulses) to each side, always starting from center, with unpredictable timing and direction with minimal bounce-back or overshoot at the end of the head impulse: that is each head impulse was "turn and stop." The amplitude of the head rotation was about 10–15 deg, and the peak head velocity of the impulse was about 140–250 deg/s, with angular accelerations of between about 3,000 deg/s^2 and 5,000 deg/s^2. The sampling frequency was 250 frames/s. Video images were analyzed online to calculate eye position using a pupil detection method based on a center-of-gravity algorithm written in LabVIEW (National Instruments, Austin). Eye velocity and head velocity were recorded for each head turn. Eye velocity was obtained from a two-point differentiator and low-pass filtered (0- to 30-Hz bandwidth). Head accelerations were obtained using a Savitzky-Golay quadratic polynomial filter with a filter length of three points (corresponding to 12 ms) to smooth and differentiate the head-velocity data. The same process was used to obtain eye accelerations from the eye velocities. Because covert saccades rarely occur on the ascending phase of head velocity and because the initial VOR gain was based on a velocity point and not the usual area under the eye velocity curve, desaccading was not needed for the calculation of the initial VOR gain. At each testing epoch, the examiner sought to give head impulses with similar peak head velocities.

Three methods of calculating VOR gain from the slow phase eye velocity were used. (1) Area VOR gain: the area under the desaccaded eye velocity curve (27) divided by the area under the head velocity curve. This is the standard area VOR gain as used in the Otometrics Impulse system.

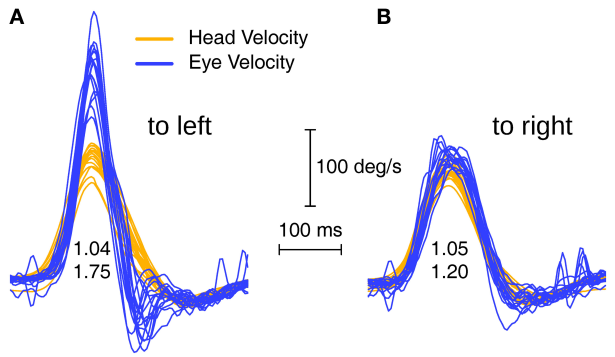

FIGURE 1 | Superimposed eye velocity and head velocity records for head impulses to the left **(A)** and right **(B)** sides of a patient with enhanced eye velocity. In this example the usual indicator of VOR gain (area VOR gain) is 1.04 for the left side and 1.05 for the right side, which does not indicate the enhanced eye velocity which is so clear in the eye velocity time series on the left. Whilst the area VOR gains are similar for both L and R, the time series of eye velocities during the head impulses are completely different. In R the eye velocity tracks head velocity almost exactly, whereas in L there is an early enhanced eye velocity during the head acceleration followed by a steep decrease in eye velocity during impulse deceleration. To quantify the enhanced eye velocity on the left we calculated a parameter called initial VOR gain, which consists of the peak eye velocity divided by the value of head velocity at the time of peak eye velocity and the initial VOR gains here are 1.75 and 1.20.

(2) The initial VOR gain defined as the peak eye velocity divided by the value of head velocity at the time of peak eye velocity. The onset of the head impulse was defined as 60 ms before the time of peak head acceleration. (3) the peak eye velocity divided by the head velocity at peak head acceleration, since this index may better reflect the effect of hydrops on cupula deflection.

In order to detect enhanced eye velocity, it is necessary to examine the time series records for individual trials–it can be concealed if only area VOR gain is examined because the eye velocity during the deceleration phase of the head impulse may cancel the enhanced eye velocity during the acceleration phase of the head impulse (see **Figure 1**). The enhanced eye velocity shown in individual trials occurs in the first part of the head impulse—from the onset to the peak head velocity (see **Figure 1**). To set an objective measure of what constitutes enhanced eye velocity we calculated the ratio of the peak eye velocity to the value of head velocity measured at the time of peak eye velocity. For this calculation, the peak eye velocity was defined as the highest eye velocity occurring in the time interval starting 40 ms before the time of peak head velocity, and ending 40 ms after the time of peak head velocity. We refer to this ratio of peak eye velocity to simultaneous head velocity as the initial VOR gain, and this was the objective measure of enhanced eye velocity used in this study.

As **Figure 1** shows, area VOR gain does not faithfully reflect the enhanced eye velocity response of these patients, which is clear on inspection of the time series eye velocity records. For example **Figure 1A** shows a patient's vHIT responses on L where the actual trajectory of eye velocity during the head impulse is unlike the usual close match to head velocity of healthy subjects, and this patient recorded an area VOR gain of 1.04 but an initial VOR gain of 1.75, justifying our use of initial VOR gain as an objective indicator of enhanced eye velocity.

Statistical Analysis

For each patient the initial VOR gain was calculated for every impulse, averaged across impulses at each testing epoch, and the averaged initial VOR gains across patients were analyzed with a one-way ANOVA with repeated measures using SPSS Version 26 (28). The data for the glycerol patients and water patients were analyzed separately. Shapiro-Wilk tests of normality (25) showed that the assumption of normality of distribution of the raw data was accepted in all conditions for both glycerol and water. Mauchly's test of sphericity (W) was not significant for both groups. The level of statistical significance was set at $p < 0.05$.

RESULTS

Reduced Initial VOR Gain After Glycerol Intake

The responses of testing 17 sides (ears) of the nine patients whose data exceeded the criterion of initial VOR gain >1.29 were analyzed. **Figure 2** shows examples of the raw data for three patients: the superimposed eye velocity and head velocity plots during standard head impulses of these patients before glycerol intake (upper two rows (A and B)) show enhanced eye velocity. Each separate image (which we term a thumbnail) shows the responses before and at hourly intervals after oral glycerol. For each set of impulses the mean initial VOR gain together with the standard error is shown beneath the impulses. The mean area VOR gain is shown to the right of the superimposed records. An example of the response of a control patient who received oral water instead of glycerol is shown in **Figure 2C**.

Figure 3 shows the average initial VOR gains at each testing epoch for patients receiving glycerol and those receiving water together with the means across the patients in the two groups (and two tailed 95% confidence intervals – gray bands). The ANOVA on the 17 glycerol ears was significant: $F = 4.72$, $p = 0.006$ with the contrast for linear trend showing that for the glycerol data there was a significant linear decrease in initial VOR gain across the testing intervals $F = 8.04$, $p = 0.012$. A total of 13/17 ears tested showed a decrease in VOR 1 h after glycerol. The ANOVA for the water control was not significant: $F = 0.454$, $p = 0.718$). Only 17 ears of nine patients were measured since the last ear did not meet the inclusion criterion of an initial VOR gain above 1.29.

Using the VOR gain specified by peak eye velocity divided by the head velocity at time of peak head acceleration also showed that glycerol caused a significant decrease in VOR gain.

Absence of Corrective Saccades After the Enhanced Eye Velocity

If eye velocity closely matches head velocity during a head impulse, then at the end of the impulse the eye will be on target, so there will be no gaze error and so no corrective saccade will be necessary. The Otometrics system (ICS Impulse) shows area gain, which is the ratio of the change in eye position to the change in head position. The change in head position is the integral of

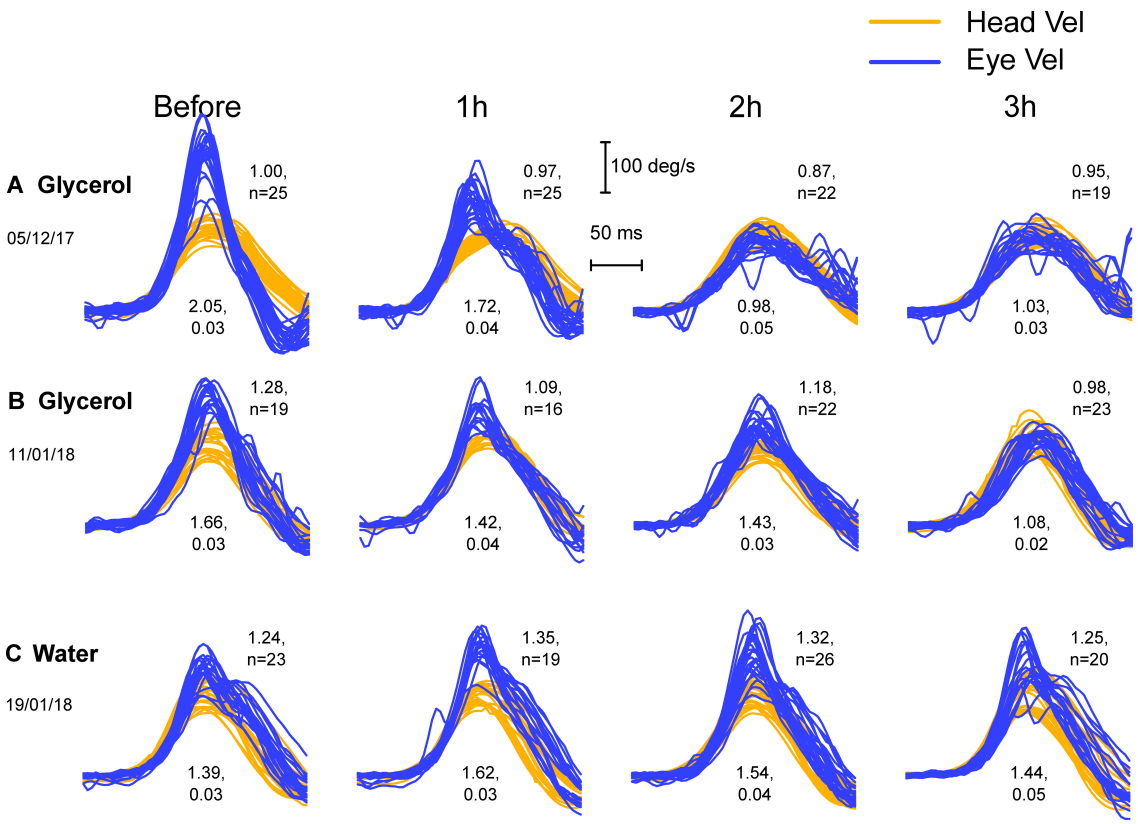

FIGURE 2 | Three examples of the successive vHIT test results (plots which we term thumbnails) of two patients **(A,B)** with enhanced eye velocity before and at hourly intervals after oral glycerol intake (upper two rows) and for another patient **(C)** before and after water intake. Each thumbnail shows the superimposed records of eye velocity (dark blue) and head velocity (light orange) during the head impulse for many trials. There appear to be inflection points in the eye velocity records during the deceleration (explained below). Before glycerol (leftmost column) the three patients all have large initial VOR gains (values shown beneath the thumbnails), reflecting the enhanced eye velocity. The decrease in enhanced eye velocity in the glycerol patients after glycerol intake is clear, whereas there is no systematic decrease in the eye velocity or the initial VOR gain in the patient receiving water.

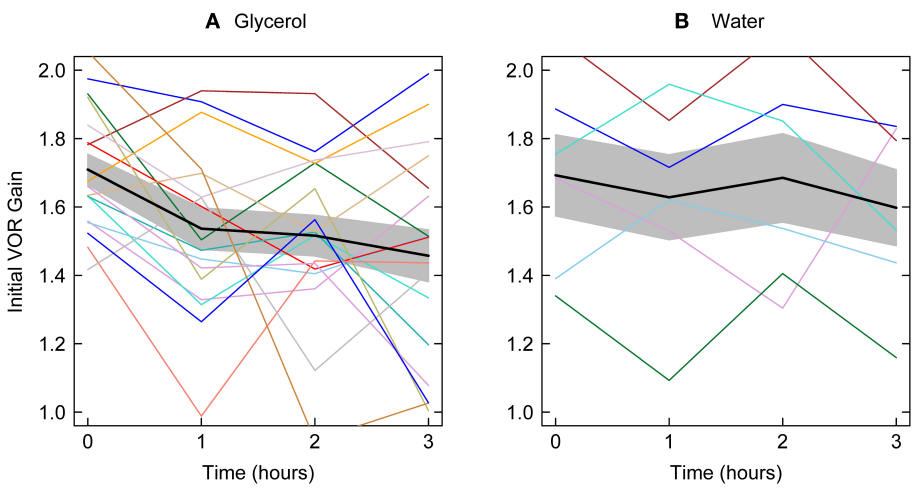

FIGURE 3 | Initial VOR gain for all patients together with mean initial VOR gain across all patients tested at each testing epoch the gray bands show two tailed 95% confidence intervals for the means. Left panel—glycerol; right panel–water. The average decrease from before to 1 h after glycerol intake is significant and there is a significant linear decrease across the test epochs. There is no significant change in initial VOR gain for patients receiving water.

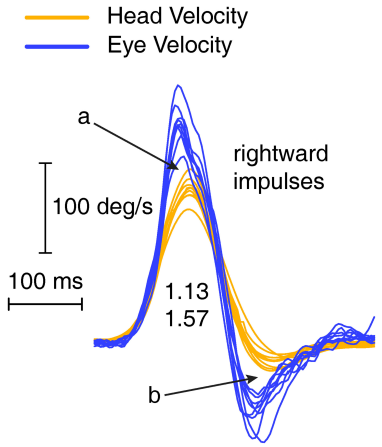

FIGURE 4 | Enhanced eye velocity (a) during acceleration may be canceled by decreased eye velocity during deceleration (b) leading to a final eye position which stays close to the target.

head velocity during the head impulse—i.e., the area under the head velocity curve. The change in head position is matched and corrected for by the change in eye position, so at the end of the impulse the eye is on the target and no saccade is necessary. However, the area gain for the entire head impulses may be close to 1, although there may be a clearly enhanced eye velocity at the start of the impulse, then in the second half of the impulse the eye velocity is regularly less than the decreasing head velocity (see **Figure 4**), thus acting to cancel out the position error caused by the enhanced eye velocity on the acceleration phase. The result is that the area between eye velocity and head velocity (arrow a in **Figure 4**) is about the same as the (opposite) area between eye velocity and head velocity in the decelerating phase (arrow b), so these two areas effectively cancel and the eye position at the end of the head impulse will be on target, so no corrective saccade will be necessary even though the trajectory of the eye velocity during the head impulse is so different from the usual response (see also **Figure 1A**). While the graphical records may show this, the area gain value may not. These examples show why we derived and used this gain measure—initial VOR gain—which reflects the enhanced eye velocity during the initial part of the head impulse.

Saccade-Like Responses

In some patients the enhancement of eye velocity during the head impulse stimulus is fairly uniform at all head velocities (see **Figure 4**). However, the records from other patients show what appears to be a saccade-like response which is added to the eye velocity during the initial head acceleration. It is a compensatory saccade and not an anticompensatory quick phase since the saccade direction is opposite to the direction of head turn. (A quick phase of nystagmus is a rapid eye movement in the same direction as head turn and so is anticompensatory). This response appears to be a very early covert saccade. Such a saccade-like response is very difficult to detect during the increasing head velocity at the start of the head impulse because the saccadic velocity is very close to the high eye velocity at the start of the head impulse. However, an inflection at the end of the saccadic-like responses (arrows in **Figure 5**) is a tell-tale sign of the addition of this saccade-like response during the head impulse. These two response modes suggest there may be two mechanisms operating to produce VOR gain enhancement. The first being the enhancement shown by fluid dynamic modeling (5), the second being a mechanism which generates this saccade-like response. We sought to try to clarify further this saccade-like mechanism and consider what may cause it.

By plotting the time series of the difference between eye velocity and head velocity during the whole head impulse (**Figure 5**, second and fourth columns) for a healthy subject (A) and patients (B and C), this saccade-like response is clearly shown in the patient records (B and C). The difference between eye velocity and head velocity effectively cancels the slow compensatory eye velocity response and leaves the saccade-like response exposed. For horizontal head turns for healthy subjects (top row), the typical records have the eye velocity matching head velocity quite closely, so the difference (E–H) curves are flat or even concave (probably because of the small effect of latency of the eye velocity response). These early saccade-like responses occur rarely in healthy subjects (**Figure 5A**) but are found and are highly repeatable in patients (e.g., arrows in **Figure 5** above).

Figure 6 shows several examples of the raw data and the corresponding plot of the difference between eye velocity and head velocity for four patients and four healthy subjects to establish the consistency of the response patterns and the usefulness of this mode of plotting the responses of head impulse testing.

DISCUSSION

These results show that there is an enhanced eye velocity during head impulse testing and that oral glycerol on average results in a significant decrease in this enhanced eye velocity. Consuming a comparable volume of water does not result in a significant decrease of enhanced eye velocity. Other evidence shows that glycerol acts to reduce ELH, so our result implies that enhanced eye velocity on vHIT testing may be an indicator of endolymphatic hydrops. In the following we consider major questions about these results—the evidence that enhanced eye velocity occurs, whether it is artifactual, the variability of patient responses, what could trigger the enhancement.

Patient Groups

The enhanced eye velocity is not restricted to patients with MD but occurs in other patient groups: some patients diagnosed as having vestibular migraine show enhanced eye velocity. This is in accord with the hydrops model put forward above because ELH occurs not only in MD but can also occur in other conditions (29, 30). The group which is poorly represented in our testing is healthy subjects because enhanced eye velocity was so rarely found in their results, as has been reported in a large study (7).

Why are there such different patterns of enhanced eye velocity responses during head impulses not seen by all clinics? We

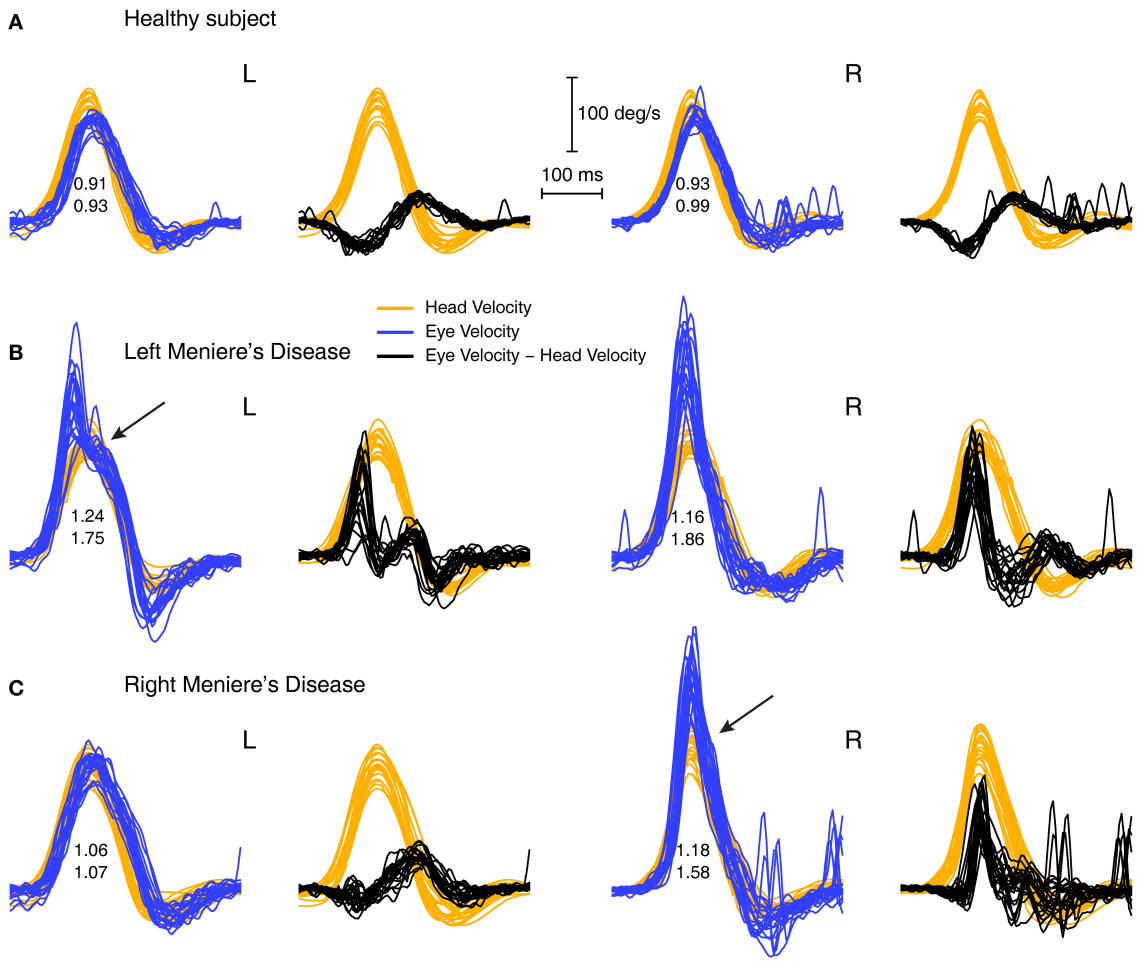

FIGURE 5 | Overlaid traces of eye velocity (blue) and head velocity (orange) and the difference between eye and head velocity (black) for head-impulse data for two patients with high VOR gain **(B,C)** and for a healthy subject **(A)**. Responses for the patients shows a pronounced peak in the difference between eye and head velocity (black traces) and we term this the "saccade-like response." In healthy subjects this difference stays close to zero or is even negative. Both sets of enhanced eye velocity for the patients show an inflection point in the eye velocity time series (shown by arrows) which would suggest the end of a saccade-like response whose point of initiation is hidden in the very rapidly increasing eye velocity during head acceleration.

consider that patient selection is an important factor. Some clinics only see patients who are well-advanced in the disease (31, 32). Other clinics test patients who are at the very earliest stage of inner ear disease (33), and it may be that the enhanced eye velocity is more salient early in the disease. Up to now VOR gains >1 tend to have been discounted as measurement error in VHIT records but see **Figure 4** of Carey et al. (6) which shows enhanced eye velocity recorded with scleral search coils so there was no goggle slippage.

Artifacts

Artifacts can occur during head impulse testing (8, 34), for example calibration errors or goggle slippage. The enhanced eye velocity we report here is not due to calibration errors or goggle slippage. There are two main reasons: the operator was very well-trained in carrying out the head impulse test and checked calibration and the tightness of the goggles whenever enhanced eye velocity occurred. Can loose straps cause a similar enhanced eye velocity? No. We have systematically loosened and tightened goggle straps without being able to duplicate the highly reliable enhanced eye velocity response pattern we have shown above.

The patient responses themselves show the enhancement is not artifactual because these responses differentially occurred in patients and not in healthy subjects. Furthermore, if it occurred in a patient it was highly likely to reappear when that patient was retested [see also Rey-Martinez et al. (4)]. Furthermore, if it were simply artifactual then it is not clear why the enhancement should systematically decrease after oral glycerol intake but not water intake.

Variability

In some patients with enhanced eye velocity there are only minimal changes in eye velocity after oral glycerol in this vestibular version of the glycerol dehydration test, just as some

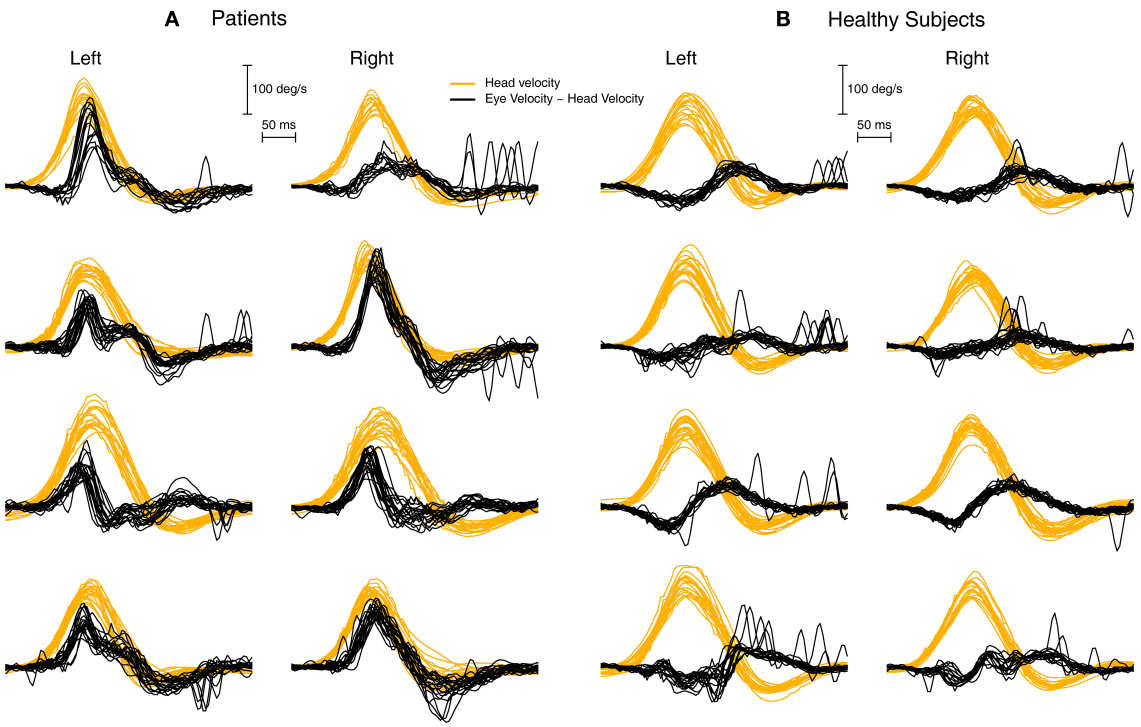

FIGURE 6 | To show the value of plotting the difference between eye velocity and head velocity for patients **(A)** and healthy subjects **(B)**. Each row shows the E-H plot for one patient and one healthy subject. The very different E-H plots between the groups is clear.

patients only show minimal changes in the auditory version of the glycerol dehydration test for ELH (35). The variability of these results is not surprising given the variability of the hydrops of the membranous labyrinth now being revealed by MRI scans (36). As is becoming clear from imaging of labyrinths with ELH, the hydrops can vary greatly in the location of greatest swelling from one individual to another—in some patients the hydrops is mainly around the utricle, in others it may be mainly around the cochlea (36).

Clearly differential enlargement of the membranous labyrinth will have very different effects on the way in which the enlarged fluid volume can affect the canal response. So we would expect that some patients with enlarged utricular volume would show large effects of glycerol on the enhanced eye velocity, whereas others with predominantly cochlear hydrops would show little effect. We do not yet have sufficiently precise estimates of the exact location of the enlarged membranous labyrinth volume to make predictions relating the hydrops to enhanced eye velocity, but this is a prediction for future research. Also, the exact effect of glycerol on the likely non-uniformly enlarged membranous labyrinth is unknown—glycerol may differentially affect different structures. The auditory glycerol dehydration test uses threshold measurement, and it has been suggested that some of the variability in that test is due to patient expectancy effects (35). Glycerol affects the objective physiological index of ELH, the ECochG, but there is still considerable variability between patients (17).

The Saccade-Like Response During Head Acceleration

In routine vHIT testing compensatory covert saccades may occur after the end of the impulse (overt saccades) or during the decreasing eye velocity of a head impulse (covert saccades).

In both cases saccades are error correcting eye movements to return the patient's gaze position to the target. Compensatory covert saccades are relatively easy to identify visually (and computationally) because the saccade direction and velocity is opposite in direction to the decreasing slow phase eye velocity in the "deceleration" phase of the head impulse, so the inflection at the start of the covert saccade is apparent (37). However, a compensatory covert saccade during the increasing eye velocity on the acceleration phase of the head impulse is difficult to detect since the saccade velocity is in the same direction as the compensatory ("slow phase") eye velocity. In that case a covert saccade is just an increment on the increasing eye velocity and so difficult to detect, although our technique of plotting the difference between eye velocity and head velocity shows this saccade-like response clearly.

The important questions are what could trigger such a consistent response pattern? These are not just anticipatory saccades since they are invariably in the correct compensatory direction, even though the direction of successive head impulses was randomized. What could trigger this response since their latency is so short? The angular jerk at the onset of the head impulse could act as a trigger. If canal receptors have enhanced

sensitivity, e.g., are jerk sensitive, they could trigger such an early rapid saccade.

In our data the patients had enhanced eye velocity during the initial part of the head impulse, and one possibility is that this is due to the fact that the transient semicircular canal receptor and afferent system (38) is sensitized. The evidence for this is shown by the comparison of initial VOR gain in normals vs. initial VOR gain in patients. So, one hypothesis is that the earliest part of the response in vHIT is due to the transient canal system—the irregular afferents synapsing on type I receptors at the crest of the crista (39–41). So, loss of these receptors—for example after systemic gentamicin which preferentially attacks type I receptors (42–44)—should lead to a poor initial response. That has been shown in patients who have received gentamicin either systemically (45) or intratympanically (6). Conversely, if those receptors were to be sensitized there should be a larger initial gain. Is there evidence for such sensitization? There is indirect evidence that these transient receptors/afferents may be sensitized in MD patients (46) who showed enhanced eye velocity response to abrupt onset galvanic stimulation (47, 48).

Another stimulus which could act as a trigger for enhanced eye velocity and the saccade-like response is tangential linear acceleration (or tangential jerk) acting on otolithic receptors.

Tangential linear acceleration during an angular rotation is defined as the product of the angular acceleration x the radius (from the axis of the rotation to the otolithic receptors), and in usual turntable testing this is insignificant because R is so small (3.76 cm) (49) and the angular acceleration is also small (perhaps 100 deg/s^2). However, with head impulse testing, the tangential linear acceleration is large because the angular acceleration is of the order of 3,000 deg/s^2. The onset of that linear acceleration or linear jerk could serve as a trigger. Tangential linear acceleration is not usually considered in animal physiological studies recording otolithic responses because the radius of animal heads is even smaller than for human heads and large angular accelerations are not usually given.

CONCLUSION

Some patients show consistent enhanced eye velocity responses on vHIT testing, and this study indicates that such enhanced eye velocity may be an indicator of endolymphatic hydrops. Oral intake of glycerol which acts to constrict the membranous labyrinth enlargement also reduces the enhanced eye velocity. The reduction of the enhanced eye velocity by glycerol serves to confirm the indication of hydrops. We have presented a measure of enhanced eye velocity—initial VOR gain–and a new technique for identifying saccade-like responses in the individual trials.

DATA AVAILABILITY STATEMENT

The raw data supporting the conclusions of this article will be made available by the authors, without undue reservation.

ETHICS STATEMENT

The studies involving human participants were reviewed and approved by MSA ENT Academy Institutional Review Board. The patients/participants provided their written informed consent to participate in this study.

AUTHOR CONTRIBUTIONS

IC conceived the study and wrote the paper. AB and IC conducted the statistical analysis. LM carried out the testing. LM, JR-M, and JD made contributions to the interpretation. All authors contributed to the manuscript and read and approved the submitted version.

FUNDING

This work was supported by a grant from the Garnett Passe and Rodney Williams Memorial Foundation (Grant L2907 RP557).

ACKNOWLEDGMENTS

Much of the work reported here has been supported by the Garnett Passe and Rodney Williams Memorial Foundation, and we are very grateful for their continued support and for the support of the National Health and Medical Research Foundation of Australia. We thank Laura Fröhlich for her helpful comments.

REFERENCES

1. Dayal VS, Mai M, Tomlinson RD. Vestibulo-ocular (VOR) abnormalities at high rotational frequencies in patients with Meniere's disease. *Otolaryngol Head Neck Surg*. (1988) 98:211–4. doi: 10.1177/019459988809800306
2. Funabiki K, Naito Y, Honjo I. Vestibulo-ocular reflex in patients with Meniere's disease between attacks. *Acta Otolaryngologica*. (1999) 119:886–91. doi: 10.1080/00016489950180225
3. Maire R, Van Melle G. Vestibulo-ocular reflex characteristics in patients with unilateral Meniere's disease. *Otol Neurotol*. (2008) 29:693–8. doi: 10.1097/MAO.0b013e3181776703
4. Rey-Martinez J, Burgess AM, Curthoys IS. Enhanced vestibulo-ocular reflex responses on vHIT. Is it a casual finding or a sign of vestibular dysfunction? *Front Neurol*. (2018) 9:866. doi: 10.3389/fneur.2018.00866
5. Rey-Martinez J, Altuna X, Cheng K, Burgess AM, Curthoys IS. Computing endolymph hydrodynamics during head impulse test on normal and hydropic vestibular labyrinth models. *Front Neurol*. (2020) 11:289. doi: 10.3389/fneur.2020.00289
6. Carey JP, Minor LB, Peng GC, Della Santina CC, Cremer PD, Haslwanter T. Changes in the three-dimensional angular vestibulo-ocular reflex following intratympanic gentamicin for Meniere's disease. *J Assoc Res Otolaryngol*. (2002) 3:430–43. doi: 10.1007/s101620010053
7. Vargas A, Ninchritz E, Golburu M, Betances F, Rey-Martinez J, Altuna X. Clinical prevalence of enhanced vestibulo-ocular reflex responses on video head impulse test. *Otol Neurotol*. (2021) 42. doi: 10.1097/MAO.0000000000003171
8. Mantokoudis G, Saber Tehrani AS, Kattah JC, Eibenberger K, Guede CI, Zee DS, et al. Quantifying the vestibulo-ocular reflex with video-oculography:

nature and frequency of artifacts. *Audiol Neurootol*. (2014) 20:39–50. doi: 10.1159/000362780
9. Zamaro E, Tehrani ASS, Kattah JC, Eibenberger K, Guede CI, Armando L, et al. VOR gain calculation methods in video head impulse recordings. *J Vestib Res*. (2020) 30:225–34. doi: 10.3233/VES-200708
10. Castro P, Esteves SS, Lerchundi F, Buckwell D, Gresty MA, Bronstein AM, et al. Viewing target distance influences the vestibulo-ocular reflex gain when assessed using the video head impulse test. *Audiol Neurootol*. (2018) 23:285–9. doi: 10.1159/000493845
11. Viirre E, Tweed D, Milner K, Vilis T. A reexamination of the gain of the vestibuloocular reflex. *J Neurophysiol*. (1986) 56:439–50. doi: 10.1152/jn.1986.56.2.439
12. Grieser B, McGarvie L, Kleiser L, Manzari L, Obrist D, Curthoys I. Numerical investigations of the effects of endolymphatic hydrops on the VOR response. *J Vestib Res*. (2014) 24:219.
13. Jansson B, Friberg U, Raskandersen H. Effects of glycerol on the endolymphatic sac - a time sequence study. *Orl-J Otorhinolaryngol Relat Spec*. (1992) 54:201–10. doi: 10.1159/000276299
14. Magliulo G, Ungari C, Dellarocca C, Muscatello M, Vingolo GM. The effect of glycerol on the guinea-pig hydropic ear. *Clin Otolaryngol*. (1991) 16:483–7. doi: 10.1111/j.1365-2273.1991.tb01045.x
15. Klockhoff I, Lindblom U. Endolymphatic hydrops revealed by glycerol test. Preliminary report. *Acta Otolaryngol*. (1966) 61:459–62. doi: 10.3109/00016486609127084
16. Klockhoff I, Lindblom U. Glycerol test in Meniere's disease. *Acta Otolaryngol*. (1966) 224:449–51. doi: 10.3109/00016486709123623
17. Moffat DA, Gibson WPR, Ramsden RT, Morrison AW, Booth JB. Transtympanic electrocochleography during glycerol dehydration. *Acta Otolaryngol*. (1978) 85:158–66. doi: 10.3109/00016487809121437
18. Ban JH, Lee JK, Jin SM, Lee KC. Glycerol pure tone audiometry and glycerol vestibular evoked myogenic potential: Representing specific status of endolymphatic hydrops in the inner ear. *Eur Arch Otorhinolaryngol*. (2007) 264:1275–81. doi: 10.1007/s00405-007-0370-5
19. Murofushi T, Matsuzaki M, Takegoshi H. Glycerol affects vestibular evoked myogenic potentials in Meniere's disease. *Auris Nasus Larynx*. (2001) 28:205–8. doi: 10.1016/S0385-8146(01)00058-X
20. Seo YJ, Kim J, Choi JY, Lee WS. Visualization of endolymphatic hydrops and correlation with audio-vestibular functional testing in patients with definite Meniere's disease. *Auris Nasus Larynx*. (2013) 40:167–72. doi: 10.1016/j.anl.2012.07.009
21. Magliulo G, Parrotto D, Gagliardi S, Cuiuli G, Novello C. Vestibular evoked periocular potentials in Meniere's disease after glycerol testing. *Ann Otol Rhinol Laryngol*. (2008) 117:800–4. doi: 10.1177/000348940811701102
22. Shojaku H, Takemori S, Kobayashi K, Watanabe Y. Clinical usefulness of glycerol vestibular-evoked myogenic potentials: preliminary report. *Acta Otolaryngol Suppl*. (2001) 545:65–8. doi: 10.1080/0001648017503 88144
23. Lopez-Escamez JA, Carey J, Chung WH, Goebel JA, Magnusson M, Mandala M, et al. Diagnostic criteria for Meniere's disease. *J Vestib Res*. (2015) 25:1–7. doi: 10.3233/VES-150549
24. Lempert T, Olesen J, Furman J, Waterston J, Seemungal B, Carey J, et al. Vestibular migraine: Diagnostic criteria. *J Vestib Res*. (2012) 22:167–72. doi: 10.3233/VES-2012-0453
25. Zar JH. *Biostatistical Analysis*. 5 ed. New Jersey: Prentice-Hall (2010).
26. MacDougall HG, Weber KP, McGarvie LA, Halmagyi GM, Curthoys IS. The video head impulse test: diagnostic accuracy in peripheral vestibulopathy. *Neurology*. (2009) 73:1134–41. doi: 10.1212/WNL.0b013e3181 bacf85
27. MacDougall HG, McGarvie LA, Halmagyi GM, Curthoys IS, Weber KP. The video Head Impulse Test (vHIT) detects vertical semicircular canal dysfunction. *PLoS ONE*. (2013) 8:e61488. doi: 10.1371/journal.pone.0061488
28. Field A. *Discovering Statistics Using IBM SPSS Statistics*. 4th ed. London: Sage (2013).
29. van der Lubbe M, Vaidyanathan A, Van Rompaey V, Postma AA, Bruintjes TD, Kimenai DM, et al. The "hype" of hydrops in classifying vestibular disorders: a narrative review. *J Neurol*. (2020) 267:197–211. doi: 10.1007/s00415-020-10278-8
30. Gurkov R, Kantner C, Strupp M, Flatz W, Krause E, Ertl-Wagner B. Endolymphatic hydrops in patients with vestibular migraine and auditory symptoms. *Eur Arch Otorhinolaryngol*. (2014) 271:2661–7. doi: 10.1007/s00405-013-2751-2
31. Yacovino DA, Finlay JB. Intra-attack vestibuloocular reflex changes in Meniere's disease. *Case Rep Otolaryngol*. (2016) 2016:2427983. doi: 10.1155/2016/2427983
32. Yacovino DA, Schubert MC, Zanotti E. Evidence of large vestibulo-ocular reflex reduction in patients with meniere attacks. *Otol Neurotol*. (2020) 41:E1133–9. doi: 10.1097/MAO.0000000000002746
33. Manzari L, Burgess AM, MacDougall HG, Bradshaw AP, Curthoys IS. Rapid fluctuations in dynamic semicircular canal function in early Meniere's disease. *Eur Arch Otorhinolaryngol*. (2011) 268:637–9. doi: 10.1007/s00405-010-1442-5
34. Mantokoudis G, Saber Tehrani AS, Wozniak A, Eibenberger K, Kattah JC, Guede CI, et al. Impact of artifacts on VOR gain measures by video-oculography in the acute vestibular syndrome. *J Vestib Res*. (2016) 26:375–85. doi: 10.3233/VES-160587
35. Arts HA, Kileny PR, Telian SA. Diagnostic testing for endolymphatic hydrops. *Otolaryngol Clin North Am*. (1997) 30:987–1005. doi: 10.1016/S0030-6665(20)30142-0
36. Gurkov R, Flatz W, Ertl-Wagner B, Krause E. Endolymphatic hydrops in the horizontal semicircular canal: a morphologic correlate for canal paresis in Meniere's disease. *Laryngoscope*. (2013) 123:503–6. doi: 10.1002/lary.23395
37. Weber KP, Aw ST, Todd MJ, McGarvie LA, Curthoys IS, Halmagyi GM. Head impulse test in unilateral vestibular loss: vestibulo-ocular reflex and catch-up saccades. *Neurology*. (2008) 70:454–63. doi: 10.1212/01.wnl.0000299117.48935.2e
38. Curthoys IS, MacDougall HG, Vidal PP, de Waele C. Sustained and transient vestibular systems: A physiological basis for interpreting vestibular function. *Front Neurol*. (2017) 8:117. doi: 10.3389/fneur.2017.00117
39. Lysakowski A, Goldberg JM. A regional ultrastructural analysis of the cellular and synaptic architecture in the chinchilla cristae ampullares. *J Comp Neurol*. (1997) 389:419–43. doi: 10.1002/(sici)1096-9861(19971222)389:3<419::aid-cne5>3.0.co;2-3
40. Lysakowski A, Goldberg JM. Ultrastructural analysis of the cristae ampullares in the squirrel monkey (Saimiri sciureus). *J Comp Neurol*. (2008) 511:47–64. doi: 10.1002/cne.21827
41. Lysakowski A, Minor LB, Fernandez C, Goldberg JM. Physiological identification of morphologically distinct afferent classes innervating the cristae ampullares of the squirrel monkey. *J Neurophysiol*. (1995) 73:1270–81. doi: 10.1152/jn.1995.73.3.1270
42. Lue JH, Day AS, Cheng PW, Young YH. Vestibular evoked myogenic potentials are heavily dependent on type I hair cell activity of the saccular macula in guinea pigs. *Audiol Neurootol*. (2009) 14:59–66. doi: 10.1159/000156701
43. Lyford-Pike S, Vogelheim C, Chu E, Della Santina CC, Carey JP. Gentamicin is primarily localized in vestibular type I hair cells after intratympanic administration. *J Assoc Res Otolaryngol*. (2007) 8:497–508. doi: 10.1007/s10162-007-0093-8
44. Hirvonen TP, Minor LB, Hullar TE, Carey JP. Effects of intratympanic gentamicin on vestibular afferents and hair cells in the chinchilla. *J Neurophysiol*. (2005) 93:643–55. doi: 10.1152/jn.001 60.2004
45. Weber KP, Aw ST, Todd MJ, McGarvie LA, Curthoys IS, Halmagyi GM. Horizontal head impulse test detects gentamicin vestibulotoxicity. *Neurology*. (2009) 72:1417–24. doi: 10.1212/WNL.0b013e3181a 18652
46. Aw ST, Aw GE, Todd MJ, Halmagyi GM. Enhanced vestibulo-ocular reflex to electrical vestibular stimulation in meniere's disease. *J Assoc Res Otolaryngol*. (2013) 14:49–59. doi: 10.1007/s10162-012-0362-z
47. Aw ST, Todd MJ, Aw GE, Weber KP, Halmagyi GM. Gentamicin vestibulotoxicity impairs human electrically evoked vestibulo-ocular reflex. *Neurology*. (2008) 71:1776–82. doi: 10.1212/01.wnl.0000335971.43443.d9
48. Aw ST, Todd MJ, Lehnen N, Aw GE, Weber KP, Eggert T, et al. Electrical vestibular stimulation after vestibular deafferentation and in vestibular schwannoma. *PLoS ONE*. (2013) 8:e82078. doi: 10.1371/journal.pone.0082078

49. Curthoys IS, Blanks RH, Markham CH. Semicircular canal functional anatomy in cat, guinea pig and man. *Acta Otolaryngol*. (1977) 83:258–65. doi: 10.3109/00016487709128843

Conflict of Interest: The authors declare that the research was conducted in the absence of any commercial or financial relationships that could be construed as a potential conflict of interest.

frontiers in Surgery

ORIGINAL RESEARCH
published: 31 May 2021
doi: 10.3389/fsurg.2021.662530

A Synchrotron and Micro-CT Study of the Human Endolymphatic Duct System: Is Meniere's Disease Caused by an Acute Endolymph Backflow?

Hao Li[1], *Gunesh P. Rajan*[2,3], *Jeremy Shaw*[4], *Seyed Alireza Rohani*[5], *Hanif M. Ladak*[6], *Sumit Agrawal*[5] *and Helge Rask-Andersen*[1]*

[1] Department of Surgical Sciences, Section of Otolaryngology and Head and Neck Surgery, Uppsala University Hospital, Uppsala, Sweden, [2] Department of Otolaryngology, Head and Neck Surgery, Luzerner Kantonsspital, Lucerne, Switzerland, [3] Department of Otolaryngology, Head and Neck Surgery Division of Surgery, Medical School, University of Western Australia, Perth, WA, Australia, [4] Centre for Microscopy, Characterisation and Analysis, Perth, WA, Australia, [5] Department of Otolaryngology-Head and Neck Surgery, Western University, London, ON, Canada, [6] Department of Medical Biophysics and Department of Electrical and Computer Engineering, Western University, London, ON, Canada

OPEN ACCESS

Edited by:
Robert Gürkov,
Bielefeld University, Germany

Reviewed by:
Daniel John Brown,
Curtin University, Australia
Alec Nicholas Salt,
Washington University in St. Louis, United States

***Correspondence:**
Helge Rask-Andersen
helge.rask-andersen@surgsci.uu.se
orcid.org/0000-0002-2552-5001

Specialty section:
This article was submitted to Otorhinolaryngology - Head and Neck Surgery, a section of the journal Frontiers in Surgery

Received: 01 February 2021
Accepted: 19 April 2021
Published: 31 May 2021

Citation:
Li H, Rajan GP, Shaw J, Rohani SA, Ladak HM, Agrawal S and Rask-Andersen H (2021) A Synchrotron and Micro-CT Study of the Human Endolymphatic Duct System: Is Meniere's Disease Caused by an Acute Endolymph Backflow? Front. Surg. 8:662530. doi: 10.3389/fsurg.2021.662530

Background: The etiology of Meniere's disease (MD) and endolymphatic hydrops believed to underlie its symptoms remain unknown. One reason may be the exceptional complexity of the human inner ear, its vulnerability, and surrounding hard bone. The vestibular organ contains an endolymphatic duct system (EDS) bridging the different fluid reservoirs. It may be essential for monitoring hydraulic equilibrium, and a dysregulation may result in distension of the fluid spaces or endolymphatic hydrops.

Material and Methods: We studied the EDS using high-resolution synchrotron phase contrast non-invasive imaging (SR-PCI), and micro-computed tomography (micro-CT). Ten fresh human temporal bones underwent SR-PCI. One bone underwent micro-CT after fixation and staining with Lugol's iodine solution (I_2KI) to increase tissue resolution. Data were processed using volume-rendering software to create 3D reconstructions allowing orthogonal sectioning, cropping, and tissue segmentation.

Results: Combined imaging techniques with segmentation and tissue modeling demonstrated the 3D anatomy of the human saccule, utricle, endolymphatic duct, and sac together with connecting pathways. The utricular duct (UD) and utriculo-endolymphatic valve (UEV or Bast's valve) were demonstrated three-dimensionally for the first time. The reunion duct was displayed with micro-CT. It may serve as a safety valve to maintain cochlear endolymph homeostasis under certain conditions.

Discussion: The thin reunion duct seems to play a minor role in the exchange of endolymph between the cochlea and vestibule under normal conditions. The saccule wall appears highly flexible, which may explain occult hydrops occasionally preceding symptoms in MD on magnetic resonance imaging (MRI). The design of the UEV and connecting ducts suggests that there is a reciprocal exchange of fluid among the utricle, semicircular canals, and the EDS. Based on the anatomic framework and previous

experimental data, we speculate that precipitous vestibular symptoms in MD arise from a sudden increase in endolymph pressure caused by an uncontrolled endolymphatic sac secretion. A rapid rise in UD pressure, mediated along the fairly wide UEV, may underlie the acute vertigo attack, refuting the rupture/K^+-intoxication theory.

Keywords: human, synchrotron radiation phase-contrast imaging, reunion duct, Bast's valve, Meniere's disease

INTRODUCTION

The etiology of Meniere's disease (MD) remains indefinite and continues to foil the afflicted and the medical profession. One reason may be the exceptional complexity of the human labyrinth, its fragile fluid system surrounded by rock-hard bone. There is also a general lack of knowledge about how organs regulate hydrostatic pressure, volume and ion homeostasis (1). The vestibular organ contains separate compartments filled with endolymph fluid. The utricle, semicircular canals, endolymphatic duct (ED), and endolymphatic sac (ES) form a phylogenetically older "pars superior," while the cochlea and saccule form the "pars inferior" (2). They are interconnected by narrow channels forming an endolymphatic duct system (EDS). The cochlea is linked to the vestibular system via the reunion duct (RD) (3, 4), the saccule to the ED via the saccular duct (SD), and the utricle to the ED via the utricular duct (UD). Consequently, the EDS may allow the exchange of fluid and solutes among the compartments and mediate pressure, thereby regulating fluid homeostasis around the sensory receptors to optimize function.

It is still uncertain if endolymph "circulates" among the partitions, and where it is produced and absorbed, which was initially thought to be confined to each partition. Seymour (2) believed that endolymph was formed in the ES and flowed through the ED to the rest of the labyrinth to insure complete filling of the phylogenetically older utricle and semicircular canals. Yet, experimental investigations suggested a reversed situation, namely, that the lateral cochlear wall secretes endolymph, and a "longitudinal flow" of endolymph exists from the cochlea to the saccule and from there to the ED and ES for reabsorption (5–8). Tracer studies rarely identified a flow toward the utricle (5), supporting Kimura's (9) findings that endolymph is secreted locally in the vestibular labyrinth (9). Endolymph may escape the utricle through the utriculo-endolymphatic valve (UEV) into the UD, ED, and ES (5). A longitudinal flow was later questioned under normal conditions (10, 11), and it was found that endolymph may instead be produced locally and absorbed in the cochlea and utricle (12). Recent molecular analyses show that the ES is essential for the normal development of endolymph volume and absorption, where pendrin, an anion exchange protein encoded by the *SLC26A4* gene, plays an important role during a critical period (13, 14).

The EDS can potentially be disrupted, leading to endolymphatic hydrops (EH), which is believed to underlie the symptoms in MD. Blockage of the RD has been described as a causative factor (15, 16) by some but denied by others (17). Experimental obstruction of the RD results in cochlear hydrops and collapse of the saccule, suggesting that both regions depend on a patent RD (8). Tracer studies indicated that endolymph may circulate from the cochlea through the RD to the ED and ES (5, 18). Collapse of the saccule and maintained utricle filling after RD blockage suggests a lack of endolymph production in the saccule consistent with the absence of an epithelial "dark cell" region or epithelia believed to secrete endolymph (19). Furthermore, experimental blockage of the ES results in EH in guinea pigs, and bony obstruction of the vestibular aqueduct (VA) has been associated with Meniere's disease (7, 17, 20). This suggests that the ES plays an important role in endolymph circulation and reabsorption.

Our knowledge of the anatomy of the human vestibular organ and EDS rests primarily on two-dimensional (2D) histologic sectioning. Reproduction of the three-dimensional (3D) anatomy may enhance our understanding of its function and clarify the pathophysiology of EH and MD. We used high-resolution synchrotron phase contrast imaging (SR-PCI) and micro-computed tomography (micro-CT) to investigate EDS in human temporal bone cadavers. Data were processed using volume-rendering software to create 3D reconstructions allowing orthogonal sectioning, cropping, and tissue segmentation. It revealed for the first time the 3D anatomy of the human UEV and its suspension to the VA. These results may shed new light on the role of the EDS in the etiology and pathophysiology of EH and MD.

Abbreviations: AAO-HNS, American Association for Head- and Neck Surgery; BM, Basilar membrane; BMIT, Bio-Medical Imaging and Therapy; CLSI, Canadian Light Source, Inc.; CC, Common crus; CT, Computerized tomography; DiceCT, Diffusible iodine-based contrast-enhanced computed tomography; ED, Endolymphatic duct; EDS, Endolymphatic duct system; EH, Endolymphatic hydrops; ES, Endolymphatic sac; LSSC, Lateral semicircular canal; MD, Meniere's disease; Micro-CT, Micro-computerized tomography; MRI, Magnetic Resonance Imaging; PSSC, Posterior semicircular canal; RD, Reunion duct; SD, Saccular duct; SR-PCI, Synchrotron-phase contrast imaging; UD, Utricular duct; UEV, Utriculo-endolymphatic valve (or Bast's valve); VA, Vestibular aqueduct.

MATERIALS AND METHODS

Ethical Statements

Human Temporal Bones

Ten fixed adult human cadaveric cochleae were used in this study. Specimens were obtained with permission from the body bequeathal program at Western University, London, Ontario, Canada in accordance with the Anatomy Act of Ontario and Western's Committee for Cadaveric Use in Research (approval No. 06092020). No staining, sectioning, or decalcification was performed on the specimens. Ethics approval for the micro-CT project was obtained from the University of Western Australia

(UWA, RA/4/1/5210), and the human temporal bones were provided by the Department of Anatomy at UWA.

SR-PCI and Imaging Technique

The SR-PCI technique used in the present investigation was recently described by Elfarnawany et al. (21) and Koch et al. (22). Each sample was scanned using SR-PCI combined with computed tomography (CT) at the Bio-Medical Imaging and Therapy (BMIT) 05ID-2 beamline at the Canadian Light Source, Inc. (CLSI) in Saskatoon, Canada. The imaging field of view was set to 4,000 × 950 pixels corresponding to 36.0 × 8.6 mm, and 3,000 projections over a 180° rotation were acquired per CT scan. CT reconstruction was performed, and the 3D image volume had an isotropic voxel size of 9 μm. The acquisition time to capture all projections per view was ∼30 min. For 3D reconstructions of the cochlear anatomy, structures were traced and color-labeled manually on each SR-PCI CT slice (∼1,400 slices per sample). The open source medical imaging software, 3D Slicer version 4.10 (www.slicer.org) (23), was used to create detailed 3D representations of the basilar membrane (BM), spiral ganglion and connective dendrites between these structures, which allowed for accurate delineation when compared to traditional 2D slices.

Micro-CT

Micro-CT was used to analyze the 3D anatomy of the nerves in the internal acoustic meatus. We used a diffusible iodine-based technique to enhance contrast of soft tissues for diffusible iodine-based contrast-enhanced computed tomography (diceCT). Increased time penetration of Lugol's iodine (aqueous I2KI, 1% I_2, 2% KI) provided possibilities to visualize between and within soft tissue structures (24). The temporal bone was fixed in a modified Karnovsky's fixative solution of 2.5% glutaraldehyde, 1% paraformaldehyde, 4% sucrose, and 1% dimethyl sulfoxide in 0.13 M of Sorensen's phosphate buffer. Soft tissue contrast was achieved by staining the sample for 14 days, as described by Culling et al. (25). The X-ray micro-CT was conducted using Versa 520 XRM (Zeiss, Pleasanton, CA, USA) running Scout and Scan software (v11.1.5707.17179). Scans were conducted at a voltage of 80 kV and 87 μA, using the LE4 filter under 0.4x optical magnification and a camera binning of 2. Source and detector positions were adjusted to deliver an isotropic

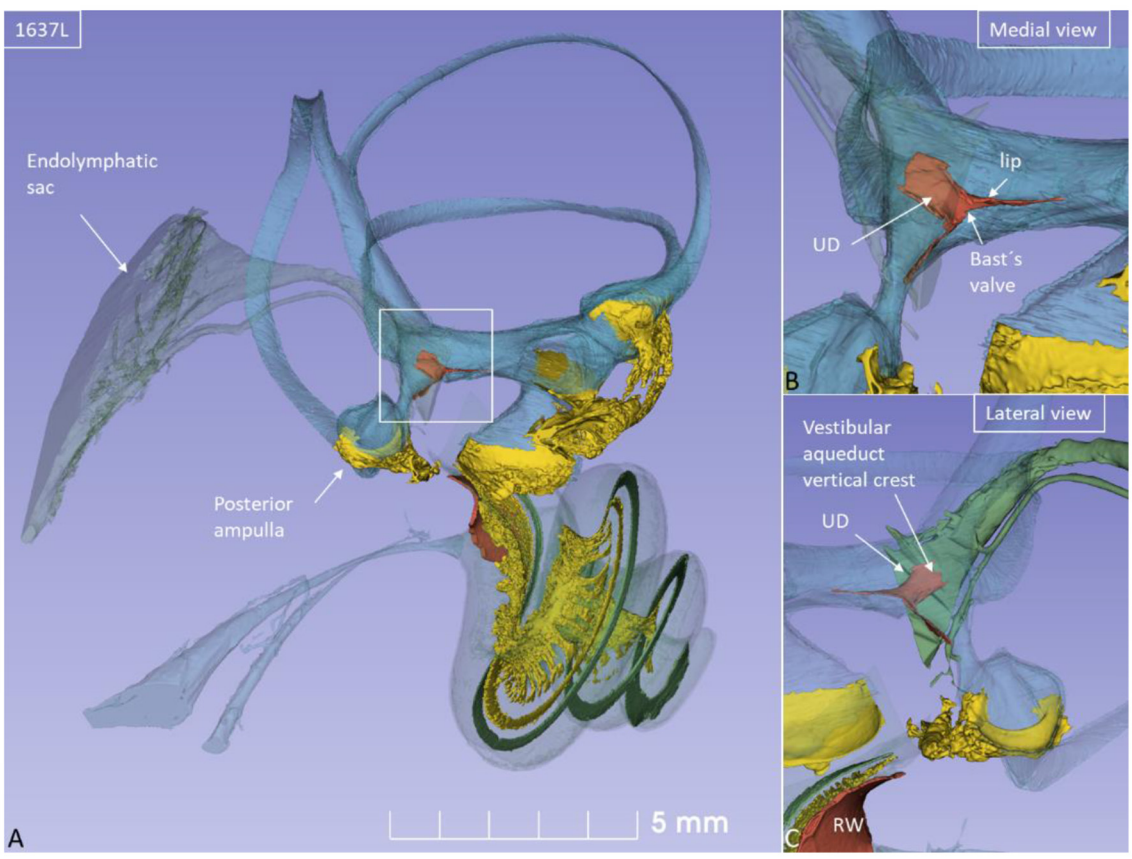

FIGURE 1 | (A) SR-PCI of a left human ear with modeling of anatomical details. Maculae and nerve structures are stained yellow. The position of the saccule and utricle and their relationship to the vestibular aqueduct (blue) are shown. **(B)** Medial view shows the position of the UEV relative to the internal aperture of the vestibular aqueduct. **(C)** Posterolateral view.

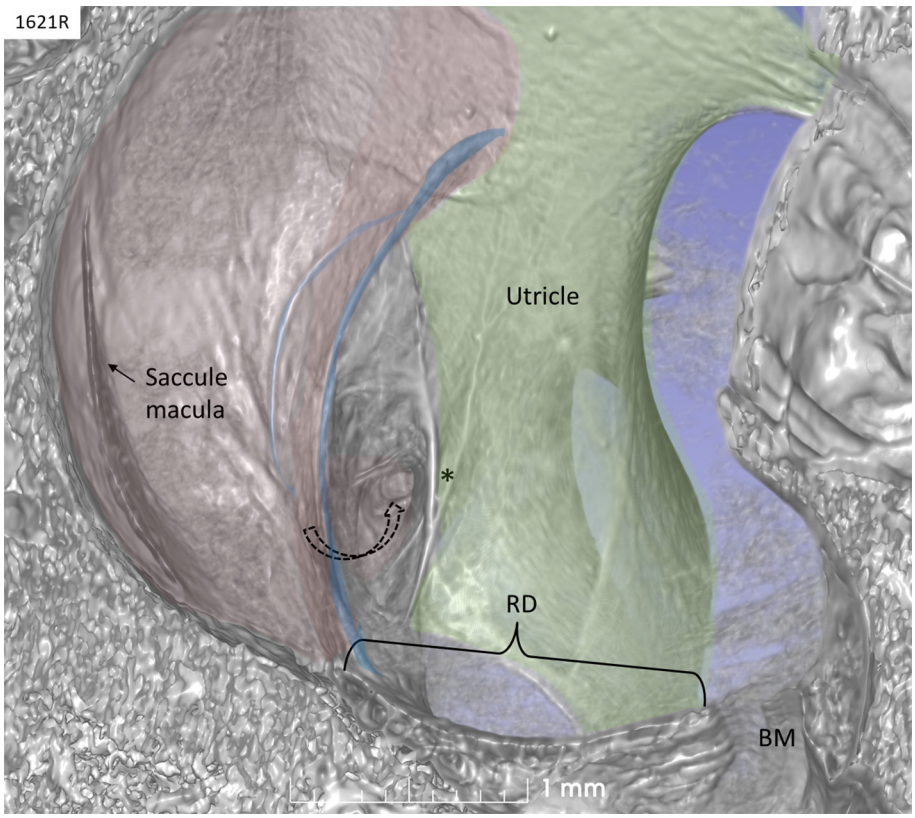

FIGURE 2 | SR-PCI of a left human ear with 3D reconstructions of saccule (red) and utricle (green) (lateral view). The entrance gate to the internal opening of the VA (broken arrow) and the UEV (*) can be seen. The saccule wall contains a reinforced semilunar portion that additionally thickens (blue) against the thinner part. The thinner part and the saccular duct are difficult to discern. BM, basilar membrane. RD, reunion duct.

voxel size of 23 μm. A total of 2,501 projections were collected over 360°, each with an exposure time of 1 s. Raw projection data were reconstructed using XM Reconstructor software (v10.7.3679.13921; Zeiss) following a standard center shift and beam hardening (0.1) correction. The standard 0.7 kernel size recon filter setting was also used. Images were imported into the 3D Slicer program (Slicer 4.6; www.slicer.org), an open-source software platform for medical image informatics, image processing, and 3D visualization. Images were resized at a scale of 4:1, and opacity and gray scale values were adjusted during volume rendering. The technique allowed reconstruction in three dimensions, and bones were made transparent and cropped.

RESULTS

Non-invasive, high-resolution SR-PCI and micro-CT reproduced both soft and bony tissues of the human cochlea and vestibular organ. Imaging and computer processing provided unique insights into the 3D anatomy of the human vestibular organ with the utricle, saccule, maculae, semicircular canals, and ES (**Figure 1**). Slicer 3D segmentations and modeling even demonstrated the orientations of the interconnecting ducts of the EDS. Positive and negative contrast enhancement improved micro-CT visualization of soft tissues, while 3D SR-PCI reproduced anatomical details without additional contrast.

The saccule was bowl-shaped and reached superiorly to the floor of the utricle to which it partially adhered. The saccule macula was placed in a pit in the medial bony wall margined posteriorly by a lip of the spherical recess. The saccular wall was thicker near the macula and had a thinner triangular-shaped part facing the middle ear (**Figures 2**, **3**).

The thicker part contained a fibrous stratum between the mesothelial and epithelial layers. It also thickened into marginal bands where the thick portion transitioned into the thinner portion. These bands reinforced the junction between the saccule and utricle. The saccule narrowed basally into a flat funnel-shaped opening to the RD. The SD exited posteriorly at the spherical recess and ran along the bony wall to the ED and the VA. Its direction was perpendicular to the RD. The thin-walled SD was sometimes difficult to visualize in 3D, but could occasionally be segmented from individual sections. The utricle lay horizontal with the macula slanting from vertical to horizontal at the nerve entry.

The rather wide UD separated from the ED soon after its entry into the labyrinth and reached the inferior part of the posteromedial wall of the utricle (**Figure 4**). The UD and UEV are viewed in **Figures 5**–**9**.

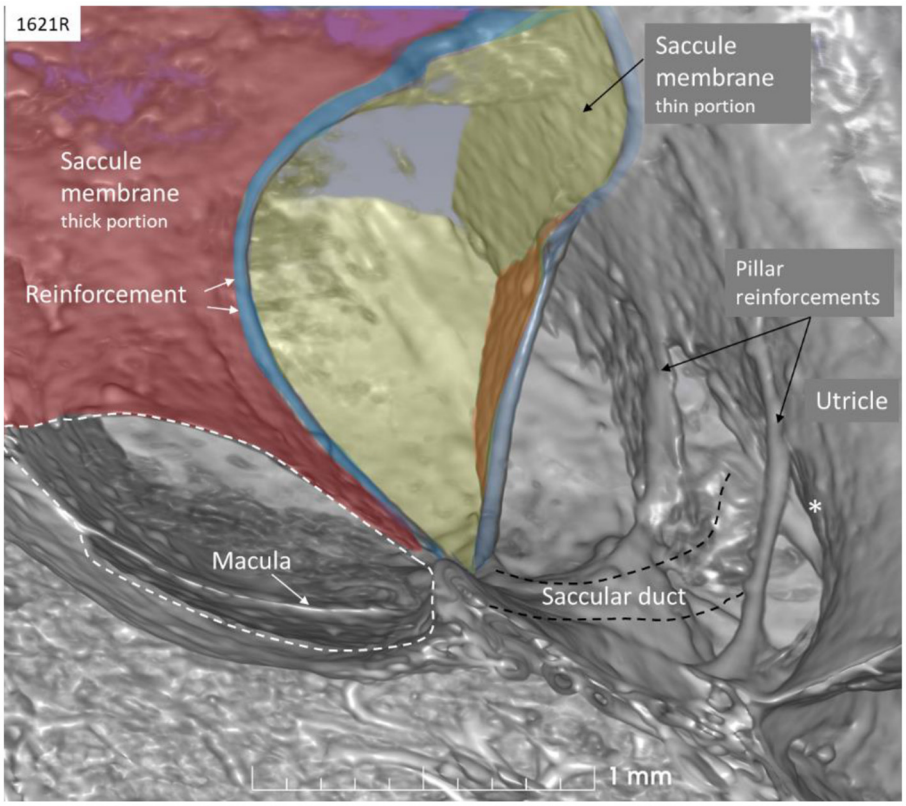

FIGURE 3 | SR-PCI of the saccule (left ear, lateral view). The wall consists of a thick (red) and thin (yellow) part separated by bands of reinforcement (blue). The thin wall appears flaccid. The SD exits near the band and runs against the ED and the UEV (*). The utricle wall is supported by several pillars attached to the internal surface of the surrounding bony wall.

The UD lumen changed from round to ovoid and slit-like (**Figures 5**, **6**). The round portion had a diameter of 0.26 × 0.24 mm in specimen 1637L, where it was best viewed. It flattened and narrowed against the UEV. The division between the UD and ED was located 0.2–0.4 mm from the internal aperture of the VA. The UEV was identified at ∼0.7 mm from the vertical crest of the VA (**Figure 4**). This distance varied, and in one specimen, the distance was 1.6 mm (2R). The valve was crescent-shaped with a superior, thicker lip attached to the inner utricle wall (**Figures 8**, **9**). The lip was suspended by a thickened reinforcement in the utricle wall (**Figures 1**, **4**, **5**, **9**). This support extended as a ligament-like suspension to the medial bony wall together with fibrous pillars. A suspensory disc stretched from the vertical crest of the VA to the lip of the valve. It was also associated with the lateral wall of the UD (**Figures 5C**, **9C**). Additional fibrous pillars connected the utricle wall with the surface of the bony wall. The mean width of the UEV was 0.69 mm (0.68, 0.65, and 0.74 mm in three measurable specimens). Several blood vessels followed the medial wall of the intra-labyrinthine ED against the VA (**Figure 6C**).

The RD was narrow and generally difficult to follow. The RD exited the caudal region of the saccule. It was best viewed with micro-CT and ran from the basal funnel of the saccule against the cochlea along the bony wall. Its smallest diameter was < 0.1 mm (**Figures 10**–**12**). It was positioned on a shallow increase of connective tissue on the spiral lamina wall and was best visualized with micro-CT since air had entered the vestibule, thus enhancing contrast. A vestibular overview show an hourglass-shaped fold (**Figure 12G**). **Figures 12A–F** shows serial micro-CT sections of the RD from the saccule to the scala media. At some points, the RD seemed collapsed. In **Figures 12G,H**, the cross-sectional diameter ranged from 0.037 to 0.074 mm. The distance between the saccule and cochlea was around 1 mm. The relation between the RD and SD is shown with micro-CT in **Figures 13A,B**. The RD runs almost perpendicular against the saccular duct. **Figure 13C** shows a horizontal section and the UEV. The saccule and cochlear endolymphatic space at the cecum vestibulare are shown in **Figure 13D**.

DISCUSSION

Saccule

The saccule resembled a vertically placed coffee bean with the convex side lying against the spherical recess and the contralateral side facing the vestibule. The superior wall was flattened, lay against the floor of the utricle, and formed an imprint. This suggests that expansion of the saccule may compress the utricle near its macula and vice versa. Basally, the inferior margin of the macula faced the entrance of the RD, where the distance between the otolith membrane and RD was in the region of 0.2–0.3 mm.

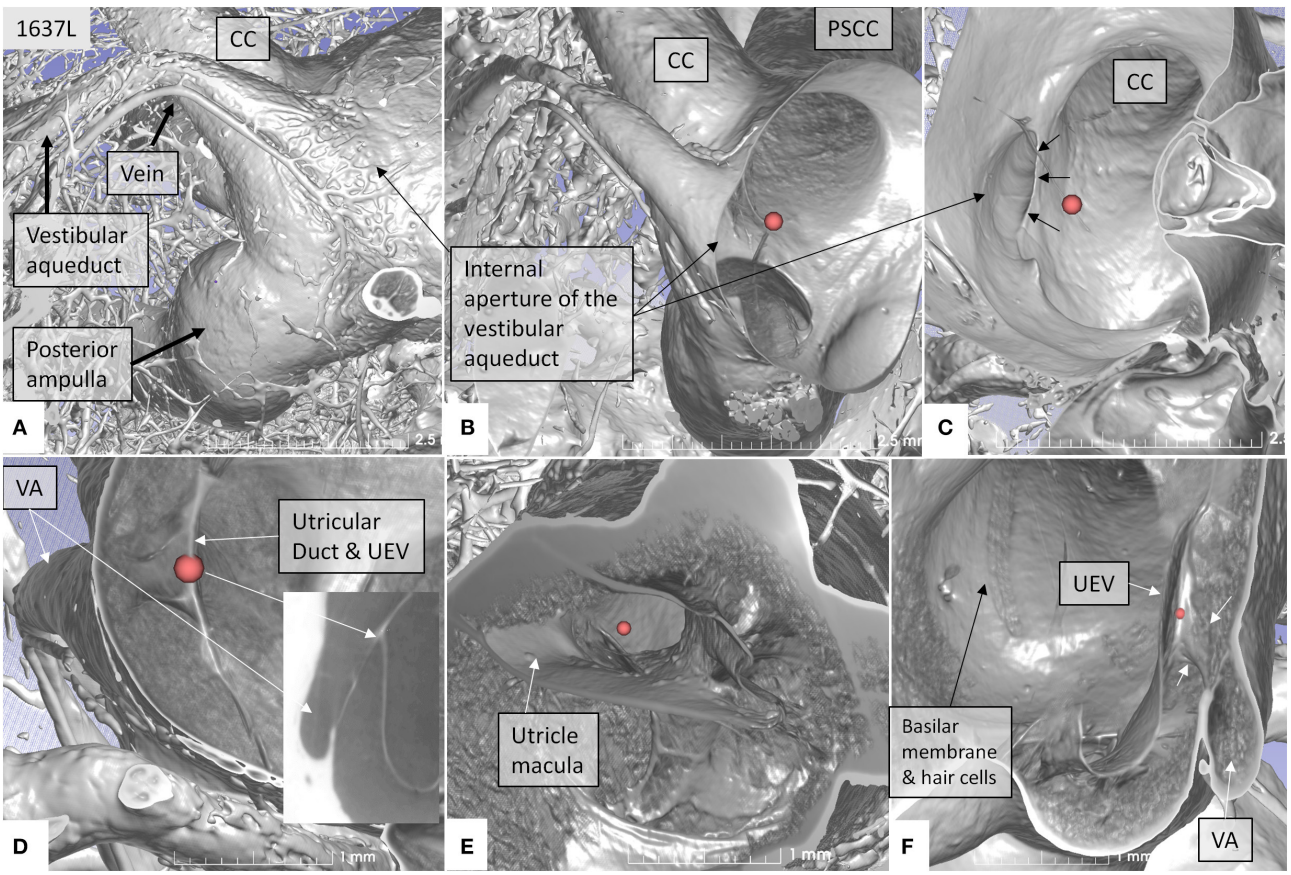

FIGURE 4 | SR-PCI showing the position of the UEV relative to the internal opening of the VA in a left bone. **(A)** Medial view shows the entrance of the VA into the vestibule. A vascular plexus surrounds the VA that drains into the vein of the VA. **(B)** Anterior cropping shows the VA and the position of the UEV (red fiducial). **(C)** Bony algorithm shows the internal opening of the VA relative to the UEV (red fiducial). **(D)** Adjusting opacity gradient reveals both the UEV and the UD (red fiducial). **(E)** Lateral view shows the position of the utricle macula and the UEV (red fiducial). **(F)** Superior view and modification of gradient opacity shows the UD (white arrows) and the UEV (red fiducial). The BM and the rows of hair cells are seen. CC, common crus; UEV, utriculo-endolymphatic valve; VA, vestibular aqueduct; PSSC, posterior semicircular canal; UD, utricular duct; BM, basilar membrane.

Here, dislodged otoconia could easily reach the RD by gravity. The saccule wall consisted of a thick and thin region where the thick part lay near the spherical recess. In lower mammals, amphibians, and fish, the saccule contains only the thin part, portentous that the macula may respond to both acoustic and static pressure (26). The orientation of the human saccular macula, the spherical recess and the re-enforced membranes were thought to shield the macula from acoustic oscillations such as stapedius-induced vibrations at large sound levels, in contrast to lower forms. The thin wall appears more flaccid and is probably more prone to dilate and collapse in MD. Ruptures may occur at the junction between the regions by increased pressure due to the resilience. The thin wall of the SD was difficult to image in 3D as it emerged near the band-like reinforcement ∼0.9 mm from the utricle floor.

Utricle and UEV

The utricle is a horizontal cylinder with several extremities. In this study, for the first time, the UEV was viewed three-dimensionally and it appeared as a fantail with a slit-like opening. Its semi-lunar shape differed somewhat from the descriptions by Bast (27) and Anson and Wilson (28). It was located near the floor of the posteromedial wall of the utricle at the internal opening of the VA, as described in humans by Bast (27, 29) and in other mammals by Hoffman and Bast (30). Wilson and Anson (31) described the valve in a 2-year-old child, and they defined it in an adult and named it the "utricular fold." We used the nomenclature of Perlman and Lindsay (32) for the UD, SD, and ED. They are alleged to form a Y-shaped type I junction in 83% of the cases, with a wide angle between the UD and ED (27). In type II (15%), the UD is short with a broad angle to the SD. In type III (2.8%), there is almost no UD at the right angle to both the SD and ED. We identified a short fan-like UD reaching the UEV with a valve facing the sinus portion of the ED.

There are several theories as to the function of the UEV. Bast (27, 29) suggested that the valve closes the pars superior to regulate endolymph volume. Bast (29) described this as follows (p. 64):

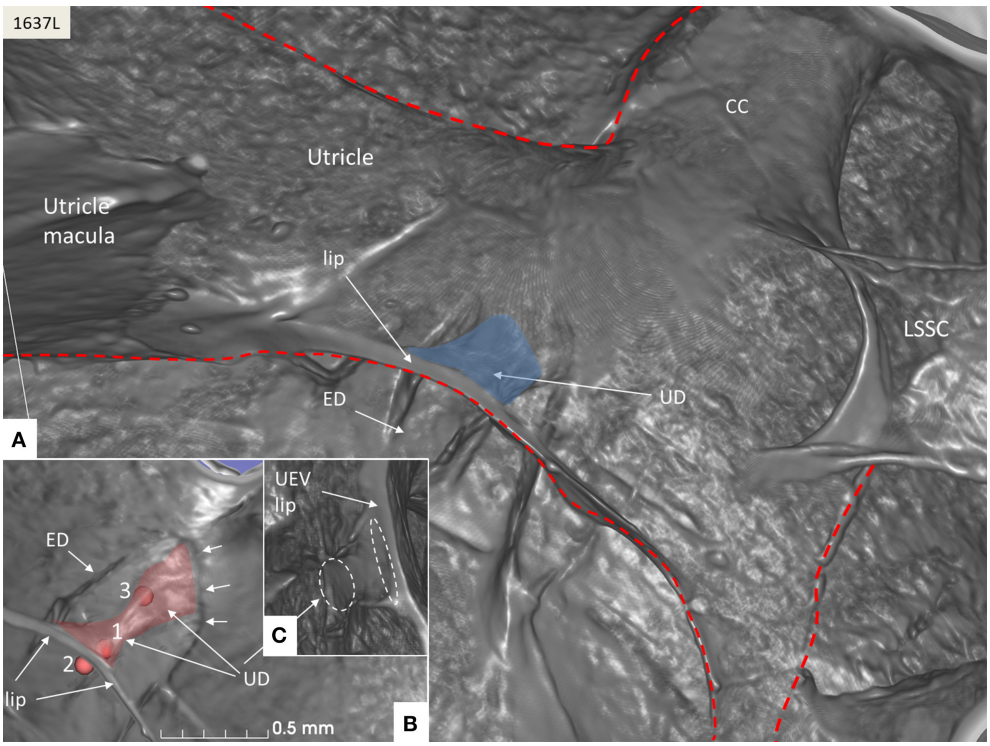

FIGURE 5 | SR-PCI of the UD (blue) at the internal aperture of the VA. **(A)** UEV lip (Bast's valve) is located near the floor of the utricle. The broken red line delineates parts of the vestibular labyrinth. **(B)** Lateral view shows the UD and the ED at the opening of the VA (small arrows). Fiducials (red) mark (1) the position of the mid-portion of the UEV, (2) where the UD reaches the base of the lip, and (3) at the division of the UD and ED. **(C)** Image shows the lateral disc running from the vertical crest of the VA to the UEV. The broken white lines depict the lumen of the UD. LSSC; lateral semicircular canal.

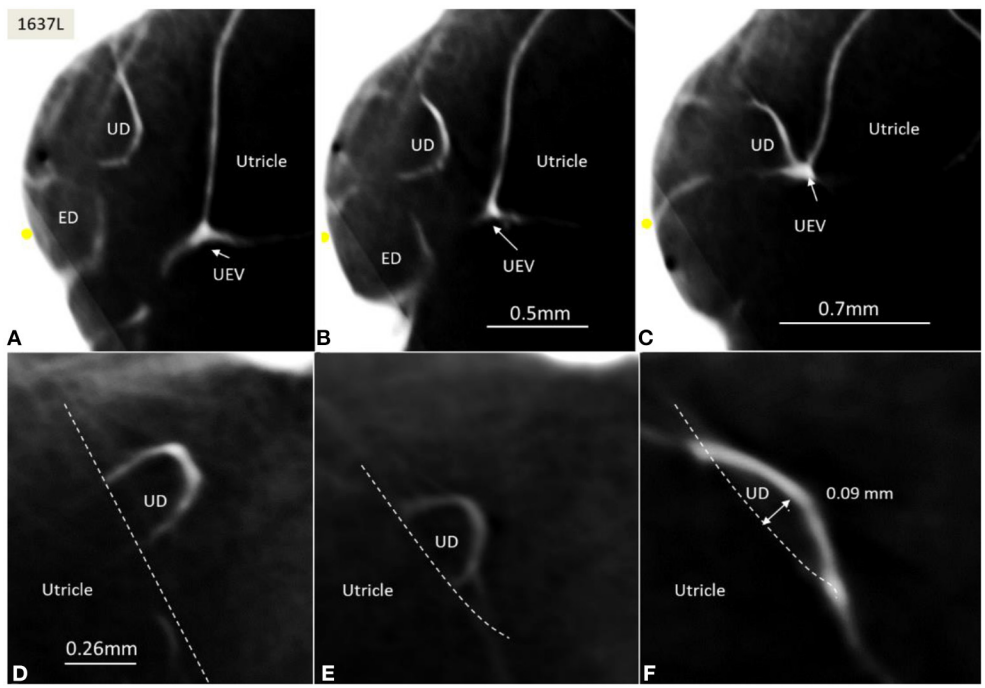

FIGURE 6 | (A–C) SR-PCI of the UD and ED at the internal aperture of the VA. The UEV is closed and connected with a membranous strand against the bony wall. **(D–F)** Lateral view shows serial sections of the UD running against the UEV. Its lumen narrows against the valve. The diameter of the UD in **(D)** is 0.32 mm.

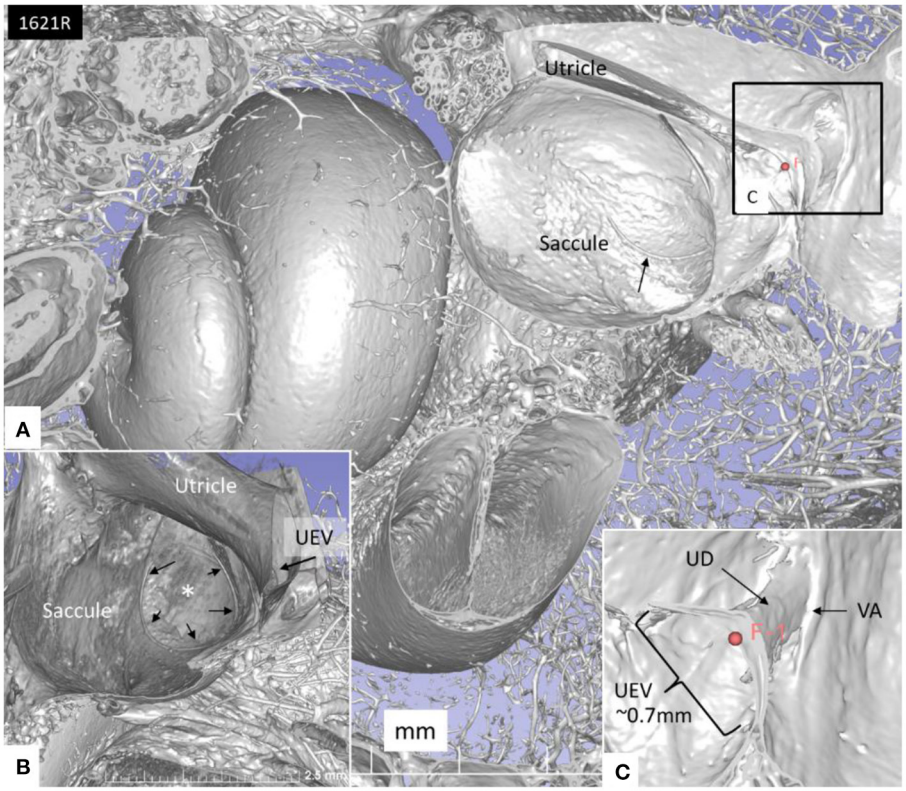

FIGURE 7 | (A) SR-PCI of the left cochlea and vestibule sectioned and viewed laterally. **(B)** The saccule wall consist of a thicker part (small black arrows) and a thinner part (*). The UEV is located in the posterior-inferior part of the utricle (arrow). **(C)** The semilunar-shaped opening of the UEV is shown in higher magnification and is marked with a red fiducial. VA, vestibular aqueduct.

> "Its position would indicate that the flow of endolymph is from the endolymphatic duct to the utricle, but this is not a necessary conclusion. If the flow is in the other direction, the slow movement of the endolymph may not affect this valve. On the other hand, in case of sudden pressure disturbance, this valve may prevent the outflow of endolymph from the utricle, thus maintaining a more constant pressure within the utricle and semicircular canals."

Bast went on to claim that fluid pressure on the valve in the utricle should force it against the opposing duct wall. This was also supported experimentally in the guinea pig, after reducing perilymph and endolymph pressure in the cochlea (33). The valve remained closed, and the utricle and semicircular canals distended even after the collapse of the saccule and cochlear duct. Bast (34) also showed cases of rupture and collapsed saccules, where the utricle was intact. The UD was firmly closed by the UEV. Despite the rupture of the saccule and collapse of the saccule and cochlear duct, the utricle did not collapse. This suggests that endolymph pressure in the utricle can be maintained independently of the pressure in the saccule and cochlear duct. It also proposes that the resolutely closed UEV is responsible for maintaining utricle pressure and therefore acts as a valve. The findings also indicate that fluid is produced in the utricle/semicircular ducts (9). Several regions within the vestibular labyrinth, such as the cupula, have the potential to secrete endolymph similar to the lateral cochlear wall (35, 36). Guild's (5) opinion was that endolymph flows from the utricle and semicircular duct to the ES.

Bast (29) found that in the fetus, the valve is lined by columnar epithelium and at the base with a highly cellular connective tissue that continued into "paralymphatic" tissue around the endolymph system between the utricle and ED. The loose tissue may permit movement of the stiffer valve in case of increased pressure in the utricle. He could not characterize the connective cells but did not exclude the possibility that smooth muscle fibers are present, but there were no indications of nerve fibers. The tissue was independent of the bone surrounding the aperture of the VA. According to Anson and Wilson (28), the fold contains areolar tissue and a fibrous web with a spear-shaped projection of periosteum projecting from the osseous wall but not into the fold proper. This was denied by Bast (27). Anson and Wilson thought that the stiffer valve or lip may not move by pressure changes, while the outer wall could close the orifice and cause movement of fluid in the UD. Schuknecht and Belal (37) studied the valve in humans and found it ideal to protect the pars superior from collapse after dehydration of the rest of the labyrinth. Bachor and Karmody (38) speculated similarly that reduced pressure in the endolymph system, secondary to collapse of the RD, may close the UEV and prevent loss of endolymph from the utricle. Our

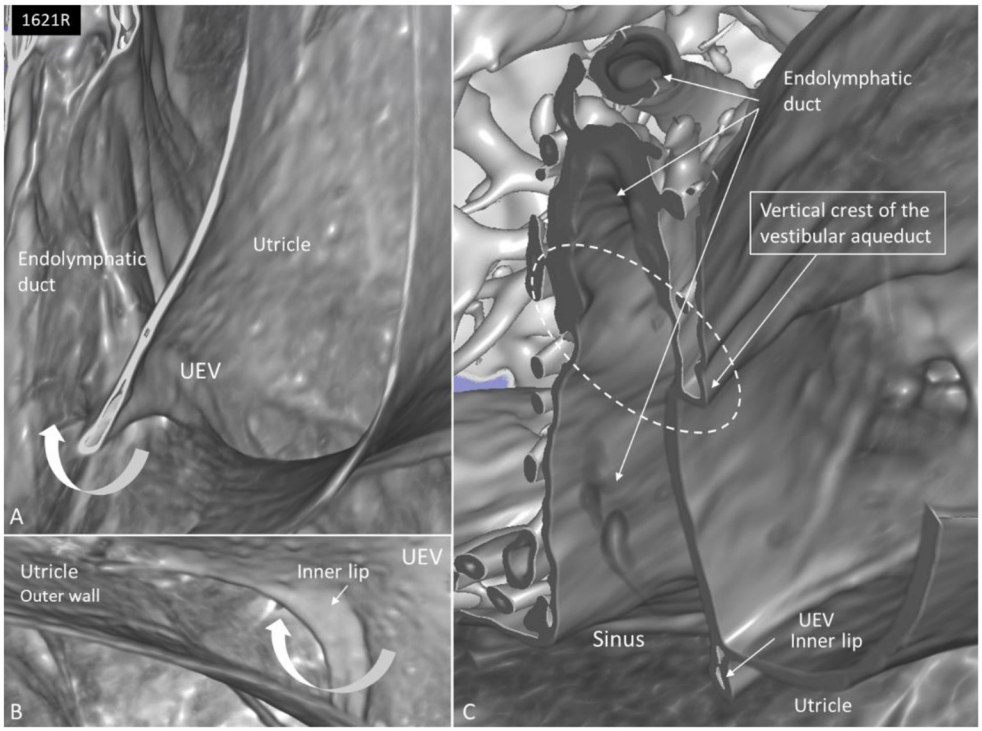

FIGURE 8 | (A) SR-PCI and higher magnification of the UEV and the slit-like opening in the utricle. **(B)** The outer utricle wall is thin but can be seen reaching the inner lip of the valve. **(C)** Coronary section shows the internal opening of the vestibular aqueduct (circle, broken lines). A membrane disc connects the vertical crest with the UEV. The epithelial wall of the UD is not visualized. The endolymphatic duct is surrounded by several blood vessels. Sinus: sinus portion of the endolymphatic duct.

study showed fibrous connections or pillars between the utricle and the inner surface of the bony labyrinth wall that may stabilize the utricle and also deter it from collapse in cases of reduced endolymph pressure.

Hofman (39) presented 3D imaging of the UEV in laboratory animals using orthogonal-plane fluorescence optical sectioning microscopy and Lim using scanning electron microscopy (40). The valve was flat and funnel-like at the utricle and ran into a narrow and short duct leading to the sinus portion of the ED. Hofman (39) described the valve as fairly rigid. The opposing utricle membrane was thin and appeared to be compliant. They speculated that the outer wall may play a greater role in the opening and closure of the valve.

SR-PCI showed the semi-lunar lip lying against its inner surface with a somewhat different shape, as shown by Bast (27) (**Figure 6**). We identified reinforcements around the lip after cropping and adjusting the opacity gradient, suggesting that it is fairly rigid (**Figure 7**). Consequently, increased pressure within the utricle would seem to open the valve through forces acting on the more flaccid part of the opposite membrane. A lowered pressure within the utricle could perhaps close it. External reduction of pressure in the SD and ED could maintain closure to avoid collapse. Conversely, an increased external pressure could force the valve to open by compressing either the flaccid membrane of the utricle or the lip. The UD was found to be partly situated on the loose basal part of the valve, suggesting a mechanism to externally open the lip (**Figure 14**). A fibrous wall from the VA was also connected to the UD and the valve to hold it in place.

The RD

The RD was first described by Viktor Hensen in 1863 (4). The Swedish anatomist Gustaf Retzius defined the RD in a newborn in 1884 as a fairly wide channel connecting the cecum vestibulare of the cochlea with the saccule (3). It contrasts with the miniscule channel described histologically by several authors. Its patency has been confirmed at serial sectioning, and both physiological and tracer studies suggest an endolymph flow or communication (5, 18, 41, 43, 44).

Earlier micro-CT did not define the human RD after manual segmentation and contrast enhancement (45). The present micro-CT imaging was able to reproduce it when air entered the vestibule. The small dimension may refute the idea of an ongoing flow under normal conditions. However, size variations may exist, and dilation can be seen after obliteration of the ED (46). Bachor and Karmody described the human RD as small, collapsed, or wide in pediatric temporal bones (38). In half of the bones, the RD was collapsed and seemed closed. They speculated that it may open when pressure increases and permanent closure may lead to hydrops. Since the RD epithelium is stratified and rests on connective tissue enhancement, it is reasonable to believe that the RD can dilate under conditions of increased endolymph

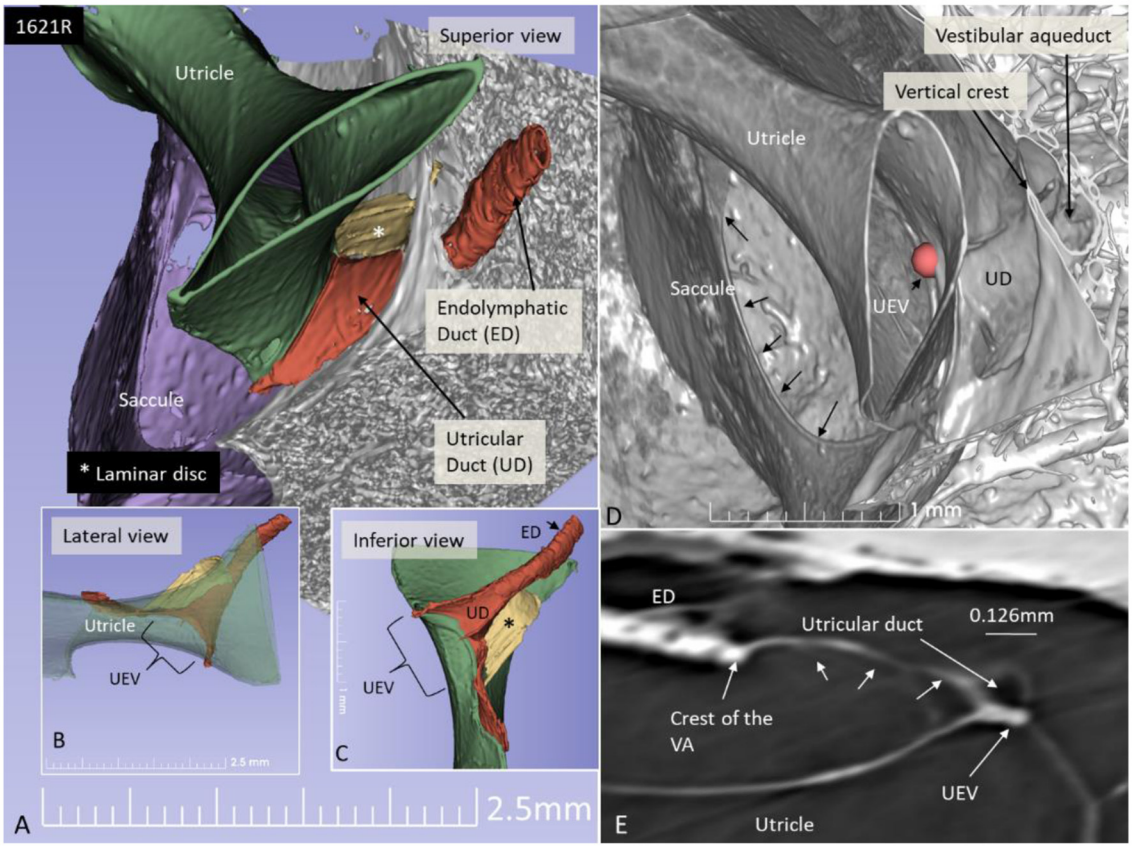

FIGURE 9 | SR-PCI 3D reconstruction and model of the posterior part of the vestibule in a left ear (superior view). **(A)** The endolymphatic duct (ED) and utricular duct (UD) can be seen. A laminar disc (*) extends from the vertical crest of the internal opening of the vestibular aqueduct (VA) to the utricle. It also covers the UD. **(B)** Lateral view of the modeled UEV is viewed through a partly transparent utricle. **(C)** Modeled UEV is viewed from inferior. **(D)** UEV is shown from inside the utricle (red fiducial). The UD wall is reinforced by the laminar disc. **(E)** Horizontal section shows the UD and UEV. The laminar disc (small arrows) runs from the vertical crest to the UEV. It keeps the UD closely associated with the UEV. Note that the UD passes on the UEV allowing increased pressure in the UD to be transmitted and may push the valve to open.

pressure and generate a flow. The thin connection may protect the cochlea from leakage of electricity to maintain cell currents at high frequencies. The endolymphatic potential has been found to be low in the vestibule except near the receptors (47, 48).

EDS in Meniere's Disease

Despite the large number of histopathological studies in MD, only a fraction seem to adhere to the AAO-HNS 1995 criteria. Hallpike and Cairns (49) described two cases where EH was prominent with excessive dilation of the saccule and scala media. There were also changes in the pars superior but no signs of blockage of the communication pathways connecting the utricle, saccule, and ED. The UEV was in its normal position, and the opening of the saccule into the ED contained a dense reddish-staining coagulum in the second case. The absence of loose connective tissue around the ES was a prominent feature. Kyoshiro Yamakawa (50) described similar findings, but there was no mention of the ES. There were edema and calculi in the stria vascularis, the RD seemed open, and the VA was large with colloid-like substance in the duct. He believed that MD symptoms were caused by an augmented pressure in the endolymph which was caused by an increased secretion from the stria vascularis.

EH is a consistent histopathological trait in patients with MD, but its role in the progress of symptoms is unclear. Blockage of the EDS, including the UEV, RD, and SD, is not overrepresented in MD. Dilation of the RD was observed in patients with EH, possibly as a result of increased cochlear hydrostatic pressure (51, 52). Lindsay (53) demonstrated a wide RD in an MD case, but its dimension was not given. According to Shimizu et al. (17) the ED was blocked in 23% in MD, while the UD was blocked in 76% in MD and 52% in normal ears. The SD was blocked in 28% in MD and 76% in normal ears. It suggests that obstruction of the UD and SD may not be the cause of EH in MD. A theory based on CT suggested that displaced saccular otoconia may block the RD, explaining symptoms in MD (54). It is conceivable that a few or even a single displaced otoconia could mechanically obstruct the RD in humans (55). According to Bachor and Karmody (38), there is no correlation between the collapse of RD and cochlear hydrops. Both wide-open and

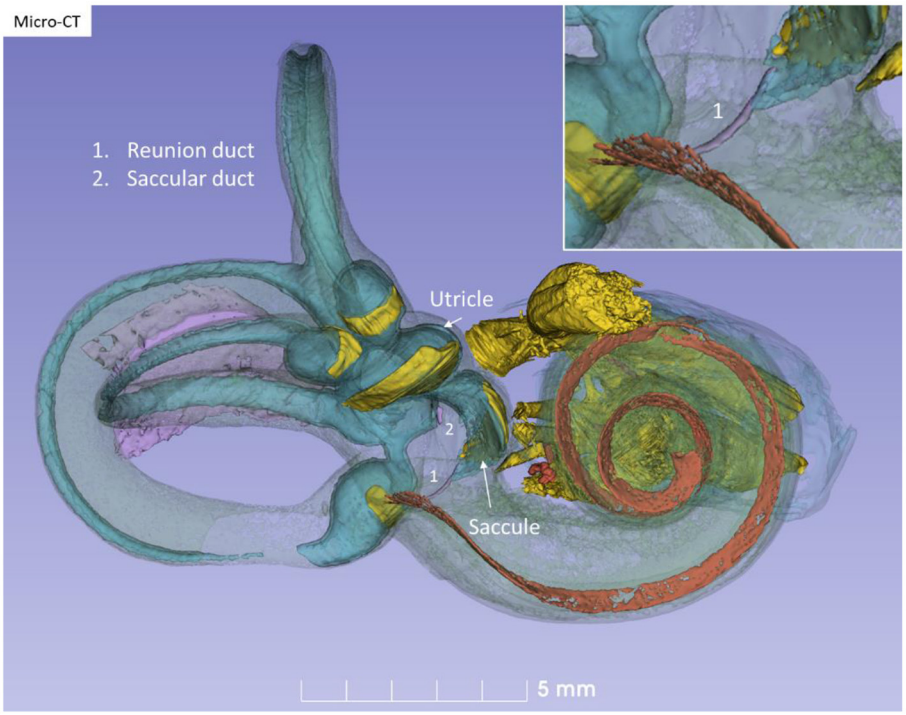

FIGURE 10 | Micro-CT and 3D modeling of a right human temporal bone (Stenver's view). The membrane labyrinth is shown in different colors after the bony capsule is made semi-transparent. The vestibular neuro-epithelium and nerves are yellow. The basilar membrane is colored red. The inset shows RD (1).

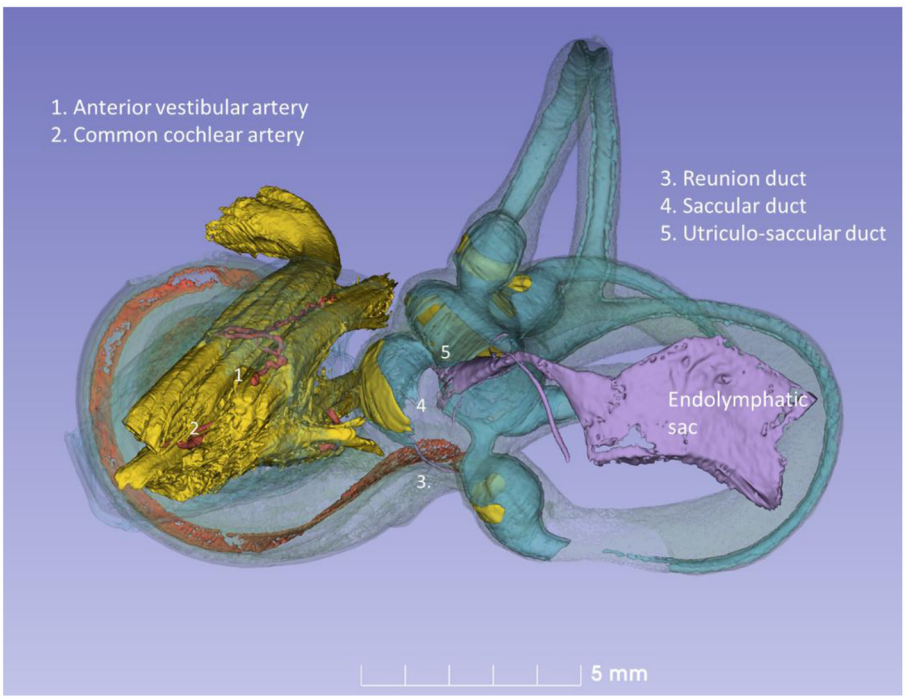

FIGURE 11 | Posterior view of the modeled inner ear shown in **Figure 10**. The position of the saccular and utricular ducts are visualized. The internal auditory canal is shown with cranial nerves and arterial blood vessels supplying the inner ear.

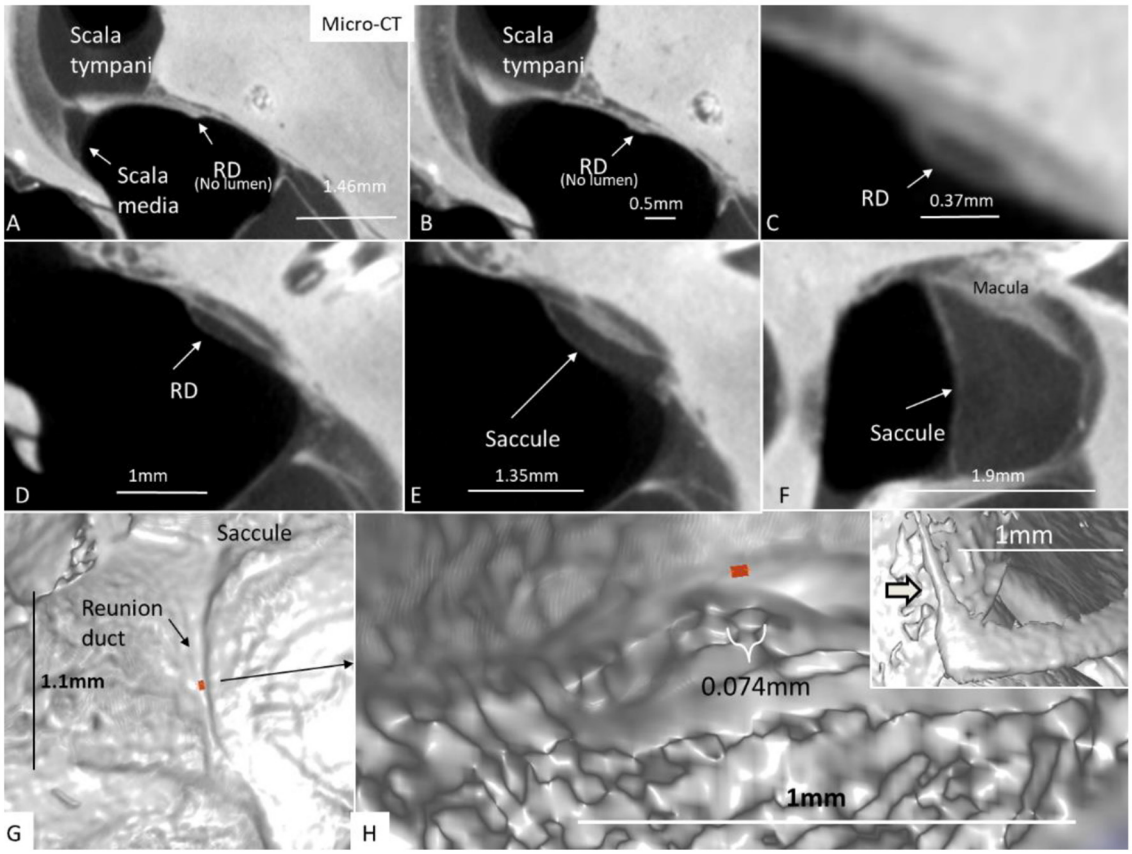

FIGURE 12 | (A–F) Micro-CT and serial sections show the reunion duct (RD) from the saccule to the cochlear duct. **(G)** Surface view of the RD. Its mid-portion is cropped and shown in **(H)** The RD diameter is less than a 10th of a millimeter. The inset in H shows the angle formed between the RD and the vestibular end of the cochlear duct.

blocked RDs were demonstrated. In patients with MD, the RD was found to have a diameter around 0.1 mm (56). Shimizu (17) showed that the RD in a patient with MD was in the range of 0.05 mm. Kitamura et al. (57) investigated five cases with EH limited to the cochlea with no verified MD. Various obliterations of the saccule and/or RD supported a longitudinal flow of the endolymph. EH depended on the location of the blockage from the RD to the ES. The present study suggests that RD may play a minor role in the exchange of endolymph between the cochlea and vestibule, but under certain conditions, it can dilate and open to maintain cochlear homeostasis.

Schuknecht and Ruther (58) showed that in 42 out of 46 ears, there was either a blockage of longitudinal flow or internal shunts causing fistulae. The UD was blocked in 12, ED in 8, endolymphatic sinus in 9, SD in 7, and RD in 27 bones. They considered that obstructions stopped longitudinal flow from both the pars superior and inferior in 21 cases, only the pars superior in 3 cases, and only the pars inferior in 16 cases. Schuknecht and Belal (37) studied the UEV in 29 human temporal bones with MD and found deposits in the lip and enlargement of the saccule compressing and closing the UD. The 3D reconstructions indicated that the endolymph volume may increase up to three times in MD (59). The relative increase was most prominent in the saccule. A possible explanation is the thin part that may expand even before pressure is built up in the utricle and maintained by the UEV. This could explain MRI findings showing occult or prominent EH preceding symptoms in some patients and in the contralateral asymptomatic ears (60–64).

The role of the ED and ES in MD is still unclear. A diminished absorption in the ED and ES could be due to mechanical obstruction or molecular or fibrotic changes (17) or disturbed vascular drainage (65). Yuen and Schuknecht (66) found no obstruction of the VA in MD and no difference in caliber compared with normal ears. The ED was smaller probably as a result of MD rather than the cause of it. A reduced radiographic visualization of the VA was described by Wilbrand (67) in MD, conceivably explained by its smaller size (68, 69). Results by Monsanto et al. (70) suggested that the UEV and SD may open as a result of retrograde pressure caused by failure of the ES to absorb endolymph. A wide-open valve could disrupt the crista function, resulting in vertigo since it would not protect against pressure fluctuations potentially harmful to the sensory epithelia. An increased pressure in the ED and ES could lead to a reversed flow of endolymph into the utricle and cause selective vestibular disturbance in MD (71).

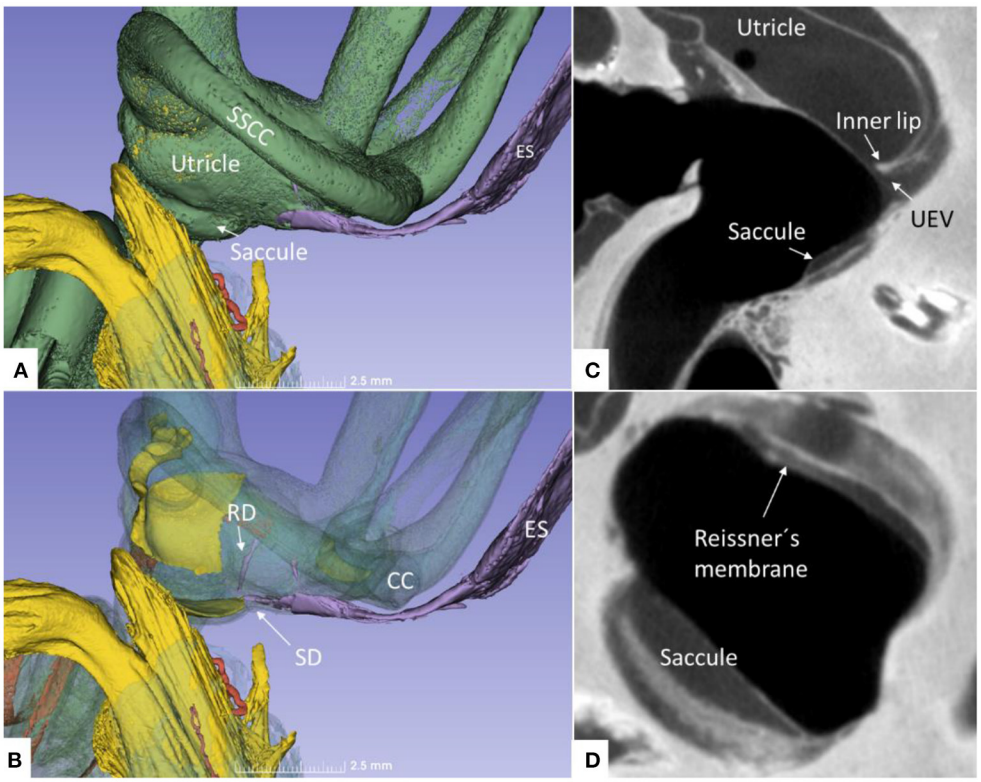

FIGURE 13 | (A) Superior close-up view of micro-CT shown in **Figure 11**. The internal aperture of the vestibular aqueduct (lilac) is seen near the common crus (CC) and the SSCC. **(B)** The saccular and reunion ducts are visible after making the bony capsule transparent. The RD runs almost perpendicular against the saccular duct. **(C)** Horizontal section of the UEV. **(D)** The saccule and cochlear endolymphatic space at the *cecum vestibulare* are shown. SSCC, superior semicircular canal; SD, saccular duct; RD, reunion duct; ES, endolymphatic sac.

Can Acute Endolymph "Backflow" Explain the Meniere Attack?

Experiments have shown that induced alterations in cochlear endolymph volume result in pronounced changes in the ES with bidirectional responses (41, 72). Acute manipulation of the systemic fluid or chronic malfunctions, such as in cochleosaccular degeneration, modify ES activity (42, 73–76). This suggests that the endolymph moves in either direction between the cochlea and ES and is reabsorbed by the ES under conditions of excess volume and secreted by conditions of volume deficiency. Thus, volume may be regulated in the entire labyrinth by the ES. Potentially, a dysfunction in the ES could lead to a volatile elevation of endolymph pressure and acute cochleo-vestibular symptoms, such as in MD. Nonetheless, there are noticeable differences in the anatomy of laboratory animals. Physiologic adaptation and human upright position may modify fluid exchange and dynamics amid the ear and cranium, with conceivable changes also in the structure of the EDS.

Imaging data suggest that the ED, VA, and UEV form a functional unit for the pars superior. This unit includes a stabilizing fibrous disc projecting from the vertical crest of the internal aperture of the VA to the UD and UEV (**Figures 5C**, **9C**). The UD is directed against and physically associated with the flexible part of the lip of the valve, indicating that the duct may force the valve to open and transmit increased endolymph/pressure into the pars superior (**Figure 14**). This framework could be particularly prone to mediating sudden escalations of ES pressure into the utricle through the relatively wide UD and UEV. The ES is an expandable bellow-like structure with an extra-osseous part comprising more than two-thirds of the total ES volume. It could mount considerable osmotic pressure gradients against the vestibular labyrinth, despite its 16 times less volume (1.85/30.4 mm^3) (69, 77, 78). A secretion–degradation system of osmotically active complexes was revealed in the ES acting within a short time frame. Secretion may be triggered by altered volume/pressure conditions in the labyrinth (73), linked to its ability to monitor endolymph (41, 42). A merocrine secretion was already observed in the human ES in an ultrastructural investigation (79). Super-resolution immunohistochemistry recently confirmed a dual absorptive–secretory capacity of the human ES (80). In a temporal bone study in MD, an unproportioned large volume of the ES contained secreted material in an otherwise smaller sac (69).

Therefore, a diminished resorption or hypersecretion of endolymph in the ES could result in a retrograde flow/pressure that underlies the acute attack of vertigo in MD. We speculate,

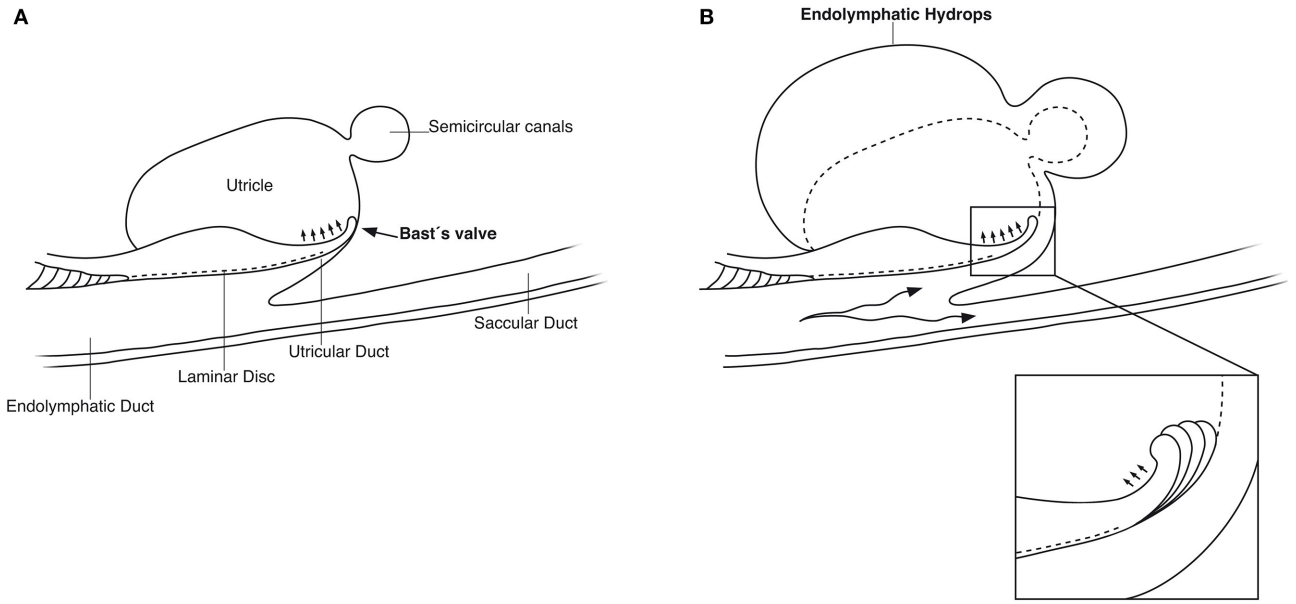

FIGURE 14 | (A) Principal drawing of the human utriculo-endolymphatic valve (Bast's valve) based on SR-PCI. The valve is structurally associated with the opening of the vestibular aqueduct through a laminar disc (interrupted line) emerging from the vertical crest of the vestibular aqueduct to the lip of the valve. The outer wall of the utricular duct faces the disc and forms the utricular fold. Between the inner and outer wall at the base of the lip, there is loose tissue allowing the valve to open (small arrows). **(B)** Hypothetical representation of the role of Bast's valve and UD in generating acute endolymphatic hypertension and hydrops in patients with MD. Increased endolymph pressure is caused by reduced reabsorption or hypersecretion in the ES, leading to a "backflow" of endolymph. It compresses the wall of the utricular duct and pushes the valve to open (inset), leading to acute EH and vertigo. Experimentally, secretion in the ES may be provoked within a short timeframe (41, 42).

based on the present morphological findings and earlier experimental studies, that acute vestibular symptoms in MD arise through a sudden fluid pressure increase and dilatation caused by a "backflow" of an overcompensated ES secreting into the utricle and semicircular canals. ES endolymph has a unique ionic composition (81), which is potentially noxious to the vestibular receptors. Dilation could lead eventually to membrane ruptures (82) additionally extending the ES response. Pressure may impact saccular and ultimately cochlear functions via the SD and RD with corresponding symptoms. Our results support Seymour's (2) notions that the ES has a supporting secretory role necessary to compensate if volume is reduced to insure complete filling of the phylogenetically older utricle and semicircular canals. Microinjections suggest that elevated hydrostatic pressure in the pars inferior or directly into the utricle result in utricle/vestibular receptor dysfunction (83). These changes were believed to be similar to sudden fluctuating changes in MD suggesting that EH is the cause of the typical symptoms (84).

Our concept could have several clinical consequences. The dysfunction of the ES may arise through hormonal disturbances, stria alterations, immune factors, etc. (85). One proposed way to relieve this dysfunction is through surgical destruction of the ES (86). Nonetheless, more studies of the UEV, EDS, and ES function in MD are necessary and could lead to novel treatment modalities against this troublesome disease. There is also a need for more studies on how these small compartments control fluid pressure and ion homeostasis.

DATA AVAILABILITY STATEMENT

The raw data supporting the conclusions of this article will be made available by the authors, without undue reservation.

AUTHOR CONTRIBUTIONS

GR and JS performed micro-CT on the human cadavers. HL performed image processing. 3D visualization of scanned objects provided by SA, HML, SR, and JS. HR-A was the head of the laboratory and planned the project, analyzed the images, and wrote the manuscript. All authors contributed to the article and approved the submitted version.

FUNDING

This study was supported by the Swedish Research Council [2017-03801], the Tysta Skolan Foundation, the Swedish hearing research foundation (hrf), and generous private funds from Arne Sundström, Sweden. Part of the research described in this paper was performed at the Bio-Medical Imaging and Therapy (BMIT) facility at the Canadian Light Source, Inc. (CLSI), which was funded by the Canada Foundation for Innovation, the Natural Sciences and Engineering Research Council of Canada, the National Research Council Canada, the Canadian Institutes of Health Research, the Government of Saskatchewan, Western Economic Diversification Canada, and the University of Saskatchewan. The project was supported by MED-EL, Innsbruck, Austria under an agreement and contract

with Uppsala University. The funder had no role in study design, data collection and analysis, decision to publish, or preparation of the manuscript.

ACKNOWLEDGMENTS

The authors acknowledge support from the Natural Sciences and Engineering Research Council of Canada and the Province of Ontario. We gratefully thank MED-EL and especially Susan Braun and Carolyn Garnham from MED-EL Innsbruck. The X-ray micro-CT scans were conducted by JS, and we wish to acknowledge the facilities and the scientific and technical assistance of Microscopy Australia at the Centre for Microscopy, Characterization & Analysis and the University of Western Australia, a facility funded by the university, state, and commonwealth governments.

REFERENCES

1. Swinburne IA, Mosaliganti KR, Upadhyayula S, Liu TL, Hildebrand DGC, Tsai TYC, et al. Lamellar junctions in the endolymphatic sac act as a relief valve to regulate inner ear pressure. *Elife.* (2017) 7:e37131. doi: 10.7554/eLife.37131
2. Seymour JC. Observations on the circulation in the cochlea. *J Laryngol Otol.* (1954) 68:689–711. doi: 10.1017/S0022215100050131
3. Retzius G. *Das Gehörorgan der Wirbelthiere: Morphologisch-Histologische STUDIEN*. Stockholm: Samson and Wallin (1884).
4. Hensen V. Zur Morphologie der Schnecke des Menschen und der Saugetiere. *Z Wiessensch Zool.* (1863) 13:481.
5. Guild SR. Circulation of the endolymph. *Laryngoscope.* (1927) 37:649–52. doi: 10.1288/00005537-192709000-00004
6. Lundquist PG, Kimura R, Wersaell J. Experiments in endolymph circulation. *Acta Otolaryngol Suppl.* (1964) 188:198. doi: 10.3109/00016486409134562
7. Kimura RS, Schuknecht HF. Membranous hydrops in the inner ear of the guinea pig after obliteration of the endolymphatic Sac. *Pr oto-rhino-laryng.* (1965) 27:343–54. doi: 10.1159/000274693
8. Kimura RS, Schuknecht HF, Ota CY, Jones DD. Obliteration of the ductus reuniens. *Acta Otolaryngol.* (1980) 89:295–309. doi: 10.3109/00016488009127141
9. Kimura RS. XLVIII: Distribution, structure, and function of dark cells in the vestibular labyrinth. *Ann Otol Rhinol Laryngol.* (1969) 78:542–61. doi: 10.1177/000348946907800311
10. Salt AN. Regulation of endolymphatic fluid volume. *Ann N Y Acad Sci.* (2001) 942:306–12. doi: 10.1111/j.1749-6632.2001.tb03755.x
11. Naftalin L, Harrison MS. Circulation of labyrinthine fluids. *J Laryngol Otol.* (1958) 72:118–36. doi: 10.1017/S0022215100053731
12. Dohlman GF. Considerations regarding the mechanism of endolymph circulation. *Adv Otorhinolaryngol.* (1973) 19:101–9. doi: 10.1159/000393982
13. Hulander M, Kiernan AE, Blomqvist SR, Carlsson P, Samuelsson EJ, Johansson BR, et al. Lack of pendrin expression leads to deafness and expansion of the endolymphatic compartment in inner ears of Foxi1 null mutant mice. *Development.* (2003) 130:2013–25. doi: 10.1242/dev.00376
14. Li X, Sanneman JD, Harbidge DG, Zhou F, Ito T, Nelson R, et al. SLC26A4 Targeted to the endolymphatic sac rescues hearing and balance in Slc26a4 mutant mice. *PLoS Genet.* (2013) 9:1003641. doi: 10.1371/journal.pgen.1003641
15. Gussen R, Adkins WY. Saccule degeneration and ductus reuniens obstruction. *Arch Otolaryngol.* (1974) 99:132–35. doi: 10.1001/archotol.1974.00780030138014
16. Sando I, Harada T, Loehr A, Sobel JH. Sudden deafness: histopathologic correlation in temporal bone. *Ann Otol Rhinol Laryngol.* (1977) 86:269–79. doi: 10.1177/000348947708600301
17. Shimizu S, Cureoglu S, Yoda S, Suzuki M, Paparella MM. Blockage of longitudinal flow in Meniere's disease: a human temporal bone study. *Acta Otolaryngol.* (2011) 131:263–8. doi: 10.3109/00016489.2010.532155
18. Rask-Andersen H, Bredberg G, Lyttkens L, Lööf G. The function of the endolymphatic duct—An experimental study using ionic lanthanum as a tracer: a preliminary report. *Ann N Y Acad Sci.* (1981) 374:11–9. doi: 10.1111/j.1749-6632.1981.tb30855.x
19. Wangemann P. Comparison of ion transport mechanisms between vestibular dark cells and strial marginal cells. *Hear Res.* (1995) 90:149–57. doi: 10.1016/0378-5955(95)00157-2
20. Paparella MM, Morizono T, Matsunaga T. Kyoshiro Yamakawa MD and temporal bone histopathology of meniere's patient reported in 1938: commemoration of the centennial of his birth. *Arch Otolaryngol Head Neck Surg.* (1992) 118:660–662. doi: 10.1001/archotol.1992.01880060110023
21. Elfarnawany M, Alam SR, Rohani SA, Zhu N, Agrawal SK, Ladak HM. Micro-CT versus synchrotron radiation phase contrast imaging of human cochlea. *J Microsc.* (2017) 265:349–57. doi: 10.1111/jmi.12507
22. Koch RW, Elfarnawany M, Zhu N, Ladak HM, Agrawal SK. Evaluation of cochlear duct length computations using synchrotron radiation phase-contrast imaging. *Otol Neurotol.* (2017) 38:e92–9. doi: 10.1097/MAO.0000000000001410
23. Fedorov A, Beichel R, Kalpathy-Cramer J, Finet J, Fillion-Robin JC, Pujol S, et al. 3D Slicer as an image computing platform for the Quantitative Imaging Network. *Magn Reson Imaging.* (2012) 30:1323–41. doi: 10.1016/j.mri.2012.05.001
24. Camilieri-Asch V, Shaw JA, Mehnert A, Yopak KE, Partridge JC, Collin SP. Dicect: a valuable technique to study the nervous system of fish. *eNeuro.* (2020) 7:1–23. doi: 10.1523/ENEURO.0076-20.2020
25. Culling CFA, Charles FA, Dunn WL. *Handbook of Histopathological and Histochemical Techniques.* London: Butterworths (1974).
26. Perlman HB. The saccule: observations on a differentiated reenforced area of the saccular wall in man. *Arch Otolaryngol Head Neck Surg.* (1940) 32:678–91. doi: 10.1001/archotol.1940.00660020683005
27. Bast TH. The utriculo-endolymphatic valve and duct and its relation to the endolymphatic and saccular ducts in man and guinea pig. *Anat Rec.* (1937) 68:75–97. doi: 10.1002/ar.1090680106
28. Anson BJ, Wilson JG. The form and structure of the endolymphatic and associated ducts in the child. *Anat Rec.* (1936) 65:485–98. doi: 10.1002/ar.1090650411
29. Bast TH. The utriculo-endolymphatic valve. *Anat Rec.* (1928) 40:61–5. doi: 10.1002/ar.1090400106
30. Hoffman EF, Bast TH. A comparative study of the utriculo-endolymphatic valve? in some of the common mammals. *Anat Rec.* (1930) 46:333–47. doi: 10.1002/ar.1090460404
31. Wilson JG, Anson BJ. The utriculo-endolymphatic valve? (bast) in a two-year-old child. *Anat Rec.* (1929) 43:145–53. doi: 10.1002/ar.1090430204
32. Perlman HB, Lindsay JR. The utriculo-endolymphatic valve. *Arch Otolaryngol Head Neck Surg.* (1936) 24:68–75. doi: 10.1001/archotol.1936.00640050075007
33. Bast TH, Eyster JAE. III. Discussion from the point of view of animal experimentation. LXXVIII. *Ann Otol Rhinol Laryngol.* (1935) 44:792–803. doi: 10.1177/000348943504400318
34. Bast TH. Function of the utriculo-endolymphatic valve: two cases of ruptured saccules in children. *Arch Otolaryngol Head Neck Surg.* (1934) 19:537–50. doi: 10.1001/archotol.1934.03790050002001
35. Kawasaki K, Yamamoto A, Omori K, Iwano T, Kumazawa T, Tashiro Y. Quantitative immunoelectron microscopic localization of Na, K-ATPase α-subunit in the epithelial cells of rat vestibular apparatus. *Hear Res.* (1992) 60:64–72. doi: 10.1016/0378-5955(92)90059-V
36. Kikuchi T, Kimura RS, Paul DL, Takasaka T, Adams JC. Gap junction systems in the mammalian cochlea. *Brain Res Rev.* (2000) 32:163–6. doi: 10.1016/S0165-0173(99)00076-4
37. Schuknecht HF, Belal AA. The utriculo-endolymphatic valve: Its functional significance. *J Laryngol Otol.* (1975) 89:985–96. doi: 10.1017/S0022215100081305
38. Bachor E, Karmody CS. The utriculo-endolymphatic valve in pediatric temporal bones. *Eur Arch Oto-Rhino-Laryngol.* (1995) 252:167–71. doi: 10.1007/BF00178106

39. Hofman R, Segenhout JM, Buytaert JAN, Dirckx JJJ, Wit HP. Morphology and function of Bast's valve: Additional insight in its functioning using 3D-reconstruction. *Eur Arch Oto-Rhino-Laryngol.* (2008) 265:153–7. doi: 10.1007/s00405-007-0424-8
40. Paparella M, Gluckman J, Meyerhof W. *Otolaryngology, 3rd ed*. Philadelphia, PA: Saunders (1991).
41. Rask-Andersen H, DeMott JE, Bagger-Sjöbäck D, Salt AN. Morphological changes of the endolymphatic sac induced by microinjection of artificial endolymph into the cochlea. *Hear. Res.* (1999) 138:81–90. doi: 10.1016/S0378-5955(99)00153-7
42. Jansson B, Friberg U, Rask-Andersen H. Effects of glycerol on the endolymphatic sac: A time-sequence study. *Orl.* (1992) 54:201–10. doi: 10.1159/000276299
43. Jahnke V, Giebel W. Untersuchungen zur durchgängigkeit des ductus reunions beim menschen. *Arch. Otorhinolaryngol.* (1975) 210:364. doi: 10.1007/BF00460088
44. Salt AN, Rask-Andersen H. Responses of the endolymphatic sac to perilymphatic injections and withdrawals: evidence for the presence of a one-way valve. *Hear Res.* (2004) 191:90–100. doi: 10.1016/j.heares.2003.12.018
45. Glueckert R, Johnson Chacko L, Schmidbauer D, Potrusil T, Pechriggl EJ, Hoermann R, et al. Visualization of the membranous labyrinth and nerve fiber pathways in human and animal inner ears using MicroCT imaging. *Front Neurosci.* (2018) 12:501. doi: 10.3389/fnins.2018.00501
46. Konishi S. The ductus reuniens and utriculo-endolymphatic valve in the presence of endolymphatic hydrops in guinea-pigs. *J Laryngol Otol.* (1977) 91:1033–45. doi: 10.1017/S0022215100084747
47. Tasaki I. Hearing. *Annu Rev Physiol.* (1957) 19:417–38. doi: 10.1146/annurev.ph.19.030157.002221
48. Schmidt RS, Fernandez C. Labyrinthine DC potentials in representative vertebrates. *J Cell Comp Physiol.* (1962) 59:311–22. doi: 10.1002/jcp.1030590311
49. Hallpike CS, Cairns H. Observations on the pathology of Ménière's syndrome. *J Laryngol Otol.* (1938) 53:625–55. doi: 10.1017/S0022215100003947
50. Yamakawa K. Hearing organ of a patient who showed Meniere's symptoms. *J Otolaryngol Soc Jpn.* (1938) 44:2310–2.
51. Altmann F, Zechner G. The pathology and pathogenesis of endolymphatic hydrops. New investigations. *Arch Klin Exp Ohren Nasen Kehlkopfheilkd.* (1968) 192:1–19. doi: 10.1007/BF00301488
52. Kohut RI, Lindsay JR. Pathologic changes in idiopathic labyrinthine hydrops: correlations with previous findings. *Acta Otolaryngol.* (1972) 73:402–12. doi: 10.3109/00016487209138959
53. Lindsay JR. Labyrinthine dropsy and Meniere'S disease. *Arch Otolaryngol Head Neck Surg.* (1942) 35:853–67. doi: 10.1001/archotol.1942.00670010861002
54. Yamane H, Sunami K, Iguchi H, Sakamoto H, Imoto T, Rask-Andersen H. Assessment of Meniere's disease from a radiological aspect saccular otoconia as a cause of Meniere's disease? *Acta Otolaryngol.* (2012) 132:1054–60. doi: 10.3109/00016489.2012.680980
55. Ross MD, Johnsson LG, Peacor D, Allard LF. Observations on normal and degenerating human otoconia. *Ann Otol Rhinol Laryngol.* (1976) 85:310–26. doi: 10.1177/000348947608500302
56. Cureoglu S, Da Costa Monsanto R, Paparella MM. Histopathology of Meniere's disease. *Oper Tech Otolayngol Head Neck Surg.* (2016) 27:194–204. doi: 10.1016/j.otot.2016.10.003
57. Kitamura K, Schuknecht HF, Kimura RS. Cochlear hydrops in association with collapsed saccule and ductus reuniens. *Ann Otol Rhinol Laryngol.* (1982) 91:5–13. doi: 10.1177/000348948209100104
58. Schuknecht HF, Rüther A. Blockage of longitudinal flow in endolymphatic hydrops. *Eur Arch Oto-Rhino-Laryngol.* (1991) 248:209–17. doi: 10.1007/BF00173659
59. Morita N, Kariya S, Deroee AF, Cureoglu S, Nomiya S, Nomiya R, et al. Membranous labyrinth volumes in normal ears and Ménière disease: a three-dimensional reconstruction study. *Laryngoscope.* (2009) 119:2216–20. doi: 10.1002/lary.20723
60. Conlon BJ, Gibson WPR. Meniere's disease: the incidence of hydrops in the contralateral asymptomatic ear. *Laryngoscope.* (1999) 109:1800–2. doi: 10.1097/00005537-199911000-00014
61. Lin MY, Timmer FCA, Oriel BS, Zhou G, Guinan JJ, Kujawa SG, et al. Vestibular evoked myogenic potentials (VEMP) can detect asymptomatic saccular hydrops. *Laryngoscope.* (2006) 116:987–92. doi: 10.1097/01.mlg.0000216815.75512.03
62. Kariya S, Cureoglu S, Fukushima H, Kusunoki T, Schachern PA, Nishizaki K, et al. Histopathologic changes of contralateral human temporal bone in unilateral Ménière's disease. *Otol Neurotol.* (2007) 28:1063–8. doi: 10.1097/MAO.0b013e31815a8433
63. Gürkov R, Pyykö I, Zou J, Kentala E. What is Menière's disease? A contemporary re-evaluation of endolymphatic hydrops. *J Neurol.* (2016) 263:71–81. doi: 10.1007/s00415-015-7930-1
64. Nakashima T, Pyykkö I, Arroll MA, Casselbrant ML, Foster CA, Manzoor NF, et al. Meniere's disease. *Nat Rev Dis Prim.* (2016) 2:1–18. doi: 10.1038/nrdp.2016.28
65. Nordström CK, Li H, Ladak HM, Agrawal S, Rask-Andersen H. A Micro-CT and synchrotron imaging study of the human endolymphatic duct with special reference to endolymph outflow and Meniere's disease. *Sci Rep.* (2020) 10:8295. doi: 10.1038/s41598-020-65110-0
66. Yuen SS, Schuknecht HF. Vestibular aqueduct and endolymphatic duct in Meniere's disease. *Arch Otolaryngol.* (1972) 96:553–5. doi: 10.1001/archotol.1972.00770090831010
67. Wilbrand HF. Menière's disease - roentgenologic diagnosis. *Arch Otorhinolaryngol.* (1976) 212:331–7. doi: 10.1007/BF00453682
68. Wilbrand HF, Stahle J, Rask-Andersen H. Tomography in Menière's disease–why and how. morphological, clinical and radiographic aspects. *Adv Otorhinolaryngol.* (1978) 24:71–93.
69. Hebbar GK, Rask-Andersen H, Linthicum FH. Three-dimensional analysis of 61 human endolymphatic ducts and sacs in ears with and without Meniere's disease. *Ann Otol Rhinol Laryngol.* (1991) 100:219–25. doi: 10.1177/000348949110000310
70. Monsanto R, Pauna HF, Kwon G, Schachern PA, Tsuprun V, Paparella MM, et al. A three-dimensional analysis of the endolymph drainage system in Ménière disease. *Laryngoscope.* (2017) 127:E170–5. doi: 10.1002/lary.26155
71. Paparella MM. Pathogenesis and pathophysiology of meniere's disease. *Acta Otolaryngol.* (1991) 111:26–35. doi: 10.3109/00016489109128041
72. Salt AN, DeMott JE. Ionic and potential changes of the endolymphatic sac induced by endolymph volume changes. *Hear Res.* (2000) 149:46–54. doi: 10.1016/S0378-5955(00)00160-X
73. Rask-Andersen H, Erwall C, Steel KP, Friberg U. The endolymphatic sac in a mouse mutant with cochleo-saccular degeneration. Electrophysiological and ultrastructural correlations. *Hear Res.* (1987) 26:177–90. doi: 10.1016/0378-5955(87)90110-9
74. Erwall C, Jansson B, Friberg U, Rask-Andersen H. Subcellular changes in the endolymphatic sac after administration of hyperosmolar substances. *Hear Res.* (1988) 35:109–18. doi: 10.1016/0378-5955(88)90045-7
75. Takumida M, Harada Y, Bagger-sjöbäck D, Rask-andersen H. Modulation of the endolymphatic sac function. *Acta Otolaryngol.* (1991) 481:129–34. doi: 10.3109/00016489109131364
76. Jansson B, Friberg U, Rask-andersen H. Endolymphatic sac morphology after instillation of hyperosmolar hyaluronan in the round window niche. *Acta Otolaryngol.* (1993) 113:741–5. doi: 10.3109/00016489309135894
77. Igarashi M, Ohashi K, Ishii M. Morphometric comparison of endolymphatic and perilymphatic spaces in human temporal bones. *Acta Otolaryngol.* (1986) 101:161–4. doi: 10.3109/00016488609132823
78. Jansson B, Friberg U, Andersen HR. Three-dimensional anatomy of the human endolymphatic Sac. *Arch Otolaryngol Neck Surg.* (1990) 116:345–9. doi: 10.1001/archotol.1990.01870030109020
79. Rask-Andersen H, Rask-Andersen H, Danckwardt-Lillieström N. Ultrastructural evidence of a merocrine secretion in the human endolymphatic SAC. *Ann Otol Rhinol Laryngol.* (1991) 100:148–56. doi: 10.1177/000348949110000211
80. Nordström CK, Danckwardt-Lillieström N, Liu W, Rask-Andersen H. "Reversed polarization" of Na/K-ATPase—a sign of inverted transport in the human endolymphatic sac: a super-resolution structured illumination microscopy (SR-SIM) study. *Cell Tissue Res.* (2020) 379:445–57. doi: 10.1007/s00441-019-03106-7

81. Mori N, Miyashita T, Inamoto R, Matsubara A, Mori T, Akiyama K, et al. Ion transport its regulation in the endolymphatic sac: suggestions for clinical aspects of Meniere's disease. *Eur Arch Otorhinolaryngol.* (2017) 274:1813–20. doi: 10.1007/s00405-016-4362-1
82. Schuknecht HF. Pathophysiology of endolymphatic hydrops. *Arch Otorhinolaryngol.* (1976) 212:253–62. doi: 10.1007/BF00453673
83. Brown DJ, Chihara Y, Wang Y. Changes in utricular function during artificial endolymph injections in guinea pigs. *Hear Res.* (2013) 304:70–6. doi: 10.1016/j.heares.2013.05.011
84. Brown DJ, Chihara Y, Curthoys IS, Wang Y, Bos M. Changes in cochlear function during acute endolymphatic hydrops development in guinea pigs. *Hear. Res.* (2013) 296:96–106. doi: 10.1016/j.heares.2012.12.004
85. Inamoto R, Miyashita T, Akiyama K, Mori T, Mori N. Endolymphatic sac is involved in the regulation of hydrostatic pressure of cochlear endolymph. *Am J Physiol Regul Integr Comp Physiol.* (2009) 297:R1610–4. doi: 10.1152/ajpregu.00073.2009
86. Gibson WPR. The effect of surgical removal of the extraosseous portion of the endolymphatic sac in patients suffering from Meniere's disease. *J Laryngol Otol.* (1996) 110:1008–11. doi: 10.1017/S0022215100135637

Conflict of Interest: The authors declare that the research was conducted in the absence of any commercial or financial relationships that could be construed as a potential conflict of interest.

frontiers in Surgery

ORIGINAL RESEARCH
published: 31 May 2021
doi: 10.3389/fsurg.2021.673847

Endolymphatic Hydrops in Fluctuating Hearing Loss and Recurrent Vertigo

Pablo Domínguez[1,2], *Raquel Manrique-Huarte*[3], *Víctor Suárez-Vega*[4], *Nieves López-Laguna*[5], *Carlos Guajardo*[3,6] *and Nicolás Pérez-Fernández*[7]*

[1] Department of Radiology, Clínica Universidad de Navarra, Pamplona, Spain, [2] Navarra Institute for Health Research (IdiSNA), Pamplona, Spain, [3] Department of Otorhinolaryngology, Clínica Universidad de Navarra, Pamplona, Spain, [4] Department of Radiology, Clínica Universidad de Navarra, Madrid, Spain, [5] Department of Emergency Medicine, Clínica Universidad de Navarra, Madrid, Spain, [6] Escuela de Fonoaudiología, Universidad Austral de Chile, Sede Puerto Montt, Valdivia, Chile, [7] Department of Otorhinolaryngology, Clínica Universidad de Navarra, Madrid, Spain

Background: Endolymphatic hydrops (EH) is the histopathological hallmark of Ménière's disease (MD) and has been found by *in vivo* magnetic resonance imaging (MRI) in patients with several inner ear syndromes without definite MD criteria. The incidence and relevance of this finding is under debate.

Purpose: The purpose of the study is to evaluate the prevalence and characteristics of EH and audiovestibular test results in groups of patients with fluctuating audiovestibular symptoms not fulfilling the actual criteria for definite MD and compare them with a similar group of patients with definite MD and a group of patients with recent idiopathic sudden neurosensory hearing loss (ISSNHL).

Material and Methods: 170 patients were included, 83 with definite MD, 38 with fluctuating sensorineural hearing loss, 34 with recurrent vertigo, and 15 with ISSNHL. The clinical variables, audiovestibular tests, and EH were evaluated and compared. Logistic proportional hazard models were used to obtain the odds ratio for hydrops development, including a multivariable adjusted model for potential confounders.

Results: No statistical differences between groups were found regarding disease duration, episodes, Tumarkin spells, migraine, vascular risk factors, or vestibular tests; only hearing loss showed differences. Regarding EH, we found significant differences between groups, with odds ratio (OR) for EH presence in definite MD group vs. all other patients of 11.43 (4.5–29.02; $p < 0.001$). If the ISSNHL group was used as reference, OR was 55.2 (11.9–253.9; $p < 0.001$) for the definite MD group, 9.9 (2.1–38.9; $p = 0.003$) for the recurrent vertigo group, and 5.1 (1.2–21.7; $p = 0.03$) for the group with fluctuating sensorineural hearing loss.

Conclusion: The percentage of patients with EH varies between groups. It is minimal in the ISSNHL group and increases in groups with increasing fluctuating audiovestibular symptoms, with a rate of severe EH similar to the known rate of progression to definite MD in those groups, suggesting that presence of EH by MRI could be related to the risk of progression to definite MD. Thus, EH imaging in these patients is recommended.

Keywords: Ménière's disease, endolymphatic hydrops, MRI, fluctuating hearing loss, recurrent vertigo, vestibular tests

OPEN ACCESS

Edited by:
Robert Gürkov, Bielefeld University, Germany

Reviewed by:
Toshihisa Murofushi, Teikyo University Mizonokuchi Hospital, Japan
Hiroshi Inui, Inui ENT Clinic, Japan
Carol A. Foster, University of Colorado Anschutz Medical Campus, United States

***Correspondence:**
Nicolás Pérez-Fernández
nperezfer@unav.es

Specialty section:
This article was submitted to Otorhinolaryngology - Head and Neck Surgery, a section of the journal Frontiers in Surgery

Received: *28 February 2021*
Accepted: *19 April 2021*
Published: *31 May 2021*

Citation:
Domínguez P, Manrique-Huarte R, Suárez-Vega V, López-Laguna N, Guajardo C and Pérez-Fernández N (2021) Endolymphatic Hydrops in Fluctuating Hearing Loss and Recurrent Vertigo. Front. Surg. 8:673847. doi: 10.3389/fsurg.2021.673847

INTRODUCTION

In recent years, the diagnostic approach to patients with Ménière's disease (MD) has undergone a major challenge. Two almost simultaneous facts explain this situation. First, the unconditional acceptance of new guidelines and criteria for the clinical diagnosis of this disease and, second, the appearance of methods for the *in vivo* visualization of endolymphatic hydrops (EH). Each aims to improve the management of patients with recurrent non-positional vertigo, but the former ignores the contribution of the latter, which, in turn, critically demands a framework of diagnosis defining a clinical perspective on the new findings in magnetic resonance imaging (MRI) of the inner ear.

The main differences between the published diagnostic criteria of MD have been critically reviewed by previous authors and show that some are extremely restrictive to a complex symptom presentation or, on the contrary, permit partial manifestations that resemble the main fluctuating nature of symptoms in the disease (1). As MD is part of a wider scenario of fluctuating hearing loss or recurrent vertigo, most of the guidelines do not consider some forms of staging or of status, both of which influence vestibular function (2) and auditory tests results (3). Another generalized deficiency in the guidelines is the absence of complete oto-neurological examinations to further categorize the level of vestibular deficit. The need for a complete otoneurologic evaluation of patients with suspected MD, at their first presentation or during follow-up, is the main conclusion of several studies that addressed particular clinical characteristics. A detailed scrutiny of symptoms has shown the existence of different subtypes or clinical variants in the unilateral (4) and bilateral (5) presentations of definite MD. This has also occurred in the case of bedside vestibular examination (6), auditory (7), and vestibular testing (8, 9).

MRI detection of EH is the result of high tech combined with complex sequence parametrization to allow the identification of the minute sensory and supporting structures of the inner ear within very hard dense bone. The imaging basis of EH relies on the fact that gadolinium-based MR contrast diffuses to the perilymph but not to the endolymph, altering the perilymph signal and allowing later discrimination between both components in MR imaging (10). At present, two sequences: "Fluid attenuated inversion recovery" (FLAIR) and "Inversion Recovery with REAL reconstruction" (REAL-IR), and two methods of contrast administration (intravenous or intratympanic) have been consolidated. This creates a source of variability that may influence the results obtained, but the technique is now widely accepted. Excellent reviews of the available techniques have also been published (11, 12). The scarce, but otherwise illustrative, number of otopathology reports on patients with any inner ear disorder representative of, or clinically ascribed to, MD is a magnificent platform for comparing results (13). It has demonstrated the importance of EH in the natural history of MD (14).

In this work, we address the EH MRI findings of patients with fluctuating auditory and vestibular symptoms, both in isolation and in combination. This is, first, a descriptive work that aims to clarify the rationale for a more in-depth evaluation of patients with fluctuating inner ear symptoms. The second purpose for this study comes from the well-known association between recurrent vestibulopathy (RV) and MD (15), as well as between fluctuating sensorineural hearing loss (FSNHL) and MD (16). In both cases, MD is expected to develop in 4% and 10–37% of the cases followed, respectively. This is the percentage of patients with EH we expect to find with MRI evaluation.

MATERIALS AND METHODS

Patients

The patients included in this work were seen at two different venues by experienced otologists–neurotologists (RMH, NPF), and all the tests included were performed for their routine care and evaluation. All data shown were retrospectively obtained from their digital medical history at both institutions. All research has been conducted in accordance with the World Medical Association's Declaration of Helsinki and in accordance with institutional and national guidelines. Patients gave written authorization for the use of their medical data for research purposes. No identifiable human data are shown.

For this study the following patients were included (**Table 1**):

1) Patients with unilateral "definite" MD according to the guidelines defined by the American Academy of Otolaryngology Head and Neck Surgery in 1995 (17), who also fulfilled the criteria of "definite" MD according to Barany 2015 (18).
2) Patients with so-called "atypical" MD. We have used a previously defined categorization that is based on the main fluctuating symptom and provides five additional groups (19). In the case of fluctuating sensorineural hearing loss (FSNHL), this can occur with a single attack of vertigo alone, with concurrent unsteadiness or without any vestibular symptoms. In the case of recurrent vertigo (RV), it may occur with fixed sensorineural hearing loss or without hearing loss (19).
3) Patients with unilateral idiopathic sudden sensorineural hearing loss (ISSNHL) without vertigo or dizziness (20).

Exclusion criteria were middle ear disease, previous surgical or intratympanic treatment and tumors, or vascular compression in the vestibular nerve.

Procedures

Clinical Data and Audiovestibular Tests

After clinical evaluation and bedside vestibular examination, tests of the vestibulo-ocular reflex (video head-impulse test or vHIT, and ocular vestibular-evoked myogenic potential or oVEMP), of the vestibulo-spinal reflex (cervical vestibular-evoked myogenic potential, or cVEMP), of nystagmus (caloric test), and of hearing (pure tone audiometry) were performed. After signing the informed consent, the MRI study was performed.

Clinical Evaluation and Bedside Testing

Data recorded for all patients included "disease duration" defined as time in years since the first typical episode of vertigo or hearing fluctuation or, in the case of ISSNHL, in days since it began as

TABLE 1 | Definitions for inclusion in this study.

Term	Original definition	References
MD definite	• Two or more definitive spontaneous episodes of vertigo lasting 20 min or longer • Audiometrically documented hearing loss on at least one occasion • Tinnitus or aural fullness in the affected ear • Other causes excluded	(17, 18)
Atypical MD cochlear (FSNHL group)	Patients with fluctuating hearing loss • Single vertigo type: with a single episode of vertigo • Unsteady type: without vertigo but with unsteadiness • No vestibular symptom type: entirely without vestibular symptoms	(19)
Atypical MD vestibular (RV group)	Patients with recurrent episodic vertigo • Hearing loss type: with complicating fixed sensorineural hearing loss • Normal hearing type: with normal hearing	(19)
Idiopathic sudden sensorineural hearing loss (ISSNHL group)	• Sensorineural hearing loss >30 dB HL, in three or more consecutive frequencies, over <72 h	(20)

MD, Ménière's disease; FSNHL, fluctuating sensorineural hearing loss; RV, recurrent vertigo; ISSNHL, idiopathic sudden sensorineural hearing loss; dB HL, decibels hearing level.

described by the patient. For fluctuating symptoms, its severity was evaluated according to the number of episodes (vertigo or hearing fluctuation) in the previous 6 months for inclusion in the study and its activity by the time (days) since the last vertigo crisis or hearing fluctuation. Additionally, the existence of drop attacks of the Tumarkin type was also considered in the case of patients with recurrent vertigo. All patients were evaluated for the existence of migraine and vascular risk factors.

Patients underwent a complete neurotological examination, and particular attention was paid to the appearance of spontaneous nystagmus behind Frenzel goggles. In addition, horizontal post head-shaking nystagmus or vibration-induced nystagmus and positional nystagmus were considered.

Audiometric Test

Audiometric findings are reported in terms of the 0.25- to 6-kHz pure-tone thresholds expressed in decibel hearing level (dB HL). In order to better analyze the results, the audiometry was divided into (a) low-frequency range threshold (0.25 kHz), (b) mean pure-tone average (PTA) for the 0.5, 1, 2, and 3 kHz, and (c) high-frequency range mean threshold (4 and 6 kHz). The affected and non-affected ears are then analyzed. For each range of frequencies, we analyze the number of patients who display a threshold lower than 50 dB HL vs. those equal or higher than 50 dB HL (21).

Vestibular Function Tests

The results of the video head impulse test (vHIT: GN Otometrics, Denmark) will be given as the gain of the vestibulo-ocular reflex and the appearance of refixation saccades obtained for head impulses in the plane of each of the three semicircular canals (SCC) of the affected and unaffected ear. The mean gain is considered normal for each of the canals in each patient evaluated when above the lower limit for the patient's age as given in the system used. In the case where the gain is found to be lower than expected, it will be considered abnormal if there are refixation saccades (overt or covert). A test is considered normal when all three SCCs are normal and abnormal when at least one of the SCCs is abnormal.

The caloric test will be considered abnormal if canal paresis (in accordance with Jongkees' formula) is above 22%.

For vestibular-evoked myogenic potential (VEMP) testing, both cervical (cVEMP) and ocular (oVEMP) tests, the normal vestibular function is defined as the presence of vestibular-evoked myogenic potentials in both ears. It is analyzed by the inter-aural asymmetry ratio [IAAR (%)] for air-conducted stimulation at 0.5 kHz. The intensity of the acoustic stimulus used is 97 dB normalized HL. A Blackman envelope was configured (rise/fall time 2 ms, plateau time 0 ms). One hundred averages were presented at a rate of 5.1/s. The cVEMP is recorded with the patients seated in an upright position. The signals obtained were rectified by the contraction value of the ECM muscle. The oVEMP is recorded with the patient sitting upright, having been instructed to look at a fixed point on the wall with an upward inclination of 35°.

Abnormal vestibular function is defined as either a unilaterally or bilaterally absent function. An absent oVEMP response is defined as EMG recordings lacking definable n10 waves, and an absent cVEMP response is defined as EMG recordings lacking definable p13 waves. The number of recordings made per subject is based on the reproducibility of the observed response. In cases in which the response is considered absent, the mean amplitude will be null (0 μV). To calculate the IAAR, the mean null values were artificially set at 1 μV, as was described in the work of Jerin et al. (22). In the case of recognized waves after stimulation of both ears, the upper limit of normal IAAR, 30%, was the criteria to define a normal or abnormal test in our locale (23).

Magnetic Resonance Imaging Endolymphatic Hydrops Evaluation

In all patients, exclusion of contraindications for MR imaging and/or intravenous contrast administration was checked prior to contrast administration. MR studies were performed in two 3T MR machines, either a Siemens Magnetom Vida (Siemens Healthineers, Erlangen, Germany) with a dedicated Siemens 20-channel head-coil, or a Siemens Magnetom Skyra with a dedicated Siemens 32-channel head coil. For this study, a REAL-IR sequence based on the previous publication by Naganawa et al. was performed (24). This was done on all patients, 4–5 h after the intravenous administration of a single dose of paramagnetic contrast material (0.1 ml/kg of Gadovist 1M, Bayer AG, Berlin, Germany) via an antecubital vein. Heavily T2-weighted cisternography images were also obtained in all patients for anatomical assessment.

MRI studies were evaluated by one of two different neuroradiologists, both with years of experience in EH imaging

evaluation. Dubious cases were resolved in consensus. Only one patient was excluded due to insufficient quality of imaging.

Cochlear EH was visually evaluated with a three-grade visual scale (none, mild, or severe) in accordance with previous work (25). Briefly, cochlear EH is evaluated at the axial slice closer to the modiolus and better depicting all cochlear turns (midmodiolar plane). In grade 0 (none), Reissner's membrane is not displaced, in grade 1 (mild), Reissner's membrane is displaced, but the scala media (cochlear duct) occupies less than half the scala vestibuli, and in grade 2 (severe), it occupies half or more of the scala vestibuli (**Figure 1**).

Vestibular EH was also visually evaluated but with a four-grade scale as previously published (12, 26). Briefly, vestibular EH is evaluated at the axial slice better depicting the horizontal semicircular canal (HSC). Grade 0 (none) corresponds to normal saccule and utricle, grade 1 (mild) corresponds to saccule dilatation but without fusion with the utricle, grade 2 (moderate) corresponds to dilated and fused saccule and utricle but with a clear rim of peripheric perilymph, and in grade 3 (severe), almost all the vestibules are occupied by endolymph (**Figure 1**).

The presence or absence of vestibular EH herniation toward the non-ampullar end of the HSC (27) and presence or absence of asymmetric perilymph hyperintensity were also recorded (28, 29).

Statistics

Quantitative variables are presented as mean values and standard deviation (SD), and categorical variables are presented as percentages (%).

For the comparison of baseline characteristics of the patients, the four groups according to Kimura's classification were used (FSNHL, RV, MD definite, and ISSNHL). The same distribution of patients was used for the comparison of audiometric thresholds below or above 50 dB HL, and for the findings in the vestibular examination. Parametric and non-parametric tests were used for comparison, as appropriate.

Logistic proportional hazard models were used to obtain the odds ratios (OR) for hydrops presence between groups. For this analysis, we first grouped participants into two categories: "definite MD" vs. "atypical MD + ISSNHL" (all other patients), considering the "atypical MD + ISSNHL" as the reference category. Afterward, we repeated the analysis using the ISSNHL group as the reference category and compared it with the other three groups: definite MD, FSNHL (merging its three diagnostic subcategories; no vestibular symptoms, unsteadiness, and vertigo), and RV (merging its two subcategories). We fitted an age- and sex-adjusted model and a multivariable adjusted model for potential confounders. The adjusted model included as covariates age, sex, vascular risk factors, hypertension, dyslipidemia, and diabetes.

A p-value below 0.05 was considered statistically significant. Analyses were performed with STATA version 13.0.

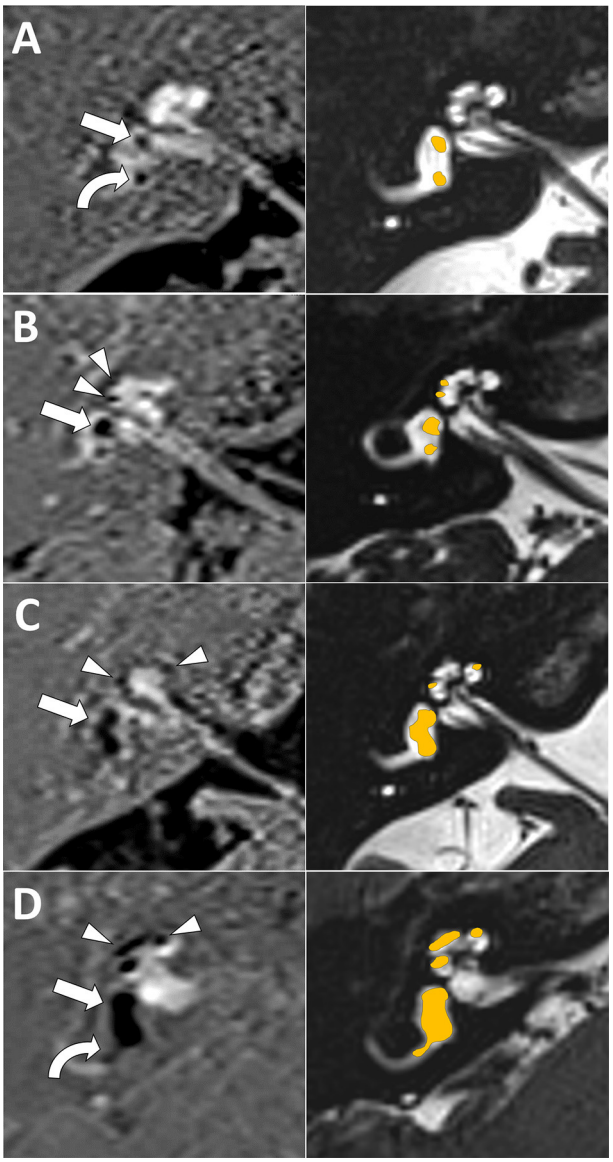

FIGURE 1 | Magnetic resonance imaging (MRI) endolymphatic hydrops (EH) visual scale examples. First column is inversion recovery with real reconstruction (REAL-IR) images for EH evaluation, second column is corresponding anatomical images with superimposed schematic colored EH as reference. **(A)** Grade 0 (normal, no EH) cochlear and vestibular EH (only normal saccule, straight arrow, and utricle, curved arrow, are seen). **(B)** Grade 1 cochlear (mild EH, arrow heads) and grade 1 vestibular EH (mild EH, with dilated saccule larger than utricle but not fused, arrow) is seen. **(C)** Grade 2 vestibular EH (moderate EH, with saccule and utricle dilated and fused, arrow); note also grade 1 cochlear EH (arrow heads). **(D)** Grade 2 cochlear (severe EH, arrow heads) and grade 3 vestibular EH (severe EH, saccule and utricle occupying almost all the vestibule, straight arrow); note also herniation toward the non-ampullary end of the horizontal semicircular canal (curved arrow).

RESULTS

We have included 170 patients of which 90 were female (52.9%) and 80 were male (47.1%). At diagnosis, the mean age was 54 ± 14 years. The right ear was affected in 78 patients, while the left was affected in 92. According to the classification used, the main patient characteristics in each group are shown in **Table 2**. Of the 170 patients included, 83 had definite MD, 38 had FSNHL (15 without vestibular symptoms, 15 with unsteadiness, and eight

TABLE 2 | Baseline characteristics of the patients.

Group		FSNHL			RV		MD definite	ISSNHL	*p*
Subgroup		**No vestibular symptoms**	**Unsteadiness**	**Vertigo**	**No HL**	**Plus HL**			
N		15	15	8	9	25	83	15	
Age, years (SD)		50.0 (14.6)	54.7 (14.5)	46.3 (22.4)	47.9 (12.8)	57.0 (16.3)	55.1 (11.9)	58.1 (7.5)	0.30
Sex (women) (%)		60	60	75	55.6	48	50.6	46.7	0.82
Side, right (%)		26.7	60.0	50.0	55.6	60.0	40.9	46.7	0.35
Disease duration, years (SD)		3.6 (4.8)	4.2 (6.7)	1.4 (1.2)	5.0 (9.8)	5.2 (6.7)	5.3 (6.2)	–	0.18
Days since last vertigo spell or hearing loss (% of the total patients in each category)	<30	6.3	6.3	5.4	4.5	11.7	55.3	13.5	0.02*
	≥30	2.2	15.6	2.2	8.9	22.2	48.9	0	
Episodes (%)	<10	100	85.7	100	88.9	73.9	79.3	–	0.59
	10–20	0	7.1	0	11.1	21.7	17.1	–	
	≥20	0	7.1	0	0	4.4	3.7	–	
Tumarkin, positive (%)		7.7	0	0	0	8.7	15.7	–	0.23
Migraine (%)	No headache	93.3	93.3	87.5	77.8	91.7	86.6	66.6	0.26
	Migraine	0	6.7	12.5	11.1	8.3	10.9	11.1	
	Tensional	6.7	0	0	11.1	0	2.4	22.2	
Vascular risk factors, presence (%)		6.7	33.3	25.0	22.2	28.0	28.1	6.7	0.36

*N, number of patients; SD, standard deviation; FSNHL, fluctuating sensorineural hearing loss; RV, recurrent vestibulopathy; MD, Ménière's disease, ISSNHL, idiopathic sudden sensorineural hearing loss; p, p-value; *statistically significant difference ($p < 0.05$); HL, hearing loss.*

with vertigo), 34 had RV (nine without SNHL and 25 with fixed SNHL), and 15 had ISSNHL. As seen from the data, the groups were homogeneous in almost all the characteristics evaluated. No statistically significant differences regarding disease duration, episodes, Tumarkin spells, migraine, or vascular risk factors are depicted. As shown in the table, for the variable "disease duration," the ISSNHL group was not included in the analysis as it was measured in days, while all others were measured in years, nor was this group included in the analysis for two other non-applicable variables: number of episodes and Tumarkin crises.

Hearing loss in each group is shown in **Figure 2** for each category of diagnosis: the results are shown for the affected and non-affected ear for each subgroup in the affected and non-affected ear, and for three categories: low frequency (0.25 kHz), mean pure tone average (PTA) for the 0.5, 1, 2, and 3 kHz and mean high frequency (4 and 6 kHz).

According to findings shown in **Table 3**, there are statistically significant differences between groups in all three frequency groups in the case of the affected ear, when comparing the percentage of patients with hearing loss lower or higher than 50 dB in each group. There are no statistically significant differences for the non-affected ear.

The results of vestibular examination are summarized in **Table 4**. As expected, there is high variability depending on the group. The rate of abnormal caloric testing is higher among RV without HL (80%) and definite MD (68.8%), but 25% of patients with FSNHL with no vestibular symptoms and 33.3% of ISSNHL showed abnormal results. The rate of abnormal vHIT in ISSNHL was also 40%. For the remaining groups, the rate of abnormal vHIT was 26.3% in the MD definite group, 25% for FSNHL plus unsteadiness, 22.2% for the FSNHL, 39.1% for the RV with HL, and 12.5% for the RV without HL group, and no abnormal vHIT for the group FSNHL with vertigo. The abnormal vHIT response for the horizontal semicircular canal of the affected ear was not specifically evaluated, but nevertheless, the discrepancies between the caloric test and vHIT (with an abnormal caloric test and a completely normal vHIT) is noteworthy in several groups. In the MD definite group, 68.8% of patients had an abnormal caloric test, but only 26.3% showed any kind of abnormality in vHIT. The rate of asymmetry in both oVEMPS and cVEMPS is higher in group FSNHL with vertigo and definite MD (33.9 and 31.6%: FSNHL with vertigo, 38.2 and 35.2%: definite MD, respectively).

Magnetic Resonance Imaging Detection of Endolymphatic Hydrops

In the clinically affected ear, cochlear hydrops was detected in 103 of 170 patients (60.6%); it was mild in 50 (29.4%) and severe in 53 (31.2%) ears. Vestibular hydrops was detected in 114 patients (67.1%), and was mild in 28 (16.5%), moderate in 52 (30.5%), and severe in 34 (20%). The distribution of findings is shown in **Table 5** and **Figure 3**. Both cochlear and vestibular hydrops were

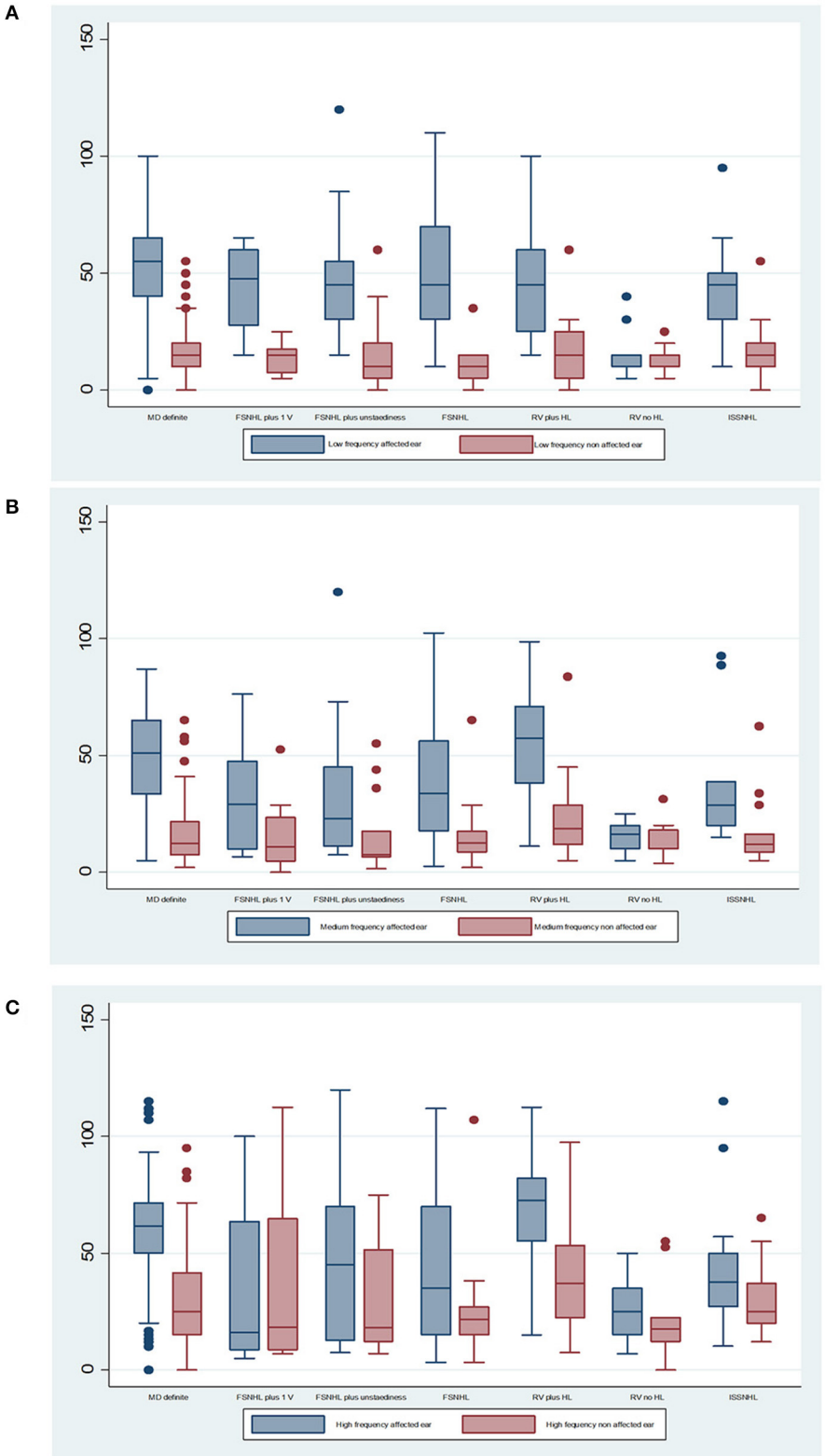

FIGURE 2 | Mean audiometric thresholds for **(A)** low frequency (0.25 kHz), **(B)** mean pure tone average (PTA) for the 0.5, 1, 2, and 3 kHz, and **(C)** mean high frequency (4 and 6 kHz). The median is the middle line of the box plot, the bottom line represents the 25th percentile, and the top line of the diagram represents the 75th percentile. The points are outlier values that indicate that the value is more than 1.5 times the interquartile range above the 75th percentile.

TABLE 3 | Distribution of patients in each category of diagnosis for audiometric threshold below or higher or equal to 50 dB hearing loss.

		FSNHL			RV		MD definite	ISSNHL	*p*
		No vestibular symptoms	Unsteadiness	Vertigo	No HL	Plus HL			
Low frequency (0.25 kHz), affected ear (%)	<50 dB	53.3	53.3	50	100	52	30.1	53.3	0.02*
	≥50 dB	46.7	46.7	50	0	48	69.9	46.7	
Low frequency (0.25 kHz), non-affected ear (%)	<50 dB	100	93.3	100	100	96	97.6	92.9	0.84
	≥50 dB	0	6.7	0	0	4	2.4	7.1	
PTA, affected ear (%)	<50 dB	73.3	80	75	100	40	48.2	86.7	0.01*
	≥50 dB	26.7	20	25	0	60	51.8	13.3	
PTA, non-affected ear (%)	<50 dB	93.3	93.3	87.5	100	96	96.4	92.8	0.9
	≥50 dB	6.7	6.7	12.5	0	4	3.6	7.1	
High frequency (4 and 6 kHz), affected ear (%)	<50 dB	66.7	60	62.5	88.9	16	24.1	73.3	0.00*
	≥50 dB	33.3	40	37.5	11.1	84	75.9	26.7	
High frequency (4 and 6 kHz), non-affected ear (%)	<50 dB	93.3	73.3	62.5	77.8	72	79.5	85.7	0.6
	≥50 dB	6.7	26.7	37.5	22.2	28	20.5	14.3	

*PTA, mean pure tone average for 0.5, 1, 2, and 3 kHz. FSNHL, fluctuating sensorineural hearing loss; RV, recurrent vestibulopathy; MD, Ménière's disease, ISSNHL, idiopathic sudden sensorineural hearing loss; p, p-value; *statistically significant difference ($p < 0.05$); HL, hearing loss.*

TABLE 4 | Summary of findings in the vestibular examination.

		FSNHL			RV		MD DEFINITE	ISSNHL
		No vestibular symptoms	Unsteadiness	Vertigo	No HL	Plus HL		
Caloric test (%)	Normal	75.0	33.3	50.0	20.0	44.4	31.3	66.7
	Abnormal	25.0	66.7	50.0	80.0	55.6	68.8	33.3
Spontaneous nystagmus (%)	Yes	8.3	21.4	87.5	11.1	26.1	37.8	14.3
	No	91.7	78.6	12.5	88.9	73.9	62.2	85.7
vHIT (%)	Normal	77.8	75.0	100.0	87.5	60.9	73.8	60.0
	Abnormal	22.2	25.0	0.0	12.5	39.1	26.3	40.0
oVEMP (mean, SD)		26.7 (11.1)	24.0 (25.2)	33.9 (17.9)	19.8 (16.9)	19.8 (16.9)	38.2 (26.9)	33.25 (23.3)
cVEMP (mean, SD)		27.4 (24.8)	27.3 (18.9)	31.6 (26.4)	15.1 (14.5)	30.8 (21.7)	35.2 (26.8)	13.0 (8.8)

FSNHL, fluctuating sensorineural hearing loss; RV, recurrent vestibulopathy; MD, Ménière's disease, ISSNHL, idiopathic sudden sensorineural hearing loss; HL, hearing loss.

detected in 94 (55%) patients in the affected ear. In **Figure 4**, the contribution (percentage) of each group to the patients without EH vs. the patients with EH is shown, and major differences are observed between groups. No EH either at the cochlea or at the vestibule was detected in 18 (47%) of the patients with FSNHL and in 11 (32%) of the patients with RV in the affected ear. In those two groups, seven (20%) and six (16%) patients, respectively, were found to have severe cochlear and/or severe vestibular EH.

Perilymphatic enhancement was observed only in the affected ear. It was detected only in the cochlea of 30 (17.6%) patients, only in the vestibule in 11 (6.5%), and in both cochlea and vestibule in 16 (9.4%). Perilymphatic enhancement was found in 13 of 46 (28.2%) ears without either cochlear or vestibular EH. Of these, three were definite MD, three were FSNHL plus unsteadiness, two were FSNHL with one vertigo spell, two were FSNHL without vestibular symptoms, two were recurrent vertigo with hearing loss, and one was ISSNHL.

In the non-affected ear, cochlear hydrops was detected in 21 (12.4%) patients; it was mild in 20 and severe in one case. Vestibular hydrops was detected in 32 (18.8%) patients and was mild in 23 (13.5%), moderate in eight (4.7%), and severe in one case (0.6%). Only in four ears were both cochlear and vestibular hydrops detected.

We observed an association between the group of patients with definite diagnosis of MD and hydrops development risk compared with patients with diagnosis of atypical MD or the ISSNHL group. Patients with definite diagnosis of MD have a significant increase in risk of hydrops in MRI compared with the atypical MD + ISSNHL group [OR 11.43 (4.5–29.02); $p < 0.001$]. After adjusting for traditional cardiovascular risk factors, we found similar results (**Table 6**). Once the reference category was

TABLE 5 | Distribution of the degree of hydrops in the affected and unaffected ear by diagnosis in number of patients.

	ISSNHL		FSNHL		RV		MD
	ISSNHL	No vestibular	Unsteadiness	1 vertigo	No SNHL	Fixed SNHL	Definite
AFF Cochlea							
No	12	10	7	6	6	11	15
Mild	3	3	8	0	3	7	26
Severe	0	2	0	2	0	7	42
AFF Vestibule							
None	12	7	8	5	5	9	10
Mild	3	6	3	1	1	2	12
Moderate	0	0	3	1	3	11	34
Severe	0	2	1	1	0	3	27
Non-AFF Cochlea							
No	11	15	12	8	7	24	72
Mild	4	0	3	0	2	1	10
Severe	0	0	0	0	0	0	1
Non-AFF Vestibule							
None	14	15	13	8	6	20	62
Mild	1	0	1	0	2	5	14
Moderate	0	0	1	0	1	0	6
Severe	0	0	0	0	0	0	1

FSNHL, fluctuating sensorineural hearing loss; RV, recurrent vestibulopathy; MD, Ménière's disease, ISSNHL, idiopathic sudden sensorineural hearing loss; SNHL, sensorineural hearing loss; AFF, affected ear; NON-AFF, non-affected ear.

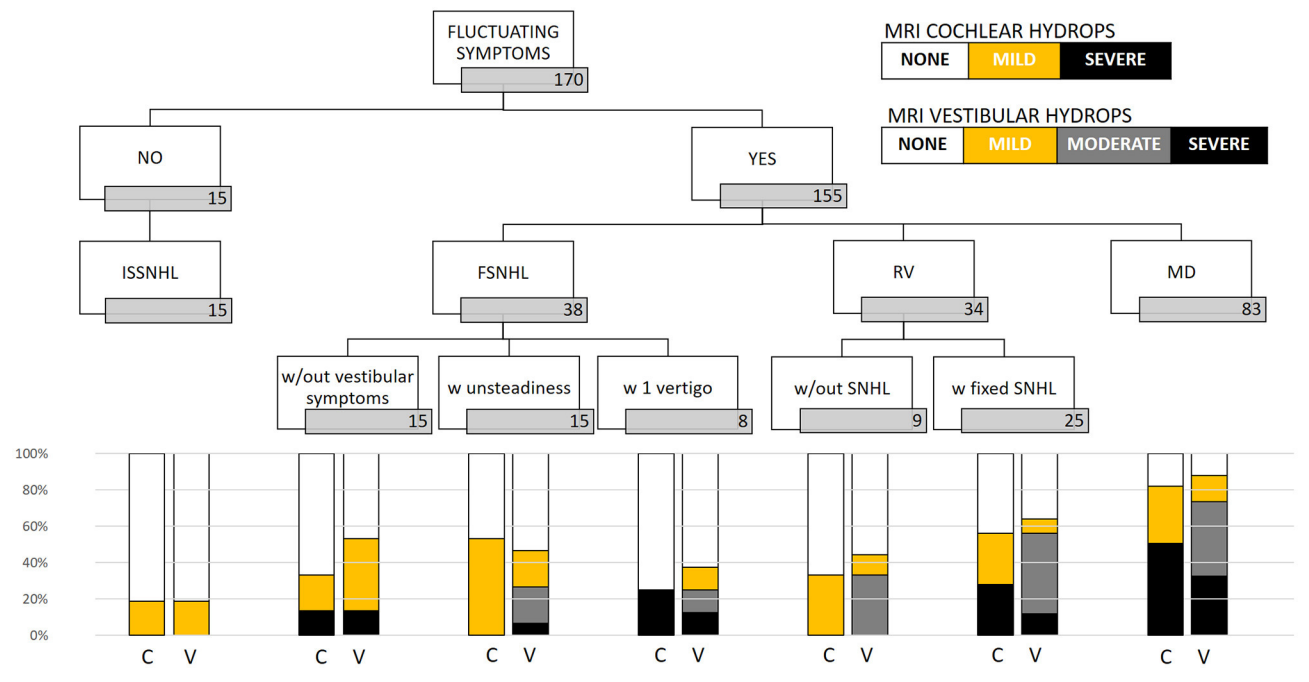

FIGURE 3 | Distribution of MRI hydrops according to category of disease in the affected ear. In the cochlea, only none, mild, and severe results are given; in the vestibule, the four (none, mild, moderate, and severe) are given. C, cochlear hydrops; V, vestibular hydrops.

changed, taking the ISSNHL group as the reference, we observed that the group with definite diagnosis of MD had a statistically significant increase in risk of hydrops [OR 55.2 (11.9–253.9); $p <$ 0.001]. To a lesser extent, we also observed a significant increase in risk for the RV group [OR 9.9 (2.1–38.9); $p = 0.003$] and for the FSNHL group [OR 5.1 (1.2–21.7); $p = 0.03$], both compared with

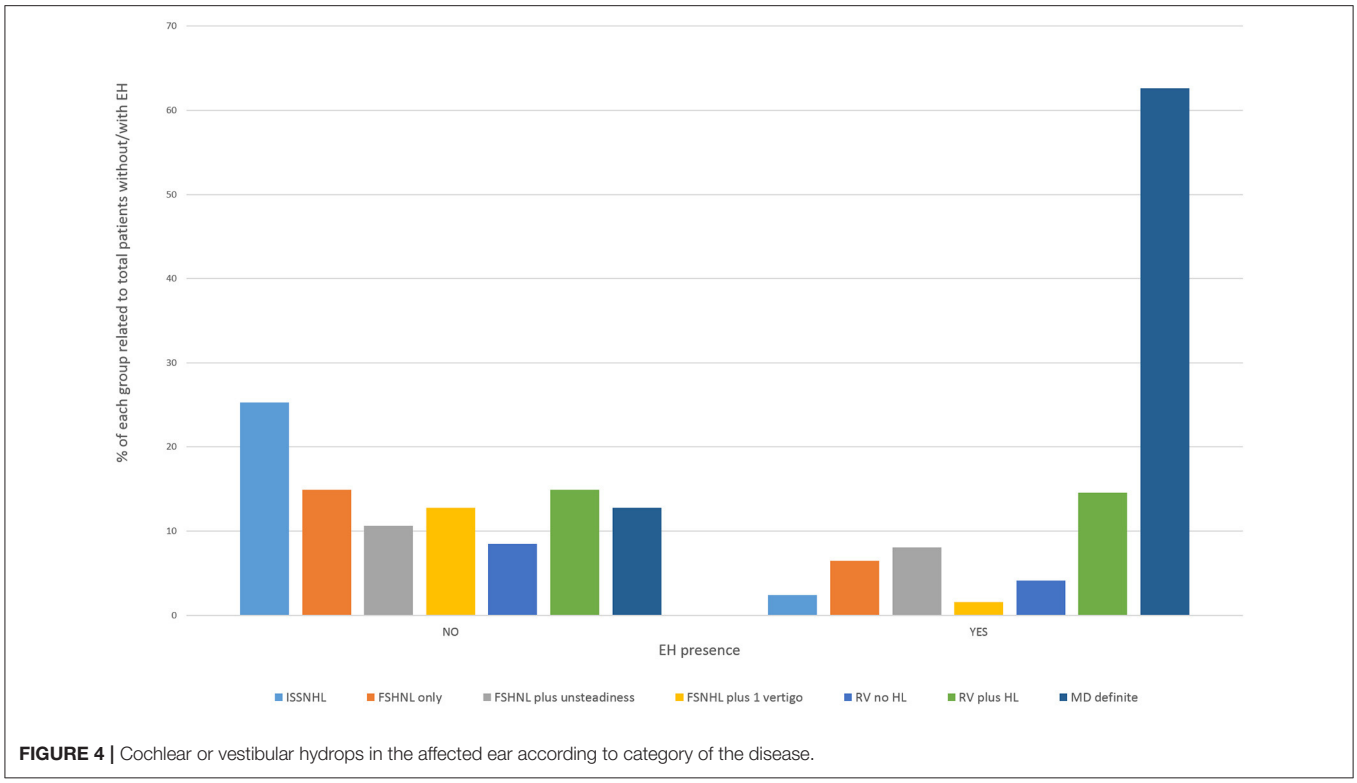

FIGURE 4 | Cochlear or vestibular hydrops in the affected ear according to category of the disease.

TABLE 6 | Odds ratio and 95% confidence intervals of hydrops according to Ménière's disease.

	MD "atypical" and ISSNHL	MD definite	*p*
N	87	83	
Adjusted for age and sex	1 (reference)	11.3 (4.4–28.8)	<0.001
Multivariable adjusted model*	1 (reference)	13.6 (4.9–37.9)	<0.001

**Multivariable adjusted: adjusted for age, sex, and vascular risk factors (hypertension, diabetes, and dyslipidaemia).*

the reference group. After adjusting for traditional cardiovascular risk factors, we found similar results in all groups (**Table 7**).

DISCUSSION

The pathological hallmark of MD is underlying EH, which was reported for the first time in 1938 (30, 31). As stated in the *Introduction* section, recent developments of high-resolution MR imaging of the inner ear have now enabled us to visualize *in vivo* EH in patients with clinical MD (32). The existing knowledge in this field supports the idea that not only is EH responsible for MD but also for other clinical malaises not fulfilling definite MD criteria (33). Previous authors (34) have also shown that, while clinical symptoms fluctuate in definite MD patients, EH is quite stable and tends to progress in the long term. We have shown in this paper that EH, as detected by MRI, is a major finding in patients with any type of inner ear disorder in which auditory or vestibular symptoms fluctuate, and its presence could, hence, imply an increased risk of evolution to definite MD in those patients.

For patients who met the criteria of definite MD (both in the AAOHNS 1995 and Barany 2015 classifications), the rate of EH is 96% in our group. These results agree with previous studies (11). The risk of EH compared with the other groups is high, especially when taking as a reference ISSNHL [OR 55.2 (11.9–253.9); $p < 0.001$]. These patients could well be screened before in particular with electrophysiological methods (frequency tuning of the VEMP), which has shown very good correlation to EH detection (21, 35).

In the case of "probable," "possible," and "atypical" MD, the norm is misunderstood. We have shown here (1) that the risk of EH among patients with definite MD is higher than in atypical MD or ISSNHL [OR 11.43 (4.5–29.2); $p < 0.001$], suggesting that the more the inner ear is clinically affected, the higher the risk an underlying EH is present and (2) that the risk of EH in the "atypical" group is lower than in the definite MD group but remains significant, taking the ISSNHL as reference. Given these findings, we believe there is an argument to promote a more detailed classification under the MD spectrum or "hydropic inner ear disease" (1). This is also based on the detailed analysis of the findings as we observe that the MRI-detected EH is more severe in cases in which the clinical presentation includes vertigo and hearing loss as shown in **Figure 3**. The presence of "severe EH" is only depicted in cases of FSNHL with vertigo (25% cochlear and 12.5% vestibular), in RV with SNHL (28% cochlear

TABLE 7 | Odds ratio and 95% confidence intervals of hydrops according to ISSNHL as the reference group.

	ISSNHL	MD definite	*P*	FSNHL	*p*	RV	*p*
N	15	83		38		34	
Adjusted for age and sex	1 (reference)	55.2 (11.9–253.9)	<0.001	5.1 (1.2–21.7)	0.03	9.9 (2.1–38.9)	0.003
Multivariable adjusted model*	1 (reference)	97.7 (15.6–611.4)	<0.001	6.9 (1.2–39.2)	0.03	14.9 (2.5–87.5)	0.003

**Multivariable adjusted: adjusted for age, sex, and vascular risk factors (hypertension, diabetes, and dyslipidemia).*

and 12% vestibular), and in definite MD (51% cochlear and 32.5% vestibular).

Over the last few years, the presence of EH in inner ear disease entities not fulfilling the clinical criteria for definite MD appears to have increased. In patients with FSNHL, previous authors demonstrated a prevalence of EH of 82.5%, being more prevalent in the vestibule than in the cochlea (36). We found cochlear EH in 39% of patients with FSNHL and vestibular EH in 47.3%. In those with RV, the number of patients with cochlear EH was 50% and with vestibular hydrops 58.8%, a very similar number to that mentioned by previous authors (37). These are patients in whom EH detection by MRI could be relevant for treatment and follow-up. From previous work, we know that the prognosis in those patients is very good (15) as the symptoms disappear, or the vertigo is resolved in 66% over a 12- to 62-month time period (38). In that work, neither age, sex, disease duration, frequency of attacks, nor time since first attack showed significant differences between the group that became inactive in the long term and those who were still active or did develop MD. The only significant difference was that, in the latter, the caloric test was much more frequently abnormal than in the former. It will be interesting to see how these patients evolve in future work.

All these data support the idea of maintaining the cochlear and vestibular categories as subtypes of MD or, at least, of introducing the location and quantity of hydrops in those cases. The utriculo-endolymphatic valve may play a role in maintaining the independence of the superior part (utricle and canals) from the inferior part (saccule and cochlear duct) (39) and be responsible of the cochlear and vestibular subtypes of MD.

Consequently, EH identification in patients with fluctuant hearing loss and recurrent vertigo cannot be dismissed in their diagnostic process. We agree that this technique should not be considered the gold standard for the diagnosis of definite MD (40) as now considered. In particular, this is observed in some cases where, after detailed medical evaluation, there is no identification of EH in the MRI as shown in our work and by others who mention that up to 10–33% of patients who fulfill the criteria for definite MD do not have MRI-demonstrable changes of hydrops (41, 42). This clinical radiologic discrepancy still reflects an incomplete understanding of the disease process and the need for additional imaging biomarkers of disease activity in MD beyond EH. It could be due to differences in phenotypes that have been defined in unilateral (4) and bilateral (5) definite MD. Additionally, taking "perilymphatic enhancement" into consideration as a marker for MD could provide a more robust diagnostic criterion (29); in our work, 13 out of 43 symptomatic ears without EH in the "atypical MD group" showed perilymphatic enhancement as the only MRI finding and, thus, could indicate added diagnostic value.

In ISSNHL, mild EH was observed in 20% of the cases. To the best of our knowledge, the evidence of EH within this clinical entity is absent (43) or very low (44). In the latter case, it was described in 2/8 of patients (one cochlear EH and the other cochlear and vestibular EH), in both cases being considered as a secondary EH. In our study, the mean time since sudden hearing loss to MRI study is always under 30 days; therefore, we cannot explain such findings as a secondary EH. Also, the rate of EH is higher in our study. This finding may be explained by two facts. First, EH is found in both affected and unaffected ears. A recent study shows how the relation of endolymphatic volume to total fluid space in the inner ear is significantly different between normal controls and of patients with ISSNHL when the cochlea of both the affected and unaffected ears were analyzed (45). Second, the imaging technique used may favor this finding. Some degree of hydrops in normal subjects is expected as slight apical cochlear EH has been described in 15% of normal subjects at the oto-pathological record (46). In our work, we used the REAL-IR MRI technique, which allows direct discrimination of bone (gray signal), perilymph (white signal), and endolymph (black signal), with robust and easy EH evaluation. Because of this, the REAL-IR sequence seems to be superior to FLAIR (in which both endolymph and bone appear black), improving slight EH detection in the cochlea where the separation between the endolymph of the scala media and the bone is minimal (47). A similar finding of slight EH has not been mentioned in normal people for the vestibule; nevertheless, should the three-grade scale for vestibular EH have been used instead of the four-grade scale, those cases with mild vestibular EH would have been considered normal. This suggests that the four-grade scale for vestibular EH could be more sensitive but less specific than the three-grade scale. We may, thus, conclude that significant EH presence in ISSNHL is still anecdotic. The continuum for sudden hearing loss has been well-evaluated in a recent nationwide survey in Japan (48) revealing that the incidence of ISSNHL was 60.9 per 100,000 population. A follow-up and in-depth study of this population may shed some light on how this malaise may evolve, including EH. As a corollary of the previous findings, we stress our interest in not incorporating normal subjects into this study as the qualitative measurement we use probably could not be able to discriminate mild cochlear EH as do quantitative newer methods (49).

That EH MRI may play a role in the diagnosis of inner ear disease is a real concept only limited by technological

accessibility, in particular, when trying to anticipate irreversible cochlear and vestibular findings, is of interest in cases of hearing loss and vertigo that may evolve into a definite MD. Our findings indicate that the expected number of patients who probably will have "definite" MD after follow-up coincides with those in whom we found both severe cochlear and severe vestibular EH. This was two (5.2%) in the case of FSNHL and three (8.8%) in the case of RV. Those patients began close follow-up and are currently being treated with diuretics. In a similar way, it has been recently shown that, in patients with ISSNHL, an increase in the endolymphatic space could render them prone to developing FSNHL (45). Also, there is a substantial number of patients with cochlear MD who will proceed to definite MD, and previous work has shown that this may occur in almost 80% of cases (50).

At this point, there may be some confusion regarding the different ways of classifying the severity of EH in MRI, and there is urgent need for agreement on a common methodology. Regarding imaging, in the case of cochlear EH, a two-grade (absent or present) or a three-grade (absent, mild, or severe) classification system is generally used. In the case of vestibular EH, a three-grade (absent, mild, or severe) classification system has been proposed by some authors (25, 42) while a four-grade scale (absent, mild, moderate, or severe) has also been used (26, 29, 51). Unfortunately, it is still not possible to evaluate EH of the semicircular canals due to its very small size and lack of spatial resolution. Occasionally, increased asymmetric hyperintensity of the perilymph is additionally found both in cochlear and vestibular compartments. This finding is interpreted as an increased diffusion of contrast material to the perilymph due to altered permeability of the blood–labyrinth barrier, presumably secondary to active inflammation (28, 29). In addition, herniation of vestibular EH toward the non-ampullar end of the horizontal semicircular canal (HSC) has been described both in histopathology and EH MRI (27). The relevance of all these MRI findings, both in themselves and in combination, requires standardization.

Regarding the vestibular tests, a discrepancy between the caloric test and vHIT was noteworthy in some groups, especially MD, as previously published (26, 52). Analysis of this dissociated response (with an altered caloric test but normal vHIT results for the HSC of the affected ear despite analyzing the function of the same vestibular organ) was not the primary goal of this study, and specific alteration of the horizontal semicircular canal was not recorded for comparison with a caloric test (only global results of normal or abnormal vHIT), and so it was not further analyzed. Nevertheless, the discrepancy between the caloric test result and vHIT has even been proposed as a marker of MD. With the results of this work, we must now consider that it may be much more common than expected also in other groups and probably be a closer relationship to hydrops than to MD itself. Also, alternative analysis of audiovestibular tests as the total number of involved vestibular end organs as done recently (9) is a promising means for evaluation of the severity of MD, and possible correlation with EH in MD and other groups should be explored in a prospective way.

As a limitation of the study, we must mention that EH was evaluated according to semiquantitative visual scales. Although volumetric evaluation of EH has been reported (53), it is not normally used in routine clinical practice, mainly because there is no dedicated software that has been developed. However, recent advances in the use of artificial intelligence with deep learning (still to be circulated) represent a major step forward for the purpose of providing an objective measure (54). Nonetheless, the correlation obtained between semiquantitative scales and volumetry is very good (55).

In this study, clinical features such as age, sex, side, disease duration, migraine, and vascular risk factors have a similar distribution among different clinical entities. Thus, patients included are homogeneous, minimizing the risk of bias in the interpretation of results so we do not consider this to be a relevant limitation.

Another limitation is that the categories were taken from an old reference, and a proper "vestibular migraine" category was not included. Of those in the group "Atypical MD Vestibular," five of 34 could have been classified as definite vestibular migraine, after reviewing the records. Only two, one in each of the categories here used, showed vestibular hydrops, which in both cases was "moderate" (56).

The transversal nature of the study also limits its conclusions, asking for longitudinal prospective studies evaluating the clinical and radiological evolution of these patients and the possible association of MRI EH in non-definite MD patients and posterior transformation to definite MD.

Also, potential correlations between audiovestibular tests and the localization of EH or with the presence of EH herniation in the semicircular canals were not analyzed and could be evaluated in future works.

CONCLUSION

MRI EH is found in a percentage of patients with fluctuating audiovestibular symptoms not fulfilling the actual diagnostic criteria for definite MD. This percentage is variable depending on the audiovestibular symptoms, from a low percentage of only slight (and even questionable) EH in ISSNHL to a moderate percentage in patients with FSNHL with one vertigo crisis or recurrent vertigo with fixed SNHL. The percentages of severe cochleovestibular EH are similar to the current reported percentages of progression to definite MD in those groups, suggesting that presence of EH by MRI could be related to the risk of progression to definite MD, and advising longitudinal follow-up studies already under way. MR EH imaging in these patients is, thus, recommended.

DATA AVAILABILITY STATEMENT

The datasets presented in this article are not readily available because they have not been uploaded to a repository, but as previously stated questions related to the accuracy or integrity of any part of the work will be appropriately investigated and resolved. Requests to access the datasets should be directed to Nicolás Pérez-Fernández, nperezfer@unav.es.

ETHICS STATEMENT

Ethical review and approval was not required for the study on human participants in accordance with the local legislation and institutional requirements. Written informed consent for participation was not required for this study in accordance with the national legislation and the institutional requirements.

AUTHOR CONTRIBUTIONS

All authors made substantial contributions to the conception and design of the work, data acquisition, analysis and/or interpretation, work draft, and critical review. All authors approved the final version to be published. All authors agreed to be accountable for the content of the work in ensuring that questions related to the accuracy or integrity of any part of the work are appropriately investigated and resolved.

FUNDING

This study was, in part, supported by the Proyectos de investigacion en salud (AES 2019). Modalidad proyectos en salud, PI19/00414, Instituto de Salud Carlos III, Ministerio de Ciencia, Innovación y Universidades, Government of Spain.

REFERENCES

1. Gurkov R, Hornibrook J. On the classification of hydropic ear disease (Menière's disease). *HNO.* (2018) 66:455–63. doi: 10.1007/s00106-018-0488-3
2. Olson J, Wolfe J. Comparison of subjective symptomatology and responses to harmonic acceleration in patients with Menière's disease. *Ann Otol Rhinol Laryngol Suppl.* (1981) 90(4 Pt3):15–7. doi: 10.1177/0003489481090 4S205
3. Perez N, Espinosa J, Fernandez S, Garcia-Tapia R. Use of distortion-product otoacoustic emissions for auditory evaluation in Menière's disease. *Eur Arch Otorhinolaryngol.* (1997) 254:329–42. doi: 10.1007/BF02630725
4. Frejo L, Martin-Sanz E, Teggi R, Trinidad G, Soto-Varela A, Santos-Perez S, et al. Extended phenotype and clinical subgroups in unilateral Meniere disease: a cross-sectional study with cluster analysis. *Clin Otolaryngol.* (2017) 42:1172–80. doi: 10.1111/coa.12844
5. Frejo L, Soto-Varela A, Santos-Perez S, Aran I, Batuecas-Caletrio A, Perez-Guillen V, et al. Clinical subgroups in bilateral Meniere Disease. *Front Neurol.* (2016) 7:182. doi: 10.3389/fneur.2016.00182
6. Marques P, Perez-Fernandez N. Bedside vestibular examination in patients with unilateral definite Ménière's disease. *Acta Otolaryngol.* (2012) 132:498–504. doi: 10.3109/00016489.2011.646357
7. Belinchon A, Perez-Garrigues H, Tenias J, Lopez A. Hearing assessment in Menière's disease. *Laryngoscope.* (2011) 121:622–6. doi: 10.1002/lary. 21335
8. Montes-Jovellar L, Guillen-Grima F, Perez-Fernandez N. Cluster analysis of auditory and vestibular test results in definite Menière's disease. *Laryngoscope.* (2011) 121:1810–7. doi: 10.1002/lary.21844
9. Huang S, Zhou H, Zhou H, Zhang J, Feng Y, Yu D, et al. A new proposal for severity evaluation of Menière's disease by using the evidence from a comprehensive battery of auditory and vestibular tests. *Front Neurol.* (2020) 11:785. doi: 10.3389/fneur.2020.00785
10. Naganawa S, Satake H, Kawamura M, Fukatsu H, Sone M, Nakashima T. Separate visualization of endolymphatic space, perilymphatic space and bone by a single pulse sequence; 3D-inversion recovery imaging utilizing real reconstruction after intratympanic Gd-DTPA administration at 3 Tesla. *Eur Radiol.* (2008) 18:920–4. doi: 10.1007/s00330-008-0854-8
11. Naganawa S, Nakashima T. Visualization of endolymphatic hydrops with MR imaging in patients with Ménière's disease and related pathologies: current status of its methods and clinical significance. *Jpn J Radiol.* (2014) 32:191–204. doi: 10.1007/s11604-014-0290-4
12. Bernaerts AA, De Foer B. Imaging of Ménière Disease. *Neuroimaging Clin N Am.* (2019) 29:19–28. doi: 10.1016/j.nic.2018.09.002
13. Ishiyama G, Lopez IA, Sepahdari AR, Ishiyama A. Meniere's disease: histopathology, cytochemistry, and imaging. *Ann N Y Acad Sci.* (2015) 1343:49–57. doi: 10.1111/nyas.12699
14. Kim S, Nam GS, Choi J. Pathophysiologic findings in the human endolymphatic sac in endolymphatic hydrops: functional and molecular evidence. *Ann Otol Rhinol Laryngol.* (2019) 128(Suppl. 6):76S83S. doi: 10.1177/0003489419837993
15. Lee H, Ahn S, Jeon S, Kim J, Park J, Hur D, et al. Clinical characteristics and natural course of recurrent vestibulopathy: a long-term follow-up study. *Laryngoscope.* (2012) 122:883–6. doi: 10.1002/lary.23188
16. Oishi N, Inoue Y, Saito H, Kanzaki S, Kanzaki J. Long-term prognosis of low-frequency hearing loss and predictive factors for the 10-year outcome. *Otolaryngol Head Neck Surg.* (2010) 142:565–9. doi: 10.1016/j.otohns.2009.12.006
17. Committee on Hearing and Equilibrium. Committee on Hearing and Equilibrium Guidelines for the Diagnosis and Evaluation of Therapy in Meniere's Disease. *Otolaryngol Head Neck Surg.* (1995) 113:181–5. doi: 10.1016/S0194-5998(95)70102-8
18. Lopez-Escamez JA, Carey J, Chung WH, Goebel JA, Magnusson M, Mandala M, et al. Diagnostic criteria for Menière's disease. *J Vestib Res.* (2015) 25:1–7. doi: 10.3233/VES-150549
19. Kimura H, Aso S, Watanabe Y. Prediction of progression from atypical to definite Ménière's disease using electrocochleography and glycerol and furosemide tests. *Acta Otolaryngol.* (2003) 123:388–95. doi: 10.1080/0036554021000028079
20. Herrera M, Garcia-Berrocal JR, Garcia-Arumi A, Lavilla MJ, Plaza G. Update on consensus on diagnosis and treatment of idiopathic sudden sensorineural hearing loss. *Acta Otorrinolaringol Esp.* (2019) 70:290–300. doi: 10.1016/j.otoeng.2018.04.007
21. Walsh R, Bath A, Bance M, Keller A, Rutka J. Consequences to hearing during the conservative management of vestibular schwannomas. *Laryngoscope.* (2000) 110:250–5. doi: 10.1097/00005537-200002010-00012
22. Jerin C, Berman A, Krause E, Ertl-Wagner B, Gürkov R. Ocular vestibular evoked myogenic potential frequency tuning in certain Menière's disease. *Hear Res.* (2014) 310:54–9. doi: 10.1016/j.heares.2014.02.001
23. Guajardo-Vergara C, Perez-Fernandez N. Air and bone stimulation in vestibular evoked myogenic potentials in patients with unilateral Ménière's disease and in controls. *Hear Balance Commun.* (2019) 17:170–8. doi: 10.1080/21695717.2019.1591009
24. Naganawa S, Kawai H, Taoka T, Sone M. Improved 3D-real inversion recovery: a robust imaging technique for endolymphatic hydrops after intravenous administration of gadolinium. *Magn Reson Med Sci.* (2019) 18:105–8. doi: 10.2463/mrms.bc.2017-0158
25. Nakashima T, Naganawa S, Pyykko I, Gibson W, Sone M, Nakata S, et al. Grading of endolymphatic hydrops using magnetic resonance imaging. *Acta Otolaryngol.* (2009) 129:5–8. doi: 10.1080/00016480902729827
26. Perez-Fernandez N, Dominguez P, Manrique-Huarte R, Calavia D, Arbizu L, Garcia-Eulate R, et al. Endolymphatic hydrops severity in magnetic resonance imaging evidences disparate vestibular test results. *Auris Nasus Larynx.* (2019) 46:210–7. doi: 10.1016/j.anl.2018.08.014
27. Gürkov R, Flatz W, Louza J, Strupp M, Ertl-Wagner B, Krause E. Herniation of the membranous labyrinth into the horizontal semicircular canal is correlated with impaired caloric response in Ménière's disease. *Otol Neurotol.* (2012) 33:1375–9. doi: 10.1097/MAO.0b013e318268d087
28. van Steekelenburg J, van Weijnen A, de Pont L, Vijlbrief O, Bommeljé C, Koopman J, et al. Value of endolymphatic hydrops and perilymph signal

intensity in suspected Ménière disease. *Am J Neuroradiol.* (2020) 41:529–34. doi: 10.3174/ajnr.A6410
29. Bernaerts A, Vanspauwen R, Blaivie C, van Dinther J, Zarowski A, Wuyts F, et al. The value of four stage vestibular hydrops grading and asymmetric perilymphatic enhancement in the diagnosis of Menière's disease on MRI. *Neuroradiology.* (2019) 61:421–9. doi: 10.1007/s00234-019-02155-7
30. Hallpike C, Cairns H. Observation on the pathology of Menierés syndrome. *Proc R Soc Med.* (1938) 31:131736. doi: 10.1177/003591573803101112
31. Yamakawa K. Hearing organ of a patient who showed Meniere's symptoms (in Japanese). *J Otolaryngol Soc Jpn.* (1938) 44:2310—2.
32. Nakashima T, Naganawa S, Sugiura M, Teranishi M, Sone M, Hayashi H, et al. Visualization of endolymphatic hydrops in patients with Meniere's disease. *Laryngoscope.* (2007) 117:415–20. doi: 10.1097/MLG.0b013e31802c300c
33. Gürkov R. Menière and friends: imaging and classification of hydropic ear disease. *Otol Neurotol.* (2017) 38:e539–44. doi: 10.1097/MAO.0000000000001479
34. Jerin C, Floerke S, Maxwell R, Gürkov R. Relationship between the extent of endolymphatic hydrops and the severity and fluctuation of audiovestibular symptoms in patients with Meniere's disease and MRI evidence hydrops. *Otol Neurotol.* (2018) 39:120–30. doi: 10.1097/MAO.0000000000001681
35. Murofushi T, Tsubota M, Kanai Y, Endo H, Ushio M. Association of cervical vestibular-evoked myogenic potential tuning property test results with MRI findings of endolymphatic hydrops in Meniere's disease. *Eur Arch Otorhinolaryngol.* (2020). doi: 10.1007/s00405-020-06410-z. [Epub ahead of print].
36. Pyykkö I, Nakashima T, Yoshida T, Zou J, Naganawa S. Meniere's disease: a reappraisal supported by a variable latency of symptoms and the MRI visualisation of endolymphatic hydrops. *BMJ Open.* (2013) 3:e001555. doi: 10.1136/bmjopen-2012-001555
37. Attyé A, Dumas G, Troprès I, Roustif M, Karkas A, Banciu E, et al. Recurrent peripheral vestibulopathy: is MRI useful for the diagnosis of endolymphatic hydrops in clinical practice? *Eur Radiol.* (2015) 25:3043–9. doi: 10.1007/s00330-015-3712-5
38. van Leeuwen R, Bruintjes T. Recurrent vestibulopathy: natural course and prognostic factors. *J Laryngol Otol.* (2010) 124:19–22. doi: 10.1017/S0022215109991009
39. Schuknecht H, Belal A. The utriculo-endolymphatic valve: its functional significance. *J Laryngol Otol.* (1975) 89:985–96. doi: 10.1017/S0022215100081305
40. Liu Y, Yang J, Duan M. Current status on researches of Meniere's disease: a review. *Acta Otolaryngol.* (2020) 140:808–12. doi: 10.1080/00016489.2020.1776385
41. Pakdaman M, Ishiyama G, Ishiyama A, Peng K, Kim H, Pope W, et al. Blood-labyrinth barrier permeability in Menière disease and idiopathic sudden sensorineural hearing loss: findings on delayed postcontrast 3D-FLAIR MRI. *Am J Neuroradiol.* (2016) 37:1903–8. doi: 10.3174/ajnr.A4822
42. Baráth K, Schuknecht B, Naldi A, Schrepfer T, Bockisch C, Hegemann S. Detection and grading of endolymphatic hydrops in Menière disease using MR imaging. *Am J Neuroradiol.* (2014) 35:1387–92. doi: 10.3174/ajnr.A3856
43. Katayama N, Yamamoto M, Teranishi M, Naganawa S, Nakata S, Sone M, et al. Relationship between endolymphatic hydrops and vestibular-evoked myogenic potential. *Acta Otolaryngol.* (2010) 130:917–23. doi: 10.3109/00016480903573187
44. Horii A, Osaki Y, Kitahara T, Imai T, Uno A, Nishike S. Endolymphatic hydrops in Meniere's diseas detected by MRI after intratympanic administration of gadolinium: comparison with sudden deafness. *Acta Otolaryngol.* (2011) 113:602–9. doi: 10.3109/00016489.2010.548403
45. Inui H, Sakamoto T, Ito T, Kitahara T. Magnetic resonance imaging of endolymphatic space in patients with sensorineural hearing loss: comparison between fluctuating and idiopathic sudden sensorineural hearing loss. *Acta Otolaryngol.* (2020) 140:345–50. doi: 10.1080/00016489.2020.1720919
46. Yamashita T, Schuknecht H. Apical endolymphatic hydrops. *Arch Otolaryngol.* (1982) 109:463–6. doi: 10.1001/archotol.1982.00790560001001
47. Suarez-Vega V, Dominguez P, Caballeros-Lam F, Leal J, Perez-Fernandez N. Comparison between high-resolution 3D-IR with real reconstruction and 3D-flair sequences in the assessment of endolymphatic hydrops in 3 tesla. *Acta Otolaryngol.* (2020) 140:883–8. doi: 10.1080/00016489.2020.1792550
48. Yoshida T, Sone M, Kitoh R, Nishio K, Ogawa K, Kanzaki S, et al. Idiopathic sudden sensorineural hearing loss and acute low-tone sensorineural hearing loss: a comparison of the results of a nationwide epidemiological survey in Japan. *Acta Otolaryngol.* (2017) 137:S38–43. doi: 10.1080/00016489.2017.1297539
49. Gerb J, Ahmadi S, Kierig E, Ertl-Wagner B, Dieterich M, Kirsh V. VOLT: a novel open-source pipeline for automatic segmentation of endolymphatic space in inner ear MRI. *J Neurol.* (2020) 267(Suppl. 1):185–96. doi: 10.1007/s00415-020-10062-8
50. Kitahara M, Takeda T, Yazawa Y, Matsubara H, Kitano H. Pathophysiology of Meniere's disease and its subvarieties. *Acta Otolaryngol Suppl.* (1984) 406:52–5. doi: 10.3109/00016488309123002
51. Gürkov R, Flatz W, Louza J, Strupp M, Ertl-Wagner B, Krause E. In vivo visualized endolymphatic hydrops and inner ear functions in patients with electrocochleographically confirmed Ménière's disease. *Otol Neurotol.* (2012) 33:1040–5. doi: 10.1097/MAO.0b013e31825d9a95
52. Hannigan I, Welgampola M, Watson S. Dissociation of caloric and head impulse tests: a marker of Meniere's disease. *J Neurol.* (2021) 268:431–9. doi: 10.1007/s00415-019-09431-9
53. Gürkov R, Berman A, Dietrich O, Flatz W, Jerin C, Krause E, et al. MR volumetric assessment of endolymphatic hydrops. *Eur Radiol.* (2015) 25:585–95. doi: 10.1007/s00330-014-3414-4
54. Cho Y, Cho K, Park C, Chung M, Kim J, Kim K, et al. Automated measurement of hydrops ratio from MRI in patients with Ménière's disease using CNN-based segmentation. *Sci Rep.* (2020) 10:7003. doi: 10.1038/s41598-020-63887-8
55. Homann G, Vieth V, Weiss D, Nikolaou K, Heindel W, Notohamiprodjo M, et al. Semi-quantitative vs. volumetric determination of endolymphatic space in Menière's disease using endolymphatic hydrops 3T-HR-MRI after intravenous gadolinium injection. *PLoS ONE.* (2015) 10:e0120357. doi: 10.1371/journal.pone.0120357
56. Lempert T, Olesen J, Furman J, Waterston J, Seemungal B, Carey J, et al. Vestibular migraine: diagnostic criteria. *J Vestib Res.* (2012) 22:167–72. doi: 10.3233/VES-2012-0453

Conflict of Interest: The authors declare that the research was conducted in the absence of any commercial or financial relationships that could be construed as a potential conflict of interest.

frontiers in Surgery

ORIGINAL RESEARCH
published: 04 June 2021
doi: 10.3389/fsurg.2021.673811

Vestibular Endolymphatic Hydrops Visualized by Magnetic Resonance Imaging and Its Correlation With Vestibular Functional Test in Patients With Unilateral Meniere's Disease

Yupeng Liu [1,2,3†], Fan Zhang [1,2,3†], Baihui He [1,2,3], Jingchun He [1,2,3], Qing Zhang [1,2,3], Jun Yang [1,2,3] and Maoli Duan [4,5*]*

[1] Department of Otorhinolaryngology-Head & Neck Surgery, Xinhua Hospital, Shanghai Jiaotong University School of Medicine, Shanghai, China, [2] Ear Institute, Shanghai Jiaotong University School of Medicine, Shanghai, China, [3] Shanghai Key Laboratory of Translational Medicine on Ear and Nose Diseases, Shanghai, China, [4] Ear Nose and Throat Patient Area, Trauma and Reparative Medicine Theme, Karolinska University Hospital, Stockholm, Sweden, [5] Division of Ear, Nose and Throat Diseases, Department of Clinical Science, Intervention and Technology, Karolinska Institutet, Stockholm, Sweden

OPEN ACCESS

Edited by:
Robert Gürkov,
Bielefeld University, Germany

Reviewed by:
Yuka Morita,
Niigata University, Japan
Sanjeev Mohanty,
MGM Health Care, India

***Correspondence:**
Jun Yang
yangjun@xinhuamed.com.cn
Maoli Duan
maoli.duan@ki.se

[†] These authors have contributed equally to this work and share first authorship

Specialty section:
This article was submitted to Otorhinolaryngology - Head and Neck Surgery, a section of the journal Frontiers in Surgery

Received: 28 February 2021
Accepted: 10 May 2021
Published: 04 June 2021

Citation:
Liu Y, Zhang F, He B, He J, Zhang Q, Yang J and Duan M (2021) Vestibular Endolymphatic Hydrops Visualized by Magnetic Resonance Imaging and Its Correlation With Vestibular Functional Test in Patients With Unilateral Meniere's Disease. Front. Surg. 8:673811. doi: 10.3389/fsurg.2021.673811

Background: Currently, 3 Tesla-MRI following intratympanic gadolinium injection has made it possible to assess the existence and the severity of hydrops in each compartment of the endolymphatic spaces *in vivo*. However, the relationship between vestibular endolymphatic hydrops (EH) visualized by MRI and vestibular functional tests, especially the correlation between caloric test, video-head impulse test, and semicircular canal hydrops, has not been well-investigated.

Objective: The purpose of this study is to investigate the relationship between the severity of EH in each compartment of otoliths and semicircular canal and the results of vestibular functional tests.

Methods: In this retrospective study, we performed three-dimensional fluid-attenuated inversion recovery (3D-FLAIR) sequences following intratympanic gadolinium injection in 69 unilateral patients with definite Menière's disease. Vestibular and lateral semicircular canal hydrops was graded on MRI using a four grade criterion. All patients underwent pure-tone audiometry, cervical vestibular evoked myogenic potential (cVEMP), ocular vestibular evoked myogenic potential (oVEMP), caloric test and video head impulse test (vHIT). The latency, amplitude and asymmetry ratio of VEMP, canal paresis (CP) and vestibulo-ocular reflex (VOR) gain of lateral semicircular canal of vHIT were collected. The correlation analysis were performed between the parameters of function test and EH.

Results: Vestibular EH showed correlations with the duration of disease ($r = 0.360$) and pure tone average ($r = 0.326$). AR of cVEMP showed correlations with Vestibular EH ($r = 0.407$). CP ($r = 0.367$) and VOR gain of lateral semicircular canal at 60 ms ($r = 0.311$) showed correlations with lateral semicircular canal hydrops.

Conclusion: EH in different compartments is readily visualized by using 3D-FLAIR MRI techniques. The degree of vestibular EH correlated with AR of cVEMP and EH in the semicircular canal ampullar affects the caloric and vHIT response in patients with unilateral Meniere's disease.

Keywords: Meniere's disease, vestibular function, MRI, endolymphatic hydrops, VEMP, vHIT, caloric test

INTRODUCTION

Ménière's disease (MD) is an idiopathic inner ear, which is characterized by recurrent attacks of vertigo, fluctuating hearing loss, tinnitus, and ear fullness. The Etiology of the disease is unclear and the pathological feature is endolymphatic hydrops (EH) (1). At present, a clinical diagnosis of MD is mainly based on the combination of medical history and auditory-vestibular function examination. With the combined application of different vestibular function examinations, clinicians can evaluate the function of saccule, the utricle, the low frequency of semicircular canal and the high frequency of semicircular canal separately by cervical vestibular-evoked myogenic potentials (cVEMP), ocular vestibular-evoked myogenic potentials (oVEMP), Caloric test, and video-head impulse test (vHIT) (2–4). Since 2007, the morphological assessment of EH in MD patients on magnetic resonance imaging (MRI) has been realized by the application of 3-dimensional fluid-attenuated inversion recovery (3D-FLAIR) sequence following the intratympanic injection of gadolinium (Gd) by Nakashima et al. (5). With the development of imaging technology, various structures of the inner ear have been observed by intratympanic or intravenous injection of contrast media.

In previous studies, many authors have reported the correlation between the degree of vestibular hydrops and vestibular function examination results in MD patients. But the conclusion is inconsistent. Guo et al. (6) reported that the asymmetry ratio (AR) of oVEMP showed correlation with the severity of vestibular EH. Katayama et al. (7) confirmed that EH was significantly associated with the disappearance of cVEMP. On the contrary, Kahn et al. (8) concluded that no significant correlation between the presence of EH and vestibular function was found in the research. The correlation between the caloric test and EH is also inconclusive. Kato et al. (9) presented that there was no significant correlation between the caloric test results and the degree of EH in the vestibule, or the lateral semicircular canal ampulla. While, Sluydts et al. (10) and Guo et al. (6) reported that the abnormal caloric tests was correlated with the severity of vestibular. Moreover, few studies have focused on the relationships between semicircular canal hydrops and vestibular-ocular reflex (VOR) recorded by video head impulse test (vHIT) (11, 12).

The purpose of this study is to elucidate the relationships between the results from cVEMP, oVEMP, the caloric test, vHIT, and EH visualized by Gd-enhanced MRI in patients with unilateral MD.

MATERIALS AND METHODS

Patients

This study was approved by the Ethics Committee of Xinhua Hospital, Shanghai Jiaotong University School of Medicine. Written informed consent was obtained from each participant. We retrospectively reviewed the medical records of 69 patients diagnosed with definite unilateral MD who were admitted to Department of Otolaryngology-Head and Neck Surgery, Xinhua Hospital, Shanghai Jiaotong University School of Medicine from March, 2018 to December, 2020. The diagnostic criteria was based on the 2015 consensus of the Barany Society (13). The inclusion criteria were as follows: (1) unilateral MD patients without complains, such as tinnitus, ear fullness, or hearing loss in the contralateral ears; (2) complete medical history record with auditory-vestibular function examinations and MRI. The exclusion criteria were as follows: (1) chronic otitis media or other middle or inner ear disease history; (2) history of middle or inner ear surgery; (3) receipt of intratympanic gentamicin or dexamethasone treatment; (4) use of vasodilators or diuretics in the previous 2 weeks; (5) patients with claustrophobia, pregnancy, or Gd allergy.

Intratympanic Gd Injection and MRI

As our previous studies described, the Gd contrast medium (Omniscan, Xudonghaipu Pharmaceutical Co. Ltd, Shanghai, China) was diluted 8-fold with saline (v/v, 1: 7). Approximately 0.4–0.6 ml of the diluted Gd was injected intratympanically. The injection was performed under a microscope. The patient then was placed in the supine position for 60 min (14).

Twenty-four hours after the Gd injection, MRI scans were performed with a 3.0 Tesla MR scanner (UMR 770, united-imaging, Shanghai, China), using a 24-channel head coil. 3D-FLAIR imaging was subsequently performed. The scan parameters for the 3D-FLAIR sequence were as follows: time of repetition = 6,500 ms, time of echo = 286.1 ms, time of inversion = 1,950 ms, flip angle = 67°, slice thickness = 0.6 mm, echo train length = 160, field of view = 200 * 200 mm, and matrix size = 256 * 256, voxel size = 0.78 * 0.78 * 1.1 mm. The scan time was 6 min 11 s. Three dimensional heavily T2-weighted spectral attenuated inversion recovery (3D-T2-SPAIR) sequence was also performed with the following parameters: voxel size = 0.65 * 0.52 * 0.76 mm, scan time = 4 min 30 s, TR = 1,300 ms, TE = 254.7 ms, flip angle = 110°, slice thickness = 0.4 mm, field of view = 200 * 200 mm, and matrix size = 384 * 384 (15).

Image Analysis

The images were evaluated by an experienced neuroradiologist who was blinded to the patient's information. The vestibule and semicircular canal were separately evaluated. The vestibular part was evaluated using the semi-quantification four-grade system proposed by Bernaerts et al. (16). In brief, a normal vestibule is described as when the saccule and utricle are visibly separately and take less than half of the surface of the vestibule. When the saccule become equal or larger than the utricle, but is not yet confluent with the utricle, vestibular hydrops grade I is defined. When there is a confluence of the saccule and utricle with still a peripheral rim enhancement of the perilymphatic space, vestibular hydrops grade II is defined. When the perilymphatic enhancement is invisible, vestibular hydrops grade III is defined. The lateral semicircular canal was evaluated by the four-grade system proposed by our team in the previous study (15). We defined Grade 0 as no hydrops when a small visible herniation which was 1/3 less than the semicircular canal with perilymph surrounding, a larger herniation (>1/3) with hydrops as Grade I and the total invisibility of crura, which often accompany the stenosis of canals as Grade II. If all semicircular canals were invisible, we defined as Grade III. Images of each grade of vestibular and lateral semicircular canal were demonstrated in **Figure 1**.

Audio-Vestibular Functional Tests

Audiometry

Pure-tone audiometry was performed in a soundproof room with the use of an audiometer (Type Madsen, Astera, Denmark). The pure-tone average (PTA) is the average of the 0.5, 1, and 2 kHz air conduction thresholds. The calculation is based on the MD guideline of China published in 2017 (17).

VEMP

VEMP tests were performed with a Bio-logic Navigator PRO auditory brainstem response diagnosis system. For cVEMP, electrodes were placed on the middle of each sternocleidomastoid muscle. The reference electrode was placed on the middle of clavicular joint and the ground electrode was placed on the nasion. The resistance between the electrodes was controlled at $<5\ k\Omega$. Tone bursts (95 dB normal hearing level [nHL], 500 Hz, rise/fall time1 ms, plateau time 2 ms, stimulation frequency 5 Hz, superposition 50 times) were delivered through headphones. Patients are instructed to raise their head from the pillow and supine head 30° after hearing a single stimulus to maintain sternocleidomastoid muscle in tension until the stimulus stops. A well-repeated wave form with p13 and n23 was defined as "Elicited." Absence of a meaningful wave form with p13 and n23 was defined as no response. The P13 potential was identified as the first positive peak in the waveform, N23 was identified as the first negative peak in the waveform, and the peak-to-peak amplitude was the P13–N23 amplitude. The latency of P13 and N23, the amplitude of P13 and N23, and the amplitude of the first positive–negative peak (P13–N23) was recorded. The percent VEMP asymmetry ratio (AR) was calculated with the following formula using the amplitude of p13–n23 on the affected side (Aa) and that on the unaffected side (Au): VEMP asymmetry (%) = 100 (Au – Aa)/(Au + Aa) %. When only one side of the oVEMP was absent, the AR was calculated as 100%. A value of AR > 40% was considered abnormal (4).

For oVEMP, the setting parameters are the same as above. The electrode was placed 1 cm below the center of the opposite eyelid. The reference electrode was placed in the lower jaw and the ground electrode was placed on the nasion. Ask the patient to gaze upward after hearing a single stimulus. Keep the eye in 25–30° angle and blink as little as possible to maintain the tension of the inferior oblique muscle until the stimulus stops. A value of AR > 40 was considered abnormal (11).

vHIT

vHIT was performed with a video-oculography device (Interacoustics, EyeSeeCam, Denmark). The subject was instructed to maintain the fixation on an earth-fixed target, which is usually straight ahead. Experienced otologists An experienced laboratory technician delivered at least 20 brief, abrupt, and unpredictable head impulses per side (10–20° angle, duration 150–200 ms, peak velocity of >150°/s). The VOR gain was defined as the ratio of the eye velocity (°/s) over the head velocity (°/s). Individual VOR gains were automatically calculated using the device software. vHIT testing was considered to be abnormal for horizontal canal if VOR gain at 60 ms was <0.8 (18).

Caloric Test

The patients were placed in supine position by raising their head 30° to keep the horizontal canal in a vertical position. The external auditory canal was irrigated with 24°C cold air for cold testing and 50°C hot air for hot testing. The induced nystagmus was recorded using electronystagmography in a dark, open-eye situation. The percentage of canal paresis (CP%) was calculated using Jongkees' formula (19). A CP% of >25% was defined as caloric weakness.

Data Analysis

All data were analyzed with SPSS v. 25 statistical software (IBM Corp., NY, US). Continuous data are presented as mean with standard deviation. The Wilcoxon rank sum test was used for non-normal data. The chi-square test was applied to compare dichotomous variables among the groups. The Spearman correlation analysis was used for categorical data to explore the correlation between the severity of hydrops on MRI and audiovestibular tests. *P*-values < 0.05 were considered significant.

RESULTS

Demographics

The study population consisted of 34 men and 35 women (40 right-sided, 29 left-sided), with ages ranging from 28 to 75 years (mean age 52.62 ± 12.11 years). The mean duration of disease was 3.43 ± 2.86 years. The mean PTA was 55.92 ± 20.56. Based on the level of hearing loss, 5 (7.2%) patients met the criteria for Stage I. Nine (13.0%) patients could be classified as stage II,

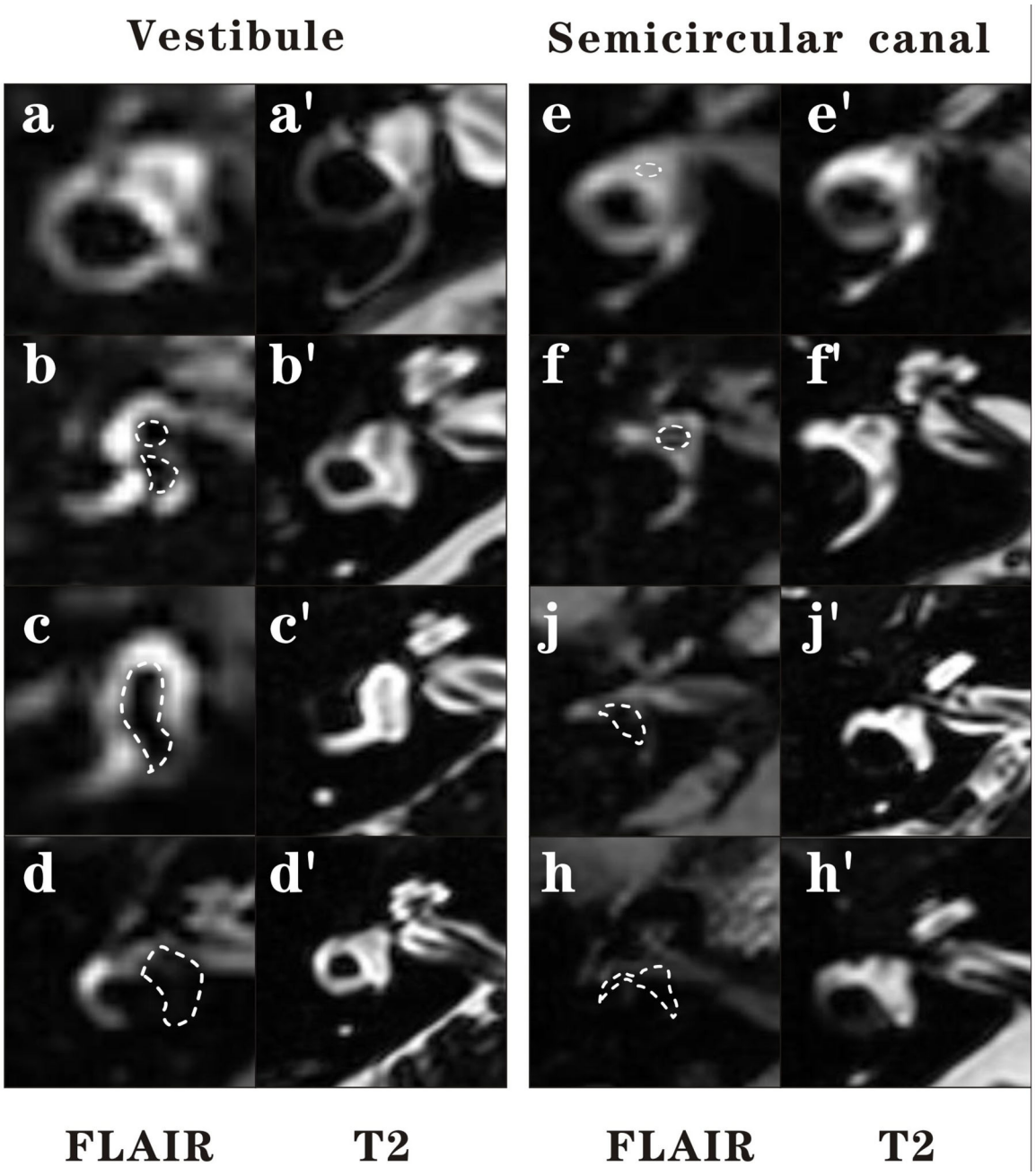

FIGURE 1 | Four grades of the vestibular EH and lateral semicircular canal EH. In this figure, 3D-FLAIR pictures **(a–h)** are shown adjacent to 3D-T2-SPAIR pictures **(a′-h′)** for each grade. For vestibule, grade 0 = No hydrops **(a)**. The saccule and utricle are visibly separately and take less than half of the surface of the vestibule. Grade 1 = Mild hydrops **(b)**. When the saccule become equal or larger than the utricle, but is not yet confluent with the utricle. Grade 2 = Moderate hydrops **(c)**. There is a confluence of the saccule and utricle with still a peripheral rim enhancement of the perilymphatic space. Grade 3 = Severe hydrops **(d)**. The perilymphatic enhancement is invisible. For lateral semicircular canal, grade 0 = No hydrops **(e)**. A small visible herniation which is 1/3 less than the semicircular canal with perilymph surrounding can be observed. Grade 1 = Mild hydrops **(f)**. A dark area occupying over 1/3 of the ampulla is observed. Grade 2 = Moderate hydrops **(g)**. The crura become dark and some of the canals become invisible with hydrops, which often accompany the stenosis of canals. Grade 3 = Severe hydrops **(h)**. All semicircular canals were invisible.

whereas Stage III and Stage IV comprised 41 (57.9%) and 14 (20.3%) of the patients, respectively. The baseline characteristics of the patient population are summarized in **Table 1**.

MRI Data

Four patients were excluded in the final data analysis because the contrast medium could not even be observed in the any

TABLE 1 | Characteristics of the study population.

Characteristics	*N* = 69
Age (years)	52.62 ± 12.11
Sex	
Male	34 (49.3%)
Female	35 (50.7%)
Affected side	
Left	29 (44.6%)
Right	40 (55.4%)
Duration of disease (years)	3.43 ± 2.86
Mean PTA (dB)	55.92 ± 20.56
Stage	
I	5 (7.2%)
II	9 (13.0%)
III	41 (57.9%)
IV	14 (20.3%)

Data are presented as mean ± standard deviation or number (%).
Staging was based on the pure-tone average at 0.5, 1, and 2 kHz.

TABLE 2 | EH grade in vestibule and lateral semicircular canal.

	Vestibule	Lateral semicircular canal
None	8	29
Grade I	14	23
Grade II	22	8
Grade III	21	5

part of membrane labyrinth. Poor permeability of the round window membrane is the most probable reason. Variable degrees of vestibular hydrops were observed in 57 of 65 (87.7%) patients in the affected ear (**Table 2**). According to the vestibular hydrops grade system, 8 (12.3%) were in grade 0, 14 (21.5%) were in grade 1, 22 (33.8%) were in grade 2, and 21 (32.3%) were in grade 3. For the ampulla hydrops of lateral semicircular canal part, 29 (44.6%) were in grade 0, 23 (35.4%) were in grade 1, 8 (12.3%) were in grade 2, and 5 (7.7%) were in grade 3. A total of three patients had normal vestibule and semicircular canal on MRI. The severity of vestibular hydrops showed correlations with the duration of disease ($r = 0.360$, $p = 0.003$) (**Figure 2A**) and PTA ($r = 0.326$, $p = 0.008$) (**Figure 2B**). Vestibular hydrops is not correlated with age of patients ($p = 0.634$). No correlations were observed between lateral semicircular canal hydrops and duration of disease ($p = 0.582$), PTA ($p = 0.348$), and age of patients ($p = 0.768$) (**Table 3**).

Correlation Between Vestibular Function Tests and MRI

VEMP

A total of 6 patients showed bilateral absence of cVEMP were excluded in the correlation analysis with hydrops on MRI. cVEMP was elicited in 48 of 65 (73.8%) patients. The P13–N23 amplitude of the affected side was significantly smaller than the contralateral side ($p < 0.05$). The mean AR of cVEMP was 0.42 ± 0.32. The Spearman correlation analysis revealed no correlations between vestibular hydrops and the latency of P13 ($p = 0.390$), the latency of N23 ($p = 0.056$), or the amplitude of P13–N23 ($p = 0.109$). Vestibular hydrops is significantly correlated with AR of cVEMP ($r = 0.407$, $p = 0.001$) (**Figure 3**).

For oVEMP, a total of 28 patients showed bilateral absence of oVEMP were excluded in the correlation analysis with hydrops on MRI. oVEMP was elicited in 26 of 65 (40.0%) patients. The P13–N23 amplitude of the affected side was significantly smaller than the contralateral side ($p < 0.05$). The mean AR of oVEMP was 0.49 ± 0.43. Vestibular hydrops showed no significance in correlation with AR of oVEMP ($p = 0.098$) (**Figure 4**). Also, there were no significant correlations between vestibular hydrops and the latency of P13 ($p = 0.976$), the latency of N23 ($p = 0.590$), the amplitude of P13–N23 ($p = 0.090$).

Caloric Test and vHIT

CP was observed in 38 of 65 (58.5%) patients. CP was significantly correlated with lateral semicircular canal hydrops ($r = 0.367$, $p < 0.003$) (**Figure 5**). No correlation was observed between CP and vestibular hydrops ($p = 0.365$).

Abnormal VOR gain was observed in 14 of 65 (21.5%) patients. The mean VOR gain on the affected side was 0.95 ± 0.19 and 1.11 ± 0.15 on the contralateral side. The VOR gain of affected side is significantly lower than the contralateral side ($p < 0.05$). VOR gain was significantly correlated with lateral semicircular canal hydrops ($r = 0.311$, $p = 0.012$) (**Figure 6**). There was no significant correlations between vestibular hydrops and VOR gains ($p = 0.243$).

DISCUSSION

The pathological change of MD is characterized by EH. Clinical diagnosis of MD is mainly based on the combination of medical history and auditory-vestibular function examination. With the development of Gd-contrasted inner ear MRI, clinicians are now able to observe this most important pathologic feature of MD by *in vivo* MRI. According to the previous studies, the accuracy for clinical diagnosed MD is 56–73% for electrocochleogram, VEMP, and caloric test (20–22). On the other hand, Gd MRI demonstrated EH in 90% of the patients with MD in a multicenter clinical study (23). The *in vivo* visualization of EH has become a powerful tool for the investigation of MD. Furthermore, the significance of EH and vestibular function tests in patients with MD has not been fully characterized yet. The recent research published by our team modified the grading system of vestibular and semicircular canal hydrops (15). The "volume-referencing" grading system showed a better correlation with the MD clinical features and had more diagnostic value than previously published methods. But the correlation between this grading system and vestibular function tests requires further research.

In this study, four patients (4/69, 14.5%) were excluded in the final data analysis because no signs of any contrast medium could be observed in any part of the endolymph. We considered the possible cause of this phenomenon is that the permeability of the

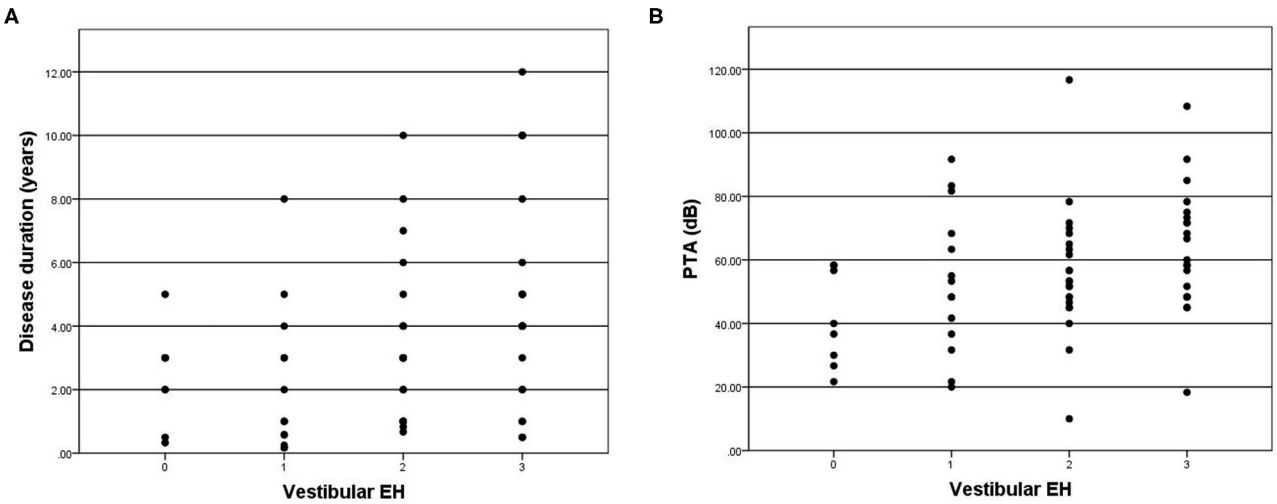

FIGURE 2 | (A) Correlation between grade of vestibular EH (x-axis) and disease duration (y-axis). The positive correlation is significant ($r = 0.360$, $p = 0.003$). **(B)** Correlation between grade of vestibular EH (x-axis) and PTA (y-axis). The positive correlation is significant ($r = 0.326$, $p = 0.008$).

round window membrane is poor and the concentration of the contrast agent into the inner ear is insufficient. Yoshioka et al. (24) evaluated the permeability of the round window membrane in 42 MD patients and 13 non-hydrop inner ear disease patients by 3D-FLAIR MRI after intratympanic Gd injection. The results showed that 13% of the patients had poor permeability of the round window membrane, and nearly half of them had calcified plaques n the tympanic membrane or inflammation in the mastoid. This proportion is similar to that of our study. The permeability of the round window membrane is an unpredictable reason for the failure of inner ear MRI after intratympanic Gd injection.

The relationship between the degree of EH and clinical features, such as duration of the disease and hearing loss was previously reported by researchers. In this study, we confirmed that vestibular EH was correlated with duration of disease and PTA. Gurkov et al. (25) reported that Patients with a longer disease duration had a higher degree of EH. A significant positive correlation between hearing loss and cochlear EH was also confirmed. But the correlation between vestibular hydrops and hearing loss or duration of disease was not mentioned. Wu et al. (26) revealed that there was a significant correlation between the duration and vestibular EH. PTA thresholds at low and middle frequencies were significantly correlated with the extent of EH in cochlea. No significant correlation was detected with the vestibular hydrops and PTA. Yang et al. (27) demonstrated both vestibular and cochlear EH were significantly correlated with PTA. But they concluded that duration of disease was not correlated with vestibular EH or cochlear EH. Fiorino et al. (28) concluded that the severity of vestibular EH is positively correlated with the course of disease, especially in patients with more than 5 years of disease duration. The results are consistent with the pathological findings of the temporal bone (29). The above results suggest that the EH in patients with MD is progressive aggravation, However, the mechanism of this phenomenon in MD remains to be further studied. The ideal method to study the correlation between the duration of disease and EH should be the large scale longitudinal study in different course of disease in the same patient. But its feasibility is limited due to the economics and ethics considerations.

TABLE 3 | Results of vHIT and Caloric test in patients.

	CP (+)	CP (–)	Total
VOR gian (+)	13	1	14
VOR gain (–)	25	26	51
Total	38	27	65

Chi-square test, correction for continuity. Statistically significant. $\chi^2 = 6.981$, $p = 0.005$. *CP, canal paresis; VOR gain, vestibulo-ocular reflex gain.*

VEMP has been gradually widely applied in the clinical diagnosis and research in various kinds of peripheral vestibular diseases. cVEMP can reflect the function of saccule and the integrity of its pathway. The pathway is from the saccule, inferior vestibular nerve, vestibular nucleus, accessory nucleus, accessory nerve to sternocleidomastoid muscle. oVEMP can reflect the function of utricle and the integrity of its pathway. The pathway is from the utricle, superior vestibular nerve, vestibular nucleus, contralateral medial longitudinal fasciculus, contralateral oculomotor nucleus to contralateral inferior oblique muscle (2). The elicited response rate of cVEMP and oVEMP was 73.8 and 40.0% in this study. The response rate of oVEMP was lower than the data previously reported (30, 31). The possible reason is that 78.2% (55 of 69) patients included in this study were in stage III and stage IV. The response rate and abnormal rate of cVEMP and oVEMP in MD increased with the progression of the disease and the severity of hearing loss (32). The latency both in cVEMP and oVEMP showed no correlations with vestibular EH in our study. Researches have revealed that the latency

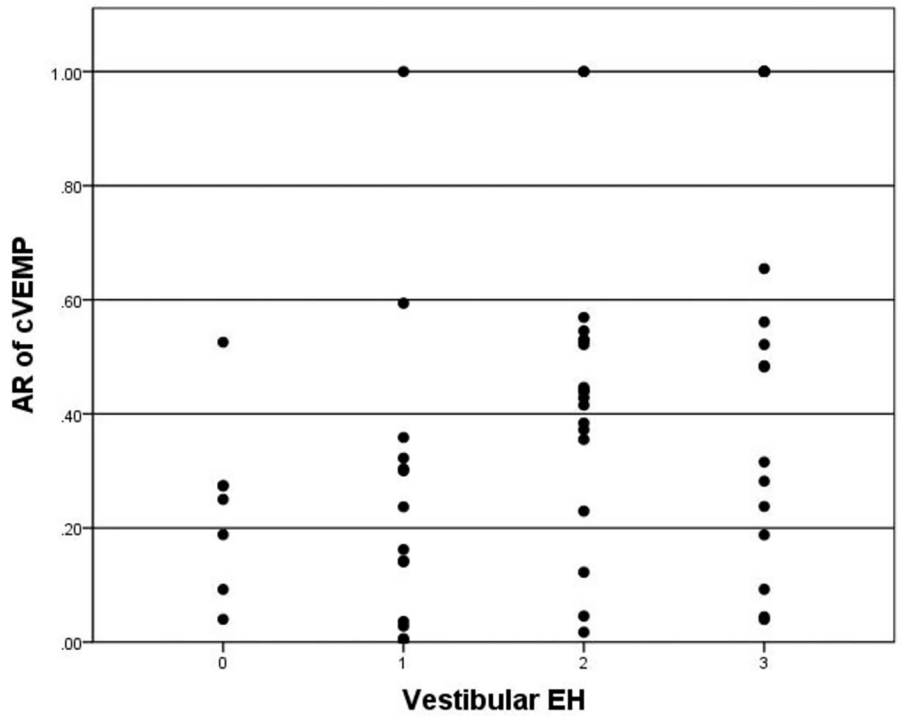

FIGURE 3 | Correlation between grade of vestibular EH (x-axis) and AR of cVEMP (y-axis). The positive correlation is significant ($r = 0.407$, $p = 0.001$).

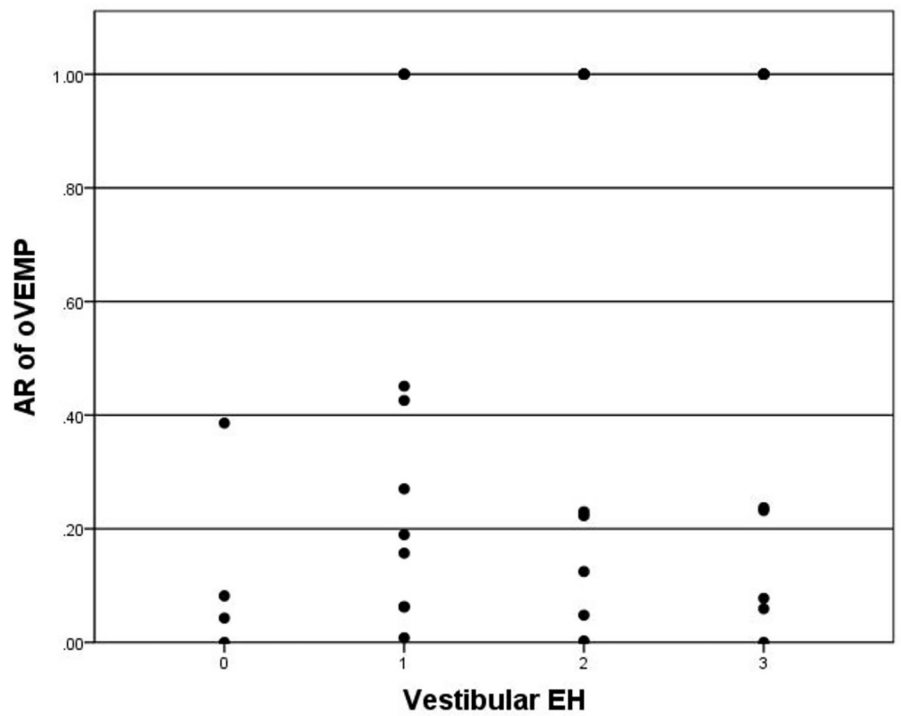

FIGURE 4 | Correlation between grade of vestibular EH (x-axis) and AR of oVEMP (y-axis). The positive correlation is insignificant ($p = 0.098$).

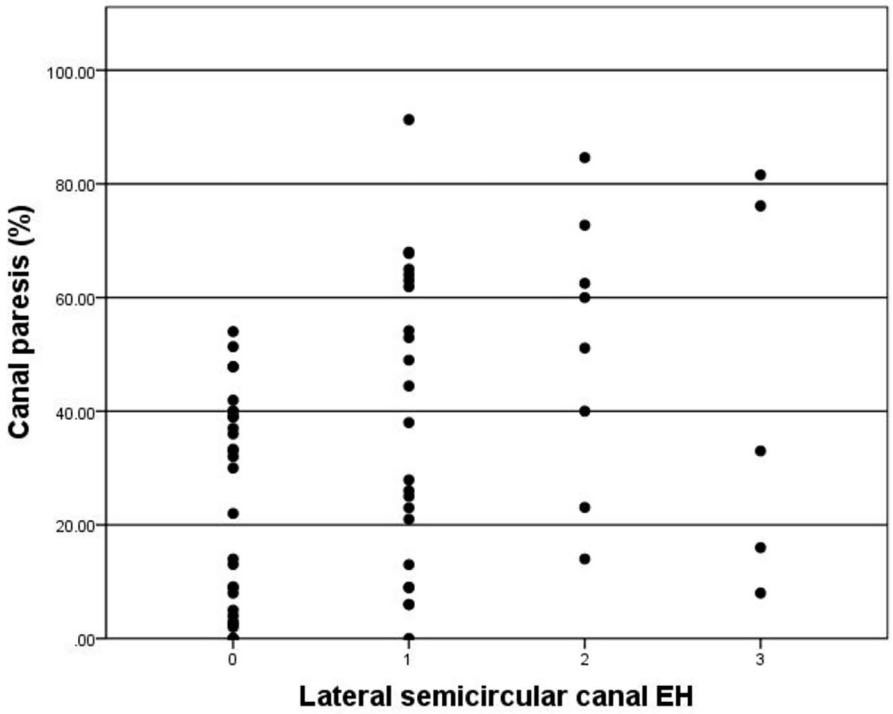

FIGURE 5 | Correlation between grade of lateral semicircular canal EH (x-axis) and CP (y-axis). The positive correlation is significant ($r = 0.367$, $p = 0.003$).

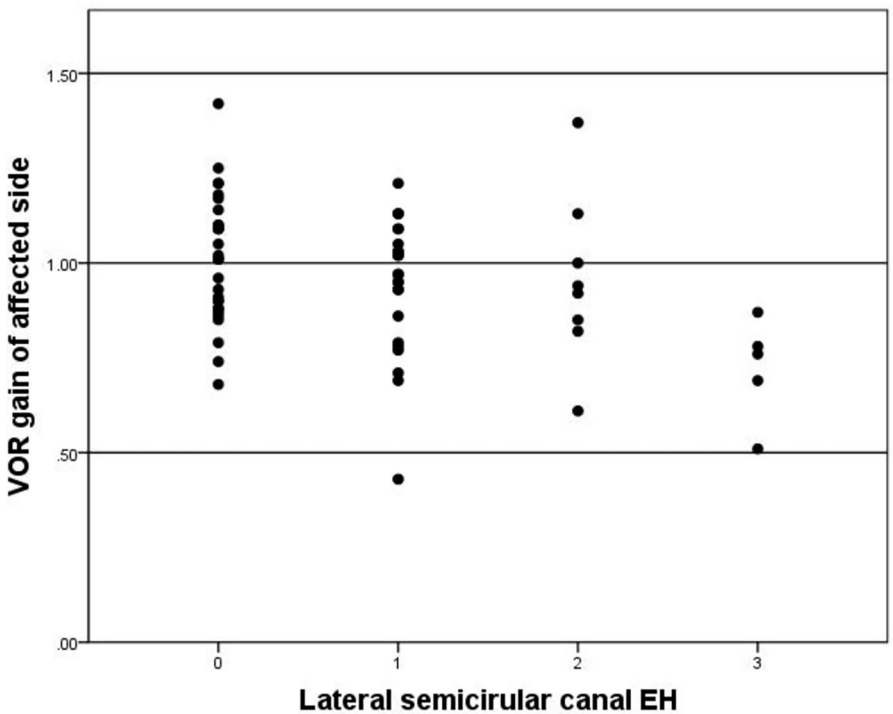

FIGURE 6 | Correlation between grade of lateral semicircular EH (x-axis) and VOR gain of affected side (y-axis). The negative correlation is significant ($r = -0.311$, $p = 0.012$).

of VEMP is prolonged due to the damage of the vestibular nerve pathway in the retrolabyrinthine (33). However, different conclusions have been made in the researches of MD patients. Johnson et al. (34) revealed that the latency of P13 was prolonged in the affected side of MD patients when compared to the contralateral side and the healthy controls. On the other hand, Murofushi et al. (35) patients with MD or vestibular neuritis hardly showed any latency prolongation in cVEMP. Whether the vestibular nerve pathway in the retrolabyrinthine of MD patients is damaged still need to be clarified in the future study. Since the amplitude of VEMP can be affected by muscle tension and subcutaneous thickness, Young et al. (36) put forward the concept of AR, and considered that AR is a more accurate method to evaluate the vestibular function of both sides, which can reflect the symmetry of vestibular function in MD patients. The present study demonstrated that AR of cVEMP was correlated with vestibular EH while AR of oVEMP was not. Gurkov et al. (25) drew a similar conclusion with our study, which indicated that patients with a more severe degree of vestibular EH also had a worse sacculus function. Guo et al. (6) have also reported that cVEMP AR was higher in MD patients with severe vestibular hydrops than in patients without vestibular hydrops. The phenomenon matches the theory that severe vestibular EH would lead to permanent morphological changes of the sensory organs, including the loss of saccular macula associated with the collapse of the saccular wall onto the otolithic membrane, which is consistent with reduced cVEMP (29). Quantitative analyses of the relationship with oVEMP values and EH degrees in vestibule in MD patients are rare. Jerin et al. (37) concluded that the 500/1,000 Hz amplitude ratio was neither correlated with the degree of endolymphatic hydrops nor with the duration of disease. The correlation between oVEMP and EH need to be further studied.

In the present study, CP was observed in 38 of 65 (58.5%) patients while abnormal VOR gain was only observed in 14 of 65 (21.5%) patients. The function of semicircular canal has frequency specificity. The caloric test was a function test at low frequency, while the VHT was a test of the high frequency. They are complementary. The abnormal rate of caloric test in patients with MD is higher than that of vHIT. The probable explanation is that the low frequency function of the semicircular canal decreased firstly, and then the high frequency function impairment occurred later in MD patients, because the caloric test examines the response of the semicircular canal at a low frequency and non-physiological stimulation, which the daily activities can not compensate for its functional decline. While the vHIT examines the high frequency function of the semicircular canal, and the frequency of head position movement stimulation in daily activities is relatively consistent with the high frequency. Vestibular compensation plays a vital role in the high frequency function impairment in patients with MD. Thus, high frequency function impairment occurs later in the duration of the disease and maintains a relative balance between the two sides (38). There were few reports of the semicircular function related to EH detected with MRI. In previous studies, Kahn et al. (8) reported no significant correlation between ampullar hydrops and vHIT by a simple two-grade canal hydrops evaluation. Gurkov et al. (25) demonstrated no significant correlation between the severity of vestibular EH and CP. Fukushima et al. (39) revealed that vestibular EH was not correlated with VOR gains, but correlated with CP. However, both CP and VOR gains of lateral semicircular canal showed significant correlations with hydrops according to the modified canal hydrops grading system proposed by our team. Although a single vHIT or caloric test has limited sensitivity to MD, especially in the early stage of the disease. But as the disease progressing, changes of CP and VOR gains of lateral semicircular canal were able to represent the degree of lateral semicircular canal hydrops to a certain extent.

These limitations should be taken into consideration is this study. First, the results of vestibular function test were short of normal healthy population in local area as reference. Adapting the standard values reported by the previous literature in the study would lead to result error. Second, the reliability of the statistical analyses would profit from a greater number of patients. Third, in this study, 78.2% of the patients were in stage III and stage IV, and most of them had significant vestibular hydrops. In some cases, it was difficult to evaluate the degree of EH in the lateral semicircular canal because of the close anatomic connection between the utricle and the ampulla of the lateral semicircular canal. The number of patients with no or mild EH was relatively small. Thus, for more precise study between canal hydrops and caloric test and vHIT, a study including more patients of stage I and stage II is necessary.

DATA AVAILABILITY STATEMENT

The raw data supporting the conclusions of this article will be made available by the authors, without undue reservation.

ETHICS STATEMENT

The studies involving human participants were reviewed and approved by The Ethics Committee of Xinhua Hospital, Shanghai Jiaotong University School of Medicine. The patients/participants provided their written informed consent to participate in this study.

AUTHOR CONTRIBUTIONS

JY and MD contributed to the study design, critically reviewed, and approved the final manuscript. YL and FZ contributed to the detailed study design and performed data acquisition, statistical analysis, and interpretation of results, drafting of the manuscript, and revised the manuscript. BH, JH, and QZ contributed to the methods of statistical analysis and critically reviewed the manuscript. All authors agree to be accountable for the content of the work, integrity, accuracy of the data, contributed to the article, and approved the submitted version.

FUNDING

This work was funded by Cross-key Projects in Medical and Engineering Fields of Shanghai Jiaotong University (No. ZH2018ZDA11) and Clinical Research Cultivation Fund of Xinhua Hospital (Nos. 17CSK03 and 18JXO04).

REFERENCES

1. Nakashima T, Pyykkö I, Arroll MA, Casselbrant ML, Foster CA, Manzoor NF, et al. Meniere's disease. *Nat Rev Dis Primers.* (2016) 2:16028. doi: 10.1038/nrdp.2016.28
2. Murofushi T. Clinical application of vestibular evoked myogenic potential (VEMP). *Auris Nasus Larynx.* (2016) 43:367–76. doi: 10.1016/j.anl.2015.12.006
3. McGarvie LA, Curthoys IS, MacDougall HG, Halmagyi GM. What does the head impulse test versus caloric dissociation reveal about vestibular dysfunction in Ménière's disease? *Ann N Y Acad Sci.* (2015) 1343:58–62. doi: 10.1111/nyas.12687
4. Egami N, Ushio M, Yamasoba T, Yamaguchi T, Murofushi T, Iwasaki S. The diagnostic value of vestibular evoked myogenic potentials in patients with Meniere's disease. *J Vestib Res.* (2013) 23:249–57. doi: 10.3233/VES-130484
5. Nakashima T, Naganawa S, Sugiura M, Teranishi M, Sone M, Hayashi H, et al. Visualization of endolymphatic hydrops in patients with Meniere's disease. *Laryngoscope.* (2007) 117:415–20. doi: 10.1097/MLG.0b013e31802c300c
6. Guo P, Sun W, Shi S, Zhang F, Wang J, Wang W. Quantitative evaluation of endolymphatic hydrops with MRI through intravenous gadolinium administration and VEMP in unilateral definite Meniere's disease. *Eur Arch Otorhinolaryngol.* (2019) 276:993–1000. doi: 10.1007/s00405-018-05267-7
7. Katayama N, Yamamoto M, Teranishi M, Naganawa S, Nakata S, Sone M, et al. Relationship between endolymphatic hydrops and vestibular-evoked myogenic potential. *Acta Otolaryngol.* (2010) 130:917–23. doi: 10.3109/00016480903573187
8. Kahn L, Hautefort C, Guichard JP, Toupet M, Jourdaine C, Vitaux H, et al. Relationship between video head impulse test, ocular and cervical vestibular evoked myogenic potentials, and compartmental magnetic resonance imaging classification in Menière's disease. *Laryngoscope.* (2020) 130:E444–52. doi: 10.1002/lary.28362
9. Kato M, Teranishi M, Katayama N, Sone M, Naganawa S, Nakashima T. Association between endolymphatic hydrops as revealed by magnetic resonance imaging and caloric response. *Otol Neurotol.* (2011) 32:1480–5. doi: 10.1097/MAO.0b013e318235568d
10. Sluydts M, Bernaerts A, Casselman JW, De Foer B, Blaivie C, Zarowski A, et al. The relationship between cochleovestibular function tests and endolymphatic hydrops grading on MRI in patients with Menière's disease. *Eur Arch Otorhinolaryngol.* (2021). doi: 10.1007/s00405-021-06610-1. [Epub ahead of print].
11. Okumura T, Imai T, Takimoto Y, Takeda N, Kitahara T, Uno A, et al. Assessment of endolymphatic hydrops and otolith function in patients with Ménière's disease. *Eur Arch Otorhinolaryngol.* (2017) 274:1413–21. doi: 10.1007/s00405-016-4418-2
12. Kitano K, Kitahara T, Ito T, Shiozaki T, Wada Y, Yamanaka T. Results in caloric test, video head impulse test and inner ear MRI in patients with Ménière's disease. *Auris Nasus Larynx.* (2020) 47:71–8. doi: 10.1016/j.anl.2019.06.002
13. Lopez-Escamez JA, Carey J, Chung WH, Goebel JA, Magnusson M, Mandalà M, et al. Diagnostic criteria for Menière's disease. *J Vestib Res.* (2015) 25:1–7. doi: 10.3233/VES-150549
14. Liu Y, Jia H, Shi J, Zheng H, Li Y, Yang J, et al. Endolymphatic hydrops detected by 3-dimensional fluid-attenuated inversion recovery MRI following intratympanic injection of gadolinium in the asymptomatic contralateral ears of patients with unilateral Ménière's disease. *Med Sci Monit.* (2015) 21:701–7. doi: 10.12659/MSM.892383
15. He B, Zhang F, Zheng H, Sun X, Chen J, Chen J, et al. The correlation of a 2D volume-referencing endolymphatic-hydrops grading system with extratympanic electrocochleography in patients with definite Ménière's disease. *Front Neurol.* (2021) 11:595038. doi: 10.3389/fneur.2020.595038
16. Bernaerts A, Vanspauwen R, Blaivie C, van Dinther J, Zarowski A, Wuyts FL, et al. The value of four stage vestibular hydrops grading and asymmetric perilymphatic enhancement in the diagnosis of Menière's disease on MRI. *Neuroradiology.* (2019) 61:421–9. doi: 10.1007/s00234-019-02155-7
17. Editorial Board of Chinese Journal of Otorhinolaryngology Head and Neck Surgery, Society of Otorhinolaryngology Head and Neck Surgery Chinese Medical Association. Guideline of diagnosis and treatment of Meniere disease (2017). *Zhonghua Er Bi Yan Hou Tou Jing Wai Ke Za Zhi.* (2017) 52:167–72. doi: 10.3760/cma.j.issn.1673-0860.2017.03.002
18. McGarvie LA, MacDougall HG, Halmagyi GM, Burgess AM, Weber KP, Curthoys IS. The video head impulse test (vHIT) of semicircular canal function–age-dependent normative values of VOR gain in healthy subjects. *Front Neurol.* (2015) 6:154. doi: 10.3389/fneur.2015.00154
19. Jongkees LB, Maas JP, Philipszoon AJ. Clinical nystagmography. A detailed study of electro-nystagmography in 341 patients with vertigo. *Pract Otorhinolaryngol (Basel).* (1962) 24:65–93.
20. Nguyen LT, Harris JP, Nguyen QT. Clinical utility of electrocochleography in the diagnosis and management of Meniere's disease: AOS and ANS membership survey data. *Otol Neurotol.* (2010) 31:455–9. doi: 10.1097/MAO.0b013e3181d2779c
21. Lamounier P, de Souza TSA, Gobbo DA, Bahmad F Jr. Evaluation of vestibular evoked myogenic potentials (VEMP) and electrocochleography for the diagnosis of Ménière's disease. *Braz J Otorhinolaryngol.* (2017) 83:394–403. doi: 10.1016/j.bjorl.2016.04.021
22. Seo YJ, Kim J, Choi JY, Lee WS. Visualization of endolymphatic hydrops and correlation with audio-vestibular functional testing in patients with definite Meniere's disease. *Auris Nasus Larynx.* (2013) 40:167–72. doi: 10.1016/j.anl.2012.07.009
23. Pyykkö I, Nakashima T, Yoshida T, Zou J, Naganawa S. Meniere's disease: a reappraisal supported by a variable latency of symptoms and the MRI visualisation of endolymphatic hydrops. *BMJ Open.* (2013) 3:e001555. doi: 10.1136/bmjopen-2012-001555
24. Yoshioka M, Naganawa S, Sone M, Nakata S, Teranishi M, Nakashima T. Individual differences in the permeability of the round window: evaluating the movement of intratympanic gadolinium into the inner ear. *Otol Neurotol.* (2009) 30:645–8. doi: 10.1097/MAO.0b013e31819bda66
25. Gurkov R, Flatz W, Louza J, Strupp M, Ertl-Wagner B, Krause E. *In vivo* visualized endolymphatic hydrops and inner ear functions in patients with electrocochleographically confirmed Meniere's disease. *Otol Neurotol.* (2012) 33:1040–5. doi: 10.1097/MAO.0b013e31825d9a95
26. Wu Q, Dai C, Zhao M, Sha Y. The correlation between symptoms of definite Meniere's disease and endolymphatic hydrops visualized by magnetic resonance imaging. *Laryngoscope.* (2016) 126:974–9. doi: 10.1002/lary.25576
27. Yang S, Zhu H, Zhu B, Wang H, Chen Z, Wu Y, et al. Correlations between the degree of endolymphatic hydrops and symptoms and audiological test results in patients with Menière's disease: a reevaluation. *Otol Neurotol.* (2018) 39:351–6. doi: 10.1097/MAO.0000000000001675
28. Fiorino F, Pizzini FB, Beltramello A, Barbieri F. Progression of endolymphatic hydrops in Ménière's disease as evaluated by magnetic resonance imaging. *Otol Neurotol.* (2011) 32:1152–7. doi: 10.1097/MAO.0b013e31822a1ce2
29. Fraysse BG, Alonso A, House WF. Menière's disease and endolymphatic hydrops: clinical-histopathological correlations. *Ann Otol Rhinol Laryngol Suppl.* (1980) 89:2–22. doi: 10.1177/00034894800896s201
30. Taylor RL, Wijewardene AA, Gibson WP, Black DA, Halmagyi GM, Welgampola MS. The vestibular evoked-potential profile of Ménière's disease. *Clin Neurophysiol.* (2011) 122:1256–63. doi: 10.1016/j.clinph.2010.11.009
31. Winters SM, Campschroer T, Grolman W, Klis SF. Ocular vestibular evoked myogenic potentials in response to air-conducted sound in Ménière's disease. *Otol Neurotol.* (2011) 32:1273–80. doi: 10.1097/MAO.0b013e31822e5ac9
32. Young YH. Potential application of ocular and cervical vestibular-evoked myogenic potentials in Meniere's disease: a review. *Laryngoscope.* (2013) 123:484–91. doi: 10.1002/lary.23640
33. Oh SY, Kim HJ, Kim JS. Vestibular-evoked myogenic potentials in central vestibular disorders. *J Neurol.* (2016) 263:210–20. doi: 10.1007/s00415-015-7860-y
34. Johnson SA, O'Beirne GA, Lin E, Gourley J, Hornibrook J. oVEMPs and cVEMPs in patients with 'clinically certain' Menière's disease. *Acta Otolaryngol.* (2016) 136:1029–34. doi: 10.1080/00016489.2016.1175663
35. Murofushi T, Shimizu K, Takegoshi H, Cheng PW. Diagnostic value of prolonged latencies in the vestibular evoked myogenic potential. *Arch Otolaryngol Head Neck Surg.* (2001) 127:1069–72. doi: 10.1001/archotol.127.9.1069
36. Young YH, Wu CC, Wu CH. Augmentation of vestibular evoked myogenic potentials: an indication for distended saccular hydrops. *Laryngoscope.* (2002) 112:509–12. doi: 10.1097/00005537-200203000-00019

37. Jerin C, Berman A, Krause E, Ertl-Wagner B, Gürkov R. Ocular vestibular evoked myogenic potential frequency tuning in certain Menière's disease. *Hear Res.* (2014) 310:54–9. doi: 10.1016/j.heares.2014.02.001
38. Agrawal Y, Minor LB. Physiologic effects on the vestibular system in Meniere's disease. *Otolaryngol Clin North Am.* (2010) 43:985–93. doi: 10.1016/j.otc.2010.05.002
39. Fukushima M, Oya R, Nozaki K, Eguchi H, Akahani S, Inohara H, et al. Vertical head impulse and caloric are complementary but react opposite to Meniere's disease hydrops. *Laryngoscope.* (2019) 129:1660–6. doi: 10.1002/lary.27580

Conflict of Interest: The authors declare that the research was conducted in the absence of any commercial or financial relationships that could be construed as a potential conflict of interest.

frontiers in Surgery

ORIGINAL RESEARCH
published: 04 June 2021
doi: 10.3389/fsurg.2021.672284

MRI With Intratympanic Gadolinium: Comparison Between Otoneurological and Radiological Investigation in Menière's Disease

Giampiero Neri[1]*, *Armando Tartaro*[2] and *Letizia Neri*[1]

[1] Neurosciences, Imaging and Clinical Sciences Department, Gabriele d'Annunzio University, Chieti, Italy, [2] Medical, Oral and Biotechnologies Sciences Department, Gabriele d'Annunzio University, Chieti, Italy

Objectives/hypothesis: To compare findings obtained using both magnetic resonance imaging plus intratympanic gadolinium and audiovestibular testing for Menière's disease.

Study design: Retrospective cohort study.

Methods: Patients with definite unilateral Menière's disease ($n = 35$) diagnosed according to 2015 Barany Criteria were included. Three-dimensional real inversion recovery (3D-real-IR) MRI was executed 24 h after intratympanic gadolinium injection to assess the presence and degree of endolymphatic hydrops. Pure tone audiometry, bithermal caloric test, head impulse test, ocular, and cervical VEMPs using air-conducted sound were performed to evaluate the level of hearing and vestibular loss. The results were compared to verify precision of the method in providing correct diagnoses.

Results: Different degrees of endolymphatic hydrops were observed in the MRI of the cochlea and vestibule in the affected ears of Menière's disease patients, even though it was impossible to radiologically distinguish the two otolithic structures separately. The correlation between the degree of linked alterations between instrumental and MRI testing was statistically significant. In particular, an 83% correspondence with audiometry, a 63% correspondence for cVEMPs and 60% correspondence for cVEMPs were seen. While for HIT the accordance was 70 and 80% for caloric bithermal test.

Conclusions: MRI using intratympanic gadolinium as a contrast medium has proved to be a reliable and harmless method, even though there is an objective difficulty in disclosing macular structures. The study revealed that there is no complete agreement between instrumental values and MRI due to the definition of the image and fluctuation of symptoms. The present work highlights the greater (but not absolute) sensitivity of otoneurological tests while MRI, although not yet essential for diagnosis, is certainly important for understanding the disease and its pathogenic mechanisms.

Keywords: magnetic resonance imaging, intratympanic gadolinium, vestibular evoked myogenic potential, head impulse test, pure tone audiometry, caloric bithermal test, posturography, Menière's disease

OPEN ACCESS

Edited by:
Robert Gürkov, Bielefeld University, Germany

Reviewed by:
Hans Thomeer, University Medical Center Utrecht, Netherlands
Jeremy Hornibrook, University of Canterbury, New Zealand

***Correspondence:**
Giampiero Neri
giampiero.neri@unich.it

Specialty section:
This article was submitted to Otorhinolaryngology - Head and Neck Surgery, a section of the journal Frontiers in Surgery

Received: *25 February 2021*
Accepted: *01 April 2021*
Published: *04 June 2021*

Citation:
Neri G, Tartaro A and Neri L (2021) MRI With Intratympanic Gadolinium: Comparison Between Otoneurological and Radiological Investigation in Menière's Disease. Front. Surg. 8:672284. doi: 10.3389/fsurg.2021.672284

INTRODUCTION

Menière's disease (MD) also called "idiopathic syndrome of endolymphatic hydrops" (EH) (1) and named after Prosper Menière (2) is a chronic inner ear disease whose symptoms are vertigo with hearing loss, tinnitus and aural pressure. Its official diagnosis is based on guideline symptoms (3) and on pure tone audiogram. Recent vestibular tests can assess dysfunctions of the cochlea, otolith organs and semicircular canals. In 2007 Nakashima (4, 5) using MRI imaging with intratympanic gadolinium demonstrated endolymphatic hydrops (6) in Menière's ears. Since then, this technique has been used to evaluate hydrops, the size and shape of endolymphatic spaces, and the severity and evolution of MD (7). Not only is endolymphatic hydrops on MRI an indicator of MD, but also of other disorders (8–10). Variability of diagnosis is reflected in epidemiological studies (11, 12) including patients in which the full range of symptoms is not present (13). A comparison between audiovestibular symptoms and tests and MRI inner ear imaging might improve MD diagnosis. In the present study the results obtained through MRI inner ear imaging were compared with audiological findings in patients with a clinical diagnosis of MD according to the 2015 Barany Criteria (3).

MATERIALS AND METHODS

This retrospective clinical study was conducted in collaboration with Biomedics Advanced Technologies Institute and Ear Nose and Throat Department of Chieti-Pescara University Hospital. The patients had a definite unilateral MD and were subjected to MRI 3T and intratympanic injection of gadolinium (Gd) (1 mmol/ml) diluted 1:7 in saline in the affected ear. The study protocol was approved by the local ethics committee. All patients signed informed consent and the study was conducted in accordance with the Declaration of Helsinki of 1975 revised in 2013.

Thirty-five (14) volunteer adult patients (19 females and 16 males) aged between 38 and 72 years (mean age 52.83) who arrived at the Hospital as out-patients for unilateral definite MD according to the 2015 Barany Criteria (3) were included in the study. Patients with bilateral MD, patients previously subjected to ear surgery, patients subjected to intratympanic treatment with gentamicin, patients with vestibular migraine, patients suffering from intracranial neoplasms, and patients in whom MRI was contraindicated were excluded from the study. No patients included in the study had acute phase MD. Three-dimensional real inversion recovery (3D-real-IR) MRI was executed 24 h after intratympanic gadolinium injection to assess the presence and degree of endolymphatic hydrops (EH). Fisher *T*-test was used for statistical evaluation.

Magnetic Resonance Imaging (MRI) was performed and the contrast medium (0.4/0.5 ml) was injected intratympanically using a 1 ml syringe with a 23G needle and a dilution of 1 cc of Gd in 7cc of saline with a 1:7 ratio. After the injection, the patient remained supine and with the head turned 45° toward the affected side, for about 30 min. Three dimensional real inversion recovery (3D-real-IR) MRI was conducted 24 h after the intratympanic gadolinium injection to assess the presence and degree of endolymphatic hydrops (EH). All tests were evaluated according to Nakashima grading (15) which is based on hydrops volume ratios in FLAIR/T2 (G) from 0 to 1 and expressed in 3 degrees of severity (**Table 1**). Since the normal ratio range of the endolymphatic area over the vestibular fluid space (sum of the endolymphatic and perilymphatic areas) was 33%, any ratio increases over 33 % were considered positive.

TABLE 1 | Hydrops visualization grading, represented by the ratio between the volumes of the contrast agent in the Flair 3D and TSE and T2 sequences.

Grading	Ratio	Results
0	0–0.33	No hydrops
1	0.33–0.66	Middle gravity hydrops
2	0.66–1	Severe hydrops

Pure tone audiometry (PA) was bone and air conducted using Amplaid audiometer. The difference between air and bone hearing thresholds (cochlear reserve) was evaluated using 250-500-1,000 frequencies, and the results were considered as indicative of MD in patients with cochlear reserve >10 Db on at least one of these frequencies.

Bithermal caloric test (BCT) was performed using the Fitzgerald Hallpike method with water at 30 and 44°C. The angular velocity of the slow phase was calculated using the Jongkees formula. Patients with a labyrinthine preponderance >20% were considered positive for labyrinth damage.

Digital Video head impulse test (vHIT) was performed on the lateral canal using only ICS Impulse vHIT GN Otometrics, (Denmark) and the VOR gains were measured taking into account mean eye velocity divided by mean head velocity during a 40 ms window centered at the time of peak head acceleration. Abnormal VOR gain was considered in the presence of corrective saccades after the head movement. The decreased gain for the horizontal canal was calculated outside the mean 2 SDs compared to normal controls (<0.70 or> 0.999) (13).

Ocular (oVEMP) and Cervical VEMPs (cVEMP) were tested using air-conducted sound and altered VEMP was considered when the amplitude of the affected side was lower or absent as compared to the opposite. Two consecutive runs were averaged to provide a final response. A Stabilometry test was performed to evaluate the level of hearing and vestibular loss.

Posturography (PG) was carried out on a baropodometric platform (Phisionorm NBP Computerized Posturographic System) a few hours before and about 20–24 h after the intratympanic injection of the contrast medium. The test was conducted with both opened and closed eyes using a foam cushion between the feet and the platform, which could alter somatosensory and proprioceptive information, and respecting an interval of 30 s between one measurement and the next.

RESULTS

In all 35 patients no hearing loss, vestibular complications or ear drum perforations after gadolinium injection could be evidenced.

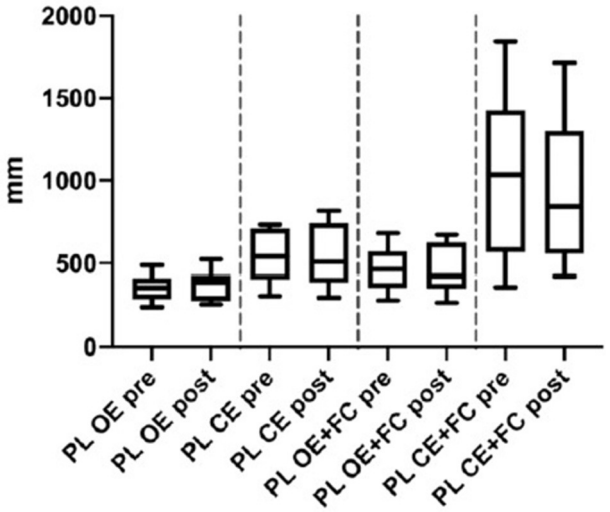

FIGURE 1 | Posturography: Path length of Menièr's patients before (pre) and 24 h- after (post) the intratympanic injection. OE, Open Eyes; CS, Closed Eyes; PC, Foam cushion under feet. Data we presented as boxes and whiskers (Tukey method).

In four patients who had all reported to have suffered from otitis in childhood, the contrast medium could not reach the labyrinth due to lack of diffusion through the round window. One of the patients (3%) refused to perform the second MRI. These five patients were excluded from the study. In the remaining 30 patients in the study group, distension of the endolymphatic spaces was observed in 22 (73%) while the labyrinth showed no signs of hydrops in the remaining eight (27%). No patients had their cochlear aqueduct lightened by gadolinium, while in all 30 patients in which the intratympanic infiltration lightened the labyrinth, gadolinium in the internal auditory canal (**Figure 1**) could be seen after 24 h.

The PA showed the presence of a constant transmission component on the 250-500-1000 frequencies that was inversely proportional to the severity of the sensorineural hearing loss (**Table 2**), with an average cochlear reserve of 22.3 dB at 250 Hz, of 12.3 Db at 500 Hz, and 5.2 Hz at 1,000 Hz. When comparing the results obtained with MRI and audiometric testing (**Table 3**) a significant correlation could be evidenced in 25 out of 30 patients (83.3%) ($p = 0.002$).

Vestibular evoked potentials were tested using air-conducted sounds and showed radiological-electrophysiological concordance in 63% of the patients (19/30) with either absent or reduced saccular (cVEMPs) bioelectric signals and in 60% of the patients with utricular (VEMPs) bioelectric signals (**Table 4**), these data being not statistically significant (0.3–0.5). On the contrary, the MRI method used was not able to distinguish the saccule from the utricle separately.

Video HIT based solely on the horizontal canal showed the presence of a significant ($p = 000.3$) correspondence in 70% of the MD patients (21/30 patients) (**Table 5**).

The bithermal caloric test showed a significant correlation between damage and radiological labyrinthine hydrops positivity

TABLE 2 | Cochlear reserve in decibels on the frequencies 250-500-1000 Hz of each patient and calculations of the average cochlear reserve.

Hz	250	500	1,000
Decibel	−15	−5	−5
	−10	−5	−5
	−40	−20	−5
	−30	−20	−10
	−15	−5	−5
	−15	−5	−5
	−35	−25	−10
	−25	−20	−5
	−45	−30	−10
	−25	−10	−5
	−25	−20	−5
	35	20	10
	−30	0	0
	−35	−10	−5
	−30	0	0
	−40	−20	−5
	−35	−15	−5
	−10	−5	−5
	−25	−20	−5
	−35	−25	−10
	−40	−20	−5
	−25	−20	−5
	−30	−20	−10
	−30	−25	−10
	−35	−10	−5
	−25	−10	−5
	−5	−5	−5
	−10	−5	−5
	−5	−5	−5
	−20	−10	−5
Average cochlear reserve	**−22.3**	**−12.3**	**−5.2**

TABLE 3 | Ratio between positive and negative patients on MRI and patients with cochlear reserve >10 dB on the frequencies 250-500-1000 Hz ($p = 0.002$) sensibility 86%.

Audiometry—MRI correspondence		
	MRI+	**MRI-**
Audiometry +	20	3
Audiometry −	2	5

of 80% (24/30) ($p = 0004$), while in 20% of the patients (6/30 patients) labyrinthine hydrops could not be demonstrated radiologically, even with a positive caloric test (**Table 6**).

In the computerized static posturography thes, the most important differences among path lengths (PL) were seen with closed eyes plus foam cushion under feet, and a significant improvement was observed 24 h after gadolinium injection (**Figure 1**) ($p = 0.011$, Cohen's $d = 0.876$, BF10 = 5.328) (data already reported elsewhere) (16).

TABLE 4 | Ratio between positive and negative patients on MRI and patients with and subjects with absent or reduced evocability of VEMPs (*p*CVEMPs = 0.3, *p*OVEMPs = 0.5).

VEMPs - MRI correspondence		
	RM +	**RM -**
C-VEMPS +	15	4
C-VEMPS -	7	4
O-VEMPS +	16	5
O-VEMPS -	6	3

TABLE 5 | Ratio between positive and negative patients on MRI and patients with corrective saccades after the head movement and decreased gain for the horizontal canal ($p = 0.003$).

vHIT - RM correspondence		
	RM+	**RM-**
HIT +	15	2
HIT -	7	6

TABLE 6 | Bithermal Caloric Test: Ratio between positive and negative patients on MRI and patients with a preponderance >20% ($p = 0.004$).

Bithermal caloric test—RM		
	RM +	**RM -**
BCT +	16	0
BCT -	6	8
Corrispondence	80%	
Discrepancy	20%	

TABLE 7 | Distribution of gadolinium in the perilymphatic spaces expressed in number of patients and percentage.

Cochlea	Vestibular spaces	Anterior SC	Posterior SC	Lateral SC
21 (70%)	27 (90%)	13 (43%)	17 (56%)	13 (43%)

Gadolinium MRI 3 Tesla did not cause any local or systemic adverse reactions. Thirty (17) of the 35 patients (86%) had a positive Gd response with contrast medium diffusion into the perilymph. Five (4) non-responders were excluded from the study. One radiologist graded the hydrops in different parts of the vestibule (**Table 7**). Contrast medium was observed in the internal auditory canal (**Figure 2**), demonstrating a communication between CSF and cochlear perilymph as described by Naganawa (18) and Kawai (19).

DISCUSSION

MD is the prototype of chronic recurrent diseases of the inner ear. Certain Meniere's disease diagnoses may be difficult despite the 2015 Barany Criteria, since they can be mimicked by other vestibular disorders. The caloric test has been the only available objective test and it has been based on the horizontal canal, and 3D-FLAIR MRI inner ear imaging and audiovestibular tests have allowed more precise diagnoses. More recently, the demonstration of inner ear hydrops by Naganawa and Nakashima (4) has granted to use MRI in MD and to disclose hydrops in migraine, trauma, sudden deafness, vestibular schwannoma, and semicircular canal dehiscence (20–22). However, doubts remain concerning the correlation between radiological and audio-vestibular findings. Pyykko et al. (9) have found a 53% sudden hearing loss in patients with EH and Katayama et al. (23) and Seoa et al. (24) have reported conflicting results as to whether cVEMPs and oVEMPs are concealed by hydrops; for caloric tests controversial findings have also been reported in literature (17, 25, 26).

Some authors have reported MD patients having a normal vHIT in the presence of a canal paresis on bithermal caloric testing. It has been hypothesized that hydropic distension allows endolymph recirculation with dissipation of its hydrostatic force and reduction of cupula displacement and nystagmus (27), and this hypothesis could have been confirmed by a direct observation of the vestibules in these patients. In the present study none of the methods, including MRI, achieved absolute diagnostic capacity. In particular, the bithermal caloric test showed a significant concordance between labyrinthine disease and radiological hydrops in 80% of the patients. The data in the present study are in line with the literature, and we and Dumas (28) have suggested that the discrepancy could be the result of either hydrops fluctuation that improves cochlear and vestibular function between attacks or of a mistaken diagnosis. The data of the present study are therefore in line with what emerges from literature, and indicate that caloric testing was able to evidence labyrinthine damage but not hydrops, as it was negative in 20–30% of the patients. Probably the reason for such discrepancy lies in the fluctuation of the hydrops in the patients in the present study during inter-critical periods, as in those by Dumas (28), which reduces the endolymphatic pressure thus improving both cochlear and vestibular function.

Evaluation of the horizontal canal using both caloric test and vHIT resulted in a reduction of agreement with MRI from 80 to 70%. The two methods stimulated the labyrinth with two different modalities, by 0.03 Hz frequencies in the caloric test, and by angular accelerations that could even reach 2,000–4,000°/s2 in the HIT (14) and this data confirm that in MD the horizontal semicircular canal maintains the ability to be stimulated on the low frequencies better than on the high ones. The most prominent feature of VOR was indeed adaptation (29). The labyrinth is able to change and improve against harmful events that might arise either slowly such as in aging, or rapidly such as in the case of lesions of the peripheral vestibular organ. In all cases, however, the labyrinthine asymmetry was reduced, but the response of the VOR to low frequencies and to low speed head movements recovered within a few weeks, while the responses to high frequency stimuli (such as HIT) were rarely complete and therefore an asymmetry to rapid head rotations persisted (30), which generated the saccadic movement toward the injured side, typical of the HIT (31).

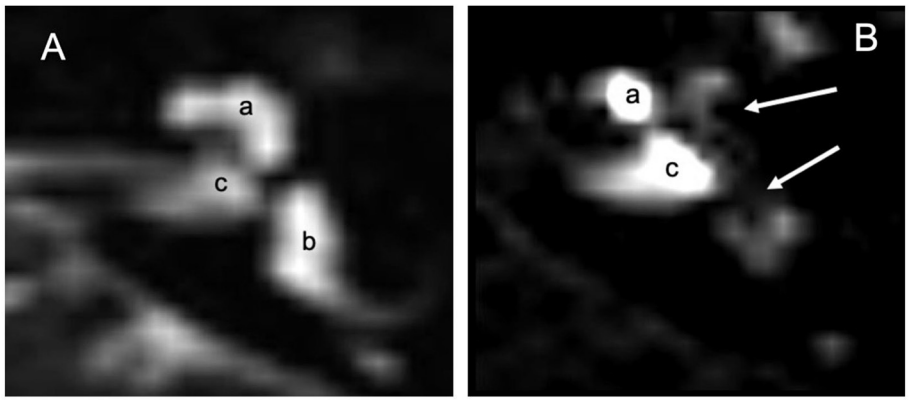

FIGURE 2 | MRI 3 Tesla: **(A)** MRI in T2 without contrast means: labyrinthine fluids including peri and endolymphatic spaces are observed (a) cochlea, (b) vestibular spaces and CSL and internal auditory canal (c). **(B)** 24 h after infiltration with the Flair technique, the contrast shows absence of gadolinium in the apical gyrus of the cochlea and vestibule (white arrows). Gd illuminates part of the cochlea (a) and the internal auditory canal (c) which seems to be the main way of diffusion of gadolinium toward the liquor spaces.

In the present study, patients were subjected to audiometric tests, and the focus was on the evaluation of low frequencies (250-500-1000), neglecting sensorineural loss resulting from MD and hearing fluctuations as they have already been widely described in the literature and represent an essential part of commonly used diagnostic criteria. Instead, the focus was on the presence or absence of cochlear reserve, which is mainly determined by the pressure of the endolymph on the platen of the stirrup and which therefore was indicative of hydrops rather than just of hearing loss. The present data show that the cochlear reserve corresponded to the MRI endolymphatic hydrops in a significant percentage of patients (83%) and therefore the cochlear reserve represents the simplest and most immediate finding that indicated hydrops regardless of sensorineural hearing loss, with a sensitivity of 86%. The spinal vestibule reflex was also evaluated using VEMPs, which did not prove to be comparable with MRI in quantifying the damage. This seems to be a consequence of the wide variability of both cervical and ocular responses in VEMPs (32), which changed according to the stage of the disease, so that in the acute phase oVEMPs increased while the cVEMPs decreased in amplitude (17) and to the vestibular nervous branch involved. Indeed, it has been observed that damage to the superior vestibular nerve results in a normal response of the cervical VEMPs and in a reduced or absent response to the ocular VEMPs while the opposite occurs with damaged inferior vestibular nerve (33–35). Both these phenomena occur because in MD the ocular VEMPs have a lower response compared to the cervical VEMPs, and it has been hypothesized that the utricle is more associated with the auditory function at low frequencies as compared to the saccule. In the present work, the posturographic evaluations showed that vestibular function not only does not worsen, but it even improves (16) after intratympanic injection, and vestibular function was certainly not linked to the Gd administration. Instead, as for audiometry, vestibular function could be linked to the pressure changes in the middle ear, which are induced by the mass of injected fluid, exerting a micro-pressure on the oval window and so modifying the dynamics inside the labyrinth as already described in Therapy with Meniett by Odqvist (36) and Gates (37).

A final observation that emerged from the imaging analysis, concerns the diffusion of the contrast medium in the internal auditory canal (IAC) (**Figure 2**). The IAC is lined with dura mater and arachnoid and it is perforated at the bottom by the vascular-nervous bundle which includes the VII and VIII cranial nerves. In IAC therefore, a natural communication exists between the cerebrospinal fluid (CSF) and perilymph (38). The MRI representations of this fluid exchange confirmed how CSF pressure changes can be transmitted to the perilymph, and therefore to the cochlea. This contiguity determines CSF pressure increases, as in gusher syndrome during stapedotomy, and in CSF pressure reductions, as in patients undergoing peritoneal ventricular shunt. Such shunts result in a low perilymphatic pressure with relative endolymphatic hydrops (39) and in variations in otoemission due to a "vacuum" in the inner ear (40, 41). These data seem to show that the relation between CSF and perilymph could be another etiopathogenetic mechanism of MD.

In the present work, intratympanic injection of Gd and subsequent 3T RM was certainly the most revolutionary way of using contrast medium in the vestibology field, as it was able to visualize endolymphatic hydrops and to ascertain not only cochlear hydrops but also a hydropic extension to the remaining parts of the posterior vestibule. However, intratympanic MRI assessment of hydrops is time-consuming, expensive and fails in about 20% of patients. The use of intravenous contrast medium could be a valid alternative to intratympanic injection as it could avoid the contrast medium diffusion problems encountered in this study. It is therefore necessary to associate imaging with electrophysiological tests, which are cheaper and easier to perform.

In this study, MRI showed results that are similar to those that have been seen for a long time with caloric tests and audiometry, which have a greater sensitivity than more recent tests such as

HIT, which however showed reduced but significantly similar findings to MRI. VEMPs, on the contrary, even though retaining all their validity, due to their wide variability could be correlated with the imaging testing which should therefore be seen as the best choice. Beyond method comparisons, it is indubitable that MRI allowed vision of the hydrops, and its added value was that it stimulated research and gave the opportunity to observe a "secret" compartment without producing cochlear damage or instability. This fact, impossible in the past opened new diagnostic, pathophysiological and therapeutic horizons. In past as well as in the present work, MRI allowed disclosure of new data, such as the possible role played by the perilymph and cerebrospinal fluid in the etiopathogenesis of MD, and MRI combined with instrumental and electrophysiological data guarantee MD monitoring over time and the effectiveness of the therapy.

DATA AVAILABILITY STATEMENT

The original contributions presented in the study are included in the article/supplementary material, further inquiries can be directed to the corresponding author/s.

ETHICS STATEMENT

The studies involving human participants were reviewed and approved by University of Chieti. The patients/participants provided their written informed consent to participate in this study.

AUTHOR CONTRIBUTIONS

GN ideate the work write the manuscript and revised the manuscript. AT performed the radiological examinations, helped write the work, and translate the paper. LN recruited the patients and provide all clinical information elaborate the data helped write the work. All authors contributed to the article and approved the submitted version.

ACKNOWLEDGMENTS

We are very grateful to Prof. Franca Daniele, from the Department of Medical, Oral and Biotechnologies Sciences of Gabriele d'Annunzio University, Chieti-Pescara, for her precious collaboration in reviewing the paper in English.

REFERENCES

1. American Academy of Otolaryngology-Head and Neck Foundation, Inc. Committee on hearing and equilibrium guidelines for the diagnosis and evaluation of therapy in Meniere's disease. *Otolaryngol Head Neck Surg.* (1995) 113:181–5. doi: 10.1016/S0194-5998(95)70102-8
2. Menière Prosper Sur une forme de surdité grave dépendant d'une lésion de l'oreille interne. In: *Bulletin de l'Académie impériale de médecine, Résumé de la lecture devant l'Académie de médecine lors de la séance du 8 janvier 1861, t. XXVI*, p. 241.
3. Lopez-Escamez JA, Carey J, Chung WH, Goebel JA, Magnusson M, Mandala M, et al. Diagnostic criteria for Meniere's disease. *J Vestib Res.* (2015) 25:1–7. doi: 10.3233/VES-150549
4. Nakashima T, Naganawa S, Sugiura M, Teranishi M, Sone M, Hayashi H, et al. Visualization of endolymphatic hydrops in patients with meniere's disease. *Laryngoscope.* (2007) 117:415–20. doi: 10.1097/MLG.0b013e31802c300c
5. Naganawa S, Sugiura M, Kawamura M, Fukatsu H, Sone M, Nakashima T. Imaging of endolymphatic and perilymphatic fluid at 3T After intratympanic administration of gadolinium-diethylene-triamine pentaacetic acid. *Am J Neuroradiol.* (2008) 29:724–6. doi: 10.3174/ajnr.A0894
6. van Steekelenburg JM, van Weijnen A, de Pont LMH, Vijlbrief OD, Bommeljé CC, Koopman JP, et al. Value of endolymphatic hydrops and perilymph signal intensity in suspected ménière disease. *AJNR Am J Neuroradiol.* (2020) 41:529–34. doi: 10.3174/ajnr.A6410
7. Li X, Wu Q, Sha Y, Dai C, Zhang R. Gadolinium-enhanced MRI reveals dynamic development of endolymphatic hydrops in Ménière's disease. *Braz J Otorhinolaryngol.* (2020) 86:165–73. doi: 10.1016/j.bjorl.2018.10.014
8. Gurkov R, Kantner C, Strupp M, Flatz W, Krause E, Ertl-Wagner B. Endolymphatic hydrops in patients with vestibular migraine and auditory symptoms. *Eur Arch Otorhinolaryngol.* (2014) 271:2661–7. doi: 10.1007/s00405-013-2751-2
9. Pyykkö I, Nakashima T, Yoshida T, Zou J, Naganawa S. Ménière's disease: a reappraisal supported by a variable latency of symptoms and the MRI visualisation of endolymphatic hydrops. *BMJ Open.* (2013) 3:e001555. doi: 10.1136/bmjopen-2012-001555
10. Conte G, Lo Russo FM, Calloni FM, Sina FM, Barozzi S, Di Berardino F, et al. MR imaging of endolymphatic hydrops in Ménière's disease: not all that glitters is gold. *Acta Otorhinolaryngologica Italica.* (2018) 38:369–76. doi: 10.14639/0392-100X-1986
11. Havia M, Kentala E, Pyykko I. Prevalence of Meniere's disease in general population of Southern Finland. *Otolaryngol Head Neck Surg.* (2005) 133:762–8. doi: 10.1016/j.otohns.2005.06.015
12. Alexander TH, Harris JP. Current epidemiology of Meniere's syndrome. *Otolaryngol Clin North Am.* (2010) 43:965–70. doi: 10.1016/j.otc.2010.05.001
13. Kim HJ, Park SH, Kim J-S, Koo JW, Kim C-Y, Kim Y-H, et al. Bilaterally abnormal head impulse tests indicate a large cerebellopontine angle tumor. *J Clin Neurol.* (2016) 12:65–74. doi: 10.3988/jcn.2016.12.1.65
14. Bartolomeo M, Biboulet R, Pierre G, Mondain M, Uziel A, Venail F. Value of the video head impulse test in assessing vestibular deficits following vestibular neuritis. *Eur Arch Otorhinolaryngol.* (2014) 271:681–8. doi: 10.1007/s00405-013-2451-y
15. Kasai S, Teranishi M, Katayama N, Sugiura M, Nakata S, Sone M, et al. Endolymphatic space imaging in patients with delayed endolymphatic hydrops. *ActaOto-Laryngologica.* (2009) 129:1169–74. doi: 10.3109/00016480802691143
16. Neri G, Bondi D, Scordella A, Tartaro A, Neri L, Cazzato F, et al. Menière's disease patients improve specific posturographic parameters following diagnostic intratympanic injection. *Am J Otolaryngol.* (2020) 41:102468. doi: 10.1016/j.amjoto.2020.102468
17. Gurkov R, Flatz W, Louza J, Strupp M, Krause E. *In vivo* visualization of endolymphatic hydrops in patients with Meniere's disease: correlation with audiovestibular function. *Eur Arch Otorhinolaryngol.* (2011) 268:1743–8. doi: 10.1007/s00405-011-1573-3
18. Naganawa S, Satake H, Iwano S, Sone M, Nakashima T. Communication between cochlear perilymph and cerebrospinal fluid through the cochlear modiolus visualized after intratympanic administration of Gd-DTPA. *Radiat Med.* (2008) 26:597–602. doi: 10.1007/s11604-008-0286-z
19. Kawai H, Naganawa S, Ishihara S, Sone M, Nakashima T. MR imaging of the cochlear modiolus after intratympanic administration of Gd-DTPA. *Magn Reson Med Sci.* (2010) 9:23–9. doi: 10.2463/mrms.9.23
20. Teranishi M, Naganawa S, Katayama N, Sugiura M, Nakata S, Sone M, et al. Image evaluation of endolymphatic space in fluctuating hearing loss without vertigo. *Eur Arch Otorhinolaryngol.* (2009) 266:1871–7. doi: 10.1007/s00405-009-0989-5

21. Poe DP, Pyykkö I. *Endolymphatic Hydrops in Patients With Superior Semicircular Canal Dehiscence Syndrome*. Iceland: Barany Society Meeting (2010).
22. Naganawa S, Kawai H, Sone M, Nakashima T, Ikeda M. Endolympathic hydrops in patients with vestibular schwannoma: visualization by non-contrast-enhanced 3D FLAIR. *Neuroradiology*. (2011) 53:1009–15. doi: 10.1007/s00234-010-0834-y
23. Katayama N, Yamamoto M, Teranishi M, Naganawa S, Nakata S, Sone M, et al. Relationship between endolymphatic hydrops and vestibular-evoked myogenic potential. *Acta Otolaryngol*. (2010) 130:917–23. doi: 10.3109/00016480903573187
24. Seoa YJ, Kimb J, Choia JY, Leea WS. Visualization of endolymphatic hydrops and correlation with audio-vestibular functional testing in patients with definite Menière's disease. *Auris Nasus Larynx*. (2013) 40:167–72. doi: 10.1016/j.anl.2012.07.009
25. Kato M, Teranishi M, Katayama N, Sone M, Naganawa S, Nakashima T. Association between endolymphatic hydrops as revealed by magnetic resonance imaging and caloric response. *Otol Neurotol*. (2011) 32:1480–5. doi: 10.1097/MAO.0b013e318235568d
26. Fiorino F, Pizzini FB, Beltramello A, Barbieri F. MRI performed after intratympanic gadolinium administration in patients with Meniere's disease: correlation with symptoms and signs. *Eur Arch Otorhinolaryngol*. (2011) 268:181–7. doi: 10.1007/s00405-010-1353-5
27. McGarvie LA, Curthoys IS, MacDougall HG, Halmagyi, GM. What does the head impulse test versus caloric dissociation reveal about vestibular dysfunction in Meniere's disease? *Ann N Y Acad Sci*. (2015) 1343:58–62. doi: 10.1111/nyas.12687
28. Dumas G, Lavieille JP, Schmerber S Vibratory test head shaking test and caloric test: a series of 87 patients. *Annalesd'Oto-laryngologie et de Chirurgie Cervico faciale Bulletin de la Societé d'Oto-laringologie des Hopitaux de Paris*. (2004) 121:22–32. doi: 10.1016/S0003-438X(04)95487-4
29. Rinaudo CN, Schubert MC, Figtree WVC, Todd CJ, Migliaccio AA. Human vestibulo-ocular reflex adaptation is frequency selective. *Neurophysiol*. (2019) 122:984–93. doi: 10.1152/jn.00162.2019
30. Cullen KE, Minor LB, Beraneck M, Sadeghi SG. Neural substrates underlying vestibular compensation: contribution of peripheral versus central processing. *J Vestib Res*. (2009) 19:171–82. doi: 10.3233/VES-2009-0357
31. Halmagyi M, Curthoys I. A clinical sign of canal paresis. *Arch Neurol*. (1988) 45:737–9. doi: 10.1001/archneur.1988.00520310043015
32. Chiarovano E, Zamith F, Vidal PP, Waele C. Ocular and cervical VEMPs: a study of 74 patients suffering from peripheral vestibular disorders. *Clin Neurophysiol*. (2011) 122:1650–9.10. doi: 10.1016/j.clinph.2011.01.006
33. Oh SY, Kim JS, Yang TH, Shin BS, Jeong SK. Cervical and ocular vestibular-evoked myogenic potentials in vestibular neuritis: comparison between air- and bone conducted stimulation. *J Neurol*. (2013) 260:2102–9.11. doi: 10.1007/s00415-013-6953-8
34. Shin BS, Oh SY, Kim JS, Kim TW, Seo MW, Lee H, et al. Cervical and ocular vestibular-evoked myogenic potentials in acute vestibular neuritis. *Clin Neurophysiol*. (2012) 123:369–75. doi: 10.1016/j.clinph.2011.05.029
35. Halmagyi GM, Webera KP, Curthoys IS. Vestibular function after acute vestibular neuritis. *Restor Neurol Neurosci*. (2010) 28:37–46. doi: 10.3233/RNN-2010-0533
36. Odkvist LM, Arlinger S, Billermark E, Densert B, Lindholm S, Wallqvist J. Effects of middle ear pressure changes on clinical symptoms in patients with Ménière's disease, a clinical multicentre placebo-controlled study. *Acta Otolaryngol Suppl*. (2000) 543:99–101. doi: 10.1080/000164800454107
37. Gates GA, Green JD Jr, Tucci DL, Telian SA. The effects of transtympanic micropressure treatment in people with unilateral ménière's disease. *Arch Otolaryngol Head Neck Surg*. (2004) 130:718–25. doi: 10.1001/archotol.130.6.718
38. Salt AN, Hale SA, Plontke SKR. Perilymph sampling from the cochlear apex: a reliable method to obtain higher purity perilymph samples from scala tympani. *J Neurosci Methods*. (2006) 153:121–9. doi: 10.1016/j.jneumeth.2005.10.008
39. Gordon AG. Endolymphatic hydrops and CSF pressure. *J Neurosurg*. (1984) 60:1332–4. doi: 10.3171/jns.1984.60.6.1332
40. Walsted A, Nielsen OA, Borum P. Hearing loss after neurosurgery. The influence of low cerebrospinal fluid pressure. *J Laryngol Otol*. (1994) 108:637–41. doi: 10.1017/S0022215100127719
41. Chomicki A, Sakka L, Avan P, Khalil T, Lemaire JJ, Chazal J. Derivation of cerebrospinal fluid: consequences on inner ear biomechanics in adult patients with chronic hydrocephalus. *Neurochirurgie*. (2007) 53:265–71. doi: 10.1016/j.neuchi.2007.04.005

Conflict of Interest: The authors declare that the research was conducted in the absence of any commercial or financial relationships that could be construed as a potential conflict of interest.

frontiers in Surgery

ORIGINAL RESEARCH
published: 16 June 2021
doi: 10.3389/fsurg.2021.680260

Cochlear Meniere's: A Distinct Clinical Entity With Isolated Cochlear Hydrops on High-Resolution MRI?

Jose E. Alonso[1†], Gail P. Ishiyama[2†], Rance J. T. Fujiwara[1], Nancy Pham[3], Luke Ledbetter[3] and Akira Ishiyama[1]*

[1] Department of Head and Neck Surgery, University of California, Los Angeles, Los Angeles, CA, United States, [2] Department of Neurology, University of California, Los Angeles, Los Angeles, CA, United States, [3] Department of Neuroradiology, University of California, Los Angeles, Los Angeles, CA, United States

OPEN ACCESS

Edited by:
Robert Gürkov,
Bielefeld University, Germany

Reviewed by:
Jeremy Hornibrook,
University of Canterbury, New Zealand
Chunfu Dai,
Fudan University, China
Peter Paul G. Van Benthem,
Leiden University Medical Center, Netherlands

***Correspondence:**
Gail P. Ishiyama
gishiyama@mednet.ucla.edu

[†] These authors share first authorship

Specialty section:
This article was submitted to Otorhinolaryngology - Head and Neck Surgery, a section of the journal Frontiers in Surgery

Received: 13 March 2021
Accepted: 10 May 2021
Published: 16 June 2021

Citation:
Alonso JE, Ishiyama GP, Fujiwara RJT, Pham N, Ledbetter L and Ishiyama A (2021) Cochlear Meniere's: A Distinct Clinical Entity With Isolated Cochlear Hydrops on High-Resolution MRI? Front. Surg. 8:680260. doi: 10.3389/fsurg.2021.680260

Objective: Describe the clinical characteristics of patients with isolated cochlear endolymphatic hydrops (EH).

Study design: Clinical case series.

Setting: Tertiary Neurotology referral clinic.

Patients: All subjects presenting to a University Neurotology clinic during a 1-year period from July 2015 until August 2016 who had isolated cochlear EH on MRI. Patients with a history of temporal bone surgery prior to the MRI were excluded.

Intervention: High-resolution delayed-intravenous contrast MRI.

Main outcome measures: Audiometric and vestibular testing, clinical history analysis.

Results: 10 subjects demonstrated *isolated*, unilateral cochlear hydrops on MRI. None of these patients met the criteria for Meniere's disease. Mean age of the group was 66.4 years and most were males (70%). Unilateral aural fullness (70%), tinnitus (80%), and hearing loss (90%) were frequently observed. Only one patient presented with unsteadiness (10%) and one patient had a single isolated spell of positional vertigo 1 month prior to the MRI (10%) but no further vertigo spells in the 4 years following the MRI. The mean PTA was 37.8 dB which was significantly decreased from the non-affected ear with PTA of 17.9 ($p < 0.001$). One patient developed vertiginous spells and unsteadiness 4 years after initial presentation and a repeat MRI revealed progression to utricular, saccular and cochlear hydrops. Vestibular testing was obtained in five patients with one patient presenting with 50% caloric paresis and all others normal. The most common treatment tried was acetazolamide in seven patients with 86% reporting subjective clinical improvement. Two out of the 10 patients had a history of migraine (20%).

Conclusions: Patients with MRI exhibiting isolated cochlear EH present with predominantly auditory symptoms: mild to moderate low-frequency hearing loss, aural fullness, tinnitus without significant vertigo. Isolated cochlear hydrops is more common in males, average age in mid-60's and there is a low comorbidity of migraine headaches. This contrasts significantly with patients with isolated saccular hydrops on MRI from our

prior studies. We believe that isolated cochlear EH with hearing loss but no vertigo is distinct from Meniere's disease or its variant delayed endolymphatic hydrops. We propose that cochlear Meniere's disease represents a distinct clinical entity that could be a variant of Meniere's disease.

Keywords: endolymphatic hydrops, cochlear Meniere's disease without vertigo, high-resolution MRI, cochlear hydrops, low-frequency hearing loss

INTRODUCTION

Meniere's disease is an inner ear disorder characterized with episodic spontaneous rotational vertigo, fluctuating hearing loss, tinnitus, and aural fullness. The diagnosis of Meniere's disease predominantly relies on clinical criteria as described by the 1995 American Academy of Otolaryngology—Head & Neck Surgery (AAO-HNS) and the 2015 Barany Society guidelines (1). Human temporal bone (HTB) studies have implicated dilation of the endolymphatic space—endolymphatic hydrops (EH)—as the nearly universal histopathological finding in Meniere's disease (2).

Cochlear hydrops or cochlear Meniere's disease was once classified as a distinct diagnostic entity, considered to be a variant of Meniere's disease without the vertigo. This group of patients previously diagnosed with cochlear Meniere's presented with a history of fluctuating auditory symptoms of aural fullness, tinnitus, and hearing loss without vertigo or vestibular symptoms (3). Despite the seemingly distinct clinical presentation of cochlear Meniere's, this entity was excluded by the Committee on Hearing and Equilibrium of the AAO-HNS in 1985 (4, 5). The histopathology of archival HTB studies of patients with a history of Meniere's disease, demonstrate that the pars inferior, the cochlea and saccule frequently display evidence of EH (6). However, it is important to evaluate for the presence and localization of EH during life in order to correlate with the clinical presentation. The question remains as to whether there is a specific histopathological correlate with isolated cochlear Meniere's.

High-resolution delayed contrast magnetic resonance imaging (MRI) has served to evaluate for endolymphatic hydrops *in vivo* to diagnose Meniere's disease and variants (7–9). High-resolution MRI imaging identification of EH involving the cochlea and vestibule is now achievable. In a study of eight patients with fluctuating hearing loss without vertigo, MRI evidence of cochlear and vestibular hydrops was identified in 100% of cases (10). A published case series of patients presenting with fluctuating aural pressure, tinnitus reported a response to medical therapy of diuretics and salt restriction in 80%, and evidence for hydrops using transtympanic electrocochleography (11). However, there has not been imaging evidence of the presence of isolated cochlear hydrops as a distinct clinical entity.

We report on a cohort of patients who display a unique set of clinical manifestations and demonstrate isolated cochlear hydrops. Importantly, little is clinically known about this entity. Herein, we aim to describe the clinical presentation of patients with isolated cochlear EH on MRI. We hypothesize that this entity is a clinically separate presentation of Meniere's disease, and we describe its clinical, audiometric, and MRI image features.

MATERIALS AND METHODS

Patient Selection

The 1995 AAO-HNS clinical guidelines were used to assign a diagnosis for definite Meniere's disease (5). A retrospective inquiry of consecutive patients who presented with audiovestibular symptoms between July 2015 and August 2016 were included. Of these, those with MRI imaging demonstrating EH of the cochlea alone were included. Patients with a past history of temporal bone surgery were excluded. With Institutional Review Board approval, a waiver of Health Insurance Portability and Accountability Act authorization, and a waiver of informed consent, a database of patients imaged with delayed intravenous contrast-enhanced 3D-FLAIR MRI was reviewed (IRB 13-000089, GI).

Data

Clinical histories, audiovestibular testing, and imaging from each patient were reviewed and recorded. Audiovestibular tests dated most closely with time of MRI were used for interpretation. The average follow-up was 16.5 months.

The pure tone average (PTA) was computed from frequencies 500, 1,000, 2,000 Hz as reported on the audiogram. Speech reception threshold (SRT) and word recognition scores (WRS) were also recorded.

Electronystagmography (ENG) testing was performed in five out of the 10 patients. Jonkee's formula was used to compute a unilateral canal paresis. A value >25% represented an abnormal response. Cervical vestibular-evoked myogenic potential (cVEMP) testing was performed in those undergoing ENG.

MRI Technique

Images were acquired as previously described (9, 12–15). In brief, a 3-Tesla Skyra unit (Siemens, Erlangen, Germany) using a 16-channel head and neck coil paired with two 4-channel surface coils positioned over bilateral ears was used following a 4-hour delay of an intravenous injection of 0.2 mmol/kg of either gadobutrol (Gadavist), or gadobenate. Cisternographic heavily T2-weighted 3-D turbo spin echo sequence (sampling perfection with application-optimized contrasts by using different flip angle evolutions: T2 SPACE) and heavily T2-weighted 3-D FLAIR

TABLE 1 | Pure tone average (PTA) of the affected ear and follow-up for each patient.

Case	PTA (dB)	Follow-up (months)
1	23	1
2	51	5
3	26	1
4	50	3
5	38	9
6	26	7
7	26	48
8	48	20
9	58.3	24
10	31.6	48

sequence (hT2w-FLAIR), and a 3-D FLAIR sequence with an inversion time of 2,050 ms, creating bright endolymph and dark perilymph were performed. A subtracted image was obtained with bright perilymph, dark endolymph, and intermediate-signal bone (9, 12, 13).

Statistical Analysis

Data were tabulated into Microsoft Excel and analyzed using Stata 15.0 (College Station, TX). Audiometric data of the affected ear were compared to the contralateral, unaffected ear. A two-tailed paired student's *t*-test was performed to assess for differences in PTA, SRT, and WRS. In all instances, p-values < 0.05 were deemed significant.

RESULTS

Demographic and Clinical Presentation

Ten patients with MRI evidence of isolated cochlear hydrops were identified and included in the study. These are cases of hydrops of the cochlear duct, but no hydrops of the saccule or the utricle. The mean age is 66.4 years with a range of 50–85 years. There were seven males (70%) and three females (30%). There was involvement of five left (50%) and five right (50%) inner ears. The mean follow-up was 16.5 months (range 1–48 months) and PTA for each patient is seen in **Table 1**.

TABLE 2 | Demographics and symptomatology; *utricular, saccular EH was identified on repeat MRI 4 years following initial presentation with isolated cochlear hydrops.

Age	**Years**
Mean +/– Std dev	66.4 +/– 11.4
Minimum	50
Maximum	85
Pure tone average	**dB**
Mean +/– Std dev	37.8 +/– 13.0
Minimum	23
Maximum	58.3
Characteristic	**Percentage (*n*)**
Sex	
Female	30% (3)
Male	70% (7)
Affected ear	
Left	50% (5)
Right	50% (5)
Symptomatology	
Aural fullness	70% (7)
Hearing loss	90% (9)
Tinnitus	80% (8)
Fluctuating hearing loss	10% (1)
Positional vertigo	10% (1)
Prolonged spontaneous vertigo	0%
Unsteadiness	10% (1)
Non-specific dizziness	10% (1)
MRI evidence of hydrops	
Cochlear	100% (10)
Utricular	11% (1)*
Saccular	11% (1)*
Electronystagmography	
Paresis or paralysis	10% (1)
Normal	40% (4)
Unknown	50% (5)
Treatment	
Acetazolomide	70% (7)
Hydrochlorothiazide	10% (1)
Betahistine	10% (1)
No treatment	10% (1)
Mean follow-up (months)	16.5; range 1–48

Auditory Symptoms

Auditory symptoms were the predominant clinical features. Ninety percent reported hearing loss, 70% endorsed ipsilateral aural fullness, and 80% complained of ipsilateral tinnitus often described it as a "hissing" or "whooshing" sound (**Table 2**). Of nine patients who reported hearing loss, only one characterized the hearing loss as fluctuating, and occurring suddenly the following day after taking a higher-than-normal dose of tadalafil (Cialis) (15). This patient with SSNHL did not clinically improve despite oral prednisone, and a subsequent MRI identified isolated cochlear hydrops. Of note, this patient had a history of migraines however the SSNHL did not occur in the setting of a migraine. The remaining patients characterized their hearing loss as gradually worsening or stable. Audiometric data commonly showed a low-frequency SNHL pattern.

Vestibular Symptoms

Vestibular symptoms were rare in these patients with isolated cochlear hydrops. No patient presented with prolonged spells of spontaneous rotational vertigo characteristic of Meniere's disease. One patient had a one-time occurrence of positional vertigo 1 month prior to the MRI imaging, and no further spells of vertigo in the ensuing subsequent 4 years of follow-up. One patient endorsed a sense of unsteadiness triggered by head positions,

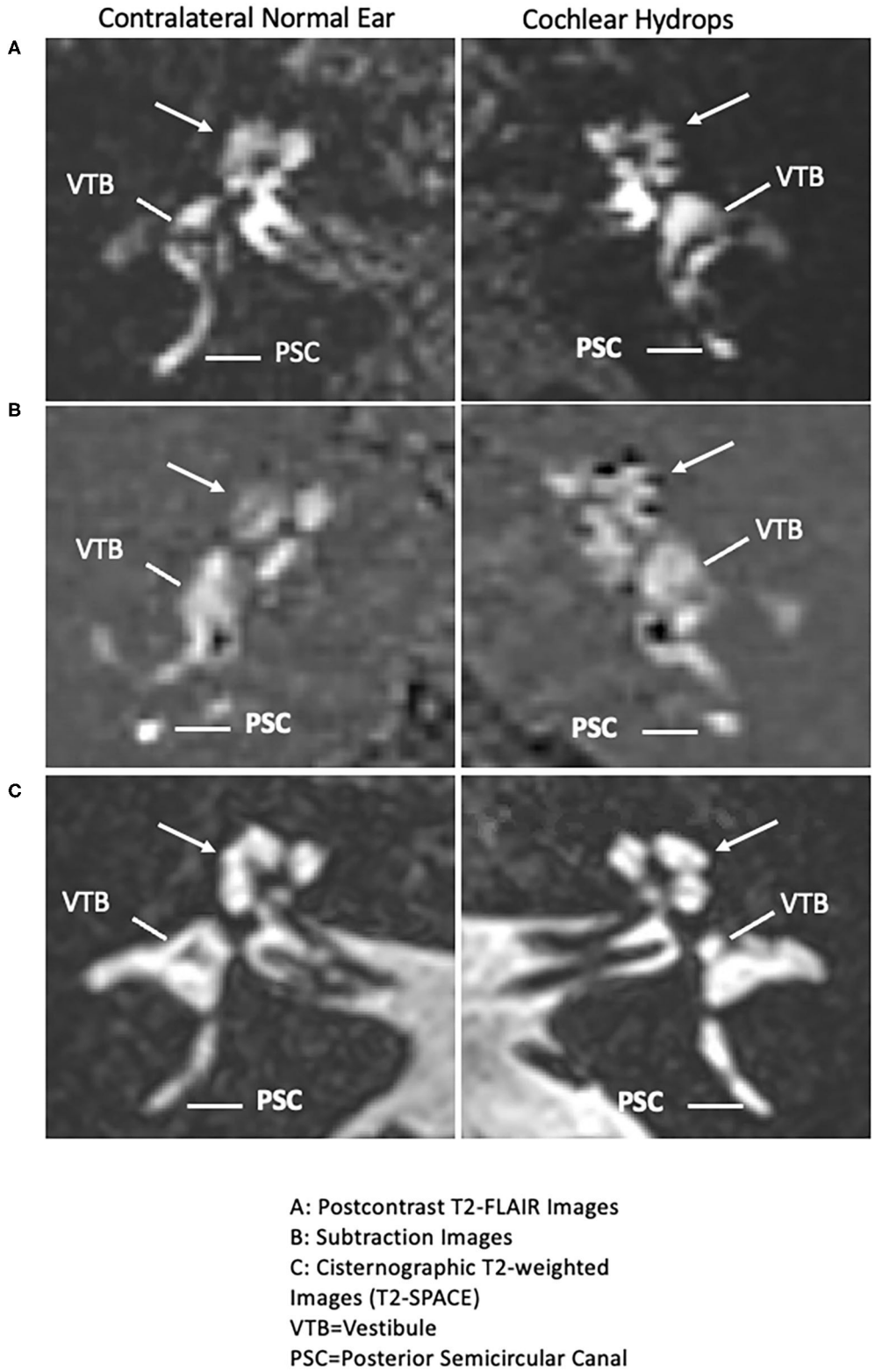

FIGURE 1 | Isolated cochlear endolymphatic hydrops on 3T MRI: *Right* column: Cochlear hydrops and *Left* column: contralateral normal ear. **(A)** (Top right panel: Cochlear hydrops), delayed postcontrast T2-FLAIR images through the cochlea demonstrate a prominent scala media signal void consistent with a dilated

(Continued)

FIGURE 1 | cochlear duct (arrow) in the left ear (Top left panel: normal contralateral side), a normal appearing cochlea in the right ear (arrow). Posterior semicircular canal (PSC) and vestibule (VTB) are labeled for reference. **(B)** (Middle right panel: cochlear hydrops), corresponding subtracted images more clearly isolate the cochlear duct (arrow) delineated against a nullified background (Middle left panel: normal contralateral side), a normal appearing cochlea in the right ear (arrow). **(C)** Bottom right panel: Cochlear hydrops and Bottom left panel: normal contralateral side): both sides on corresponding cisternographic T2-weighted images (T2 SPACE), provided for anatomic reference, demonstrate normal fluid signal within the vestibule and cochlea on the disease side and the normal contralateral side, indicating isolated cochlear hydrops.

with a duration of several minutes and no further spells noted during follow-up.

Cochlear Hydrops on MRI Testing

All patients displaying evidence of cochlear hydrops with contrast-enhanced MRI of the internal auditory canal in the time span covering July 2015 until August 2016 were included. There were no temporal bone, internal auditory canal, or cerebellopontine angle lesions. Isolated cochlear hydrops as depicted by hT2w-FLAIR sequence is seen in **Figure 1**. Of note, one patient who demonstrated isolated cochlear hydrops in the first MRI developed utricular, saccule, and cochlear hydrops on repeat imaging 4 years after their initial presentation along with recurrent spells of vertigo and worsening hearing loss. The progression from isolated cochlear hydrops to utricular, saccular and cochlear hydrops on imaging 4 years later is seen in **Figure 2**.

Comorbidity of Migraine

There were 2 (20%) patients with a comorbidity of migraine headaches as defined the International Headache Society criteria. No patients met the criteria for vestibular migraines. Both patients with a history of migraine were male. The patient who complained of non-specific unsteadiness had a history of migraine headaches, but there was no association of the migraine headaches with either the auditory or unsteadiness symptoms.

Progression to Meniere's Disease in One Patient

One patient out of the 10 with unilateral cochlear hydrops exhibited progression to Meniere's disease 4 years later. At the time of the first MRI, he complained of long-standing unilateral aural fullness, tinnitus, and hearing loss. Approximately 4 years later, he developed worsening unilateral auditory symptoms and recurrent spells of vertigo and MRI revealed progression to utricular, saccular, and cochlear hydrops (**Figure 2**). There were no drop attacks in our cohort.

Audiometry

All patients had audiometric testing for review and are presented per the standardized hearing outcomes format as previously described in Gurgel et al. (14). One hundred percent of patients exhibited sensorineural patterns of hearing loss (**Figure 3**). Of these, 70% (seven of 10 patients) showed low-frequency, up-sloping SNHL, and 20% (two of 10 patients) showed a flat SNHL pattern and one patient (10%) had a down-sloping SNHL. The average PTA in the affected ear is 37.8 ± 13.0 dB (range 23–58.3 dB). Mean SRT was 36.0 ± 22.5 dB (range 10–80). Mean WRS in the affected ear were excellent at 80% (range 16–100%) and the median was 96%. The PTA in the affected ear (37.8 ± 13.0) was significantly worse than in the unaffected ear (17.9 ± 7.1) ($p < 0.001$). The SRT in the affected ear (36.0 ± 22.5) was significantly worse than in the unaffected ear (23.0 ± 16.9) ($p = 0.001$). The WRS in the affected ear (80.0 ± 27.5) was also significantly worse than in the unaffected ear (93.2 ± 15.3) ($p = 0.02$) (**Table 3**).

Vestibular Testing

Five of 10 patients underwent ENG testing. Caloric testing revealed one patient with 50% paresis on the ipsilateral side. This patient had one time episode of positional vertigo 1 month prior to the MRI but no subsequent vertigo. All other patients had normal caloric testing results. Vestibular-evoked myogenic potential responses were normal in all subjects.

DISCUSSION

Isolated cochlear hydrops on MRI has an apparent distinct clinical entity. All patients in the present study with isolated cochlear endolymphatic hydrops with no vestibular hydrops exhibited symptomatology of unilateral stable hearing loss, aural fullness, and tinnitus. The PTA ranged from mild to moderate low-frequency hearing loss (average 42 dB), with only one patient in the profound category. This contrasts to patients with sudden SNHL, which PTA may range between 58.9 and 86.4 dB and typically affected in multiple consecutive frequencies (15–17). In addition, patients with sudden SNHL typically have less recovery of hearing if higher frequencies are involved compared with sudden SNHL in the low frequencies. This may reflect a predominance of hydrops as causative of low frequency sudden SNHL, which may be more likely to fluctuate. The most common pattern of hearing loss in the cochlear hydrops cohort was a low frequency SNHL in eight out of 10 patients (80%), with one patient having a flat SNHL and one patient having a downsloping SNHL. Of note, the patient with a flat SNHL pattern had a low frequency hearing loss in an audiogram documented 2 years prior to the MRI at the onset of the auditory symptoms. In the cochlear hydrops cohort, low-frequency SNHL was common pattern with 85.7% clinically responding to acetazolamide with improvement in subjective tinnitus and hearing. However, in those who underwent repeat audiogram, the hearing loss remained stable.

Of interest, one of the 10 patients characterized the hearing loss as sudden in onset, with improvement using acetazolamide. While one of the patients had sudden hearing loss, this group of patients is distinct from the patients with the idiopathic sudden hearing loss which presents generally with an abrupt hearing loss without fluctuation. The temporal bones from patients with a history of sudden SNHL demonstrate findings of severe atrophy of the organ of Corti and tectorial membrane without endolymphatic hydrops (18). A recent study using

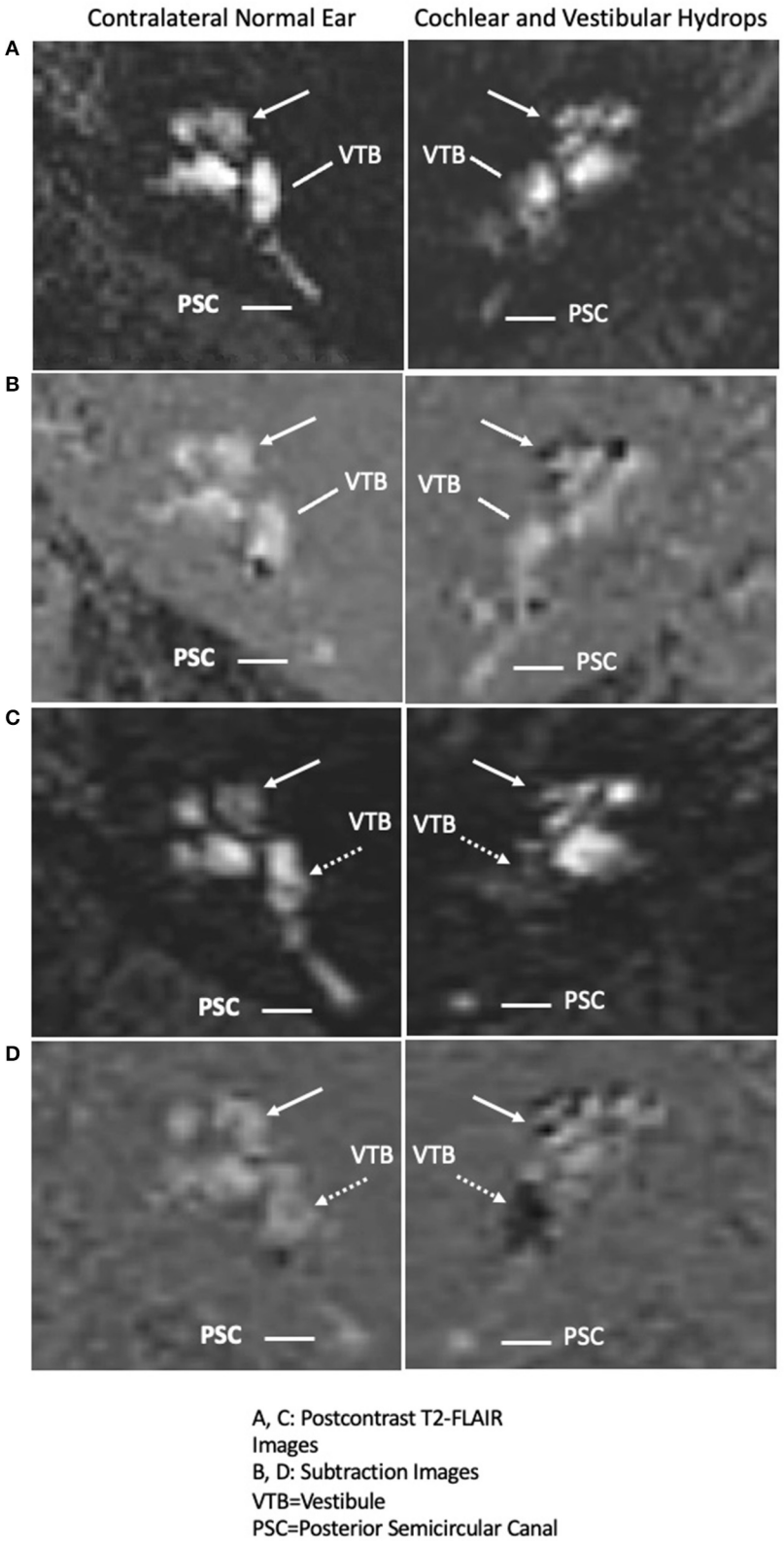

FIGURE 2 | Interval progression of cochlear endolymphatic hydrops in 2015 to cochlear and vestibular endolymphatic hydrops in 2019 on 3T MRI: *Right* column: Endolymphatic hydrops and *Left* column: contralateral normal ear. **(A)** (Right panel: Cochlear hydrops in 2015 MRI), delayed postcontrast T2-FLAIR images through

(Continued)

FIGURE 2 | the cochlea demonstrate a prominent scala media signal void consistent with a dilated cochlear duct (arrow) in the right ear (Left panel: normal contralateral side), a normal appearing cochlea in the left ear. Posterior semicircular canal (PSC) and vestibule (VTB) are labeled for reference. **(B)** (Right panel: Cochlear hydrops in 2015 MRI), corresponding subtracted images more clearly isolate the cochlear duct delineated against a nullified background (Left panel: normal contralateral side), a normal appearing cochlea in the left ear. **(C)** (Right panel: Cochlear and Vestibular hydrops in 2019 MRI), delayed postcontrast T2-FLAIR images demonstrate a prominent cochlear duct and vestibule signal void consistent with cochlear (arrow) and vestibular (dashed arrow) hydrops in the right ear (Left panel: normal contralateral side), normal appearance of the cochlea and vestibule. **(D)** (Right panel: Cochlear and Vestibular hydrops in 2019 MRI), corresponding subtracted images more clearly isolate the cochlear duct (arrow) and vestibule (dashed arrow) against a nullified background in the right ear (Left panel: normal contralateral side), normal subtracted images of the cochlea and vestibule in the left ear.

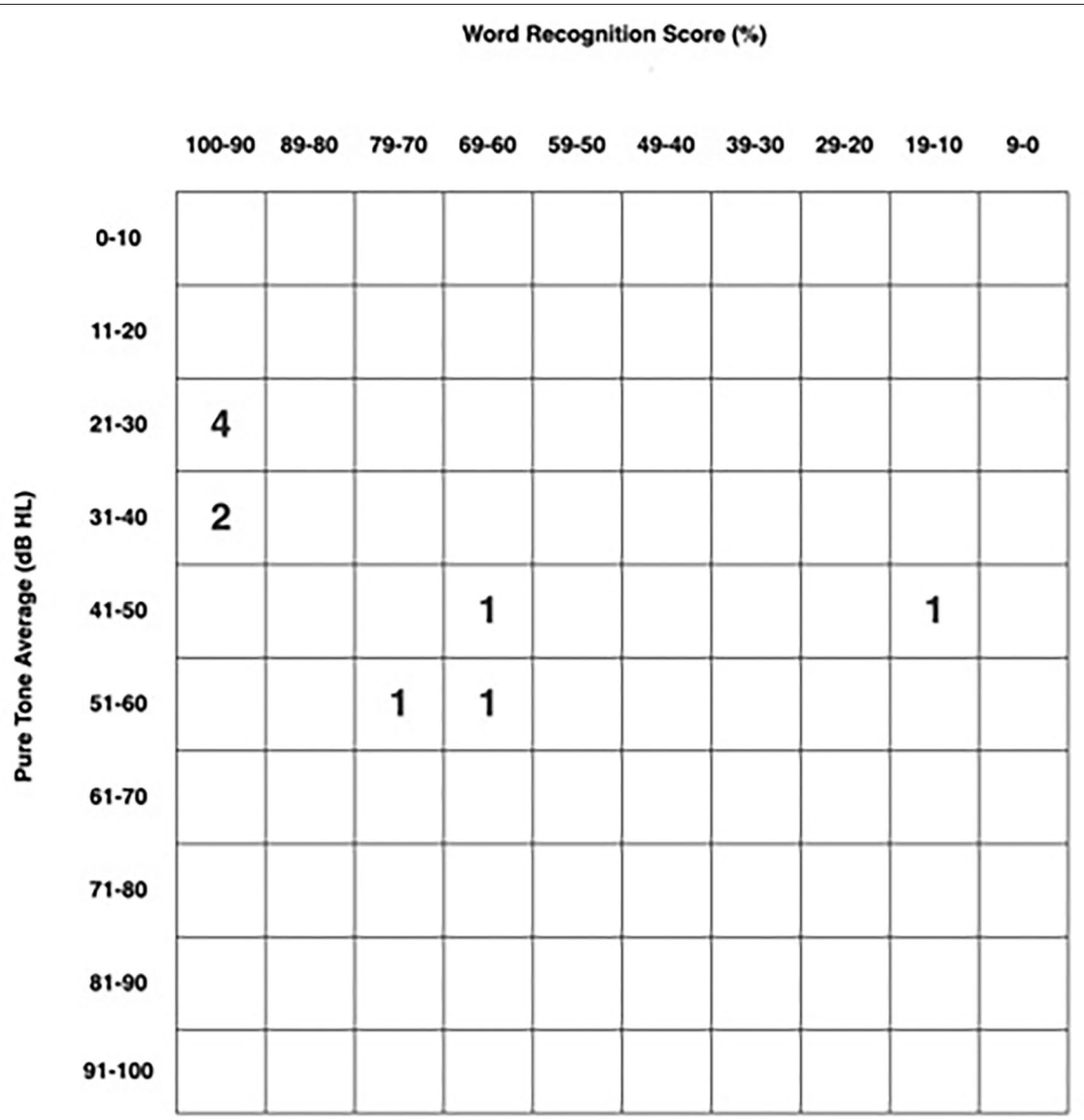

FIGURE 3 | Standardized audiometric scattergram of 10 patients.

high-resolution delayed contrast MRI imaging demonstrated that patients with sudden SNHL do not have endolymphatic hydrops (19).

Only one of the 10 patients reported vertigo in our study at the time of isolated cochlear hydrops on MRI. By description, this may have been a bout of benign paroxysmal positional vertigo. Another patient had a sense of unsteadiness predominantly with head movements. One other patient developed spells of vertigo 4 years later, and MRI revealed a progression to vestibular and cochlear hydrops. This patient is indicative of the potential for cochlear hydrops to present as a specific entity but may in some cases be early Meniere's disease.

The present study cohort have similar clinical presentations to a report by Nozawa et al. which identified prominent unilateral aural fullness, tinnitus, hearing loss in 50 patients with unilateral low-frequency SNHL. In their study, 33% described dizziness or unsteady sensation that was not fluctuating (20). Another separate retrospective study of 137 patients endorsed prominent unilateral auditory symptoms with approximately one-third unsteadiness or dizzy sensation immediately after rising (21). Both studies report a female predominance which differs from the present study of isolated cochlear hydrops which was 70% male. The clinical profile of symptoms is distinct from those of Meniere's disease characterized by spells of vertigo accompanied by reduced hearing, tinnitus, and aural fullness.

The management of the symptoms of isolated cochlear hydrops in this cohort was similar to that used for Meniere's disease. Notably, six out of 7 patients (85.7%) who were treated with acetazolamide reported significant improvement or resolution of symptoms. Of note, improvement in tinnitus and hearing was more commonly observed whereas aural fullness appeared to persist and respond poorly to medical management. One patient who clinically presented with tadalafil-related sudden SNHL with MRI evidence of isolated cochlear hydrops failed a course of prednisone, and subsequently had symptom improvement with acetazolamide (22). The rationale for using acetazolamide is based on an animal model where guinea pigs were administered oral acetazolamide and demonstrated reduced endolymphatic hydrops compared to those without treatment (23). Furthermore, patient's with Meniere's disease who respond to acetazolamide demonstrated reversal of endolymphatic hydrops with treatment based on MRI imaging (13).

There was one patient who presented with unilateral hearing loss, fullness, and tinnitus without vertigo had an MRI showing isolated cochlear hydrops, and would be diagnosed with cochlear Meniere's. Four years later, this patient had full spectrum Meniere's disease with recurrent spells of vertigo and unsteadiness and worsening auditory symptoms. The MRI progressed, consistent with ipsilateral cochlear, saccular, and utricular hydrops (**Figure 2**). This presentation has some overlapping features of delayed endolymphatic hydrops (DEH) which was first described by Nadol et al. (24). In DEH, episodic spells of vertigo occur 1–68 years following a preceding instance of sudden profound deafness (25). HTB studies have similarly identified EH on histopathologic analysis in DEH (25). However, this patient's initial hearing loss was mild at 26 dB. We speculate this patient progressed from cochlear EH to Meniere's disease, and that a subset of the isolated cochlear hydrops patients may represent an early form of Meniere's disease. Similarly, in our study of isolated saccular hydrops, one patient presented first with only sudden SNHL and then 3 years later developed full spectrum Meniere's disease with recurrent spells of room-spinning vertigo and the MRI demonstrated cochlear, saccular, and utricular hydrops (26).

It is particularly instructive to compare the present study cohort of patients with MRI demonstrating isolated cochlear hydrops to patients presenting with isolated saccular hydrops from our prior study. In the case of isolated saccular hydrops, the clinical presentation is the full spectrum of Meniere's disease with 12 out of 18 patients meeting criteria for Meniere's disease and four out of 18 meeting criteria for delayed endolymphatic hydrops (26). Thus, the presence of endolymphatic hydrops in the saccule in the case of sudden SNHL may be predictive of the development of Meniere's disease. Also, 22% of those with isolated saccular hydrops had a history of Tumarkin falls. This contrasts with the present study cohort of patients with isolated cochlear hydrops. There were no cases in the cochlear hydrops cohort meeting the criteria for Meniere's disease or delayed endolymphatic hydrops, and no cases of Tumarkin falls. In one patient, the isolated cochlear hydrops progressed to cochlear and vestibular hydrops with recurrent vertigo spells. Further studies may identify factors involved in progression of the endolymphatic hydrops.

TABLE 3 | Statistical analysis of audiometric data between affected and non-affected ear.

Outcome	Mean (SD)		*P*-value
	Affected ear	Non-affected ear	
PTA	37.8 (13.0)	17.9 (7.1)	<0.001
SRT	36.0 (22.5)	23.0 (16.9)	0.001
WRS	80.0 (27.5)	93.2 (15.3)	0.02

PTA, pure tone average; SRT, speech recognition threshold; WRS, word recognition score.

In the present study of all patients with isolated cochlear hydrops, audiovestibular testing demonstrates a low-frequency hearing loss pattern in 80%, similar to saccular hydrops (83%) with a similar degree of hearing impairment with isolated saccular hydrops mean PTA 54 dB vs. isolated cochlear hydrops 37.8 dB and WRS 59 vs. 80%. In both isolated saccular hydrops and isolated cochlear hydrops, there is a history of unilateral tinnitus, aural fullness and subjective response to diuretic therapy. Furthermore, there is a distinction in the incidence of migraine headaches which was significantly lower in our cohort compared to saccular hydrops patients (22 vs. 61%). Demographically, it appears cochlear hydrops more often affects men (mean age 67.6 years, 78% male). However, females were the majority in isolated saccular hydrops (mean age 60.8 years, 61% female) (26). Larger studies are indicated to evaluate these demographic differences between patients with isolated cochlear hydrops and those with isolated saccular hydrops.

VEMP testing identified normal responses in the present study of isolated cochlear hydrops. It is possible that endolymphatic hydrops localizing only to the cochlea is associated with preservation of VEMP responses. A multivariable analysis of the VEMP responses noted that that EH of the vestibule had a greater effect on the decrement of VEMP responses than EH of the cochlea (27). Of the five patients in the cohort of cochlear hydrops who had vestibular testing, one patient had 50% ipsilateral caloric paresis presenting with one single spell of positional vertigo. In Gurkov et al., the degree of audiovestibular hydrops correlated with a progressive loss of auditory function, and a trend toward decrement of amplitude of VEMP (27). The presence of isolated saccular hydrops was indicative of

Meniere's disease, and correspondingly 53% of those tested had a significant caloric paresis and 29% had reduced or absent VEMP responses (26).

In fifty-percent of our patients, an increased FLAIR signal in the perilymphatic space was noted in the inner ear with cochlear EH. In a previous study, our group attributed this radiographic finding to an increased blood-labyrinthine barrier permeability (28). Furthermore, extensive endothelial cell damage and the presence of oxidative stress markers were identified in a histopathologic analysis of human utricular macula from patients who underwent surgery for intractable Meniere's disease or delayed EH. These findings could represent a pathophysiologic mechanism or contribute to an increased permeability of the blood-labyrinthine barrier, and the subsequent development of EH (28, 29).

Migraine as a comorbidity was seen in only two of nine patients, and both were male with one patient endorsing non-specific dizziness or unsteadiness in addition to ipsilateral fluctuating mild hearing loss. Previous case studies reported a possible pathophysiologic link between migraine and sudden SNHL in a subset of idiopathic sudden hearing loss (30). There is one case report of MRI evidence of bilateral EH involving the vestibule and cochlea has been demonstrated in a patient with bilateral fluctuating hearing loss, tinnitus, without vertigo who may represent early bilateral Meniere's disease (31). Our cohort further contrasts with patients with Meniere's disease with migraine who frequently have bilateral subjective fluctuating hearing loss with a return to baseline normal hearing, and have an earlier age of symptom onset (32, 33). In the majority of cases of isolated cochlear hydrops, the symptoms were responsive to acetazolamide. The 20% comorbidity of migraines in the present study of isolated cochlear hydrops is not greater than the incidence in the general population. Additionally, in the two cases of comorbidity of migraines and cochlear hydrops, the migraines were not temporally associated with the inner ear symptoms. In contrast, Gurkov et al. study of 249 patients with MRI confirmed Meniere's disease, about 20% had migraine visual aura (phosphenes) simultaneous with the vertigo spells and more than half of the patients reported that headaches occurred in association with their vertigo (34).

There are limitations inherent to the current study. An element of selection bias exists as our cohort consists of patients who present to a tertiary university Neurotology clinic with hearing loss and or audiovestibular symptoms, and thus there is a high pre-test probability for endolymphatic hydrops. Further studies would be to conduct more extended follow-up to enable symptom tracking, treatment response, and the possibility to monitor for the evolution of symptoms and MRI findings.

DATA AVAILABILITY STATEMENT

The data analyzed in this study is subject to the following licenses/restrictions: they contain protected health information. Requests to access these datasets should be directed to jalonso@mednet.ucla.edu.

AUTHOR CONTRIBUTIONS

GI and AI: contributed to the conception and design of the project. JA: organized the database. JA and RF: performed the statistical analysis. NP and LL: contributed to the collection and refinement of radiologic images. All authors contributed to manuscript revision, read, and approved the submitted version.

REFERENCES

1. Lopez-Escamez JA, Carey J, Chung WH, Goebel JA, Magnusson M, Mandala M, et al. Classification committee of the Barany Society; Japan Society for Equilibrium Research; European Academy of Otology and Neurotology; Equilibrium Committee of the American Academy of Otolaryngology- Head and Neck Surgery; Korean Balance Society. Diagnostic criteria for Meniere's disease. *J Vestib Res.* (2015) 35:1–7. doi: 10.1016/j.otorri.2015.05.005
2. Hallpike CS, Cairns H. Observations on the pathology of Meniere's syndrome. *J Laryngol Otol.* (1938) 53:625–55. doi: 10.1017/S0022215100003947
3. Williams HL, Horton BT, Day LA. Endolymphatic hydrops without vertigo: its differential diagnosis and treatment. *Archiv Otolaryngol.* (1950) 51.4:557–81. doi: 10.1001/archotol.1950.00700020580008
4. Pearson BW, Brackmann DE. Committee on Hearing and Equilibrium guidelines for reporting treatment results in Meniere's disease. *Otolaryngol Head Neck Surg.* (1985) 93:579–81. doi: 10.1177/019459988509300501
5. American Academy of Otolaryngology-Head and Neck Foundation. Committee on Hearing and Equilibrium guidelines for the diagnosis and evaluation of therapy in Meniere's disease. *Otolaryngol Head Neck Surg.* (1995) 113:181–5. doi: 10.1016/S0194-5998(95)70102-8
6. Okuno T, Sando I. Localization, frequency, and severity of endolymphatic hydrops and the pathology of the labyrinthine membrane in Menière's disease. *Ann Otol Rhinol Laryngol.* (1987) 96:438–45. doi: 10.1177/000348948709600418
7. Naganawa S, Sugiura M, Kawamura M, Fukatsu H, Sone M, Nakashima T. Imaging of endolymphatic and perilymphatic fluid at 3T after intratympanic administration of gadolinium-diethylene-triamine pentaacetic acid. *Am J Neuroradiol.* (2008) 29:724–6. doi: 10.3174/ajnr.A0894
8. Nakashima T, Naganawa S, Sugiura M, Teranishi M, Sone M, Hayashi H, et al. Visualization of endolymphatic hydrops in patients with Meniere's disease. *Laryngoscope.* (2007) 117:415–20. doi: 10.1097/MLG.0b013e318 02c300c
9. Sepahdari AR, Ishiyama G, Vorasubin N, Peng KA, Linetsky M, Ishiyama A. Delayed intravenous contrast-enhanced 3D FLAIR MRI in Meniere's disease: correlation of quantitative measures of endolymphatic hydrops with hearing. *Clin Imaging.* (2015) 39:26–31. doi: 10.1016/j.clinimag.2014. 09.014
10. Teranishi M, Naganawa S, Katayama N, Sugiura M, Nakata S, Sone M, et al. Image evaluation of endolymphatic space in fluctuating hearing loss without vertigo. *Eur Arch Otorhinolaryngol.* (2009) 266:1871–7. doi: 10.1007/s00405-009-0989-5
11. Dornhoffer JL. Diagnosis of cochlear Ménière's disease with electrocochleography. *J Otorhinolaryngol Relat Spec.* (1998) 60:301–5. doi: 10.1159/000027614
12. Naganawa S, Yamazaki M, Kawai H, Bokura K, Sone M, Nakashima T. Visualization of endolymphatic hydrops in Ménière's disease with single-dose intravenous gadolinium-based contrast media using heavily T(2)-weighted 3D-FLAIR. *Magn Reson Med Sci.* (2010) 9:237–42. doi: 10.2463/mrms.9.237
13. Sepahdari AR, Vorasubin N, Ishiyama G, Ishiyama A. Endolymphatic hydrops reversal following acetazolamide therapy: demonstration with delayed intravenous contrast-enhanced 3D-FLAIR MRI. *Am J Neuroradiol.* (2016) 37:151–4. doi: 10.3174/ajnr.A4462

14. Gurgel RK, Jackler RK, Dobie RA, Popelka GR. A new standardized format for reporting hearing outcome in clinical trials. *Otolaryngol Head Neck Surg*. (2012) 147:803–7. doi: 10.1177/0194599812458401
15. Lim HJ, Kim YT, Choi SJ, Lee JB, Park HY, Park K, et al. Efficacy of 3 different steroid treatments for sudden sensorineural hearing loss: a prospective, randomized trial. *Otolaryngol Head Neck Surg*. (2013) 148:121–7. doi: 10.1177/0194599812464475
16. Tsounis M, Psillas G, Tsalighopoulos M, Vital V, Maroudias N, Markou K. Systemic, intratympanic and combined administration of steroids for sudden hearing loss. A prospective randomized multicenter trial. *Eur Arch Otorhinolaryngol*. (2018) 275:103–10. doi: 10.1007/s00405-017-4803-5
17. Rauch SD, Halpin CF, Antonelli PJ, Babu S, Carey JP, Gantz BJ, et al. Oral vs. intratympanic corticosteroid therapy for idiopathic sudden sensorineural hearing loss: a randomized trial. *JAMA*. (2011) 305:2071–9. doi: 10.1001/jama.2011.679
18. Schuknecht HF. *Pathology of the Ear*. Philadelphia, PA: Lea and Febiger (1993).
19. Pakdaman MN, Ishiyama G, Ishiyama A, Peng KA, Kim HJ, Pope WB, et al. Blood labyrinthine barrier permeability in Meniere's disease and idiopathic sudden sensorineural hearing loss: findings on delayed postcontrast 3D-FLAIR MRI. *Am J Neuroradiol*. (2016) 37:1903–8. doi: 10.3174/ajnr.A4822
20. Nozawa I, Imamura S, Mizukoshi A, Honda H, Okamoto Y. Clinical study of acute low-tone sensorineural hearing loss: survey and analysis of glycerol test and orthostatic test. *Ann Otol Rhinol Laryngol*. (2002) 111:160–4. doi: 10.1177/000348940211100209
21. Imamura S, Nozawa I, Imamura M, Murakami Y. Clinical observations on acute low-tone sensorineural hearing loss. Survey and analysis of 137 patients. *Ann Otol Rhinol Laryngol*. (1997) 106:746–50. doi: 10.1177/000348949710600906
22. Wester JL, Ishiyama G, Karnezis S, Ishiyama A. Sudden hearing loss after cialis (tadalafil) use: a unique case of cochlear hydrops. *Laryngoscope*. (2018) 128:2615–8. doi: 10.1002/lary.27428
23. Shinkawa H, Kimura RS. Effect of diuretics on endolymphatic hydrops. *Acta Otolaryngol*. (1986) 101:43–52. doi: 10.3109/00016488609108606
24. Nadol JB Jr, Weiss AD, Parker SW. Vertigo of delayed onset after sudden deafness. *Ann Otol Rhinol Laryngol*. (1975) 84:841–6. doi: 10.1177/000348947508400617
25. Schuknecht HF, Gulya AJ. Endolymphatic hydrops. An overview and classification. *Ann Otol Rhinol Laryngol Suppl*. (1983) 106:1–20. doi: 10.1177/00034894830920S501
26. Maxwell A, Ishiyama G, Karnezis S, Ishiyama A. Isolated saccular hydrops on high-resolution MRI is associated with full spectrum Meniere's disease. *Otol Neurotol*. (2021) 2021:3051. doi: 10.1097/MAO.0000000000003051
27. Katayama N, Yamamoto M, Teranishi M, Naganawa S, Nakata S, Sone M, et al. Relationship between endolymphatic hydrops and vestibular-evoked myogenic potential. *Acta Otolaryngol*. (2010) 130:917–23. doi: 10.3109/00016480903573187
28. Gurkov R, Flatz W, Louza J, Strupp M, Krause E. *In vivo* visualization of endolymphatic hydrops in patients with Meniere's disease: correlation with audiovestibular function. *Eur Arch Otorhinolaryngol*. (2011) 268:1743–8. doi: 10.1007/s00405-011-1573-3
29. Ishiyama G, Lopez IA, Ishiyama P, Vinters HV, Ishiyama A. The blood labyrinthine barrier in the human normal and Meniere's disease macula utricle. *Sci Rep*. (2017) 7:253. doi: 10.1038/s41598-017-00330-5
30. Ishiyama G, Wester J, Lopez IA, Beltran-Parrazal L, Ishiyama A. Oxidative stress in the blood labyrinthine barrier in the macula utricle of Meniere's disease patients. *Front Physiol*. (2018) 9:1068. doi: 10.3389/fphys.2018.01068
31. Viirre ES, Baloh RW. Migraine as a cause of sudden hearing loss. *Headache*. (1996) 36:24–8. doi: 10.1046/j.1526-4610.1996.3601024.x
32. Liu IY, Ishiyama A, Sepahdari AR, Johnson K, Ishiyama G. Bilateral endolymphatic hydrops in a patient with migraine variant without vertigo: a case report. *Headache*. (2017) 57:455–9. doi: 10.1111/head.12976
33. Cha YH, Brodsky J, Ishiyama G, Sabatti C, Baloh RW. The relevance of migraine in patients with Meńière's disease. *Acta Otolaryngol*. (2007) 127:1241–5. doi: 10.1080/00016480701242469
34. Gurkov R, Jerrin C, Flatz W, Maxwell R. Clinical manifestations of hydropic ear disease (Meniere's). *European Arch Oto-Rhino-Laryngol*. (2019) 276:27–40. doi: 10.1007/s00405-018-5157-3

Conflict of Interest: The authors declare that the research was conducted in the absence of any commercial or financial relationships that could be construed as a potential conflict of interest.

frontiers in Surgery

ORIGINAL RESEARCH
published: 21 June 2021
doi: 10.3389/fsurg.2021.682245

Visualization of Endolymphatic Hydrops in Patients With Unilateral Idiopathic Sudden Sensorineural Hearing Loss With Four Types According to Chinese Criterion

Huan Qin[1,2,3†], *Baihui He*[1,2,3†], *Hui Wu*[1,2,3], *Yue Li*[1,2,3], *Jianyong Chen*[1,2,3], *Wei Wang*[1,2,3], *Fan Zhang*[1,2,3], *Maoli Duan*[4,5*] and *Jun Yang*[1,2,3*]

[1] Department of Otorhinolaryngology Head and Neck Surgery, Xinhua Hospital, Shanghai Jiaotong University School of Medicine, Shanghai, China, [2] Ear Institute, Shanghai Jiaotong University School of Medicine, Shanghai, China, [3] Shanghai Key Laboratory of Translational Medicine on Ear and Nose Diseases, Shanghai, China, [4] Department of Otolaryngology Head and Neck, Audiology and Neurotology, Karolinska University Hospital, Stockholm, Sweden, [5] Division of Ear, Nose and Throat Diseases, Department of Clinical Science, Intervention and Technology, Karolinska Institute, Stockholm, Sweden

OPEN ACCESS

Edited by:
Robert Gürkov,
Bielefeld University, Germany

Reviewed by:
Hans Thomeer,
University Medical Center Utrecht, Netherlands
Conrad Riemann,
Bielefeld Clinic, Germany

***Correspondence:**
Jun Yang
yangjun@xinhuamed.com.cn
Maoli Duan
maoli.duan@ki.se

[†] These authors share first authorship

Specialty section:
This article was submitted to Otorhinolaryngology - Head and Neck Surgery, a section of the journal Frontiers in Surgery

Received: 18 March 2021
Accepted: 10 May 2021
Published: 21 June 2021

Citation:
Qin H, He B, Wu H, Li Y, Chen J, Wang W, Zhang F, Duan M and Yang J (2021) Visualization of Endolymphatic Hydrops in Patients With Unilateral Idiopathic Sudden Sensorineural Hearing Loss With Four Types According to Chinese Criterion. Front. Surg. 8:682245. doi: 10.3389/fsurg.2021.682245

Objective: The aim of this study is to evaluate the possible value of endolymphatic hydrops (EH) in patients with unilateral idiopathic sudden sensorineural hearing loss (UISSNHL) with four types according to audiometry.

Methods: Seventy-two patients (40 men and 32 women; age range, 28–78 years; mean age: 50.0 ± 12.9 years) with UISSNHL were admitted retrospectively into this study. Based on the pure tone audiometry before treatment, the hearing loss of all these patients were categorized into four types: low-frequency group (LF-G), high-frequency group (HF-G), flat group (F-G), and total deafness group (TD-G). The average time from symptom onset to the first examination was 6.9 ± 4.4 days (1–20 days). 3D-FLAIR MRI was performed 24 h after intratympanic injection of gadolinium (Gd) within 1 week after the UISSNHL onset. The incidence of EH in the affected ears based on four types of hearing loss were analyzed using the Chi-square test, and the possible relationship with vertigo and prognosis were also assessed.

Results: Eleven of 21 patients (52.4%) in LF-G had the highest EH-positive rate, followed by 18.2% in HF-G, 11.8% in F-G, and 17.4% in TD-G. The significant difference was found in the four groups ($P = 0.018$). The EH rate of LF-G was statistically significantly higher than that of F-G and TD-G ($P = 0.009$, $P = 0.014$), respectively. After being valued by the volume-referencing grading system (VR scores), the EH level was represented by the sum scores of EH. In LF-G, no statistically significant difference was found in the prognosis of ISSNHL patients between with the EH group and the no EH group ($P = 0.586$). The symptom "vertigo" did not correlate with EH and prognosis.

Conclusions: EH was observed in UISSNHL patients by 3D-FLAIR MRI. EH may be responsible for the pathology of LF-G but not related to prognosis. It might be meaningless to assess EH in other hearing loss types, which might be more related to the blood-labyrinth dysfunction.

Keywords: idiopathic sudden sensorineural hearing loss, endolymphatic hydrops, low-frequency hearing loss, magnetic resonance imaging, prognosis

INTRODUCTION

Sudden sensorineural hearing loss (SSNHL) is defined as a subset of disorder in which hearing loss is sensorineural and occurs within 72 h, affecting ∼5–27 per 100,000 people annually (1). Furthermore, SSNHL is one of the most frequently recognized otolaryngological emergencies (2). About 90% of patients with SSNHL have no identifiable cause for the hearing loss (1). Rather than the possible tumor, trauma, or other causes identifiable according to patients' history (2), the exact etiology and pathological mechanism of idiopathic sudden sensorineural hearing loss (ISSNHL) have not been clarified (3). Hypothesis causes of ISSNHL mainly focused on micro-circulation disorders, viral infection, or autoimmune diseases (3). However, the possible relationship between EH and hearing loss was also mentioned early in 2002 (4); however, few articles published to support due to the limited imaging techniques.

The study of the correlation of EH with ISSNHL started prospering not only because the imaging of EH was successfully settled by the three-dimensional fluid-attenuated inversion recovery (3D-FLAIR) magnetic resonance imaging (MRI) by Nagawama et al. (5) and Nakashima et al. (6) but also due to the progressive understanding of EH in Ménière's disease (MD). Foster and Breeze (7) concluded EH as a cofactor of MD with other possible stimuli like ischemia. Venous drainage had an influence on both ISSNHL and MD reported in 2008, also suggesting the possible relationship between EH and ISSNHL (8). Chen et al. (9) reported that EH was observed in four of seven ISSNHL patients with vertigo. Okazaki et al. (10) found that cochlear EH and vestibular EH were observed in 66 and 41% of the affected ears with ISSNHL, respectively. Zheng et al. (11) claimed that the presence of EH may be a secondary reaction following the impairment of the inner ears with pantonal ISSNHL (a German classification in which the hearing level at all frequencies decreases to the approximate degree between 35 and 120 dB) because no correlation between vertigo and prognosis was found.

In the present study, 3D-FLAIR MRI of membranous labyrinth after intratympanic gadolinium (Gd) injection was performed and EH was assessed according to the volume-referencing grading system (VR scores) proposed in our previous study (12). The EH was analyzed in four types of unilateral ISSNHL (UISSNHL) according to a Chinese guideline published in 2015 (13), which is adjusted from the classification standard proposed by Sheehy (14) and mentioned in a Chinese multicenter study (15). The purpose of this study is to find the EH distribution in four types of UISSNHL and to preliminarily explore the possible value of EH among different types.

MATERIALS AND METHODS

Subjects

In this retrospective study, 72 patients (40 men and 32 women; age range, 28–78 years; mean age: 50.0 ± 12.9 years) were enrolled from March 2017 to June 2020 in the Department of Otolaryngology-Head and Neck Surgery, Xinhua Hospital, Shanghai Jiaotong University School of Medicine. All patients met the following inclusion criteria; the first three criteria were from the 2015 Chinese guideline (**Table 1**) (13): (1) patients had experienced a UISSNHL and had an audiometry within 72 h; (2) the cause of hearing loss was unclear after detailed history collection; (3) the extent of hearing loss was at least 20 dB HL in at least two contiguous frequencies with no air-bone conduction gap [compared to the 2019 AAO-HNS criteria (1): hearing loss consists of a decrease in hearing of 30 dB HL affecting at least three consecutive frequencies]; and (4) 3D-FLAIR MRI was done within 1 week of the onset of hearing loss. Exclusion criteria included were the following: (1) a history of (fluctuating or acute) sensorineural hearing loss; (2) patients with vertigo caused by benign paroxysmal positional vertigo, MD, and vestibular schwannoma; (3) a history of previous otologic surgery, middle ear disease, cranial disease, or head trauma; (4) otalgia in bilateral ears; and (5) an allergy to Gd. Before detailed history collection, MRI examination, and treatment, the informed consent was obtained from each participant. The information included age, sex, affected side were collected.

TABLE 1 | Criteria for diagnosis of ISSNHL.

Main symptoms
Sudden onset
Sensorineural hearing loss
Unknown etiology
For reference
Hearing loss ≥ 20 dB HL in at least two adjacent frequencies occurred suddenly within 72 h
Mostly unilateral hearing loss, few bilateral onset occurred simultaneously or successively
May be accompanied by tinnitus, stuffy feeling of ear, abnormal feeling of skin around the ear
May be accompanied by vertigo, nausea, and vomiting
No cranial nerve symptoms other than from cranial nerve VIII
Definite diagnosis: all of the above main symptoms are present

These criteria were assessed by the Society of Otorhinolaryngology Head and Neck Surgery Chinese Medical Association of China in 2015.

Pure-Tone Audiometry

Pure-tone audiometry was performed in a soundproof room with the use of an audiometer (Type Madsen, Astera, München, Denmark). According to the 2015 Chinese guideline (13), the diagnosis of UISSNHL was established and divided into four groups: (1) low-frequency group (LF-G): hearing loss at frequencies under 1 k Hz with the least reduction by 20 dB HL at 250 and 500 Hz; (2) high-frequency group (HF-G): hearing loss at frequencies of 2 k Hz or above with the least reduction by 20 dB HL at 4 and 8 k Hz; (3) flat group (F-G): hearing loss at all frequencies (250–8 k Hz) and the average hearing threshold was ≤80 dB HL; and (4) total deafness group (TD-G): hearing loss at all frequencies (250–8 k Hz) with the mean threshold ≥81 dB HL. The examples of audiograms in four types are shown in **Figure 1**. The audiometry was collected both before and 1

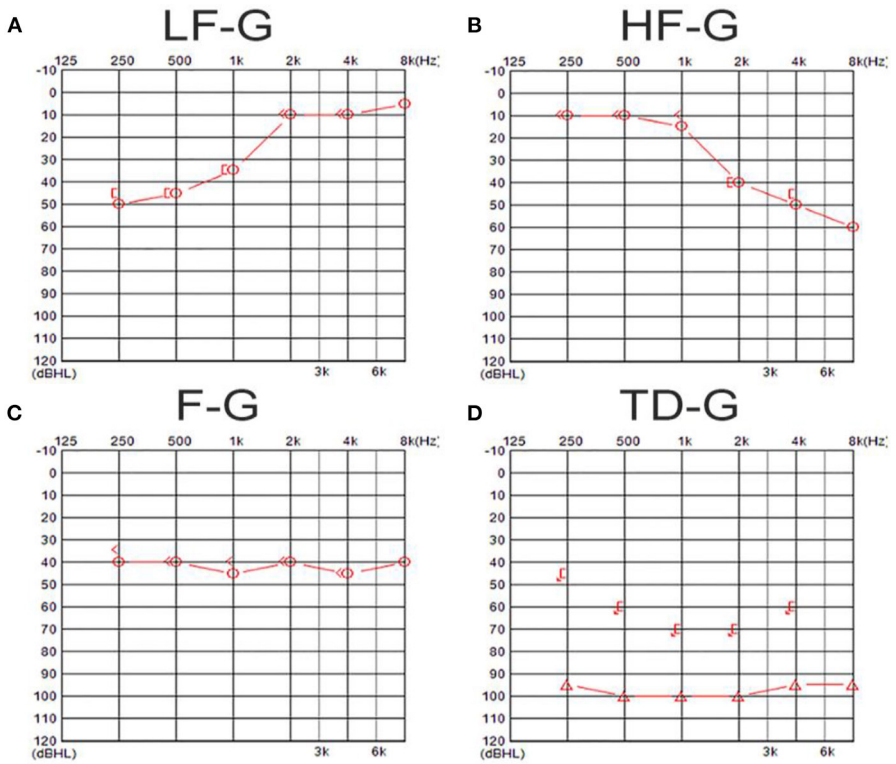

FIGURE 1 | The examples of audiograms in four types of UISSNHL. **(A)** Shows an audiogram of a patient in LF-G in which hearing loss was over 20 dB HL in 250–1 k-Hz frequencies; **(B)** shows an audiogram of a patient in HF-G in which hearing loss was over 20 dB HL in 2–8 k-Hz frequencies; **(C)** exhibits an audiogram of a patient in F-G in which hearing loss was at all frequencies and the average hearing threshold was ≤80 dB HL; **(D)** shows an audiogram belonging to a patient in TD-G in which hearing loss at all frequencies was ≥81 dB HL.

month after the treatment. The pure tone average (PTA) was calculated as the average threshold of those damaged frequencies: 250–1 k Hz in LF-G; 2–8 k Hz in HF-G; and 250–8 k Hz in F-G and TD-G.

Intratympanic Gd Injection and MRI Analysis

Gd was diluted eight-fold with saline (v/v = 1:7) and injected intra-tympanically (0.5 ml) through the inferior–posterior quadrant of the tympanic membrane bilaterally using a 23-G needle and a 1-ml syringe under an oto-endoscope. The patient was then placed in the supine position for 60 min.

3D-FLAIR MRI was performed on a 3-Tesla scanner (uMR 770, United Imaging, Shanghai, China) 24 h after intratympanic Gd injection with a 24-channel head coil. Three-dimensional heavily T2-weighted spectral attenuated inversion recovery (3D-T2-SPAIR, T2) and 3D-FLAIR imaging were subsequently performed. The main scan parameters for the 3D-FLAIR sequence were as follows: time of repetition (TR) = 6,500 ms, time of echo (TE) = 286.1 ms, time of inversion = 1,950 ms, scan time = 6 min and 11 s. The main scan parameters for 3D-T2-SPAIR sequence were as follows: TR = 1,300 ms, TE = 254.7 ms, scan time = 4 min and 30 s (12). The degree of EH of each part of the inner ear (include vestibule, cochlea, and semicircular canals) was assessed separately into four grades (**Table 2**), while VR scores were assigned and the EH were presented as the sum scores of each part according to our previous study (12) (**Figure 2**). The EH were estimated double-blinded by two experienced radiologists by which if there was any discrepancy, it would be double-checked by one senior otologist.

Treatment

Different treatment protocols were administered variously for four hearing loss types according to the 2015 Chinese guideline (13). The main regimen for patients was intravenous dexamethasone. To achieve a better prognosis, hyperbaric oxygenation (16) and intratympanic dexamethasone injection (17) were used as the auxiliary therapies for patient. The treatment duration lasted for 10 days.

Outcome Assessment

The therapeutic effect of UISSNHL is graded as follows (13): (1) Complete recovery: the follow-up audiometry returns to normal or reaches the healthy ear level or the level before the disease; (2) remarkable effect: the affected frequencies increase by more

TABLE 2 | Four gradings of the EH in the cochlea, vestibule, and semicircular canals.

Grade	Cochlea	Vestibule	Semicircular canals (SCC)
None	The scala media (dark area in the cochlea) could not be viewed.	The saccule and utricle (two dark areas in the vestibule) are separate; Saccule is smaller than the utricle.	The SCC is clearly visible; A narrow dark area (<1/3 of the ampulla) is visible.
Grade I	The scala media expand but still shapes as a triangle.	The saccule becomes larger than utricle; The saccule not confluent with utricle.	The SCC is clearly visible; The dark area occupies over one-third of the ampulla.
Grade II	The scala media expands into circle.	A confluence appears; Surrounding perilymph is still visible.	The ampulla becomes dark; Some of the SCC narrow or become invisible.
Grade III	No signal could be viewed in the scala media.	No signal could be viewed in the vestibule.	No signal could be viewed in the SCC.

**The grading algorithm is summarized from VR scores in previous He's work (12).*

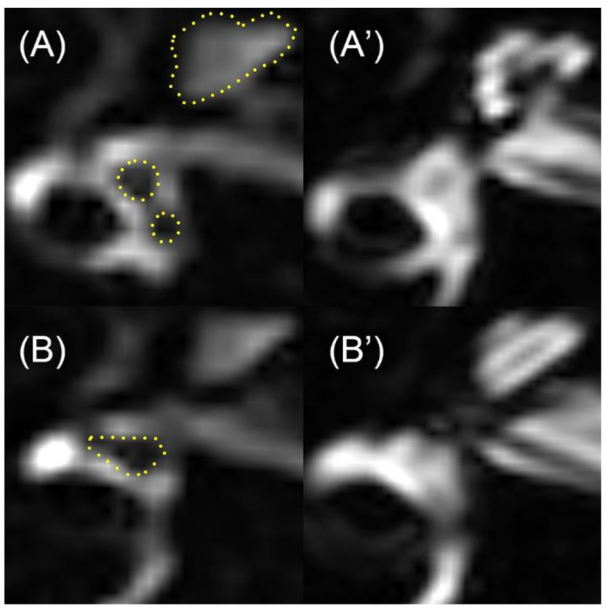

FIGURE 2 | An example of the EH in an UISSNHL patient. This patient belonged to LF-G. 3D-FLAIR images on the left were compared with T2 images on the right. The evaluation was as follows: cochlea-grade I (three points). The cochlea in **(A)**, especially the apical part of each turn, was smaller than the highlighted line, which was the outline of cochlea in T2 sequence in **(A')**. Vestibule-grade I (four points) and semicircular canals-grade I (five points): because the black area in **(B)** is over one-third of the whole ampulla, shown in **(B')**. Therefore, the sum EH level of this patient was 12 points.

than 30 dB HL on average; (3) effective: the average hearing loss frequency rises by 15–30 dB HL; and (4) invalid: the mean improvement of affected frequencies is <15 dB HL. In this study, in order to facilitate statistical analysis, complete recovery or remarkable effect was collected as effective.

Statistical Analysis

Descriptive statistics were done for age, sex, affected side, the incidence of vertigo, and PTA in UISSNHL patients. The nonparametric analysis and paired *t*-test were done for the two-group analysis while one-way ANOVA was used for four-group analysis. The logistic analysis was used to exclude the possible confounding factors. The possible relationships among EH, vertigo, and prognosis were compared by the Chi-square test and Fisher's exact test for categorical variables. $P < 0.05$ was statistically significant. Statistical analyses were conducted by using SPSS 22.0 for Windows software (IBM, Chicago, IL, USA).

RESULTS

Clinical Characteristics of UISSNHL Patients

The clinical characteristics of the enrolled 72 patients and the distribution of the four hearing-loss groups are listed in **Table 3**. Among 72 UISSNHL ears, TD-G (31.9%) was the most common hearing loss type, LF-G (29.2%) and F-G (23.6%) were less common while HF-G (15.3%) consisted of the least of all. Vertigo manifested as a single rotational vertigo, swaying vertigo, which occurred 1 day before the hearing decline or after hearing decline and lasted from several hours to several days. The onset was not related to the head position, and the attack did not recur after recovery. The age of the four groups had no significant difference ($P > 0.05$). The patients with UISSNHL were divided into three groups according to their ages: <40 years old, 40–60 years old, and > 60years old. At the same time, EH of three groups were statistically analyzed by the Chi-square test, and no significant correlation was found ($p > 0.05$). Gender and affected sides were evenly distributed in each group ($P > 0.05$). Some patients reported a concomitant symptom of vertigo in each group in which TD-G had the highest rate. The average time from symptom onset to the first examination was 6.9 ± 4.4 days (1–20 days). The results of PTA before treatment and after treatment were described. The patients in LF-G had the lightest hearing loss level, while patients in TD-G had the most severe hearing loss. However, the highest effectiveness was in patients of LF-G (85.7%).

An analysis of the relationship between vertigo and hearing loss in four types is shown in **Table 4**, and there was no difference between vertigo and hearing loss types ($P = 0.56$).

TABLE 3 | Characteristics of UISSNHL patients.

	LF-G	HF-G	F-G	TD-G
Patients [*n* (%)]	21 (29.2)	11 (15.3)	17 (23.6)	23 (31.9)
Age (years)	54.1 ± 8.3	49.2 ± 11.3	50.1 ± 12.5	47.3 ± 8.6
Gender (*n*)				
Male	12	7	8	13
Female	9	4	9	10
Affected side (*n*)				
Right	13	8	6	8
Left	8	3	11	15
Vertigo [*n* (%)]	5 (23.4)	3 (27.2)	6 (35.3)	10 (43.5)
PTA (dB HL)				
Pretreatment	45.8 ± 5.2	51.7 ± 6.9	61.6 ± 8.4	98.9 ± 9.0
Post-treatment	21.2 ± 9.4	34.0 ± 9.8	49.5 ± 15.0	86.3 ± 16.7
Effectiveness [*n* (%)]	18 (85.8)	6 (54.5)	6 (35.3)	8 (34.8)
EH of <40 years old [*n* (%)]	1 (0.05)	1 (9.1)	0	0
EH of 40–60 years old [*n* (%)]	9 (42.3)	0	1 (5.9)	4 (17.4)
EH of >60 years old [n (%)]	1 (0.05)	1 (9.1)	1 (5.9)	0
Total EH [*n* (%)]	11 (52.4)	2 (18.2)	2 (11.8)	4 (17.4)

n, means number.

TABLE 4 | An analysis of the relationship between vertigo and hearing loss types.

Vertigo or not	UISSNHL types (*n*)			
	LF-G	HF-G	F-G	TD-G
Vertigo group	5	3	6	10
No vertigo group	16	8	11	13
P	0.56			

The comparison was done between the "vertigo" group and the "no vertigo" group. There was no difference when comparing the "vertigo" group and the "no vertigo" group. The P-value was derived from the Chi-square test.

EH Evaluation and MRI Association With Clinical Characteristics

No side effects such as tympanic membrane perforation, infection, and other complications after the intratympanic injection of Gd-DTPA were observed. The Gd-DTPA demonstration rate was 100% (72/72) in both the affected ears and the normal ears. The incidence of EH is shown in **Table 1**, and LF-G had the highest EH-positive rate by 52.4%. The EH rate of LF-G was higher than that of F-G and TD-G, and the difference was statistically significant ($P = 0.009$, P=0.014), respectively. Then, EH were estimated and the distribution of EH grading according to VR scores is exhibited in **Figure 2**. The total EH level was estimated by the sum score of three parts of the inner ear, namely, cochlea, vestibule, and semicircular canal. Of all EH-positive patients with UISSNHL, gradings of EH were mild or moderate hydrops (**Figure 2**) with the maximum score of EH as 37 points (12). No significant difference was found among HF-G, F-G, and TD-G in EH sum scores ($P > 0.05$). Cochlear EH and vestibular EH were more detectable than EH in semicircular canals in most patients (**Figure 3**).

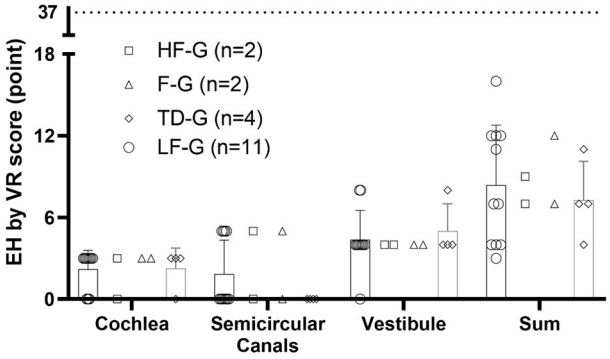

FIGURE 3 | EH grading in three parts of the inner ear and the sum of VR scores. EH in cochlea were scored 0, 3, 6, and 9 for four grades while those in vestibule were scored 0, 4, 8, and 12 and those in the semicircular canals as 0, 5, 10, and 16 according to the volume-referencing scores (12). The sum score of three parts represented EH in the entire inner ear. The scatter plot showed the scores in each part of each patient, while the histogram presented for TD-G and LF-G represented mean and SD. In this study, most UISSNHL patients had mild or moderate EH as the maximum score of EH was 37 points.

TABLE 5 | An analysis of the relationship between vertigo and EH in LF-G.

Vertigo or not	EH in LF-G	
	EH positive (*n*)	No EH (*n*)
Vertigo group	2	1
No vertigo group	9	9
P	0.311	

The comparison was done between the "vertigo" group and the "no vertigo" group. There was no difference when comparing the "vertigo" group and the "no vertigo" group. P-value was derived from Fisher's exact test.

There was no statistically significant relationship between EH with gender ($P = 0.402$) and age ($P = 0.116$) using logistic regression analysis. After judging the grading of each part in the inner ear and added into sum to represent the total EH level of each patient, no significant difference of the sum EH score was found in EH patients with four types ($P = 0.081$). Therefore, we separated patients into no EH group and EH-positive group for analysis. Since LF-G had the largest positive rate of EH, the related analyses were mainly done in this group.

The possible influence of the vertigo symptom on EH was analyzed (**Table 5**). The EH rate was higher in the vertigo group (67%) than that in the no vertigo group (50%). However, the no correlation between vertigo and EH in LF-G was found.

The Prognosis Analysis

Analysis of the relationship between EH and prognosis of all groups and LF-G is shown in **Table 6**. The effectiveness rate of all groups with positive EH (63%) was higher than that of all groups without EH (49%). Furthermore, the effectiveness rate of LF-G with positive EH (82%) was lower than that of LF-G without EH (90%). However, there was no significant difference between EH-positive rate in the effective group and the invalid group both

TABLE 6 | An analysis of the relationship between EH and prognosis of all group and LF-G.

EH	Prognosis of all groups		Prognosis of LF-G	
	Effectiveness (*n*)	Invalidation (*n*)	Effectiveness (*n*)	Invalidation (*n*)
Positive	12	7	9	2
None	26	27	9	1
p	0.291		0.414	

The comparison was done between the "positive" group and "none" groups. There was no difference when comparing the "positive" group and the "none" group. P-value was derived from the Chi-square test.

TABLE 7 | An analysis of the relationship between vertigo and prognosis in LF-G.

Vertigo or not	Prognosis in LF-G	
	Effectiveness (*n*)	Invalidation (*n*)
Vertigo group	3	2
No vertigo group	15	1
P	0.128	

The comparison was done between the "vertigo" group and the "no vertigo" group. There was no difference when comparing the "vertigo" group and the "no vertigo" group. P-value was derived from Fisher's exact test.

in all UISSNHL patients and in LF-G patients ($P = 0.291$, $P = 0.414$).

The possible relationship of vertigo and prognosis was also analyzed. The effectiveness rate of LF-G with vertigo (60%) was lower than that of LF-G without vertigo (93%). However, no significant difference was found in the effectiveness rate between the vertigo group and the patients with no vertigo in LF-G ($P = 0.128$; **Table 7**).

DISCUSSION

Our study confirmed that EH does appear in UISSNHL patients and had the closest correlation to the low-frequency hearing loss. Among the possible pathological mechanisms discussed in the guideline referencing the German guideline (18), the low-frequency hearing loss is supposed to be most likely correlated with cochlear or vestibular EH (11). Indeed, early in 1990, the possible relationship between SSNHL and EH was firstly studied on human temporal bone by Yoon et al. (19). They observed 4 of 11 temporal bones from eight patients with SSNHL, and the EH-positive rate for ISSNHL accordingly was 28.6%. Filipo et al. (20) reported greater SP/AP ratios in electrocochleography of ISSNHL patients with low frequency and flat audiometric profiles, suggesting a close relationship of EH and ISSNHL. The exploration of ISSNHL with EH almost stagnated until the visualization of EH with 3D-FLAIR was established (6). Duan et al. (21, 22) firstly demonstrated that MRI can clearly visualize inner ear imaging in animal studies. Subsequently, Nagawama et al. (5) were the first to mention the 3D-FLAIR sequences and firstly attempt EH imaging in ISSNHL patients (23). The low availability (faint enhancement) of EH imaging in ISSNHL patients 4 h after intravenous Gd reported by Nakashima's research group (23) might limit other researchers' interest until in 2017 they broke their own point of view (10). Given that few studies were done to explore the EH relationship with SSNHL, Horri et al. (24) reported that two of eight ISSNHL patients (excluding low-frequency SNHL) had EH in 2011 and Chen et al. (9) reported that EH exists in four of seven ISSNHL patients with vertigo in 2012. These researchers used intratympanic Gd which was claimed by Yamasaka et al. (25) by which intratympanic Gd provided stronger signals and had no remarkable side effect. The latest study about EH and ISSNHL was published in 2019 by Zheng et al. (11) who reported a difference of EH in affected ears and unaffected ears and considered EH in pantonal ISSNHL (analog to F-G and TD-G in this study) to be the secondary EH.

In the present study, the EH rate of total UISSNHL was 26.4% and only patients in LF-G had a higher rate of EH (52.4%). However, Okazaki et al. (10) observed EH positivity in 66% cochlea and 41% vestibule in ISSNHL (low-frequency SNHL patients were excluded). Their results varied a lot from low onset of EH in ISSNHL in three types (HF-G, F-G, and TD-G) in the present study. The high positive rate might be due to the scanning method they used, hydrops after 4 h intravenous Gd, which exhibited the EH images according to the reversed endolymph and perilymph signals (26). Acute labyrinth inflammation with protein exudate, or blood-labyrinth barrier (BLB) causing Gd diffusion in both endolymph and perilymph (27), could explain the low detection rate of EH in ISSNHL in three types in the present study using the endolymph imaging 3D-FLAIR sequence (28). Indeed, 3D-FLAIR scans were studied in the bleeding of ISSNHL 10 min after intravenous Gd injection in many studies (29–35), which might reflect the possible inflammation and BLB in the inner ear as firstly mentioned by Sugira et al. (29). Zhu et al. (33) did not recommend 4 h after intravenous Gd injection as a time point to image the inner ear in ISSNHL patients since there were no significant signal intensity changes between the images 10 min and 4 h after Gd injection using the 1.5-T MRI, in which EH were not discussed. Kim et al. (36) also showed no significant difference in signal intensity in the affected ears. However, Byun et al. (37) and Min et al. (38) suggested that the higher signal intensity observed in ISSNHL patients 4 h after Gd indicated a poor prognosis. Byun et al. (37) claimed that a higher signal intensity was shown in 4-h Gd-injection imaging than that in 10-min imaging. The increased signal intensity caused by increased permeability (due to BLB) suggested an increase in inner ear damage. The signal intensity in the inner ear after 24 h intratympanic Gd was never discussed because there might be a difference in round-window permeability (39). Therefore, 3D-FLAIR after intratympanic Gd may have limitations in observing the difference of signal intensity to predict the permeability of BLB and the prognosis of ISSNHL. Relatively, 3D-FLAIR after 4 h intravenous Gd might be more suitable for ISSNHL without LF-G.

Interestingly, the recent Japanese researchers excluded the low-frequency hearing loss while analyzing ISSNHL, as mentioned above (10, 24). A nationwide epidemiological survey

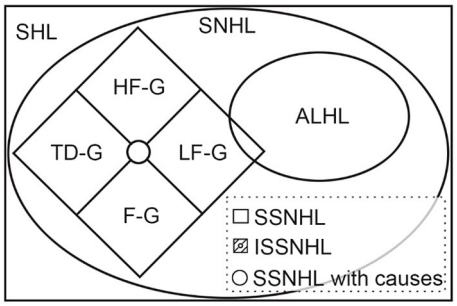

FIGURE 4 | Subtype sets of the sudden hearing loss (SHL).

in Japan published in 2017 claimed that ISSNHL and acute low-tone sensorineural hearing loss (ALHL) belong to different inner ear diseases (40). ALHL is characterized by acute-onset low tone hearing loss often associated with tinnitus, ear fullness, and/or autophony, without vertigo, and its cause remains unknown (40). According to the 2019 AAO-HNS guideline and 2015 Chinese guideline, we considered there to be an intersection between ISSNHL and ALHL (**Figure 4**). ISSNHL patients with low-frequency hearing loss without vertigo were also ALHL and ALHL patients corresponding to the onset time and hearing loss definition which could be called ISSNHL. The LF-G in the present study might be divided into ISSNHL with vertigo and ALHL.

This figure shows the relationship among different acronyms related to sudden hearing loss. Among them, the definitions of SHL, SNHL, SSNHL, and ISSNHL were clearly explained in the 2019 AAO-HNS guideline (41) and the 2015 Chinese guideline (13). Sudden hearing loss (SHL) is defined as a rapid-onset subjective sensation of hearing impairment in one or both ears, while sensorineural hearing loss (SNHL) only means hearing loss without a conductive hearing loss (41). Furthermore, sudden SNHL (SSNHL) is a subset of SNHL developed within 72 h, which is the same in the 2019 AAO-HNS guideline (41) and the 2015 Chinese guideline (13). However, hearing loss definition varied in two guidelines. HF-G, LF-G, F-G, and TD-G were the abbreviations of four groups defined by the 2015 Chinese guideline (13). ALHL was defined according to the 2017 epidemiological survey in Japan. Although ALHL is separated from ISSHNL in the Japanese definition, there should be an overlap according to their definition.

Cochlear hydrops begins at the apical turn of the cochlea and extends to the vestibule, causing the low-frequency hearing loss ahead of vertigo (42). Shimono et al. (43) also reported that EH was observed in the cochlea and vestibule in ALHL. Furthermore, EH is a definite pathological feature and might be a cofactor of MD according to the comprehensive review from 1938 to 2012 (7). Ma et al. (44) conducted a comparison between ALHL and ISSNHL (low-frequency hearing loss excluded) and discovered that ALHL patients had higher IgE with an enhanced SP/AP ratio of electrocochleography, which was an index relating to EH in MD (12, 44). However, follow-up for ALHL patients was recommended because patients who presented with ALHL and concomitant tinnitus or had recurrent episodes of ALHL were more likely to develop MD than other ALHL patients (45). Junicho et al. (46) considered the ALHL as a subtype of ISSNHL. They reported that only 8.5% of 177 ALHL patients developed MD and concluded that not all low-tone ISSNHL patients suffered from EH even if they had vertigo attack at the onset. In summary, ALHL or ISSNHL patients with low frequency hearing loss might have EH in some patient and even develop MD with recurrent vertigo; however, the correlation was not definite. In our study, the 72 patients of ISSNHL ranged in age from 28 to 78. As the prevalence of MD is mostly between 40 and 60 years of age (47), the younger age group is less prone to be affected by MD. In order to reduce the bias, the patients with ISSNHL were divided into three groups (<40 years old, 40–60 years old, and >60 years old), and at the same time, EH of three groups were statistically analyzed by the Chi-square test, but no significant correlation was found ($p > 0.05$).

We concluded a similar result as the vertigo seemed to have no relationship for the EH-positive rate and the effectiveness in LF-G. Zheng et al. (11) had the same conclusion in 2009 and supposed that EH might be a secondary reaction of inner ear impairment. However, Yu et al. (48) made a META analysis in 2008 and found that ISSNHL patients with vertigo had a lower recovery rate of hearing than the ones without vertigo, while in the subgroup of these researches in which the patients were under the intratympanic corticosteroids injection, vertigo had no correlation with recovery rate of hearing. The intratympanic corticosteroids used as a treatment method might eliminate the prognostic difference. Also, the steroid–diuretic combination therapy was more effective than the steroid or diuretic treatments alone reported by Morita et al. (49), which also suggests a close correlation with EH and ALHL.

Consequently, 3D-FLAIR after 24 h intratympanic Gd showed 52.4% EH positivity in LF-G patients, and we recommended this scanning strategy for LF-G patients of ISSNHL. However, for the other three groups of patients, EH imaging was not recommended due to the low detection rate and no difference in effectiveness. Alternatively, 3D-FLAIR 10 min or 4 h after intravenous injection with the signal intensity assessment was recommended due to the possible BLB hypothesis.

This study has some limitations that should be highlighted. First, our ISSNHL patient sample size was considerably small after being divided into four groups. Second, the contrast MRI was not performed after treatment, which might show the EH changes and be helpful for understanding the possible etiology and pathogenesis of ISSNHL. Third, time delays between disease onset and MRI evaluation may be a confounder of the percentages of EH. At last, during our treatment and up to 1–2 months of follow-up of the patients, no patient ended having MD, but long-term follow-up results were not reported in this study.

DATA AVAILABILITY STATEMENT

The raw data supporting the conclusions of this article will be made available by the authors, without undue reservation.

ETHICS STATEMENT

The studies involving human participants were reviewed and approved by Ethics Committee of Xinhua Hospital (Approval No. XHEC-D-2021-029). The patients/participants provided their written informed consent to participate in this study.

AUTHOR CONTRIBUTIONS

JY and MD contributed to the study design and critically reviewed and approved the final manuscript. HQ performed the data acquisition. HQ and BH contributed to the detailed study design and statistical analysis, interpretation of the results, drafting of the manuscript, and revision of the manuscript. HW and WW contributed to the study design, data acquisition, and statistical analysis. YL, JC, and FZ contributed to the methods of statistical analysis and critically reviewed the manuscript. All the authors contributed to the article and approved the submitted version.

FUNDING

This work was funded by Cross-key Projects in Medical and Engineering Fields of Shanghai Jiaotong University (No. ZH2018ZDA11) and Clinical Research Cultivation Fund of Xinhua Hospital (Nos. 17CSK03 and 18JXO04).

ACKNOWLEDGMENTS

The authors wish to thank all the coworkers at the Department of Otolaryngology-Head and Neck Surgery and the Department of Radiology in Xinhua Hospital, Shanghai, China, for their contributions to this study.

REFERENCES

1. Chandrasekhar SS, Tsai Do BS, Schwartz SR, Bontempo LJ, Faucett EA, Finestone SA, et al. Clinical practice guideline: sudden hearing loss (update) executive summary. *Otolaryngol Head Neck Surg.* (2019) 161:195–210. doi: 10.1177/0194599819859883
2. Lloyd SK. Sudden sensorineural hearing loss: early diagnosis improves outcome. *Br J Gen Pract.* (2013) 63:e592–4. doi: 10.3399/bjgp13X670877
3. Kim MB, Lim J, Moon IJ. Anatomical and pathological findings of magnetic resonance imaging in idiopathic sudden sensorineural hearing loss. *J Audiol Otol.* (2020) 24:198–203. doi: 10.7874/jao.2020.00157
4. Tran BH. Endolymphatic deafness: a particular variety of cochlear disorder. *ORL J Otorhinolaryngol Relat Spec.* (2002) 64:120–4. doi: 10.1159/000057790s
5. Naganawa S, Komada T, Fukatsu H, Ishigaki T, Takizawa O. Observation of contrast enhancement in the cochlear fluid space of healthy subjects using a 3D-FLAIR sequence at 3 Tesla. *Eur Radiol.* (2006) 16:733–7. doi: 10.1007/s00330-005-0046-8
6. Nakashima T, Naganawa S, Sugiura M, Teranishi M, Sone M, Hayashi H, et al. Visualization of endolymphatic hydrops in patients with Meniere's disease. *Laryngoscope.* (2007) 117:415–20. doi: 10.1097/MLG.0b013e31802c300c
7. Foster CA, Breeze RE. Endolymphatic hydrops in Ménière's disease: cause, consequence, or epiphenomenon? *Otol Neurotol.* (2013) 34:1210–4. doi: 10.1097/MAO.0b013e31829e83df
8. Ciccone MM, Scicchitano P, Gesualdo M, Cortese F, Zito A, Manca F, et al. Idiopathic sudden sensorineural hearing loss and ménière syndrome: the role of cerebral venous drainage. *Clin Otolaryngol.* (2018) 43:230–9. doi: 10.1111/coa.12947
9. Chen X, Zhang XD, Gu X, Fang ZM, Zhang R. Endolymphatic space imaging in idiopathic sudden sensorineural hearing loss with vertigo. *Laryngoscope.* (2012) 122:2265–8. doi: 10.1002/lary.23452
10. Okazaki Y, Yoshida T, Sugimoto S, Teranishi M, Kato K, Naganawa S, et al. Significance of endolymphatic hydrops in ears with unilateral sensorineural hearing loss. Otol *Neurotol.* (2017) 38:1076–80. doi: 10.1097/MAO.0000000000001499s
11. Zheng YX, Liu AG, Wang XL, Hu Y, Zhang YF, Peng LY. The role of endolymphatic hydrops in patients with pantonal idiopathic sudden sensorineural hearing loss: a cause or secondary reaction. *Curr Med Sci.* (2019) 39:972–7. doi: 10.1007/s11596-019-2130-3
12. He B, Zhang F, Zheng H, Sun X, Chen J, Chen J, et al. The correlation of a 2D volume-referencing endolymphatic-hydrops grading system with extra-tympanic electrocochleography in patients with definite ménière's disease. *Front Neurol.* (2021) 11:1881. doi: 10.3389/fneur.2020.595038
13. Surgery. EBoCJoOHaN, society of otorhinolaryngology head and neck surgery CMA. Guideline of diagnosis and treatment of sudden deafness (2015). *Zhonghua Er Bi Yan Hou Tou Jing Wai Ke Za Zhi.* (2015) 50:443–7. doi: 10.3760/cma.j.issn.1673-0860.2015.06.002
14. Sheehy JL. Vasodilator therapy in sensory-neural hearing loss. *Laryngoscope.* (1960) 70:885–914. doi: 10.1288/00005537-196007000-00002
15. Group Cshlm-ccs. Prospective clinical multi-center study on the treatment of sudden deafness with different typings in China. *Zhonghua Er Bi Yan Hou Tou Jing Wai Ke Za Zhi.* (2013) 48:355–61. doi: 10.3760/cma.j.issn.1673-0860.2013.05.002
16. Bennett MH, Kertesz T, Perleth M, Yeung P, Lehm JP. Hyperbaric oxygen for idiopathic sudden sensorineural hearing loss and tinnitus. *Cochrane Database Syst Rev.* (2012) 10:Cd004739. doi: 10.1002/14651858.CD004739.pub4
17. Battaglia A, Lualhati A, Lin H, Burchette R, Cueva R. A prospective, multi-centered study of the treatment of idiopathic sudden sensorineural hearing loss with combination therapy versus high-dose prednisone alone: a 139 patient follow-up. *Otol Neurotol.* (2014) 35:1091–8. doi: 10.1097/mao.0000000000000450
18. Michel O. Deutsche Gesellschaft fur Hals-Nasen-Ohren-Heilkunde K-uH-C. The revised version of the german guidelines "sudden idiopathic sensorineural hearing loss". *Laryngorhinootologie.* (2011) 90:290–3. doi: 10.1055/s-0031-1273721
19. Yoon TH, Paparella MM, Schachern PA, Alleva M. Histopathology of sudden hearing loss. *Laryngoscope.* (1990) 100:707–15. doi: 10.1288/00005537-199007000-00006s
20. Filipo R, Cordier A, Barbara M, Bertoli GA. Electrocochleographic findings: Meniere's disease versus sudden sensorineural hearing loss. *Acta Otolaryngol Suppl.* (1997) 526:21–3. doi: 10.3109/00016489709124015
21. Counter S, Bjelke B, Borg E, Klason T, Chen Z, Duan MJN. Magnetic resonance imaging of the membranous labyrinth during *in vivo* gadolinium (Gd-DTPA-BMA) uptake in the normal and lesioned cochlea. *Neuroreport.* (2000) 11:3979–83. doi: 10.1097/00001756-200012180-00015
22. Duan M, Bjelke B, Fridberger A, Counter S, Klason T, Skjönsberg A, et al. Imaging of the guinea pig cochlea following round window gadolinium application. *Neuroreport.* (2004) 15:1927–30. doi: 10.1097/00001756-200408260-00019
23. Tagaya M, Teranishi M, Naganawa S, Iwata T, Yoshida T, Otake H, et al. 3 Tesla magnetic resonance imaging obtained 4 hours after intravenous gadolinium injection in patients with sudden deafness. *Acta Otolaryngol.* (2010) 130:665–9. doi: 10.3109/00016480903384176
24. Horii A, Osaki Y, Kitahara T, Imai T, Uno A, Nishiike S, et al. Endolymphatic hydrops in Meniere's disease detected by MRI after intratympanic administration of gadolinium: comparison with sudden deafness. *Acta Oto-Laryngol.* (2011) 131:602–9. doi: 10.3109/00016489.2010.548403

25. Yamazaki M, Naganawa S, Tagaya M, Kawai H, Ikeda M, Sone M, et al. Comparison of contrast effect on the cochlear perilymph after intratympanic and intravenous gadolinium injection. *Am J Neuroradiol*. (2012) 33:773–8. doi: 10.3174/ajnr.A2821
26. Naganawa S, Yamazaki M, Kawai H, Bokura K, Sone M, Nakashima T. Imaging of Meniere's disease after intravenous administration of single-dose gadodiamide: utility of subtraction images with different inversion time. *Magn Reson Med Sci*. (2012) 11:213–9. doi: 10.2463/mrms.11.213
27. Berrettini S, Seccia V, Fortunato S, Forli F, Bruschini L, Piaggi P, et al. Analysis of the 3-dimensional fluid-attenuated inversion-recovery (3D-FLAIR) sequence in idiopathic sudden sensorineural hearing loss. *JAMA Otolaryngol Head Neck Surg*. (2013) 139:456–64. doi: 10.1001/jamaoto.2013.2659
28. Naganawa S, Sugiura M, Kawamura M, Fukatsu H, Sone M, Nakashima T. imaging of endolymphatic and perilymphatic fluid at 3T after intratympanic administration of gadolinium-diethylene-triamine pentaacetic acid. *Am J Neuroradiol*. (2008) 29:724–6. doi: 10.3174/ajnr.A0894
29. Sugiura M, Naganawa S, Teranishi M, Nakashima T. Three-dimensional fluid-attenuated inversion recovery magnetic resonance imaging findings in patients with sudden sensorineural hearing loss. *Laryngoscope*. (2006) 116:1451–4. doi: 10.1097/01.mlg.0000228005.78187.23
30. Tanigawa T, Tanaka H, Sato T, Nakao Y, Katahira N, Tsuchiya Y, et al. 3D-FLAIR MRI findings in patients with low-tone sudden deafness. *Acta Otolaryngol*. (2010) 130:1324–8. doi: 10.3109/00016489.2010.496461
31. Lee HY, Jung SY, Park MS, Yeo SG, Lee SY, Lee SK. Feasibility of three-dimensional fluid-attenuated inversion recovery magnetic resonance imaging as a prognostic factor in patients with sudden hearing loss. *Eur Arch Otorhinolaryngol*. (2012) 269:1885–91. doi: 10.1007/s00405-011-1834-1
32. Tanigawa T, Shibata R, Tanaka H, Gosho M, Katahira N, Horibe Y, et al. Usefulness of three-dimensional fluid-attenuated inversion recovery magnetic resonance imaging to detect inner-ear abnormalities in patients with sudden sensorineural hearing loss. *J Laryngol Otol*. (2015) 129:11–5. doi: 10.1017/s0022215114003028
33. Zhu H, Ou Y, Fu J, Zhang Y, Xiong H, Xu Y. A comparison of inner ear imaging features at different time points of sudden sensorineural hearing loss with three-dimensional fluid-attenuated inversion recovery magnetic resonance imaging. *Eur Arch Otorhinolaryngol*. (2015) 272:2659–65. doi: 10.1007/s00405-014-3187-z
34. Lee JI, Yoon RG, Lee JH, Park JW, Yoo MH, Ahn JH, et al. Prognostic value of labyrinthine 3D-flair abnormalities in idiopathic sudden sensorineural hearing loss. AJNR Am *J Neuroradiol*. (2016) 37:2317–22. doi: 10.3174/ajnr.A4901
35. Lee JW, Park YA, Park SM, Kong TH, Park SY, Bong JP, et al. Clinical features and prognosis of sudden sensorineural hearing loss secondary to intralabyrinthine hemorrhage. *J Audiol Otol*. (2016) 20:31–5. doi: 10.7874/jao.2016.20.1.31
36. Kim TY, Park DW, Lee YJ, Lee JY, Lee SH, Chung JH, et al. Comparison of inner ear contrast enhancement among patients with unilateral inner ear symptoms in MR images obtained 10 minutes and 4 hours after gadolinium injection. *Am J Neuroradiol*. (2015) 36:2367–72. doi: 10.3174/ajnr.A4439
37. Byun H, Chung JH, Lee SH, Park CW, Park DW, Kim TY. The clinical value of 4-hour delayed-enhanced 3D-FLAIR MR images in sudden hearing loss. *Clin Otolaryngol*. (2019) 44:336–42. doi: 10.1111/coa.13305
38. Min X, Gu H, Zhang Y, Li K, Pan Z, Jiang T. Clinical value of abnormal MRI findings in patients with unilateral sudden sensorineural hearing loss. *Diagn Interv Radiol*. (2020) 26:429–36. doi: 10.5152/dir.2020.19229
39. Yoshioka M, Naganawa S, Sone M, Nakata S, Teranishi M, Nakashima T. Individual differences in the permeability of the round window: evaluating the movement of intratympanic gadolinium into the inner ear. *Otol Neurotol*. (2009) 30:645–8. doi: 10.1097/MAO.0b013e31819bda66
40. Yoshida T, Sone M, Kitoh R, Nishio SY, Ogawa K, Kanzaki S, et al. Idiopathic sudden sensorineural hearing loss and acute low-tone sensorineural hearing loss: a comparison of the results of a nationwide epidemiological survey in Japan. *Acta Otolaryngol*. (2017) 137(Suppl. 565):S38–43. doi: 10.1080/00016489.2017.1297539
41. Chandrasekhar SS, Tsai Do BS, Schwartz SR, Bontempo LJ, Faucett EA, Finestone SA, et al. Clinical practice guideline: sudden hearing loss (update). *Otolaryngol Head Neck Surg*. (2019) 161(1_Suppl):S1–45. doi: 10.1177/0194599819859885
42. Thai-Van H, Bounaix MJ, Fraysse B. Menière's disease: pathophysiology and treatment. *Drugs*. (2001) 61:1089–102. doi: 10.2165/00003495-200161080-00005
43. Shimono M, Teranishi M, Yoshida T, Kato M, Sano R, Otake H, et al. Endolymphatic hydrops revealed by magnetic resonance imaging in patients with acute low-tone sensorineural hearing loss. *Otol Neurotol*. (2013) 34:1241–6. doi: 10.1097/MAO.0b013e3182990e81
44. Ma Y, Sun Q, Zhang K, Bai L, Du L. High level of IgE in acute low-tone sensorineural hearing loss: a predictor for recurrence and Meniere Disease transformation. *Am J Otolaryngol*. (2021) 42:102856. doi: 10.1016/j.amjoto.2020.102856
45. Stölzel K, Droste J, Voß LJ, Olze H, Szczepek AJ. Comorbid symptoms occurring during acute low-tone hearing loss (AHLH) as potential predictors of Menière's disease. *Front Neurol*. (2018) 9:884. doi: 10.3389/fneur.2018.00884
46. Junicho M, Aso S, Fujisaka M, Watanabe Y. Prognosis of low-tone sudden deafness - does it inevitably progress to Meniere's disease? *Acta Otolaryngol*. (2008) 128:304–8. doi: 10.1080/00016480601002096
47. Basura GJ, Adams ME, Monfared A, Schwartz SR, Antonelli PJ, Burkard R, et al. Clinical practice guideline: Ménière's disease. *Otolaryngol Head Neck Surg*. (2020) 162:1–55. doi: 10.1177/0194599820909438
48. Yu H, Li H. Association of vertigo with hearing outcomes in patients with sudden sensorineural hearing loss: a systematic review and meta-analysis. *JAMA Otolaryngol Head Neck Surg*. (2018) 144:677–83. doi: 10.1001/jamaoto.2018.0648
49. Morita S, Suzuki M, Iizuka K. A comparison of the short-term outcome in patients with acute low-tone sensorineural hearing loss. *ORL J Otorhinolaryngol Relat Spec*. (2010) 72:295–9. doi: 10.1159/000314695

Conflict of Interest: The authors declare that the research was conducted in the absence of any commercial or financial relationships that could be construed as a potential conflict of interest.

frontiers in Surgery

ORIGINAL RESEARCH
published: 22 June 2021
doi: 10.3389/fsurg.2021.671624

Novel Magnetic Resonance Imaging-Based Method for Accurate Diagnosis of Meniere's Disease

Taeko Ito[1†], Takashi Inoue[2†], Hiroshi Inui[1,3], Toshiteru Miyasaka[4], Toshiaki Yamanaka[1], Kimihiko Kichikawa[4], Noriaki Takeda[5], Masato Kasahara[2], Tadashi Kitahara[1] and Shinji Naganawa[6]*

[1] Department of Otolaryngology-Head and Neck Surgery, Nara Medical University, Kashihara, Japan, [2] Institute for Clinical and Translational Science, Nara Medical University, Kashihara, Japan, [3] Inui ENT Clinic, Sakurai, Japan, [4] Department of Radiology, Nara Medical University, Kashihara, Japan, [5] Department of Otolaryngology, University of Tokushima Graduate School of Medicine, Tokushima, Japan, [6] Department of Radiology, Nagoya University Graduate School of Medicine, Nagoya, Japan

Background: Pathologically, Meniere's disease symptoms are considered to be associated with endolymphatic hydrops. Examinations revealing endolymphatic hydrops can be useful for accurate Meniere's disease diagnosis. We previously reported a quantitative method for evaluating endolymphatic hydrops, i.e., by measuring the volume of the endolymphatic space using three-dimensional magnetic resonance imaging (MRI) of the inner ear. This study aimed to confirm the usefulness of our methods for diagnosing Meniere's disease. Here, we extracted new explanatory factors for diagnosing Meniere's disease by comparing the volume of the endolymphatic space between healthy volunteers and patients with Meniere's disease. Additionally, we validated our method by comparing its diagnostic accuracy with that of the conventional method.

Methods and Findings: This is a prospective diagnostic accuracy study performed at vertigo/dizziness centre of our university hospital, a tertiary hospital. Eighty-six patients with definite unilateral Meniere's disease and 47 healthy volunteers (25 and 33 males, and 22 and 53 females in the control and patient groups, respectively) were enrolled. All participants underwent 3-Tesla MRI 4 h after intravenous injection of gadolinium to reveal the endolymphatic space. The volume of the endolymphatic space was measured and a model for Meniere's disease diagnosis was constructed and compared with models using conventional criteria to confirm the effectiveness of the methods used. The area under the receiver operating characteristic curve of the method proposed in this study was excellent (0.924), and significantly higher than that derived using the conventional criteria (0.877). The four indices, sensitivity, specificity, positive predictive value, and negative predictive value, were given at the threshold; all of these indices achieved higher scores for the 3D model compared to the 2D model. Cross-validation of the models revealed that the improvement was due to the incorporation of the semi-circular canals.

Conclusions: Our method showed high diagnostic accuracy for Meniere's disease. Additionally, we revealed the importance of observing the semi-circular canals for Meniere's disease diagnosis. The proposed method can contribute toward providing effective symptomatic relief in Meniere's disease.

Keywords: Meniere's disease, magnetic resonance imaging, endolymphatic hydrops, diagnostic strategy, ROC analysis

OPEN ACCESS

Edited by:
Paul van de Heyning, University of Antwerp, Belgium

Reviewed by:
Neil Donnelly, University of Cambridge, United Kingdom
Michihiko Sone, Nagoya University Hospital, Japan
Bert De Foer, Sint Augustinus Hospital, Belgium

***Correspondence:**
Taeko Ito
taeito@naramed-u.ac.jp

†These authors have contributed equally to this work

Specialty section:
This article was submitted to Otorhinolaryngology - Head and Neck Surgery, a section of the journal Frontiers in Surgery

Received: *24 February 2021*
Accepted: *19 May 2021*
Published: *22 June 2021*

Citation:
Ito T, Inoue T, Inui H, Miyasaka T, Yamanaka T, Kichikawa K, Takeda N, Kasahara M, Kitahara T and Naganawa S (2021) Novel Magnetic Resonance Imaging-Based Method for Accurate Diagnosis of Meniere's Disease. Front. Surg. 8:671624. doi: 10.3389/fsurg.2021.671624

INTRODUCTION

Meniere's disease (MD) is a common disease characterized by recurrent vertigo/dizziness and cochlear symptoms (hearing loss, tinnitus, and aural fullness). Since a well-constructed clinical guideline for MD has already been reported (1) patients with MD can receive appropriate treatment once the correct diagnosis has been reached. In 2015, new criteria for MD diagnosis were established by a collaborative working group led by the Barany Society (2). In the Barany criteria, MD diagnosis is mainly based on patients' subjective symptoms. Therefore, for accurate diagnosis and appropriate treatment, obtaining an accurate medical history and clarification of patients' complaints are essential. However, this can be challenging, since patient complains are often vague. In fact, 40–80% of patients are not definitively diagnosed in the long term, thus leading to inadequate treatment, (3) administration of unnecessary medicine, and increases in medical costs, which are significant problems worldwide. Thus, examinations that help reach an accurate diagnosis with minimal requirements for specialist training are desirable.

In 1938, Yamakawa (4) and Hallpike and Cairns (5) independently reported the finding of endolymphatic hydrops in the temporal bones of patients with MD; hence, objective examinations that can reveal endolymphatic hydrops are considered to be useful for diagnosing MD, and many investigators have attempted to establish them. Electrocochleography and glycerol and furosemide testing are used for diagnosing endolymphatic hydrops, but the positivity rate of these tests among patients with MD is ∼50% (6–12). Because of the low ratios, these tests cannot be components of the diagnostic criteria of MD, and it is considered difficult to clinically detect endolymphatic hydrops in patients with MD by morphological examinations.

In 2006, the Nagoya University group succeeded in visualizing the endolymphatic space using 3-Tesla MRI after intravenous gadolinium injection (13) (inner ear MRI [ieMRI]). Subsequently, a convenient method of grading endolymphatic hydrops on ieMRI was proposed (14). Using this grading, the positive ratio of endolymphatic hydrops on ieMRI was found to be 70–100% (15–17) suggesting that it could be a diagnostic criterion of MD. Although this grading has the advantage of being convenient, it has the limitation of being a qualitative evaluation, using only one slice of ieMRI, with the plane for image analysis varying depending on the head position and anatomical differences in the skull, and restricted to a particular part of the inner ear, neglecting the semi-circular canals (SCCs). To allow ieMRI to be a component of the diagnostic criteria of MD, it is required to establish a quantitative method to measure endolymphatic hydrops in the whole inner ear and identify the explanatory factors for their grading; hence, we started to measure the volumes of inner ears and endolymphatic space in 2016 (18–20). In these previous studies, to quantitatively observe endolymphatic hydrops in the whole inner ear, we reported a method of constructing high-quality three-dimensional images of ieMRI (ie3DMRI) and the volume of the endolymphatic space.

In the present study, we compared the volume of the endolymphatic space between patients with MD and healthy controls using the ie3DMRI method, thereby extracting new and reliable explanatory factors for diagnosing MD. These factors can help clinicians to diagnose MD with accuracy.

METHODS

The Medical Ethics Committee of our university approved this study (certificate number: 0889). Written informed consent was obtained from each participant, including healthy volunteers.

Patients and Controls

We enrolled 86 patients diagnosed with unilateral Meniere's disease (uMD), according to the Barany criteria (2) and American Academy of Otolaryngology-Head and Neck Surgery (21) at the vertigo/dizziness center of our university hospital between July 2014 and December 2018. As controls, 47 healthy volunteers participated in the present study, and data related to both ears ($n = 94$) of each volunteer were included in the statistical analysis. Control volunteers had no history of hearing loss, vertigo, middle or inner ear diseases, cranial disease, head trauma, renal disease, or heart disease. The controls were not using any medications at the time. Both patients and controls had no history of allergy to gadolinium.

MRI Observation

MRI measurements were acquired 4 h after intravenous administration of a single dose (0.1 mmol/kg body weight) of gadolinium-diethylenetriaminepentaacetic acid dimethylamide (Magnescope; Guerbet, Tokyo, Japan) (15). A 3-Tesla MRI unit (MAGNETOM Verio; Siemens, Erlangen, Germany) with a 32-channel array head coil was used. The sequences, proposed by Naganawa et al. (22) specific to endolymphatic and perilymphatic fluids were adopted. A radiologist (with 14 years of experience) and two otolaryngologists (with 12 and 29 years of experience), who were blinded to the clinical progress of the patients, evaluated the MRI findings independently. If their evaluations differed, a third otolaryngologist (with 31 years of experience) made the final decision.

Conventional Two-Dimensional Evaluation of Endolymphatic Hydrops

The criteria proposed by Nakashima et al. (14) and Kahn et al. (23) were adopted. According to the criteria by Naganawa et al. we classified the endolymphatic hydrops in the cochleae and vestibules as none, mild, or significant. In the present study, both mild and significant were defined as positive: the existence of endolymphatic hydrops. Additionally, we evaluated the endolymphatic hydrops using the criteria by Kahn et al. and classified them as none, grade I, or grade II; grade I, or grade II was defined as positive in the present study.

Volumetric Measurement of Total Fluid Space and Endolymphatic Space

Volumetric measurement of the total fluid space and endolymphatic space was performed in accordance with

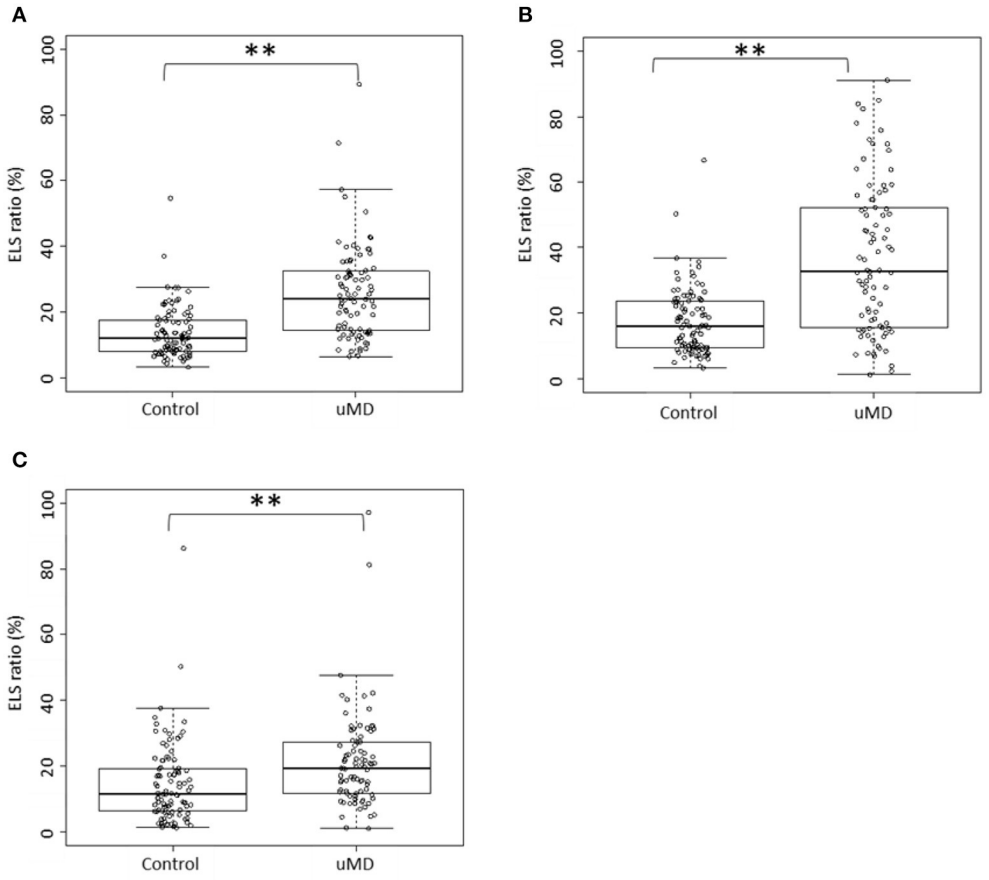

FIGURE 1 | Distribution of the ELS ratio. **(A)**: cochlea; **(B)**: vestibule; **(C)**: SCCs. In the cochleae, the ELS ratios of controls and patients with uMD were 8.15% (median) and 22.50%, respectively **(A)**. In the vestibules, the ELS ratios of controls and patients with uMD were 16.25 and 32.85%, respectively **(B)**. In the SCCs, the ELS ratios of controls and patients with uMD were 11.65 and 19.50%, respectively **(C)**. The ELS ratios of patients with uMD were significantly higher than those of controls in the cochleae, vestibules, and SCCs. $^{**}p < 0.001$, Mann–Whitney U test.

our previously published methods (18–20) on our workstation (Virtual Place; AZE, Ltd., Tokyo, Japan). In this protocol, the endolymphatic space voxels have negative signal values and the perilymph space voxels have positive signal values. The volume of the total fluid space was acquired using a software to count voxels automatically. Then, the ratio of the volume of the endolymphatic space to that of the total fluid space was calculated ("ELS ratio"). We performed these measurements three times, and the average was used for calculation. In the present study, we evaluated the SCCs in addition to the cochlea and vestibule, which is the conventional method used.

Statistical Methods

All P-values were two sided, and P-values of 0·05 or lower were considered statistically significant. All statistical analyses were performed using R, Version 3.5.2 (24). The minimum number of subjects was determined from the number of explanatory variables in logistic regression analysis; $n = 70$ for patients with uMD and $n = 35$ for controls. We examined sex and age differences between patients and controls using Fisher's exact test and the Mann–Whitney U test, respectively. The ELS ratio between controls and patients with uMD was compared using the Mann–Whitney U test. The association between patient background and the morbidity of uMD was investigated using multivariate logistic regression analysis. A model to diagnose uMD was developed on the basis of the receiver operating characteristic (ROC) curve using multivariate logistic regression analyses, and the difference in the areas under the curve (AUCs) was statistically compared using Delong's test. Moreover, we evaluated the index of net reclassification improvement (NRI) (25) and performed cross-validation among models.

RESULTS

Patient Background

There were 25 and 33 men and 22 and 53 women in the control and patient groups, respectively. The mean age of controls and patients with uMD was 58.4 ± 16.3 and 56.9 ± 14.7 years, respectively. There were no significant differences between the

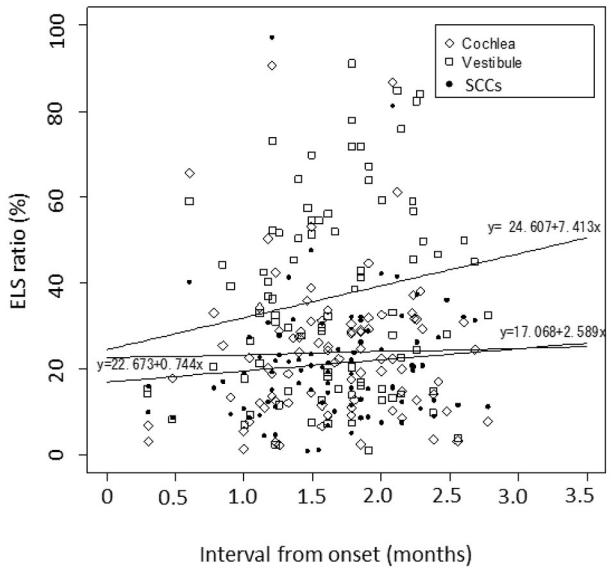

FIGURE 2 | Correlation between the interval from the onset of uMD to MRI observation. Using an interval of days on a linear scale, the logarithmic day (x) is scaled as $x = \log_{10}(1 + \text{interval})$. The simple linear regression analyses summarize the data as follows: the ELS ratios (y) showed a slightly increasing trend with time, but there were no significant changes; $y = 22.673 + 0.744x$ with $P = 0.83$ for the cochleae, $y = 24{\cdot}607 + 7{\cdot}413x$ with $p = 0.11$ for the vestibules, and $y = 17.068 + 2.589x$ with $p = 0.38$ for the SCCs. Diamond: cochlea, square: vestibule, dot: SCCs.

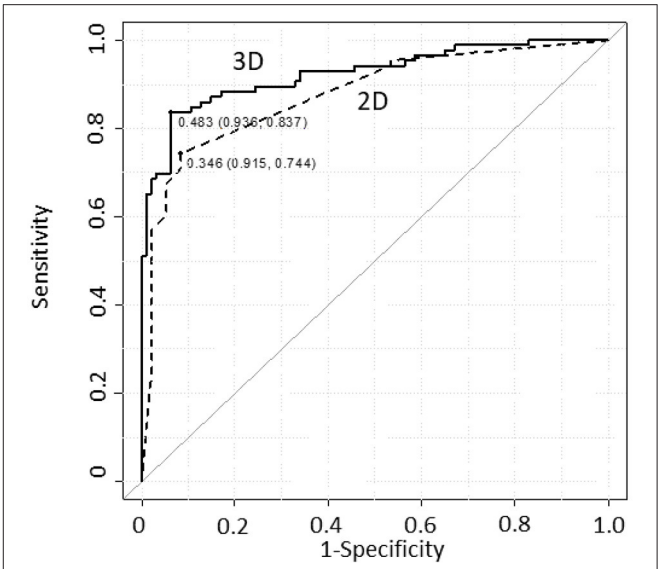

FIGURE 3 | ROC curve comparison for MD diagnostic accuracy between the models. The AIC values were 161.3 and 155.7 with the 2D and 3D models, respectively. The AUC values were 0.877 and 0.924 with the 2D and 3D models, respectively. For the 3D model, both AIC and AUC values were improved compared with those for the 2D model. 2D Model: MD∼Sex + EHV + EHC. 3D Model: MD∼Sex + Vv + Cv + Sv + Vi + Si + VCi + Vh + Vr + Cr + VCr + Ir + Vr2 + Cr2 + Vr:Cr + Sr:VCr + VCr:Ir. Dotted line: 2D model, continuous line: 3D model.

controls and patients with uMD (sex; $p = 0.11$, Fisher's exact test, age; $p = 0.47$, Mann–Whitney U test).

ELS Ratio of Controls and Patients With uMD

The Box and bee swarm plots in **Figures 1A–C** show the ELS ratio of controls and patients with uMD. In the cochleae, the ELS ratio of controls was 8.15 [4.93–14.45]% (median [interquartile range]) and that of patients with uMD was 22.50 [12.20–31.12]% (**Figure 1A**). In the vestibules, the ELS ratio of controls was 16.25 [9.70–23.65]% and that of patients with uMD was 32.85 [15.75–52.20]% (**Figure 1B**). In the SCCs, the ELS ratio of controls was 11.65 [6.45–19.25]% and that of patients with uMD was 19.50 [11.90–27.15]% (**Figure 1C**). Among all parts of the inner ears, there were significant differences between controls and patients with uMD ($p < 0.001$, Mann–Whitney U test).

Relationship Between the ELS Ratio and the Interval From Onset of MD to MRI Observation

Figure 2 shows the correlation between the interval from the onset of uMD to MRI observation and the ELS ratio in the cochleae/vestibules/SCCs. Using an interval of days on a linear scale, the logarithmic day (x) was scaled as $x = \log_{10}(1 + \text{interval})$. The ELS ratios (y) showed a slightly increasing trend with time, but there were no significant changes ($p = 0.83$ in the cochleae, $p = 0.11$ in the vestibules, and $p = 0.38$ in the SCCs).

Contribution of the Background Factors

Multivariate logistic regression analyses were performed with uMD as an objective variable and sex, age, and the volumes of endolymphatic hydrops in the cochleae/vestibules/SCCs as explanatory variables (**Supplementary Table 1**). The odds ratio of being female was significantly higher in patients with uMD; sex was a confounding factor for a causality pathway toward MD and should be included as an adjustment factor in model building for diagnosing uMD. The ELS ratio in SCCs was not a significant factor in this analysis.

Model Building for MD Diagnosis

Logistic regression models were built for diagnosing MD. We introduced an abridged notation to describe logistic regression equations, abbreviating the regression coefficients and expressing the first-order interaction between predictors A_1 and A_2 as A_1:A_2. Consider $Y \sim A_1 + A_2 + A_1{:}A_2$ as an example; this notation denotes $logit\{P/(1\text{-}P)\} = \beta_0 + \beta_1 A_1 + \beta_2 A_2 + \beta_c A_1 \cdot A_2$. Here, the objective and dichotomous variable Y is predicted by the probability P at which Y gains 1 and β represents a regression coefficient. Each regression coefficient for each predictor is determined using the maximum likelihood estimation based on a set of predictors for given observational data.

The results obtained from the conventional evaluation of endolymphatic hydrops on ieMRI (15) were applied to a logistic regression model to diagnose MD. An objective and dichotomous variable is *MD*, determined according to the Barany criteria (2). Predictors were *Sex, EHV*, and *EHC*, where *EHV* and *EHC*

TABLE 1 | Comparison of MD diagnostic accuracy between the models.

Subjects: uMD +control	Threshold	Sensitivity	Specificity	Positive predictive value	Negative predictive value	AUC	*p*-value	*p*-value by NRI	AIC
2D model	0.346	0.744	0.915	0.889	0.796	0.877			161.3
3D model	0.483	0.837	0.936	0.923	0.863	0.924	$p = 0.07$	$p < 0.001$	155.7

Each threshold value was determined as the closest top-left point on the ROC curve. The four indices of sensitivity, specificity, positive predictive value, and negative predictive value were given at the threshold; all of these indices achieved higher scores for the 3D model. The AIC value improved from 161.3 to 155.7 (2D−3D model), and the AUC value improved from 0.877 to 0.924 (2D−3D model).

were the morbidity indicators of endolymphatic hydrops in the vestibule and cochlea, respectively. Values of these variables were given as 0, 0.5, or 1 for no, mild, or significant endolymphatic hydrops, respectively, according to the conventional grading (14). The objective variable *MD* was predicted with Equation (1) [2D model], where the interaction term *EHV:EHC* was omitted because trial calculations showed that it was not correlated with the objective variable *MD*:

$$MD \sim Sex + EHV + EHC \quad (1)$$

We built a logistic regression model from a set of volumes of vestibules, cochleae, or SCCs and their ELS, evaluated using the ie3DMRI technique. Seven independent predictors were used: *Sex* (Sex), *Vv* (vestibular volume), *Cv* (cochlear volume), *Sv* (SCC volume), *V*h (ELS volume in the vestibule), *Ch* (ELS volume in the cochlea), and *Sh* (ELS volume in the SCC). Each of other predictors was defined as a function of the seven independent predictors and selected from the standpoint of medicine: $Vi = 1/Vv$, $Vr = Vh \cdot Vi$, $Vr2 = Vr^2$, $Ci = 1/Cv$, $Cr = Ch \cdot Ci$, $Cr2 = Cr^2$, $Si = 1/Sv$, $Sr = Sh \cdot Si$, $Sr2 = Sr^2$, $VCi = 1/(Vv + Cv)$, $VCr = (Vh + Ch) \cdot VCi$, $VCr2 = VCr^2$, $Ii = 1/(Vv + Cv + Sv)$, $Ir = (Vh + Ch + Sh) \cdot Ii$, $Ir2 = Ir^2$.

To improve the MD diagnostic accuracy, we selected predictors in the logistic regression model to maximize the AUC of the ROC curve and to minimize Akaike's information criterion (25) (AIC) using the data from 94 ears of controls and 86 ears of patients with uMD. The model validity was confirmed using a cross-validation method of "leave-one-out calculation." The result is presented using Equation (2) [3D model] (**Supplementary Table 2**).

$$MD \sim Sex + Vv + Cv + Sv + Vi + Si + VCi + Vh + Vr + Cr + VCr + Ir + Vr2 + Cr2 + Vr{:}Cr + Sr{:}VCr + VCr{:}Ir \quad (2)$$

Comparison of uMD Diagnostic Accuracy of Models

We conducted MD diagnosis on 86 ears of patients with uMD and 94 ears of controls and compared the diagnostic accuracy between the two models. **Figure 3** shows ROC curves and thresholds for MD diagnosis, with a solid line plotted according to the logistic regression model, based on Equation (2) [3D model], and a dotted line according to the conventional method, (21) based on Equation (1) [2D model] for reference.

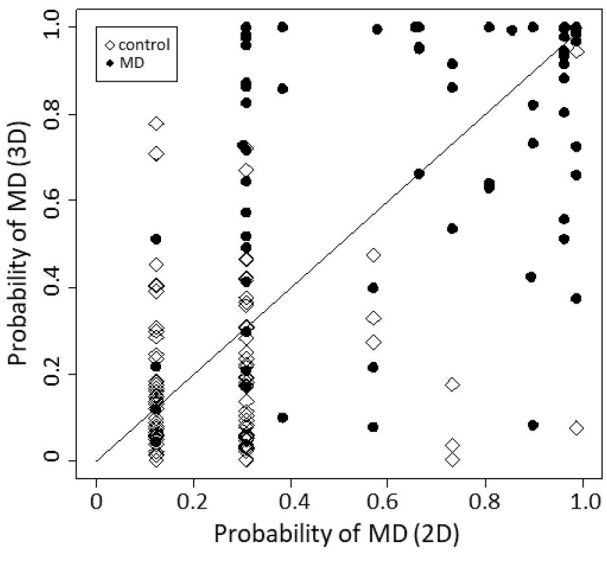

FIGURE 4 | Reclassification plot, a basis for the NRI test. The diagnostic accuracy was significantly improved by the 3D model compared with the 2D model ($p < 0.001$, continuous NRI test).

The MD diagnostic accuracies of the two models were tabulated and compared (**Table 1**). Each threshold value was determined as the closest top-left point on the ROC curve. The four indices, i.e., sensitivity, specificity, positive predictive value, and negative predictive value, were given at the threshold; all of these indices achieved higher scores for the 3D model. The AIC value improved from 161.3 to 155.7 (2D−3D model), and the AUC value improved from 0.877 to 0.924 (2D−3D model); however, Delong's test showed that the AUC difference was not significant.

Figure 4 is a reclassification plot showing the diagnostic improvement with the 3D model compared with the 2D model. Based on the evaluation, the following continuous NRI test was carried out, and the improvement in diagnostic accuracy was statistically confirmed ($p < 0.001$).

A cross-validation procedure (26) was conducted (**Supplementary Table 3**), in which the AICs, AUCs, and mean square errors were calculated for the models' varying explanatory terms. The mean square error was evaluated using the leave-one-out method as the mean square of the difference

between the estimated MD probability and the definite diagnosis for the remaining subjects. The selected 3D model minimized the AIC and mean square error, implying that improvement in MD diagnostic accuracy of the selected 3D model from the 2D model was achieved by the incorporation of terms related to SCCs and the interaction between the cochleae, vestibules, and SCCs.

Sensitivity and Specificity of the Selected 3D Model and the 2D Model

The sensitivity of the selected 3D model and the 2D model was 0.83 (71/86) and 0.74 (64/86), respectively. The specificity of the selected 3D model and the 2D model was 0.94 (88/94) and 0.93 (87/94), respectively.

DISCUSSION

In the present study, we confirmed that our method using ie3DMRI strongly supported the diagnosis of MD with a high level of accuracy. Additionally, when we optimized the MD diagnostic formulae, incorporating the ELS ratio of the SCCs and the interaction among the whole inner ear, cochleae, vestibules, and SCCs, the ROC curves significantly improved. Cross-validation of the models showed that the improvement was due to the incorporation of both SCCs and the interaction between the cochleae and vestibules, although the ELS ratio in the SCCs was not a significant factor for MD. This implies that the ELS ratio in the SCCs and its interaction with the cochleae and vestibules are associated with morbidity in MD. Moreover, we succeeded in incorporating the interaction between the ELS ratio of the cochleae, vestibules, and SCCs in the MD diagnosis, whereas the conventional grading could evaluate endolymphatic hydrops only in the cochlea and vestibule. In fact, some patients with intractable MD had endolymphatic hydrops in the SCCs; in our previous study, symptomatic relief was associated with the disappearance of endolymphatic hydrops in the SCCs after endolymphatic sac drainage (20). Sugimoto et al. also reported that some patients showed endolymphatic hydrops herniation into the SCCs (27). Taken together, we should not neglect the endolymphatic space in SCCs while diagnosing MD and elucidating the causes of MD symptoms.

Wu et al. and Gürkov et al. reported that endolymphatic hydrops showed progressive deterioration during the disease duration from the data of 41 (28) and 54 patients, (29) respectively. In the present study ($n = 86$), although the ELS ratio tended to increase with time, no significant changes were noted. Based on the results in the present study, our method has the potential to distinguish individuals with MD from those without, even in the early stages of disease progression.

One of the limitations of this study was that symptoms were not included in our analysis. The Barany criteria, which are presently the most reliable criteria, emphasize the importance of interpreting the characteristics of vertigo/dizziness in diagnosing MD (2). Inclusion of data related to the characteristics of vertigo/dizziness in the statistical analysis may have led to more accurate results. In the present study, however, we decided to exclude these factors to evaluate the usefulness of ie3DMRI *per se*. A high rate of accurate diagnosis can be reached when combining the method in the present study with the conventional strategy for MD diagnosis. Misdiagnoses of vertigo/dizziness especially by non-specialists are major concerns, resulting in increased medical costs (3, 30). The method in the present study could also provide valuable feedback to non-specialists and residents who wish to polish their vertigo diagnostic skills. Another limitation was that not all patients with MD had endolymphatic hydrops and not all patients with endolymphatic hydrops had MD. The results indicated a factor other than endolymphatic hydrops caused the MD symptoms in some cases. The relationship between MD symptoms and endolymphatic hydrops remains unclear. When the causes of MD symptoms are revealed, they should be included to the factors entered in MD diagnostic models, which can lead to improved MD diagnosis accuracy and symptom relief for a larger number of patients.

For a long time, researchers studying MD have attempted to elucidate the mechanisms of endolymphatic hydrops formation and the relationship between symptoms and changes in the condition of endolymphatic hydrops. Volumetric measurement of ELS, which is objective, and quantitative observation of endolymphatic hydrops in patients has the potential to elucidate these issues in the future.

DATA AVAILABILITY STATEMENT

The original contributions presented in the study are included in the article/**Supplementary Material**, further inquiries can be directed to the corresponding author/s.

ETHICS STATEMENT

The studies involving human participants were reviewed and approved by The Medical Ethics Committee of Nara Medical University. The patients/participants provided their written informed consent to participate in this study.

AUTHOR CONTRIBUTIONS

TIt and TIn contributed equally to the manuscript. TIt, TIn, and TK have full access to all of the data in the present study and take responsibility for the integrity of the data and the accuracy of the data analysis. TIt, TIn, TY, KK, NT, MK, TK, and SN were involved in the study conception and design. TIn provided statistical expertise. TIt and TIn drafted the manuscript. TIt, TK, and SN are the guarantors. All the authors participated in the interpretation of the results and critical revision of the manuscript.

FUNDING

This work was supported by JSPS KAKENHI Grant Number 18K09354 Grant-in-Aid for Scientific Research (C), Grant-in-Aid for Early-Career Scientists (Grant Number 20K18260), AMED under Grant Number JP20dk0310092, and Health and Labour Sciences Research Grant for Research on Rare and Intractable Diseases (Grant Number 20FC1048) from the Ministry of Health, Labour, and Welfare of Japan.

ACKNOWLEDGMENTS

This work was supported by JSPS KAKENHI Grant Number 18K09354 Grant-in-Aid for Scientific Research (C), Grant-in-Aid for Early-Career Scientists (Grant Number 20K18260), AMED under Grant Number JP20dk0310092, and Health and Labour Sciences Research Grant for Research on Rare and Intractable Diseases (Grant Number 20FC1048) from the Ministry of Health, Labour, and Welfare of Japan.

SUPPLEMENTARY MATERIAL

The Supplementary Material for this article can be found online at: https://www.frontiersin.org/articles/10.3389/fsurg.2021.671624/full#supplementary-material

REFERENCES

1. Sajjadi H, Paparella MM. Meniere's disease. *Lancet.* (2008) 372:406–14. doi: 10.1016/S0140-6736(08)61161-7
2. Lopez-Escamez JA, Carey J, Chung WH, Goebel JA, Magnusson M, Mandala M, et al. Diagnostic criteria for Meniere's disease. *J Vestibular Res.* (2015) 25:1–7. doi: 10.3233/VES-150549
3. Geser R, Straumann D. Referral and final diagnoses of patients assessed in an academic vertigo center. *Front Neurol.* (2012) 3:169. doi: 10.3389/fneur.2012.00169
4. Yamakawa K. Hearing organ of a patient who showed Meniere's symptoms. *J Otolaryngol Soc Jpn.* (1938) 44:2310–2.
5. Hallpike CS, Cairns H. Observations on the Pathology of Meniere's Syndrome: (Section of Otology). *Proc R Soc Med.* (1938) 31:1317–36. doi: 10.1177/003591573803101112
6. Coats AC. The summating potential and Meniere's disease. *I. Summating potential amplitude in Meniere and non-Meniere ears. Arch Otolaryngol.* (1981) 107:199–208. doi: 10.1001/archotol.1981.00790400001001
7. Ferraro JA, Tibbils RP. SP/AP area ratio in the diagnosis of Meniere's disease. *Am J Audiol.* (1999) 8:21–8. doi: 10.1044/1059-0889(1999/001)
8. Gibson WP, Moffat DA, Ramsden RT. Clinical electrocochleography in the diagnosis and management of Meneere's disorder. *Audiology.* (1977) 16:389–401. doi: 10.3109/00206097709071852
9. Klockhoff I. The effect of glycerin on fluctuant hearing loss. *Otolaryngol Clin North Am.* (1975) 8:345–55. doi: 10.1016/S0030-6665(20)32772-9
10. Sauer RC, Kaemmerle AW, Arenberg IK. The prognostic value of the glycerol test: a review of 60 ears with unidirectional inner ear valve implants. *Otolaryngol Clin North Am.* (1980) 13:693–701. doi: 10.1016/S0030-6665(20)32328-8
11. Snyder JM. Predictability of the glycerin test in the diagnosis of Meniere's disease. *Clin Otolaryngol Allied Sci.* (1982) 7:389–97. doi: 10.1111/j.1365-2273.1982.tb01402.x
12. Tsunoda R, Fukaya T, Komatsuzaki A. The furosemide test and vestibular status in Meniere's disease. *Acta Otolaryngol.* (1998) 118:157–60. doi: 10.1080/00016489850154847
13. Naganawa S, Komada T, Fukatsu H, Ishigaki T, Takizawa O. Observation of contrast enhancement in the cochlear fluid space of healthy subjects using a 3D-FLAIR sequence at 3 Tesla. *Eur. Radiol.* (2006) 16:733–7. doi: 10.1007/s00330-005-0046-8
14. Nakashima T, Naganawa S, Pyykko I, Gibson WP, Sone M, Nakata S, et al. Grading of endolymphatic hydrops using magnetic resonance imaging. *Acta Otolaryngol Suppl.* (2009) (2009) 560:5–8. doi: 10.1080/00016480902729827
15. Ito T, Kitahara T, Inui H, Miyasaka T, Kichikawa K, Ota I, et al. Endolymphatic space size in patients with Meniere's disease and healthy controls. *Acta Otolaryngol.* (2016) 136:879–82. doi: 10.3109/00016489.2016.1169556
16. Morimoto K, Yoshida T, Sugiura S, Kato M, Kato K, Teranishi M, et al. Endolymphatic hydrops in patients with unilateral and bilateral Meniere's disease. *Acta Otolaryngol.* (2017) 137:23–8. doi: 10.1080/00016489.2016.1217042
17. Naganawa S, Yamazaki M, Kawai H, Bokura K, Iida T, Sone M, et al. MR imaging of Meniere's disease after combined intratympanic and intravenous injection of gadolinium using HYDROPS2. *Magn Res Med Sci.* (2014) 13:133–7. doi: 10.2463/mrms.2013-0061
18. Inui H, Sakamoto T, Ito T, Kitahara T. Magnetic resonance volumetric measurement of endolymphatic space in patients without vertiginous or cochlear symptoms. *Acta Otolaryngol.* (2016) 136:1206–12. doi: 10.1080/00016489.2016.1204663
19. Inui H, Sakamoto T, Ito T, Kitahara T. Volumetric measurements of the inner ear in patients with Meniere's disease using three-dimensional magnetic resonance imaging. *Acta Otolaryngol.* (2016) 136:888–93. doi: 10.3109/00016489.2016.1168940
20. Ito T, Inui H, Miyasaka T, Shiozaki T, Matsuyama S, Yamanaka T, et al. Three-dimensional magnetic resonance imaging reveals the relationship between the control of vertigo and decreases in endolymphatic hydrops after endolymphatic sac drainage with steroids for Meniere's Disease. *Front Neurol.* (2019) 10:46. doi: 10.3389/fneur.2019.00046
21. Committee on Hearing and Equilibrium guidelines for the diagnosis and evaluation of therapy in Meniere's disease. American Academy of Otolaryngology-Head and Neck Foundation, Inc. *Otolaryngol Head Neck Surg.* (1995) 113:181–5. doi: 10.1016/S0194-5998(95)70102-8
22. Naganawa S, Yamazaki M, Kawai H, Bokura K, Sone M, Nakashima T. Imaging of Meniere's disease after intravenous administration of single-dose gadodiamide: utility of subtraction images with different inversion time. *Magn Reson Med Sci.* (2012) 11:213–9. doi: 10.2463/mrms.11.213
23. Kahn L, Hautefort C, Guichard JP, Toupet M, Jourdaine C, Vitaux H, et al. Relationship between video head impulse test, ocular and cervical vestibular evoked myogenic potentials, and compartmental magnetic resonance imaging classification in meniere's disease. *Laryngoscope.* (2019) 130:E444–52. doi: 10.1002/lary.28362
24. R RCT. *A Language and Environment for Statistical Computing. R Foundation for Statistical Computing, Vienna, Austria.* Available online at: https://www.R-project.org/ (accessed June 10, 2021).
25. Pencina MJ, D'Agostino RB Sr., D'Agostino RB Jr., Vasan RS. Evaluating the added predictive ability of a new marker: from area under the ROC curve to reclassification and beyond. *Stat Med.* (2008) 27:157–72; discussion 207–12. doi: 10.1002/sim.2929
26. Allen DM. Mean square error of prediction as a criterion for selecting variables. *Technometrics.* (1971) 13:469–75. doi: 10.2307/1267161
27. Sugimoto S, Yoshida T, Teranishi M, Kobayashi M, Shimono M, Naganawa S, et al. Significance of endolymphatic hydrops herniation into the semicircular canals detected on MRI. *Otol Neurotol.* (2018) 39:1229–34. doi: 10.1097/MAO.0000000000002022
28. Wu Q, Dai C, Zhao M, Sha Y. The correlation between symptoms of definite Meniere's disease and endolymphatic hydrops visualized by magnetic resonance imaging. *Laryngoscope.* (2016) 126:974–9. doi: 10.1002/lary.25576
29. Gurkov R, Flatz W, Louza J, Strupp M, Ertl-Wagner B, Krause E. *In vivo* visualized endolymphatic hydrops and inner ear functions in patients with electrocochleographically confirmed Meniere's disease. *Otol Neurot.* (2012) 33:1040–5. doi: 10.1097/MAO.0b013e31825d9a95
30. Grill E, Strupp M, Muller M, Jahn K. Health services utilization of patients with vertigo in primary care: a retrospective cohort study. *J Neurol.* (2014) 261:1492–8. doi: 10.1007/s00415-014-7367-y

Conflict of Interest: The authors declare that the research was conducted in the absence of any commercial or financial relationships that could be construed as a potential conflict of interest.

frontiers in Surgery

ORIGINAL RESEARCH
published: 20 July 2021
doi: 10.3389/fsurg.2021.667248

MR Imaging of Cochlear Modiolus and Endolymphatic Hydrops in Patients With Menière's Disease

Rita Sousa[1], Carla Guerreiro[1], Tiago Eça[2], Jorge Campos[3] and Leonel Luis[2,4]*

[1] Neuroradiology Department, Centro Hospitalar Universitário Lisboa Norte, Lisbon, Portugal, [2] Otorhinolaryngology Department, Centro Hospitalar Universitário Lisboa Norte, Lisbon, Portugal, [3] Imaging Department, Red Cross Hospital, Lisbon, Portugal, [4] Clinical Physiology Translational Unit, Institute of Molecular Medicine, University of Lisbon, Lisbon, Portugal

Background: Menière's disease (MD) is an inner ear disorder characterized by recurrent episodes of spontaneous vertigo, unilateral low-frequency sensorineural hearing loss, tinnitus, and aural fullness. Current diagnosis still often has to rely on subjective and audiometric criteria only, although endolymphatic hydrops is recognized as the pathophysiological substrate of the disease, having been demonstrated in anatomical pathological studies and by magnetic resonance (MRI). The modiolus has a close functional and anatomical relationship with the cochlear nerve and membranous labyrinth and can be evaluated with MRI but no data exist on the modiolar size in MD.

Purpose: Our purpose is to examine the following hypothesis. Is cochlear modiolus smaller in symptomatic ears in MD?

Methods: We used a retrospective 3 Tesla MR study (heavily T2-weighted 3D fast asymmetric spin-echo images and 0.5 mm slice thickness) comparing the mean modiolar area (MMA) in the index and best ears of eight patients with definite MD based on audiometric data. The obtained MMA values were compared against the audiometric data and the presence of vestibular endolymphatic hydrops.

Results: No differences were seen in MMA between best and worst ears. Ears with a pure tone average (PTA) ≥25 dB and more pronounced endolymphatic hydrops showed lower MMA (not statistically significant). Two patients with extreme endolymphatic hydrops showed a noteworthy ipsilateral decrease in the cochlear modiolus area.

Conclusion: No differences were seen in MMA between best and worst ears in definite MD. Worse hearing function (PTA ≥ 25dB) and more pronounced endolymphatic hydrops seem to be associated with lower MMA. This might be related to bone remodeling as a consequence of endolymphatic hydrops. Further research is needed to corroborate and explore these findings.

Keywords: Menière's disease, endolymphatic hydrops, cochlear modiolus, magnetic resonance inner ear, membranous labyrinth

OPEN ACCESS

Edited by:
Robert Gürkov, Bielefeld University, Germany

Reviewed by:
Wilhelm Flatz, Ludwig Maximilian University of Munich, Germany
Andrés Soto-Varela, Complejo Hospitalario Universitario de Santiago, Spain

****Correspondence:***
Rita Sousa
ritafsousa1@gmail.com

Specialty section:
This article was submitted to Otorhinolaryngology - Head and Neck Surgery, a section of the journal Frontiers in Surgery

Received: *12 February 2021*
Accepted: *17 May 2021*
Published: *20 July 2021*

Citation:
Sousa R, Guerreiro C, Eça T, Campos J and Luis L (2021) MR Imaging of Cochlear Modiolus and Endolymphatic Hydrops in Patients With Menière's Disease. Front. Surg. 8:667248. doi: 10.3389/fsurg.2021.667248

INTRODUCTION

MD is a chronic disease with a prevalence of 200–500 per 100,000 individuals (1), characterized by a recurrent clinical syndrome of audiovestibular symptoms, namely spontaneous vertigo, unilateral hearing loss, aural fullness, and tinnitus (2).

Prosper Ménière, in 1861, was the first to recognize the inner ear at the origin of the symptoms (3), with endolymphatic hydrops only later, in 1937, being described by British (4) and Japanese (5) researchers.

Nowadays its cause remains undetermined, but the pathophysiological substrate seems to be the increase in the endolymphatic space of the membranous labyrinth, partially occupying the usual space of the perilymph. The molecular mechanism of the endolymphatic hydrops is still unknown, although genetic and inflammatory factors have been referred (6). ELH has been known to be the pathological basis of various pathophysiological changes of inner ear function (7).

Nowadays, endolymphatic hydrops can be demonstrated with MR (8), but current diagnostic criteria still remain symptom based and do not consider vestibular evaluation nor demonstration of endolymphatic hydrops (9), although this has been debated controversially (2).

Given the audiometric deterioration in the disease and the close relation of the modiolus with the endolymphatic space, a change in the structure of cochlear modiolus might be expected at least in symptomatic ears of patients with MD.

Some theories refer to an inflammatory mediated process in endolymphatic structures with micro ruptures of the membranous labyrinth, causing a sudden mixture between the perilymph and endolymph, resulting in physical and chemical changes in the cochlear and vestibular system (10, 11). This chronic process could result in a reactive bone process of hyperostosis and an increase of cochlear modiolus size. On the other side, a decrease of cochlear modiolus size could be explained by bone remodeling as a result of chronic increased pressure caused by enlarged endolymphatic space, at least in long-term disease or in cases with more pronounced endolymphatic hydrops.

Because we could not find sufficient data in relation to this question in the literature and clarify these controversial hypotheses, we decided to investigate the size of cochlear modiolus in 16 ears of eight patients with clinical definite MD.

MATERIALS AND METHODS

All studies were performed in a 3 Tesla MRI scanner (Philips Achieva–Philips Medical Systems, Best, Netherlands), using an 8-channel head coil. Thin-section heavily T2-weighted 3D fast spin-echo, TR 1500/TE 200, echo train length 61, field of view 150, slice thickness 0.5 mm, axial slab matrix 256, voxel size 0.5 AP/0.7 RL/0.5 FH and scan time 4.34 min.

Thin section MR images of 16 ears of eight patients with definite MD were obtained. Patients were all recruited from the outpatient otoneurological department of Hospital Santa Maria (Lisbon). They were clinically evaluated by one senior (LL) and one junior (TE) otoneurologist who classified the patients with definite MD according to the clinical Barany Society criteria (8) and defined the "symptomatic" (or "index") and "asymptomatic" ("best") ears according to clinical/audiometric evaluation. In each patient, the "index ear" was considered the one with a higher pure tone average (at 500 dB, 1,000 dB, 2,000 dB, and 4,000 dB), similar to the recently published concept of the "index ear" for MD (12).

In our study, we used a volumetric T2 acquisition with 0.5 mm thickness. Two neuroradiologists, blinded to the clinical diagnosis, independently evaluated the area of the cochlear modiolus on the MR console, using multiplanar reformatting. This area was measured in the axial slice in which the cochlear modiolus was visualized at its maximum size from the thin section T2-weighted images (midmodiolar level). A region of interest was manually drawn and measured by each radiologist twice: the measured area outlined the low signal trapezoidal or triangular shape at the axis of the basal turn of the cochlea, or the middle and basal turn, excluding the thin free part of the osseous spiral lamina and interscalar septum (13, 14). The average of the two measurements was obtained for each radiologist and the final value was obtained by averaging the values obtained by each radiologist.

Additionally, the vestibular endolymphatic space was evaluated, based on MR images obtained with HYDROPS protocol 4 h after intravenous injection of a single dose of gadolinium, as previously described (15).

The area of vestibular endolymphatic space and the area of the total membranous labyrinth was manually traced by a radiologist, using multiplanar reformatting, according to the plane of the lateral semicircular canal (including the ampulla in the measurement), using volumetric acquisitions (the volumetric HYDROPS and T2, respectively). The final value was obtained as the percentage of endolymphatic area to total labyrinth area. We couldn't quantify cochlear endolymphatic space because of image quality limitations. All image evaluation procedures were performed by researchers blinded to the clinical data of the patients.

The two groups were compared using the Mann-Whitney *U* test. A *p*-value of 0.05 was considered statistically significant. Interrater reliability was also assessed using the intraclass correlation coefficient (ICC).

RESULTS

Cochlear modiolus area, PTA, and vestibular endolymphatic space were registered in **Table 1** for "index" and "best" ears. We tried to avoid the terms symptomatic and asymptomatic because some "asymptomatic" ears are not truly healthy and some show elevated PTA (higher than 25dB) (patients two, six, seven, and eight). This is explained by the tendency of bilateral affection in the disease (16, 17).

Three MD patients were male and five were female. Ages ranged from 47 to 52 in MD group (mean age of 48). Disease duration ranged from 2 to 24 years (mean duration of 7 years). All patients had spontaneous vertigo attacks lasting from 20 min to 12 h and fluctuating symptoms; number of vertigo attacks ranged from 2 to 10 episodes/year; and postural instability between

TABLE 1 | PTA, mean modiolus area, vestibular endolymphatic hydrops, and disease duration of worst and best ears of eight patients with clinical criteria of definite MD.

	Ear group	PTA (dB)	Mean modiolus area (mm^2)	Vestibular endolymphatic hydrops (%)	Disease duration (years)	Number of vertigo attacks (nr/year)	Duration of vertigo attacks	Fluctuating symptoms	Instability between attacks
Patient 1	Index	55	3.10	82	3	6	20 min–12 h	Hypoacusia Tinnitus	No
	Best	15	3.53	66					
Patient 2	Index	69	3.69	86	1	10	20 min–12 h	Hypoacusia Aural fullness Tinnitus	No
	Best	28	3.93	50					
Patient 3	Index	55	3.94	63	6	3	20 min–12 h	Hypoacusia Aural fullness Tinnitus	No
	Best	7	3.76	61					
Patient 4	Index	41	3.82	47	5	5	20 min–12 h	Tinnitus Aural fullness	Yes
	Best	13	3.76	57					
Patient 5	Index	41	3.59	21	2	3	20 min-12 h	Hypoacusia Aural fullness Tinnitus	No
	Best	13	3.46	29					
Patient 6	Index	59	3.46	70	2	2	20 min–12 h	Hypoacusia Aural fullness Tinnitus	No
	Best	53	3.34	58					
Patient 7	Index	61	3.21	50	24	5	20 min–12 h	Hypoacusia Aural fullness Tinnitus	Yes
	Best	30	3.36	35					
Patient 8	Index	39	3.03	28	13	3	20 min–12 h	Tinnitus Aural fullness	No
	Best	28	3.28	57					

attacks was described by two patients (**Table 1**). Pure tone average audiometry (PTA) ranged from 15 to 55 dB (mean PTA of 44dB).

The MMA in this MD population was 3.52 mm^2 (3.03 to 3.94 mm^2). Interrater reliability was good: ICC = 0.90, with a 95% confidence interval (0.59–0.97). We did not find differences of MMA between "index ears" (3.51 mm^2) and "best ears" groups (3.52 mm^2) (**Figure 1**), but ears with PTA higher than 25dB had smaller modiolus areas, although this is not a statistically significant finding ($p = 0.3320$).

Vestibular endolymphatic hydrops was present in 88% of patients with definite MD (7/8 patients). Vestibular endolymphatic hydrops was found in 11/16 ears (69%) according to Barath's criteria (18) (cut-off of 50%) and 13/16 ears (81%) according to Nakashima's criteria (19) (cut-off of 33%).

Mean vestibular endolymphatic space was 56% in symptomatic ears and 52% in asymptomatic ears. We got slightly smaller modiolus in "index" endolymphatic hydrops ears, although this is not a statistically significant finding (**Figure 2**).

When we analyzed PTA, modiolus area, and endolymphatic space for each individual patient, we found a consistently decreased modiolar area in the index ears in only three patients (patients one, two, and seven), but this was more evident in patients one and two, which interestingly had more extreme endolymphatic hydrops and a higher number of acute episodes and a relatively recent diagnosis of the disease (**Figures 3**, **4**, **Table 1**). Patient seven had a longer disease duration and described persistent postural instability (**Table 1**).

DISCUSSION

According to previous histological studies (11), the cochlear modiolus has a base of 4 mm and a height of 3, which gives an area of 6 mm^2 if we assume it has a triangular shape, which is not always true. Naganawa et al. first measured cochlear modiolus with MRI in 1999 in asymptomatic healthy volunteers (13); they used a 1.5 Tesla scanner, surface coils, matrix of 512, and 0.8 mm slice thickness, and their measurements showed areas ranging from 4.1 to 5.8 mm^2 in healthy subjects, which is slightly smaller than previously documented. These values are in discrepancy with those previously obtained with CT (14) but they can be explained by limitations inherent to the CT technique. With CT

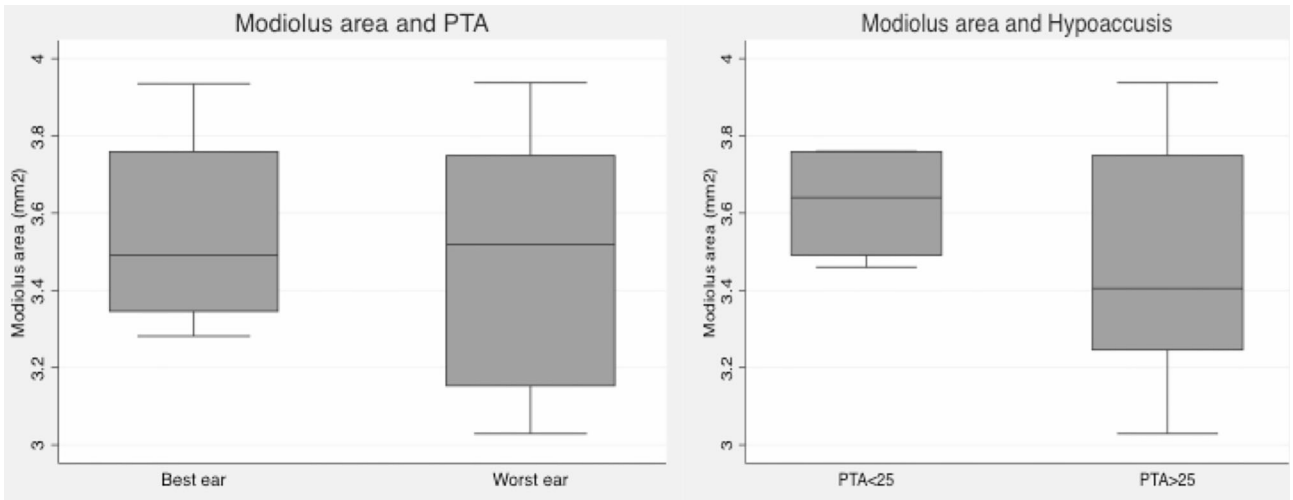

FIGURE 1 | Box plot graphics. Left: Mean modiolar area in best and index ears (based on PTA): no differences were found. Right: Mean modiolar area in ears with normal PTA (<25dB) and with hearing loss (≥25dB): ears with PTA≥25 have smaller modiolus areas, but differences were not statistically significant.

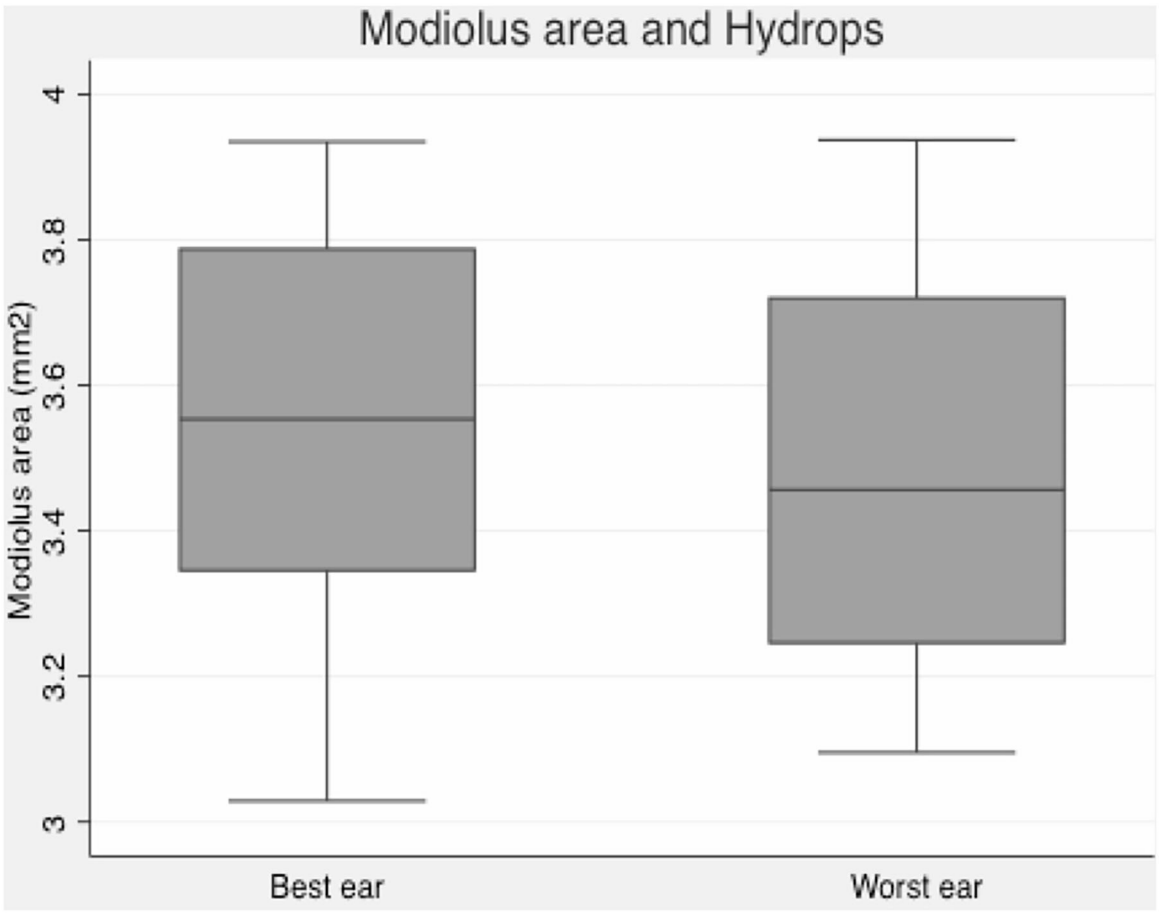

FIGURE 2 | Box plot graphic. Modiolus area and endolymphatic hydrops–slightly smaller modiolus in ears with more pronounced vestibular hydrops.

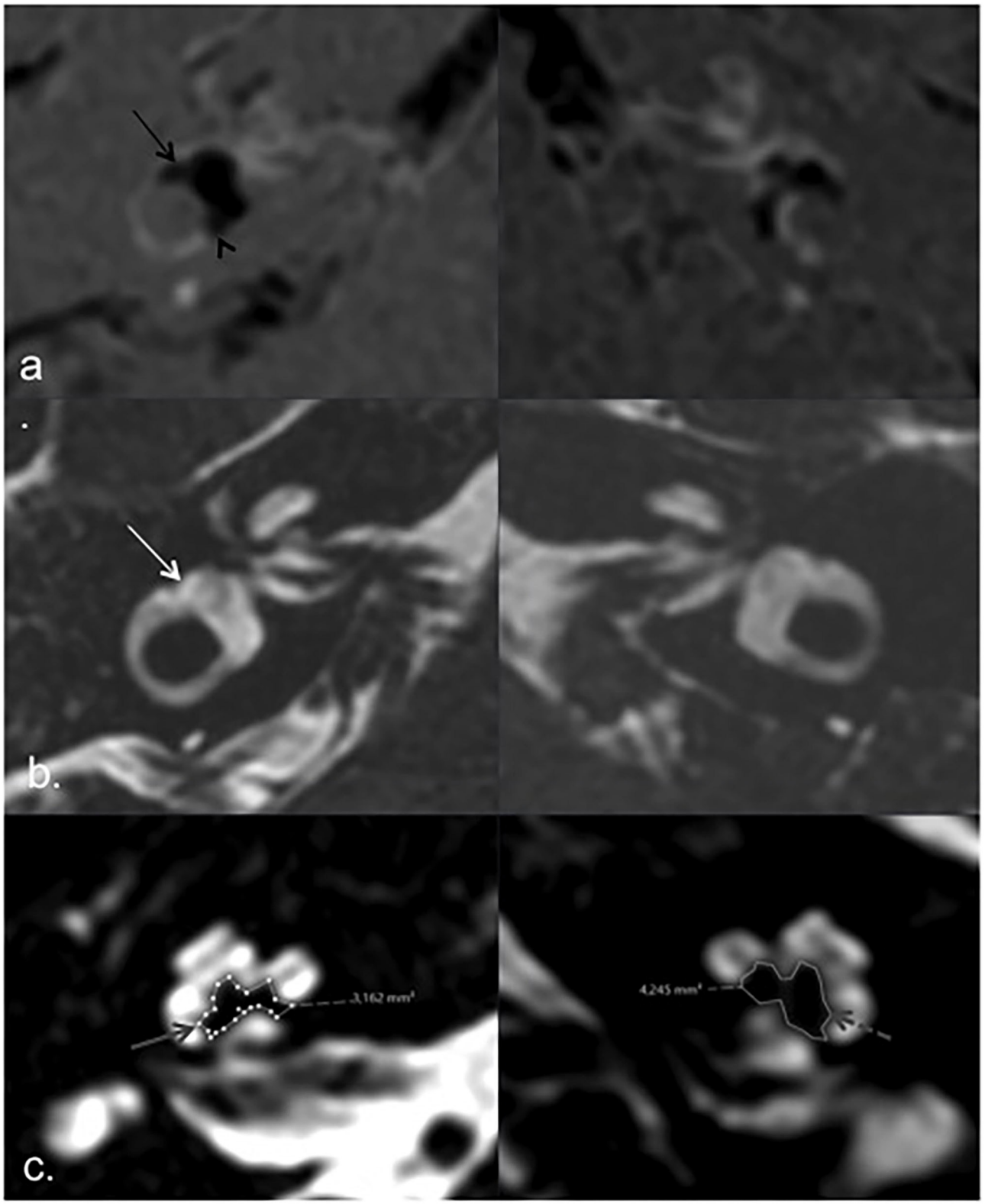

FIGURE 3 | MRI of patient 2. HYDROPS **(a)** and T2 3D TSE **(b)** axial images according to lateral semicircular canal plane, showing endolymphatic (black arrows) and total vestibular labyrinth (white arrow) respectively. Extreme right vestibular endolymphatic hydrops with herniation of endolymph into de ampullary (black arrow) and non-ampullary (black arrowhead) endings of the lateral semicircular canal in right ear (index ear). Axial T2 image according to the greater axis of cochlear modiolus **(c)**, showing marked asymmetric modiolar areas, smaller on the right side (solid gray arrow) compared to the left asymptomatic side (dashed gray arrow).

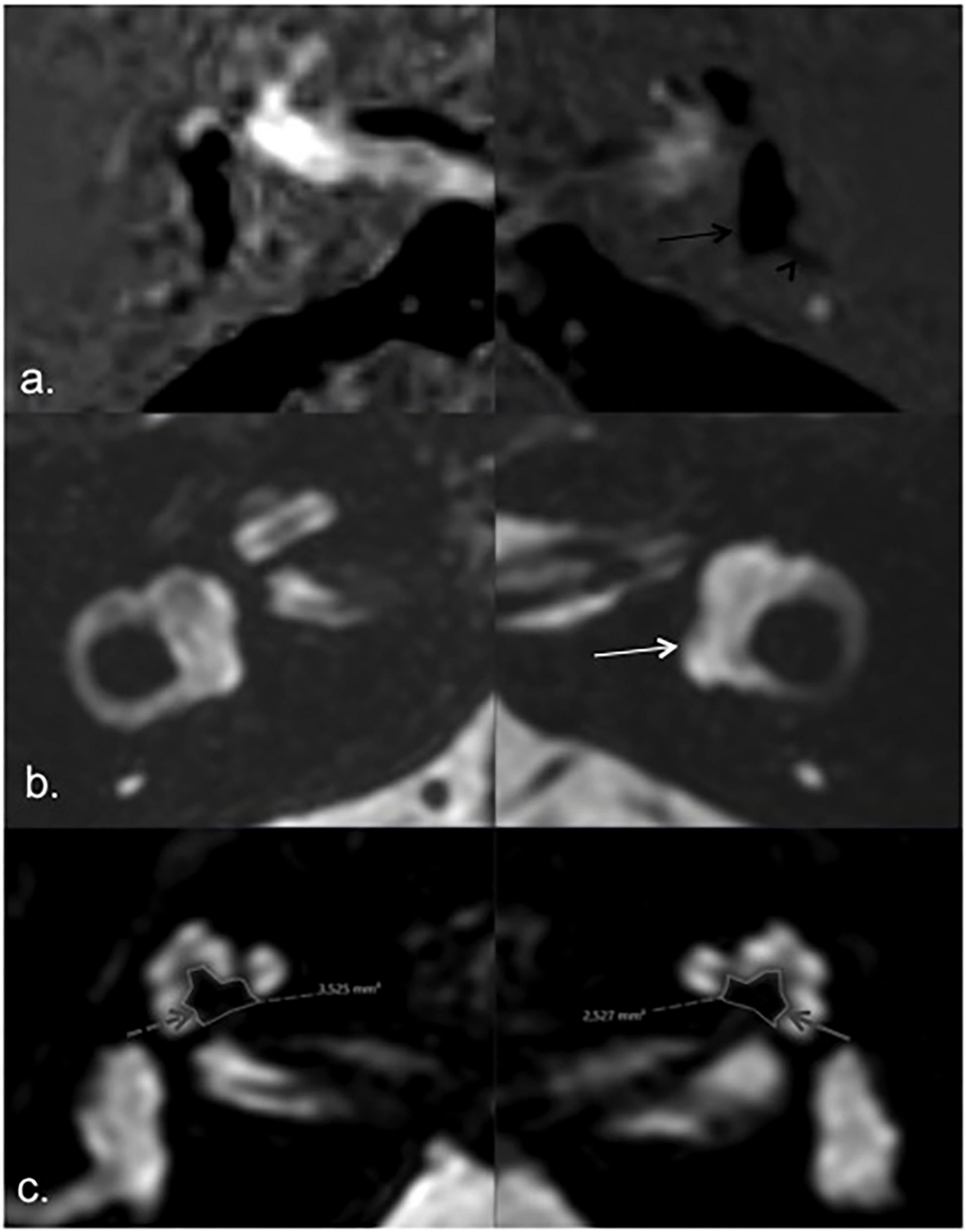

FIGURE 4 | MRI of patient 1. HYDROPS **(a)** and T2 **(b)** axial images showing endolymphatic (black arrow) and total membranous labyrinth (white arrow) respectively; bilateral vestibular endolymphatic hydrops, more pronounced on the left side (a. black arrow) with herniation of the utricle into the non-ampullary limb of the lateral semicircular canal (black arrowhead). Axial T2 image according to the greater axis of cochlear modiolus **(c)**, showing marked asymmetric modiolar areas, smaller on the left side (index ear) (solid gray arrow) compared to the left asymptomatic side (dashed gray arrow).

one can only measure the calcified portion of modiolus, which can explain lower modiolar areas in some ears.

To our knowledge, no data exist regarding cochlear modiolar size in MD, although it has been studied in patients with large endolymphatic duct and sac (13). Naganawa et al. (13) found a decrease in the size of the modiolus in 8 of 12 patients with large endolymphatic sac and duct and modiolus >4 mm^2 in 4 of 12 ears; all the 10 ears of healthy volunteers showed modiolus areas >4 mm^2. These data suggested that hearing loss in patients with large endolymphatic duct and sac might be caused by microscopic changes that are not visible on MRI and do not support the theory that hearing loss was caused by hydrostatic subarachnoid pressure into the labyrinth through a deficient modiolus.

In our study we used a 3-tesla MR scanner and a thinner slice thickness (0.5 mm) (instead of 0.8 mm used by Naganawa) in order to decrease the partial volume effect. Naganawa et al. (13), however, used surface coils, a smaller field of view, and larger matrix size. The same method of measuring the maximum cross-sectional area of the cochlear modiolus was applied (13), excluding the osseous spiral lamina and interscalar septum. Similarly, two observers manually measured the areas twice and the mean value of all measurements was used for analysis. Although there is a substantial subjectivity inherent to human judgment in defining the region of interest, especially in defining the base of the triangle on MR, our interobserver agreement was good with this method.

A volumetric measurement should be more precise, but we would need higher-quality images. As this was a retrospective study, we did not have data from a group of healthy volunteers (it would be difficult to reproduce the same conditions in the new available MR scanner). For this reason, we can only compare our MD data with healthy volunteers data from previous histological (11, 20) and MR (14) data. Our data showed mean areas of 3.52 mm^2 (3.03–3.94 mm^2), which seems to be lower than in the healthy population. However, we cannot make definite conclusions regarding this and future prospective controlled studies can confirm this finding with greater confidence: we will expect a global decrease in modiolus size in index and non-index ears in MD compared to the healthy asymptomatic control group.

In this study, we did not find significant statistical differences in MMA between "asymptomatic" and index ears in MD. Maybe this can be related to the fact that the "asymptomatic" or "best" ear is not truly healthy in some patients as we can see from the PTA records. This explains why a slight decrease in MMA is seen in ears with PTA higher than 25 dB or in ears with larger endolymphatic spaces. This aspect was more evident in two particular patients (patients one and two) even in relatively short-term disease (3 and 1 years, respectively). Our endolymphatic space areas refer to the vestibular component only because of image quality limitations in cochlear endolymphatic space.

Increased hydrostatic pressure can explain these findings, based on increased endolymph fluid and decreased microvascular supply (stria vascularis), causing bone remodeling and demineralization, respectively. This aspect has been demonstrated in previous histological studies (11, 20) and should also be corroborated in future MR investigations with a larger sample of patients with MD, or even better, with a larger sample of patients with hydropic ear disease. We think a study that aims to compare MMA between ears with and without endolymphatic hydrops (not only MD) can show significant differences, as the presumed underlying mechanism of modiolar decrease is present (bone remodeling), independently of the (subjective) clinical diagnosis. However, this might be observed mainly in more pronounced endolymphatic hydrops cases or in long-standing ones. We emphasize that the time and duration of the disease were determined based on the time of the disease from the definitive diagnosis. In both cases, the patients presented with audiovestibular symptoms 6 and 5 years before the definitive diagnosis (although the diagnosis of definite MD is relatively recent).

In fact, it seems MD is an entity whose clinical criteria have some inherent diagnostic subjectivity based on symptoms only, and MD seems to include a wide range of distinct etiologies, being difficult to unify in a single entity. Endolymphatic hydrops seems to be present in most patients with a clinical diagnosis but also in other patients with an incomplete clinical picture of MD or secondary to other etiologies (congenital, tumors, trauma, among others), which has lead to the concept of Hydropic Ear Disease, encompassing all typical and atypical variants of MD in one logical framework (21–23). For these reasons, in further studies, it should be interesting to study this particular subject of cochlear modiolus size in a population with documented hydropic ear (21–23), as suggested by our two cases of extreme hydrops and decreased modiolar size.

CONCLUSIONS

In the last years, a lot has been published regarding imaging in MD, mainly related to endolymphatic hydrops, which is the pathophysiological correlate of the disease. Endolymphatic hydrops is present in the greater majority of MD patients but can be also be found in other entities. Recently other additional imaging signs have been shown to increase the specificity of endolymphatic hydrops in MD (besides the diagnosis remains clinical only), such as the increased intensity of the perilymphatic space after gadolinium injection in the index ear (24), which represents an increase in the permeability of the hemato-perilymphatic barrier. In this study, we focused on another still unexplored finding: cochlear modiolus size and its relationship with endolymphatic hydrops.

The modiolus area is not significantly different between the index and best ears in MD, which can be explained by the tendency of bilateral affection of the disease and might reflect its systemic nature. However, the modiolus area seems to be smaller in ears with extreme endolymphatic hydrops, causing worse hearing function in patients with clinical criteria for definite MD, which can be justified by increased hydrostatic pressure resulting in bone remodeling of cochlear modiolus and cochlear nerve endings damage. MR imaging of the cochlear modiolus

deserves more investigation, however, especially in patients with endolymphatic hydrops, with or without fulfillment of traditional clinical criteria for MD (termed "hydropic disease") (21, 22). Assessment of the modiolus area may be a useful evaluation finding, easy to assess, with a high inter-observer agreement, which favors its applicability in clinical practice. Although this study has limitations inherent to its retrospective design, such as a reduced number of patients and the absence of a healthy control group, it raises new clues regarding imaging in MD/ hydropic disease that have been previously unreported. Further controlled and prospective studies, with a larger number of patients, are needed to corroborate and explore these findings.

DATA AVAILABILITY STATEMENT

The original contributions presented in the study are included in the article/supplementary material, further inquiries can be directed to the corresponding author.

ETHICS STATEMENT

The studies involving human participants were reviewed and approved by Comissão de Ética da Faculdade de Medicina da Universidade de Lisboa. The patients/participants provided their written informed consent to participate in this study.

AUTHOR CONTRIBUTIONS

RS, CG, TE, JC, and LL contributed to conception and design of the study. RS and CG evaluated the MR images. TE and LL made the clinical evaluation. RS and CG organized the database. CG performed the statistical analysis. RS wrote the first draft of the manuscript. RS, CG, and TE wrote sections of the manuscript. All authors contributed to manuscript revision, read, and approved the submitted version.

REFERENCES

1. Havia M, Kentala E, Pykko I. Prevalence of menière's disease in general population of Southern Finland. *Otolaryngol Head Neck Surg.* (2005) 133:762–8. doi: 10.1016/j.otohns.2005.06.015
2. Gurkov R, Hornibrook J. On the classification of hydropic ear disease (Meniere's disease). *HNO.* (2018) 66:455–63. doi: 10.1007/s00106-018-0488-3
3. Atkinson M. Menière's original papers reprinted with an English translation with commentaries and bibliographical sketch. *Acta Otolaryngol.* (1961) 162:1–78.
4. Hallpike CS, Cairns H. Observations on the pathology of the menière's syndrome. *Pro R Soc Med.* (1938) 31:1317–36. doi: 10.1177/003591573803101112
5. Yamakawa K. Uber die pathologische veranderung bei einem menière-kranken. *Proc 42nd Ann Meet Oto-Rhino-Laryngol Soc Japan.* (1938) 4:2310–2.
6. Frejo L, Requena T, Owawa S, Gallego-Martinez A, Martinez-Bueno M, Aran I, et al. Regulation of Fn14 receptor and NF-kB underlies inflammation in ménière's disease. *Front Immunol.* (2017) 8:1739. doi: 10.3389/fimmu.2017.01739
7. Gluth MB. On the relationship between Meniere's disease and endolymphatic hydrops. *Otol Neurotol.* (2020) 41:242–9. doi: 10.1097/MAO.0000000000002502
8. Pyykko I, Zou J, Gürkov R, Naganawa S, Nakashima T. Imaging of temporal bone. *Adv Otorhinolaryngol.* (2019) 82:12–31. doi: 10.1159/000490268
9. Lopez-Escamez JA, Carey J, Chung WH, Goebel JA, Magnussen M, Mandala M, et al. Diagnostic criteria for menière's disease. *J Vestib Res.* (2015) 25:1–7. doi: 10.3233/VES-150549
10. Schuknecht HF. Meniere'disease: a correlation of symptomatology and pathology. *Laryngoscope.* (1963) 73:651–5. doi: 10.1288/00005537-196306000-00002
11. Bruce P. Anatomy of the cochlea. In: *Surgical Anatomy of the Ear and Temporal Bone*. New York, NY: Thieme Medical Pub (1989) p. 151–60.
12. Gurkov R, Todt I, Jadeed R, Sudhoff H, Gehl HB. Laterality of audiovestibular symptoms predicts laterality of endolymphatic hydrops in hydropic ear disease (meniere). *Otol Neurotol.* (2020) 41:e1140–4. doi: 10.1097/MAO.0000000000002775
13. Naganawa S, Ito T, Iwayama T, Fukatsu H, Ishigaki T, Nakashima T, et al. MR imaging of the cochlear modiolus: area measurement in normal subjects and in patients with a large endolymphatic duct and sac. *Radiology.* (1999) 231:819–23. doi: 10.1148/radiology.213.3.r99dc05819
14. Lemmerming MM, Mancuso AA, Antonelli PJ, Kubilis PS. Normal modiolus: CT appearance in patients with large vestibular aqueduct. *Radiology.* (1997) 204:213–9. doi: 10.1148/radiology.204.1.9205250
15. Naganawa S, Yamazaki M, Kawai H, Bokura K, Sone M, Nakashima T. Visualization of endolymphatic hydrops in menière's disease with single dose intravenous gadolinium-based contrast media using heavily T2-weighted 3D FLAIR. *Magn Res Sci.* (2010) 9:237–42. doi: 10.2463/mrms.9.237
16. Stahle J, Friberg U, Svedberg A. Long-term progression of meniere's disease. *Am J Otol.* (1989) 10:170–3.
17. Pyykko I, Nakashima T, Yoshida T, Zou J, Naganawa S. Meniere's disease: a reappraisal supported by a variable latency of symptoms and the MRI visualisation of endolymphatic hydrops. *BMJ Open.* (2013) 3:e001555. doi: 10.1136/bmjopen-2012-001555
18. Barath K, Schuknecht B, Naldi AM, Schrepfer T, Bockisch CJ, Hegemann SC. Detection and grading of endolymphatic hydrops in ménière's disease using MR imaging. *AJNR Am J Neuroradiol.* (2014) 35:1387–92. doi: 10.3174/ajnr.A3856
19. Nakashima T, Naganawa S, Sugiura M, Teranishi M, Sone M, Hayashi H, et al. Visualization of endolymphatic hydrops in patients with menière's disease. *Laryngoscope.* (2007) 117:415–20. doi: 10.1097/MLG.0b013e31802c300c
20. Kariya S, Cureoglu S, Fukushima H, Nomiya S, Nomiya R, Schachem PA, et al. Vascular findings in the stria vascularis in patients with unilateral and bilateral ménière's disease: a histopathologic temporal bone study. *Otol Neurotol.* (2009) 30:1006–12. doi: 10.1097/MAO.0b013e3181b4ec89
21. Gurkov R, Pykko I, Zou J, Kentala E. What is menière's disease? A contemporary re-evaluation of endolymphatic hydrops. *J Neurol.* (2016) 263(Suppl. 1): S71–81. doi: 10.1007/s00415-015-7930-1
22. Gurkov, R. Menière and friends: imaging and classification of hydropic ear disease. *Otol Neurotol.* (2017) 38:e539–44. doi: 10.1097/MAO.0000000000001479
23. Gurkov R, Jerin C, Flatz W, Maxwell R. Clinical manifestations of hydropic ear disease (ménière's). *Eur Arch Otorhinolaryngol.* (2019) 276:27–40. doi: 10.1007/s00405-018-5157-3
24. Stekelenburg JM, Weijnen A, Pont LMH, Vijbrief OD, Bommelié CC, Koopman JP, et al. Value of endolymphatic hydrops and perilymph signal intensity in suspected menière disease. *AJNR Am J Neuroradiol.* (2020) 41:529–34. doi: 10.3174/ajnr.A6410

Conflict of Interest: The authors declare that the research was conducted in the absence of any commercial or financial relationships that could be construed as a potential conflict of interest.

frontiers in Surgery

MINI REVIEW
published: 23 August 2021
doi: 10.3389/fsurg.2021.700271

Advanced Imaging of the Vestibular Endolymphatic Space in Ménière's Disease

Diego Zanetti[1,2*†], *Giorgio Conte*[3†], *Elisa Scola*[3†], *Silvia Casale*[3†], *Giorgio Lilli*[1,2†] *and Federica Di Berardino*[1,2†]

[1] Audiology Unit, Department of Specialistic Surgical Sciences, Fondazione IRCCS Ca' Granda Ospedale Maggiore Policlinico, University of Milan, Milan, Italy, [2] Audiology Unit, Department of Clinical Sciences and Community Health, Fondazione IRCCS Ca' Granda Ospedale Maggiore Policlinico, University of Milan, Milan, Italy, [3] Neuroradiology Unit, Fondazione IRCCS Ca' Granda Ospedale Maggiore Policlinico, Milan, Italy

OPEN ACCESS

Edited by:
Robert Gürkov,
Bielefeld University, Germany

Reviewed by:
Sebastian Christoph Roesch,
Paracelsus Medical University, Austria
Hans Thomeer,
University Medical Center
Utrecht, Netherlands

***Correspondence:**
Diego Zanetti
diego.zanetti.bs@gmail.com

†ORCID:
Diego Zanetti
orcid.org/0000-0002-8116-4108
Giorgio Conte
orcid.org/0000-0002-1562-7389
Elisa Scola
orcid.org/0000-0001-9056-4122
Silvia Casale
orcid.org/0000-0002-6286-7537
Giorgio Lilli
orcid.org/0000-0002-6109-5037
Federica Di Berardino
orcid.org/0000-0001-7514-5624

Specialty section:
This article was submitted to Otorhinolaryngology-Head and Neck Surgery, a section of the journal Frontiers in Surgery

Received: 25 April 2021
Accepted: 19 July 2021
Published: 23 August 2021

Citation:
Zanetti D, Conte G, Scola E, Casale S, Lilli G and Di Berardino F (2021) Advanced Imaging of the Vestibular Endolymphatic Space in Ménière's Disease. Front. Surg. 8:700271. doi: 10.3389/fsurg.2021.700271

The diagnosis of "definite" Ménière's disease (MD) relies upon its clinical manifestations. MD has been related with Endolymphatic Hydrops (EH), an enlargement of the endolymphatic spaces (ES) (cochlear duct, posterior labyrinth, or both). Recent advances in Magnetic Resonance (MR) imaging justify its increasing role in the diagnostic workup: EH can be consistently recognized in living human subjects by means of 3-dimensional Fluid-Attenuated Inversion-Recovery sequences (3D-FLAIR) acquired 4 h post-injection of intra-venous (i.v.) Gadolinium-based contrast medium, or 24 h after an intratympanic (i.t.) injection. Different criteria to assess EH include: the comparison of the area of the vestibular ES with the whole vestibule on an axial section; the saccule-to-utricle ratio ("SURI"); and the bulging of the vestibular organs toward the inferior 1/3 of the vestibule, in contact with the stapedial platina ("VESCO"). An absolute link between MD and EH has been questioned, since not all patients with hydrops manifest MD symptoms. In this literature review, we report the technical refinements of the imaging methods proposed with either i.t. or i.v. delivery routes, and we browse the outcomes of MR imaging of the ES in both MD and non-MD patients. Finally, we summarize the following imaging findings observed by different researchers: blood-labyrinthine-barrier (BLB) breakdown, the extent and grading of EH, its correlation with clinical symptoms, otoneurological tests, and stage and progression of the disease.

Keywords: magnetic resonance imaging, hydrops, membranous labyrinth, ear, vestibule

INTRODUCTION

Ménière's disease (MD) is thought to be an unbalance of inner ear fluids, manifesting as fluctuating sensorineural hearing loss (SNHL), recurrent vertigo spells, tinnitus, and ear fullness (1). It affects between 200 and 500 persons every 100,000 inhabitants in Western countries (2). Endolymphatic Hydrops (EH), a swelling of the endolymphatic space (ES) that occupies part of the perilymphatic space (PS) constitutes the pathological landmark of the disease (3). It encompasses the cochlear duct and the saccule, sometimes extending to the semicircular canals (SCC) and utricle.

In 1995, the American Academy of Otolaryngology—Head and Neck Surgery (AAO-HNS) re-established the guidelines for the assessment of MD (4). In 2015 (5), a new consensus was reached on 2 main forms of MD "definite" and "probable" MD. Diagnosis of **definite** MD is obtained upon two or more vertigo spells limited to a period between 20 min and 12 h, associated with unilateral

low-frequencies SNHL, tinnitus and intermittent ear fullness. **Probable** MD is defined by more than 2 vertigo spells lasting between 20 min and 1 day and ipsilateral intermittent ear fullness. To evaluate the presence of EH, electrocochleography (ECochG) is able to identify, through an acoustic stimulation, the increase of the endolymphatic pressure with bulging of the Reissner's membrane in case of EH. Other electrophysiological tests, such as the vestibular evoked myogenic potentials (VEMPs) and video head impulse test (vHIT) might be useful, but their role is still controversial.

Recent reports confirm that the otoneurological responses correlate well with the magnetic resonance imaging (MRI) showing that the EH starts from the saccule and then progresses to the SCC (6).

In the past, imaging studies were still obtained to exclude retrocochlear disorders, such as vestibular nerve schwannomas. New developments of MRI techniques (7) have enabled visualization of EH in humans by means of 3 Tesla (3T) scanners and Gadolinium (Gd) administered either intravenously (i.v.) (8) or intratympanically (i.t.) (9, 10). However, the diagnostic accuracy of EH by MRI is disputed, mainly owing to the disparities in the inclusion and diagnostic criteria.

The clinical consequences of a correct assessment of EH would represent a significant leap forward, by providing a more reliable tool to differentiate between MD and non-MD diseases of the inner ear (11, 12) to follow-up the untreated clinical evolution of the disease (13) or to test different pharmacological or surgical protocols (14, 15). The purpose of this review of the literature is to understand the reliability of MRI in detecting EH in the population of suspected MD patients with insights of the contemporary technological advances and to compare the imaging findings with the natural history of the disease and the outcome of treatments. Furthermore, we discuss the newest MR protocols to assess EH and the commonest MRI findings in different vestibular disorders.

Literature Search Strategy

According to the PRISMA guidelines (16), the scientific literature of the last decade was browsed with the aim of identifying studies describing the MR findings in "definite" MD patients (see the PRISMA flowchart in the additional digital content).

The following search queries were used in Medline, Cochrane database, Scopus and EMBASE (from 2010 to Present): "*Ménière*" *OR* "*endolymphatic hydrops*" AND "*magnetic resonance*" OR "*MR*." The search was restricted to articles that provided at least an abstract in English. References of the selected publications were also examined to extract any further relevant article. The retrieved articles were considered eligible if they provided results of MR in patients with "definite" MD (4) or to the 2015 Consensus Statement (5). Two of the co-Authors (FDB and GL) separately reviewed all articles and excluded those with unclear clinical diagnostic criteria. Other exclusion criteria were studies on animals, case reports, personal (expert) opinions, metanalysis, different diagnostic criteria, studies where diagnosis of "definite" MD was lacking; studies not assessing hydrops by accepted MRI techniques; and studies not reporting the status of the contralateral (unaffected) ear.

The following information were outsourced from the selected studies: first author, year of publication, total number of subjects enrolled, MRI techniques and peculiar MRI findings related with the presence of hydrops in the affected vs. unaffected ears.

Literature Search Results

The initial search yielded a total of 219 articles: 97 articles in PubMed, 91 in EMBASE, 27 in Scopus and none in the Cochrane Library. After excluding duplicates and those not respecting the inclusion criteria, 77 articles were left; among these, 47 were included by relevance. These 47 papers were carefully analyzed for the purposes of this study. Six of them were review studies and were only considered for the general overview of the topic.

The main features of each of the 41 remaining articles are reported in **Table 1**: 8 out of 41 studies performed an i.t. administration of Gd, 27 only an i.v. delivery and 3 studies performed both simultaneously; 3 studies dealt with post-acquisition processing of images.

The MR images were acquired 4 h after the i.v administration in 26 out of 27 studies, and 24 h after the i.t. injection in 8 out of 11 trials (8 i.t. only and 3 i.t. + i.v).

A 3T machine was used in 40 out of 41 studies. The most common MRI technique to identify EH was the 3D FLAIR ($n =$ 38/41 original studies).

The selected method to assess the degree of EH was the VES/vestibule ratio $> 30\%$ in 28 studies, $> 50\%$ in 3 studies, the SURI in 4 studies, the VESCO only in 1 study.

The sensitivity, specificity, PPV and NPV of the techniques in correctly identifying EH were reported in 37 out of 41 studies.

Side effects of Gd administration were reported in 3 of 1,578 patients (sum of all articles), all of them with the i.t. routes.

DISCUSSION

The published papers on MRI of the inner ear have almost doubled during the last 10 years, confirming the interest in the subject and the potentiality of the innovative methods. However, the role of MRI in differentiating between different inner ear diseases remains to be established. Based on general opinion in the field, we considered reasonable to report on the volumetric detection of EH rather than generic imaging of MD.

The MRI identification of the fluid compartments of the inner ear can be achieved by either intratympanic or intravenous administration of Gd (8).

The Intra-Tympanic Gadolinium Injection

It has been the first method proposed in the literature to study the inner ear spaces (9, 54). The i.t.-Gd delivery method utilizes an i.t. injection of 0.4–0.7 ml of an 8-fold dilution of the Gd solution into the tympanic cavity. The contrast medium diffuses into the perilymph through the round window membrane (RWM), but not in the endolymph, producing the so-called perilymph positive image (PPI). Considering the diffusion dynamics, the MRI scans are obtained 1 day after the i.t. injection. The method of choice is based on T2-weighted scans with the 3D Fluid-Attenuated-Inversion-Recovery (3D-FLAIR)

TABLE 1 | Summary of literature review (last decade) on MRI in Meniere's disease (MD).

References	year	# of pts	MRI method	MR findings	Notes
Fiorino et al. (10)	2011	32	3T 3D-FLAIR after i.t. Gd	Degree of EH in cochlea and the semicircular canals directly proportional to MD duration	
Gürkov et al. (17)	2012	41	3D IR-TSE	Correlation of EH (Likert scale) with duration of MD, degree of SNHL, saccular dysfunction	ECochG, VEMPs, VNG
Claes et al. (14)	2012	12	3T 3D-FLAIR after i.t. Gd	Correlation between TT-ECoG and EH grading on MRI	
Naganawa et al. (18)	2012	24	3T 3D-FLAIR after i.v.Gd → HYDROPS2	Subtraction of MR cisternography from PPI facilitated recognition of the ES	Scan time 40% < than HYDROPS
Sano et al. (19)	2012	10	3T 3D-FLAIR after i.v.Gd 4 h delayed acquisition	Increased Gd enhancement in symptomatic ears.	Better resolution after 4 h
Naganawa et al. (20)	2013	10	HYDROPS-Mi2 after i.v. Gd	Multiplied MRC onto HYDROPS → better visualization of ES and PS on a single volumetric image in EH+ pts	CNR ratio increase 200 fold
Seo et al. (21)	2013	26	3T 3D-FLAIR 24 h after IT.Gd	EH in the cochlea (81%) and saccule (69%). Correlation with auditory and vestibular testing	Audiometry, VEMPs, ECochG
Naganawa et al. (22)	2014	10	i.t. Gd Real-IR + i.v. 3D FLAIR	Superiority of combined administration vs. i.v. Gd alone	
Barath et al. (23)	2014	53	i.v. Gd 3T 4 h 3D-real IR	EH in 90% on the clinically affected and in 22% on the clinically silent side	
Liu et al. (24)	2015	30	3T 3D-FLAIR after IT Gd	EH also in 23.3% of asymptomatic ears	
Sepahdari et al. (25)	2015	41	i.v. Gd 3D-FLAIR + MIP	MIP superior to 2D images for EH assessment	
Suga et al. (13)	2015	12	3T 3d-FLAIR 24 h after i.t. Gd + 4 h after i.v. Gd	EH reduction at 1 yr correlates with symptoms recovery	
Hornibrook et al. (26)	2015	57	3T 3d-real IR 24 h after i.t. Gd	High correlation between ECochG (tone bursts) and EH at MRI	vs. 45 other pathologies
Bykowski et al. (27)	2015	6	3T 2d-FIESTA + T1SE 24 h after i.t. Gd	Using a 3-inch surface coil preserves high resolution within a clinically acceptable acquisition time	
Attyé et al. (28)	2015	132	3T 3d-FLAIR 4 h after i.v. Gd	Similar pathophysiological mechanism in RPV and MD	EH in RPV/MD
Wu et al. (29)	2016	54	3T 3D-FLAIR vs. 3D-real IR after i.t. Gd	Low-tone hearing thresholds correlates with severity of EH in the cochlea.	EH progressed over time.
Pakdaman et al. (30)	2016	32	3T 3d-FLAIR 4 h after i.v. Gd + T2 SPACE	Increased BLB permeability in MD	vs. 11 pts with sudden SNHL
Keller et al. (31)	2017	85	3D FIESTA + 2D SPACE	Conventional MRI without Gd allows detection of EH	
Choi et al. (32)	2017	46	3T 3D-FLAIR MRC after i.v.Gd and HYDROPS-Mi2	Degree of EH in MD vs. VN patients	Correlation with caloric tests
Attyé et al. (11)	2017	30	3T 3d-FLAIR 4 h after i.v. Gd	SURI: most specific criterion for imaging of EH	vs. 30 healthy ear
Okumura et al. (33)	2017	21	3T CISS + 2d-FLAIR 4 h after i.v. Gd	70% EH + low correlation with VEMPS and VNG	
Yoshida et al. (34)	2017	42	3T 3d-FLAIR 4 h after i.v. Gd	Prevalence of vestibular EH significantly higher in MD	vs. healthy ears
Conte et al. (12)	2018	22	3T 3D-FLAIR 4 h after i.v. Gd	New criterion of EH assessment: VESCO	vs. normal ears.
Wesseler et al. (35)	2018	31	3T 3D-FLAIR-SPAIR 24 h after i.t. Gd	MRI more accurate than caloric test, vHIT, and cVEMP.	MR scan for hydrops after 24 h
Bier et al. (36)	2018	10	MRC+VISTA-IR+ HYDROPS 4 h after i.v. Gd	EH gradient along the cochlea	
Quatre et al. (37)	2019	41	3T 3D-FLAIR 4 h after i.v. Gd	Comparison with audio-vestibular tests: ECochG and DPOAEs correlated with EH	ECochG, shift-DPOAE, cVEMPs

(Continued)

TABLE 1 | Continued

References	year	# of pts	MRI method	MR findings	Notes
Pérez-Fernández et al. (38)	2019	22	3T 3D-FLAIR 4 h after i.v. Gd	Degree of vEH correlates with vestibular deficit	vHIT, VEMPs, audiometry
Bernaerts et al. (39)	2019	148	3T 3D-FLAIR 4 h after i.v. Gd	4 degrees of EH. Combined with perilymphatic enhancement: Sensitivity 79.5% Specificity 93.6%	
Ito et al. (15)	2019	20	3T 3D-FLAIR + MRC 4 h after i.v. Gd	Reduction of EH 2 ys after endolymphatic sac drainage and local steroids	pre- and post-surgery MR
Eliezer et al. (40)	2019	30	3T 3D-FLAIR + SSFP 4 h after i.v. Gd	In acute vestibular deficits	vs. healthy ears
Guo et al. (41)	2019	56	3T T2-SPACE and Real-IR 4 h after i.v. Gd	Degree of EH correlates with audiometry and VEMPs	oVEMP and PTA correlates with cochlear EH
Ohashi et al. (42)	2020	15	HYDROPS-Mi2 + 3D-real IR images	Measurement of endolymphatic volume	Comparison of 2 techniques
Gerb et al. (43)	2020	105	3T 3D-FLAIR + CISS 4 h after i.t. Gd	VOLT: new algorithm for automatic segmentation of MR images	All pts with acute vertigo (incl. MD)
Nahmani et al. (44)	2020	16	3T 3D-FLAIR 4 h after i.v. Gd Variable Flip Angle-	Reliable in evaluating BLB breakdown and ES	
Cho et al. (45)	2020	226	INHEARIT on archived datasets	Feasibility of automated EH ratio measurements	Automatic segmentation + calculation of EH
van Steekelenburg (46)	2020	220	3T 3D-FLAIR + SPACE 4 h after i.v. Gd	EH in 91.9% of MD vs. 7% in other vertigo.	Combination of PPI and EH in MD
Pai et al. (47)	2020	31	3T 3D-FLAIR 4 h after i.v. Gd	Correlation of EH finding at MR with diseased ear	
Fukushima et al. (48)	2020	55	3T 3D-FLAIR and HYDROPS-Mi2 4 h after i.v. Gd	Progression of vestibular EH over 2–3 years	MR repeated annually
Kahn et al. (49)	2020	31	3T 3D-FLAIR 4 h after i.v. Gd	EH: Cochlear 88%, saccular 91%, utricular 50%, ampullar 8.5%. No correlation with VEMPs/vHIT. Severity of EH correlated with SNHL	vs. 26 healthy ears
Gürkov et al. (50)	2021	30	1.5T 3D-FLAIR Hydrops 24 h after i.t. Gd	Reliability of 1.5T fast identification and grading of EH	
He et al. (51)	2021	50	3T 3D-FLAIR 4 h after i.v. Gd	3D-FLAIR MRI + PT- ECochG more sensitive than ECochG alone for EH	PT- ECochG
Zhang et al. (52)	2021	24	3T 3D-FLAIR 4 h after i.v. Gd	Degree of EH correlates with hearing threshold	Extratympanic
Sluydts et al. (53)	2021	78	3T 3D-FLAIR 4 h after i.v. Gd	Only severe cochlear and vestibular EH are associated with cochleovestibular dysfunction	Audiometry, caloric tests, VEMPs, vHIT

BLB, blood-labyrinth barrier; CISS, continuous Interference Steady-State; CNR, contrast-to-noise ratio; ECochG or TT-ECochG, trans-tympanic electro-cocleography; EH, endolymphatic hydrops; ES, endolymphatic space; FLAIR, Fluid Attenuated Inversion Recovery; hT2w-VISTA-IR, heavily T2-weighted volume isotropic turbo spin echo acquisition inversion recovery; HYDROPS, Hybrid of the reversed image of the positive endolymph signal and native image of positive perilymph signal; HYDROPS-Mi2, multiplication of HYDROPS with MRC; INEARHIT, Inner Ear Hydrops Estimation via Artificial Intelligence; MIIRMR, medium inversion time inversion recovery imaging with magnitude reconstruction; MIP, maximum intensity projections; IR-TSE, Inversion Recovery Turbo Spin-Echo; MRC, magnetic resonance cisternography; PEI, positive endolymph image; PPI, positive perilymph image; PS, perilympahtic space; PT- ECochG, peri-tympanic electro-cocleography; RPV, Recurrent peripheral vestibulopathy; SNHL, sensorineural hearing loss; SPACE, sampling perfection with application-optimized contrasts by using different flip angle evolutions; SPAIR, Spectral Attenuated Inversion Recovery; SSFP, steady-state free precession sequences; SURI, Inversion of the saccule to utricle area ratio; 3D-REAL-IR, 3D-inversion-recovery turbo spin-echo with real reconstruction; VEMPs, vestibular-evoked myogenic potentials (oVEMPs: ocular, cVEMPS: cervical); VESCO, vestibular endolymphatic space contacting the oval window; VHIT, video Head Impulse Test; VNG, video-nystagmography; VN, vestibular neuritis.

algorithm, which lowers the endolymph signal in respect to the adjacent perilymph. Variations to the flip angle can be applied. If the inversion time of the 3D-FLAIR is shortened, the perilymph signal is suppressed and that of the endolymph is enhanced, obtaining a positive endolymphatic image (PEI). Another technique, namely 3D-inversion-recovery turbo spin-echo (TSE) with real reconstruction (3D-real IR) (55) creates a sharp contrast between the inner ear fluids (the positive perilymph vs. the negative endolymph) and the neighboring bone that results as null.

Given the known entry routes and kinetics of drugs from the middle to the inner ear, the most suitable and reliable method to investigate the vestibular EH (vEH) and the cochlear EH (cEH) is that described by Nakashima et al. (9). In contrast, Carfrae et al. (54) and Shi et al. (55) denied an additional value of Gd delivered directly to the middle ear during surgery: vEH and cEH were detected only in 25 and 16% of patients, respectively, possibly owing to the dilution of the contrast medium. In many countries, the i.t. delivery of Gd is still off-label; moreover, some patients are reluctant to undergo bilateral injections of their tympanic membranes. Thus, the puncture is limited to the affected ear, leaving the contralateral uninvestigated.

Wu et al. (29) administered a bilateral i.t. injection of Gd: the presence of vEH was detected in two thirds of the ears with clinical symptoms of MD, while cEH in 8%. A few studies tested the simultaneous delivery of Gd through the i.t. and the i.v. routes: Iida et al. (56) demonstrated the presence of both vEH and cEH in 67% of the contralateral asymptomatic ears. Naganawa et al. (22) used 3D-real IR images for the i.t.-Gd side and the so-called HYDROPS sequences ("*Hybrid of the reversed image of the positive endolymph signal and native image of positive perilymph signal*") for i.v perfusion. Only HYDROPS images were able to demonstrate vEH in 89% and cEH in 67% of all symptomatic ears, respectively. The i.t. administration is able to show the presence of EH in other audiological disorders (26, 57), even if at a very low rate.

To improve the acquisition and analysis of the images, Bykowski et al. (27) applied 8-channel surface coils to acquire 3D-FLAIR images after an i.t. injections in six patients with definite MD. By varying the inversion times, they were able to judge the fluid-suppression ability of each sequence, in all the six patients tested.

The Intra-Venous Gadolinium Perfusion

Although the i.t.- Gd technique has the great benefit of enhancing the visualization of the perilymph (35), the i.v.-Gd delivery route has several advantages: lesser invasiveness (although major complications can still occur); reduced operating times (4 h for a comprehensive MRI study); bilateral examination in a single test session. It consists in the intravenous perfusion of a fixed (per weight) dose of Gd (between 0.1 and 0.2 ml/Kg) that rather quickly diffuses in the perilymph without spreading to the endolymph, depending on the permeability of the blood-labyrinth barrier (BLB) (58), thus creating a PPI. The 2 most popular scanning sequences, 3D-real IR and 3D-FLAIR are substantially equivalent, although the latter is more sensitive to less concentrated dilutions of Gd (12).

Noteworthy, a correct visualization of the inner ear compartments relies upon the inversion time. After the normal MR standards are established in healthy controls, MR images can be immediately analyzed after acquisition or they can be scrutinized after processing. Post-processing includes subtraction of the PEI (a 3D FLAIR sequence) from the PPI. HYDROPS and HYDROPS2 (22) are then reconstructed and can be juxtaposed to the corresponding MR cisternography images to obtain the HYDROPS-Mi2 and HYDROPS2-Mi2 images, respectively, which show increased contrast compared to background noise (42). The combination of "*maximum intensity projection*" (MIP) and 3D-FLAIR further adds robustness to the assessment of EH.

The main concern about either technique of MRI of EH is the correct identification of the vestibular organs, which requires a thorough knowledge of the radiological anatomy. During the last decade, a number of different methods to detect hydrops have been proposed, raising also a vivid debate among research groups.

Nakashima et al. (59) initially described the vestibular endolymphatic space (VES) by calculating the ratio between the endolymphatic organs and the whole vestibule in an axial projection. They defined the vEH as "*absent*" when the ratio was <33%, "*mild*" when 34-50% and "*significant*" if >50%. In addition, they evaluated the cochlear ES (cES) by measuring the displacement of the Reissner's membrane. They defined the cEH as "*mild*" if the displacement did not exceed the scala vestibuli (SV), or "*significant*" when the cES exceeded the SV.

In clinical studies, the first problem encountered with the VES/vestibule ratio was that mild vEH was not only reported in the greatest majority of symptomatic ears of MD patients, but also in more than half of the asymptomatic contralateral ears (19, 34, 58, 60). Moreover, EH has been detected also in healthy individuals (11, 61, 62), and this challenges its correlation with MD (63).

A few studies also raise the issue of specificity: mild vEH was identified even in symptomatic ears of patients with otological diseases other than MD (19), such as recurrent peripheral vestibulopathy and unilateral labyrinthine deficit (28, 40).

Nevertheless, the sensitivity of i.v. Gd-enhanced MR with 4 h delayed acquisitions is very high (>95%); thus, a significant VES/vestibule ratio might represent a potential indicator of MD even before a clear clinical diagnosis has been established. In fact, severe vEH was always excluded the ears of clinically silent MD patients (30) and mild vEH was in the very low range (below 20%) in healthy volunteers. Considering a VES/vestibule ratio > 50% (instead of 30%) may reduce its sensitivity but can represent a more reliable rule-in criteria for MD, allowing to differentiate MD from unaffected ears and from other auricular diseases.

Although Nakashima's criteria are universally accepted, other cut-off values for vEH have been suggested: Sepahdari et al. (25) used a VES/vestibule ratio of 45% (2 SD above the mean) in a group of patients with sudden SNHL and found vEH in 6/12 (50%), concluding that it was inconsistent for the assessment of MD in sudden SNHL. Another study (34) claimed that even a lower ratio of 41.9% yielded an absolute specificity of 100% in differentiating hydropic from normal ears, still retaining a high sensitivity (88.5%). They also studied the asymptomatic ears and

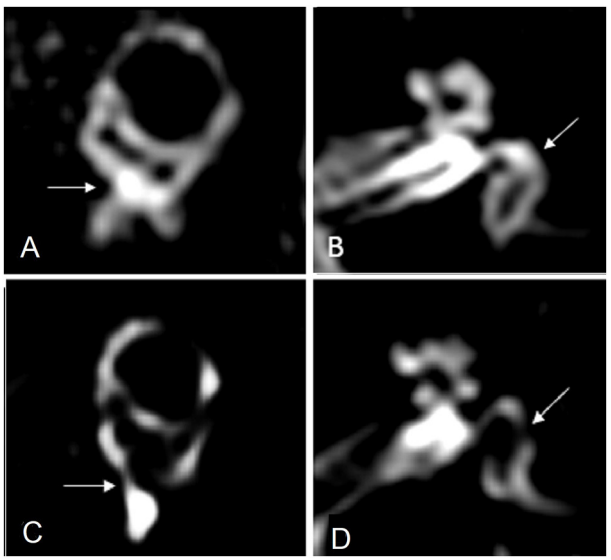

FIGURE 1 | (A) MR imaging oblique sagittal reconstruction parallel to the superior semicircular canal of a healthy ear shows superiorly the vestibular endolymphatic space and inferiorly the perilymph filling the inferior third of the vestibule with preservation of the perilymph signal medial to the oval window (arrow). **(B)** MR imaging axial reconstruction parallel to the lateral semicircular canal at the inferior third of the vestibule in a healthy subject, showing the vestibule filled by the perilymph (arrow). **(C)** MR imaging oblique sagittal reconstruction parallel to the superior semicircular canal in a patient with Menière disease shows enlargement of the vestibular endolymphatic space bulging into the inferior third of the vestibule and contacting the oval window (arrow), with the consequent absence of the normal perilymph signal. **(D)** MR imaging axial reconstruction parallel to the lateral semicircular canal at the inferior third of the vestibule shows the vestibular endolymphatic space contacting the oval window, "VESCO" (arrow).

ascertained cEH in 46% of MD patients and 33% of healthy subjects.

Other research groups graded the EH with a criterium based on the morphology of the saccule (11, 28, 40). Using a ratio between the area of the saccule and that of the utricle (SURI) >50%, they were able to differentiate the ears of 30 patients with MD from normal controls, with a sensitivity of 50% and specificity of 100. The reliability of post-contrast imaging in detecting EH was very high in Eliezer et al. study (64) by means of 3D-FLAIR and 4 h delayed acquisition, with much greater efficiency than the 3D FIESTA sequences.

Conte et al. (12) compared the imaging outcomes in 49 subjects, half of which had suffered a sudden SNHL, and the remaining were afflicted by definite MD. Using the 4-h delayed 3D-FLAIR protocol, 2 independent examiners observed that in MD patients the saccule was swollen and protruded in the lower part of the vestibule, arriving in contact with the footplate of the stapes. They named this finding "VESCO" an acronym of "*vestibular endolymphatic space contacting the oval window*." The VESCO showed an optimal specificity but a low sensitivity (81%) in differentiating MD ears from other inner ear diseases. **Figure 1** details the regular membranous labyrinth anatomy in a 3T Gd-FLAIR axial scan in one of our healthy adult volunteers and depicts the VESCO in one of our symptomatic MD patients.

Recent Advances

A number of technical innovations have been recently added to the MR armamentarium to improve the identification of EH, such as the Variable and Constant Flip Angle-Delayed 3D-FLAIR Sequences (44) or the i.t.-Gd "*medium inversion time inversion recovery imaging with magnitude reconstruction*" (MIIRMR) (65).

In order to eliminate the subjective (examiner's) bias, new automated images segmentation processing algorithms have been introduced (43, 66), also associated with deep-learning models based on Artificial Intelligence (45). By adding the quantification of perilymphatic enhancement to the grading of EH, van Steekelenburg et al. (46) recently reported to improve the positive predictive value of Gd-enhanced MRI from 0.92 to 0.97 in the confirmation of definite MD.

The majority of ongoing studies is currently aimed at targeting the correlation between the morphologic findings and the symptomatology ("the whole symptoms triad") and, especially, with the results of the functional audio-vestibular testing and with the outcomes of treatment (37, 41, 48, 51, 52, 62, 63, 67). In general, the literature agrees that the presence of EH at MRI, independently from the cut-off values for definition of vEH, strongly correlates with the side of the disease in MD patients (47, 50), but it lacks specificity in differentiating MD from other inner ear disturbances, in the absence of clinical/instrumental confirmation (64). It seems that the MRI demonstration of EH is a necessary but not sufficient condition to assess a diagnosis of MD. Nevertheless, it is highly improbable that EH is only casually associated with MD, because the causative relationship is too stringent (2).

The present review has some limitations: the reported populations are rather heterogenous in diagnostic criteria and definition of MD; some studies include very small patients' samples, thus a metanalysis was not feasible. In contrast, the review offers an insight of the latest technological developments.

In conclusion, current MR imaging methods allow to clearly depict the ES vs. the PS, in both the cochlear and vestibular compartments with multiple dedicated protocols. MRI of the ES can be comfortably obtained by means of i.v. administration of Gd and late (4 h) acquisitions. Thus, the more invasive and off-label i.t. injection of Gd, is considered by most Authors a 2nd-line investigative tool.

Although the role of EH in MD has been questioned by recent research, and its presence may not always be considered pathological, current MR imaging yields a very high sensitivity in detecting it. As quantitative indexes alone are probably insufficient to establish an MRI diagnosis of MD, more accurate criteria based on the morphology of the endolymphatic organs are required. A 3 Tesla MR scanner is essential for the purpose of identifying the subtle morphological variations of the ES in MD and to correlate the findings with the clinical history and audio-vestibular testing. The newest techniques proposed in the last years appear to be promising tools and deserve to be further investigated, especially focusing on the features, prevalence and role of EH in different inner ear disorders and on the relevance of other findings (BLB breakdown, methemoglobin, and inflammatory deposits) in the ES.

AUTHOR CONTRIBUTIONS

GC defined the literature search strategy, evaluated the articles relevance, and revised the manuscript. ES scrutinized the retrieved articles for inclusion/exclusion in the systematic review. SC scrutinized the retrieved articles for inclusion/exclusion in the systematic review and provided the MR images with captions. GL prepared the draft of the manuscript. FDB revised the manuscript and checked references and table. DZ designed the study, revised, and edited the final version of the manuscript. All authors contributed to the article and approved the submitted version.

FUNDING

The costs of publication will be covered by Associazione Progetto Udire OdV, a charity supporting the research on deafness and vestibular disorders, listed in the Lombardy Region registry of non-profit organizations.

SUPPLEMENTARY MATERIAL

The Supplementary Material for this article can be found online at: https://www.frontiersin.org/articles/10.3389/fsurg.2021.700271/full#supplementary-material

REFERENCES

1. Basura GJ, Adams ME, Monfared A, Schwartz SR, Antonelli PJ, Burkard R, et al. Clinical practice guideline: Ménière's disease. *Otolaryngol Head Neck Surg.* (2020) 162:S1–55. doi: 10.1177/0194599820909438
2. Gürkov R, Pyykö I, Zou J, Kentala E. What is Menière's disease? A contemporary re-evaluation of endolymphatic hydrops. *J Neurol.* (2016) 263(Suppl. 1):S71–81. doi: 10.1007/s00415-015-7930-1
3. Merchant SN, Adams JC, Nadol JB Jr. Pathophysiology of Meniere's syndrome: are symptoms caused by endolymphatic hydrops? *Otol Neurotol.* (2005) 26:74–81. doi: 10.1097/00129492-200501000-00013
4. Committee on Hearing and Equilibrium guidelines for the diagnosis and evaluation of therapy in Menière's disease. American Academy of Otolaryngology-Head and Neck Foundation, Inc. *Otolaryngol Head Neck Surg.* (1995) 113:181–5. doi: 10.1016/S0194-5998(95)70102-8
5. Lopez-Escamez JA, Carey J, Chung WH, Goebel JA, Magnusson M, Mandala M, et al. Diagnostic criteria for Meniere's disease. *J Vestib Res.* (2015) 25:1–7. doi: 10.3233/VES-150549
6. Sobhy OA, Elmoazen DM, Abd-Elbaky FA. Towards a new staging of Ménière's disease: a vestibular approach. *Acta Otorhinolaryngol Ital.* (2019) 39:419–28. doi: 10.14639/0392-100X-2461
7. Reinshagen KL, Curtin HD. Radiological assessment of the vestibular system. *Oper Tech Otolaryngol.* (2019) 30:171–9. doi: 10.1016/j.otot.2019.07.011
8. Naganawa S, Nakashima T. Visualization of endolymphatic hydrops with MR imaging in patients with Ménière's disease and related pathologies: current status of its methods and clinical significance. *Jpn J Radiol.* (2014) 32:191–204. doi: 10.1007/s11604-014-0290-4
9. Naganawa S, Sugiura M, Kawamura M, Fukatsu H, Sone M, Nakashima T. Imaging of endolymphatic and perilymphatic fluid at 3T after intratympanic administration of gadolinium-diethylene-triamine pentaacetic acid. *AJNR Am J Neuroradiol.* (2008) 29:724–6. doi: 10.3174/ajnr.A0894
10. Fiorino F, Pizzini FB, Beltramello A, Mattellini B, Barbieri F. Reliability of magnetic resonance imaging performed after intratympanic administration of gadolinium in the identification of endolymphatic hydrops in patients with Ménière's disease. *Otol Neurotol.* (2011) 32:472–7. doi: 10.1097/MAO.0b013e31820e7614
11. Attyé A, Eliezer M, Boudiaf N, Tropres I, Chechin D, Schmerber S, et al. MRI of endolymphatic hydrops in patients with Meniere's disease: a case-controlled study with a simplified classification based on saccular morphology. *Eur Radiol.* (2017) 27:3138–46. doi: 10.1007/s00330-016-4701-z
12. Conte G, Caschera L, Calloni S, Barozzi S, Di Berardino F, Zanetti D, et al. MR imaging in Menière disease: is the contact between the vestibular endolymphatic space and the oval window a reliable biomarker? *AJNR Am J Neuroradiol.* (2018) 39:2114–9. doi: 10.3174/ajnr.A5841
13. Suga K, Kato M, Yoshida T, Nishio N, Nakada T, Sugiura S, et al. Changes in endolymphatic hydrops in patients with Ménière's disease treated conservatively for more than 1 year. *Acta Otolaryngol.* (2015) 135:866–70. doi: 10.3109/00016489.2015.1015607
14. Claes G, Van den Hauwe L, Wuyts F, Van de Heyning P. Does intratympanic gadolinium injection predict efficacy of gentamicin partial chemolabyrinthectomy in Menière's disease patients? *Eur Arch Otorhinolaryngol.* (2012) 269:413–8. doi: 10.1007/s00405-011-1644-5
15. Ito T, Inui H, Miyasaka T, Shiozaki T, Matsuyama S, Yamanaka T, et al. Three-dimensional magnetic resonance imaging reveals the relationship between the control of vertigo and decreases in endolymphatic hydrops after endolymphatic sac drainage with steroids for Meniere's disease. *Front Neurol.* (2019) 10:46. doi: 10.3389/fneur.2019.00046
16. Moher D, Liberati A, Tetzlaff J, Altman DG, The PRISMA Group. Preferred reporting items for systematic reviews and meta-analyses: the PRISMA statement. *PLoS Med.* (2009) 6:e1000097. doi: 10.1371/journal.pmed.1000097
17. Gürkov R, Flatz W, Louza J, Strupp M, Ertl-Wagner B, Krause E. *In vivo* visualized endolymphatic hydrops and inner ear functions in patients with electrocochleographically confirmed Ménière's disease. *Otol Neurotol.* (2012) 33:1040–5. doi: 10.1097/MAO.0b013e31825d9a95
18. Naganawa S, Yamazaki M, Kawai H, Bokura K, Sone M, Nakashima T. Imaging of Ménière's disease by subtraction of MR cisternography from positive perilymph image. *Magn Reson Med Sci.* (2012) 11:303–9. doi: 10.2463/mrms.11.303
19. Sano R, Teranishi M, Yamazaki M, Isoda H, Naganawa S, Sone M, et al. Contrast enhancement of the inner ear in magnetic resonance images taken at 10 minutes or 4 hours after intravenous gadolinium injection. *Acta Otolaryngol.* (2012) 132:241–6. doi: 10.3109/00016489.2011.639085
20. Naganawa S, Yamazaki M, Kawai H, Bokura K, Sone M, Nakashima T. Imaging of Ménière's disease after intravenous administration of single-dose gadodiamide: utility of multiplication of MR cisternography and HYDROPS image. *Magn Reson Med Sci.* (2013) 12:63–8. doi: 10.2463/mrms.2012-0027
21. Seo YJ, Kim J, Choi JY, Lee WS. Visualization of endolymphatic hydrops and correlation with audio-vestibular functional testing in patients with definite Meniere's disease. *Auris Nasus Larynx.* (2013) 40:167–72. doi: 10.1016/j.anl.2012.07.009
22. Naganawa S, Yamazaki M, Kawai H, Bokura K, Iida T, Sone M, et al. MR imaging of Ménière's disease after combined intratympanic and intravenous injection of gadolinium using HYDROPS2. *Magn Reson Med Sci.* (2014) 13:133–7. doi: 10.2463/mrms.2013-0061
23. Baráth K, Schuknecht B, Naldi AM, Schrepfer T, Bockisch CJ, Hegemann SC. Detection and grading of endolymphatic hydrops in Menière disease using MR imaging. *AJNR Am J Neuroradiol.* (2014) 35:1387–92. doi: 10.3174/ajnr.A3856
24. Liu Y, Jia H, Shi J, Zheng H, Li Y, Yang J, et al. Endolymphatic hydrops detected by 3-dimensional fluid-attenuated inversion recovery MRI following intratympanic injection of gadolinium in the asymptomatic contralateral ears of patients with unilateral Ménière's disease. *Med Sci Monit.* (2015) 21:701–7. doi: 10.12659/MSM.892383
25. Sepahdari AR, Ishiyama G, Vorasubin N, Peng KA, Linetsky M, Ishiyama A. Delayed intravenous contrast-enhanced 3D FLAIR MRI in Meniere's disease: correlation of quantitative measures of endolymphatic hydrops with hearing. *Clin Imaging.* (2015) 39:26–31. doi: 10.1016/j.clinimag.2014.09.014
26. Hornibrook J, Flook E, Greig S, Babbage M, Goh T, Coates M, et al. MRI inner ear imaging and tone burst electrocochleography in the diagnosis of Ménière's disease. *Otol Neurotol.* (2015) 36:1109–14. doi: 10.1097/MAO.0000000000000782

27. Bykowski J, Harris JP, Miller M, Du J, Mafee MF. Intratympanic contrast in the evaluation of Menière disease: understanding the limits. *AJNR Am J Neuroradiol.* (2015) 36:1326–32. doi: 10.3174/ajnr.A4277
28. Attyé A, Dumas G, Troprès I, Roustit M, Karkas A, Banciu E, et al. Recurrent peripheral vestibulopathy: is MRI useful for the diagnosis of endolymphatic hydrops in clinical practice? *Eur Radiol.* (2015) 25:3043–9. doi: 10.1007/s00330-015-3712-5
29. Wu Q, Dai C, Zhao M, Sha Y. The correlation between symptoms of definite Meniere's disease and endolymphatic hydrops visualized by magnetic resonance imaging. *Laryngoscope.* (2016) 126:974–9. doi: 10.1002/lary.25576
30. Pakdaman MN, Ishiyama G, Ishiyama A, Peng KA, Kim HJ, Pope WB, et al. Blood-labyrinth barrier permeability in Menière disease and idiopathic sudden sensorineural hearing loss: findings on delayed postcontrast 3D-FLAIR MRI. *AJNR Am J Neuroradiol.* (2016) 37:1903–8. doi: 10.3174/ajnr.A4822
31. Keller JH, Hirsch BE, Marovich RS, Branstetter BF 4th. Detection of endolymphatic hydrops using traditional MR imaging sequences. *Am J Otolaryngol.* (2017) 38:442–6. doi: 10.1016/j.amjoto.2017.01.038
32. Choi JE, Kim YK, Cho YS, Lee K, Park HW, Yoon SH, et al. Morphological correlation between caloric tests and vestibular hydrops in Ménière's disease using intravenous Gd enhanced inner ear MRI. *PLoS ONE.* (2017) 12:e0188301. doi: 10.1371/journal.pone.0188301
33. Okumura T, Imai T, Takimoto Y, Takeda N, Kitahara T, Uno A, et al. Assessment of endolymphatic hydrops and otolith function in patients with Ménière's disease. *Eur Arch Otorhinolaryngol.* (2017) 274:1413–21. doi: 10.1007/s00405-016-4418-2
34. Yoshida T, Sugimoto S, Teranishi M, Otake H, Yamazaki M, Naganawa S, et al. Imaging of the endolymphatic space in patients with Ménière's disease. *Auris Nasus Larynx.* (2018) 45:33–8. doi: 10.1016/j.anl.2017.02.002
35. Wesseler A, Óvári A, Javorkova A, Kwiatkowski A, Meyer JE, Kivelitz DE. Diagnostic value of the magnetic resonance imaging with intratympanic gadolinium administration (IT-Gd MRI) versus audio-vestibular tests in Menière's disease: IT-Gd MRI makes the difference. *Otol Neurotol.* (2019) 40:e225–32. doi: 10.1097/MAO.0000000000002082
36. Bier G, Bongers MN, Schabel C, Heindel W, Ernemann U, Hempel JM. *In vivo* assessment of an endolymphatic hydrops gradient along the cochlea in patients with Menière's disease by magnetic resonance imaging-a pilot study. *Otol Neurotol.* (2018) 39:e1091–9. doi: 10.1097/MAO.0000000000002016
37. Quatre R, Attyé A, Karkas A, Job A, Dumas G, Schmerber S. Relationship between audio-vestibular functional tests and inner ear MRI in Meniere's disease. *Ear Hear.* (2019) 40:168–76. doi: 10.1097/AUD.0000000000000584
38. Pérez-Fernández N, Dominguez P, Manrique-Huarte R, Calavia D, Arbizu L, Garcia-Eulate R, et al. Endolymphatic hydrops severity in magnetic resonance imaging evidences disparate vestibular test results. *Auris Nasus Larynx.* (2019) 46:210–7. doi: 10.1016/j.anl.2018.08.014
39. Bernaerts A, Vanspauwen R, Blaivie C, van Dinther J, Zarowski A, Wuyts FL, et al. The value of four stage vestibular hydrops grading and asymmetric perilymphatic enhancement in the diagnosis of Menière's disease on MRI. *Neuroradiology.* (2019) 61:421–9. doi: 10.1007/s00234-019-02155-7
40. Eliezer M, Maquet C, Horion J, Gillibert A, Toupet M, Bolognini B, et al. Detection of intralabyrinthine abnormalities using post-contrast delayed 3D-FLAIR MRI sequences in patients with acute vestibular syndrome. *Eur Radiol.* (2019) 29:2760–9. doi: 10.1007/s00330-018-5825-0
41. Guo P, Sun W, Shi S, Zhang F, Wang J, Wang W. Quantitative evaluation of endolymphatic hydrops with MRI through intravenous gadolinium administration and VEMP in unilateral definite Meniere's disease. *Eur Arch Otorhinolaryngol.* (2019) 276:993–1000. doi: 10.1007/s00405-018-05267-7
42. Ohashi T, Naganawa S, Takeuchi A, Katagiri T, Kuno K. Quantification of endolymphatic space volume after intravenous administration of a single dose of gadolinium-based contrast agent: 3D-real inversion recovery versus HYDROPS-Mi2. *Magn Reson Med Sci.* (2020) 19:119–24. doi: 10.2463/mrms.mp.2019-0013
43. Gerb J, Ahmadi SA, Kierig E, Ertl-Wagner B, Dieterich M, Kirsch V. VOLT: a novel open-source pipeline for automatic segmentation of endolymphatic space in inner ear MRI. *J Neurol.* (2020) 267(Suppl 1):185–96. doi: 10.1007/s00415-020-10062-8
44. Nahmani S, Vaussy A, Hautefort C, Guichard JP, Guillonet A, Houdart E, et al. Comparison of enhancement of the vestibular perilymph between variable and constant flip angle-delayed 3D-FLAIR sequences in Menière disease. *AJNR Am J Neuroradiol.* (2020) 41:706–11. doi: 10.3174/ajnr.A6483
45. Cho YS, Cho K, Park CJ, Chung MJ, Kim JH, Kim K, et al. Automated measurement of hydrops ratio from MRI in patients with Ménière's disease using CNN-based segmentation. *Sci Rep.* (2020) 10:7003. doi: 10.1038/s41598-020-63887-8
46. van Steekelenburg JM, van Weijnen A, de Pont LMH, Vijlbrief OD, Bommeljé CC, Koopman JP, et al. Value of endolymphatic hydrops and perilymph signal intensity in suspected Ménière disease. *AJNR Am J Neuroradiol.* (2020) 41:529–34. doi: 10.3174/ajnr.A6410
47. Pai I, Mendis S, Murdin L, Touska P, Connor S. Magnetic resonance imaging of Ménière's disease: early clinical experience in a UK centre. *J Laryngol Otol.* (2020) 134:302–10. doi: 10.1017/S0022215120000626
48. Fukushima M, Ueno Y, Kitayama I, Akahani S, Inohara H, Takeda N. Assessment of the progression of vertical semicircular canal dysfunction and increased vestibular endolymphatic hydrops in patients with early-stage Ménière disease. *JAMA Otolaryngol Head Neck Surg.* (2020) 146:789–800. doi: 10.1001/jamaoto.2020.1496
49. Kahn L, Hautefort C, Guichard JP, Toupet M, Jourdaine C, Vitaux H, et al. Relationship between video head impulse test, ocular and cervical vestibular evoked myogenic potentials, and compartmental magnetic resonance imaging classification in menière's disease. *Laryngoscope.* (2020) 130:E444–52. doi: 10.1002/lary.28362
50. Gürkov R, Lutsenko V, Babkina T, Valchyshyn S, Situkho M. Clinical high-resolution imaging and grading of endolymphatic hydrops in hydropic ear disease at 1.5 T using the two-slice grading for vestibular endolymphatic hydrops in less than 10 min. *Eur Arch Otorhinolaryngol.* (2021). doi: 10.1007/s00405-021-06731-7. [Epub ahead of print].
51. He B, Zhang F, Zheng H, Sun X, Chen J, Chen J, et al. The correlation of a 2D volume-referencing endolymphatic-hydrops grading system with extra-tympanic electrocochleography in patients with definite ménière's disease. *Front Neurol.* (2021) 11:595038. doi: 10.3389/fneur.2020.595038
52. Zhang W, Hui L, Zhang B, Ren L, Zhu J, Wang F, et al. The correlation between endolymphatic hydrops and clinical features of Meniere disease. *Laryngoscope.* (2021) 131:E144–50. doi: 10.1002/lary.28576
53. Sluydts M, Bernaerts A, Casselman JW, De Foer B, Blaivie C, Zarowski A, et al. The relationship between cochleovestibular function tests and endolymphatic hydrops grading on MRI in patients with Menière's disease. *Eur Arch Otorhinolaryngol.* (2021). doi: 10.1007/s00405-021-06610-1. [Epub ahead of print].
54. Carfrae MJ, Holtzman A, Eames F, Parnes SM, Lupinetti A. 3 Tesla delayed contrast magnetic resonance imaging evaluation of Ménière's disease. *Laryngoscope.* (2008) 118:501–5. doi: 10.1097/MLG.0b013e31815c1a61
55. Shi S, Zhou F, Wang W. 3D-real IR MRI of Meniere's disease with partial endolymphatic hydrops. *Am J Otolaryngol.* (2019) 40:589–93. doi: 10.1016/j.amjoto.2019.05.015
56. Iida T, Teranishi M, Yoshida T, Otake H, Sone M, Kato M, et al. Magnetic resonance imaging of the inner ear after both intratympanic and intravenous gadolinium injections. *Acta Otolaryngol.* (2013) 133:434–8. doi: 10.3109/00016489.2012.753640
57. Gürkov R. Menière and friends: imaging and classification of hydropic ear disease. *Otol Neurotol.* (2017) 38:e539–44. doi: 10.1097/MAO.0000000000001479
58. Tagaya M, Yamazaki M, Teranishi M, Naganawa S, Yoshida T, Otake H, et al. Endolymphatic hydrops and blood-labyrinth barrier in Ménière's disease. *Acta Otolaryngol.* (2011) 131:474–9. doi: 10.3109/00016489.2010.534114
59. Nakashima T, Naganawa S, Sugiura M, Teranishi M, Sone M, Hayashi H, et al. Visualization of endolymphatic hydrops in patients with meniere's disease. *Laryngoscope.* (2007) 117:415–20. doi: 10.1097/MLG.0b013e31802c300c
60. Nakashima T, Naganawa S, Pyykko I, Gibson WP, Sone M, Nakata S, et al. Grading of endolymphatic hydrops using magnetic resonance imaging. *Acta Otolaryngol Suppl.* (2009) 560:5–8. doi: 10.1080/00016480902729827
61. Gluth MB. On the relationship between Menière's disease and endolymphatic hydrops. *Otol Neurotol.* (2020) 41:242–9. doi: 10.1097/MAO.0000000000002502
62. Van der Lubbe MFJA, Vaidyanathan A, Van Rompaey V, Postma AA, Bruintjes TD, Kimenai DM, et al. The "hype" of hydrops in classifying

vestibular disorders: a narrative review. *J Neurol.* (2020) 267(Suppl. 1):197–211. doi: 10.1007/s00415-020-10278-8

63. Morita Y, Takahashi K, Ohshima S, Yagi C, Kitazawa M, Yamagishi T, et al. Is vestibular Meniere's disease associated with endolymphatic hydrops? *Front Surg.* (2020) 7:601692. doi: 10.3389/fsurg.2020.601692
64. Eliezer M, Poillon G, Horion J, Lelion P, Gerardin E, Magne N, et al. MRI diagnosis of saccular hydrops: comparison of heavily-T2 FIESTA-C and 3D-FLAIR sequences with delayed acquisition. *J Neuroradiol.* (2019). doi: 10.1016/j.neurad.2019.04.005. [Epub ahead of print].
65. Zou J, Wang Z, Chen Y, Zhang G, Chen L, Lu J. MRI detection of endolymphatic hydrops in Meniere's disease in 8 minutes using MIIRMR and a 20-channel coil after targeted gadolinium delivery. *World J Otorhinolaryngol Head Neck Surg.* (2020) 5:180–7. doi: 10.1016/j.wjorl.2019.04.001
66. Vaidyanathan A, van der Lubbe MFJA, Leijenaar RTH, van Hoof M, Zerka F, Miraglio B, et al. Deep learning for the fully automated segmentation of the inner ear on MRI. *Sci Rep.* (2021) 11:2885. doi: 10.1038/s41598-021-82289-y
67. Lee J, Kim ES, Lee Y, Lee K, Yoon DY, Ju YS, et al. Quantitative analysis of cochlear signal intensity on three-dimensional and contrast-enhanced fluid-attenuated inversion recovery images in patients with Meniere's disease: correlation with the pure tone audiometry test. *J Neuroradiol.* (2019) 46:307–11. doi: 10.1016/j.neurad.2019.03.010

Conflict of Interest: The authors declare that the research was conducted in the absence of any commercial or financial relationships that could be construed as a potential conflict of interest.

Publisher's Note: All claims expressed in this article are solely those of the authors and do not necessarily represent those of their affiliated organizations, or those of the publisher, the editors and the reviewers. Any product that may be evaluated in this article, or claim that may be made by its manufacturer, is not guaranteed or endorsed by the publisher.

frontiers in Surgery

ORIGINAL RESEARCH
published: 05 October 2021
doi: 10.3389/fsurg.2021.687490

Measurements From Ears With Endolymphatic Hydrops and 2-Hydroxypropyl-Beta-Cyclodextrin Provide Evidence That Loudness Recruitment Can Have a Cochlear Origin

*Shannon M. Lefler[1], Robert K. Duncan[2], Shawn S. Goodman[3], John J. Guinan Jr.[4,5] and Jeffery T. Lichtenhan[1]**

[1] Department of Otolaryngology, Washington University School of Medicine in St. Louis, Saint Louis, MO, United States, [2] Department of Otolaryngology-Head and Neck Surgery, Kresge Hearing Research Institute, University of Michigan, Ann Arbor, MI, United States, [3] Department of Communication Sciences and Disorders, University of Iowa, Iowa City, IA, United States, [4] Eaton-Peabody Laboratories, Massachusetts Eye and Ear, Boston, MA, United States, [5] Department of Otolaryngology, Harvard Medical School, Boston, MA, United States

OPEN ACCESS

Edited by:
Robert Gürkov,
Bielefeld University, Germany

Reviewed by:
A. B. Zulkiflee,
University Malaya Medical Centre, Malaysia
Paul Hinckley Delano,
University of Chile, Chile

***Correspondence:**
Jeffery T. Lichtenhan
jlichtenhan@gmail.com

Specialty section:
This article was submitted to Otorhinolaryngology–Head and Neck Surgery, a section of the journal Frontiers in Surgery

Received: 29 March 2021
Accepted: 02 September 2021
Published: 05 October 2021

Citation:
Lefler SM, Duncan RK, Goodman SS, Guinan JJ Jr and Lichtenhan JT (2021) Measurements From Ears With Endolymphatic Hydrops and 2-Hydroxypropyl-Beta-Cyclodextrin Provide Evidence That Loudness Recruitment Can Have a Cochlear Origin. Front. Surg. 8:687490. doi: 10.3389/fsurg.2021.687490

Background: Loudness recruitment is commonly experienced by patients with putative endolymphatic hydrops. Loudness recruitment is abnormal loudness growth with high-level sounds being perceived as having normal loudness even though hearing thresholds are elevated. The traditional interpretation of recruitment is that cochlear amplification has been reduced. Since the cochlear amplifier acts primarily at low sound levels, an ear with elevated thresholds from reduced cochlear amplification can have normal processing at high sound levels. In humans, recruitment can be studied using perceptual loudness but in animals physiological measurements are used. Recruitment in animal *auditory-nerve* responses has never been unequivocally demonstrated because the animals used had damage to sensory and neural cells, not solely a reduction of cochlear amplification. Investigators have thus looked for, and found, evidence of recruitment in the auditory central nervous system (CNS). While studies on CNS recruitment are informative, they cannot rule out the traditional interpretation of recruitment originating in the cochlea.

Design: We used techniques that could assess hearing function throughout entire frequency- and dynamic-range of hearing. Measurements were made from two animal models: guinea-pig ears with endolymphatic-sac-ablation surgery to produce endolymphatic hydrops, and naïve guinea-pig ears with cochlear perfusions of 13 mM 2-Hydroxypropyl-Beta-Cyclodextrin (HPBCD) in artificial perilymph. Endolymphatic sac ablation caused low-frequency loss. Animals treated with HPBCD had hearing loss at all frequencies. None of these animals had loss of hair cells or synapses on auditory nerve fibers.

Results: In ears with endolymphatic hydrops and those perfused with HPBCD, auditory-nerve based measurements at low frequencies showed recruitment compared

to controls. Recruitment was not found at high frequencies (> 4 kHz) where hearing thresholds were normal in ears with endolymphatic hydrops and elevated in ears treated with HPBCD.

Conclusions: We found compelling evidence of recruitment in auditory-nerve data. Such clear evidence has never been shown before. Our findings suggest that, in patients suspected of having endolymphatic hydrops, loudness recruitment may be a good indication that the associated low-frequency hearing loss originates from a reduction of cochlear amplification, and that measurements of recruitment could be used in differential diagnosis and treatment monitoring of Ménière's disease.

Keywords: endolymphatic hydrops, low-frequency hearing, loudness recruitment, auditory nerve overlapped waveform, 2-hydroxypropyl-beta-cyclodextrin

INTRODUCTION

Dynamic range alterations accompany disorders of many sensory systems including the auditory system. The dynamic range of hearing is altered when trauma or disease elevates the thresholds of low-level sounds, but the loudness of high-level sounds is within normal limits. An elevated threshold with an abnormally fast growth of loudness that achieves normal loudness at high levels is called "recruitment" [e.g., (1–3)]. Recruitment demonstrates that audiometric sensorineural hearing loss is more complex than a simple linear reduction of sound, such as from disorders of the middle ear or the use of hearing-protective devices (e.g., ear muffs or earplugs). In animal models, recruitment is typically studied with measurements of physiologic responses (e.g., auditory nerve compound action potentials -CAPs), not by perceptual loudness. Here we use the term "response recruitment" to distinguish recruitment measured by a physiologic response from "loudness recruitment" which is recruitment measured by a subjective or psychophysical method.

The traditional proposed pathophysiologic mechanism of recruitment is that cochlear amplification has been reduced. Cochlear amplification is a process that increases basilar-membrane (BM) vibrations by mechanisms that saturate at high levels. Cochlear amplification improves sensitivity to low-level sounds, but does not appear to play an important role in responses to high-level sounds. Cochlear amplification requires outer-hair-cell (OHC) electromotility, and functional impairment or loss of OHCs produces hearing threshold elevation (i.e., hearing loss) that can be many tens of dB. In contrast to low-level responses, most auditory responses to high-level sounds are unaffected by reductions of cochlear amplification. Thus, a reduction of cochlear amplification results in hearing threshold elevation but normal responses to high-level sounds with a resulting higher rate of response growth (i.e., in recruitment).

The traditional interpretation of recruitment originated from measurements of BM motion. Reductions in cochlear amplification, such as from damage or stimulation of olivocochlear efferents, change the growth of BM motion with sound level, with vibration threshold being elevated but the motion remaining within normal limits for high-level sounds [e.g., (4, 5)]. Following reductions of cochlear amplification, measurements of both loudness and BM motion show increased thresholds, increased growth with sound level and normal amplitudes at high levels. *The striking similarity between these is the main source of the traditional interpretation that recruitment has a cochlear origin* [e.g., (6, 7)].

There have been no published data showing clear response recruitment in measurements from the auditory nerve of damaged or diseased ears in which the damage was restricted to a reduction of cochlear amplification (8, 9). The lack of auditory-nerve data showing recruitment may be a consequence of the lack of animal models with reduced cochlear amplification but preserved synaptic activity between inner hair cells (IHCs) and auditory nerve fibers. For example, cochleae that have been treated with salicylate or acoustic overexposure can have reduced cochlear amplification, but can also have impairment of IHCs and the IHC synapses with auditory nerve fibers [e.g., (10, 11)]. The lack of data showing unequivocal recruitment in auditory nerve measurements has led investigators to reject the traditional interpretation that loudness recruitment originates in the cochlea and to consider alternative origins such as that loudness recruitment originates in the auditory central nervous system (CNS) [e.g., (8)].

We hypothesized that a pure reduction of cochlear amplification, without damage to IHCs, auditory nerve fibers, or endocochlear potential, would show recruitment that arises in the cochlea and is manifested in auditory-nerve responses. Here we show recruitment in auditory-nerve measurements from two guinea pig models: (1) guinea-pig ears that underwent surgery to ablate the endolymphatic sac, a procedure that induces endolymphatic hydrops that can be seen histologically at 30 postoperative days and that causes low-frequency hearing threshold elevation soon after the ablation (12–14), and (2) naïve (i.e., never operated on) animals that underwent cochlear perfusions of 13 mM 2-Hydroxypropyl-Beta-Cyclodextrin (HPBCD) in artificial perilymph. HPBCD can be used to treat Niemann-Pick type C disease, Alzheimer's disease, and atherosclerosis, but causes hearing loss [(15) p. 1,017]. Ears with endolymphatic hydrops and animals that underwent acute cochlear perfusion with low-dose HPBCD did not have

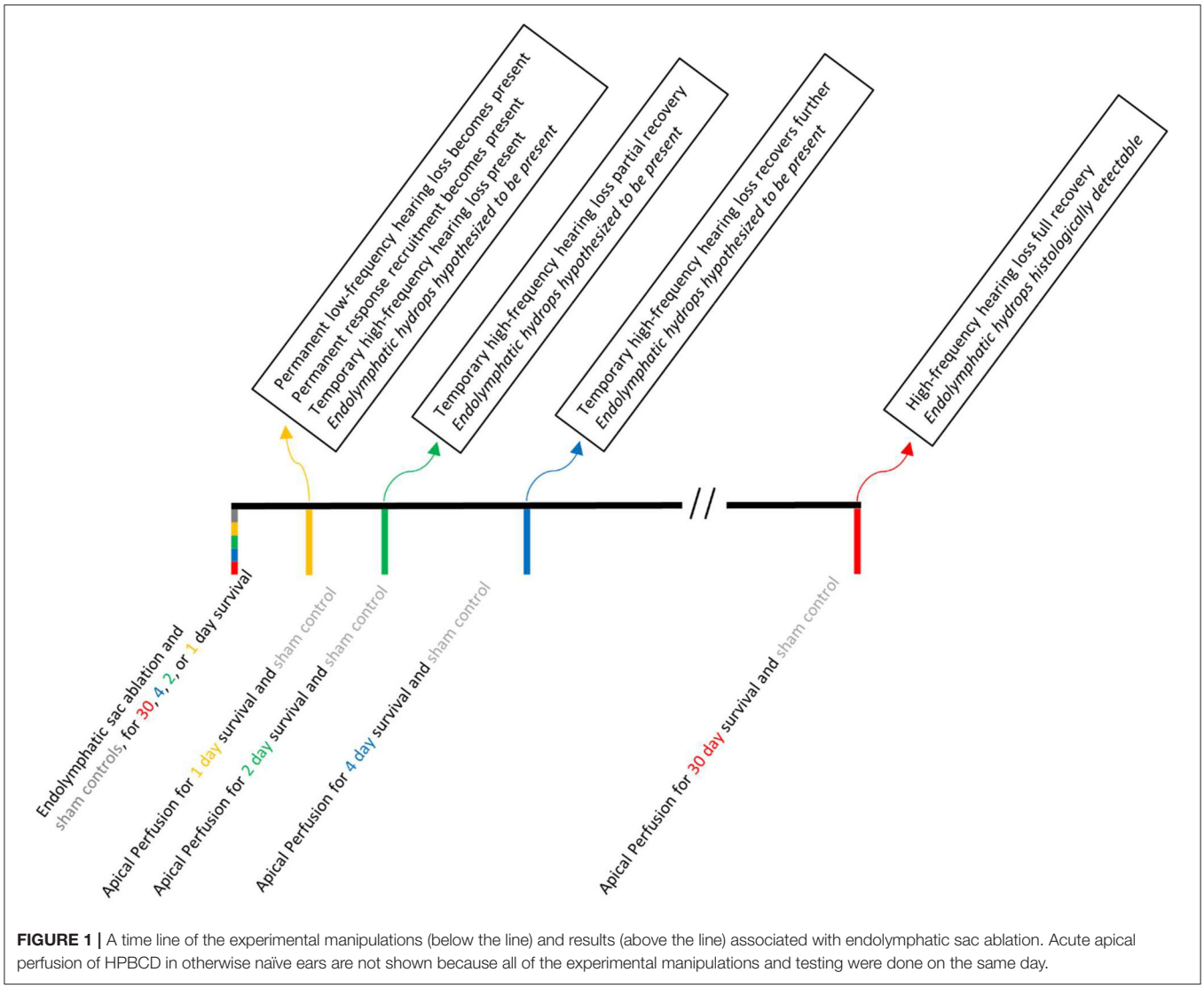

FIGURE 1 | A time line of the experimental manipulations (below the line) and results (above the line) associated with endolymphatic sac ablation. Acute apical perfusion of HPBCD in otherwise naïve ears are not shown because all of the experimental manipulations and testing were done on the same day.

loss of cochlear hair cells or afferent auditory nerve synapses, and the hearing loss appears to arise from a reduction of cochlear amplification (14, 16). Ears with endolymphatic hydrops as well as those treated acutely with HPBCD are thus well suited to address the question of whether the traditional interpretation of recruitment is correct. Moreover, if the degree of response recruitment correlates with the severity of endolymphatic hydrops, it is possible that clinical measurements of loudness recruitment can be used as a functional assessment of the presence of endolymphatic hydrops in patients with Ménière's disease.

METHODS

Overview

The right ears of NIH-strain pigmented guinea pigs of either sex weighing at least 400 g were used. Animals were assigned to one of two groups: an endolymphatic-sac-surgery group or an HPBCD group. We provided the full details of the endolymphatic sac surgery in a video-based publication (14). The key steps are to visualize the extra-osseous portion of the endolymphatic sac, to use fine picks to destroy the intraosseous portion of the endolymphatic sac, and to fully disarticulate it from the extra-osseous portion. Middle ear structure was not disrupted during the endolymphatic sac ablation surgery. The endolymphatic sac group had 43 guinea pigs, with two animals used here for the first time and 38 used previously in Lee et al. (12) or Valenzuela et al. (13, 14). The eight control animals for the endolymphatic sac group (four sham surgery and four naïve) were also used in Lee et al. (12) and Valenzuela et al. (13, 14). The sham surgery involved visualizing the endolymphatic duct though not ablating it. Results from sham-surgery and naïve animals were found to be similar (12). Operated animals underwent a second surgery to make cochlear function measurements at pre-defined postoperative time points: 1, 2, 4, or 30 days (**Figure 1**). The number of animals used in each figure is provided in its legend.

Three guinea pigs received cochlear perfusions of HPBCD. The surgery for the HPBCD animals was nearly identical to the surgery to make cochlear function measurements in the endolymphatic sac animals, with one additional step to directly administer HPBCD in artificial endolymph using the apex-to-base cochlear perfusion technique that is routinely used in our lab (16–21). Control measurements for the HPBCD group were made from each ear before perfusion.

Cochlear histology was done on the animals with endolymphatyic sac ablation (both ears), ears with HPBCD perfusions, and selected ears from control animals. The histological procedure is fully described in Lee et al. (12) where it was used to assess endolymphatic hydrops and in Lichtenhan et al. (16) where it was used to assess structural integrity following HPBCD. The histological assessment did not reveal any sensory cell loss and the immunohistoflurescence-based confocal microscopy did not show any cochlear synapse loss following endolymphatic sac ablation. At present, we do not know the origin of the low-frequency hearing loss associated with endolymphatic hydrops in guinea pigs, although we speculate that it is due to endolymphatic hydrops that does not show up in histology (12). This animal model is consistent with findings from human temporal bone studies of patients with Ménière's disease (22).

Sound Calibration

During the experiments, a hollow ear bar (5, 0.322 cm i.d.) was attached to the bony portion of the right ear canal using a stereotaxic device. One end of the bar was wrapped in a portion of the cut ear canal soft tissue to form a sound delivery port with no acoustic leaks. Stimuli were presented via an ER-10X (Etymotic Research) probe connected to the other end of the hollow ear bar. Prior to the experiments, the sound delivery system was calibrated using a 1/8" GRAS type 40P reference microphone and custom-made coupling device. To calibrate system output, the hollow ear bar was coupled to one end of a cavity having dimensions and volume similar to the bony portion of the ear canal, and the reference microphone was coupled to the opposite end. Stimuli were played through the ER-10X probe loudspeakers into the ear bar and measured by the reference microphone. A transfer function for the sound source to sound pressure at the plane of the tympanic membrane was obtained and applied to all stimuli used in this experiment.

The ER-10X probe microphone was used for recording otoacoustic emissions, not for setting stimulus levels. The ER-10X probe microphone was calibrated using a copper tube (1.83 m; 0.635 cm i.d.) that was closed at one end and had a sound source placed in the opposite end. The ER-10X probe and a reference microphone (1/8" GRAS type 40P) were sealed in small holes located ∼2.5 cm from the sound source. The probe and reference microphones were located opposite to each other and perpendicular to the long axis of the tube. The microphone inlet (probe) and diaphragm (reference) were flush with the wall of the tube. A train of click stimuli was played through the sound source, and the incident wave was measured simultaneously by the probe and reference microphones. Clicks were spaced in time to allow internal reflections in the tube to decay into the noise floor before the next click in the train was presented. Measurements were averaged and temporally windowed to include the incident wave only. A transfer function of the ER-10X probe microphone relative to the reference microphone was created and used to achieve a flat probe microphone response from 0.1 to 34 kHz.

Physiologic Measurements

Animals were sedated with an intraperitoneal injection of 100 mg/kg Inactin hydrate (i.e., thiobutabarbital sodium), after which the head and neck areas were shaved. A tracheotomy was done to artificially ventilate and sustain anesthesia with ∼1.2% of isoflurane in oxygen gas. Ventelation volume was adjusted to maintain 5% end-tidal CO2. A pulse oximeter (Capno True Amp, Bluepoint Medical) was used to monitor O2 saturation, expired CO2 level, and heart rate. A DC-powered heating blanket and rectal thermometer system (Homeothermic Blanket with Flexible Probe from Harvard Apparatus) monitored and maintained body temperature at 38°C. The double-walled sound attenuated room where physiologic measurements were made was heated so that the area immediately around the animal was ∼25°C. The guinea pig's head was secured with a bite bar, snout clamp, a hollow ear bar on the right side, and solid ear bar on the left side. When in the supine position, a canula was inserted into the left jugular vein and Lactated Ringer solution (0.5 mL/h) was administered to maintain hydration. The right bulla was accessed ventrally by removing soft tissue and the jaw.

Cochlear function measurements were made using Auditory Research Lab audio software (ARLas, https://github.com/myKungFu). A computer running custom MATLAB software (The MathWorks, Inc., Natick, MA) and the software utility Playrec (23) was used. Stimuli were generated in MATLAB, digitized at 96 kHz, presented to a 24-bit sound card (RME Fireface 802) and routed to an acoustic probe system (ER-10X) that was coupled to the hollow ear bar. Otoacoustic emission (OAE) measurements were made using the acoustic probe system connected to the sound card. Once the ear bars were in place and the head secured, the bulla was opened slightly and OAE measurements were made. The round-window-niche electrode was positioned. Vecuronium bromide (0.1 mg / kg) was administered through the jugular-vein cannula to prevent middle ear muscle contractions. Auditory Nerve Overlapped Waveform (ANOW) and auditory nerve compound action potentials (CAP) measurements were made (details below). These round-window-electrode voltage measurements were band pass filtered at 0.1–3 kHz and amplified 10,000 times (GRAS CP511, Astro-Med, Inc.).

Otoacoustic Emission Measurements

Distortion product otoacoustic emissions (DPOAEs) at 2f1-f2 were measured with paired primary tones that had durations of 1 s, frequencies f2/f1 = 1.22 and levels L1 & L2 of 60 and 50 dB SPL, respectively. f2 frequencies ranged from 1 to 30 kHz in 2 kHz steps, with 12 repetitions presented at each step. Noise floor measurements were made using the standard error of the DPOAE amplitude converted to dB SPL.

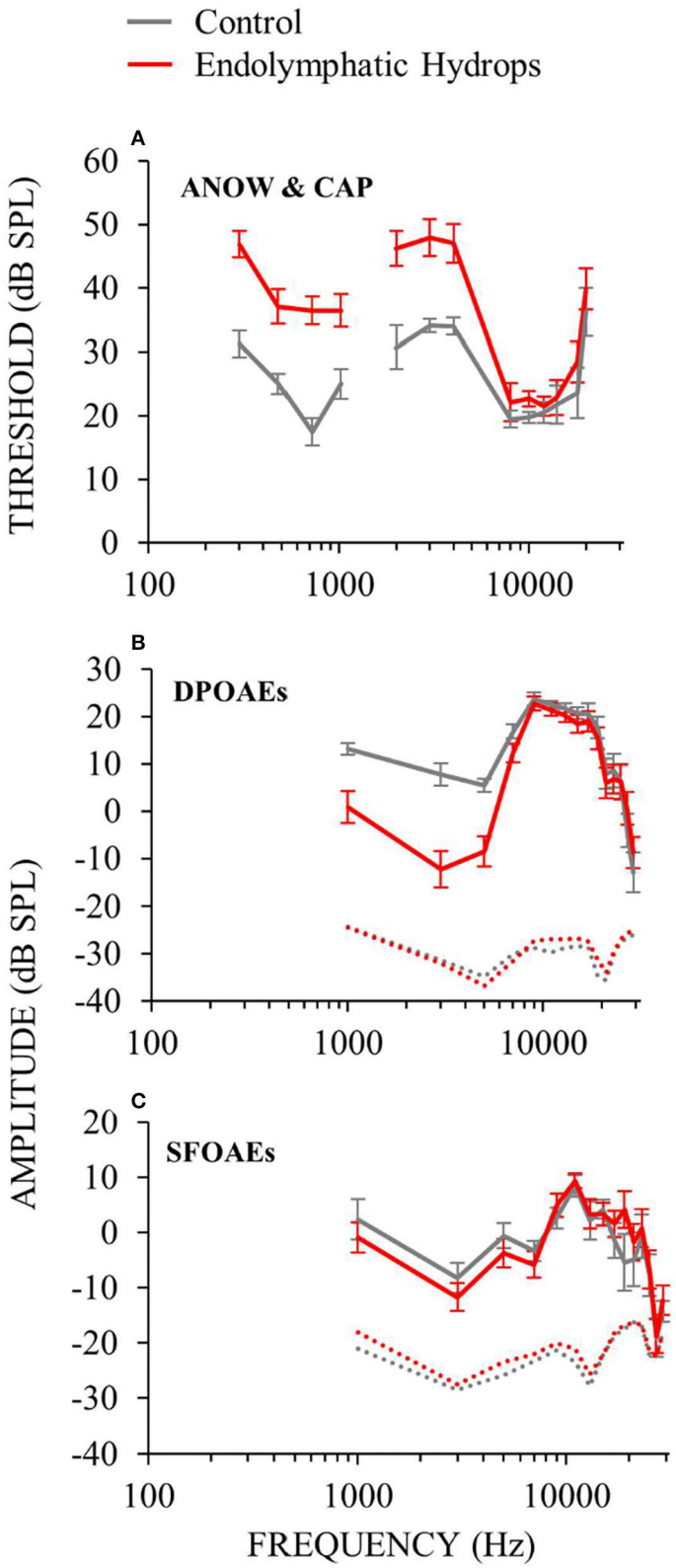

FIGURE 2 | Cochlear function measurements from experimental (red) and control (gray) animals. Data from the right ears of 18 guinea pigs 30 days after ablation of the endolymphatic sac, and from 8 control animals, 4 of which had undergone sham surgery. Error bars are one standard error of the mean. Operated animals had hearing dysfunction at low (≤ 1) and mid (2–4 kHz) frequencies, but not high frequencies. See elevated hearing thresholds **(A)**, decreased DPOAEs **(B)** and decreased SFOAEs **(C)**.

Stimulus frequency otoacoustic emission (SFOAEs) were evoked with probe tones having 250 ms duration, 10 ms rise/fall, and 40 dB SPL sound level. The double-evoked extraction method was used, with a suppressor tone presented 50 Hz above the SFOAE frequency at a level of 60 dB SPL (24–26). The double-evoked method eliminates the stimulus along with system distortion, leaving the otoacoustic emission. Probe tones ranged from 1 to 30 kHz in 2 kHz steps and were presented with 24 repetitions. Noise floor measures were estimated using the standard error of the mean of the SFOAE measurements converted to dB SPL.

Measurements of Auditory-Nerve Responses

Measurements of auditory-nerve responses were made with an Ag/AgCl ball electrode placed in the round-window niche (non-inverting) and platinum needle electrodes placed in the exposed musculature of the right jaw (inverting) and neck (ground).

ANOW Measurements and Calculations

ANOW measurements were made with tone bursts (33.3 ms duration) presented in alternating polarity (92 repetitions) at 300, 480, 720, and 1,020 Hz. In this report, these frequencies will be referred to as 300, 500, 700, and 1,000 Hz, respectively. The cochlear microphonic follows the sinusoidal stimuli, but neural excitation occurs mostly during one phase of the tone, for low-frequency tones of low- to moderate-levels. Averaging the response of alternating tone bursts cancels the cochlear microphonic and overlaps the phase-locked neural firing. The ANOW measurements used only the second harmonic of the overlapped response, which selects the auditory-nerve response (27). Recorded ANOW waveforms were bandpass filtered using an FIR filter (600–1,600 Hz passband). Filtered waveforms were corrected for filter group delay and checked for high-amplitude artifacts using a quartile-based detection method (28). The temporal locations of artifacts were recorded, but the artifacts were not removed. Weighted least-squares fits were used to determine the coefficients associated with sinusoids of twice the probe frequency in cosine and (minus) sine phase. The weights on each waveform sample were set to 1 (no artifact) or 0 (artifact present). This method removed the effects of short, infrequent artifacts while preserving the rest of the information in the waveforms, as well as avoiding splatter from edge discontinuities. ANOW waveforms were fit individually, and the resulting coefficients were stored as vectors in complex rectangular form (in a manner similar to complex Fourier coefficients, but at a single frequency). The mean of the stored coefficients was taken as the signal, and the standard error of the mean was taken as the noise floor. ANOW magnitude and phase were computed in the usual way as the square root of the sum of the squares of the real and imaginary parts, and as the four-quadrant arctangent of the ratio of imaginary and real parts.

CAP Measurements and Calculations

CAP measurements were made in response to tone bursts with 13.9 ms durations (1.0 ms rise/fall) presented with 128 repetitions of alternating polarity. Tone burst presentations were interleaved with periods of silence (13.9 ms duration), so that each alternating-polarity pair was presented at a repetition rate of 14.38/s. The sound level of the tone bursts were varied from 10 to 80 dB SPL in 5 dB steps.

Recorded CAP waveforms were bandpass filtered using an FIR filter (150–1,500 Hz passband). Filtered waveforms were corrected for filter group delay and checked for high-amplitude artifacts using a quartile-based detection method. Waveforms containing artifacts were removed from subsequent analysis. An automated peak-picking algorithm identified the amplitudes and latencies of N1 and P1 for each waveform. Results from the automated algorithm accurately reflected the investigators visual assessments of the amplitudes and latencies.

Curve Fitting to Response-Amplitude-vs.-Sound-Level Functions

CAP recordings were obtained in 5 dB steps from 10 to 80 dB SPL. For each test frequency, this resulted in 14 peak-to-peak amplitude and peak-delay values. In order to characterize the growth of these values as a function of stimulus level, amplitude and delay were fit (separately) with weighted smoothing splines. The smoothing coefficient (0.005) was determined empirically by examining many data sets and choosing a single value that, across animals, yielded an appropriate amount of smoothing while still retaining essential features of the level series. The weighting values were the signal-to-noise ratio at each stimulus level. The weighting values were set to zero for responses with signal-to-noise ratios of < 6 dB. The spline fit was interpolated to yield values with 1-dB spacing, and these densely-spaced spline curves were differentiated to give growth rates. A similar process was used to find the growth rates of ANOW responses, except that the RMS magnitude (in dB) of the response was used instead of peak-to-peak amplitude, and the phase delay of the response was used instead of the peak delays of the CAP waveform. Our slope measure of "response recruitment" was calculated as the median of the derivative values at sound levels at and above threshold for each frequency of each ear.

RESULTS

Recruitment in Ears With Endolymphatic Hydrops

Cochlear function measurements from animals 30 days after endolymphatic sac ablation that induced endolymphatic hydrops are shown in **Figure 2**. Auditory neural threshold measurements were made with ANOWs for low frequencies ($\leq$ 1 kHz) and with CAPs for mid (2–4 kHz) and high frequencies (8–20 kHz; **Figure 2A**). Thresholds were elevated relative to control for low- and mid-frequencies and were within normal limits for high-frequencies (**Figure 2A**). This configuration is similar to that found in human patients with Ménière's disease (22). OAE measurements were made only at frequencies $\geq$ 1 kHz, due to poor signal-to-noise ratios at lower frequencies. DPOAE amplitudes were decreased relative to controls for mid-frequencies (1–4 kHz), and were

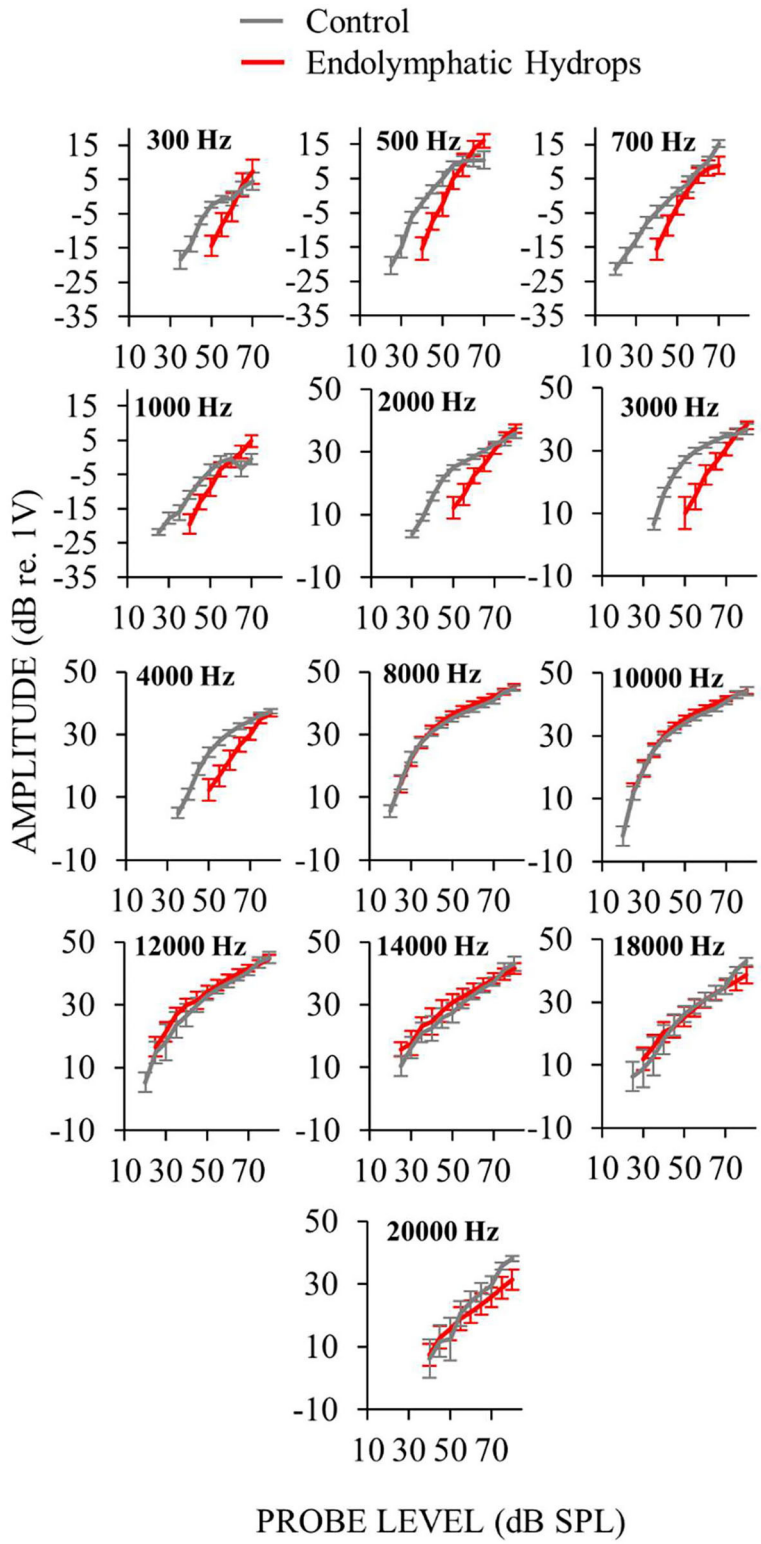

FIGURE 3 | Auditory-nerve response amplitudes from ears with endolymphatic sac ablation (red) and control ears (gray) as functions of sound level for many frequencies. Measurements at low-frequencies (≤ 1 kHz) were made with ANOW and at mid- and high-frequencies (2–4 and ≥ 8 kHz) were made with CAPs. Only measurements that were at, and above, threshold are plotted. Control animals were naïve or underwent a sham-surgery. Points are averages from 18 (low frequencies) or 15 (mid and high frequencies) ears with endolymphatic sac ablation, and eight control ears. Error bars are one standard error of the mean. Response recruitment was seen at low and mid frequencies in that thresholds were elevated but responses converged to near normal at high-levels.

within normal limits for other frequencies (**Figure 2B**). SFOAE amplitudes did not differ significantly from controls (**Figure 2C**). These OAE results are similar to those we have reported previously (12, 14). Overall, ablation of the endolymphatic sac and the resulting endolymphatic hydrops were associated with low- and mid-frequency hearing dysfunction.

Auditory-nerve responses (ANOW at low frequencies, and CAPs at mid and high frequencies) from ears with endolymphatic sac ablation and from control animals, were measured over a wide range of sound levels (**Figure 3**). This enabled the assessment of cochlear neural response recruitment throughout the frequency range of hearing. *Ears with endolymphatic sac ablation showed response recruitment at low and mid frequencies in that thresholds were elevated, response amplitude grew faster than normal with level, and supra-threshold responses were within the normal range.* At high sound levels, response amplitudes for low and mid frequencies in ears with endolymphatic sac ablation were occasionally hyper-responsive compared to control (i.e., 0.3, 0.5, and 1 kHz in **Figure 3**). At high frequencies, CAP amplitudes from ears with endolymphatic sac ablation were essentially indistinguishable from control ears, except that responses at 20 kHz were reduced compared to controls at the highest stimulus levels.

To measure response-growth (slopes), the auditory-nerve response-amplitude vs. sound-level functions of individual ears were fit with smoothing splines, and the spline slopes were calculated. Although the slopes varied with sound level, compact estimates of the overall growth rates were obtained by taking the *median* slope of each function. This slope metric allowed comparison of rates of growth across multiple frequencies and animals. For each frequency, **Figure 4** shows the median across ears of the median slopes. The median slope values for ears with endolymphatic sac ablation (red in **Figure 4**) were higher than controls (gray) for low ($\leq$ 1 kHz) and mid (2–4 kHz) frequencies, and were little different than control ears for high ($\geq$ 8 kHz) frequencies (**Figure 4**). The steeper slopes in the ears with endolymphatic sac ablation are consistent with these ears having response recruitment at low and mid frequencies. In contrast, the lower slopes of the control ears are consistent with the more compressive growth produced by cochlear amplification.

Comparing the data in **Figures 2**, **4** shows that frequencies with hearing loss (i.e., low and mid frequencies) are associated with high-slope response vs. sound-level functions, i.e. with response recruitment. In **Figure 5** we explore this further. **Figures 5A,B** show example plots (at 0.5 and 12 kHz), of the slope metric for recruitment for each ear that had endolymphatic sac ablation, as a function of its hearing threshold at that frequency. At these two frequencies, ears with higher thresholds had higher slopes of their response growths, as would be necessary for the responses of all ears reach the same high amplitude at high sound levels. For all tested frequencies, linear-regression lines were fit to similar plots, and from each plot (one plot for each frequency and condition) we calculated linear regression coefficients. The results, in **Figure 5C**, show that the dependence on hearing threshold of the slope metric of response recruitment was greater at low and mid frequencies (where hearing thresholds were elevated) compared to high frequencies (where hearing thresholds were on average within normal limits). Linear-regression slope coefficients from the operated ears differed significantly (at the 0.05 level) from zero, at five of the seven low and mid frequencies (i.e., for frequencies of *0.3, 0.5,* 0.7, 1, *2, 3, and 4* kHz, with the probabilities that the slopes differed from zero being respectively: *0.014, 0.0016*, 0.174, 0.193, *0.00031, 0.000028, and 0.024*). In contrast, for high-frequencies in the operated ears, no regression slope differed from zero at the 0.05 level. In the control ears, except at the highest frequency tested, no regression slope differed from zero at the 0.05 level. Interestingly, at the lowest frequencies, the control-ear data have negative regression slopes, a pattern opposite that of the operated ears, although these negative averages were not statistically significantly different from zero. Overall, *these results suggest that clinical measurements of recruitment in patients suspected of having endolymphatic hydrops should be focused on those frequencies associated with hearing threshold elevation.*

Histology in Ears With the Endolymphatic Sac Removed

Both functional and histological assessments were completed on eight ears that had the endolymphatic sac removed and on seven control ears. For each ear, we measured: (1) the average of the threshold shifts at low frequencies ($\leq$ 1 kHz) to assess hearing loss, (2) the median at low frequencies of the slope metrics for response recruitment, and (3) the average of scala media cross sectional area in mid-modiolar sections (**Figure 6**) of the apical cochlear half (i.e., cochlear turns 2.5–4), to assess endolymphatic hydrops in the part of the (cochlea that has low characteristic-frequencies (20, 29).

The degree of low-frequency *response* recruitment varied with the severity of apical endolymphatic hydrops (**Figure 7A**), consistent with the hypothesis that *loudness* recruitment varies with the severity of endolymphatic hydrops. While the correlation for operated ears hinges on two ears that had scala-media areas that were similar to unoperated ears, it was still statistically significant ($p = 0.026$). If all ears are considered, the correlation becomes highly statistically significant ($p = 0.0014$).

The degree of response recruitment varied with the extent of low-frequency hearing loss (**Figure 7B**), which was shown in a different way in **Figure 5**. Scala media area varied with low-frequency hearing threshold (**Figure 7C**), as was shown in Lee et al. (12), now with two additional animals (filled red symbols). Adding the two animals changed the regression very little: the regression results with the two animals removed were $y = 0.014x + 0.4376$; $R^2 = 0.5731$, similar to the values in **Figure 7C**. Overall, the **Figure 7** results suggest that both *the degree of response recruitment and the low-frequency hearing loss may provide non-invasive assessments of the severity of endolymphatic hydrops.*

Recruitment in Ears Treated With HPBCD

To further explore whether auditory-nerve response recruitment originates from attenuation of cochlear amplification, we

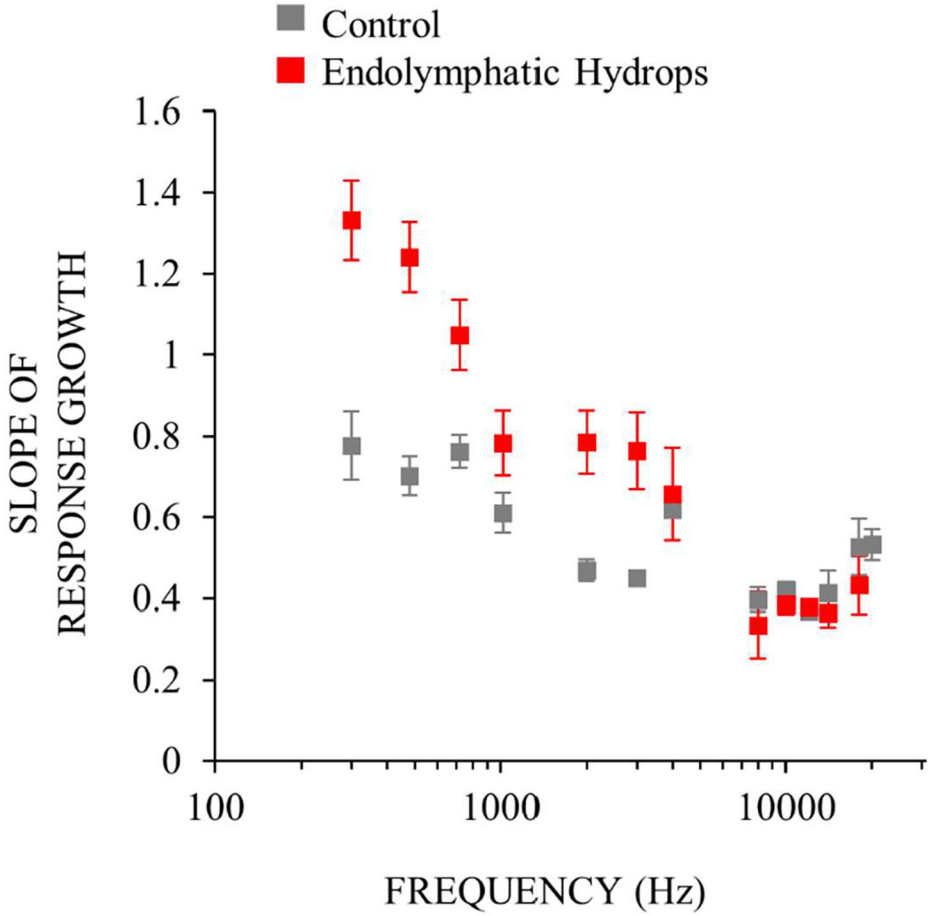

FIGURE 4 | Neural response recruitment quantified by the median slopes of response-amplitude vs. sound-level functions, vs. frequency. Points are medians. Error bars are one standard error of the mean. Data from ears with endolymphatic sac ablation are red, and from control ears are gray. Data are from the same measurements as **Figure 3**.

perfused HPBCD through three otherwise naïve cochleae, and measured cochlear function before and after the perfusions. HPBCD in low-doses (13 mM) has been shown to reduce OHC function while producing little or no change in IHC function or endocochlear potential (16). Auditory-nerve responses were used to quantify hearing threshold using ANOWs for low frequencies ($\leq$ 1 kHz) and CAPs for mid (2–4 kHz) and high frequencies (8–20 kHz). Thresholds were elevated relative to control for all frequencies tested (**Figure 8A**), consistent with our previous HPBCD data (16). DPOAEs and SFOAEs at frequencies $\geq$ 1 kHz were decreased at all tested frequencies (**Figures 8B,C**), again consistent with our previous HPBCD data (16). Overall, the effects of acute cochlear perfusions of low-dose HPBCD were consistent with the changes being due to a reduction of cochlear amplification (30).

Auditory-nerve response amplitudes were assessed over a wide range of sound levels in the three ears perfused with HPBCD. While HPBCD elevated neural thresholds throughout the frequency range of guinea pig hearing, response recruitment was seen only at low frequencies ($\leq$ 1 kHz). Post-perfusion thresholds were elevated but post-perfusion response amplitudes were similar to pre-perfusion amplitudes at high sound levels (**Figures 9A–D**). In contrast, post-perfusion measurements at mid- and high-frequencies had elevated thresholds and high-level amplitudes that were far below the range of pre-perfusion amplitudes (**Figures 9E–H**). Pre-perfusion responses were sometimes non-monotonic with sound level, but post-perfusion measurements were generally monotonic (**Figure 9**). The elevated neural thresholds and decreases in moderate-sound-level neural amplitudes in ears perfused with HPBCD are similar to our previous results (16); this is the first report of auditory-nerve responses evoked by *high sound levels* before and after HPBCD perfusion. In contrast to ears that had the endolymphatic sac removed (**Figure 2**), post-HPBCD-perfusion high-level response amplitudes were *not* hyper-responsive compared to control for any frequency tested (**Figure 9**).

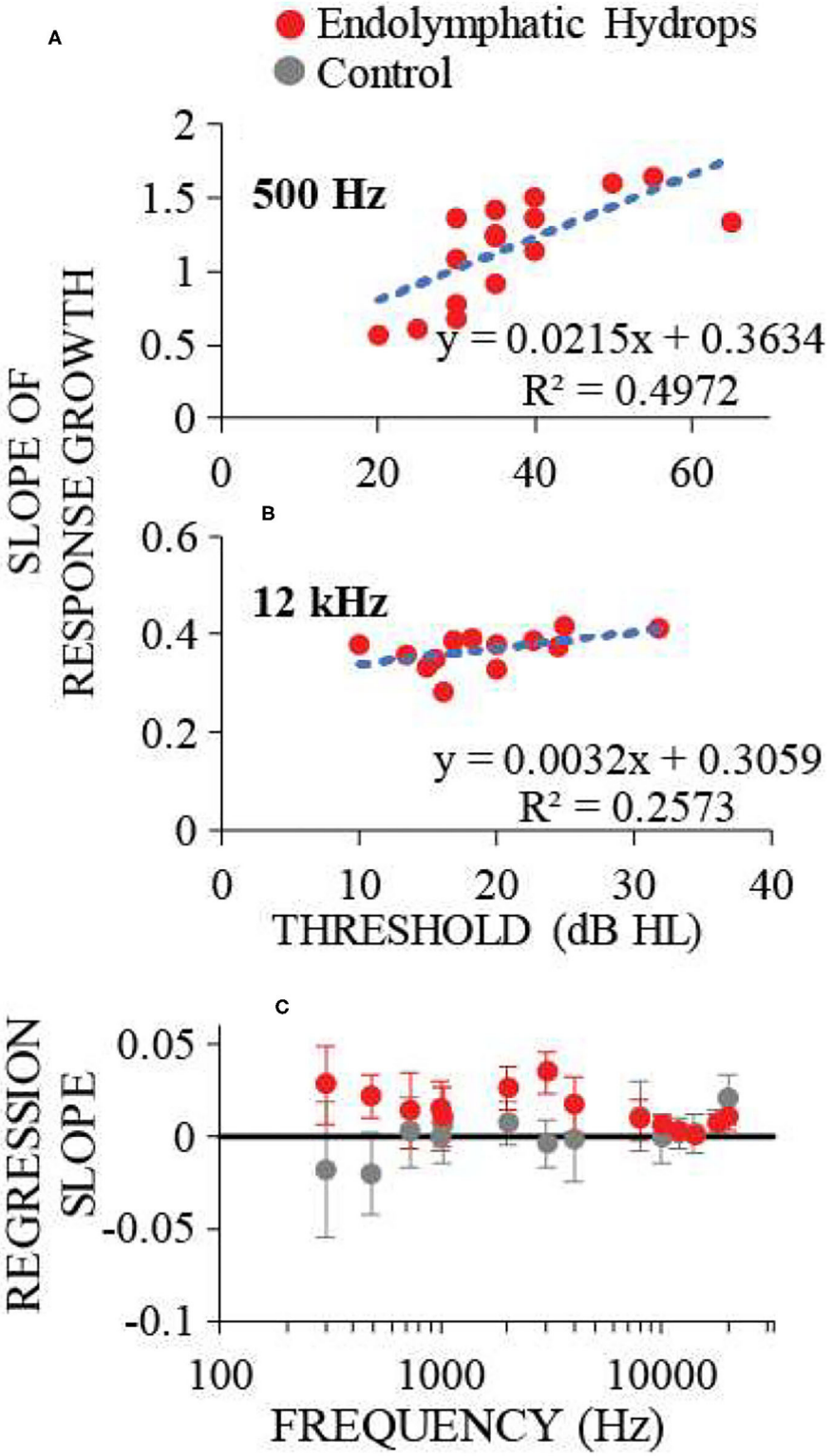

FIGURE 5 | The dependence on hearing threshold of the slope metric of response recruitment. **(A,B)** show the slope metric for response recruitment vs. the threshold of that ear at the test frequency, for two example frequencies with one point for each ear operated on to remove the endolymphatic sac. Dotted lines are linear regressions to the points; regression line coefficients and the R^2 value for the regression are shown at the panel lower right. **(C)** shows the regression-line slope coefficients averaged across ears for each frequency, for operated (red) and control (gray) ears. Error bars are 95% confidence intervals. Response recruitment varied with hearing threshold at low and mid frequencies where hearing thresholds were elevated, but not at high frequencies where hearing thresholds were within normal limits.

FIGURE 6 | Images of mid-modiolar sections from a guinea pig that survived 30 days after a surgery to ablate the endolymphatic sac on the right side. The scala media of the right cochlea (right column) was enlarged (red) compared to that in the normal left side (left column) scala media (blue). The scala-media areas are shown in color at top and, from the same cochleae, uncolored at bottom.

Recruitment in Operated Ears a Few Days After Endolymphatic Sac Ablation

In some animals, response recruitment was assessed a few days (i.e., 1, 2, or 4) following surgery to ablate the endolymphatic sac. Endolymphatic sac ablation produces endolymphatic hydrops that can be seen in histology at 30 postoperative days but not at a few postoperative days (12). In Lee et al. (12), we reported finding elevated hearing thresholds at low- and mid-frequencies in the first few postoperative days, and concluded that low- and mid-frequency hearing loss preceded histologically-verifiable endolymphatic hydrops. Here we address the question of whether response recruitment also precedes the development of histologically-verifiable hydrops.

In ears assessed a few days following surgery, response recruitment at low frequencies was generally present at all postoperative days (**Figure 10**). In operated ears, CAP responses to high-level, low- and mid-frequency sounds were occasionally hyper-responsive compared to controls (e.g., **Figure 10** at 500 Hz). In contrast, at high-frequencies response recruitment was not robustly present during the first few postoperative days. Overall these results show that endolymphatic sac ablation that causes low-frequency hearing loss and endolymphatic hydrops at 30 postoperative days, also produced response recruitment at low and mid frequencies during the first few postoperative days, even though endolymphatic hydrops cannot be seen in histology at this time.

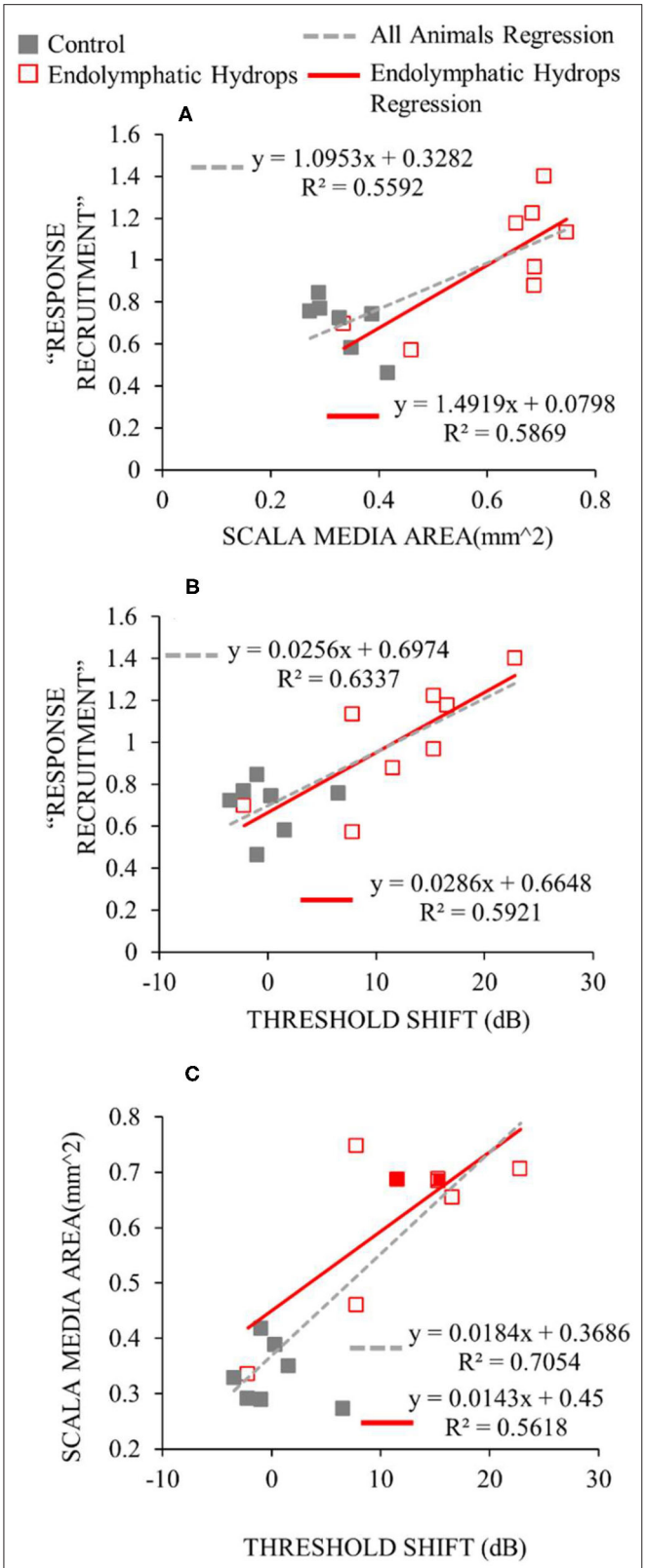

FIGURE 7 | Functional and histological assessments compared. For the y-axis of **(A,B)**, the median slopes of the response growths were averaged across low frequencies (≤ 1 kHz). For the x-axis of **(A)**, the scala media area was *(Continued)*

FIGURE 7 | averaged across turns in the apical cochlear half. For the x-axis of **(B,C)**, the threshold shift is the average threshold at low frequencies relative to the low-frequency average of the control ears. Data from operated ears are red and from control ears are gray. The red lines show the linear regressions to the data of the same color, while the gray dashed lines show the regressions to all the data from both control and operated ears. The linear regression parameters and the square of the Pearson's correlation coefficient are shown in each panel.

DISCUSSION

Response Recruitment Can Originate in the Cochlea

Our results show that response recruitment can have a cochlear origin and that perceptual loudness recruitment can result from attenuation of cochlear amplification. Before the results presented here, recruitment had not been convincingly shown in physiologic measurements from the auditory nerve (8, 9). Activation the medial olivocochlear efferent reflex produces recruitment in auditory-nerve CAP measurements [e.g., (31)]. However, in normal hearing, activation of medial olivocochlear efferents involves the auditory CNS, and efferent effects have not been considered as a demonstration of a cochlear origin of recruitment. The conclusion that the low-frequency response recruitment in **Figures 3**, **9** originated from reduced cochlear amplification rests critically on there being no dysfunction in the IHCs or their synapses with afferent auditory nerve fibers. Other reports have found hair cell and synaptic loss in ears 4–6 months after endolymphatic sac ablation (32, 33). In contrast, we have previously shown that endolymphatic hydrops does not affect IHCs, OHCs or counts of afferent synapses during the first 30 postoperative days (12, 14), which is consistent with results from human temporal bone studies of patients with Ménière's disease (22).

We assessed whether cochlear perfusions of low-dose HPBCD caused alterations of cochlear responses that are consistent with the toxicity being confined to the OHCs. Low-dose treatments of HPBCD are known to cause OHC dysfunction (16). While HPBCD elevated hearing thresholds throughout the frequency range of hearing, response recruitment occurred only at low frequencies with characteristic-frequency places in the apical half of the cochlea. It appears that acute low-dose HPBCD cochlear perfusions cause OHC-only dysfunction only in the apical cochlear half. A research question to be addressed is: do clinical patients with hearing loss from treatment with HPBCD, who had normal ears before treatment, have loudness recruitment for low-frequency sounds.

From an assessment of CAP waveforms, we found suggestive evidence that HPBCD may affect IHC function in the high-frequency basal cochlear half (16). This suggestive evidence of IHC dysfunction resulted from a 27 mM HPBCD concentration that was far higher than the 13 mM concentration used here (16). In some species, under some conditions, IHC loss has been reported following treatments with higher concentrations of HPBCD (e.g., 2,000 mg/kg delivered subcutaneously), but not with low HPBCD concentrations (34–36). In these other

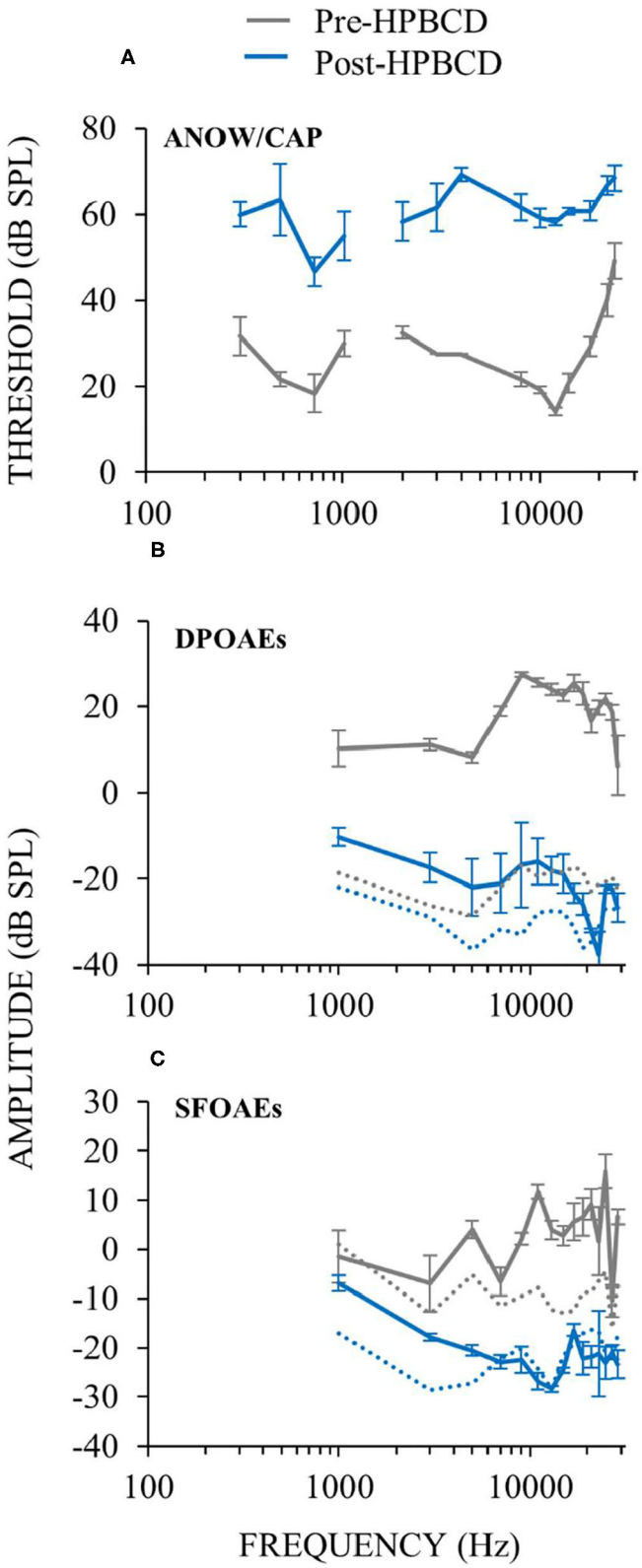

FIGURE 8 | Cochlear function measurements from before (gray) and after (blue) cochlear perfusion with HPBCD in artificial perilymph. Data are averages from three animals. Error bars are one standard error of the mean. HPBCD elevated hearing thresholds **(A)**, decreased DPOAEs **(B)** and decreased SFOAEs **(C)**. OAE noise floors (dotted lines in **B,C**) for pre-HPBCD measurements were higher than post-HPBCD treatment because a paralytic was administered after the pre-HPBCD measurements.

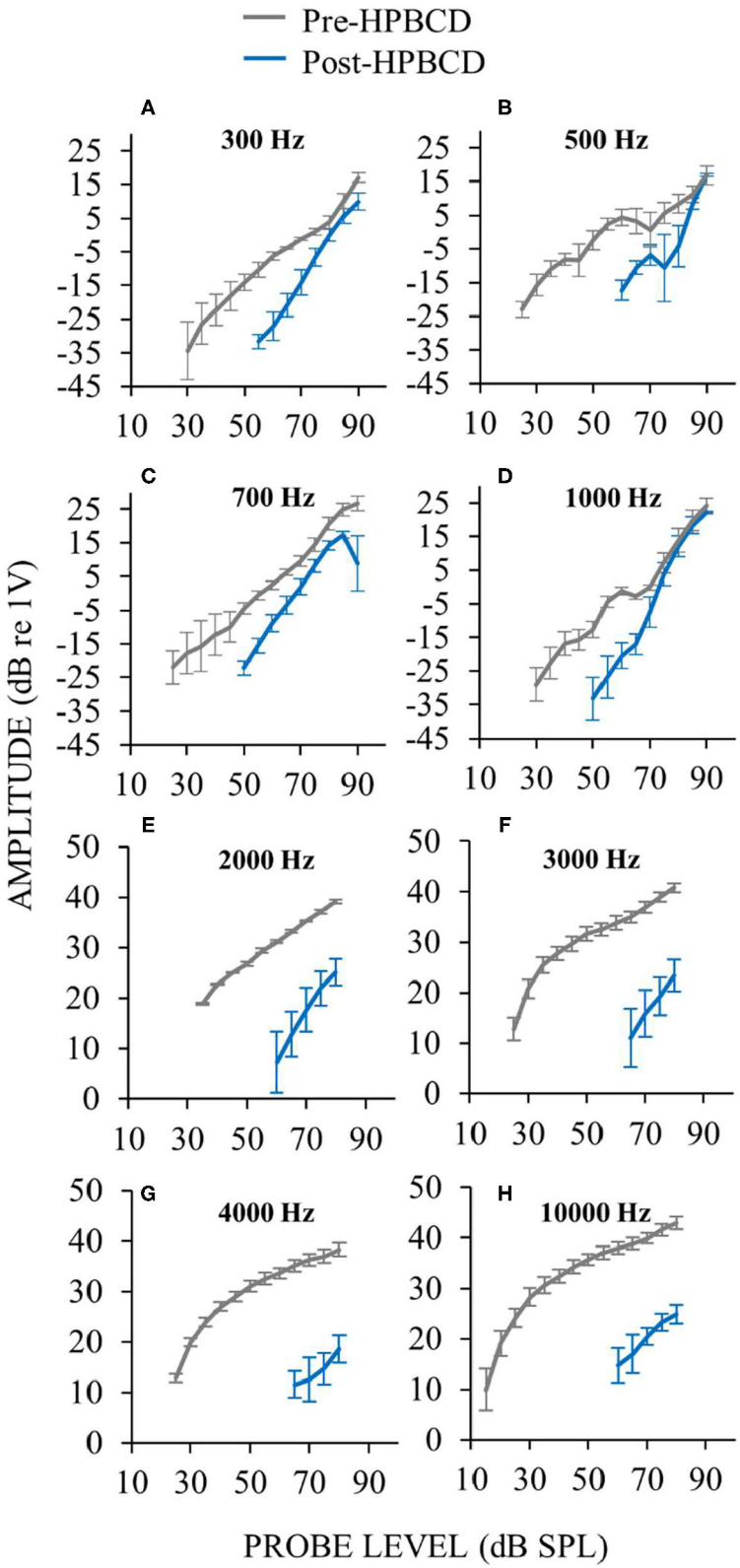

FIGURE 9 | Auditory-nerve responses over a wide range of frequencies and sound level before (gray) and after (blue) cochlear perfusion with 13 mM HPBCD. ANOW was used at low frequencies 300 Hz **(A)**, 500 Hz **(B)**, 700 Hz **(C)**, 1,000 Hz **(D)**, CAPs were used for mid and high frequencies 2,000 Hz **(E)**, 3,000 Hz **(F)**, and 4,000 Hz **(G)**. Only one exemplar high frequency plot is shown (10 kHz, **H**) because plots from all high frequencies were similar. Data are averages from three ears. Error bars are one standard error of the mean. Response recruitment was seen only at low frequencies.

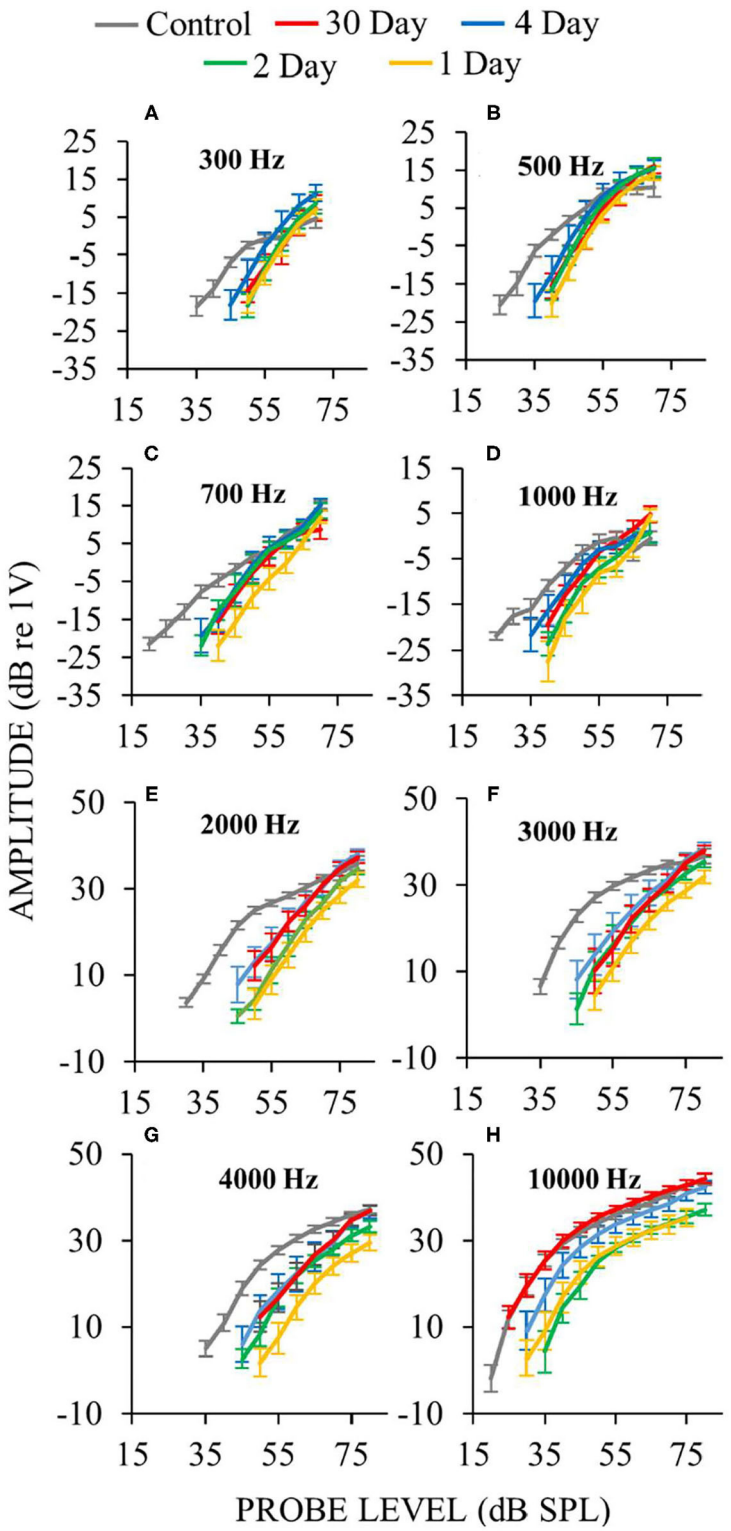

FIGURE 10 | Auditory-nerve response amplitudes vs. sound-level during the first few days following endolymphatic sac surgery. Low-frequency measurements were made with ANOWs at 300 Hz **(A)**, 500 Hz **(B)**, 700 Hz **(C)**, 1,000 Hz **(D)**, mid- and high- frequency measurements were made with CAPs at 2,000 Hz **(E)**, 3,000 Hz **(F)**, 4,000 Hz **(G)**, and 10,000 Hz **(H)**. Data from eight control animals that were either naïve or underwent a sham surgery. Error bars are one standard error of the mean. The number of ears used for ANOW measurements at 30, 4, 2, and 1 postoperative days are, respectively, 17, 10, 6, and 10. The number of ears used for CAP measurements at 30, 4, 2, and 1 postoperative days are respectively 14, 10, 6, and 10. Response recruitment can be seen at low frequencies during the earliest (1–4) postoperative days before endolymphatic hydrops has been detected, indicating that response recruitment can precede the development of histologically detectable endolymphatic hydrops.

reports, functionally meaningful IHC loss following high-dose HPBCD administration occurred in the high-frequency basal cochlear half, not the low-frequency apical cochlear half where we found response recruitment. Another study showed that the effects of HPBCD on IHC loss were not instantaneous, but were delayed by up to 8 weeks (36). These studies also found species differences with HPBCD treatment, although they did not assess low-frequency hearing (34–36). At present, there are no reports showing that acute low-dose HPBCD affects IHC structure or function in the low-frequency apical cochlear half. Overall, the low-frequency response recruitment we found in ears acutely treated with HPBCD is adequately explained by HPBCD affecting OHC function only.

Response Recruitment in the Auditory CNS

Following cochlear damage, measurements of CNS responses have shown that compensatory mechanism(s) in the CNS increase central-auditory gain such that responses to high-level sound can be restored to a near-normal loudness. The combination of hearing threshold elevation and central-gain increase can produce response recruitment [e.g., (37, 38)]. This response recruitment in the CNS has been interpreted as an origin perceptual loudness recruitment that is an alternative to, or in addition to, a cochlear origin (39). Measurements from the cochlear nucleus following acoustic trauma showed that, at high sound levels, neurons with "chopper" excitation properties had firing rates that were within, or sometimes greater than, normal values, which suggests that the cochlear nucleus is the most caudal origin of CNS-based changes that give rise to recruitment (40). Following destruction of IHCs or auditory nerve fibers by neurotoxic drugs, inferior colliculus field potentials were reduced less than those from the auditory nerve, which points to at least a partial recruitment mechanism between the periphery and midbrain (41–43). After almost complete ototoxic destruction of IHCs or auditory nerve fibers, measurements from the auditory cortex can be within normal limits, or even hyper-responsive, which shows adaptive restoration of responses in the auditory CNS (41, 42, 44). Together, these results suggest that the neuronal signal from a damaged cochlea is progressively amplified as it is relayed up through the CNS to the auditory cortex. The experimental manipulations used by investigators when measuring auditory-CNS responses, such as acoustic trauma and ototoxic drugs, have also been shown to be associated with or cause *behavioral* manifestations of loudness recruitment or hyperacusis (38, 45–47). In summary, an increase in central gain may be a source of loudness recruitment. We do not dispute the interpretation that recruitment can originate in the CNS. However, studies showing CNS recruitment do not rule out that recruitment can also have a cochlear origin.

Larger-Than-Normal Responses and Hyperacusis

In ears with endolymphatic hydrops stimulated at low-frequencies and at high sound levels, we occasionally found that gross neural responses were larger than control responses (e.g., **Figure 3**, 500 Hz and 1 kHz, and **Figure 10**, 300 Hz and 500 Hz). Responses to loud sounds that are larger than normal have been interpreted as showing hyperacusis, i.e., uncomfortably loud or painful responses [e.g., (38, 41, 48)]. Compared to control responses, it is unclear exactly how much higher a response must be before accurate identification of hyperacusis is achieved. The relationship between physiologic response measurements and the perception of loudness is not completely understood, nor is the relationship between behavioral measurements and hyperacusis [e.g., (49)]. Perhaps response measurements throughout the entire auditory system need to be considered to fully assess the physiology of perceptual loudness. Measurements from the auditory efferents could also be considered in such an assessment, as they play a role in the perception of loudness, recruitment, hyperacusis, and hyper-responsiveness related to tinnitus (50, 51).

CLINICAL IMPLICATIONS

Clinical measurement that objectively quantify loudness recruitment could be helpful to differentially diagnose endolymphatic hydrops, and to track the progression of the condition as it worsens or improves from treatment. Our data provide some guidance for how to use loudness measurements. First, ear-specific (not binaural) loudness measurements should be made, since most patients with endolymphatic hydrops are unilaterally affected, and binaural-based assessment would involve the better ear. Second, for the assessment of endolymphatic hydrops, physiologic measurements of *cochlear* recruitment may be more useful than measurements of behavioral recruitment, considering that the auditory central auditory nervous system can be a source recruitment and this could obscure cochlear recruitment [e.g., (37, 40, 41)]. It is not known how recruitment in the cochlea vs. in the CNS influences overall recruitment. Third, loudness recruitment measurements should be done only at those frequencies that have hearing threshold elevation. At frequencies not associated with elevated hearing threshold, the slope of our response amplitude-by-sound-level functions did not differ from control (**Figures 3**, **4**). This indicates that clinicians should not test everyone with the same, or standard, frequencies because a patient might not have hearing loss (and thus not cochlear loudness recruitment) at that frequency. Forth, to identify a condition that affects the perception of loudness by attenuating cochlear amplification, OAEs alone are probably not helpful. While it has been shown that the "disparate OAE profile" (DPOAE amplitudes are reduced while SFOAE amplitudes are normal) may identify ears with endolymphatic hydrops and Ménière's disease cf. (12, 14, 52), it is not understood how OAEs from diseased ears can be used to objectively assess the perception of loudness. Fifth, cochlear microphonic measurements do not entirely originate from OHC physiologic responses (18, 53), which reduces their value for determining response recruitment. In summary, our results indicate that the combination of low-frequency hearing loss and loudness recruitment should be helpful to early identify endolymphatic hydrops and assess its severity once it develops.

Measurements of loudness recruitment should be useful in patients with Ménière's disease, considering that Ménière's patients often experience the effects of loudness recruitment. It is widely known that fitting hearing aids to patients with

Ménière's disease is challenging because of their reduced dynamic range [e.g., (54, 55)]. Approaches to quantify loudness need to be developed that can be used consistently across laboratories and clinics (56). These approaches should take into account the factors outlined in the previous paragraph and the results shown in our figures.

DATA AVAILABILITY STATEMENT

The original contributions presented in the study are included in the article/supplementary material, further inquiries can be directed to the corresponding authors.

ETHICS STATEMENT

The animal study was reviewed and approved by Washington University Institutional Animal Care and Use Committee.

AUTHOR CONTRIBUTIONS

JG and JL conceived experiment. SL, SG, and JL collected data. SL, RD, SG, JG, and JL interpreted results, wrote the manuscript, and approved the manuscript. JL drafted the manuscript. All authors contributed to the article and approved the submitted version.

FUNDING

Research reported in this publication was supported by the National Institute of Deafness and Other Communication Disorders within the National Institutes of Health R01 DC014997 (JL).

REFERENCES

1. Jerger J, Shedd JL, Harford E. On the detection of extremely small changes in sound intensity. *AMA Arch Otolaryngol.* (1959) 69:200–11. doi: 10.1001/archotol.1959.00730030206015
2. Buus S, Florentine M. Growth of loudness in listeners with cochlear hearing losses: recruitment reconsidered. *J Assoc Res Otolaryngol.* (2002) 3:120–39. doi: 10.1007/s101620010084
3. Moore BC. Testing the concept of softness imperception: loudness near threshold for hearing-impaired ears. *J Acoust Soc Am.* (2004) 115:3103–11. doi: 10.1121/1.1738839
4. Robles L, Ruggero MA. Mechanics of the mammalian cochlea. *Physiol. Rev.* (2001) 81:1305–52. doi: 10.1152/physrev.2001.81.3.1305
5. Ota T, Nin F, Choi S, Muramatsu S, Sawamura S, Ogata G, et al. Characterization of the static offset in the travelling wave in the cochlear basal turn. *Pflugers Arch.* (2020) 472:625–35. doi: 10.1007/s00424-020-02373-6
6. Zhang M, Zwislocki JJ. OHC response recruitment and its correlation with loudness recruitment. *Hearing Res.* (1995) 85:1–10. doi: 10.1016/0378-5955(95)00026-Z
7. Preyer S, Gummer AW. Nonlinearity of mechanoelectrical transduction of outer hair cells as the source of nonlinear basilar-membrane motion and loudness recruitment. *Audiol Neurootol.* (1996) 1:3–11. doi: 10.1159/000259185
8. Heinz MG, Issa JB, Young ED. Auditory-nerve rate responses are inconsistent with common hypotheses for the neural correlates of loudness recruitment. *J Assoc Res Otolaryngol.* (2005) 6:91–105. doi: 10.1007/s10162-004-5043-0
9. Sheppard A, Hayes SH, Chen GD, Ralli M, Salvi R. Review of salicylate-induced hearing loss, neurotoxicity, tinnitus and neuropathophysiology. *Acta Otorhinolaryngol Ital.* (2014) 34:79–93.
10. Ruel J, Chabbert C, Nouvian R, Bendris R, Eybalin M, Leger CL, et al. Salicylate enables cochlear arachidonic-acid-sensitive NMDA receptor responses. *J Neurosci.* (2008) 28:7313–23. doi: 10.1523/JNEUROSCI.5335-07.2008
11. Liberman MC, Dodds LW. Single-neuron labeling and chronic cochlear pathology. III. Stereocilia damage and alterations of threshold tuning curves. *Hear Res.* (1984) 16:55–74. doi: 10.1016/0378-5955(84)90025-X
12. Lee C, Valenzuela CV, Goodman SS, Kallogjeri D, Buchman CA, Lichtenhan JT. Early detection of endolymphatic hydrops using the auditory nerve overlapped waveform (ANOW). *Neuroscience.* (2020) 425:251–66. doi: 10.1016/j.neuroscience.2019.11.004
13. Valenzuela CV, Lee C, Buchman CA, Lichtenhan JT. Revised surgical approach to induced endolymphatic hydrops in the guinea pig. *J of Visualized Experiments.* (2020) 4:160. doi: 10.3791/60597
14. Valenzuela CV, Lee C, Mispagel A, Bhattacharyya A, Lefler SM, Payne S, et al. Is cochlear synapse loss an origin of low-frequency hearing loss associated with endolymphatic hydrops? *Hearing Res.* (2020) 398:108099. doi: 10.1016/j.heares.2020.108099
15. Crumling MA, Liu L, Thomas PV, Benson J, Kanicki A, Kabara L, et al. Hearing loss and hair cell death in mice given the cholesterol-chelating agent hydroxypropyl-beta-cyclodextrin. *PLoS ONE.* (2012) 7:e53280. doi: 10.1371/journal.pone.0053280
16. Lichtenhan JT, Hirose K, Buchman CA, Duncan RK, Salt AN. Direct administration of 2-Hydroxypropyl-Beta-Cyclodextrin into guinea pig cochleae: effects on physiological and histological measurements. *PLoS ONE.* (2017) 12:e0175236. doi: 10.1371/journal.pone.0175236
17. Salt AN, Lichtenhan JT, Gill RM, Hartsock JJ. Large endolymphatic potentials from low-frequency and infrasonic tones in the guinea pig. *J Acoust Soc of Am.* (2013) 133:1561–71. doi: 10.1121/1.4789005
18. Lichtenhan JT, Hartsock JJ, Gill RM, Guinan JJ Jr, Salt AN. The auditory nerve overlapped waveform (ANOW) originates in the cochlear apex. *J Assoc Res Otolaryngol.* (2014) 15:395–411. doi: 10.1007/s10162-014-0447-y
19. Lichtenhan JT, Hartsock J, Dornhoffer JR, Donovan KM, Salt AN. Drug delivery into the cochlear apex: improved control to sequentially affect finely spaced regions along the entire length of the cochlear spiral. *J Neurosci Methods.* (2016) 273:201–9. doi: 10.1016/j.jneumeth.2016.08.005
20. Lee C, Guinan JJ, Rutherford MA, Kaf WA, Kennedy KM. Cochlear compound action potentials from high-level tone bursts originate from wide cochlear regions that are offset toward the most sensitive cochlear region. *J Neurophysiol.* (2019) 121:1018–33. doi: 10.1152/jn.00677.2018
21. Goodman SS, Lee C, Guinan JJ, Lichtenhan JT. The spatial origins of cochlear amplification assessed by stimulus-frequency otoacoustic emissions. *Biophys J.* (2020) 118:1183–95. doi: 10.1016/j.bpj.2019.12.031
22. Nadol JB. Disorders of unknown or multiple causes. In: Merchant SN, Nadol JB, editor, *Schuknecht's Pathology of the Ear, 3rd Edn.* Shelton, CT: People's Medical Publishing House (2010). p. 572–630.
23. Humphrey R. *Playrec Version 2.1. 1.* 11 (2015).
24. Keefe DH. Double-evoked otoacoustic emissions. I. Measurement theory and nonlinear coherence. *J Acoust Soc Am.* (1998) 103:3489–98. doi: 10.1121/1.423057
25. Keefe DH, Ling R. Double-evoked otoacoustic emissions. II. Intermittent noise rejection, calibration and ear-canal measurements. *J Acoust Soc Am.* (1998) 103:3499–508. doi: 10.1121/1.423058
26. Schairer KS, Fitzpatrick D, Keefe DH. Input-output functions for stimulus-frequency otoacoustic emissions in normal-hearing adult ears. *J Acoust Soc Am.* (2003) 114:944–66. doi: 10.1121/1.1592799
27. Lichtenhan JT, Cooper NP, Guinan JJ. A new auditory threshold estimation technique for low frequencies: proof of concept. *Ear and Hear.* (2013) 34:42. doi: 10.1097/AUD.0b013e31825f9bd3
28. Goodman SS, Fitzpatrick DF, Ellison JC, Jesteadt W, Keefe DH. High-frequency click-evoked otoacoustic emissions and behavioral thresholds in humans. *J Acoust Soc Am.* (2009) 125:1014–32. doi: 10.1121/1.3056566

29. Tsuji J, Liberman MC. Intracellular labeling of auditory nerve fibers in guinea pig: central and peripheral projections. *J Comp Neurol.* (1997) 381:188–202. doi: 10.1002/(SICI)1096-9861(19970505)381:2<188::AID-CNE6>3.0.CO;2-#
30. Takahashi S, Homma K, Zhou Y, Nishimura S, Duan C, Chen J, et al. Susceptibility of outer hair cells to cholesterol chelator 2-hydroxypropyl-β-cyclodextrine is prestin-dependent. *Sci Rep.* (2016) 23:6:21973. doi: 10.1038/srep21973
31. Gifford ML, Guinan JJ Jr. Effects of electrical stimulation of medial olivocochlear neurons on ipsilateral and contralateral cochlear responses. *Hear Res.* (1987) 29:179–94. doi: 10.1016/0378-5955(87)90166-3
32. Bixenstine PJ, Maniglia MP, Vasanji A, Alagramam KN, Megerian CA. Spiral ganglion degeneration patterns in endolymphatic hydrops. *Laryngoscope.* (2008) 118:1217–23. doi: 10.1097/MLG.0b013e31816ba9cd
33. Momin SR, Melki SJ, Alagramam KN, Megerian CA. Spiral ganglion loss outpaces inner hair cell loss in endolymphatic hydrops. *Laryngoscope.* (2010) 120:159–65. doi: 10.1002/lary.20673
34. Liu X, Ding D, Chen GD, Li L, Jiang H. 2-hydroxypropyl-β-cyclodextrin ototoxicity in adult rats: rapid onset and massive destruction of both inner and OHCs above a critical dose. *Neurotox Res.* (2020) 38:808–23. doi: 10.1007/s12640-020-00252-7
35. Ding D, Manohar S, Jiang H, Salvi R. Hydroxypropyl-β-cyclodextrin causes massive damage to the developing auditory and vestibular system. *Hear Res.* (2020) 396:108073. doi: 10.1016/j.heares.2020.108073
36. Ding D, Jiang H, Salvi R. Cochlear spiral ganglion neuron degeneration following cyclodextrin-induced hearing loss. *Hear Res.* (2021) 400:108125. doi: 10.1016/j.heares.2020.108125
37. Resnik J, Polley DB. Fast-spiking GABA circuit dynamics in the auditory cortex predict recovery of sensory processing following peripheral nerve damage. *Elife.* (2017) 6:e21452. doi: 10.7554/eLife.21452
38. Auerbach BD, Radziwon K, Salvi R. Testing the central gain model: loudness growth correlates with central auditory gain enhancement in a rodent model of hyperacusis. *Neuroscience.* (2019) 407:93–107. doi: 10.1016/j.neuroscience.2018.09.036
39. Salvi R, Auerbach BD, Lau C, Chen, Y.-C., Manohar S, et al. Functional neuroanatomy of salicylate- and noise-induced tinnitus and hyperacusis. *Curr Top Behav Neurosci.* (2020) 51:133–60. doi: 10.1007/7854_2020_156
40. Cai S, Ma WL, Young ED. Encoding intensity in ventral cochlear nucleus following acoustic trauma: implications for loudness recruitment. *J Assoc Res Otolaryngol.* (2009) 10:5–22. doi: 10.1007/s10162-008-0142-y
41. Chambers AR, Resnik J, Yuan Y, Whitton JP, Edge AS, Liberman MC, et al. Central gain restores auditory processing following near-complete cochlear denervation. *Neuron.* (2016) 89:867–79. doi: 10.1016/j.neuron.2015.12.041
42. Salvi R, Sun W, Ding D, Chen GD, Lobarinas E. Inner hair cell loss disrupts hearing and cochlear function leading to sensory deprivation and enhanced central auditory gain. *Front Neurosci.* (2017) 10:621. doi: 10.3389/fnins.2016.00621
43. Wake M, Takeno S, Mount RJ, Harrison RV. Recording from the inferior colliculus following cochlear inner hair cell damage. *Acta Otolaryngol.* (1996) 116:714–20. doi: 10.3109/00016489609137912
44. Qiu C, Salvi R, Ding D, Burkard R. Inner hair cell loss leads to enhanced response amplitudes in auditory cortex of unanesthetized chinchillas: evidence for increased system gain. *Hear Res.* (2000) 139:153–71. doi: 10.1016/S0378-5955(99)00171-9
45. Sun W, Deng A, Jayaram A, Gibson B. Noise exposure enhances auditory cortex responses related to hyperacusis behavior. *Brain Res.* (2012) 1485:108–16. doi: 10.1016/j.brainres.2012.02.008
46. Chen G, Lee C, Sandridge SA, Butler HM, Manzoor NF, Kaltenbach JA. Behavioral evidence for possible simultaneous induction of hyperacusis and tinnitus following intense sound exposure. *J Assoc Res Otolaryngol.* (2013) 14:413–24. doi: 10.1007/s10162-013-0375-2
47. Zhang C, Flowers E, Li JX, Wang Q, Sun W. Loudness perception affected by high doses of salicylate-A behavioral model of hyperacusis. *Behav Brain Res.* (2014) 271:16–22. doi: 10.1016/j.bbr.2014.05.045
48. Auerbach BD, Rodrigues PV, Salvi RJ. Central gain control in tinnitus and hyperacusis. *Front Neurol.* (2014) 5:206. doi: 10.3389/fneur.2014.00206
49. Knudson IM, Melcher JR. Elevated acoustic startle responses in humans: relationship to reduced loudness discomfort level, but not self-report of hyperacusis. *J Assoc Res Otolaryngol.* (2016) 17:223–35. doi: 10.1007/s10162-016-0555-y
50. Knudson IM, Shera CA, Melcher JR. Increased contralateral suppression of otoacoustic emissions indicates a hyperresponsive medial olivocochlear system in humans with tinnitus and hyperacusis. *J Neurophysiol.* (2014) 112:3197–208. doi: 10.1152/jn.00576.2014
51. Wilson US, Sadler KM, Hancock KE, Guinan JJ Jr, Lichtenhan JT. Efferent inhibition strength is a physiological correlate of hyperacusis in children with autism spectrum disorder. *J Neurophysiol.* (2017) 118:1164–72. doi: 10.1152/jn.00142.2017
52. Abdala C, Suresh C, Luo P, Shera CA. Developing a join SFOAE + DPOAE diagnostic profile. *Asso. Res. Otolaryngol. Abstr.* (2020) 493:307.
53. Chertoff ME, Kamerer AM, Peppi M, Lichtenhan JT. An analysis of cochlear response harmonics: contribution of neural excitation. *J Acoust Soc Am.* (2015) 138:2957–63. doi: 10.1121/1.4934556
54. Valente M, Mispagel K, Valente LM, Hullar T. Problems and solutions for fitting amplification to patients with Ménière's disease. *J Am Acad Audiol.* (2006) 17:6–15. doi: 10.3766/jaaa.17.1.2
55. Basura GJ, Adams ME, Monfared A, Schwartz SR, Antonelli PJ, Burkard R, et al. Clinical practice guideline: ménière's disease executive summary. *Otolaryngol Head Neck Surg.* (2020) 162:415–34. doi: 10.1177/0194599820909439
56. Punch J, Joseph A, Rakerd B. Most comfortable and uncomfortable loudness levels: six decades of research. *Am J Audiol.* (2004) 13:144–57. doi: 10.1044/1059-0889(2004/019)

Conflict of Interest: The authors declare that the research was conducted in the absence of any commercial or financial relationships that could be construed as a potential conflict of interest.

Publisher's Note: All claims expressed in this article are solely those of the authors and do not necessarily represent those of their affiliated organizations, or those of the publisher, the editors and the reviewers. Any product that may be evaluated in this article, or claim that may be made by its manufacturer, is not guaranteed or endorsed by the publisher.

frontiers in Surgery

ORIGINAL RESEARCH
published: 22 October 2021
doi: 10.3389/fsurg.2021.672865

The Additional Value of Endolymphatic Hydrops Imaging With Intratympanic Contrast for Diagnostic Work-Up—Experience From a Neurotology Center in Austria

Lennart Weitgasser[1]*, *Anna O'Sullivan*[1,2], *Alexander Schlattau*[3] and *Sebastian Roesch*[1]

[1] Department of Otorhinolaryngology, Head and Neck Surgery, Paracelsus Medical University, Salzburg, Austria, [2] Institute of Experimental Neuroregeneration, Paracelsus Medical University, Salzburg, Austria, [3] Department of Radiology, Paracelsus Medical University, Salzburg, Austria

OPEN ACCESS

Edited by:
Robert Gürkov,
Bielefeld University, Germany

Reviewed by:
Katharina Stölzel,
University Medical Center Hamburg-Eppendorf, Germany
Maksym Situkho,
Kolomiychenko Otolaryngology Institute of National Academy of Medical Sciences, Ukraine

***Correspondence:**
Lennart Weitgasser
l.weitgasser@salk.at

Specialty section:
This article was submitted to Otorhinolaryngology - Head and Neck Surgery, a section of the journal Frontiers in Surgery

Received: 26 February 2021
Accepted: 27 September 2021
Published: 22 October 2021

Citation:
Weitgasser L, O'Sullivan A, Schlattau A and Roesch S (2021) The Additional Value of Endolymphatic Hydrops Imaging With Intratympanic Contrast for Diagnostic Work-Up—Experience From a Neurotology Center in Austria. Front. Surg. 8:672865. doi: 10.3389/fsurg.2021.672865

Objective: To illustrate the merit of hydrops imaging during clinical workup of dizziness and balance disorders.

Background: Ever since the first description of *in-vivo* endolymphatic hydrops imaging in 2007, this diagnostic tool has been implemented in an increasing number of centers. The more experience in its clinical application is gathered, the more it is possible to critically assess its potential value for the diagnostic workup. This article intends to provide information about the experience of handling and utilization of endolymphatic hydrops imaging in one of the first centers in Austria.

Methods: Retrospective analysis and review of clinical cases.

Results: Based on our experience of endolymphatic hydrops imaging (EHI), which was established in cooperation between our departments of radiology and otorhinolaryngology in 2017, we have exclusively used intratympanic application of a contrast agent prior to magnetic resonance imaging, as this approach provides high quality imaging results. In 42.6% of cases, EHI could lead to the diagnosis of MD or HED. Since precise vestibular examination is still necessary, EHI is not a tool to replace the clinical examination but rather to add significantly to the interpretation of the results.

Conclusion: Endolymphatic hydrops imaging represents a valuable, safe and well-applicable tool for evaluating cases with inconclusive clinical results. However, its potential additional diagnostic benefits rely on a correct indication based on prior thorough vestibular investigations.

Keywords: hydrops, imaging, dizziness, vertigo, Menière, magnetic resonance imaging, intratympanic

INTRODUCTION

The diagnostic work-up of recurrent vestibular disorders still represents a challenging task, due to their variable clinical presentation or inconsistent diacritic results. Symptomatic and historically based classification systems may be helpful tools, especially in Menière's disease (MD) with its classical triad of rotatory vertigo, low-frequency hearing loss as well as tinnitus or aural fullness.

However, in several cases symptoms do not present themselves in a way such that a satisfactory conclusion is possible. Vestibular and cochlear manifestations may occur completely independent from each other but also monosymptomatic forms of the disease seem to be existent.

Endolymphatic hydrops represents the anatomical correlate of a multifaceted clinical picture and provides a common ground for different perspectives on the actual cause and pathophysiology in the context of MD and diseases of the human labyrinth.

Ever since the first description of the visualization of endolymphatic hydrops in 2005 by Zou et al. (1), the scientific interest and the number of publications in this field have been constantly growing.

Contrast-enhanced, high-resolution magnetic resonance imaging (MRI) is capable of visualizing the endolymphatic hydrops (ELH) *in-vivo*, which reveals the pathophysiological basis of the clinical syndrome originally described by Prosper Menière (2–4). Based not only on symptomatic but also on imaging characteristics, a new terminology was proposed (5, 6) to sum up this spectrum of disorders as "Hydropic Ear Disease" (HED).

In our clinic, we began performing specific MRI (named "hydrops MRI") in patients with suspected ELH in 2017. Before this time, we generally referred to typical symptoms of MD and occasionally used electrocochleography for the diagnostic work-up. The introduction of hydrops MRI has enabled us to improve the diagnostic accuracy and subsequent care for patients with recurrent vestibular symptoms.

The purpose of this article is to illustrate the establishment and application of hydrops imaging at a tertiary neurotology referral center and critically evaluate its potential benefits for diagnostics.

MATERIALS AND METHODS

Course of Action and Decision-Making Prior to Hydrops Imaging

The selection of patients for hydrops imaging at our center is based on the following criteria and preconditions:

Potential candidates are adult patients, presenting with typical symptoms, suspicious for HED, according to the 1995 AAO-HNS Guidelines and the Equilibrium Committee Amendment (7, 8). Clinical presentation is supposed to include recurrent episodes of rotatory vertigo, lasting for minutes to hours and/or aural symptoms like fullness, tinnitus and sensorineural hearing loss (SNHL), ideally audiometrically documented. However, as it is well-known that symptoms may occur completely independent from each other and to a variable in extend, a simultaneous presence cannot be expected in every patient. Therefore, the diagnostic evaluation may not be straight-forward.

Patients chosen for hydrops imaging are those with symptoms, suspicious of ELH, indecisive diagnostic results and first referral at our center. However, patients with distinct clinical symptoms for years, clearly fulfilling diagnostic criteria for MD, and comprehensive diagnostic results do not qualify for hydrops imaging, since additional diagnostic value for the individual is not expected.

The first diagnostic step for this group of patients remains history taking and distinct vestibular examination. Other causes of vestibular dysfunction or vestibular disease, as well as diseases of the central nervous system initially need to be excluded. We therefore rely on the execution of the HINTS exam, followed by subsequent otoscopy, audiometric and vestibular investigations, such as videonystagmography (VNG), video-head-impulse-test (vHIT) and vestibular evoked myogenic potentials (VEMPs) testing. Moreover, neurological and, if necessary, psychological investigations are performed by the appropriate departments.

Pre-interventional Arrangements

At our center, the application of the contrast medium for displaying the perilymphatic space during the MRI is administered exclusively intratympanically. Therefore, the definition of an "index ear" is mandatory. This definition is based on previous clinical and diagnostic findings, which consist of laterality of low-frequency hearing loss, tinnitus or aural fullness, missing caloric response during VNG and/or decreased VEMPs. In case of bilateral symptoms, the side more severely affected is selected.

Clinical circumstances representing a contraindication for intratympanic administration of any agent, such as acute otitis media or recent trauma or surgery, need to be excluded prior to application.

Informed consent is obtained, including specifically, the information about an "off-label use" of the contrast agent being applied intratympanically.

Intratympanic Application of the Contrast Agent

Gadoteric acid with a concentration of 279.3 mg/ml is diluted 1:10 with a sodium chloride 0.9% isotonic solution. Around 20 min prior to intratympanic administration, a solution of 10% lidocaine is applied to the tympanic membrane and the auditory canal, providing fully coverage (e.g., by pump spray or directly poured). Lidocaine will be completely removed by suction, subsequently. A volume of 0.4–0.5 ml of the diluted gadoteric acid is then administered through the anterior/superior quadrant of the tympanic membrane into the middle ear. Patients remain lying with their head turned to the contralateral side for 30 min after application and are advised not to speak to reduce an efflux of contrast fluid through the Eustachian tube. The MRI is performed the following day, but within 24 h after application of the contrast agent.

An audiometric control to exclude potential harm on inner ear function through the contrast agent or noise-exposure through MRI is performed routinely within 7 days of examination.

MRI Technique and Evaluation Process

Radiological evaluation is performed with a 3 Tesla MR machine (Achieva, Philips Medical Systems™). Interpretation of all imaging results have been carried out by the same radiologist—author A.S. The acquired sequences are a coronal fluid attenuated inversion recovery (FLAIR, slice thickness 4 mm), an axial T1 (2.0 mm) and diffusion weighted imaging (DWI, slice thickness 4 mm, b:0, b:1000, ADC maps) over the whole neurocranium

for general diagnostic purposes (i.e., to exclude stroke or other cerebral pathologies). An isometric post contrast axial T1 black blood sequence (voxel size 0.8 mm) is performed for general diagnostic purposes (i.e., to exclude vestibular schwannoma) and for the inner ear an isometric axial T2 (1.0 mm voxel size). Our diagnostic "Menière" sequence is an isometric inversion recovery sequence (T1 weighted, voxel size 0.8 mm, TE: 354 ms, TR: 7,600 ms), which shows contrast enhancement of the perilymphatic structures of the vestibular system and the cochlea after intratympanic contrast agent administration. ELH is displayed indirectly as peripherally displaced or missing enhancement of the structures (**Figure 1**). The radiologist reports on the likeliness of ELH and if presumed positive, the anatomical sites affected. In order to provide comprehensible data, imaging results were reviewed and in case of ELH, the grading system of Baráth et al. (9) was applied to the results (**Table 1**).

RESULTS

Since 2017 we performed endolymphatic hydrops imaging (EHI) in 13 patients (6 female, 7 male), aged between 34 and 76 (mean 54.7 years) at the time of examination. Median duration of symptoms was 12 months. Mean pure-tone average for frequencies 500, 1,000, 2,000 and 4,000 Hz on the index ear was 43.5 dB HL. ELH was detected in six patients (46.2%). In seven patients (53.8%), no sign of ELH was apparent. In one case, analysis could not be performed appropriately due to technical problems. In this specific case the "black-blood sequence" was analyzed but showed no sign of ELH. Intratympanic application of contrast agent has been well-tolerated by all patients. Except slight, self-limiting vertigo during or shortly after its application in some patients, no side effects have been reported. Audiometric follow-up, around 7 days after intervention, showed no worsening of hearing thresholds. In all confirmed cases, ELH was located in both, the cochlea and the vestibule.

Referring to the proposed classification from Gürkov et al. (5, 6) for HED, we assigned the six patients with confirmed ELH to a group based on their individual anamnesis and symptoms. Consequently, five patients were classified as certain primary endolymphatic hydrops (PHED) of the cochleo-vestibular type and one patient as the cochlear type. In the group without confirmed ELH, six patients showed symptoms appropriate to the cochleo-vestibular type and one patient to the cochlear type. **Table 1** shows a summary of the patients' individual symptoms and clinical data.

DISCUSSION

We consider the right selection of patients for endolymphatic hydrops imaging (EHI) as crucial for meaningful results. Until now, we performed EHI in selected patients with unclear, recurring vestibular and/or cochlear symptoms, where allocation of symptoms to a specific disease was not possible on a sole clinical basis. In accordance with recent literature (6) we try to avoid nomenclature like "atypical" MD, by focusing on the potential pathophysiological background with the help of EHI.

We did not define a specific period of symptom duration before undertaking EHI, yet. To date, we are performing EHI only for initial diagnosis and do not use it for follow-up examinations. Moreover, in patients with typical symptoms of MD, who already had a cerebellopontine angle MRI, we do not repeat specific EHI. If MRI results are not present thus far (and in general every patient with "idiopathic" vestibular or cochlear symptoms should get an MRI at least once), EHI can be added with the patient's approval.

The established methods for contrast agent administration are the intravenous or intratympanic application. We prefer the intratympanic application due to its better uptake into the perilymphatic space and therefore, improved radiological assessment (10). Moreover, potential gastro-intestinal adverse effects or failure of renal function reported after systemic, intravenous application can be precluded through local, intratympanic administration. Disadvantages of this method compared to the intravenous application are the additional time and effort needed, the inconvenience for the patient and that this procedure is classified as an off-label use. Moreover, if both ears are to be examined, bilateral intratympanic application of the contrast agent is necessary. Even though this procedure can be useful to detect an asymptomatic ELH on the contralateral side or to evaluate a patient with symptoms in both ears, we follow the approach emphasized by a recent study of Gürkov et al. (11) and strictly perform EHI unilaterally, namely on the more affected side, the so called "index ear." Despite the off-label use of intratympanic application of gadoteric acid, we have not found any reports in literature, nor did we experience any severe side effects in our patients thus far (12, 13).

A multicenter evaluation of Pyykkö et al. demonstrated ELH in 90% of patients with typical symptoms of MD and even 75% of patients with unilateral symptoms showed bilateral ELH in EHI. In monosymptomatic patients ELH was detected in 55–90% (10). In our group, about half of the patients did not show ELH in the MRI. The difference in numbers might originate from the time point when EHI was performed. Our patients were asymptomatic at the time the MRI was performed and the moment to detect ELH may have passed. In a report by Shi et al. (14), EHI was consistently performed 1 week after the patient suffered from acute symptoms like a vertigo attack or hearing loss. The authors report of a detection rate for ELH of 100% in the affected ear in 198 patients. Therefore, it may be ideal to perform EHI directly after onset of symptoms, but in the clinical routine fast availability of MRI for "elective indication" is not always possible. This may be a potential explanation for the reduced number of detected ELH in our patient group.

One of our patients with suspected MD and a known allergy to gadoteric acid did not receive EHI in consideration of the risk-benefit-ratio and concerning the fact that the procedure is classified as an off-label-use, although it seems unlikely that the local application of a small amount of contrast agent into the middle ear would cause a systemic allergic reaction compared to an intravenous application.

The quality of the evaluation of the images highly depends on the radiologist's skills and experience. A possible source of error which influences the quality can be an insufficient application of the contrast agent, like insufficient filling of the middle ear.

FIGURE 1 | MRI (inversed recovery) of a right inner ear, axial plane. **(A)** Evidence of cochlear (arrow) and vestibular hydrops (dotted arrow). Endolymphatic space is clearly visible by its hypointense (dark) signal, compared to the hyperintense (bright) signal of the contrast-enhanced perilymphatic space. **(B)** Evidence of cochlear (arrow) and vestibular hydrops; saccule (dashed arrow) and utricle (dotted arrow). **(C)** Regular contrast enhanced perilymphatic space of vestibule and cochlea; no enlargement of endolymphatic space.

TABLE 1 | Patient's individual symptoms and diagnostic results; grading according to Baráth et al.

Nr.	Age	Sex	ELH in MRI	Location & grading of ELH	Index ear	Vertigo	Aural fullness	Tinnitus	SNHL	FQ	vHIT	Caloric response	cVEMPs
1	76	f	yes	coch I/vest I	R	spinning	none	none	R	all	normal	R <	R <
2	68	m	yes	coch II/vest II	L	spinning	L	L	L	all	L <	symmetric	inconclusive
3	64	m	yes	coch I/vest I	L	none	none	L	L	low	normal	L <	L <
4	61	m	yes	coch II/vest II	L	spinning	L	L	L	all	normal	L <	L <
5	48	f	yes	coch I/vest I	R	swaying	R	R	R	all	normal	R <	symmetric
6	43	f	none	None	L	swaying + spinning	none	L	L	all	normal	L <	not done
7	42	f	none	None	L	spinning	none	L	L	low	normal	L <	not done
8	36	m	yes	coch I/vest I	R	swaying	R	R	R	low	normal	R <	R <
9	34	f	none	None	R	swaying + spinning	R	R	R	low	normal	R <	symmetric
10	73	m	none	None	L	spinning	None	L	B, L<R	low + high	normal	L <	L <
11	66	m	none	None	L	spinning	L	L	L	low	normal	L <	L <
12	57	m	none	None	R	spinning	R	R	R	low	normal	R <	L <
13	44	f	none	None	R	daze feeling	R	R	R	low	normal	R <	not done

f, female; m, male; ELH, endolymphatic hydrops; MRI, magnetic resonance imaging; coch cochlea, vest vestibule, SNHL, sensorineural hearing loss; FQ, frequencies affected from SNHL, vHIT video head impulse test, cVEMPs cervical vestibular evoked myogenic potentials; R, right; L, left; B, bilateral, < decrease in comparison to contralateral side.

Other mitigating factors are swallowing, speaking, or moving the head, which leads to a faster elimination of contrast agent from the middle ear cavity. A difference in the patient's individual permeability of the round window (e.g., after infections, surgery etc.) may also account for diverging results. Currently, a duration of 24 h after intratympanic application of gadoteric acid seems to be the optimal scan time for EHI (15). Previous studies have shown a significant correlation between low-frequency hearing thresholds and the grade of ELH, otherwise no correlation have been found between ELH and the severity of vestibular symptoms (e.g., frequency of vertigo attacks) (9, 14). In our group, two of six patients with verified ELH had low-frequency hearing loss, while in the remaining four all frequencies were decreased. However, all patients without confirmed ELH showed at least low-frequency hearing loss on the index ear. In case of negative EHI, a control MRI could be considered subsequently, e.g., if progression of symptoms occurs. To date, we do not have a clear recommendation regarding this situation.

Personal View on the Topic

In our opinion EHI is a very beneficial procedure, which improves the diagnostic workup of various inner ear dysfunctions in patients with suspected ELH. Proof of ELH by EHI helps to remove uncertainties and visualize the cause of the disease, therefore, making it more comprehensible for patients and healthcare providers alike. Subsequently, patients are better equipped to understand and accept their disease. The psychological strain of patients, who suffer from an unknown or suspected disease, can be reduced by making a clear diagnosis, which can prevent repeated consultations and examinations ("doctor shopping"). With a diagnosis and the visualization of its cause, it is easier

to convey therapeutic measures to the patient, especially in case of destructive methods (e.g., gentamicin). For the previous 3 years, we have performed EHI only with intratympanic application of gadoteric acid and considering the lack of side effects, as well as the improved radiological assessment, we do not see a clear benefit for implementing the intravenous method.

Our current number of cases is small, but we are highly motivated to expand the usage of this diagnostic procedure. Due to its recent and ongoing development we think that in the future the value of this imaging technique will increase, not only for patients with MD like symptoms, but also for other clinical entities, which are associated with the endolymphatic system (e.g., enlarged vestibular aqueduct). Finally, we want to emphasize our clear belief in the scientific value of this method, potentially contributing to the clarification of unanswered questions within the field.

CONCLUSION

Endolymphatic hydrops imaging is a valuable method for the diagnostic workup in patients with recurring vestibular and auditory symptoms as described in MD, but inconclusive clinical examination results. In these cases diagnosis of MD or HED, respectively, can be based on the additional presence of ELH in EHI. As an early diagnosis of MD or HED can lead to more specific treatment and less costs for further diagnostics in the long run, we think that EHI should be performed more frequently during primary assessment than has previously been the norm. However, the indication to perform EHI and its final evaluation of results rely on initially thorough vestibular diagnostics. Open questions, like an optimum point in time for EHI, the potential value of repeatedly performed investigations for follow-up examinations or treatment evaluation, as well as the interpretation of missing hydrops in cases of distinct clinical findings need to be addressed in the future.

DATA AVAILABILITY STATEMENT

The raw data supporting the conclusions of this article will be made available by the authors, without undue reservation.

ETHICS STATEMENT

Ethical review and approval was not required for the study on human participants in accordance with the local legislation and institutional requirements. Written informed consent for participation was not required for this study in accordance with the national legislation and the institutional requirements.

AUTHOR CONTRIBUTIONS

LW and SR established idea and content of the article. AO'S and LW collected and analyzed data. AS provided technical information. All authors contributed equally to this work and discussed results and contributed to the manuscript at all stages.

REFERENCES

1. Zou J, Pyykkö I, Bjelke B, Dastidar P, Toppila E. Communication between the perilymphatic scalae and spiral ligament visualized by *in vivo* MRI. *Audiol Neurootol.* (2005) 10:145–52. doi: 10.1159/000084024
2. Atkinson M. Ménière's original papers reprinted with an english translation with commentaries and biographical sketch. *Acta Otolaryngo.* (1961) 162:1–78.
3. Hallpike CS, Cairns H. Observations on the pathology of ménière's syndrome: (Section of Otology). *Proc R Soc Med.* (1938) 31:1317–36. doi: 10.1177/003591573803101112
4. Yamakawa K. Über die pathologische Veränderung bei einem Menière-Kranken. *J Otorhinolaryngol Soc Jpn*. (1938) 44:2310–2.
5. Gürkov R, Pyykö I, Zou J, Kentala E. What is Menière's disease? A contemporary re-evaluation of endolymphatic hydrops. *J Neurol.* (2016) 263(Suppl. 1):S71–81. doi: 10.1007/s00415-015-7930-1
6. Gürkov R, Hornibrook J. On the classification of hydropic ear disease (Menière's disease). Zur Klassifikation der hydropischen Ohrerkrankung (M. Menière). *HNO.* (2018) 66:455–63. doi: 10.1007/s00106-018-0488-3
7. Monsell EM, Balkany TA, Gates GA, Goldenberg RA, Meyerhoff WL, House JW. Committee on hearing and equilibrium guidelines for the diagnosis and evaluation of therapy in Menière's disease. American academy of otolaryngology-head and neck foundation, Inc. *Otolaryngol Head Neck Surg.* (1995) 113:181–5. doi: 10.1016/S0194-5998(95)70102-8
8. Goebel JA. 2015 equilibrium committee amendment to the 1995 AAO-HNS guidelines for the definition of Ménière's disease. *Otolaryngol Head Neck Surg.* (2016) 154:403–4. doi: 10.1177/0194599816628524
9. Baráth K, Schuknecht B, Naldi AM, Schrepfer T, Bockisch CJ, Hegemann SC. Detection and grading of endolymphatic hydrops in Menière disease using MR imaging. *AJNR Am J Neuroradiol.* (2014) 35:1387–92. doi: 10.3174/ajnr.A3856
10. Pyykkö I, Nakashima T, Yoshida T, Zou J, Naganawa S. Meniere's disease: a reappraisal supported by a variable latency of symptoms and the MRI visualisation of endolymphatic hydrops. *BMJ Open.* (2013) 3:e001555. doi: 10.1136/bmjopen-2012-001555
11. Gürkov R, Todt I, Jadeed R, Sudhoff H, Gehl HB. Laterality of audiovestibular symptoms predicts laterality of endolymphatic hydrops in hydropic ear disease (Menière). *Otol Neurotol.* (2020) 41:e1140–4. doi: 10.1097/MAO.0000000000002775
12. Louza J, Krause E, Gürkov R. Hearing function after intratympanic application of gadolinium-based contrast agent: a long-term evaluation. *Laryngoscope.* (2015) 125:2366–70. doi: 10.1002/lary.25259
13. Louza JP, Flatz W, Krause E, Gürkov R. Short-term audiologic effect of intratympanic gadolinium contrast agent application in patients with Ménière's disease. *Am J Otolaryngol.* (2012) 33:533–7. doi: 10.1016/j.amjoto.2011.12.004

14. Shi S, Guo P, Li W, Wang W. Clinical features and endolymphatic hydrops in patients with MRI evidence of hydrops. *Ann Otol Rhinol Laryngol.* (2019) 128:286–92. doi: 10.1177/0003489418819551
15. Naganawa S, Nakashima T. Visualization of endolymphatic hydrops with MR imaging in patients with Ménière's disease and related pathologies: current status of its methods and clinical significance. *Jpn J Radiol.* (2014) 32:191–204. doi: 10.1007/s11604-014-0290-4

Conflict of Interest: The authors declare that the research was conducted in the absence of any commercial or financial relationships that could be construed as a potential conflict of interest.

Publisher's Note: All claims expressed in this article are solely those of the authors and do not necessarily represent those of their affiliated organizations, or those of the publisher, the editors and the reviewers. Any product that may be evaluated in this article, or claim that may be made by its manufacturer, is not guaranteed or endorsed by the publisher.

frontiers in Surgery

ORIGINAL RESEARCH
published: 04 November 2021
doi: 10.3389/fsurg.2021.758947

Hydropic Ear Disease: Correlation Between Audiovestibular Symptoms, Endolymphatic Hydrops and Blood-Labyrinth Barrier Impairment

Lisa M. H. de Pont[1,2], Josephine M. van Steekelenburg[1], Thijs O. Verhagen[1,3,4], Maartje Houben[1,3], Jelle J. Goeman[5], Berit M. Verbist[2], Mark A. van Buchem[2], Claire C. Bommeljé[3], Henk M. Blom[3,4,6] and Sebastiaan Hammer[1]**

[1] Department of Radiology, Haga Teaching Hospital, The Hague, Netherlands, [2] Department of Radiology, Leiden University Medical Center, Leiden, Netherlands, [3] Department of Otorhinolaryngology, Haga Teaching Hospital, The Hague, Netherlands, [4] Department of Otorhinolaryngology, Leiden University Medical Center, Leiden, Netherlands, [5] Department of Biomedical Data Sciences, Leiden University Medical Center, Leiden, Netherlands, [6] Department of Otorhinolaryngology, Antwerp University Hospital, Antwerp, Belgium

Research Objective: To investigate the correlation between clinical features and MRI-confirmed endolymphatic hydrops (EH) and blood-labyrinth barrier (BLB) impairment.

Study Design: Retrospective cross-sectional study.

Setting: Vertigo referral center (Haga Teaching Hospital, The Hague, the Netherlands).

Methods: We retrospectively analyzed all patients that underwent 4 h-delayed Gd-enhanced 3D FLAIR MRI at our institution from February 2017 to March 2019. Perilymphatic enhancement and the degree of cochlear and vestibular hydrops were assessed. The signal intensity ratio (SIR) was calculated by region of interest analysis. Correlations between MRI findings and clinical features were evaluated.

Results: Two hundred and fifteen patients with MRI-proven endolymphatic hydrops (EH) were included (179 unilateral, 36 bilateral) with a mean age of 55.9 yrs and median disease duration of 4.3 yrs. Hydrops grade is significantly correlated with disease duration ($P < 0.001$), the severity of low- and high-frequency hearing loss (both $P < 0.001$), and the incidence of drop attacks ($P = 0.001$). Visually increased perilymphatic enhancement was present in 157 (87.7%) subjects with unilateral EH. SIR increases in correlation with hydrops grade ($P < 0.001$), but is not significantly correlated with the low or high Fletcher index ($P = 0.344$ and $P = 0.178$ respectively). No significant differences were found between the degree of EH or BLB impairment and vertigo, tinnitus or aural fullness.

Conclusion: The degree of EH positively correlates with disease duration, hearing loss and the incidence of drop attacks. The BLB is impaired in association with EH grade, but without clear contribution to the severity of audiovestibular symptoms.

Keywords: endolymphatic hydrops, blood-labyrinth barrier, magnetic resonance imaging, clinical features, audiovestibular function

OPEN ACCESS

Edited by:
Robert Gürkov,
Bielefeld University, Germany

Reviewed by:
Michihiko Sone,
Nagoya University Hospital, Japan
Chunfu Dai,
Fudan University, China
Pablo D. Dominguez,
University Clinic of Navarra, Spain

****Correspondence:***
Lisa M. H. de Pont
l.depont@hagaziekenhuis.nl;
l.m.h.de_pont@lumc.nl
Sebastiaan Hammer
s.hammer@hagaziekenhuis.nl

Specialty section:
This article was submitted to Otorhinolaryngology - Head and Neck Surgery, a section of the journal Frontiers in Surgery

Received: *15 August 2021*
Accepted: *12 October 2021*
Published: *04 November 2021*

Citation:
de Pont LMH, van Steekelenburg JM, Verhagen TO, Houben M, Goeman JJ, Verbist BM, van Buchem MA, Bommeljé CC, Blom HM and Hammer S (2021) Hydropic Ear Disease: Correlation Between Audiovestibular Symptoms, Endolymphatic Hydrops and Blood-Labyrinth Barrier Impairment. Front. Surg. 8:758947. doi: 10.3389/fsurg.2021.758947

INTRODUCTION

Menière's disease (MD) is a refractory otologic disorder that predominantly manifests in adults between 40 and 60 years of age (1, 2). Its typical features are recurrent vertigo spells associated with fluctuating cochlear symptoms in the affected ear (3–6). The disease may affect one ear, albeit bilaterality has been reported in 2–73% of cases (7). MD is strongly associated with endolymphatic hydrops (EH): a distention of the endolymphatic space of the inner ear due to accumulation of endolymph fluid (8). Although a certain diagnosis of EH is reserved for post-mortem temporal bone histology, the Equilibrium committee of the AAO-HNS has provided clinical guidelines to aid the diagnosis of MD in living patients (5, 9).

The most striking features of MD are rotatory vertigo and hearing loss, which show great variability among patients with respect to onset, duration and severity (10, 11). Vertigo attacks can last from several minutes to hours, and are often incapacitating due to their unpredictability and impact on quality of life (12). In initial stages of the disease, hearing loss is typically reversible after each vertigo attack, but profound and permanent hearing loss ultimately develops (13). Additionally, patients may experience a myriad of symptoms consisting of (but not limited to) tinnitus, aural fullness, or a sudden fall without loss of consciousness known as drop attacks (14–16). Migraine and autoimmune diseases are common comorbidities, reported in up to 16 and 11% of patients respectively (17–21).

Despite their strong association, the relationship between EH and MD remains unclear. In the last decade, the application of delayed gadolinium (Gd)-enhanced MRI has provided novel insights in the clinical effect of EH (22–30). The degree of EH is reported to correspond with disease duration and the degree of sensorineural hearing loss in MD patients (27, 28, 31, 32). Contrarily, no correlation has emerged between EH and tinnitus, aural fullness, or the frequency and duration of vertigo attacks (23, 30). The absence of a clear correlation has led to the belief that other mechanisms beyond EH must play a role in the production of audiovestibular symptoms.

Recent literature has introduced novel MRI parameters that may help clarify the clinical-MRI inconsistency. Increased perilymph signal intensity (SI) at 4 h-delayed Gd-enhanced 3-dimensional fluid-attenuated inversion recovery (3D FLAIR) MRI is a frequent concomitant finding in patients with EH (32–36). The underlying pathophysiological process is assumed to be impairment of the blood-labyrinth barrier (BLB), leading to increased permeability and leakage of Gd from capillaries into the perilymphatic spaces (32, 37). The increased perilymphatic enhancement is well-visualized on 3D FLAIR, due to its high sensitivity to changes in T1-shortening induced by gadolinium-based contrast media (38). Previous studies investigating this FLAIR hyperintensity have reported that the concurrent finding of EH and BLB impairment slightly increases specificity for MD compared with EH alone (34, 35). The importance of this MRI parameter is further emphasized by the notion that BLB impairment may be the sole MRI correlate in a small percentage of MD patients without EH (35, 36). Furthermore, normalization of the FLAIR hyperintensity has been observed in coincidence with improved vestibulocochlear function in several inflammatory inner ear conditions (39–41). The above-mentioned findings suggest that BLB impairment may provide additional clinical information about HED and may potentially bring new insights to the individual severity of audiovestibular symptoms.

Extensive literature from the past two decades has demonstrated that virtually all patients with clinically overt MD show EH on MRI, for which different subjective EH grading systems have been used (34, 35, 42–44). However, probably the most important gain from hydrops MRI is the demonstration of EH in clinically atypical or non-classifiable cases according to the current AAO-HNS criteria (34, 45). These findings highlight the diagnostic relevance of MR imaging, particularly in the clinical setting where the current AAO-HNS criteria appear to be insufficient—e.g., subjects with isolated cochlear or vestibular symptoms. This concept has sparked aspirations to abandon the symptom-based classification and to adapt a diagnostic system that incorporates the MRI-objectivation of EH. In 2018, Gürkov et al. proposed the classification of Hydropic Ear Disease (HED): an imaging-based classification system that is based upon the demonstration of EH and that acknowledges the wide spectrum of audiovestibular symptoms associated with this pathological substrate (8, 46). However, the clinical utility of this system relies on the value of imaging-derived parameters in this clinical spectrum.

The objective of this study was therefore to investigate the correlation between clinical features and labyrinthine abnormalities in patients with MRI-proven hydropic ear disease, with emphasis on EH and BLB-impairment.

MATERIALS AND METHODS

Patients

We retrospectively identified all patients who underwent 4 h-delayed Gd-enhanced 3D FLAIR MRI at our institution from February 2017 to March 2019. The commonest clinical indication for inner ear MRI was recurrent vertigo with fluctuating aural symptoms suspected of MD. Three-hundred eighty-nine patients were eligible for inclusion. Exclusion criteria were <18 years old ($N = 1$), previous middle or inner ear surgery ($N = 17$), prior ablative treatment of the ear with gentamicin injections ($N = 10$) or a technically inadequate MRI examination ($N = 11$). We also excluded patients with coexisting conditions that may cause fluctuating audiovestibular symptoms, such as otosclerosis ($N = 2$) and vestibular schwannoma ($N = 2$).

MRI Protocol

Imaging examinations were carried out on a 3T MRI scanner (Magnetom Skyra; Siemens, Erlangen, Germany) with a 20-channel array head coil, 4 h after intravenous gadolinium administration (30 mL gadoterate meglumine, Dotarem; Guerbet, Aulnay-sous-Bois, France) (34). Patients were evaluated in the supine position with additional fixation between the patient's head and receiver coil to reduce motion artifacts. We acquired a 3D FLAIR sequence to differentiate endolymph from perilymph with the following parameters:

TABLE 1 | Grading of endolymphatic hydrops on 4 h-delayed Gd-enhanced 3D FLAIR MRI.

Grade	Vestibule	Cochlea
0	Normal-sized saccule and utricle	No displacement of Reissner's membrane
1	The saccule is equal in size or larger than the utricle, but not confluent	Dilation of the scala media with partial obliteration of the scala vestibuli
2	Confluence of saccule and utricle that encompasses >50% of the vestibule	Complete obliteration of the scala vestibuli
3	Total effacement of the perilymphatic space in the vestibule	n.a.

n.a. indicates not applicable.

FOV = 190 mm, section thickness 0.8 mm, TR = 6,000 ms, TE = 177 ms, number of excitations 1, TI 2,000 ms, flip angle 180°, matrix 384 × 384, bandwidth 213 Hz/pixel, turbo factor 28, voxel size 0.5 × 0.5 × 0.8 mm, resulting in an acquisition time of 14 min. High-resolution T2 sampling perfection with application-optimized contrasts by using different flip angle evolution (SPACE sequence; Siemens) images of the inner ear were obtained for anatomic reference of the entire labyrinthine fluid space. The scan parameters for the T2 SPACE sequence were as follows: FOV 160 mm, section thickness 0.5 mm, TR 1,400 ms, TE 155 ms, number of excitations 1, flip angle 120°, matrix 320 x 320, bandwidth 289 Hz/pixel, turbo factor 96, voxel size 0.5 × 0.5 × 0.5, and acquisition time 5 min.

MRI Evaluation

Visual Assessment

Images were independently evaluated by two observers: one head and neck radiologist (SH) and one PhD student (LP) with, respectively, 4.5 and 3 years of experience in hydrops MRI, who were blinded to the clinical data. The presence of endolymphatic hydrops was graded on a 4-point scale for vestibular hydrops and a 3-point scale for cochlear hydrops, respectively (**Table 1**). The *summative EH score* was calculated as the sum of cochlear and vestibular EH grades per patient to reflect global EH severity, which could range from 0 to 5.

Post-contrast signal intensity of the perilymph was visually scored as normal (symmetrical) or increased (asymmetrical). Any discrepancy was resolved by consensus reading.

Quantitative Analysis

Quantitative measurements of the perilymph signal intensity were performed by one observer (LP) blinded to the clinical data. A freehand region of interest (ROI) was drawn on an axial section in the basal cochlear turn of both ears. In this region, quantification of perilymph enhancement was considered most reliable as the scala tympani is less affected by the morphological distortion from EH compared with other perilymphatic structures and this structure remains visible regardless of the degree of EH. In addition, the scala tympani visually appears the largest in the basal turn of the cochlea and is therefore easiest to contour in this region. An additional circular ROI of 0.6 mm^2 was placed in the left middle cerebellar peduncle (**Figure 1**). The signal intensity ratio (SIR) of the basal cochlear turn to that of the middle cerebellar peduncle was calculated.

Clinical Symptoms and Pure-Tone Audiometry

Clinical diagnoses were independently evaluated by 2 otorhinolaryngologists (HB and CB), who were blinded to the MRI results, according to the latest AAO-HNS criteria (5). Patients who did not fulfill the clinical criteria for probable or definite MD were assigned the clinical diagnosis *other disease*, which was considered an umbrella term for non-classifiable cases and patients with other vertigo-associated diseases (e.g., vestibular neuritis, vestibular migraine). Any discrepancy was resolved by consensus reading.

Information on the presence of audiovestibular symptoms and results from pure-tone audiometry (PTA) was collected from medical records. Age was defined as age at time of MRI. Unless otherwise specified, we calculated disease duration as the time elapsed from the first appearance of vertigo *or* hearing loss until MRI at our hospital. The frequency of vertigo attacks was calculated as the number of attacks per month. The duration of vertigo was divided into the following five categories: (1) <20 min; (2) 20 min to 12 h; (3) 12–24 h; (4) more than 24 h; and (5) variable duration. For hearing loss analysis, we selected the most recent PTA before or after MRI with a maximum time interval of 1 year. We documented hearing function in the form of low and high Fletcher indexes (the average hearing loss at the frequencies 0.5–1.0–2.0 kHz and 1.0–2.0–4.0 kHz, respectively).

Statistical Analysis

Statistical analyses were performed using SPSS Statistics (version 24, IBM, Chicago, Illinois, USA). The level of significance was set at $P < 0.05$. Inter-observer agreement on the presence and grading of EH (3-point scale for the cochlea and 4-point scale for the vestibule) was estimated using Cohen's kappa (κ) coefficient. We considered a κ value >0.80 as excellent agreement. The Kolmogorov-Smirnov test was used to test the data for normal distribution. Data are presented as median [min-max] *or* mean ± standard deviation. Means and medians were compared between two independent groups by a Student *t* test and Mann-Whitney *U* test, respectively. The chi-square test was used to compare gender distribution and the prevalence of symptoms and comorbidities among groups with different hydrops grades. A Kruskall-Wallis *H* test was used to compare median EH scores and SIR across groups with different duration of vertigo attacks. The Wilcoxon rank-test was used to compare SIR and Fletcher indexes between both ears from unilateral EH patients. Correlation between (normally and not-normally distributed) continuous variables were assessed using the Pearson and Spearman correlation coefficients. Correlation between continuous and ordinal variables were assessed using the Jonckheere-Terpstra test of trend, which is a rank-based test that can be used to assess the significance of a trend in the data (e.g., as EH deteriorates, does hearing loss also deteriorate). Unless otherwise specified, correlation tests between

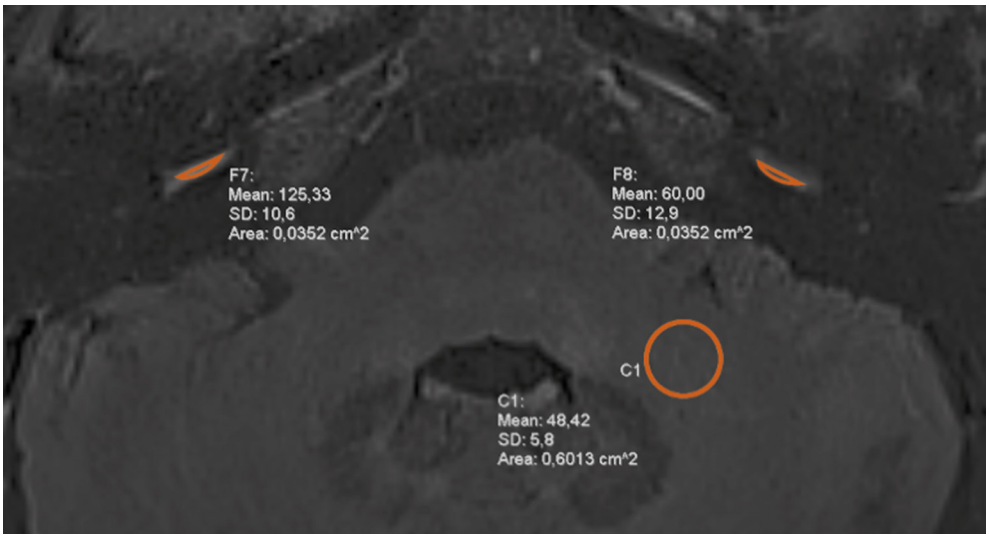

FIGURE 1 | Signal intensity measurements at 4 h-delayed contrast-enhanced 3D FLAIR MRI. Symmetrical regions of interest (ROI) were drawn in the basal cochlear turn of each ear and a circular ROI was placed in the left middle cerebellar peduncle. The measurements were used to calculate the signal intensity ratio (SIR).

MRI findings and clinical features were performed solely in patients with unilateral EH.

RESULTS

Subject Characteristics

EH was observed in 215 patients (62.1%). Patient characteristics are listed in **Table 2**. The remaining 131 patients (37.9%) had no apparent EH and were excluded from further analysis. A summary of the clinical diagnoses of the included and excluded patients is provided in **Table 3**. Interobserver agreement for the clinical diagnosis was substantial ($\kappa = 0.78$).

MRI Findings

Inter-observer Reliability

Interobserver reliability was excellent: $\kappa = 0.88$ for cochlear EH, $\kappa = 0.95$ for vestibular EH, $\kappa = 0.83$ for visual assessment of perilymph enhancement.

Endolymphatic Hydrops

All 215 patients demonstrated EH in their clinically affected ear, including 179 patients (83.3%) with unilateral EH (101 right, 78 left) and 36 patients with bilateral EH (16.7%). Concurrent vestibular and cochlear EH was most prevalent (144 patients, 67%). Isolated vestibular or cochlear hydrops was present in 53 (24.7%) and 18 (8.4%) patients, respectively. The degree of cochlear hydrops is strongly associated with the degree of vestibular hydrops, as revealed by the Spearman correlation coefficient ($r_s = 0.553$; $P < 0.001$).

Among the 36 patients with bilateral EH, 21 (58.3%) had symptoms in the contralateral hydropic ear and 15 (41.7%) were clinically silent on the contralateral side. Asymptomatic EH appeared more frequently in the vestibule (80%) than in the cochlea (26.7%).

TABLE 2 | Clinical characteristics of patients with HED ($n = 215$).

Male/female, *n* (%)	101/114 (47/53)
Unilateral/bilateral EH, *n* (%)	179/36 (83/17)
Mean age, *y*	55.9 ± 0.9
Mean age of onset, *y*	47.5 ± 1.1
Vertigo, *n* (%)	212 (98.6)
Subjective hearing loss, *n* (%)	208 (96.7)
Tinnitus, *n* (%)	196 (91.2)
Aural fullness, *n* (%)	144 (67.0)
Median disease duration, *y*	4.25 [0.04–45.9]
Median duration hearing loss, *y*	5.1 [0.03–42.0]
Median duration vertigo, *y*	3.9 [0.04–45.9]
Migraine, *n* (%)	24 (11.2)
Autoimmune diseases, *n* (%)	14 (6.5)
Cardiovascular risk factors	
High blood pressure, *n* (%)	37 (17.2)
Dyslipidemia, *n* (%)	20 (9.3)
Type II diabetes, *n* (%)	12 (5.6)
History of smoking, *n* (%)	15 (7.0)

HED, Hydropic Ear Disease; EH, endolymphatic hydrops; N, number; Y, year.

Post-contrast Perilymph Signal Intensity

Visually increased perilymphatic enhancement (PE) was present in 157 patients (87.7%) with unilateral EH (**Figure 2**). Quantitative BLB measurements confirmed a significant higher median SIR in affected ears of unilateral EH patients compared with their contralateral non-hydropic ears ($P < 0.001$; **Table 4**). In addition, there was a statistically significant trend of higher median SIR among increasing summative EH score ($T_{jt} = 7.896{,}000$; $z = 4{,}104$; $P < 0.001$; **Figure 3**). This trend was stronger for vestibular EH ($T_{jt} = 5.640{,}000$; $z = 2{,}945$;

TABLE 3 | Clinical diagnosis of the included and excluded patients according to the 2015 AAO-HNS criteria.

	Subjects with EH (included)	Subjects without EH (excluded)	*N* (%)
Unilateral definite MD	174	6	180 (52.0%)
With contralateral asymptomatic ear	167	6	
With contralateral symptomatic ear	7	0	
Bilateral definite MD	17	4	21 (6.1%)
Unilateral probable MD	11	9	20 (5.8%)
With contralateral symptomatic ear	10	9	
With contralateral asymptomatic ear	1	0	
Bilateral probable MD	0	1	1 (0.3%)
Unilateral other disease	8	55	63 (18.2%)
Bilateral other disease	5	56	61 (17.6%)
Total	215	131	346 (100%)

EH, endolymphatic hydrops; MD, Menière's disease; other disease, other vertigo-associated diseases and non-classifiable cases.

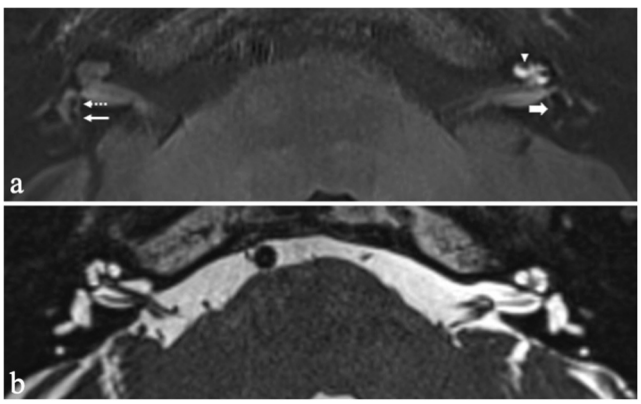

FIGURE 2 | Axial 4 h-delayed Gd-enhanced 3D FLAIR MRI **(a)** and axial heavily T2 weighted sequence **(b)** in a patient with recurrent vertigo attacks and left-sided sensorineural hearing loss. The affected left ear demonstrates dilation of the scala media with complete obliteration of the scala vestibuli compatible with grade 2 cochlear hydrops (arrow head). The saccule and utricle in the left ear are confluent indicative of grade 2 vestibular hydrops (thick arrow). A thin rim of surrounding perilymph remains visible. Compare with a normal saccule (dashed arrow) and utricle (thin arrow) in the right ear. Also note the increased perilymphatic enhancement in the cochlea of the left ear, suggestive of BLB impairment.

$P = 0.003$) than cochlear EH ($T_{jt} = 1.943{,}000$; $z = 1{,}896$; $P = 0.058$). Among the 22 patients with unilateral EH that did not demonstrate visually increased PE in their affected ear, 14 patients (63.6%) had isolated vestibular or isolated cochlear EH.

Among the 15 bilateral EH patients with unilateral symptoms, the symptomatic ears demonstrated a mean SIR of 1.6 ± 0.8 compared with a mean SIR of 1.2 ± 0.5 in their symptomatic ear, which was statistically significant ($P < 0.005$). In addition, symptomatology in these patients was also correlated with a higher summative EH score [median EH score 1 (1–4) vs. 3 (1–5), $P < 0.05$].

TABLE 4 | Median SIR in hydropic and non-hydropic ears from 179 patients with unilateral HED.

	Hydropic ears	Contralateral ears	*P*-value
Median SIR	1.40 [0.68–5.52]	1.05 [0.47–2.94]	<0.001

SIR, signal intensity ratio; HED, Hydropic Ear Disease.

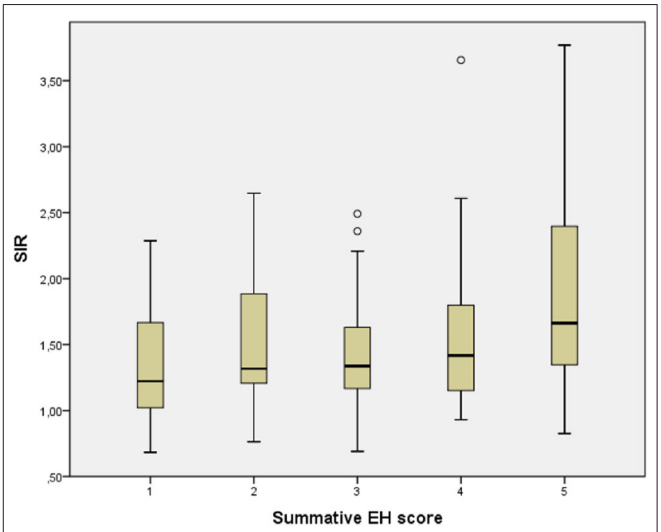

FIGURE 3 | Correlation between signal intensity ratio (SIR) and summative endolymphatic hydrops (EH) score in unilateral hydropic ear disease (HED). A Jonckheere-Terpstra rank-test revealed a significant trend toward a higher median SIR among increasing EH score ($P < 0.001$).

Correlation Between MRI Findings and Clinical Characteristics

Clinical Symptoms

Most patients reported concomitant vestibular and cochlear symptoms (212 patients, 98.6%). Three patients (1.4%) had isolated cochlear symptoms.

The clinical features from patients with unilateral EH are summarized in **Table 5**. There were no significant differences in the prevalence of hearing loss, tinnitus, or aural fullness in groups with different EH grades ($P = 0.780$; $P = 0.900$; $P = 0.200$). The median SIR also did not differ between hydropic ears with and without tinnitus or aural fullness ($P = 0.947$ and $P = 0.185$). Information on the frequency or duration of vertigo attacks was available in 102 (57.0%) and 166 (92.7%) patients with unilateral EH, respectively. No significant correlation was found between the degree of EH or SIR and the frequency of vertigo attacks ($P = 0.188$ and $P = 0.165$, respectively). Regarding the duration of vertigo, the majority of cases (84.9%) had vertigo episodes lasting between 20 min and 12 h. No significant differences were noted in summative EH score or median SIR across groups with different duration of vertigo attacks ($P = 0.431$ and $P = 0.380$, respectively).

A comparison of clinical features between unilateral and bilateral EH patients is summarized in **Table 6**. No differences were found in the presence of aural symptoms (hearing loss,

TABLE 5 | Clinical features in unilateral HED stratified by the summative EH score.

	Grade 1	Grade 2	Grade 3	Grade 4	Grade 5	*P*-value/*P*-value for trend
Mean age, y	54.6 ± 2.2	58.8 ± 3.0	56.1 ± 1.9	54.5 ± 2.0	56.4 ± 1.7	0.732
Median disease duration, y	1.7 [0.1–30.0]	2.3 [0.2–30.0]	3.3 [0.04–24.8]	9.8 [0.25–33.0]	5.8 [0.33–29.0]	<0.001
Subjective hearing loss, *n* (%)	34 (94)	21 (100)	44 (98)	29 (97)	46 (98)	0.78
Vertigo, *n* (%)	34 (94)	21 (100)	45 (100)	29 (97)	47 (100)	0.2
Median nr of attacks per month	6.0 [0.3–28.0]	2.3 [0.3–14.0]	4.0 [0.08–70.0]	3.5 [1.0–28.0]	4.0 [0.16–16.0]	0.188
Duration of vertigo attacks						0.843
<20 min	1	1	2	1	2	
20 min–12 h	27	16	38	22	38	
12–24 h	1	1	0	1	0	
>24 h	1	1	1	0	0	
Variable duration	3	1	1	4	3	
Missing	3	1	3	2	4	
Tinnitus, *n* (%)	32 (89)	20 (95)	42 (93)	28 (93)	44 (94)	0.9
Aural fullness, *n* (%)	26 (72)	13 (62)	36 (80)	18 (60)	28 (60)	0.2
Drop attacks, *n* (%)	0 (0)	0 (0)	1 (0.02)	4 (13.3)	7 (14.9)	0.013

HED, Hydropic Ear Disease; EH, endolymphatic hydrops.

TABLE 6 | Clinical differences between unilateral and bilateral HED patients.

	Unilateral EH	Bilateral EH	*P*-value
Mean age, *y*	55.9 ± 12.3	55.6 ± 14.2	0.870
Mean age of onset, *y*	48.13 ± 1.12	44.02 ± 3.08	0.145
Median disease duration, *y*	4.04 [0.04–33.0]	6.08 [0.3–45.9]	0.241
Hearing loss	*Hydropic ear*	*Worst ear*	
Median low Fletcher	48 [2–120]	53.5 [5–120]	0.190
Median high Fletcher	50 [2–120]	51 [5–120]	0.167
Median nr of vertigo attacks per month	4.0 [0.08–70]	2.0 [0.04–30.0]	0.100

HED, Hydropic Ear Disease; EH, endolymphatic hydrops.

TABLE 7 | Characteristics of unilateral HED patients with and without drop attacks.

	Drop attacks *N* = 12	No drop attacks *N* = 167	*P*-value
Male/female, *n* (%)	8/4 (67/33)	78/89 (47/53)	0.236
Mean age, *y*	55.0 ± 4.2	56.0 ± 0.9	0.780
Median disease duration, *y*	9.5 [3.2–23.2]	3.8 [0.04–33.0]	0.007
Median summative EH score	5.0 [3–5]	3.0 [1–5]	0.001
Median Cochlear EH score	2.0 [1–2]	1.0 [0–2]	0.013
Median Vestibular EH score	3.0 [2–3]	2.0 [0–3]	0.001
Median SIR	1.6 [0.83–3.66]	1.4 [0.68–5.52]	0.403
Median Low Fletcher	60 [45–72]	47 [2–120]	0.027
Median High Fletcher	58 [27–68]	48 [2–120]	0.191

HED, Hydropic Ear Disease; SIR, signal intensity ratio; EH, endolymphatic hydrops.

tinnitus, aural fullness) between patients with unilateral or bilateral EH. Additionally, no significant differences were noted in duration or frequency of vertigo attacks ($P = 0.831$ and $P = 0.100$, respectively).

Drop Attacks

Among patients with unilateral EH, drop attacks (DA) were reported by 12 subjects (**Table 7**). There were no statistically significant differences in sex or age between patients with and without DA ($P = 0.236$; $P = 0.780$). However, the DA group had a longer disease duration than patients without DA ($P = 0.007$). In all 12 patients with DA, MRI revealed concurrent cochlear and vestibular EH, which was both graded as either moderate or significant. The cochlear and vestibular EH grades, as well as the *summative* EH scores, were significantly higher in the DA group. Notably, DA was only reported in patients with a *summative* EH score of 3 or more. Additionally, patients with DA showed significantly greater hearing loss in the low and medium frequencies (low Fletcher 60 vs. 47, $P = 0.027$). No significant differences were noted at high frequencies between patients with and without DA (High Fletcher 58 vs. 48, $P = 0.191$).

Comorbidities

Hypertension was the most frequent cardiovascular risk factor and present in 37 (17.2%) unilateral EH patients (18 men; 19 women), followed by dyslipidemia (9%) and smoking (7%). Twenty-four patients (11.2%) had a history of migraine. No significant differences in the prevalence of co-morbidities were noted between patients with unilateral or bilateral EH (data not shown).

TABLE 8 | Hearing loss in unilateral HED stratified by the summative EH score.

Pure-tone audiometry	Grade 1 *N* = 35	Grade 2 *N* = 18	Grade 3 *N* = 39	Grade 4 *N* = 26	Grade 5 *N* = 43	*P*-value for trend
Median low Fletcher index	28.0 [2–120]	38 [20–75]	45 [12–120]	58 [5–75]	60 [22–85]	<0.001
Median high Fletcher index	26.5 [2–120]	42.0 [20–65]	51.0 [7–120]	60.0 [13–75]	60.0 [30–95]	<0.001
Missing	1	3	6	4	4	

HED, Hydropic Ear Disease; EH, endolymphatic hydrops.

Disease Duration

Information on disease duration was available in 142 unilateral HED patients (90.4%) and 27 bilateral HED patients (75%). In patients with unilateral EH, the Jonckheere-Terpstra test for trend revealed that the degree of EH increases significantly with longer disease duration (**Table 5**, $P < 0.001$ for the summative EH score; $P < 0.001$ for vestibular EH; $P = 0.041$ for cochlear EH). Among patients with a summative EH score of 5, the median disease duration was lower than would be expected. We performed an intra-cluster analysis of patients with a summative EH score of 5 with the aim of identifying factors associated with rapid EH progression. However, no correlation was found between disease duration and gender ($P = 0.218$), age ($P = 0.137$), vertigo attack frequency ($P = 0.161$), drop attacks ($P = 0.705$), SIR ($P = 0.939$), tinnitus ($P = 0.081$), aural fullness ($P = 0.891$), or sensorineural hearing loss ($P = 0.823$ for low Fletcher index, $P = 0.886$ for high Fletcher index).

Patients with bilateral EH did not demonstrate a statistically significant longer disease duration than patients with unilateral EH (6.1 yrs vs. 4.0 yrs; $P = 0.241$).

Pure Tone Audiometry

In 161 patients (89.9%) with unilateral EH and 36 patients with bilateral EH (100%), PTA was performed within 1 year of the MRI examination with a median time interval of 36 days (0–340 days). Of note, most patients (116/161, 72%) had undergone PTA within 2 months of the MRI examination.

In 161 unilateral EH patients, the average low Fletcher index was 48 dB [2; 120] in the hydropic ears and 13 dB [0–98] in the contralateral non-hydropic ears ($P < 0.001$). The high Fletcher index was 50 dB [2–120] in the hydropic ears and 17 dB [0–120] in the contralateral non-hydropic ears ($P < 0.001$). The Jonckheere-Terpstra test for trend showed that the low and high Fletcher indexes were significantly correlated with increasing summative EH score ($P < 0.001$ and $P < 0.001$; **Table 8**). A partial correlation was run to determine the relationship between SIR and hearing loss whilst controlling for EH. First, we performed a square root (sqrt) transformation of the low and high Fletcher indexes to reduce the skewness of our original data. The partial correlation revealed no statistically significant correlation between SIR and low Fletcher ($P = 0.344$) or high Fletcher ($P = 0.178$), respectively. We therefore did not demonstrate an additive effect of SIR on the extent of sensorineural hearing loss in HED patients.

The worst ear from bilateral EH patients demonstrated a median low Fletcher index of 53.5 dB [5–120] and median high Fletcher index of 51 dB [5–120]. These hearing thresholds were not significantly different from the low and high Fletcher indexes from the hydropic ears of unilateral EH patients ($P = 0.190$ and $P = 0.167$, respectively).

DISCUSSION

In the present study, we explored the relationship between cochleovestibular symptoms and intralabyrinthine abnormalities in a large cohort of patients with HED. We demonstrated the association between EH grade and hearing loss, as well as their progressive deterioration with respect to disease duration. Similar correlations have been shown by a couple of radiological studies (23, 27, 28, 30, 33) and a histological study on temporal bones from MD patients (47). Contrarily, previous radiological studies by Xie et al. ($N = 117$) and Fiorino et al. ($N = 18$) revealed no significant correlation between the severity of sensorineural hearing loss and EH grade, as revealed by MRI after intratympanic Gd-administration in definite MD patients (48, 49). Although the precise reason for this discrepancy is unknown, possible explanations may be different patient selection and sample sizes, or the use of a different MRI protocol and/or visual grading method for EH. Interestingly, our study revealed that there are cases with severe EH and hearing loss despite having a short disease duration and vice versa. These findings indicate that in some patients the hydropic process and hearing loss deteriorate rapidly, while others have a slow and gradual progression. Similar findings have previously been shown (50). Therefore, we hypothesize that factors other than duration are associated with the progression of EH. However, we did not identify factors associated with rapid EH progression. Further study is needed to explore these temporal patterns, which could have important implications in understanding the pathophysiology of HED.

Tinnitus and aural fullness have received less attention in literature, as emphasis is often placed on more prominent symptoms such as hearing loss and vertigo. However, it was previously reported that 19% of MD patients rank tinnitus as their most severe symptom and 38% considers aural fullness as a severe problem (51, 52). The identification of an *in vivo* correlate would provide important insights in the individually perceived severity of clinical disease. However, in contrast to hearing loss, our data did not demonstrate a correlation between EH grade and the presence of tinnitus or aural fullness. Notably, our study design did not cover qualitative measures of tinnitus or aural fullness, such as the perceived loudness or intensity.

The etiology of vertigo spells in HED also remains elusive. A myriad of theories have previously been proposed, including mechanical pressure or chemical imbalance/intoxication within the inner ear (53–56). Herein, we did not demonstrate a significant correlation between the extent of EH and the frequency or duration of vertigo attacks. It can therefore be concluded that merely the presence of EH does not elicit vertigo, which agrees with previous studies (23, 30). Schuknecht suggested that ruptures of the membranous labyrinth are the cause of vertigo spells, which would theoretically decrease the endolymph volume (57). However, a previous case report has revealed no large changes in EH on consecutive MRIs despite ongoing vertigo attacks (58). Of note, it was previously suggested that the fluctuations in EH may potentially be too small to be detected by MRI (23). Regarding the time course of vertigo attacks, our data contradicts previous suppositions that the number of attacks diminish over time (59). We did not observe a relationship between disease duration and the frequency or duration of vertigo attacks, which supports previous findings by Havia et al. and Jerin et al. (30, 60). It is worth noting that, although data on the *presence* of symptoms was well-documented in electronic patient files, we were unable to retrieve information on the *duration* of vestibular or cochlear symptoms in 21% of patients. Also, in hindsight, the categories we used to classify the duration of vertigo attacks were rather wide. The majority of patients fell within the 2nd category (vertigo attacks lasting 20 min to 12 h) and we did not account for further subanalysis.

In literature, there are conflicting views regarding the origin and evolution of EH. A previous meta-analysis of temporal bone reports from 184 MD patients demonstrated a cochleocentric distribution, where EH begins in the cochlear apex and from there progresses to involve the saccule, utricle and semicircular canals (61). The typical occurrence of low-frequency hearing loss in early stages of MD might be explained by these histopathological findings (57). On the contrary, in most of the radiologic literature, EH predominates in the vestibule (10, 62, 63). In our study, isolated cochlear EH was a scarce finding and less prevalent than isolated vestibular EH, which supports the hypothesis that EH originates in the vestibule. It was recently reported that a 3D real IR sequence is superior to 3D FLAIR in the assessment of cochlear EH due to its ability to distinguish endolymph from surrounding bone (64). Therefore, we cannot exclude that the lower prevalence of cochlear EH in our study cohort may be due to lower sensitivity of 3D FLAIR to cochlear EH. In addition, a golden standard for the assessment and quantification of EH is currently lacking. Although 3- and 4-point visual grading systems are often utilized to assess EH, and are subject to ongoing refinement, further developments are desired to enable objective volumetric quantification of EH.

Previous studies have addressed the development of bilateral EH in MD patients and reported variable prevalence rates ranging from 21 to 75%, which is thought to increase with disease duration (10, 23). In our study, bilateral EH was present in 36 (16.7%) of patients. We did not reveal significant differences in disease duration or age between patients with unilateral or bilateral EH and we were therefore unable to confirm the hypothesis. Nevertheless, the occurrence of bilaterality has led to the supposition that EH is a systemic disease and associations with genetic factors and several comorbidities have been reported in literature, particularly migraine and autoimmune diseases (21). In our study, migraine and autoimmune diseases were present in 11.2 and 6.5% of cases, respectively. Among the cardiovascular risk factors, hypertension was the most common comorbidity and reported in 17.2% of patients (17.8% in men; 16.7% in women). In comparison, the prevalence of arterial hypertension in the general Dutch population was estimated at 29.9% in men and 15.6% in women (65). Additionally, the prevalence of migraine in Europe and a broad group of autoimmune diseases in Denmark were estimated at 37.6 and 7.6–9.4%, respectively (66, 67). Therefore, an association between EH and autoimmune diseases, migraine or hypertension cannot be substantiated from our data.

The association between EH and BLB impairment at 4 h-delayed Gd-enhanced MRI has previously been demonstrated (32–36). In the present study, visually increased perilymphatic enhancement was present in 157 (87.7%) of unilateral HED patients. Furthermore, the degree of BLB impairment was significantly associated with EH grade. The BLB is indicated as the essential structure for the maintenance of inner ear fluid homeostasis by selectively regulating the passage of ions between the vasculature and inner ear (68). Based on this knowledge, it has been postulated that destruction of the labyrinthine barriers causes the formation of EH (33). However, previous studies have demonstrated that increased BLB permeability may also be present in non-hydropic ears from patients with sudden sensorineural hearing loss (SSNHL) or vestibular neuritis (36, 69). Therefore, it can also be deduced that BLB impairment does not necessarily lead to the formation of EH. Regardless of their actual pathophysiological processes, both EH and BLB impairment are likely markers of disordered labyrinthine homeostasis. Interestingly, it has been demonstrated on MRI that patients with SSNHL may show improvement of symptoms in parallel with resolution of the FLAIR hyperintensity (40). This close correspondence between MRI findings and clinical features in SSNHL patients raises the question whether this might also apply to patients with EH, though the underlying pathophysiological mechanisms are likely different. However, we evaluated the isolated effect of SIR on the degree of sensorineural hearing loss and did not demonstrate a significant correlation between SIR and low or high Fletcher indexes. Thus, a putative association between SIR and hearing loss in HED patients cannot be supported from this data. Our results are in agreement with Suzuki et al., who used the SIR of the basal cochlear turn against the cerebellar hemisphere as marker of BLB permeability and found no significant correlation with hearing thresholds (70). On the contrary, Kahn et al. did report a significant correlation between BLB impairment and worse hearing levels (71). In their study, however, they performed a visual assessment of BLB integrity and did not control for the potential confounding effect of EH. In addition to hearing loss, we also did not find a significant correlation between SIR and tinnitus, aural fullness, or the frequency and duration of vertigo attacks. It is worth noting that our retrospective study design inherently did not acknowledge certain clinical factors that could have potentially

influenced the MRI results, such as the time elapsed between the MRI examination and the last vertigo attack or intratympanic corticosteroid injections. Longitudinal radiological and clinical assessment could offer a better characterization of the dynamic alteration of MRI parameters in relation to treatment strategies and symptomatology.

Drop attacks are known to occur in a subset of MD patients, although the reported incidence is variable with rates ranging from 13.5 to 72%, depending on the definition used (16, 24, 72). In our study, drop attacks were present in 7.4% of unilateral HED patients. We found that drop attacks were associated with a longer disease course and higher grades of EH compared to patients without DA's. The DA group also demonstrated greater hearing loss than non-DA patients, which may be attributed to the longer disease duration and greater degree of EH. Similar observations were previously made by Wu et al. (16). Contrarily, the median SIR was not significantly different between patients with and without DA. Although the pathophysiological mechanisms of drop attacks are unknown, mechanical stimulation of the otolithic organs (saccule and/or utricle) by endolymphatic pressure gradients is currently the most widely accepted etiology (73, 74). The finding that DA occurs in patients with a greater degree of EH seems to support this theory.

The rationale behind MR imaging of EH is based on a desire to seek improved diagnostic precision and better understand how labyrinthine abnormalities affect the function of the inner ear. In addition, the possibility that imaging-derived data could serve as a surrogate marker of disease progression and therapeutic efficacy has become attractive. A critical aspect when considering the use of an MRI as a surrogate parameter is validation: the degree of EH and/or BLB impairment must show a correlation with the presence and severity of audiovestibular symptoms. Investigating the clinical picture from a morphologic point of view (i.e., Hydropic Ear Disease) allows assessment of this pathologic stage across the entire clinical spectrum. Although some correlations have been found, the degree of EH and BLB impairment incompletely characterize the whole phenotype of HED, especially regarding the incidence and severity of vertigo attacks. If a more explicit radiologic-clinical correlation can be established, then this information could potentially be used to better predict disease progression, monitor treatment response, and aid the development of novel treatment strategies.

CONCLUSION

In this retrospective study, we have investigated the clinical picture of patients with MRI-evidence of hydropic ear disease with or without BLB impairment. In our study population, the degree of EH correlates with disease duration, the severity of sensorineural hearing loss and the incidence of drop attacks. BLB is impaired in association with EH grade, but without clear contribution to the severity of audiovestibular symptoms.

DATA AVAILABILITY STATEMENT

The original contributions presented in the study are included in the article, further inquiries can be directed to the corresponding author/s.

ETHICS STATEMENT

Ethical review and approval was not required for the study on human participants in accordance with the local legislation and institutional requirements. Written informed consent for participation was not required for this study in accordance with the national legislation and the institutional requirements.

AUTHOR CONTRIBUTIONS

LP, JS, and SH contributed to the conception and design of the manuscript. LP, SH, TV, MH, HB, and CB acquired the data. JG helped shape and verify the statistical methods. LP performed the statistical analysis and drafted the manuscript. All authors contributed to the article and approved the submitted version.

FUNDING

Related to the research being submitted: SH: Radiology Research Fund from the Radiological Society of the Netherlands, to assess the technical feasibility of MRI-evaluated endolymphatic hydrops and allow development and optimization of imaging techniques. The funder was not involved in the study design, collection, analysis, interpretation of data, the writing of this article or the decision to submit it for publication. Not related to the research being submitted: BV: grants from Oticon and Advanced Bionics paid to institution.

REFERENCES

1. Harcourt J, Barraclough K, Bronstein AM. Meniere's disease. *BMJ*. (2014) 349:g6544. doi: 10.1136/bmj.g6544
2. Gürkov R, Pyykö I, Zou J, Kentala E. What is Menière's disease? A contemporary re-evaluation of endolymphatic hydrops. *J Neurol*. (2016) 263(suppl. 1):S71–81. doi: 10.1007/s00415-015-7930-1
3. Hallpike C, Cairns H. Observations on the pathology of Meniere's syndrome. *Proc R Soc Med*. (1938) 31:1317–36. doi: 10.1177/003591573803101112
4. Yamakawa K. Über die pathologische Veränderung bei einem Menière-Kranken. Proceedings of 42nd Annual Meeting Oto-Rhino-Laryngol Soc Japan. *J Otolaryngol Soc Jpn*. (1938) 4:2310–2.
5. Goebel JA. 2015 Equilibrium Committee amendment to the 1995 AAO-HNS guidelines for the definition of Ménière's disease. *Otolaryngol Head Neck Surg*. (2016) 154:403–4. doi: 10.1177/0194599816628524
6. Lopez-Escamez JA, Carey J, Chung WH, Goebel JA, Magnusson M, Mandalà M, et al. Diagnostic criteria for Menière's disease. *J Vestib Res Equilib Orientat*. (2015) 25:1–7. doi: 10.3233/VES-150549
7. House JW, Doherty JK, Fisher LM, Derebery MJ, Berliner KI. Meniere's disease: prevalence of contralateral ear involvement. *Otol Neurotol*. (2006) 27:355–61. doi: 10.1097/00129492-200604000-00011
8. Gürkov R. Menière and friends: imaging and classification of hydropic ear disease. *Otol Neurotol*. (2017) 38:e539–44. doi: 10.1097/MAO.0000000000001479

9. Committee on Hearing and Equilibrium guidelines for the diagnosis and evaluation of therapy in Meniere's disease. American Academy of Otolaryngology-Head and Neck Foundation, Inc. *Otolaryngol Head Neck Surg*. (1995) 113:181–5. doi: 10.1016/S0194-5998(95)70102-8
10. Pyykkö I, Nakashima T, Yoshida T, Zou J, Naganawa S. Ménière's disease: a reappraisal supported by a variable latency of symptoms and the MRI visualisation of endolymphatic hydrops. *BMJ Open*. (2013) 3:1555. doi: 10.1136/bmjopen-2012-001555
11. Phillips JS, Murdin L, Rea P, Sutton L. Clinical subtyping of Ménière's disease. *Otolaryngol Head Neck Surg*. (2018) 159:407–9. doi: 10.1177/0194599818773077
12. Pullen RL. Navigating the challenges of Meniere disease. *Nursing*. (2017) 47:38–45. doi: 10.1097/01.NURSE.0000520504.06428.ce
13. Rauch SD. Clinical hints and precipitating factors in patients suffering from Meniere's disease. *Otolaryngol Clin North Am*. (2010) 43:1011–7. doi: 10.1016/j.otc.2010.05.003
14. Nakashima T, Pyykkö I, Arroll MA, Casselbrant ML, Foster CA, Manzoor NF, et al. Meniere's disease. *Nat Rev Dis Prim*. (2016) 2:16028. doi: 10.1038/nrdp.2016.28
15. Gürkov R, Kantner C, Strupp M, Flatz W, Krause E, Ertl-Wagner B. Endolymphatic hydrops in patients with vestibular migraine and auditory symptoms. *Eur Arch Oto Rhino Laryngol*. (2014) 271:2661–7. doi: 10.1007/s00405-013-2751-2
16. Wu Q, Li X, Sha Y, Dai C. Clinical features and management of Meniere's disease patients with drop attacks. *Eur Arch Oto Rhino Laryngol*. (2019) 276:665–72. doi: 10.1007/s00405-018-5260-5
17. Teggi R, Carpini SD, Zagato L. Endolymphatic hydrops and ionic transporters: genetic and biohumoral aspects. *J Neurol*. (2019) 266:47–51. doi: 10.1007/s00415-019-09399-6
18. Teggi R, Battista RA, Di Berardino F, Familiari M, Cangiano I, Gatti O, et al. Evaluation of a large cohort of adult patients with ménière's disease: bedside and clinical history. *Acta Otorhinolaryngol Ital*. (2020) 40:444–9. doi: 10.14639/0392-100X-N0776
19. Saberi A, Nemati S, Amlashi TT, Tohidi S, Bakhshi F. Phonophobia and migraine features in patients with definite meniere's disease: pentad or triad/tetrad? *Acta Otolaryngol*. (2020) 140:548–52. doi: 10.1080/00016489.2020.1749299
20. Frejo L, Soto-Varela A, Santos-Perez S, Aran I, Batuecas-Caletrio A, Perez-Guillen V, et al. Clinical subgroups in bilateral meniere disease. *Front Neurol*. (2016) 7:182. doi: 10.3389/fneur.2016.00182
21. Gazquez I, Soto-Varela A, Aran I, Santos S, Batuecas A, Trinidad G, et al. High prevalence of systemic autoimmune diseases in patients with menière's disease. *PLoS ONE*. (2011) 6:e26759. doi: 10.1371/journal.pone.0026759
22. Nakashima T, Naganawa S, Sugiura M, Teranishi M, Sone M, Hayashi H, et al. Visualization of endolymphatic hydrops in patients with Meniere's disease. *Laryngoscope*. (2007) 117:415–20. doi: 10.1097/MLG.0b013e31802c300c
23. Shi S, Guo P, Li W, Wang W. Clinical features and endolymphatic hydrops in patients with MRI evidence of hydrops. *Ann Otol Rhinol Laryngol*. (2019) 128:286–92. doi: 10.1177/0003489418819551
24. Gürkov R, Jerin C, Flatz W, Maxwell R. Clinical manifestations of hydropic ear disease (Menière's). *Eur Arch Oto Rhino Laryngol*. (2019) 276:27–40. doi: 10.1007/s00405-018-5157-3
25. Maxwell ĀAK, Ishiyama G, Karnezis S, Ishiyama A. Isolated saccular hydrops on high-resolution MRI is associated with full spectrum Meniere's disease. *Otol Neurotol*. (2021) 42:876–82. doi: 10.1097/MAO.0000000000003051
26. Sluydts M, Bernaerts A, Casselman JW, De Foer B, Blaivie C, Zarowski A, et al. The relationship between cochleovestibular function tests and endolymphatic hydrops grading on MRI in patients with Menière's disease. *Eur Arch Oto Rhino Laryngol*. (2021). doi: 10.1007/s00405-021-06610-1. [Epub ahead of print].
27. Attyé A, Eliezer M, Medici M, Tropres I, Dumas G, Krainik A, et al. *In vivo* imaging of saccular hydrops in humans reflects sensorineural hearing loss rather than Meniere's disease symptoms. *Eur Radiol*. (2018) 28:2916–22. doi: 10.1007/s00330-017-5260-7
28. Sepahdari AR, Ishiyama G, Vorasubin N, Peng KA, Linetsky M, Ishiyama A. Delayed intravenous contrast-enhanced 3D FLAIR MRI in Meniere's disease: correlation of quantitative measures of endolymphatic hydrops with hearing. *Clin Imaging*. (2015) 39:26–31. doi: 10.1016/j.clinimag.2014.09.014
29. Nakashima T, Naganawa S, Teranishi M, Tagaya M, Nakata S, Sone M, et al. Endolymphatic hydrops revealed by intravenous gadolinium injection in patients with Ménière's disease. *Acta Otolaryngol*. (2010) 130:338–43. doi: 10.3109/00016480903143986
30. Jerin C, Floerke S, Maxwell R, Gürkov R. Relationship between the extent of endolymphatic hydrops and the severity and fluctuation of audiovestibular symptoms in patients with Menière's disease and MRI evidence of hydrops. *Otol Neurotol*. (2018) 39:e123–30. doi: 10.1097/MAO.0000000000001681
31. Gürkov R, Flatz W, Louza J, Strupp M, Ertl-Wagner B, Krause E. *In vivo* visualized endolymphatic hydrops and inner ear functions in patients with electrocochleographically confirmed Ménière's disease. *Otol Neurotol*. (2012) 33:1040–5. doi: 10.1097/MAO.0b013e31825d9a95
32. Tagaya M, Yamazaki M, Teranishi M, Naganawa S, Yoshida T, Otake H, et al. Endolymphatic hydrops and blood-labyrinth barrier in Meniere's disease. *Acta Otolaryngol*. (2011) 131:474–9. doi: 10.3109/00016489.2010.534114
33. Zhang W, Xie J, Hui L, Li S, Zhang B. The correlation between endolymphatic hydrops and blood-labyrinth barrier permeability of Meniere disease. *Ann Otol Rhinol Laryngol*. (2021) 130:578–84. doi: 10.1177/0003489420964823
34. Van Steekelenburg JM, van Weijnen A, de Pont LMH, Vijlbrief OD, Bommeljé CC, Koopman JP, et al. Value of endolymphatic hydrops and perilymph signal intensity in suspected Ménière disease. *Am J Neuroradiol*. (2020) 41:529–34. doi: 10.3174/ajnr.A6410
35. Bernaerts A, Vanspauwen R, Blaivie C, van Dinther J, Zarowski A, Wuyts FL, et al. The value of four stage vestibular hydrops grading and asymmetric perilymphatic enhancement in the diagnosis of Menière's disease on MRI. *Neuroradiology*. (2019) 61:421–9. doi: 10.1007/s00234-019-02155-7
36. Pakdaman MN, Ishiyama G, Ishiyama A, Peng KA, Kim HJ, Pope WB, et al. Blood-labyrinth barrier permeability in menière disease and idiopathic sudden sensorineural hearing loss: findings on delayed postcontrast 3D-FLAIR MRI. *Am J Neuroradiol*. (2016) 37:1903–8. doi: 10.3174/ajnr.A4822
37. Zou J, Li M, Zhang Y, Zheng G, Chen D, Chen S, et al. Transport augmentation through the blood-inner ear barriers of guinea pigs treated with 3-nitropropionic acid and patients with acute hearing loss, visualized with 3.0 T MRI. *Otol Neurotol*. (2011) 32:204–12. doi: 10.1097/MAO.0b013e3182016332
38. Naganawa S. The Technical and clinical features of 3D-FLAIR in neuroimaging. *Magn Reson Med Sci*. (2015) 14:93–106. doi: 10.2463/mrms.2014-0132
39. Mark AS, Chapman JC, Seltzer S, Fitzgerald DC, Nelson-Drake J, Gulya AJ. Labyrinthine enhancement on gadolinium-enhanced magnetic resonance imaging in sudden deafness and vertigo: correlation with audiologic and electronystagmographic studies. *Ann Otol Rhinol Laryngol*. (1992) 101:459–64. doi: 10.1177/000348949210100601
40. Seltzer S, Mark AS. Contrast enhancement of the labyrinth on MR scans in patients with sudden hearing loss and vertigo: evidence of labyrinthine disease. *Am J Neuroradiol*. (1991) 12:13–6.
41. Sone M, Mizuno T, Naganawa S, Nakashima T. Imaging analysis in cases with inflammation-induced sensorineural hearing loss. *Acta Otolaryngol*. (2009) 129:239–43. doi: 10.1080/00016480802226163
42. Nakashima T, Naganawa S, Pyykko I, Gibson WPR, Sone M, Nakata S, et al. Grading of endolymphatic hydrops using magnetic resonance imaging. *Acta Otolaryngol Suppl*. (2009) 560:5–8. doi: 10.1080/00016480902729827
43. Baráth K, Schuknecht B, Monge Naldi A, Schrepfer T, Bockisch CJ, Hegemann SCA. Detection and grading of endolymphatic hydrops in Menière disease using MR imaging. *Am J Neuroradiol*. (2014) 35:1387–92. doi: 10.3174/ajnr.A3856
44. Attyé A, Eliezer M, Boudiaf N, Tropres I, Chechin D, Schmerber S, et al. MRI of endolymphatic hydrops in patients with Meniere's disease: a case-controlled study with a simplified classification based on saccular morphology. *Eur Radiol*. (2017) 27:3138–46. doi: 10.1007/s00330-016-4701-z
45. Teranishi M, Naganawa S, Katayama N, Sugiura M, Nakata S, Sone M, et al. Image evaluation of endolymphatic space in fluctuating hearing loss without vertigo. *Eur Arch Oto Rhino Laryngol*. (2009) 266:1871–7. doi: 10.1007/s00405-009-0989-5
46. Gürkov R, Hornibrook J. On the classification of hydropic ear disease (Menière's disease). *HNO*. (2018) 66:455–63. doi: 10.1007/s00106-018-0488-3
47. Okuno T, Sando I. Localization, frequency, and severity of endolymphatic hydrops and the pathology of the labyrinthine membrane in

meniere's disease. *Ann Otol Rhinol Laryngol*. (1987) 96:438–45. doi: 10.1177/000348948709600418
48. Xie W, Shu T, Liu J, Peng H, Karpeta N, Marques P. The relationship between clinical characteristics and magnetic resonance imaging results of Ménière disease : a prospective study. *Sci Rep*. (2021) 11:7212. doi: 10.1038/s41598-021-86589-1
49. Fiorino F, Pizzini FB, Beltramello A, Barbieri F. MRI performed after intratympanic gadolinium administration in patients with Meniere's disease: correlation with symptoms and signs. *Eur Arch Oto Rhino Laryngol*. (2011) 268:181–7. doi: 10.1007/s00405-010-1353-5
50. Zhang Y, Liu B, Wang R, Jia R, Gu X. Characteristics of the cochlear symptoms and functions in Meniere's disease. *Chin Med J*. (2016) 129:2445–50. doi: 10.4103/0366-6999.191767
51. Yoshida T, Stephens D, Kentala E, Levo H, Auramo Y, Poe D, et al. Tinnitus complaint behaviour in long-standing Menière's disorder: its association with the other cardinal symptoms. *Clin Otolaryngol*. (2011) 36:461–7. doi: 10.1111/j.1749-4486.2011.02381.x
52. Levo H, Kentala E, Rasku J, Pyykkö I. Aural fullness in ménière's disease. *Audiol Neurotol*. (2014) 19:395–9. doi: 10.1159/000363211
53. Sando I, Orita Y, Hirsch BE. Pathology and pathophysiology of Meniere's disease. *Otolaryngol Clin North Am*. (2002) 35:517–28. doi: 10.1016/S0030-6665(02)00020-8
54. Paparella MM. Pathogenesis of meniere's disease and meniere's syndrome. *Acta Otolaryngol*. (1983) 406:10–25. doi: 10.3109/00016488309122996
55. Silverstein H. The effects of perfusion the perilymphatic space with artificial endolymph. *Ann Otol Rhinol Laryngol*. (1970) 79:754–65. doi: 10.1177/000348947007900408
56. Gibson WPR. Hypothetical mechanism for vertigo in Meniere's disease. *Otolaryngol Clin North Am*. (2010) 43:1019–27. doi: 10.1016/j.otc.2010.05.013
57. Schuknecht HF. Meniere's disease: a correlation of symptomatology and pathology. *Laryngoscope*. (1963) 73:651–65. doi: 10.1288/00005537-196306000-00002
58. Fukushima M, Akahani S, Inohara H, Takeda N. Stability of endolymphatic hydrops in ménière disease shown by 3-Tesla Magnetic Resonance Imaging during and after Vertigo Attacks. *JAMA Otolaryngol*. (2019) 145:583–5. doi: 10.1001/jamaoto.2019.0435
59. Perez-Garrigues H, Lopez-Escamez JA, Perez P, Sanz R, Orts M, Marco J, et al. Time course of episodes of definitive vertigo in Ménière's disease. *Arch Otolaryngol Head Neck Surg*. (2008) 134:1149–54. doi: 10.1001/archotol.134.11.1149
60. Havia M, Kentala E. Progression of symptoms of dizziness in Ménière's disease. *Arch Otolaryngol*. (2004) 130:431–5. doi: 10.1001/archotol.130.4.431
61. Pender DJ. Endolymphatic hydrops and Meniere's disease: a lesion meta-analysis. *J Laryngol Otol*. (2014) 128:859–65. doi: 10.1017/S0022215114001972
62. Shi S, Zhou F, Wang W. 3D-real IR MRI of Meniere's disease with partial endolymphatic hydrops. *Am J Otolaryngol*. (2019) 40:589–93. doi: 10.1016/j.amjoto.2019.05.015
63. Fiorino F, Pizzini FB, Beltramello A, Barbieri F. Progression of endolymphatic hydrops in Meniere's disease as evaluated by magnetic resonance imaging. *Otol Neurotol*. (2011) 32:1152–7. doi: 10.1097/MAO.0b013e31822a1ce2
64. Manuel V, Vega S, Dominguez P, Caballeros FM, Leal JI, Perez-fernandez N. Comparison between high-resolution 3D-IR with real reconstruction and 3D-flair sequences in the assessment of endolymphatic hydrops in 3 tesla. *Acta Otolaryngol*. (2020) 140:883–8. doi: 10.1080/00016489.2020.1792550
65. Wang X, Bots ML, Yang F, Sun J, He S, Hoes AW, et al. A comparison of the prevalence and clustering of major cardiovascular risk factors in the Netherlands and China. *Eur J Prev Cardiol*. (2016) 23:1766–73. doi: 10.1177/2047487316648474
66. Katsarava Z, Mania M, Lampl C, Herberhold J, Steiner TJ. Poor medical care for people with migraine in Europe – evidence from the Eurolight study. *J Headache Pain*. (2018) 19:1–9. doi: 10.1186/s10194-018-0839-1
67. Cooper GS, Bynum MLK, Somers EC. Recent insights in the epidemiology of autoimmune diseases: improved prevalence estimates and understanding of clustering of diseases. *J Autoimmun*. (2009) 33:197–207. doi: 10.1016/j.jaut.2009.09.008
68. Ishiyama G, Lopez IA, Ishiyama P, Vinters H V., Ishiyama A. The blood labyrinthine barrier in the human normal and Meniere's disease macula utricle. *Sci Rep*. (2017) 7:253. doi: 10.1038/s41598-017-00330-5
69. Eliezer M, Maquet C, Horion J, Gillibert A, Toupet M, Bolognini B, et al. Detection of intralabyrinthine abnormalities using post-contrast delayed 3D-FLAIR MRI sequences in patients with acute vestibular syndrome. *Eur Radiol*. (2019) 29:2760–9. doi: 10.1007/s00330-018-5825-0
70. Suzuki H, Teranishi M, Sone M, Yamazaki M, Naganawa S, Nakashima T. Contrast enhancement of the inner ear after intravenous administration of a standard or double dose of gadolinium contrast agents. *Acta Otolaryngol*. (2011) 131:1025–31. doi: 10.3109/00016489.2011.598552
71. Kahn L, Hautefort C, Guichard JP, Toupet M, Jourdaine C, Vitaux H, et al. Relationship between video head impulse test, ocular and cervical vestibular evoked myogenic potentials, and compartmental magnetic resonance imaging classification in menière's disease. *Laryngoscope*. (2019) 130:E444–52. doi: 10.1002/lary.28362
72. Kentala E, Havia M, Pyykkö I. Short-lasting drop attacks in Meniere's disease. *Otolaryngol Head Neck Surg*. (2001) 124:526–30. doi: 10.1067/mhn.2001.115169
73. Baloh RW, Jacobson K, Winder T. Drop attacks with Meniere's syndrome. *Ann Neurol*. (1990) 28:384–7. doi: 10.1002/ana.410280314
74. Calzada AP, Lopez IA, Ishiyama G, Ishiyama A. Otolithic membrane damage in patients with endolymphatic hydrops and drop attacks. *Otol Neurotol*. (2012) 33:1593–8. doi: 10.1097/MAO.0b013e318271c48b

Conflict of Interest: The authors declare that the research was conducted in the absence of any commercial or financial relationships that could be construed as a potential conflict of interest.

Publisher's Note: All claims expressed in this article are solely those of the authors and do not necessarily represent those of their affiliated organizations, or those of the publisher, the editors and the reviewers. Any product that may be evaluated in this article, or claim that may be made by its manufacturer, is not guaranteed or endorsed by the publisher.

frontiers in Surgery

CASE REPORT
published: 08 December 2021
doi: 10.3389/fsurg.2021.727672

Enhanced Eye Velocity With Backup Saccades in vHIT Tests of a Menière Disease Patient: A Case Report

Maria Montserrat Soriano-Reixach[1,2]*, *Jorge Rey-Martinez*[1,2], *Xabier Altuna*[1,2] and *Ian Curthoys*[3]

[1] Neurotology Unit, Department of Otorhinolaryngology Head and Neck Surgery, Donostia University Hospital, Donostia-San Sebastian, Spain, [2] Biodonostia Health Research Institute, Otorhinolaryngology Area, Osakidetza Basque Health Service, San Sebastián, Spain, [3] Vestibular Research Laboratory, School of Psychology, The University of Sydney, Sydney, NSW, Australia

Reduced eye velocity and overt or covert compensatory saccades during horizontal head impulse testing are the signs of reduced vestibular function. However, here we report the unusual case of a patient who had enhanced eye velocity during horizontal head impulses followed by a corrective saccade. We term this saccade a "backup saccade" because it acts to compensate for the gaze position error caused by the enhanced velocity (and enhanced VOR gain) and acts to return gaze directly to the fixation target as shown by eye position records. We distinguish backup saccades from overt or covert compensatory saccades or the anticompensatory quick eye movement (ACQEM) of Heuberger et al. (1) ACQEMs are anticompensatory in that they are in the same direction as head velocity and so, act to take gaze off the target and thus require later compensatory (overt) saccades to return gaze to the target. Neither of these responses were found in this patient. The patient here was diagnosed with unilateral definite Meniere's disease (MD) on the right and had enhanced VOR (gain of 1.17) for rightward head impulses followed by backup saccades. For leftwards head impulses eye velocity and VOR gain were in the normal range (VOR gain of 0.89). As further confirmation, testing with 1.84 Hz horizontal sinusoidal head movements in the visual-vestibular (VVOR) paradigm also showed these backup saccades for rightwards head turns but normal slow phase eye velocity responses without backup saccades for leftwards had turns. This evidence shows that backup saccades can be observed in some MD patients who show enhanced eye velocity responses during vHIT and that these backup saccades act to correct for gaze position error caused by the enhanced eye velocity during the head impulse and so have a compensatory effect on gaze stabilization.

Keywords: Meniere's disease, backup saccades, enhanced eye velocity, endolymphatic hydrops, vHIT, case report, VOR (vestibulo-ocular reflex)

OPEN ACCESS

Edited by:
Ilmari Pyykkö,
Tampere University, Finland

Reviewed by:
A. B. Zulkiflee,
University Malaya Medical Centre, Malaysia
Klaus Jahn,
Schoen Clinic Bad Aibling, Germany

***Correspondence:**
Maria Montserrat Soriano-Reixach
mariiasoriano@gmail.com

Specialty section:
This article was submitted to Otorhinolaryngology - Head and Neck Surgery, a section of the journal Frontiers in Surgery

Received: *19 June 2021*
Accepted: *15 November 2021*
Published: *08 December 2021*

Citation:
Soriano-Reixach MM, Rey-Martinez J, Altuna X and Curthoys I (2021) Enhanced Eye Velocity With Backup Saccades in vHIT Tests of a Menière Disease Patient: A Case Report. Front. Surg. 8:727672. doi: 10.3389/fsurg.2021.727672

INTRODUCTION

Video head impulse testing of healthy subjects usually results in the eye velocity matching the head velocity, so vestibulo-ocular response (VOR) gain is about 1.0 and gaze remains on the earth fixed target. Vestibular hypofunction causes reduced eye velocity during the impulse, with corrective (compensatory) saccades—either overt or covert—to correct the gaze error and return gaze to the

earth fixed target. Recently there have been reports of enhanced eye velocity (and so enhanced VOR gain) during head impulse testing of some patients with Menière's Disease (MD) (2–4). Such enhanced eye velocity could be caused by peripheral vestibular disease, such as endolymphatic hydrops related diseases or central vestibular dysfunction, such as cerebellar disease (5). Or the enhancement could be due to a recording artifact (6).

In usual vHIT testing of patients with vestibular hypofunction and reduced eye velocity during the head impulse, the corrective saccade is called compensatory since it returns the gaze to the target by canceling out the gaze position error caused by the inadequate eye velocity. In the case of enhanced eye velocity, a corrective saccade is also necessary to return gaze to the fixation target. Therefore, this corrective saccade is also compensatory in the sense that it cancels the gaze position error caused by the enhanced eye velocity. Although this saccade is compensatory, it is in the opposite direction to the common compensatory saccade recorded in patients with vestibular hypofunction. To avoid confusion we have used the term "backup saccade" to refer to this corrective saccade after enhanced eye velocity. Until now, when enhanced vestibular slow phase eye velocity during head impulses have been observed on vHIT testing, no corrective backup saccades have been described (3). In this case report we describe, for what we think is the first time, a patient with definite MD with enhanced eye velocity (and so enhanced VOR gain) during head impulse testing, who showed compensatory saccades ("backup saccades"). These backup saccades were observed on clinical HIT tests, recorded on head impulse testing using vHIT and further confirmed by their occurrence during visual-vestibular reflex (VVOR) testing.

CASE REPORT

A 74-year-old woman, with left eye amblyopia and no other medical history of interest, was diagnosed with unilateral definite Menière's disease (MD) of the right ear in 2016 according to the following Bárány Society diagnostic criteria for MD7: (1) Two or more spontaneous episodes of vertigo, each lasting 20 min to 12 h, (2) Low-medium frequency sensorineural hearing loss in one ear, defining the affected ear, on at least one occasion prior, (3) Fluctuating aural symptoms (hearing, tinnitus, or fullness) in the affected ear, (4) Not better accounted for by another vestibular diagnosis (7).

During the last 5 years she reported unilateral right fluctuating low and had mid-frequency hearing loss (**Figure 1**) with mild sensorineural hearing loss of the right ear (PTA 40 dB-HL). She had normal hearing of the left ear [pure tone average (PTA), 20 dB-HL according to BIAP 2017 (www.biap.org)]. During this 5-year period, the fluctuating hearing loss on the right was accompanied by recurrent vertigo attacks lasting 30–60 min with tinnitus and fullness in the right ear. These attacks occurred monthly before medical treatment. Good control of vertigo attacks was achieved with Betahistine (16 mg every 8 h) and four doses of intratympanic corticoid of Dexamethasone (1.5 ml with a dilution of 15 mg/ml) to the right ear on two occasions (2017 and 2019). In the most recent consultation, she reported occasional vertigo attacks with mild instability, which did not interfere with her daily life. The cerebral and posterior fossa magnetic resonance images showed no alterations; also, no other general or neurological symptoms were presented during the 5-year period.

On physical examination, bilateral otoscopy was normal and her smooth pursuit appeared normal at bedside testing. On horizontal head impulse testing with the instruction to fixate an earth fixed target, she showed corrective saccades when her head was turned to the affected (right) side (**Supplementary Video 1**), but no corrective saccades for leftwards head impulses. vHIT testing using ICS Impulse system showed exactly what was happening. During rightwards head impulses the patient had enhanced slow phase eye velocity (i.e., with eye velocity greater than head velocity, so VOR gains for the right were >1) (**Figure 2**, **Supplementary Video 2**). VOR gain was calculated using the area under the desaccaded eye velocity record divided by the area under the head velocity curve for VOR gain measurement as is standard for the ICS Impulse system. **Figure 1** shows that at the end of each rightward head impulse there was a corrective saccade which acted to eliminate the gaze position error caused by the enhanced eye velocity and so this saccade is compensatory. As is clear from **Figure 1**, saccades rarely occurred during the rightward head turn, so desaccading was not required for VOR gain calculation. The measured VOR gain for rightward impulses was 1.17, and for leftward impulses was 0.89. As discussed above, we termed this unusual saccade a "backup saccade" to distinguish it from the usual overt or covert saccades, which act to correct for gaze position error when there is reduced slow phase eye velocity in patients with vestibular hypofunction. The backup saccade acts to correct gaze position error, with the key point being that here the gaze position error is due to vestibular hyperfunction rather than vestibular hypofunction. That result is very clearly shown by the eye position records (**Figure 4**).

This patient also showed backup saccades during rightward head movements in low frequency visual vestibular (VVOR) testing (**Figure 3**) at a frequency of 1.84 Hz. The measured VOR gain on the right side was 1.07 and 0.91 on the left (using the gain calculation method published by Rey-Martinez et al. and Soriano-Reixach et al. (2, 8).

The backup saccade we report here is distinctly different from the anticompensatory quick eye movements (ACQEM) reported by Heuberger et al. (1) during head impulse testing of some patients with Meniere's Disease for the following reasons;

> ACQEMs occur during the head impulse and take the gaze off the target, in the direction of the head velocity and so are anticompensatory in the sense that the ACQEM will take gaze off the fixation target and so require a corrective saccade at the end of the head impulse to return gaze to the earth fixed target. These corrective saccades after ACQEMs are clearly shown in Heuberger **Figure 1**. In contrast, backup saccades occur at the end of the head impulse and return gaze to the target directly and so are compensatory. They act to correct the gaze position error entailed by enhanced eye velocity during the head impulse (**Figures 2**, **4**).
>
> The latency for the ACQEM is consistently around 96 ms from the onset of the head impulse by

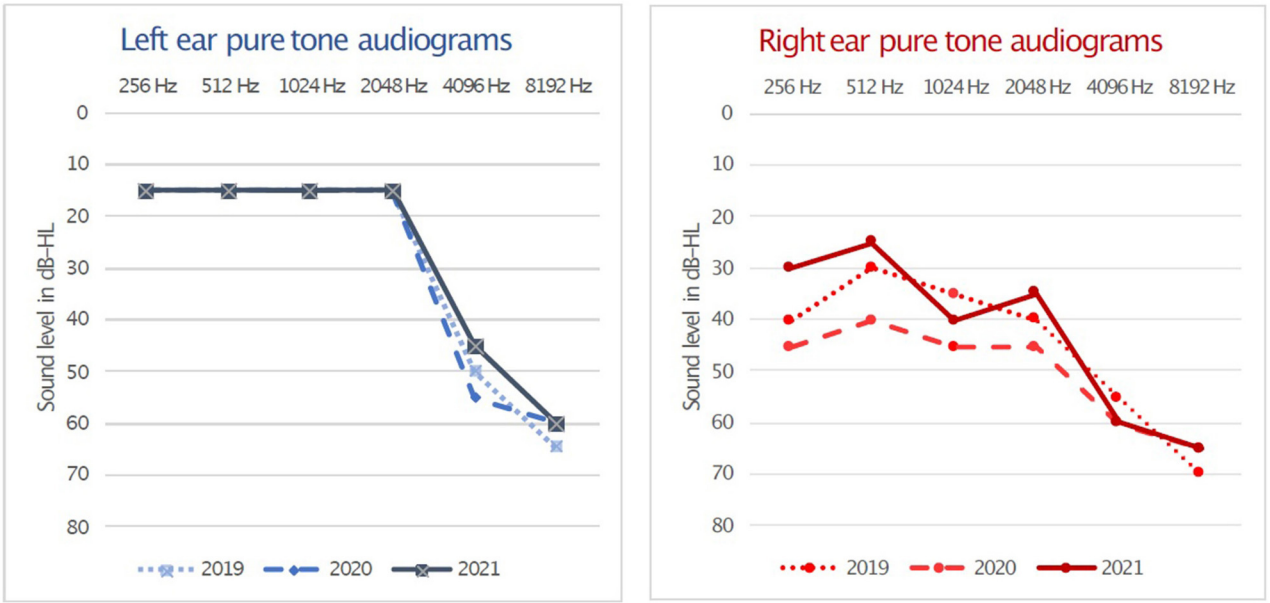

FIGURE 1 | Right and left pure tone air-conduction audiograms from the last 3 years. Unilateral right fluctuating low and mid-frequencies hearing loss with a PTA 40 dB-HL is present at testing in 2019, 2020, and 2021 while normal hearing was obtained in left ear on these occasions with a PTA of 20 dB-HL. Hearing loss levels and PTA calculation methods according to BIAP 2017 (www.biap.org).

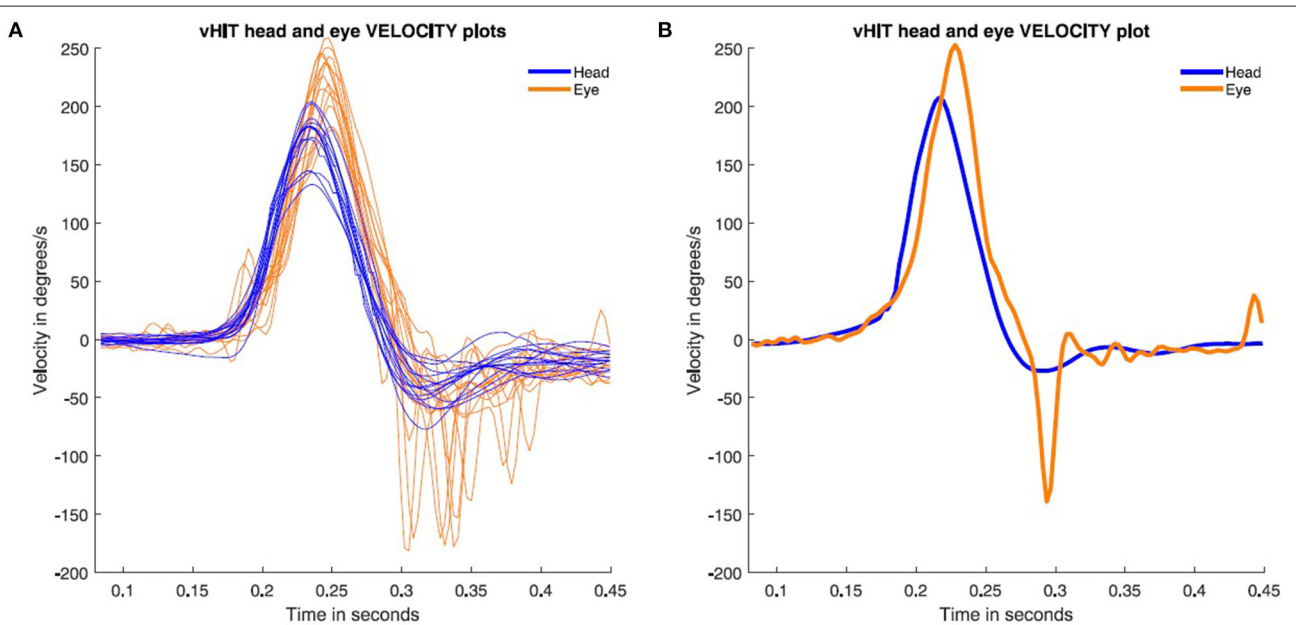

FIGURE 2 | Rightward video head impulse test responses performed during the patient's most recent test (2021). The eye velocity (orange) is enhanced compared to head velocity (blue). This will result in the eye being off target and in order to correct that gaze position error (**Figure 4**) the eye makes a compensatory backup saccade. **(A)** All the right-side impulses are plotted with backup saccades present on all impulses. **(B)** A single rightward head impulse to show the onset of the backup saccade exactly.

Heuberger et al. (1), whereas the backup saccade has a longer variable latency of around 150–200 ms (see **Figure 1**).

We also note that the backup saccade is distinctly different from the very early compensatory "saccade-like" response reported by Curthoys et al., in some MD patients with enhanced eye velocity

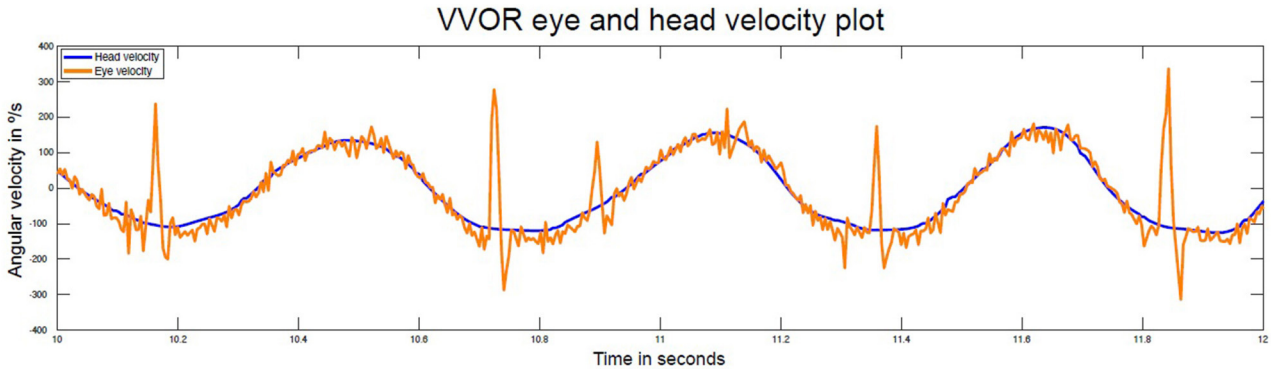

FIGURE 3 | Time series of head and eye velocity during the visual vestibular-ocular (VVOR) interaction test at 1.84 Hz. There is evidence of enhanced eye velocity for rightward head turns and backup saccades are present in each rightward head turn. Normal eye velocity responses occur for leftward head rotations. In this VVOR figure, negative velocity values are assigned to right direction movement velocity. The VOR gain for the right and left sides were 1.07 and 0.91, respectively.

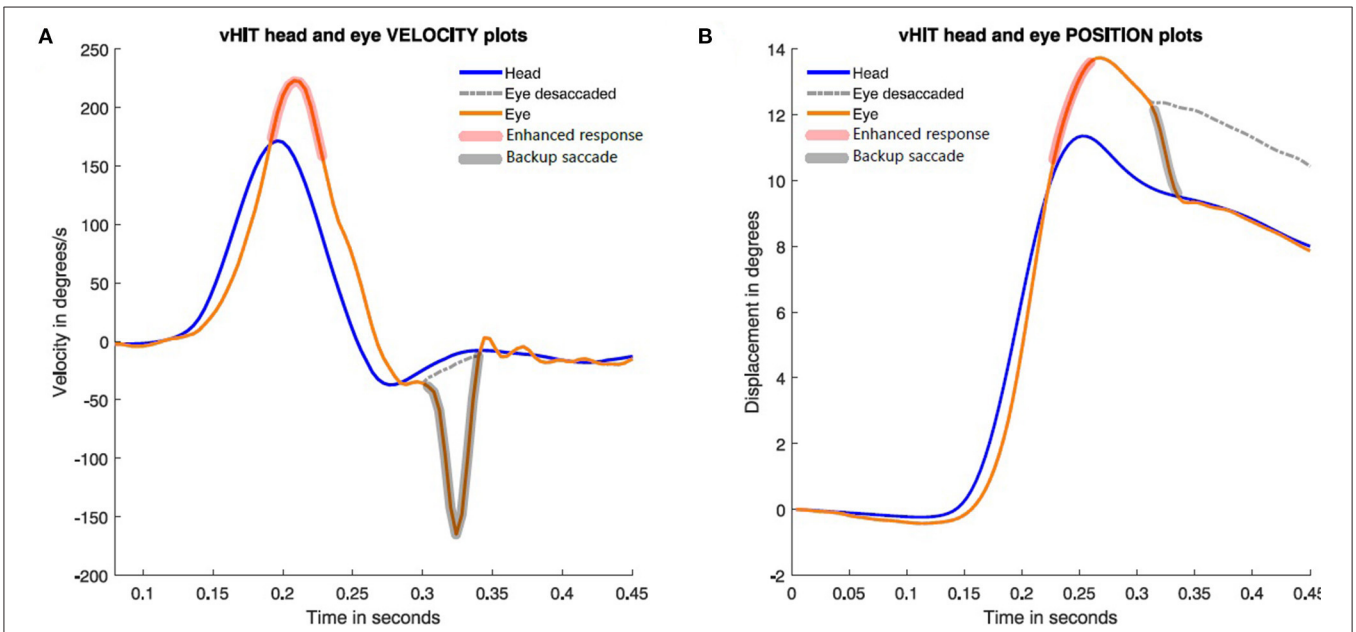

FIGURE 4 | Time series plots of eye velocity and corresponding eye position during a single rightward head impulse to show how the backup saccade corrects for the gaze position error. In **(A)**, the enhanced eye velocity (red shadow brush) is followed at the end of the head impulses by a backup saccade (black shadow brush). In **(B)**, head and eye position during the impulse are plotted. The dashed line shows eye position without backup saccade.

(3). The latency of these "saccade-like" responses is very short and much shorter than ACQEMs and backup saccades, as well as being in the opposite direction to ACQEMs. In the Curthoys et al. study, it was suggested that the enhanced eye velocity might be due to hydrops, in accord with the effect of glycerol and modeling and imaging data (9). However, another possibility is that cerebellar dysfunction could result in enhanced VOR gain (5). Alternatively the enhanced eye velocity may be due to a calibration error (6). That is unlikely because it would affect both leftward and rightward eye velocity responses, whereas backup saccades were only found on rightward head impulses.

In the clinical series published by Vargas et al. it was reported that of 56 patients with MD, 39.6% of them had enhanced VOR responses on vHIT testing, but in most of these cases with enhanced VOR gain none presented backup saccades as reported here. Only two cases in that clinical series (one of them being the case presented here), had evident backup saccades (i.e., only 8.6% of the MD patients with enhanced VOR gain on vHIT). Why are backup saccades not more commonly seen in patients with enhanced eye velocity? It has been suggested that this could be due to the very different eye velocity trajectories

during the increasing head velocity and decreasing head velocity phases of the head impulse [Curthoys et al. (3); **Figure 1**]. It may be that the eye position error during the acceleration phase may be partially corrected by the eye position error during the deceleration phase, resulting in such a small final eye position error that it is not necessary for any correction.

The main limitation of this case report is the possible effect of left eye amblyopia on right eye recorded vHIT responses. At this moment, we did not find any bibliographic reference about the possible effect of contralateral amblyopia on vHIT testing, but this and many of the previous discussed questions should be investigated on further research as other possible cause associated with the reversed backup saccades.

A recent report confirming the presence of very early saccade responses during active head impulses has highlighted the future need for detailed examination of these various saccades or saccade-like responses during head impulse testing, including consideration of a factor which has been shown to affect saccades—the patient's age (10, 11).

CONCLUSION

Backup saccades can be observed in some MD patients with enhanced eye vHIT responses. These backup saccades are compensatory but are in the opposite direction to the usual compensatory saccades recorded in patients with reduced vestibular function.

DATA AVAILABILITY STATEMENT

The data in this article is not readily available due to consent needed to use patient data. Reasonable requests can be made to the corresponding author/s.

ETHICS STATEMENT

The studies involving human participants were reviewed and approved by Donostia University Hospital. The patients/participants provided their written informed consent to participate in this study. Written informed consent was obtained from the individual(s) for the publication of any potentially identifiable images or data included in this article.

AUTHOR CONTRIBUTIONS

MS-R and JR-M contributed to conception and design of the study and organized the database. JR-M performed the statistical analysis and wrote sections of the manuscript. MS-R wrote the first draft of the manuscript. All authors contributed to manuscript revision, read, and approved the submitted version.

SUPPLEMENTARY MATERIAL

The Supplementary Material for this article can be found online at: https://www.frontiersin.org/articles/10.3389/fsurg.2021.727672/full#supplementary-material

Supplementary Video 1 | Examples of backup saccades during rightward head impulses.

Supplementary Video 2 | External video of vHIT testing. Backup saccades are evident in the absence of observable recording artifacts such as google slippage.

REFERENCES

1. Heuberger M, Saglam M, Todd NS, John K, Schneider E, Lehnen N, et al. Covert anti-compensatory quick eye movements during head impulses. *PLoS ONE.* (2014) 9:e93086. doi: 10.1371/journal.pone.0093086
2. Rey-Martinez J, Batuecas-Caletrio A, Matiño E, Trinidad-Ruiz G, Altuna X, Perez-Fernandez N. Mathematical methods for measuring the visually enhanced vestibulo-ocular reflex and preliminary results from healthy subjects and patient groups. *Front Neurol.* (2018) 9:69. doi: 10.3389/fneur.2018.00069
3. Curthoys IS, Manzari L, Rey-Martinez J, Dlugaiczyk J, Burgess AM. Enhanced eye velocity in head impulse testing-a possible indicator of endolymphatic hydrops. *Front Surg.* (2021) 8:666390. doi: 10.3389/fsurg.2021.666390
4. Vargas A, Ninchritz E, Goiburu M, Betances F, Rey-Martinez J, Altuna X. Clinical prevalence of enhanced vestibulo-ocular reflex responses on video head impulse test. *Otol Neurotol.* (2021) 42:e1160–9. doi: 10.1097/MAO.0000000000003171
5. Kheradmand A, Zee DS. The bedside examination of the vestibulo-ocular reflex (VOR): an update. *Rev Neurol.* (2012) 168:710–9. doi: 10.1016/j.neurol.2012.07.011
6. Mantokoudis G, Saber AS, Kattah JC, Eibenberger K, Guede CI, Zee DS, et al. Quantifying the vestibulo-ocular reflex with video-oculography: nature and frequency of artifacts. *Audiol Neurotol.* (2015) 20:39–5. doi: 10.1159/000362780
7. Lopez-Escamez JA, Carey J, Chung WH, Goebel JA, Magnusson M, Mandalà M, et al. Diagnostic criteria for Menière's disease. *J Vestib Res.* (2015) 25:1–7. doi: 10.3233/VES-150549
8. Soriano-Reixach MM, Prieto-Matos C, Perez-Fernandez N, Rey-Martinez J. Effects of parameters of video head impulse testing on visually enhanced vestibulo-ocular reflex and vestibulo-ocular reflex suppression. *Clin Neurophysiol.* (2020) 131:1839–47. doi: 10.1016/j.clinph.2020.04.169
9. Rey-Martinez J, Altuna X, Cheng K, Burgess AM, Curthoys IS. Computing endolymph hydrodynamics during head impulse test on normal and hydropic vestibular labyrinth models. *Front Neurol.* (2020) 21:289–98. doi: 10.3389/fneur.2020.00289
10. Sjögren J, Karlberg M, Hickson C, Magnusson M, Fransson PA, Tjernström F. Short-latency covert saccades – the explanation for good dynamic visual performance after unilateral vestibular loss? *Front Neurol.* (2021) 45:695064. doi: 10.3389/fneur.2021.695064
11. Agarwal Y, Schubert MC, Migliaccio AA, Zee DS, Schneider E, Lehnen N, et al. Evaluation of quantitative head impulse testing using search coils versus video-oculography in older individuals. *Otol Neurotol.* (2014) 35:283–8. doi: 10.1097/MAO.0b013e3182995227

Conflict of Interest: The authors declare that the research was conducted in the absence of any commercial or financial relationships that could be construed as a potential conflict of interest.

Publisher's Note: All claims expressed in this article are solely those of the authors and do not necessarily represent those of their affiliated organizations, or those of the publisher, the editors and the reviewers. Any product that may be evaluated in this article, or claim that may be made by its manufacturer, is not guaranteed or endorsed by the publisher.

frontiers in Surgery

ORIGINAL RESEARCH
published: 12 January 2022
doi: 10.3389/fsurg.2021.673323

Imaging Analysis of Patients With Meniere's Disease Treated With Endolymphatic Sac-Mastoid Shunt Surgery

Yawei Li[1,2], *Yafeng Lv*[1,2], *Na Hu*[3], *Xiaofei Li*[1,2], *Haibo Wang*[1,2]* *and Daogong Zhang*[1,2]*

[1] *Department of Otolaryngology-Head and Neck Surgery, Shandong Provincial Ear, Nose and Throat Hospital, Cheeloo College of Medicine, Shandong University, Jinan, China,* [2] *Shandong Provincial Vertigo & Dizziness Medical Center, Jinan, China,* [3] *Department of Radiology, Shandong Provincial Ear, Nose and Throat Hospital, Cheeloo College of Medicine, Shandong University, Jinan, China*

Objective: Endolymphatic sac surgery is effective in treating intractable Meniere's disease (MD), but the underlying mechanism is still unknown. Our study investigated the mechanism by which endolymphatic sac-mastoid shunt (EMS) surgery is effective in treating MD by means of imaging.

Methods: The experiment included 19 patients with intractable MD who underwent 3D-fluid-attenuated inversion recovery (FLAIR) MRI with a 3-Tesla unit 6 h after intravenous administration of gadolinium, before EMS, and 2 years after the surgery. The enhanced perilymphatic space in the bilateral cochlea, vestibule, and canals was visualized and compared with that in the endolymphatic space by quantitatively scoring the scala vestibuli of the cochlea and by measuring the developing area of the vestibules quantitatively.

Results: Gadolinium was present in the perilymph of the inner ear in the cochlea, vestibules, and canals of all patients. At the 2-year follow-up, 14 (73.68%) patients had vertigo control. Both before and 2 years after surgery, significant differences were observed in the scala vestibuli scores and the area of vestibular perilymph between the affected and healthy sides. The scala vestibuli scores and the area of vestibular perilymph, however, did not differ when comparing them before and after surgery.

Conclusions: According to our results, endolymphatic hydrops was not significantly reduced by surgery. The mechanism by which EMS controls vertigo might be unrelated to the improvement in hydrops.

Keywords: imaging, analysis, Meniere's disease, endolymphatic sac-mastoid shunt, surgery

OPEN ACCESS

Edited by:
Shinji Naganawa,
Nagoya University, Japan

Reviewed by:
Akira Ishiyama,
University of California, Los Angeles, United States
Steven D. Rauch,
Harvard Medical School, United States

***Correspondence:**
Haibo Wang
whboto11@163.com
Daogong Zhang
zhangdaogong1978@163.com

Specialty section:
This article was submitted to Otorhinolaryngology - Head and Neck Surgery, a section of the journal Frontiers in Surgery

Received: *27 February 2021*
Accepted: *03 December 2021*
Published: *12 January 2022*

Citation:
Li Y, Lv Y, Hu N, Li X, Wang H and Zhang D (2022) Imaging Analysis of Patients With Meniere's Disease Treated With Endolymphatic Sac-Mastoid Shunt Surgery. Front. Surg. 8:673323. doi: 10.3389/fsurg.2021.673323

INTRODUCTION

Endolymphatic hydrops was definitively diagnosed only by histopathological examination after death until Gadolinium (Gd)-enhanced inner ear MRI was introduced. Following intratympanic Gd injection, a 3-T MRI scan showed the first distinct images of endolymphatic hydrops in a patient with Meniere's disease (MD) in 2007 (1). Later, Nakashima (2) proposed a three-stage grading system for hydrops by evaluating the vestibular space and cochlea via dilated endolymphatic spaces and detected a percentage of endolymphatic hydrops that ranged from 47% (3) to ∼90% (4–6)

on the symptomatic side, and an elevated percentage also in the asymptomatic ear. Fukuoka also used 3D-fluid-attenuated inversion recovery (FLAIR) MRI following bilateral intratympanic Gd to semi-quantitatively evaluate endolymphatic hydrops in patients with MD (7). None of the patients who underwent this imaging method experienced any changes in hearing level or new-onset tinnitus, suggesting that this technique is a safe and powerful tool for the diagnosis of MD.

Endolymphatic sac surgery, first described by Portmann in 1927 (8), has been used to treat patients with medically refractory MD (9). Technical details of sac surgery can vary and include decompression of the sac alone, placement of a shunt between the endolymphatic sac and cerebrospinal fluid (CSF) space, and placement of a shunt between the endolymphatic sac and the mastoid air cells (endolymphatic sac-mastoid shunt; EMS). Endolymphatic sac shunt procedures became popular in the 1960s, following the success of the House's subarachnoid shunting procedure. However, the mechanism of EMS for this disease remains unclear. By comparing the imaging results before and after EMS surgery, we aimed to investigate the mechanism by which it is effective in vertigo control. Although some scholars have studied the mechanism of sac surgery by imaging, the results varied and the mechanism remained unclear.

TABLE 1 | Patient demographics, PTA (before and after surgery), and vertigo class.

			Vertigo Attack			PTA (dB HL)	
Patient no	Age	Sex	Pre-op	Post-op	Vertigo class	Pre-op	Post-op
1	45	F	2	0	A	40	30
2	57	F	10	2	B	65	60
3	46	M	15	4	B	45	50
4	50	F	5	0	A	47.5	45
5	43	F	3	0	A	32.5	25
6	39	F	10	0	A	31.25	25
7	53	M	20	0	A	80	45
8	47	F	12	1	B	75	30
9	56	M	5	0	A	55	40
10	47	F	2	0	A	65	35
11	41	F	7	0	A	57.5	80
12	52	M	2	0	A	65	70
13	42	F	15	4	B	35	35
14	45	M	20	8	B	40	35
15	42	M	12	10	D	30	35
16	50	F	5	6	D	55	55
17	43	M	10	9	D	60	75
18	55	M	10	11	D	45	30
19	44	M	13	15	D	45	50

MATERIALS AND METHODS

Clinical Data

According to the diagnostic criteria formulated by the Classification Committee of the Bárány Society, 19 patients clinically diagnosed with unilateral Meniere's disease and admitted to the Department of Otolaryngology-Head and Neck Surgery of Shandong Provincial ENT Hospital between January 2017 and January 2018 were enrolled in our study. The selection criteria were as follows: (1) All patients had a diagnosis of unilateral definite Meniere's disease; (2) brainstem audiometry and brain magnetic resonance scans were used to rule out cerebellopontine angle tumor or other intracranial diseases; (3) middle ear disease was ruled out. The exclusion criteria were as follows: (1) Patients who had a history of allergy of Gd or pregnancy were prohibited from parting in this study; (2) Patients were excluded if they had undergone previous surgical treatment for the inner disease. The average age of the group was 47.21 $\pm$ 5.39, with nine men and 10 women. The number of vertigo spells and the hearing levels of each case is listed in **Table 1**. All patients had received standard medical treatment for at least 1 year but continued to experience recurrent vertigo. They agreed to undergo EMS surgery and to participate in this study, by providing written informed consent. Before the surgery and 2 years after it, all patients received intravenous Gd injection, followed by 3D-FLAIR MRI.

EMS

After complete mastoidectomy under general anesthesia, the sigmoid sinus and posterior fossa dura were skeletonized. The horizontal and posterior semi-circular canals were identified. The endolymphatic sac was identified as a thickened portion of the dura, usually deep and inferior to the posterior semicircular canal, anterior to the sigmoid sinus, and superior to the jugular bulb. The lateral aspect of the sac was incised, and a silver clip was placed into the sac, extending into the mastoid cavity.

Imaging Method

A total of 19 patients underwent intravenous injection of Gd (0.4 ml/kg). We obtained 3D-FLAIR MRI scans 6 h after injection using a GE Discovery 750w 3T MRI scanner with an eight-channel phased-array coil. The parameters for 3D-FLAIR included: repetition time (TR) = 9,000 ms, echo time (TE) = 82.3 ms, inversion time (TI) = 2,500 ms, echo train length (ETL) = 140, BW = 35.7 kHz, matrix size = 256 $\times$ 256, number of excitation (NEX) = 2, slice thickness = 1.6 mm, field of view (FOV) = 20.5 cm $\times$ 17.4 cm, and a scan time of 5 min 46 s. The parameters for 3D-T2 weighted scan included: TR = 2,500 ms, TE = 102 ms, ETL = 120, BW = 41.7 kHz, matrix size = 256 $\times$ 256, NEX = 2, slice thickness = 1 mm, FOV = 20.5 cm $\times$ 17.4 cm and a scan time of 2 min 41 s. Two experienced radiologists blinded to the patient diagnosis independently reviewed the 3D-FLAIR axial findings of the bilateral inner ears of all patients. Scores for the cochlea were as follows: (1) a score of 2 indicated that the scala tympani/scala vestibuli had developed well; (2) a score of 1 indicated that the scala tympani/scala vestibuli had developed uneven or thinner; (3) a score of 0 indicated that the scala

tympani/scala vestibuli was unclear or could not be visualized. Briefly, the scope of imaging was the perilymphatic area of the largest imaging section of the bilateral vestibules. Areas for the vestibule perilymph were calculated as the mean of three measurements (area of perilymph = the entire area of the vestibule – area of endolymphatic) (**Figure 1**). In a preliminary study, 32 patients with unilateral MD were intratympanically injected with Gd, followed by 3D-FLAIR MRI, which showed significant differences in scala vestibuli scores but not scala tympani scores, and area of vestibular perilymph on the affected and healthy sides (10). Therefore, this study measured scala vestibuli scores and area of vestibular perilymph for the purpose of grading. We reconstructed the images of 3D-FLAIR by using Volume View processing technology.

Statistical Analysis

All statistical analyses were performed using SPSS 17 statistical software. Scala vestibuli scores were compared using the Wilcoxon signed-rank sum tests, and the area of vestibular perilymph was compared using paired sample *t*-tests. Before and after surgery, scala vestibuli scores were compared using the Mann-Whitney U test, and area of vestibular perilymph using paired sample *t*-tests. Measured values are expressed as mean ± *SD*. All statistical analyses were performed with a *P*-value <0.05, which was considered statistically significant.

RESULTS

Gadolinium (Gd) was observed in almost all parts of the perilymph in the cochlea, vestibule, and canals of 19 patients. Our measuring method was based on the earlier method proposed by Nakashima in 2009 but was not identical. Before surgery, the scala vestibuli score on the affected side was 0.57 ± 0.52, and 1.66 ± 0.5 on the healthy side. On the affected side, the area of vestibular perilymph was 5.73 ± 2.99 mm^2, while it was 8.89 ± 2.52 mm^2 on the healthy side. The differences in scala vestibuli scores ($Z = 3.426$, $P < 0.05$) and area of vestibular perilymph ($t = 2.65$, $P < 0.05$) on the affected and healthy sides were statistically significant.

Two years after EMS, the scala vestibuli score on the affected side was 0.64 ± 0.67, and 1.64 ± 0.67 on the healthy sides. At this time, the area of vestibular perilymph on the affected side was 5.7 ± 2.89 mm^2, while it was 8.52 ± 2.54 mm^2 on the healthy side. The differences in scala vestibuli scores ($Z = 2.869$, $P < 0.05$) and area of vestibular perilymph ($t = 2.39$, $P < 0.05$) on the affected and healthy sides were also statistically significant. The differences in scala vestibuli scores before and after surgery on

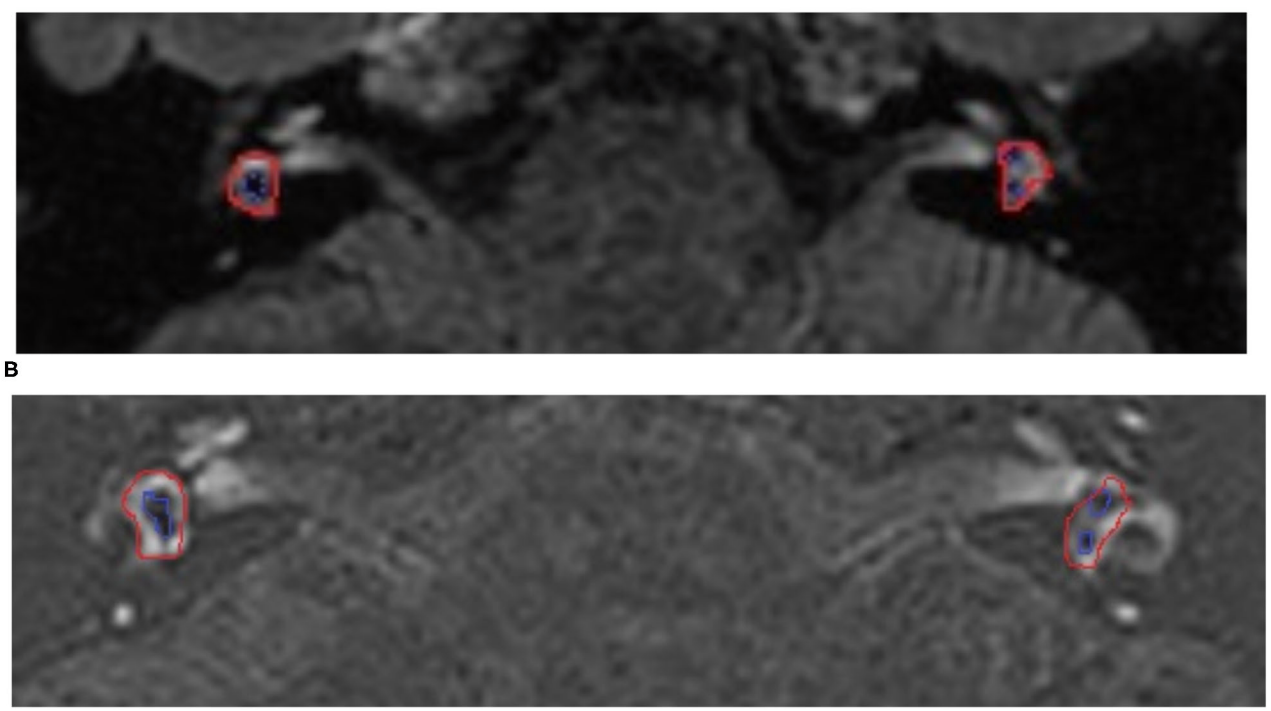

FIGURE 1 | The 3D-fluid-attenuated inversion recovery (FLAIR) MRI views of a 50-year-old woman with Meniere's disease (MD) on the right side before and after surgery. The long-term control of vertigo 2 years after the operation was class A. **(A)** MRI before the operation, the red line indicated the entire vestibular area, while the blue line indicated the endolymphatic area. The low density of the vestibular on the right was larger than the left, showing vestibular hydrops on the right side. **(B)** MRI after the operation, the low density of the vestibular on the right was still larger than the left, but did not vary after surgery. This result indicated the vestibular hydrops was not alleviated before and after surgery.

both the affected (Z =0.447, $P > 0.05$) and healthy ($Z = 0.000$, $P > 0.05$) sides, however, did not differ significantly. Similarly, the area of vestibular perilymph before and after surgery on both the affected ($t = 0.74$, $P > 0.05$) and healthy ($t = 0.66$, $P > 0.05$) sides did not differ significantly. The detailed data of scala vestibuli scores and area of vestibular perilymph of 19 patients before and after surgery were shown in **Tables 2**, **3**. Among the 19 patients, nine patients (47.37%) achieved class A control, and five patients (26.32%) achieved class B control.

DISCUSSION

Meniere's disease (MD) is a complicated inner ear disease, and endolymphatic hydrops is thought to be the pathological basis for this condition. As we could not visually observe hydrops *in vivo*, imaging methods have been applied to detect the condition of endolymph, perilymph, and endolymphatic sac hydrops. Both 3D-FLAIR and 3D-real IR (inversion recovery) MRI can differentiate the endolymphatic space from the perilymphatic space, but the latter is not as sensitive as the former to the low density of Gd, so we used 3D-FLAIR MRI as the preferred imaging method (11, 12). However, some authors have questioned this imaging method because inversion time can affect the area of the endolymphatic space (13, 14), so different inversion times could result in differences in imaging results and accordingly affect the assessment of hydrops. Liu applied 2,350 ms as the inversion time to detect the condition of hydrops in patients with endolymphatic shunt surgery, and in this study, they found that patients who underwent shunt surgery continued to have endolymphatic hydrops (15).

The mechanism of sac surgery for vertigo control remains unclear. Gibson reported that an abnormal fluid in the inner ear caused the endolymphatic sac to secrete glycoproteins, causing drainage of the endolymph toward the sac by which vertigo is caused (16). Scholars have questioned that if hydrops can be alleviated, symptoms such as vertigo, ear fullness, or tinnitus can be controlled. However, a post-mortem histopathological study of the temporal bone of 15 patients who had undergone EMS found endolymphatic hydrops in all patients (17). Interestingly, although the endolymphatic sac was not exposed in five of these patients, four experienced postoperative control of vertigo. In the other eight patients, the endolymphatic sac was exposed, but the drainage tube was not embedded in the endolymphatic sac cavity; of these eight patients, four showed postoperative control of vertigo. In only two patients, the endolymphatic sac was exposed, and the drainage tube was embedded in the cavity of

TABLE 2 | Preoperative and postoperative 3D-FLAIR MRI comparison of the affected and healthy sides of 19 patients with Meniere's disease ($x \pm s$).

	Affected ear pre-op	Affected ear post-op	Unaffected ear pre-op	Unaffected ear post-op
Scala vestibuli score	0.57 ± 0.52	0.64 ± 1.66	0.66 ± 0.50	1.64 ± 0.67
Area of vestibular perilymph	5.73 ± 2.99	5.70 ± 2.89	8.89 ± 2.52	8.52 ± 2.54

TABLE 3 | Detailed data of 19 patients.

	Scala vestibuli score (point)				Area of vestibular perilymph (mm^2)			
Patient	Affected pre-op	Affected post-op	Healthy pre-op	Healthy post-op	Affected pre-op	Affected post-op	Healthy pre-op	Healthy post-op
1	1	1	2	3	5.46	5.23	10.34	10.89
2	0	0	2	2	3.12	3.07	9.43	9.46
3	1	1	2	2	6.01	5.99	12.63	13.21
4	0	0	1	2	10.89	10.75	7.01	6.99
5	1	2	1	2	6.41	5.98	8.70	8.73
6	1	0	1	1	5.27	5.34	7.25	7.26
7	1	0	1	1	4.38	4.36	8.96	8.46
8	0	0	1	1	5.03	4.89	5.99	6.59
9	1	1	1	2	2.09	2.03	11.80	10.23
10	0	0	2	2	3.13	3.49	10.03	9.15
11	0	0	2	0	1.79	1.78	11.84	10.23
12	0	0	2	2	4.01	4.23	13.09	13.54
13	0	1	2	2	6.23	6.19	4.89	3.26
14	1	1	2	2	10.78	10.61	11.89	10.01
15	1	1	2	2	10.45	10.45	8.30	5.68
16	1	2	2	2	3.25	3.33	6.53	7.26
17	1	1	1	2	5.78	5.86	5.45	7.58
18	0	0	1	0	4.27	4.28	8.09	6.01
19	1	1	2	2	10.69	10.64	7.01	7.23

the endolymphatic sac, but neither of them showed postoperative vertigo control. Therefore, the control of vertigo was not related to the condition of the endolymphatic sac. This procedure may only reinforce the vertigo threshold. In 1977, Torok suggested that the placebo effect might be a factor in vertigo control (18). Thus, in conclusion, endolymphatic sac surgery was found to not control vertigo by relieving hydrops.

Following the changes in imaging parameters before and after EMS surgery, we found that the mechanism of vertigo control was not due to the improvement in hydrops. In 2013, Uno et al. reported changes in endolymphatic hydrops after endolymph sac surgery, which were observed with 3D-FLAIR MRI after intratympanic injection of Gd. Although only 28.6% of patients had negative hydrops after sac surgery, all patients had vertigo suppression. However, in 2014, Liu (19) found that endolymphatic hydrops in the cochlea and vestibule improved 3 months after endolymphatic sac decompression, which is contrary to our results. This result might have been due to the different surgical approaches and observation times. Pender performed a meta-analysis of MD to demonstrate that endolymphatic hydrops began in the cochlea, followed by the saccule, utricle, ampullae, and finally affected the semicircular canals (20). This finding might have affected our results because we chose the timepoints as before surgery and 2 years after surgery for comparison. Moreover, the extent of hydrops was reported to be unrelated to the surgical approach or the condition of sac exposure, confirming that endolymphatic sac surgery could not relieve hydrops but could control vertigo (18).

In conclusion, our findings indicate that the mechanism of EMS surgery does not involve the improvement of hydrops. In the future, the further examination must be conducted in clinics to confirm the relationship between endolymphatic hydrops and vertigo control, and to provide new theories for the mechanism of MD. As for the potential of surgery to affect hydrops, a large number of cases with or without surgery should be accumulated, and further comparisons should be made.

DATA AVAILABILITY STATEMENT

The original contributions presented in the study are included in the article/supplementary material, further inquiries can be directed to the corresponding author/s.

ETHICS STATEMENT

Written informed consent was obtained from the individual(s) for the publication of any potentially identifiable images or data included in this article.

AUTHOR CONTRIBUTIONS

YLi contributed to the conception of the work. YLv and XL contributed to the surgery. YLi collected data and performed the analysis. NH contributed to the part of imaging. HW and DZ contributed to the study design. All authors contributed to the article and approved the submitted version.

FUNDING

This work was supported by Shandong Provincial Natural Science Foundation (No. ZR2020MH179) and Taishan Scholars Program of Shandong Province (No. ts20130913).

REFERENCES

1. Nakashima T, Naganawa S, Sugiura M, Teranishi M, Sone M, Hayashi H, et al. Visualization of endolymphatic hydrops in patients with Meniere's disease. *Laryngoscope.* (2007) 117:415–20. doi: 10.1097/MLG.0b013e31802c300c
2. Nakashima T, Naganawa S, Pyykko I, Gibson WP, Sone M, Nakata S, et al. Grading of endolymphatic hydrops using magnetic resonance imaging. *Acta Otolaryngol Suppl.* (2009) 129:5–8. doi: 10.1080/00016480902729827
3. Hornibrook J, Flook E, Greig S, Babbage M, Goh T, Coates M, et al. inner ear imaging and tone burst electrocochleography in the diagnosis of Ménière's disease. *Otol Neurotol.* (2015) 36:1109–14. doi: 10.1097/MAO.0000000000000782
4. Baráth K, Schuknecht B, Naldi AM, Schrepfer T, Bockisch CJ, Hegemann SC. Detection and grading of endolymphatic hydrops in Menière disease using MR imaging. *AJNR Am J Neuroradiol.* (2014) 35:1387–92. doi: 10.3174/ajnr.A3856
5. Ilmari P, Tsutomu N, Tadao Y, Zou J, Naganawa S. Meniere's disease: a reappraisal supported by a variable latency of symptoms and the MRI visualisation of endolymphatic hydrops. *BMJ Open.* (2013) 3:e001555. doi: 10.1136/bmjopen-2012-001555
6. Naganawa S, Yamazaki M, Kawai H, Bokura K, Sone M, Nakashima T. Visualization of endolymphatic hydrops in Ménière's disease after single-dose intravenous gadolinium-based contrast medium: timing of optimal enhancement. *Magn Reson Med Sci.* (2012) 11:43–51. doi: 10.2463/mrms.11.43
7. Fukuoka H, Tsukada K, Miyagawa M, Oguchi T, Takumi Y, Sugiura M, et al. Semi-quantitative evaluation of endolymphatic hydrops by bilateral intratympanic gadolinium-based contrast agent (GBCA) administration with MRI for Meniere's disease. *Acta Oto-laryngol.* (2010) 130:10–6. doi: 10.3109/00016480902858881
8. Portmann G. The saccus endolymphaticus and an operation for draining the same for the relief of vertigo. 1927. *J Laryngol Otol.* (1991) 105:1109–12. doi: 10.1017/S0022215100118365
9. Söderman AC, Ahlner K, Bagger-Sjöbäck D, Bergenius J. Surgical treatment of vertigo–the Karolinska Hospital policy. *Am J Otol.* (1996) 17:93–8.
10. Zhang DG, Shi HL, Fan ZM, Wang GB, Han YC, Li YW, et al. Visualization of endolymphatic hydrops in 3D-FLAIR MRI after intratympanic Gd-DTPA administration in Meniere's disease patients. *Zhonghua Er Bi Yan Hou Tou Jing Wai Ke Za Zhi.* (2013) 48:628–33.
11. Nakashima T, Naganawa S, Katayama N, Teranishi M, Nakata S, Sugiura M, et al. Clinical significance of endolymphatic imaging after intratympanic gadolinium injection. *Acta Otolaryngol Suppl.* (2009) 560:9–14. doi: 10.1080/00016480902729801
12. Naganawa S, Yamazaki M, Kawai H, Bokura K, Sone M, Nakashima T. Estimation of perilymph enhancement after intratympanic administration of Gd-DTPA by fast T1-mapping with a dual flip angle 3D spoiled gradient echo sequence. *Magn Reson Med Sci.* (2013) 12:223–8. doi: 10.2463/mrms.2012-0071
13. Eliezer M, Gillibert A, Tropres I, Krainik A, Attyé A. Influence of inversion time on endolymphatic hydrops evaluation in 3D-FLAIR imaging. *J Neuroradiol.* (2017) 44:339–43. doi: 10.1016/j.neurad.2017.06.002
14. Attyé A, Eliezer M, Boudiaf N, Tropres I, Chechin D, Schmerber S, et al. of endolymphatic hydrops in patients with Meniere's disease: a case-controlled study with a simplified classification based on saccular morphology. *Eur Radiol.* (2017) 27:3138–46. doi: 10.1007/s00330-016-4701-z

15. Liu IY, Sepahdari AR, Ishiyama G, Ishiyama A. High resolution MRI shows presence of endolymphatic hydrops in patients still symptomatic after endolymphatic shunt surgery. *Otol Neurotol.* (2016) 37:1128–30. doi: 10.1097/MAO.0000000000001144
16. Gibson WP. The effect of surgical removal of the extraosseous portion of the endolymphatic sac in patients suffering from Menière's disease. *J Laryngol Otol.* (1996) 110:1008–11. doi: 10.1017/S0022215100135637
17. Torok N. Old and new in Ménière disease. *Laryngoscope.* (1977) 87:1870–7. doi: 10.1002/lary.1977.87.11.1870
18. Chung JW, Fayad J, Linthicum F, Ishiyama A, Merchant SN. Histopathology after endolymphatic sac surgery for Ménière's syndrome. *Otol Neurotol.* (2011) 32:660–4. doi: 10.1097/MAO.0b013e31821553ce
19. Liu F, Huang W, Chen Q, Meng X, Wang Z, He Y. Noninvasive evaluation of the effect of endolymphatic sac decompression in Ménière's disease using magnetic resonance imaging. *Acta Oto-laryngol.* (2014) 134:666–71. doi: 10.3109/00016489.2014.885118
20. Pender DJ. Endolymphatic hydrops and Ménière's disease: a lesion meta-analysis. *J Laryngol Otol.* (2014) 128:859–65. doi: 10.1017/S0022215114001972

Conflict of Interest: The authors declare that the research was conducted in the absence of any commercial or financial relationships that could be construed as a potential conflict of interest.

frontiers in Surgery

ORIGINAL RESEARCH
published: 04 February 2022
doi: 10.3389/fsurg.2022.747517

Vestibular Aqueduct Morphology and Meniere's Disease—Development of the "Vestibular Aqueduct Score" by 3D Analysis

*Laurent Noyalet[1], Lukas Ilgen[1], Miriam Bürklein[1], Wafaa Shehata-Dieler[1], Johannes Taeger[1], Rudolf Hagen[1], Tilmann Neun[2], Simon Zabler[3], Daniel Althoff[4] and Kristen Rak[1]**

[1] Department of Oto-Rhino-Laryngology, Plastic, Aesthetic and Reconstructive Head and Neck Surgery and the Comprehensive Hearing Center, University of Würzburg, Würzburg, Germany, [2] Institute for Diagnostic and Interventional Neuroradiology, University of Würzburg, Würzburg, Germany, [3] Department of X-ray Microscopy, University of Würzburg, Würzburg, Germany, [4] Fraunhofer Development Center for X-ray Technology, Würzburg, Germany

Improved radiological examinations with newly developed 3D models may increase understanding of Meniere's disease (MD). The morphology and course of the vestibular aqueduct (VA) in the temporal bone might be related to the severity of MD. The presented study explored, if the VA of MD and non-MD patients can be grouped relative to its angle to the semicircular canals (SCC) and length using a 3D model. Scans of temporal bone specimens (TBS) were performed using micro-CT and micro flat panel volume computed tomography (mfpVCT). Furthermore, scans were carried out in patients and TBS by computed tomography (CT). The angle between the VA and the three SCC, as well as the length of the VA were measured. From these data, a 3D model was constructed to develop the vestibular aqueduct score (VAS). Using different imaging modalities it was demonstrated that angle measurements of the VA are reliable and can be effectively used for detailed diagnostic investigation. To test the clinical relevance, the VAS was applied on MD and on non-MD patients. Length and angle values from MD patients differed from non-MD patients. In MD patients, significantly higher numbers of VAs could be assigned to a distinct group of the VAS. In addition, it was tested, whether the outcome of a treatment option for MD can be correlated to the VAS.

Keywords: vestibular aqueduct (VA), 3D analysis, temporal bone, saccotomy, computed tomography, Meniere's disease

OPEN ACCESS

Edited by:
Robert Gürkov, Bielefeld University, Germany

Reviewed by:
Jeremy Hornibrook, University of Canterbury, New Zealand
Daogong Zhang, Shandong Provincial ENT Hospital, China

***Correspondence:**
Kristen Rak
Rak_K@ukw.de

Specialty section:
This article was submitted to Otorhinolaryngology - Head and Neck Surgery, a section of the journal Frontiers in Surgery

Received: *26 July 2021*
Accepted: *03 January 2022*
Published: *04 February 2022*

Citation:
Noyalet L, Ilgen L, Bürklein M, Shehata-Dieler W, Taeger J, Hagen R, Neun T, Zabler S, Althoff D and Rak K (2022) Vestibular Aqueduct Morphology and Meniere's Disease—Development of the "Vestibular Aqueduct Score" by 3D Analysis. Front. Surg. 9:747517. doi: 10.3389/fsurg.2022.747517

INTRODUCTION

Meniere's disease (MD) typically presents as attacks of vertigo lasting from minutes to hours, fluctuating hearing, tinnitus and aural pressure. Variations in these symptoms can make the diagnosis difficult in some cases (1). There are different theories on the pathogenesis of MD based on the endolymphatic hydrops (EH) theory. EH describes an increase of the endolymph inducing an expansion of the cochlear endolymphatic space, resulting in a protrusion of Reissner's membrane into the scala vestibuli.

One hypothesis is, that the EH is triggered by a disturbed absorption of endolymph in the endolymphatic sac (ES). This might happen in patients with a reduced sac lumen, a constricted ductal lumen or a scarred sac.

Another theory states, that the increase of endolymph can also be caused by a disturbance of the active ion transport, which is essential for the composition of the endolymph, resulting in a calcium-rich endolymph and a disturbed electrochemical potential (2). This theory is underlined by the fact, that in patients suffering from MD, the stria vascularis, which regulates the ion concentration, has shown an altered blood supply (3).

In addition, there are different theories attempting to explain how an MD attack develops. An acute attack might occur, when endolymph and perilymph mix due to a permeability disturbance of the inner ear barriers or a rupture of the Reissner's membrane (4). An additional theory postulates, that an MD attack can also occur as a result of blockage of the endolymphatic duct, causing the endolymph to flow in the utricle through the valve of Bast, resulting in vertigo (5).

For diagnosis of MD the AAO-HNS criteria from 1995 (6), later revised in 2015 by the Barany society (7), are commonly used. Based on the duration of vertigo, documented low- to mid-frequency hearing loss and fluctuating aural symptoms like tinnitus or hearing, the patient is categorized in definite or probable MD. Alternatively the Gibson score, which is a 10-point scale of the classical MD symptoms (vertigo, aural fulness, tinnitus and hearing loss) can be used (8).

In addition to the above mentioned clinical symptoms electrocochleography (EcochG) can help in the diagnosis of MD. EcochG refers to the recording of the acoustic evoked cochlear potentials generated by the outer hair cells as well as the auditory nerve action potential. In MD the presence of EH can be evaluated using this technique (9).

3-Tesla-MRI has also proved to be of value in detecting the presence of EH. By local or intravenous application of Gadolinium (Gd), the endolymph can be distracted from the perilymph, since the endolymph has different characteristics of Gd uptake, resulting in an endolymph notch in the Gd rich perilymph (10–12).

Studies have also shown a genetic link to the development of MD. This type of MD, the familial MD, can be linked to different mutated genes or alleles (13).

For MD there are several treatment options, depending on the extent and severity of the symptoms. The current guidelines initially suggest drug therapy. Betahistine in combination with antiemetics and antinauseants for the acute seizure showed good results (14). In case of persistent symptoms, the next step can be a function preserving operation, like the saccotomy, in which the ES is decompressed or opened. This therapy has been reported to be satisfactory, if the ES is not fibrous (15). Another option is transtympanic Gentamycin application, which selectively affects the sensory epithelium of the vestibular organ (16). This mode of therapy results in good vertigo control, with only low risk of consecutively hearing loss (14). When all treatment modalities fail, a neurectomy of the vestibular nerve, or if the patient has already lost hearing, a complete extraction of the membranous labyrinth can be done (17).

The vestibular auquaeduct (VA) is a bony channel that runs from the vestibulum of the inner ear, to the posterior surface of the petrous bone. The VA has an average length of about 6.95–11.86 mm (18, 19) and is divided into proximal short and longer distal parts, which are both positioned at an angle of 90–135° to each other (20). The VA contains the endolymphatic duct (ED), which is filled with endolymph and ends blind as the endolymphatic sac (ES) in a dura duplication. The ES is divided into a proximal, middle (pars rugosa) and distal part. The pars rugosa represents the active part, with a multi-layered secretory epithelium (21). As reported by Eckhard et al. (22), the epithelium of the ES is important for maintaining Na^+ concentration of the endolymph and volume balance. In addition, this study was the first to describe that the VA in MD patients can be classified into 2 groups; developmentally hypoplastic and degenerative, depending on the angle of the entry and the exit. Particularly noticeable were VA of the hypoplastic type, as these were exclusively found in MD patients with an angle of >140° (20, 22). The authors proposed that due to the reduced area of the epithelium, EH can occur. Similar findings have been previously published describing that the size of the VA influences the extent of the ES (23) and is reduced in MD patients, specifically in volume and length (18, 19). The epithelial layers of the ES in MD have also been described to be pathologically altered. Ikeda and Sando (23) found fibrotic changes with much higher rates in the VA of MD patients.

Based on these studies, the aim of the present paper was to investigate VA morphology using different imaging modalities. For reference, micro-CT was applied and compared to two different clinically available imaging modalities; micro flat panel volume computed tomography (mfpVCT) and multi-slice computed tomography (CT). From these data a clinically suitable model for grouping the VA morphology according to a newly developed "vestibular aqueduct score" (VAS) was developed by application of a virtual 3D model based on the angle relative to the semicircular canals (SCC). Furthermore, it was evaluated, as a first test of the VAS whether the score might be used to group the outcome of patients who were treated by saccotomy, with respect to their success in reduction of symptoms.

METHODS

Temporal Bone Specimens

Temporal bone specimens (TBS) were used for the development of this specialized methodology. Ten TBS were scanned in an experimental micro-CT with a slice thickness of 18 μm, which served as a reference. In addition, 37 specimens were examined by CT with a slice thickness of 600 μm, plus an additional mfpVCT scan with 197 μm slices. There were 35 specimens from the right side, and two from the left side.

Patient Selection

For control measurements, 42 CT temporal bone scans were used from selected patients with normal hearing and vestibular function. All patients received radiological imaging prior to middle cranial fossa operations for vestibular neurinoma surgery of the contralateral ear. In addition, 52 patients, who had a confirmed MD diagnosis according to the AAO-HNS classification (24), Gibson Score (25) or positive Ecohgh results for MD, were selected for the study group. All 52 patients were treated by saccotomy (26) and were examined by CT and cranial

magnet resonance imaging for exclusion of a retrocochlear lesion. Anamnestic data were used and stored anonymously. The study was conducted in concordance with local guidelines and principles of the Declaration of Helsinki and Good Clinical Practice and was approved by the local ethics committee at the University of Würzburg (20191127/02).

Imaging

Micro-CT measurements were performed using a MetRIC setup with the following parameters: Tube voltage = 120 kV; power = 4 W; exposure time = 200 ms; 15 averaged images; 2 mm aluminum and 0.38 mm silicon filters; slice thickness = 18 μm (27). CT scans were recorded by the multi-slice scanner SOMATOM Definition AS+ (Siemens Healthcare AG) with the following parameters: Tube voltage = 120 kV; tube current = 38 mA; pitch = 0.55; collimation = 0.6 mm; slice thickness = 600 μm. mfpVCT scans were performed on an Axiom Artis (Siemens Healthcare AG) using the following parameters: 20s DynaCT head protocol; tube voltage = 109 kV; tube current = 42 mA; pulse length = 3.5 ms; rotation angle = 200°; frame angle step = 0.4°/frame; slice thickness = 197 μm.

Imaging Processing

The images were saved as DICOM files and imported into the Horos® Medical Viewer (version 3.3.5) and 3D Slicer® (version 4.10.2) for processing. The 3D Curved MPR (multiplanar reconstruction) function in Horos® was used to determine the length of the VA from the entrance at the vestibule up to the exit at the ES. The axial plane was always selected as the display plane (**Figure 1**). Each point was placed in the middle of the lumen.

The freely available software 3D Slicer® was used to create a 3D model of the inner ear. As described in the work of Dhanasingh, Dietz (28), the Segment Editor Tool was used as the basis for creating a 3D model of the SCC and the VA. First, the region of the SCC and the VA was selected *via* the function "Crop Volume" and "Create New Annotation ROI" and cropped to this region with the settings Isotropic Spacing, Spacing Scale 0.5, Interpolator Linear and Interpolated Cropping. In the Segment Editor, the threshold function can then be used to adjust the gray value so that the SCC and VA are marked as accurately as possible. The marked threshold range was saved as a mask ("Use for masking") and manually traced. This process was always done in the axial plane first and then in the other planes. With the existing 3D model (**Figure 1**), the extension "Angle Planes" made it possible to define 2 planes, and to measure an angle between these planes using the Python Interactor (Text Code Angle 3D Slicer) (29). With respect to the planes, both the cutting plane of the VA and one of the SCC were used, and then the angle in between was then measured (see **Supplementary Video 1**).

Saccotomy

The standard procedure of saccotomy includes an antrotomy followed by a mastoidectomy with thinning out the bone over the dura of the posterior fossa and exposing the sigmoid sinus. For identification of the ES, the lateral SCC is thinned out until the endost and the so called "blue line" is visible. Then the posterior semicircular canal and its endost are identified. Afterwards the posterior SCC is hypothetically bisected by a line, drawn in the same direction as the blue line of the lateral SCC. The ES can be than be identified dorsally to the caudal half of the posterior SCC and medially to sigmoid sinus as a duplicate of the dura. Finally, the ES is slit to open, and a silicone triangle inserted, which results in permanent drainage of perilymph from the ES into the mastoid.

Statistical Analysis

Descriptive data analysis (mean value, 95% confidence interval (CI) and standard deviation) was performed with Microsoft Excel. The paired *T*-test and the two-sample *T*-test were employed to test for statistical significance. Null hypothesis was rejected if p was determined smaller than 0.05. In addition, the intraclass correlation (ICC) and Cronbach alpha were evaluated using SPSS (IBM). According to Koo and Li (30), a correlation of >0.9 for the ICC was considered to be adequate. As a test model, two-fold mixed with absolute agreement and a confidence interval of 95% was used. For the Cronbach Alpha, values of $\alpha >$ 0.9 were considered to be highly reliable. When three or more groups were compared the one-way ANOVA was used. The 3D diagrams were created with Excel using a template (31), and for other diagrams Graphpad Prism 8.3® was used.

RESULTS

Comparison of Angle and Length of the VA Between Micro-CT and mfpVCT in TBS

To establish the method, angle measurements of the VA in relation to all the SCC were performed in 10 TBS scanned by micro-CT images (18 μm). In addition, mfpVCT (197 μm) was performed which is the imaging modality with the highest possible resolution in humans. Data are presented in **Table 1**.

All measurements were performed twice to check reliability. Evaluation of the T-test with dependent samples of the 1st and 2nd test series from both recordings consistently showed no statistically significant differences (micro-CT: $p = 0.46$, ICC = 0.99, $\alpha = 0.99$; mfpVCT: $p = 0.15$, ICC = 0.99, $\alpha = 0.99$) and a difference of 0.3° for micro-CT and mfpVCT, so the null hypothesis was accepted.

When comparing the results of angle measurements of the micro-CT and mfpVCT images, there were no significant differences (lat SCC: difference = 0.07°, $p = 0.94$; post SCC: difference = 1.7°, $p = 0.11$; ant SCC: difference = 0.3°, $p =$ 0.43). Thus, the mfpVCT images can be used as a reference. The intraclass correlation and the Cronbach alpha were also evaluated and showed a correlation coefficient of greater than 0.9 (ICC = 0.98–0.99) and $\alpha > 0.9$ ($\alpha = 0.97$–0.99) when comparing the series of measurements and comparing micro-CT to mfpVCT, which complies with a very reliable result (**Figure 2A**).

The comparison of the VA length determination of micro-CT and mfpVCT showed no significant differences (difference = 0.5 mm, $p = 0.1$, ICC = 0.93, $\alpha = 0.92$). The values of the micro-CT were slightly longer than those of the mfpVCT since the exact entry into the vestibule is shown only in the micro-CT (**Figure 1D**). Nevertheless, the mfpVCT is sufficiently accurate (**Figure 2A**).

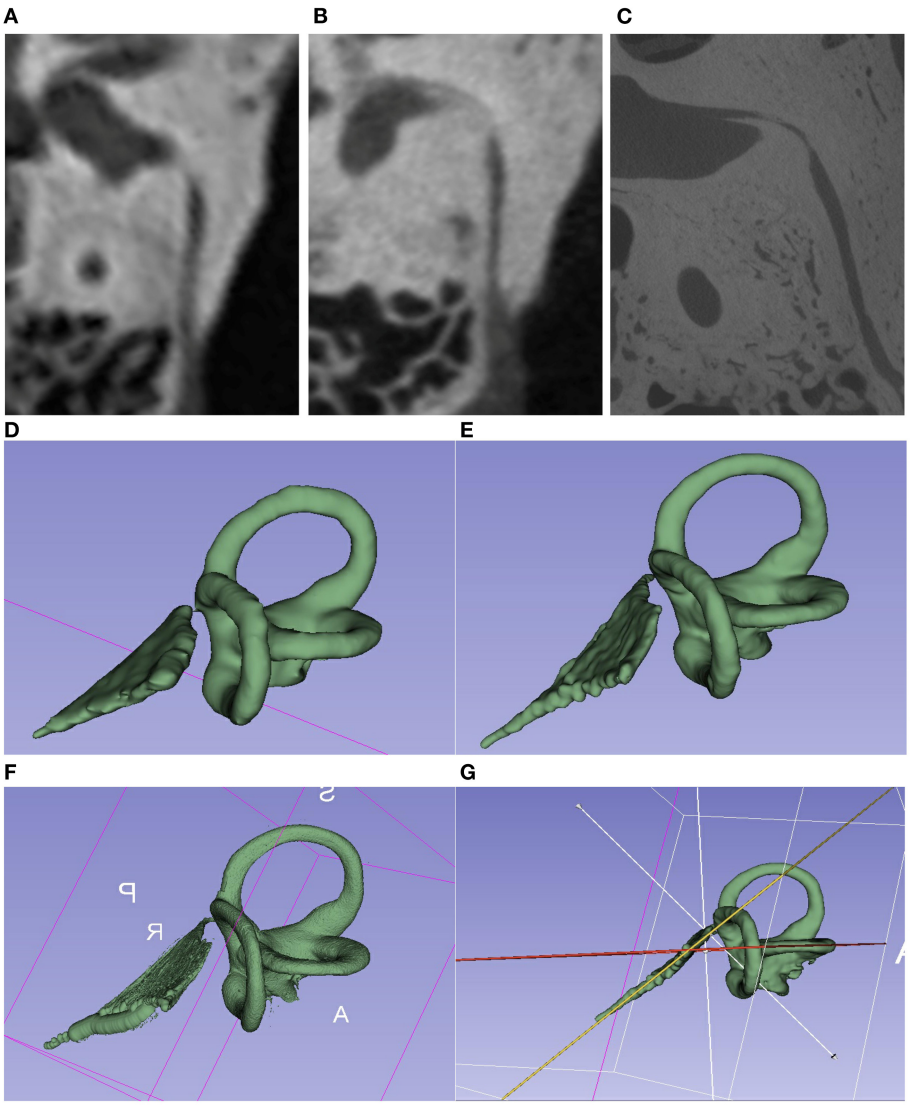

FIGURE 1 | Comparison of the imaging techniques of the same TBS. **(A–C)** Images of different image quality [**(A)** = CT 600 µm; **(B)** = mfpVCT 197 µm 600 µm; **(C)** = micro-CT 18 µm]. VA seen in its full length in the axial plane. **(E–G)** 3D model created with the 3D slicer software using the segment editor tool. [**(D)** = CT; **(E)** = mfpVCT; **(F)** = micro-CT]. **(G)** Presentation of the angle measurement technique.

Comparison of Angle and Length Between mfpVCT and CT in TBS

Normally, only lower-resolution images of patients are clinically available, so it was necessary to check whether the results of the high-resolution TBS images were consistent even with thicker layers. To investigate this, 37 TBS (including the 10 TBS scanned by micro-CT) were scanned by mfpVCT and CT. All data are presented in **Table 1**.

The angle measurements were performed twice with the result that both series were nearly identical (CT: difference = 0.3°, p = 0.2, ICC = 0.98, α = 0.99). The measurements of the angle in CT showed no significant differences compared to mfpVCT (lat SCC: difference = 0.1°, p = 0.87; post SCC: difference = 1.1°, p = 0.15; ant SCC: difference = 0.8°, p = 0.2; α = 0.94–0.97, ICC = 0.94–0.97). The comparison of the length determination of mfpVCT and CT showed significantly shorter values in CT (difference = 0.5 mm, p = 0.03, ICC = 0.88, α = 0.87) (**Figure 2B**).

A correlation analysis was performed between the length of the VA and the respective angle. Only for the lateral SCC there was a clear tendency (r^2 = 0.32, p = 0.0003), showing that with a higher angle, the VAVA were relatively smaller. For the other SCC, there was no correlation (r^2 = 0.17, p = 0.03) (**Figure 2C**).

Angle and Length Measurements in Patients

Measurements in patients were performed in CT scans. The VA length in non-MD patients was 9.3 mm (range: 5–16.1 mm, SD:

TABLE 1 | Anamnestic data of saccotomy patients before and after surgery.

	Preoperatively		Postoperatively > 6 weeks	Postoperatively < 6 weeks
Vertigo	100%	Ø	38%	28%
		<	32%	36%
		=	30%	36%
Tinnitus	98%	Ø	71%	60%
		=	29%	40%
Aural fullness	82%	Ø	77%	68%
		=	23%	32%

After surgery is divided into less than and greater than 6 weeks. "Ø" = no symptoms; "<" = less symptoms than before surgery; "=" = symptoms like or worse than before surgery.

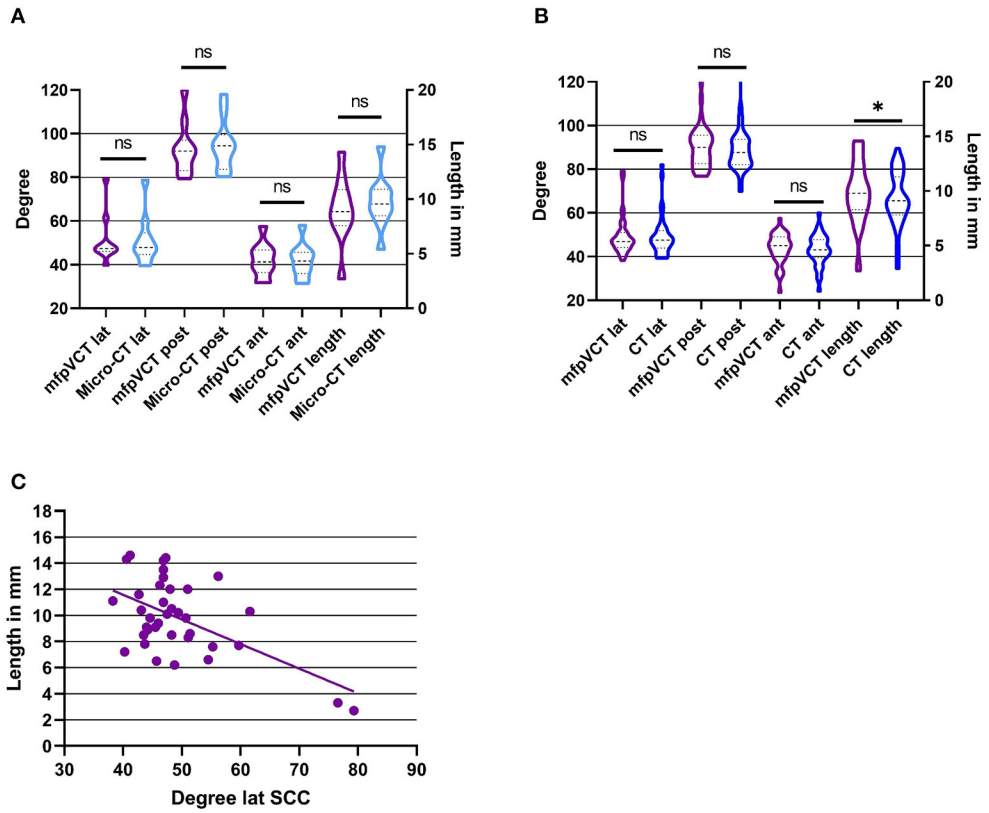

FIGURE 2 | Results of angle and length measurements of the TB specimen in comparison with the different image techniques. **(A)** mfpVCT and micro-CT ($n = 10$), **(B)** mfpVCT and CT ($n = 37$), and **(C)** Correlation of length and angle of the lateral SCC and the VA. *$p < 0.05$.

2.4 mm, 95% CI: 8.8–10.4 mm), and the angle to the lateral SCC was 55° (range: 35.6–92.6° mm, SD: 13°, 95% CI: 52.5–60.8°), the posterior 93.9° (range: 79.6–147.1°, SD: 14°, 95% CI: 92.6–102.1°) and the anterior 43.7° (range: 30.3–59.2°, SD: 7°, 95% CI: 41–45.6°).

The VA length in MD patients was 7.9 mm (range: 3.6–13.0 mm, SD: 2.4 mm, 95% CI: 7.3–8.6 mm). The angle to the lateral SCC was 71.4° (range: 29.5°–125°, SD: 19.4°, CI: 67.1°–77.5°), the posterior 102.7° (range: 57.5°–157.8°, SD: 20.8°, CI: 97.9°–109.6°), and the anterior 37.8° (range: 4.4°–75°, SD: 15.2°, CI: 33.2°–41.7°).

In comparison with the non-MD patients, there is a significant difference between the results of the lateral SCC (difference: 16.4°, $p = 0.0001$), the anterior SCC (difference: 5.9°, $p = 0.03$) and length (difference: 1.4 mm, $p = 0.03$). For the posterior SCC (difference: 8.8°, $p = 0.1$) no significant difference was found (**Figure 3**).

Development of the VAS

To facilitate the comparison of the angle measurement results of the VA, a score was developed using the mean value and twice the standard deviation of the angle measurements to form a 3D

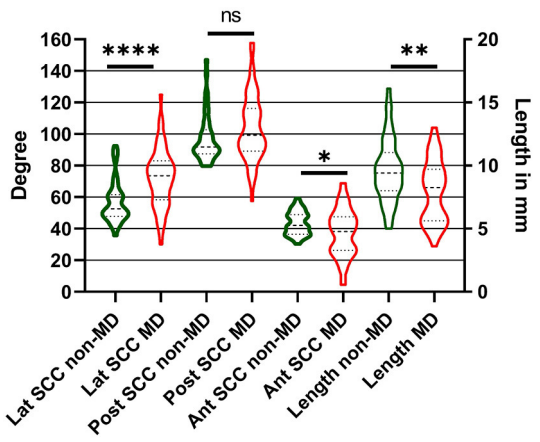

FIGURE 3 | Results of angle and length measurements of MD and non-MD patients in comparison. Width of the bars show the distribution. Differences between the measurements were significant for the lateral and anterior SCC and the length between MD and non-MD patients. *$p < 0.05$; **$p < 0.01$; ****$p < 0.0001$.

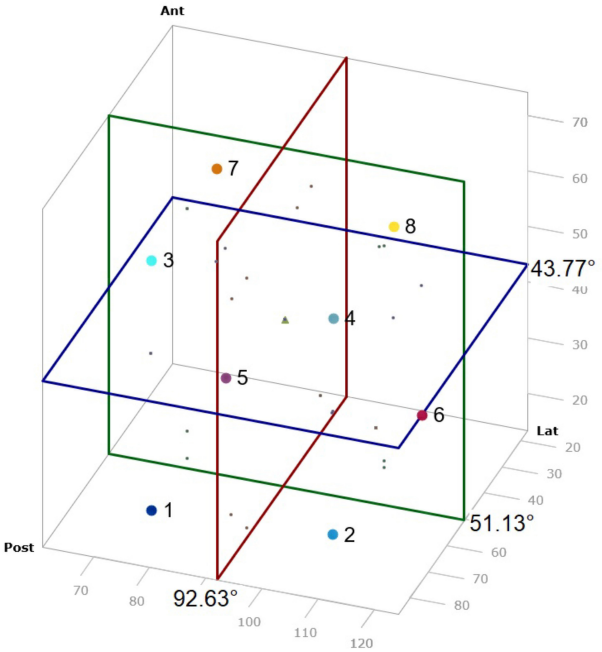

FIGURE 4 | VA score scheme as 3D diagram. Points mark the different VAS groups.

diagram, and then dividing this into 8 cubes which represents the various VAS groups. Therefore, all SCC angle results could be represented in one value and results were categorized. Each axis of the 3D diagram was divided into lower and higher than the mean value to obtain 8 groups (**Figure 4**). The averaged mean value of all non-MD VA and TBS was used, which included 79 datasets. These were 51.13° ± 20.4° (2x SD) (range: 35.6–92.6°, SD: 10.2°, 95% CI: 49.7–54.3°) (lateral SCC), 92.63° ± 24.6° (2x SD) (range: 75–147.1°, SD: 12.3°, 95% CI: 89.6–95.1°) (posterior SCC) and 43.77° ±14° (2x SD) (range: 23.6–59.2°, SD: 7°, 95% CI: 42.1–45.3°) (anterior SCC).

Assignment of the VA to the VAS

The VA of the 10 TBS, measured by micro-CT, were assigned to the respective groups 1–8 of the VAS: 1 (10%), 2 (10%), 4 (10%), 5 (20%), 6 (20%), 7 (10%), 8 (20%) (**Figure 5A**). The VA of the 37 TBS, measured by mfpVCT, could be matched to the respective groups 1 (5%), 2 (16%), 3 (2%), 5 (14%), 6 (5%), 7 (32%) 8 (26%) (**Figure 5B**). The non-MD VA could be matched to the VAS: 1 (29%), 2 (19%), 3 (5%), 4 (5%), 5 (7%), 6 (2%), 7 (14%), 8 (19%) (**Figure 5C**) and the VA of MD patients to the VAS: 1 (17%), 2 (44%), 3 (6%), 4 (17%), 7 (8%), 8 (8%) (**Figure 5D**). Analysis by heat map displayed an even distribution in TBS and non-MD patients, whereas VAS of MD patients grouped mainly in VAS 2.

Anamnestic Data MD Patients

The medical history of each patient was evaluated both preoperatively and postoperatively according to the scheme of the Gibson score and AAO-HNS criteria. Patients received an EcochG for diagnosis. This showed definite EH in 81.6%, marginal evidence in 12.2%, and no evidence of EH was found in 6.2% of the cases. The hearing level was also examined. The pure tone audiogram was evaluated at 500, 1,000, 2,000 and 4,000 Hz at initial evaluation, just before and after surgery. PTA^4 hearing threshold (AC) of 46 dB HL was calculated at initial presentation and a PTA^4 bone conduction threshold of 44 dB HL. This deteriorated until before surgery (time period 126 weeks) to 67 dB HL (AC) and 60 dB HL BC. Analysis of the data with ANOVA, showed a significant difference in the progression of hearing loss from initial hearing test to after surgery ($p = 0.01$).

Correlation VAS and Outcome Saccotomy

To apply the VAS in a clinical setting, MD patients who were operated by saccotomy were chosen. In every operation, it was possible to expose the ES. Results of the saccotomy were categorized as successful and not successful. The success criteria were defined as follows; patients who reported being completely free of vertigo or just mild persistent vertigo were considered successful. Patients who continued to suffer from dizziness (same or worse than before surgery) were considered unsuccessful.

Post-surgical evaluation timeframes were divided in to up to 6 weeks and more than 6 weeks after surgery. The success rate of the saccotomy in the observation period <6 weeks was 72% and more than 6 weeks, 64% (**Table 1**). In 8 patients, it was stated that the petrous bone was very compact, 11 patients had a fibrous sac.

To correlate the outcome of the saccotomy with the VAS, the success rate of each VAS group was calculated. The lowest success rate in the observation period <6 weeks was in VAS 8 with 50% and 2 with 70% (**Figure 6A**). After the period of 6 weeks, VAS 4 showed a success rate of only 33%. The other groups did not differ much (**Figure 6B**).

DISCUSSION

In the present study, it was shown that it is possible to measure the angle of the VA relative to the three SCC in CT scans as

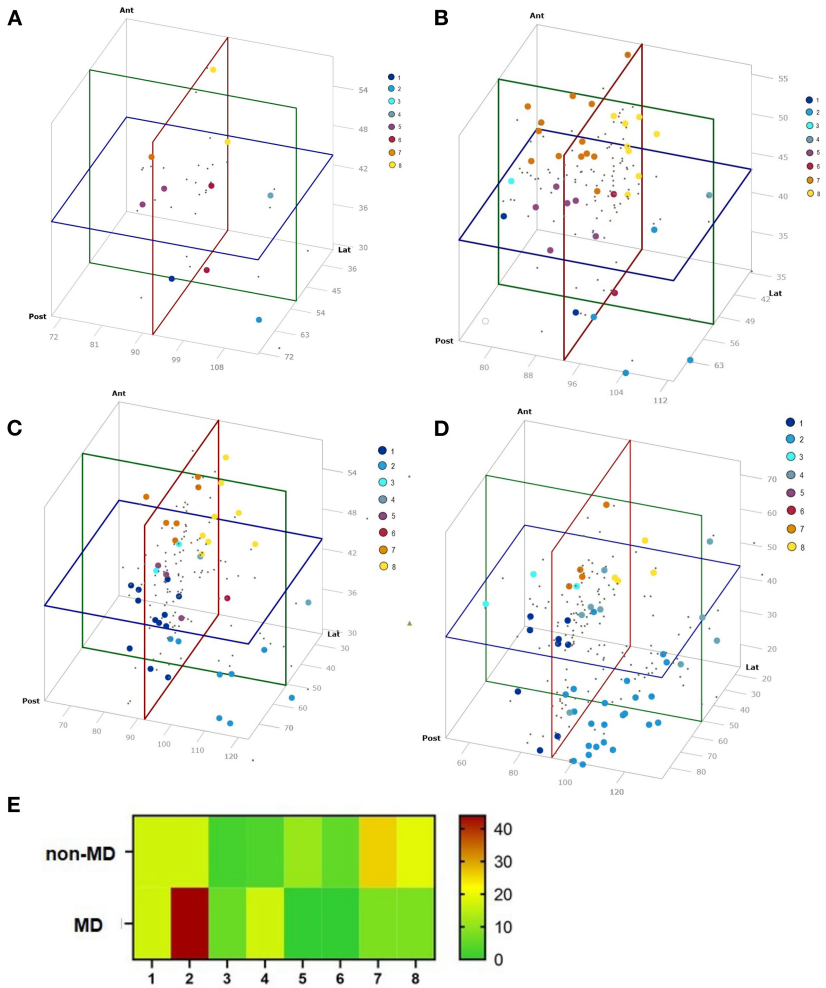

FIGURE 5 | Results of the angle measurements visualized in a 3D diagram. Colors represent the VAS group. **(A)** TBS micro-CT ($n = 10$), **(B)** TBS mfpVCT ($n = 37$), **(C)** non-MD patients ($n = 42$), **(D)** MD patients ($n = 52$), and **(E)** Distribution of each group according to the VAS. MD patients are concentrated in group 2, as compared to non-MD patients and TBS, where the distribution is more balanced.

a feasible and comparable method to other imaging modalities with higher resolution. The values were significantly different in MD patients compared to non-MD patients, which resulted in a different distribution of the VA according to a newly developed VAS score (**Figure 5E**). These results, and especially the improved method of grouping the VA with respect to their position to the SCC in the VAS offers a novel approach for more differentiated diagnostics of MD. It might also be of further clinical relevance since the newest theory of the cause of an MD attack is based on anatomical changes of the endolymphatic duct, in particular a reduction of the lumen, which results in overfilling of the endolymphatic sinus and a potential discharge of endolymph through the valve of Blast into to utricle (5). Consequently, the morphological changes might be more prominent in specific groups of the VAS, resulting in a higher rate of MD or an altered susceptibility to treatment options.

Many studies have already attempted to more accurately identify the pathophysiology of MD. Bachinger et al. (20) showed that the VA in MD patients can have a different position, and in other studies (22, 32, 33) it was recently shown that narrow bony VA favors EH, and thus the morphology of the VA plays a role in the expression of MD. These works were facilitated by new and improved imaging technologies such as high-resolution CT data.

A possible limitation of all radiologically based studies in the field of MD is the slice thickness of the images. Particularly when the slice thickness increases, the VA, with its very narrow lumen, is often not easily or no longer recognizable (**Figure 1**). In the study by Stahle and Wilbrand (19), only 65% of the VAs of the ears affected by MD were visible, whereas 81% of the VAs of the ear not affected by MD were clearly detectable. They stated that a better imaging technique is necessary to perform a reliable delineation of VAs. To further address this problem, different imaging modalities were investigated. It was shown that the angle of the VA to the SCCs can be detected without significant differences in CT, but the length differed significantly between mfpVCT and MSCT because of the reduced resolution. For this

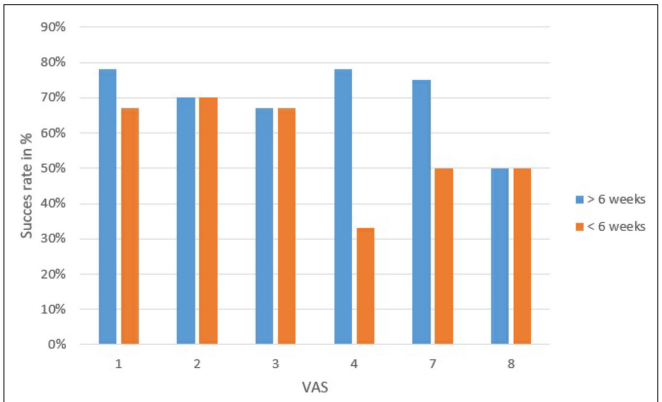

FIGURE 6 | Outcome of the saccotomy compared to each VAS divided into 6 weeks before and after surgery. Successful outcome means that patients have not vertigo or better tan before operation. VAS 4 had the most patients with unsuccessful treatment.

reason, the length of the VA was not used for the development of the VAS score.

To our knowledge, the measurement of the angles of VA to the 3 SCCs has not yet been published before. All SCCs were used as markers because they are at a constant angle to the axes of the body. As early as 1974, Wilbrand measured the angle between anterior SCC and VA (34). Thirty-five unselected temporal bones were examined, in which an average angle of 45° between the VA and anterior SCC was found. This corresponds very well with the results presented here (**Table 1**) and is a further confirmation that VA angle measurements provide reliable results. Another observation reported by his group was that longer aqueducts showed a smaller angle between the entrance and exit path of the VA compared to shorter aqueducts. The results showed that there was also a tendency toward a correspondence between angle size and length. Similar to the present study, a correlation between the angles of the lateral SCC and the length of the VA could be determined (**Figure 2C**), which shows that these two values are probably the two most important for identification of different anatomical variations of the VA.

Based on the results from the TBS, it was revealed that CT images with a higher slice thickness (600 µm), which are normally performed in the clinical setting, can be used to perform angle measurements and to create a 3D model. Both the results of the mfpVCT and the MSCT corresponded to the reference of the micro-CT.

For the 3D model, the mean plus two SD of angle measurements performed in non-MD patients and TB specimens ($n = 79$) was chosen since they represent VA not affected by MD. It cannot be ruled out that an MD patient could have potentially been included in the anonymously used TBS, but none of the angles were different from the group of non-MD patients, which represent a group of the contralateral side of vestibular schwannoma patients not suffering from MD. Consequently, the angle measurements of the 79 VA can thus be used as a control. The mean plus two SD was chosen since in normally distributed data, which the angle measurements are, this range represents 94.45% of the data. Following these statistical considerations, the VAS should be able to group the angle values of the VA in relation to the SCC in an appropriate mode. Indeed, this was shown by the fact that the VAS scores of the TBS and non-MD patients had a broad and even distribution, whereas 90% of MD patients were assigned to the groups 1, 2 and 8 (**Figure 5E**).

The results of the angle measurements showed significant differences between non-MD and MD VA with higher angle values to the lateral and posterior SCC and lower values to the anterior SCC in MD VA. Moreover, the standard deviation was higher in MD patients, because of a much larger range of the results.

Interestingly, there were 10 aqueducts within the MD group which were particularly noticeable with a very short length (<5.5 mm), and a flat angle to the lateral (<74°) and posterior SCC (<110°). They were assigned to group 2 and 4 of the VA score. They resemble the "hypoplastic" type described by Bachinger et al. (20). In their study, they divided the VA into hypoplastic and degenerative with respect to their angle between the entrance and exit of the VA. This allowed the two different types of disease pathologies to be distinguished. In this method of classification, only the group of hypoplastic VA can be clearly assigned to MD, since the form of the degenerative type corresponds to that of normal adults.

The present investigation was performed using a new measurement technique known as the "3D Curved MPR" (35). It is the first time that the VA length has been analyzed using this technique, but the results are (**Table 1**) similar to those reported in the literature (18, 19).

One obstacle to the presented method is that it still cannot be used in everyday clinical practice. As the 3D Slicer software is at present only suitable for scientific purposes, this method cannot yet be used as a clinical diagnostic tool in its current form since calculations must still be done manually. Therefore, a system will be required which automatically marks the SCC and VA and can display them in 3D, thus facilitating use in clinical practice.

MD patients treated with saccotomy were included because these patients had a full set of diagnosis prior to surgery. To include as much data as possible for this work, all existing anamnestic parameters were noted and based on these data, the Gibson score and AAO-HNS was calculated. However, problems with these diagnostic guidelines are the interpretation of the scores and their dependence on patient's information, since not all parameters can be measured clinically. This is why an additional score with radiological features might help to distinguish patients more clearly and help with the diagnosis of MD, as the Hydrops MRI, which has been shown to be applicable (36).

By using the data of the success of saccotomy a first test was performed for the application of the VAS. As shown in **Figure 6**, patients in VAS score 4 are the group of patients with the lowest success rate (33%). In contrary, patients grouped patients grouped to VAS score 1 to 3 are those with the best success rates. However, it has to be mentioned that due to uncertainty surrounding whether saccotomy is a valid treatment for MD (37), and the relative small number of patients, these data have to be interpreted with caution. In the future, further studies correlating

the VAS with other findings, such as effectiveness of different therapies, but also with the variant symptoms of MD, should be performed on larger series of patients to determine whether the VAS is a valid tool to stage MD patients.

CONCLUSION

By the application of different imaging modalities, it could be shown that angle measurements of the VA are reliable and can be used to enhance the diagnosis of patients with MD. Length and angle results from these patients differed from non-MD patients. From the angle measurements of the temporal bone specimen and the non-MD patients, a 3D model was constructed, and the VAS score developed. This score offers a new method for grouping MD patients with respect to the morphology of their VA, making it possible to group MD patients, for example, with regard to the success of a specific MD treatment.

DATA AVAILABILITY STATEMENT

The raw data supporting the conclusions of this article will be made available by the authors, without undue reservation.

ETHICS STATEMENT

The studies involving human participants were reviewed and approved by Ethic Comittee of University Wuerzburg Institute for Pharmacology and Toxicology Versbacherstraße 9, 97078 Wuerzburg, Germany. Written informed consent for participation was not required for this study in accordance with the national legislation and the institutional requirements.

AUTHOR CONTRIBUTIONS

LN developed, executed and analyzed the measurements, and wrote the manuscript. LI helped with statistical analysis, x-rays, and writing the manuscript. MB, WS-D, JT, and RH helped developing the method and contributed anamnestic data. TN, SZ, and DA performed the x-rays. KR helped creating the method, performing measurements and analysis, and wrote the manuscript. All authors contributed to manuscript revision, read, and approved the submitted version.

FUNDING

This publication was supported by the Open Access Publication Fund of the University of Wuerzburg.

ACKNOWLEDGMENTS

We thank Barbara Vona, Institute of Human Genetics, Universitätsmedizin Göttingen for her assistance in proofreading the English language.

SUPPLEMENTARY MATERIAL

The Supplementary Material for this article can be found online at: https://www.frontiersin.org/articles/10.3389/fsurg.2022.747517/full#supplementary-material

REFERENCES

1. Hallpike CS, Cairns H. Observations on the pathology of meniere's syndrome: (Section of Otology). *Proc R Soc Med.* (1938) 31:1317–36. doi: 10.1177/003591573803101112
2. Salt AN, DeMott J. Endolymph calcium increases with time after surgical induction of hydrops in guinea-pigs. *Hear Res.* (1994) 74:115–21. doi: 10.1016/0378-5955(94)90180-5
3. Kariya S, Cureoglu S, Fukushima H, Nomiya S, Nomiya R, Schachern PA, et al. Vascular findings in the stria vascularis of patients with unilateral or bilateral Meniere's disease: a histopathologic temporal bone study. *Otol Neurotol.* (2009) 30:1006–12. doi: 10.1097/MAO.0b013e3181b4ec89
4. Schuknecht HF. Pathophysiology of endolymphatic hydrops. *Archiv oto-rhino-laryngology.* (1976) 212:253–62. doi: 10.1007/BF00453673
5. Gibson WP. Hypothetical mechanism for vertigo in Meniere's disease. *Otolaryngol Clin North Am.* (2010) 43:1019–27. doi: 10.1016/j.otc.2010.05.013
6. Committee on Hearing and Equilibrium guidelines for the diagnosis and evaluation of therapy in Meniere's disease. American academy of otolaryngology-head and neck foundation, Inc. *Otolaryngol Head Neck Surg.* (1995). 113:181–5. doi: 10.1016/S0194-5998(95)70102-8
7. Lopez-Escamez JA, Carey J, Chung WH, Goebel JA, Magnusson M, Mandala M, et al. Diagnostic criteria for Meniere's disease. *J Vestib Res.* (2015) 25:1–7. doi: 10.3233/VES-150549
8. Gibson W. The 10-Point score for the clinical diagnosis of ménière's disease. *Surgery of the Inner Ear.* (1991) 11:21.
9. Gibson WP, Moffat DA, Ramsden RT. Clinical electrocochleography in the diagnosis and management of Meneere's disorder. *Audiology.* (1977) 16:389–401. doi: 10.3109/00206097709071852
10. Nakashima T, Naganawa S, Teranishi M, Tagaya M, Nakata S, Sone M, et al. Endolymphatic hydrops revealed by intravenous gadolinium injection in patients with Meniere's disease. *Acta Otolaryngol.* (2010) 130:338–43. doi: 10.3109/00016480903143986
11. Homann G, Vieth V, Weiss D, Nikolaou K, Heindel W, Notohamiprodjo M, et al. Semi-quantitative vs. volumetric determination of endolymphatic space in Meniere's disease using endolymphatic hydrops 3T-HR-MRI after intravenous gadolinium injection. *PLoS ONE.* (2015) 10:e0120357. doi: 10.1371/journal.pone.0120357
12. Gurkov R, Berman A, Dietrich O, Flatz W, Jerin C, Krause E, et al. MR volumetric assessment of endolymphatic hydrops. *Eur Radiol.* (2015) 25:585–95. doi: 10.1007/s00330-014-3414-4
13. Gallego-Martinez A, Espinosa-Sanchez JM, Lopez-Escamez JA. Genetic contribution to vestibular diseases. *J Neurol.* (2018) 265(Suppl 1):29–34. doi: 10.1007/s00415-018-8842-7
14. Strupp M, Brandt T, Brevern Mv, Dieterich M, Eckhardt-Henn DA, Straumann D, et al. *Kapitel: Hirnnervensyndrome und Schwindel Schwindel—Therapie.* Deutsche Gesellschaft für Neurologie (2012).
15. Wilschowitz M, Sanchez-Hanke M, Ussmuller J. [The value of saccotomy in Meniere disease. a long-term analysis of 42 cases]. *HNO.* (2001) 49:180–7. doi: 10.1007/s001060050730
16. Espinosa-Sanchez JM, Lopez-Escamez JA. The pharmacological management of vertigo in Meniere disease. *Expert Opin Pharmacother.* (2020) 21:1753–63. doi: 10.1080/14656566.2020.1775812
17. Jackler RK, Whinney D. A century of eighth nerve surgery. *Otol Neurotol.* (2001) 22:401–16. doi: 10.1097/00129492-200105000-00023
18. Rizvi SS, Smith LE. Idiopathic endolymphatic hydrops and the vestibular aqueduct. *Ann Otol Rhinol Laryngol.* (1981) 90:77–9. doi: 10.1177/000348948109000120
19. Stahle J, Wilbrand HF. The temporal bone in patients with Meniere's disease. *Acta Otolaryngol.* (1983) 95:81–94. doi: 10.3109/00016488309130919

20. Bachinger D, Luu NN, Kempfle JS, Barber S, Zurrer D, Lee DJ, et al. Vestibular aqueduct morphology correlates with endolymphatic sac pathologies in Meniere's disease-a correlative histology and computed tomography study. *Otol Neurotol.* (2019) 40:e548–55. doi: 10.1097/MAO.0000000000002198
21. Rask-Andersen H, Stahle J. Lymphocyte-macrophage activity in the endolymphatic sac. an ultrastructural study of the rugose endolymphatic sac in the guinea pig. *ORL J Otorhinolaryngol Relat Spec.* (1979) 41:177–92. doi: 10.1159/000275458
22. Eckhard AH, Zhu M, O'Malley JT, Williams GH, Loffing J, Rauch SD, et al. Inner ear pathologies impair sodium-regulated ion transport in Meniere's disease. *Acta Neuropathol.* (2019) 137:343–57. doi: 10.1007/s00401-018-1927-7
23. Ikeda M, Sando I. Endolymphatic duct and sac in patients with Meniere's disease. a temporal bone histopathological study. *Ann Otol Rhinol Laryngol.* (1984) 93:540–6. doi: 10.1177/000348948409300603
24. Lopez-Escamez JA, Carey J, Chung WH, Goebel JA, Magnusson M, Mandala M, et al. [Diagnostic criteria for Meniere's disease consensus document of the Barany Society, the Japan Society for equilibrium research, the European Academy of Otology and Neurotology (EAONO), the American Academy of Otolaryngology-Head and Neck Surgery (AAO-HNS) and the Korean Balance Society]. *Acta Otorrinolaringol Esp.* (2016) 67:1–7. doi: 10.1016/j.otorri.2015.05.005
25. Gibson WP, Arenberg IK. *The 10-point score for the Clinical Diagnosis of M'eni'ere's Disease*. London: Kugler Publications (1991).
26. Wetmore SJ. Endolymphatic sac surgery for Meniere's disease: long-term results after primary and revision surgery. *Arch Otolaryngol Head Neck Surg.* (2008) 134:1144–8. doi: 10.1001/archotol.134.11.1144
27. Baranowski T, Dobrovolskij D, Dremel K, Hölzing A, Lohfink G, Schladitz K, et al. Local fiber orientation from X-ray region-of-interest computed tomography of large fiber reinforced composite components. *Composit Sci Technol.* (2019) 183:107786. doi: 10.1016/j.compscitech.2019.107786
28. Dhanasingh A, Dietz A, Jolly C, Roland P. Human inner-ear malformation types captured in 3D. *J Int Adv Otol.* (2019) 15:77–82. doi: 10.5152/iao.2019.6246
29. Lopinto J, Vimort J-B. *Angle Planes Extension* (2019).
30. Koo TK, Li MY. A guideline of selecting and reporting intraclass correlation coefficients for reliability research. *J Chiropr Med.* (2016) 15:155–63. doi: 10.1016/j.jcm.2016.02.012
31. Pope A. *3d XY Scatter Chart*. (2004). Available online at: http://www.andypope.info/charts/3drotate.htm
32. Gibson WPR. Meniere's Disease. *Adv Otorhinolaryngol.* (2019) 82:77–86. doi: 10.1159/000490274
33. Valvassori GE, Dobben GD. Multidirectional and computerized tomography of the vestibular aqueduct in Meniere's disease. *Ann Otol Rhinol Laryngol.* (1984) 93(6 Pt 1):547–50. doi: 10.1177/000348948409300604
34. Wilbrand HF, Rask-Andersen H, Gilstring D. The vestibular aqueduct and the para-vestibular canal. an anatomic and roentgenologic investigation. *Acta Radiol Diagn (Stockh).* (1974) 15:337–55. doi: 10.1177/028418517401500401
35. Schurzig D, Timm ME, Lexow GJ, Majdani O, Lenarz T, Rau TS. Cochlear helix and duct length identification—evaluation of different curve fitting techniques. *Cochlear Implants Int.* (2018) 19:268–83. doi: 10.1080/14670100.2018.1460025
36. Gurkov R, Pyyko I, Zou J, Kentala E. What is Meniere's disease? a contemporary re-evaluation of endolymphatic hydrops. *J Neurol.* (2016) 263 Suppl 1:S71–81. doi: 10.1007/s00415-015-7930-1
37. Pullens B, Giard JL, Verschuur HP, van Benthem PP. Surgery for Meniere's disease. *Cochrane Database Syst Rev.* (2010) 1:CD005395. doi: 10.1002/14651858.CD005395.pub2

Conflict of Interest: The authors declare that the research was conducted in the absence of any commercial or financial relationships that could be construed as a potential conflict of interest.

frontiers | Frontiers in Surgery

REVIEW
published: 28 April 2022
doi: 10.3389/fsurg.2022.874971

Consensus on MR Imaging of Endolymphatic Hydrops in Patients With Suspected Hydropic Ear Disease (Meniere)

Yupeng Liu[1,2,3], *Ilmari Pyykkö*[4], *Shinji Naganawa*[5], *Pedro Marques*[6], *Robert Gürkov*[7], *Jun Yang*[1,2,3]* *and Maoli Duan*[8,9]*

[1] Department of Otorhinolaryngology-Head and Neck Surgery, Xinhua Hospital, Shanghai Jiaotong University School of Medicine, Shanghai, China, [2] Ear Institute, Shanghai Jiaotong University School of Medicine, Shanghai, China, [3] Shanghai Key Laboratory of Translational Medicine on Ear and Nose Diseases, Shanghai, China, [4] Hearing and Balance Research Unit, Field of Otolaryngology, Faculty of Medicine and Health Technology, School of Medicine, Tampere University, Tampere, Finland, [5] Department of Radiology, Nagoya University Graduate School of Medicine, Nagoya, Japan, [6] Unit of Otorhinolaryngology, Department of Surgery and Physiology, University of Porto Medical School, Porto, Portugal, [7] ENT Centre at Red Cross Square, University of Munich, Munich, Germany, [8] Ear Nose and Throat Patient Area, Trauma and Reparative Medicine Theme, Karolinska University Hospital, Stockholm, Sweden, [9] Division of Ear, Nose and Throat Diseases, Department of Clinical Science, Intervention and Technology, Karolinska Institutet, Stockholm, Sweden

OPEN ACCESS

Edited by:
Haralampos Gouveris, Johannes Gutenberg University Mainz, Germany

Reviewed by:
Arata Horii, Niigata University, Japan
Toshihisa Murofushi, Teikyo University Mizonokuchi Hospital, Japan

***Correspondence:**
Jun Yang
yangjun@xinhuamed.com.cn
Maoli Duan
maoli.duan@ki.se

Specialty section:
This article was submitted to Otorhinolaryngology - Head and Neck Surgery, a section of the journal Frontiers in Surgery

Received: *13 February 2022*
Accepted: *28 March 2022*
Published: *28 April 2022*

Citation:
Liu Y, Pyykkö I, Naganawa S, Marques P, Gürkov R, Yang J and Duan M (2022) Consensus on MR Imaging of Endolymphatic Hydrops in Patients With Suspected Hydropic Ear Disease (Meniere). Front. Surg. 9:874971. doi: 10.3389/fsurg.2022.874971

Endolymphatic hydrops (EH) is considered the histological hallmark of Meniere's disease. Visualization of EH has been achieved by special sequences of inner ear magnetic resonance imaging (MRI) with a gadolinium-based contrast agent *via* intravenous or intratympanic administration. Although it has been applied for more than 10 years since 2007, a unified view on this technique has not yet been achieved. This paper presents an expert consensus on MRI of endolymphatic hydrops in the following aspects: indications and contra-indications for patient selection, methods of contrast-agent administration (intravenous or intratympanic), MRI sequence selection, the specific scanning parameter settings, and standard image evaluation methods and their advantages and disadvantages. For each part of this consensus, a comment is attached to elucidate the reasons for the recommendation.

Keywords: Meniere's disease, magnetic resonance imaging, endolymphatic hydrops, consensus, gadolinium

INTRODUCTION

Meniere's disease (MD) is a disease complex of multifactorial etiology. As no objective methods exist for diagnosis, the Committee on Hearing and Equilibrium of the American Academy of Otolaryngology-Head & Neck Surgery (AAO-HNS) suggests the use of symptom-based guidelines for the diagnosis of MD (1) which has been supported by the Barany Society (2). MD is believed to originate in the inner ear, and endolymphatic hydrops (EH) can be demonstrated in histological preparations or with MRI, though the etiology of the disease is unknown (3) and most likely multifactorial. EH is considered the histological hallmark of MD. In the early days, histopathological post-mortem studies were considered the only way to confirm the diagnosis of MD (4). In the past decades, direct visualization of EH in living subjects was achieved by special sequences of inner ear magnetic resonance imaging (MRI) with a gadolinium-based contrast agent (GBCA) *via* intravenous, intratympanic, or their combined administration with 3 Tesla magnetic

resonance imaging (3T MRI) (5). Clinicians have used different MRI algorithms and visualization methods to confirm and classify EH in MD patients (6). In the clinical guideline proposed by the Japan Society for Equilibrium Research in 2020, EH on MRI was regarded as an objective sign for "certain" MD in the diagnostic criteria of MD (7). As a result of the accumulated experience with EH imaging in patients with symptoms of inner ear disorders, the concept of hydropic ear disease (HED) was developed, unifying the various clinical manifestations in patients with EH as well as the primary and secondary etiologies of EH into one comprehensive taxonomy (8–10).

The endolymphatic space forms a closed liquid circulation system, which is separated from the perilymph. After intratympanic injection or intravenous administration, GBCA is absorbed through the round and oval windows, or the blood labyrinth barrier, respectively, and distributed in the perilymph fluid after entering the inner ear. By changing the water proton relaxation rate of local tissues, GBCA can enhance the image contrast ratio between gadolinium-containing tissues and the gadolinium-free tissues to reflect the morphological changes of the surrounding structures (11). Since GBCA primarily enters the perilymphatic space and not the endolymphatic space, the image of the perilymph fluid can be distinguished from the endolymph fluid by looking at the presence (perilymphatic space) and absence (endolymphatic space) of GBCA in the inner ear (12). Currently, 3-dimensional fluid-attenuated inversion recovery (3D-FLAIR) and 3-dimensional real inversion recovery (3D-real IR) sequences are most widely used with various scan parameters. Regarding grading of EH, different grading scales for evaluating the degree of EH have been proposed. Prior to the upcoming 8th International Symposium on Meniere's Disease and Inner Ear Disorders, shifted to occur in April 2023, an international consensus group of experts in inner ear imaging has come together to work out recommendations for the use of endolymphatic hydrops imaging. This consensus includes the following aspects: contrast agent selection, application of contrast agent, indications and contraindications, MR sequence(s), scan parameters, and image evaluation.

CONSENSUS OF THE COMMITTEE

Indications/Contra-Indications

Patients who fulfill the 1995 AAO-HNS criteria of "possible," "probable," or "definite" MD or patients who fulfill the Barany Society criteria of "probable" or "definite" MD can be included. Patients with fluctuating symptoms of inner ear dysfunction without a definite diagnosis despite specialized neurotological function testing and conventional cranial MRI may be candidates for EH imaging, depending on the therapeutic consequences of a potentially confirmed diagnosis of HED. Both patients suffering from an acute attack of vertigo and patients in a stable stage are eligible for MRI examination (13). Patients enrolled in clinical trials concerned with the therapeutic efficacy of interventions in HED should receive EH imaging as one of the trial outcome parameters. Furthermore, EH imaging is recommended before invasive and/or destructive treatments such as intratympanic gentamicin injections, endolymphatic sac surgery, semicircular canal occlusion, labyrinthectomy, and vestibular neurectomy (14, 15). However, patients who meet MRI contraindications due to mental or drug incompliances should not undergo MRI examination. The incidence of adverse reactions to GBCA is low, occurring in approximately one in 10,000–40,000 injections. Severe, life-threatening anaphylactoid reactions to GBCA are rare. Intravenous application of GBCA should be forbidden in patients with severe gadolinium allergy, severe chronic kidney disease, and acute renal injury (16). Intratympanic application of GBCA should be used cautiously in these patients as well but those with kidney problems could tolerate the very low amount of intratympanic GBCA. We recommend patients with a history of chronic otitis media, otitis media with effusion or tympanic membrane perforation, or with a history of middle ear surgery for intravenous application of GBCA before MRI examination. Patients who are severely overweight or suffer from claustrophobia may hinder imaging with 3T MRI scanners. The clinician should weigh the importance of an MRI-confirmed diagnosis of EH against the potential risks in each individual patient.

Comments

The symptoms of MD are diverse. Some patients have symptoms of vertigo and/or types of hearing loss different from those in the currently recommended clinical MD criteria (AAO-HNS 1995 and Barany Society), and they do not strictly meet the current diagnostic criteria. The reason for variability in complaints is not well-understood though it is reasonable to assume that the variability may be associated with different genotypes, comorbidities, and primary vs. secondary etiologies (8). For these patients, inner ear imaging technology can help clinicians to identify whether it is a disease related to EH, to provide a reference for an informed choice of treatment options.

Type and Application of Contrast Agents

Commonly used MRI contrast agents include gadoterate megluminate, gadobutrol, gadobenate dimeglumine, gadopentetic acid dimeglumine, and gadodiamide. All of the contrast agents mentioned above, except gadoterate megluminate, were reported to be safe for intratympanic and intravenous injection (17–24). There are still insufficient data about the effect of contrast agent type on the quality of MRI images aimed at detecting EH. From clinical experience, not many differences in image quality seem to be present among contrast agents. We therefore recommend that currently, clinicians do not need to pay special attention to the type of gadolinium contrast agents. However, further research is needed on this topic.

Generally, both intratympanic and intravenous injection of GBCA can be used. Based on the existing clinical experience and clinical safety studies, we recommend that the contrast medium should be diluted eightfold in saline solution before intratympanic injection (25). However, it has not been established yet whether higher concentrations of GBCA intratympanically applied may cause ototoxicity in the clinical application. The tympanic cavity should be filled with the contrast agent for better absorption through the oval

window and round window. Before injection of the GBCA, an anterior-superior puncture of the tympanic membrane should be performed, creating an "overpressure valve" for the middle ear gas during the injection of the GBCA and avoiding excessive middle ear pressure build-up which may cause pain and transient vertigo in the patient. For the injection, an ultra-thin cannula with a diameter of 0.4 mm is recommended in order to avoid a potentially persisting perforation of the ear drum (26). Clinicians should ask patients to remain in a supine position with the head turned by 45 degrees toward the contralateral side for 30 min after injection. Speaking and swallowing should be avoided as much as possible during this period. MRI is recommended to be performed 24 h after the intratympanic administration (27, 28).

Intravenous GBCA administration is also a suitable route of delivery. A single intravenous dose of GBCA (0.1 mmol/kg body weight) should be administered intravenously. Intravenous administration of double-dose GBCA might be considered when the pulse sequence optimization is not mature enough to visualize EH with single-dose GBCA. However, taking into account the gadolinium deposition issue in the brain, a single dose of macrocyclic-type agents is recommended (29), especially in patients undergoing multiple EH imaging evaluations such as participants in clinical trials. Furthermore, the use of a double dose of GBCA is not approved in some countries. MRI is recommended to be performed 4 h after intravenous application of GBCA (30, 31).

Comments

Currently, there is a shortage of high-quality studies to compare the visualization of the inner ear between intratympanic and intravenous dosing of GBCA, though general opinion suggests better imaging with the intratympanic approach (32, 33). However, the intratympanic method has some restrictions as GBCA is not registered for intratympanic use by national pharmaceutical agencies. An appropriate approach should be chosen with consideration of the clinical characteristics of each patient. Some patients would not accept intratympanic injection when they have access to the intravenous method as an alternative. Due to the difference of the permeability of the round and oval windows, the signal intensity of the perilymph after intratympanic injection may have larger inter-individual differences than that after intravenous injection (34). Also, a single intratympanic injection to the affected side would not enable bilateral observation of both ears. Duan et al. first reported in 2004 that using round window application of GBCA showed no affection in auditory brainstem response thresholds in animal study, indicating that gadolinium is non-toxic to the guinea pig cochlea (24). Intratympanic administration of GBCA has also been reported to be well-tolerated in humans (35–37). The application of intratympanic injection is limited in patients with some diseases such as external ear malformation, acute otitis media, and tympanic membrane perforations.

MRI Sequence and Scanning Parameters

We recommend the 3D-FLAIR sequence and 3D-real IR sequence (38) as a basic imaging sequence that can characterize the signal differences between the contrast-enhanced perilymph and non-contrast-enhanced endolymph. Subtraction of two kinds of images with slightly different inversion time is frequently employed to produce 3D-real IR images (39). One is 3D-FLAIR, which provides a positive perilymph signal. The other employs a shorter inversion time to produce a positive endolymph image (40). The subtraction of these two kinds of images is called a HYDROPS (HYbriD of Reversed image Of Positive endolymph signal and native image of positive perilymph Signal) image. Many reports with hydrops images can be found using single-dose intravenous GBCA (41, 42). The advantage of the 3D-real IR sequence is that clinicians are able to identify the signals from the endolymph space, perilymph space, and surrounding bone tissues on one single unprocessed 3D-real IR image. The endolymph space and surrounding bone tissues cannot be separated using the 3D-FLAIR sequence. However, the 3D-FLAIR sequence is superior to the 3D-real IR sequence in cases where GBCA was insufficiently distributed into the perilymphatic space after an intratympanic injection (32). 3D-real IR imaging now can be performed even with single-dose intravenous GBCA (43).

Repetition time (TR), echo time (TE), inversion time (TI), readout flip angle (FA), field of view (FOV), slice thickness, and matrix size are the main scan parameters in the MRI of EH. Different parameters were previously proposed by clinicians from different medical centers in the world. For intratympanic GBCA administration, when the GBCA concentration in the labyrinth is high, the adjustments of pulse sequence parameters are not so strict. However, for single-dose intravenous administration, parameters should be strictly defined. Otherwise, meaningful results cannot be expected. Slight changes of the parameters might ruin the entire study. Successful parameters can be found in a previous review paper (32).

Comments

Clinicians, radiologists, and MRI technicians could adjust the parameters depending on the actual situation in the MR examination to acquire acceptable EH images, however, a test scan and verification are necessary before the clinical study if the newly adjusted protocol is applied.

How to Evaluate Images

Several grading systems were proposed to visually evaluate and compare the relative areas of the non-enhanced endolymphatic space vs. the contrast-enhanced perilymph space. The classic three-grade scale proposed by Nakashima is most commonly used in current literature. In this grading system, the vestibule and cochlea are analyzed separately (44). Regarding the cochlea, no hydrops is present when the Reissner's membrane remains *in situ* between the endolymph-containing scala media and perilymph-containing scala vestibuli. A mild hydrops is defined by a slight displacement of Reissner's membrane without exceeding the area of the scala vestibule. A significant endolymphatic hydrops is present when the area of the scala media is larger than that of the scala vestibuli. It is recommended to evaluate the axial plane of the cochlea in MRI so as to maximize the visualization of the three turns of the cochlea. Concerning the vestibule, no hydrops is present when the ratio

of the endolymphatic area over the sum of the endolymphatic and perilymphatic areas is <1/3. A mild hydrops is present when the ratio of the endolymphatic area over the whole vestibular fluid space ranges between 1/3 and 1/2. A significant hydrops is present when the ratio of the endolymphatic area exceeds 1/2 (44). This classification method is based on the temporal bone specimen study where the area ratio of endolymphatic space to the vestibular fluid ranged from 26.5 to 39.4% (mean 33.2%). This proportion is also confirmed by endolymphatic space imaging in healthy volunteers (29). Based on this three-stage grading, a modified four-stage grading of cochlear hydrops has then been proposed by Gürkov et al. (45, 46): grade 0 = the endolymph is not/hardly visible, grade 1 = the endolymph is clearly visible as round hypointense regions, grade 2 = the perilymph is further displaced by the endolymph but the perilymph still has a crescent appearance, grade 3 = a perilymph with a flat appearance.

Extension of EH into the semicircular canals (SCC) was first observed by Gürkov et al. (47, 48) and linked to caloric hypofunction to the SCC, but the pathophysiological significance of this EH feature is still not entirely resolved.

Another semi-quantitative grading system called "SURI" (saccule to utricle ratio inversion) is proposed as a marker of EH. In this grading system, grade 0 is defined when no saccular abnormality is observed (SURI<1). Grade 1 is defined when SURI≥1. Grade 2 is defined when the saccule is not visible (49). The three-grade scale of cochlea hydrops and four-grade scale of vestibular hydrops proposed by Bernaerts et al. might be considered as a combination of Nakashima's system and the "SURI" system (18). In the evaluation of cochlea hydrops, each grade is defined based on the location of Reissner's membrane. A normal vestibule is defined when the saccule and utricle are visibly separately and take up less than half of the surface of the vestibule. Vestibular hydrops grade I is defined when the saccule becomes equal or larger than the utricle. Vestibular hydrops grade II is defined when there is a confluence of the saccule and utricle, with still a peripheral rim enhancement of the perilymphatic space. Vestibular hydrops grade III is defined when perilymphatic enhancement is no longer visible. This grading system could provide an accurate description of the severity of EH in different parts of the otolith organs.

Based on this vestibular EH grading, a four-stage grading for EH using two axial images/slices has been proposed for use in EH imaging with a 1.5 Tesla scanner and intratympanic GBCA administration. This grading takes into account the more inferior location of the sacculus with respect to the utriculus and the general predilection for vestibular EH to affect the sacculus in the earliest stage of disease evolution: grade 0 = the sacculus in the inferior vestibulum is not/hardly visible; grade 1 = the sacculus in the inferior vestibulum appears with a round shape; grade 2 = endolymph in the inferior vestibulum has completely displaced the perilymph, but the superior vestibulum still has a clear perilymph signal; grade 3 = the perilymph signal is virtually lost on both slices (50).

Inui et al. (51–53) proposed a quantitatively 3D measurement to evaluate the volume of the inner ear endolymphatic space (ELS) in a more accurate way. Positive perilymph images (PPI) and positive endolymph images (PEI) were transferred, and PEI images were subtracted from the PPI images and the images were reconstructed using a specialized workstation. Accurate measurement of EH is helpful in the further study of the relationship between EH and the clinical manifestation and functional results of MD.

Comments

Currently, quantification of the degree of cochlear hydrops is still difficult because the cochlear endolymphatic space is divided into different cochlear turns, and each space is quite small. The existing imaging technology is not enough to fully distinguish the cochlear endolymphatic space of all the cochlear turns, especially the apical turns. The semi-quantitative classification system based on the location of Reissner's membrane, which was first proposed by Nakashima, is still considered to be the most convenient method for the evaluation of cochlear hydrops. This classification allows for the visualization of EH in subjects without MD maybe indicating that the endolymphatic space in living organisms is not as tightly regulated as suggested (as also pressure of the eyes) (6). However, evaluation of the vestibule with a high sensitivity for EH specific for MD can be achieved with this method. The Gürkov classification seems suitable for rapid clinical assessment, being based on typical morphological features of different degrees of EH severity. The "SURI" grading system and Bernaerts system have their advantages in vestibular hydrops evaluation. However, these EH grading methods evaluate EH in the cochlea and vestibule separately without considering the extent of the endolymph space distension throughout the entire inner ear. Also, evaluation of semicircular canal EH is not included. Recently, He et al. (54) established a 2D volume-referencing EH grading system in which the volume ratio and the semicircular canals are taken into consideration to better represent the total EH of inner ears. Clinicians can combine the results of MRI and audio-vestibular function tests (electrocochleogram (ECochG), cervical vestibular evoked myogenic potentials (cVEMP), and ocular vestibular evoked myogenic potentials (oVEMP) to evaluate the severity of the disease comprehensively. Also, as indicated above, focusing on quantitative saccule hydrops and utricle hydrops changes for individual patients in a longitudinal imaging study design would provide valuable information for further understanding of the pathophysiological changes in MD patients. A histopathologic study revealed that hydrops initially involves the cochlear duct and the saccule. With the progression of pathology, the utricle and semicircular canals will be involved subsequently (55).

AUTHOR CONTRIBUTIONS

JY and MD contributed to the study design and critically reviewed and approved the final manuscript. YL contributed to the detailed study design, drafting of the manuscript, and revised the manuscript. IP, SN, PM, and RG critically reviewed the manuscript. All authors agreed to be accountable for the content of the work, contributed to the article, and approved the submitted version.

REFERENCES

1. Goebel JA. 2015 Equilibrium committee amendment to the 1995 AAO-HNS guidelines for the definition of Ménière's disease. *Otolaryngol Head Neck Surg.* (2016) 154:403–4. doi: 10.1177/0194599816628524
2. Lopez-Escamez JA, Carey J, Chung WH, Goebel JA, Magnusson M, Mandalà M, et al. Diagnostic criteria for Menière's disease. *J Vestib Res.* (2015) 25:1–7. doi: 10.3233/VES-150549
3. Nakashima T, Pyykkö I, Arroll MA, Casselbrant ML, Foster CA, Manzoor NF, et al. Meniere's disease. *Nat Rev Dis Primers.* (2016) 2:16028. doi: 10.1038/nrdp.2016.28
4. Committee on Hearing and Equilibrium guidelines for the diagnosis and evaluation of therapy in Menière's disease. American Academy of Otolaryngology-Head and Neck Foundation, Inc. *Otolaryngol Head Neck Surg.* (1995) 113:181–5. doi: 10.1016/S0194-5998(95)70102-8
5. Iida T, Teranishi M, Yoshida T, Otake H, Sone M, Kato M, et al. Magnetic resonance imaging of the inner ear after both intratympanic and intravenous gadolinium injections. *Acta Otolaryngol.* (2013) 133:434–8. doi: 10.3109/00016489.2012.753640
6. Yoshida T, Sugimoto S, Teranishi M, Otake H, Yamazaki M, Naganawa S, et al. Imaging of the endolymphatic space in patients with Ménière's disease. *Auris Nasus Larynx.* (2018) 45:33–8. doi: 10.1016/j.anl.2017.02.002
7. Iwasaki S, Shojaku H, Murofushi T, Seo T, Kitahara T, Origasa H, et al. Diagnostic and therapeutic strategies for Meniere's disease of the Japan Society for Equilibrium Research. *Auris Nasus Larynx.* (2021) 48:15–22. doi: 10.1016/j.anl.2020.10.009
8. Gürkov R, Jerin C, Flatz W, Maxwell R. Clinical manifestations of hydropic ear disease (Menière's). *Eur Arch Otorhinolaryngol.* (2019) 276:27–40. doi: 10.1007/s00405-018-5157-3
9. Gürkov R, Hornibrook J. On the classification of hydropic ear disease (Menière's disease). *HNO.* (2018) 66:455–63. doi: 10.1007/s00106-018-0488-3
10. Gürkov R, Pyykö I, Zou J, Kentala E. What is Menière's disease? A contemporary re-evaluation of endolymphatic hydrops. *J Neurol.* (2016) 263(Suppl. 1):S71–81. doi: 10.1007/s00415-015-7930-1
11. Caravan P, Ellison JJ, McMurry TJ, Lauffer RB. Gadolinium(III) chelates as MRI contrast agents: structure, dynamics, and applications. *Chem Rev.* (1999) 99:2293–352. doi: 10.1021/cr980440x
12. Pyykkö I, Zou J, Poe D, Nakashima T, Naganawa S. Magnetic resonance imaging of the inner ear in Meniere's disease. *Otolaryngol Clin North Am.* (2010) 43:1059–80. doi: 10.1016/j.otc.2010.06.001
13. Fukushima M, Akahani S, Inohara H, Takeda N. Stability of endolymphatic hydrops in Ménière disease shown by 3-tesla magnetic resonance imaging during and after vertigo attacks. *JAMA Otolaryngol Head Neck Surg.* (2019) 145:583–85. doi: 10.1001/jamaoto.2019.0435
14. Landen M, Bernaerts A, Blaivie C, Vanspauwen R, Deckers F, De Foer B. Downgrading of endolymphatic hydrops on MRI after intratympanic corticosteroid therapy in a patient with Menière's disease. *Otol Neurotol.* (2020) 41:e638–40. doi: 10.1097/MAO.0000000000002603
15. Higashi-Shingai K, Imai T, Okumura T, Uno A, Kitahara T, Horii A, et al. Change in endolymphatic hydrops 2 years after endolymphatic sac surgery evaluated by MRI. *Auris Nasus Larynx.* (2019) 46:335–45. doi: 10.1016/j.anl.2018.10.011
16. Beckett KR, Moriarity AK, Langer JM. Safe use of contrast media: what the radiologist needs to know. *Radiographics.* (2015) 35:1738–50. doi: 10.1148/rg.2015150033
17. Eliezer M, Poillon G, Gillibert A, Horion J, Cruypeninck Y, Gerardin E, et al. Comparison of enhancement of the vestibular perilymph between gadoterate meglumine and gadobutrol at 3-Tesla in Meniere's disease. *Diagn Interv Imaging.* (2018) 99:271–77. doi: 10.1016/j.diii.2018.01.002
18. Bernaerts A, Vanspauwen R, Blaivie C, van Dinther J, Zarowski A, Wuyts FL, et al. The value of four stage vestibular hydrops grading and asymmetric perilymphatic enhancement in the diagnosis of Menière's disease on MRI. *Neuroradiology.* (2019) 61:421–29. doi: 10.1007/s00234-019-02155-7
19. Fiorino F, Mattellini B, Vento M, Mazzocchin L, Bianconi L, Pizzini FB. Does the intravenous administration of frusemide reduce endolymphatic hydrops? *J Laryngol Otol.* (2016) 130:242–7. doi: 10.1017/S0022215115003527
20. Hornibrook J, Flook E, Greig S, Babbage M, Goh T, Coates M, et al. MRI inner ear imaging and tone burst electrocochleography in the diagnosis of Ménière's disease. *Otol Neurotol.* (2015) 36:1109–14. doi: 10.1097/MAO.0000000000000782
21. Shi H, Li Y, Yin S, Zou J. The predominant vestibular uptake of gadolinium through the oval window pathway is compromised by endolymphatic hydrops in Ménière's disease. *Otol Neurotol.* (2014) 35:315–22. doi: 10.1097/MAO.0000000000000196
22. Sugimoto S, Yoshida T, Teranishi M, Okazaki Y, Naganawa S, Sone M. The relationship between endolymphatic hydrops in the vestibule and low-frequency air-bone gaps. *Laryngoscope.* (2018) 128:1658–62. doi: 10.1002/lary.26898
23. Counter SA, Bjelke B, Borg E, Klason T, Chen Z, Duan ML. Magnetic resonance imaging of the membranous labyrinth during in vivo gadolinium (Gd-DTPA-BMA) uptake in the normal and lesioned cochlea. *Neuroreport.* (2000) 11:3979–83. doi: 10.1097/00001756-200012180-00015
24. Duan M, Bjelke B, Fridberger A, Counter SA, Klason T, Skjönsberg A, et al. Imaging of the guinea pig cochlea following round window gadolinium application. *Neuroreport.* (2004) 15:1927–30. doi: 10.1097/00001756-200408260-00019
25. Nakashima T, Naganawa S, Sugiura M, Teranishi M, Sone M, Hayashi H, et al. Visualization of endolymphatic hydrops in patients with Meniere's disease. *Laryngoscope.* (2007) 117:415–20. doi: 10.1097/MLG.0b013e31802c300c
26. Gürkov R, Holzer M. Intratympanale Applikation von Medikamenten. *HNO Nachrichten.* (2020) 50:42–5. doi: 10.1007/s00060-020-7096-z
27. Wesseler A, Óvári A, Javorkova A, Kwiatkowski A, Meyer JE, Kivelitz DE. Diagnostic value of the magnetic resonance imaging with intratympanic gadolinium administration (IT-Gd MRI) versus audio-vestibular tests in Menière's disease: IT-Gd MRI makes the difference. *Otol Neurotol.* (2019) 40:e225–32. doi: 10.1097/MAO.0000000000002082
28. Pyykkö I, Zou J, Gürkov R, Naganawa S, Nakashima T. Imaging of temporal bone. *Adv Otorhinolaryngol.* (2019) 82:12–31. doi: 10.1159/000490268
29. Taoka T, Naganawa S. Gadolinium-based contrast media, cerebrospinal fluid and the glymphatic system: possible mechanisms for the deposition of gadolinium in the brain. *Magn Reson Med Sci.* (2018) 17:111–9. doi: 10.2463/mrms.rev.2017-0116
30. Shi S, Zhou F, Wang W. 3D-real IR MRI of Meniere's disease with partial endolymphatic hydrops. *Am J Otolaryngol.* (2019) 40:589–93. doi: 10.1016/j.amjoto.2019.05.015
31. Morimoto K, Yoshida T, Sugiura S, Kato M, Kato K, Teranishi M, et al. Endolymphatic hydrops in patients with unilateral and bilateral Meniere's disease. *Acta Otolaryngol.* (2017) 137:23–8. doi: 10.1080/00016489.2016.1217042
32. Naganawa S, Nakashima T. Visualization of endolymphatic hydrops with MR imaging in patients with Ménière's disease and related pathologies: current status of its methods and clinical significance. *Jpn J Radiol.* (2014) 32:191–204. doi: 10.1007/s11604-014-0290-4
33. Conte G, Lo Russo FM, Calloni SF, Sina C, Barozzi S, Di Berardino F, et al. MR imaging of endolymphatic hydrops in Ménière's disease: not all that glitters is gold. *Acta Otorhinolaryngol Ital.* (2018) 38:369–76. doi: 10.14639/0392-100X-1986
34. Yoshioka M, Naganawa S, Sone M, Nakata S, Teranishi M, Nakashima T. Individual differences in the permeability of the round window: evaluating the movement of intratympanic gadolinium into the inner ear. *Otol Neurotol.* (2009) 30:645–8. doi: 10.1097/MAO.0b013e31819bda66
35. Louza JP, Flatz W, Krause E, Gürkov R. Short-term audiologic effect of intratympanic gadolinium contrast agent application in patients with Ménière's disease. *Am J Otolaryngol.* (2012) 33:533–7. doi: 10.1016/j.amjoto.2011.12.004
36. Louza J, Krause E, Gürkov R. Audiologic evaluation of Menière's disease patients one day and one week after intratympanic application of gadolinium contrast agent: our experience in sixty-five patients. *Clin Otolaryngol.* (2013) 38:262–6. doi: 10.1111/coa.12087
37. Louza J, Krause E, Gürkov R. Hearing function after intratympanic application of gadolinium-based contrast agent: a long-term evaluation. *Laryngoscope.* (2015) 125:2366–70. doi: 10.1002/lary.25259
38. Naganawa S, Satake H, Kawamura M, Fukatsu H, Sone M, Nakashima T. Separate visualization of endolymphatic space, perilymphatic space and bone by a single pulse sequence; 3D-inversion recovery imaging utilizing real

reconstruction after intratympanic Gd-DTPA administration at 3 Tesla. *Eur Radiol.* (2008) 18:920–4. doi: 10.1007/s00330-008-0854-8
39. Naganawa S, Yamazaki M, Kawai H, Bokura K, Sone M, Nakashima T. Imaging of Ménière's disease after intravenous administration of single-dose gadodiamide: utility of subtraction images with different inversion time. *Magn Reson Med Sci.* (2012) 11:213–9. doi: 10.2463/mrms.11.213
40. Naganawa S, Sugiura M, Kawamura M, Fukatsu H, Sone M, Nakashima T. Imaging of endolymphatic and perilymphatic fluid at 3T after intratympanic administration of gadolinium-diethylene-triamine pentaacetic acid. *AJNR Am J Neuroradiol.* (2008) 29:724–6. doi: 10.3174/ajnr.A0894
41. Ito T, Inoue T, Inui H, Miyasaka T, Yamanaka T, Kichikawa K, et al. Novel magnetic resonance imaging-based method for accurate diagnosis of Meniere's disease. *Front Surg.* (2021) 8:671624. doi: 10.3389/fsurg.2021.671624
42. Naganawa S, Suzuki K, Nakamichi R, Bokura K, Yoshida T, Sone M, et al. Semi-quantification of endolymphatic size on MR imaging after intravenous injection of single-dose gadodiamide: comparison between two types of processing strategies. *Magn Reson Med Sci.* (2013) 12:261–9. doi: 10.2463/mrms.2013-0019
43. Naganawa S, Kawai H, Taoka T, Sone M. Improved 3D-real inversion recovery: a robust imaging technique for endolymphatic hydrops after intravenous administration of gadolinium. *Magn Reson Med Sci.* (2019) 18:105–8. doi: 10.2463/mrms.bc.2017-0158
44. Nakashima T, Naganawa S, Pyykko I, Gibson WP, Sone M, Nakata S, et al. Grading of endolymphatic hydrops using magnetic resonance imaging. *Acta Otolaryngol Suppl.* (2009) 129:5–8. doi: 10.1080/00016480902729827
45. Gürkov R, Flatz W, Louza J, Strupp M, Krause E. *In vivo* visualization of endolyphatic hydrops in patients with Meniere's disease: correlation with audiovestibular function. *Eur Arch Otorhinolaryngol.* (2011) 268:1743–8. doi: 10.1007/s00405-011-1573-3
46. Gürkov R, Flatz W, Louza J, Strupp M, Ertl-Wagner B, Krause E. *In vivo* visualized endolymphatic hydrops and inner ear functions in patients with electrocochleographically confirmed Ménière's disease. *Otol Neurotol.* (2012) 33:1040–5. doi: 10.1097/MAO.0b013e31825d9a95
47. Gürkov R, Flatz W, Ertl-Wagner B, Krause E. Endolymphatic hydrops in the horizontal semicircular canal: a morphologic correlate for canal paresis in Ménière's disease. *Laryngoscope.* (2013) 123:503–6. doi: 10.1002/lary.23395
48. Gürkov R, Flatz W, Louza J, Strupp M, Ertl-Wagner B, Krause E. Herniation of the membranous labyrinth into the horizontal semicircular canal is correlated with impaired caloric response in Ménière's disease. *Otol Neurotol.* (2012) 33:1375–9. doi: 10.1097/MAO.0b013e318268d087
49. Attyé A, Eliezer M, Boudiaf N, Tropres I, Chechin D, Schmerber S, et al. MRI of endolymphatic hydrops in patients with Meniere's disease: a case-controlled study with a simplified classification based on saccular morphology. *Eur Radiol.* (2017) 27:3138–46. doi: 10.1007/s00330-016-4701-z
50. Gürkov R, Lutsenko V, Babkina T, Valchyshyn S, Situkho M. Clinical high-resolution imaging and grading of endolymphatic hydrops in hydropic ear disease at 1.5 T using the two-slice grading for vestibular endolymphatic hydrops in less than 10 min. *Eur Arch Otorhinolaryngol.* (2022) 279:751–7. doi: 10.1007/s00405-021-06731-7
51. Inui H, Sakamoto T, Ito T, Kitahara T. Magnetic resonance-based volumetric measurement of the endolymphatic space in patients with Meniere's disease and other endolymphatic hydrops-related diseases. *Auris Nasus Larynx.* (2019) 46:493–7. doi: 10.1016/j.anl.2018.11.008
52. Inui H, Sakamoto T, Ito T, Kitahara T. Magnetic resonance imaging of endolymphatic hydrops in patients with unilateral Meniere's disease: volume ratio and distribution rate of the endolymphatic space. *Acta Otolaryngol.* (2021) 141:1033–7. doi: 10.1080/00016489.2021.1968488
53. Inui H, Kitahara T, Ito T, Sakamoto T. Magnetic resonance 3D measurement of the endolymphatic space in 100 control human subjects. *J Int Adv Otol.* (2021) 17:536–40. doi: 10.5152/iao.2021.21317
54. He B, Zhang F, Zheng H, Sun X, Chen J, Chen J, et al. The correlation of a 2D volume-referencing endolymphatic-hydrops grading system with extra-tympanic electrocochleography in patients with definite Ménière's disease. *Front Neurol.* (2021) 11:595038. doi: 10.3389/fneur.2020.595038
55. Okuno T, Sando I. Localization, frequency, and severity of endolymphatic hydrops and the pathology of the labyrinthine membrane in Menière's disease. *Ann Otol Rhinol Laryngol.* (1987) 96:438–45. doi: 10.1177/000348948709600418

Conflict of Interest: The authors declare that the research was conducted in the absence of any commercial or financial relationships that could be construed as a potential conflict of interest.

Publisher's Note: All claims expressed in this article are solely those of the authors and do not necessarily represent those of their affiliated organizations, or those of the publisher, the editors and the reviewers. Any product that may be evaluated in this article, or claim that may be made by its manufacturer, is not guaranteed or endorsed by the publisher.

Advantages of publishing in Frontiers

OPEN ACCESS
Articles are free to read for greatest visibility and readership

FAST PUBLICATION
Around 90 days from submission to decision

HIGH QUALITY PEER-REVIEW
Rigorous, collaborative, and constructive peer-review

TRANSPARENT PEER-REVIEW
Editors and reviewers acknowledged by name on published articles

Frontiers
Avenue du Tribunal-Fédéral 34
1005 Lausanne | Switzerland

Visit us: www.frontiersin.org
Contact us: frontiersin.org/about/contact

REPRODUCIBILITY OF RESEARCH
Support open data and methods to enhance research reproducibility

DIGITAL PUBLISHING
Articles designed for optimal readership across devices

FOLLOW US
@frontiersin

IMPACT METRICS
Advanced article metrics track visibility across digital media

EXTENSIVE PROMOTION
Marketing and promotion of impactful research

LOOP RESEARCH NETWORK
Our network increases your article's readership